Synthetic Approaches to Heterocyclic Systems of Pharmaceutical Relevance

Thesis submitted to the University of Strathclyde as part of the assessment towards a degree of Doctor of Philosophy

Luke Green

2021

Abstract

Heterocycles are a privileged motif in pharmaceutically relevant compounds and are found in more than 85% of biologically-active molecules.[1] As such, understanding the roles of these moieties and improving access to them is of upmost importance in drug discovery.

Chapter I provides a conformational analysis of the novel, heterocyclic cyclopropylpyran (3-oxabicyclo[4.1.0]heptane, CPP) moiety with five-membered heterocyclic compounds. Previous conformational and synthetic studies of the CPP moiety with six-membered systems showed that this was bioisosteric with morpholine in kinase inhibitors, due to coplanar conformations.[2,3] A hypothesis was developed and suggested that overlap of π-like orbitals in the cyclopropyl ring with those in the heteroaromatic π-system was in part responsible for the coplanarity, supported by quantum mechanical (QM) modelling. Application of QM modelling and subsequent synthesis of furans, pyrroles and isoxazoles with three pyran analogues (CPP, dihydropyran (DHP) and tetrahydropyran (THP)) provided very little evidence for electronic effects, with the smaller five-membered systems allowing coplanar conformations for all furan and isoxazole pyran analogues, as shown in Figure 1. This included the THP analogues, which crystallised twisted with six-membered systems.

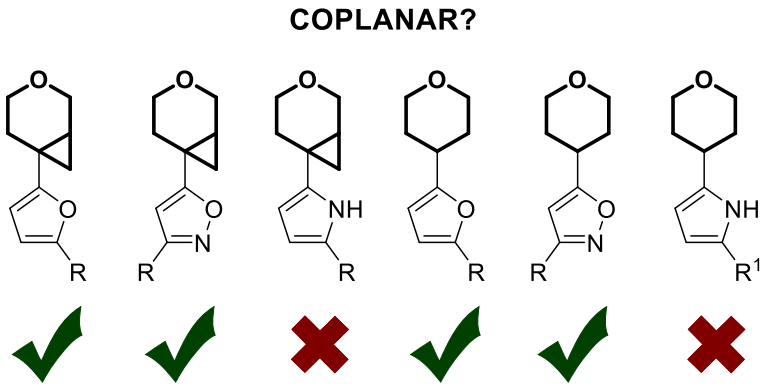

Figure 1. Summary of the key outcomes of the conformational analysis.

Following this, an enantioselective synthesis of the bicyclo[4.1.0]heptane moiety was investigated, aimed at accessing an intermediate to enable installation of the CPP moiety onto a range of heterocyclic systems (Figure 2). Gold-catalysed cycloisomerisation of 1,6-enynes gave the desired 3-azabicyclo[4.1.0]hept-4-enes with good enantioselectivities. Optimisation of this method led to the discovery of a scalable one-pot cycloisomerisation-reduction process, followed by oxidation of a vinyl group to a carboxylic acid in one step. Preliminary studies into the use of this acid as a means of installing the azabicyclo[4.1.0]heptane moiety gave mixed results; however, a potassium trifluoroborate salt could be accessed and successfully implemented in subsequent Suzuki-Miyaura cross-coupling reactions with 2-bromopyridine.

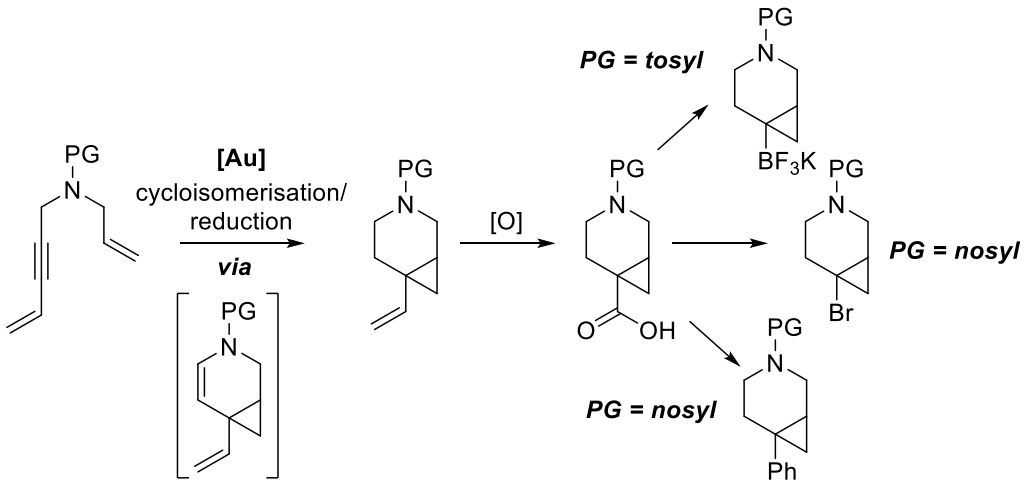

Figure 2. Summary of functionalisation of the 1,6-enyne moiety to give intermediates enabling the installation of the azabicyclo[4.1.0]heptane moiety.

Chapter II reports a modern adaptation of the Huisgen approach to 1,3,4-oxadiazoles, a heterocyclic motif which finds application in biologically active molecules and electron transporting materials in organic light emitting diodes. Current synthetic methods towards this scaffold are known within the literature; however, these may require toxic and difficult to handle reagents, alongside the use of bespoke intermediates.

An under-utilised approach towards this moiety is the Huisgen reaction wherein a 5-substituted tetrazole and acid chloride or acid anhydride are combined under high temperatures to afford the 1,3,4-oxadiazole *via* a nitrile imine intermediate. Implementation of flow photochemistry with a UV-B lamp under significantly more mild reaction conditions was found to facilitate the formation of the nitrile imine intermediate. Furthermore, integration of benign carboxylic acid starting materials represented a significant advancement in the applicability of this approach, which has been exemplified by a broad substrate scope and comparable efficiency to existing approaches.

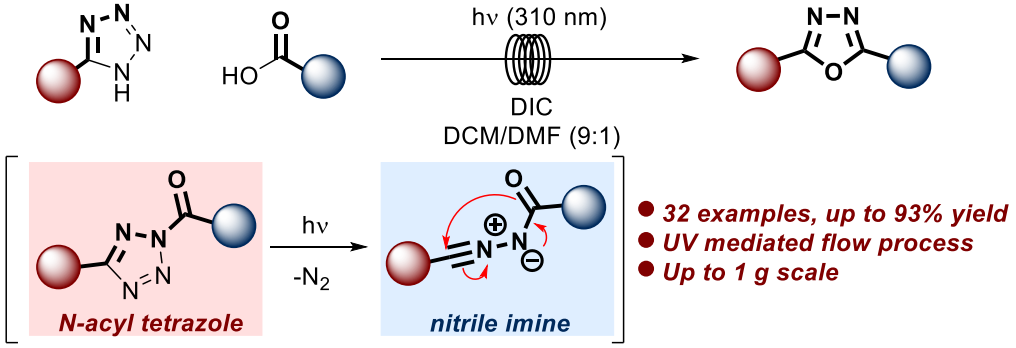

Scheme 1. Summary of the photochemical Huisgen reaction in flow.

This research has been subsequently published: L. Green *et al*., *Chem. Eur. J.*, 2020, **26**, 14866-14870.[4]

Acknowledgements

To begin with, I would like to thank both of my supervisors, Dr Craig Jamieson and Dr Simon Peace. Your support and guidance throughout my studies has been invaluable and allowed me to continually learn and develop my skills. The time you have both given to project discussions and the trust in me to take ownership of my research is something for which I am truly grateful. I have thoroughly enjoyed the knowledge you have instilled upon me; be it the state of Motherwell FC, insights into horse racing or, most importantly, the world of chemistry and pharmaceuticals. Thank you for making my studies enjoyable and I am glad to have had the pleasure of working with you both.

I would also like to thank Dr Heather Hobbs for welcoming me into the laboratory and allowing me to integrate into the team. Your project knowledge and help with day-to-day questions was vital and allowed me to hit the ground running. I am also grateful to Dr Declan Summers who provided initial support on my project and took the time to help me understand the intricacies of the CPP data.

To everyone that allowed me to obtain the necessary data: Dr Sandeep Pal, Dr Alan Kennedy, the chiral analytical group and the global spectroscopy group, thank you for your time and patience.

Prof. Harry Kelly, your enthusiasm for the scheme, passion for development and investment in the students is truly appreciated. Along with Prof. William Kerr, thank you for allowing me to be part of this scheme, it has been a privilege to be a member of such a unique research environment. Thanks also to Prof. Kerr who examined both my 9- and 21-month reports and pushed me to improve both my technique and confidence.

Thank you to Andrea Malley and Abby Mullord who have allowed me to attend conferences and have been very supportive in the administration side of the scheme.

Finally, I would not have been able to do this without the unwavering support of my family and friends. Throughout the difficult times, they have stood by me and encouraged me to pursue my goals. In particular, I am grateful to my fiancée Alisia who has been a constant source of encouragement and support. I would not have been able to do this without you, thank you.

Contents

Abbreviations

AO	Atomic Orbital
ATP	Adenosine Triphosphate
B3LYP	Becke 3-Parameter (Exchange), Lee, Yang and Parr
BEI	Binding Efficiency Index
BINAP	(1,1′-Binaphthalene-2,2′-diyl)bis(diphenylphosphine)
Bn	Benzyl
Boc	*tert*-Butyloxycarbonyl
BPin	Boronic Acid Pinacol Ester
CAN	Ceric Ammonium Nitrate
CataXCium A®	Di(1-adamantyl)-*n*-butylphosphine
Cbz	Carboxybenzyl
CDI	1,1′-Carbonyldiimidazole
CFL	Compact Fluorescent Lamps
COX-2	Cyclooxygenase 2
CPP	Cyclopropylpyran (3-oxabicyclo[4.1.0]heptane)
CPPip	Cyclopropylpiperidine (3-azabicyclo[4.1.0]heptane)
CRO	Contract Research Organisation
DBU	1,8-Diazabicyclo[5.4.0]undec-7-ene
DCC	Dicyclohexylcarbodiimide
DCE	Dichloroethane
DCM	Dichloromethane
DFT	Density Functional Theory
DHP	Dihydropyran
DIBAL-H	Diisobutylaluminium hydride

DIC	*N*,*N*'-Diisopropylcarbodiimide
DIPEA	*N*,*N*-Diisopropylethylamine
DMAP	4-(*N*,*N*-Dimethylamino)pyridine
DMF	*N*,*N*-Dimethylformamide
DMP	Dess–Martin Periodinane
DMSO	Dimethyl Sulfoxide
EDCI	*N*-(3-Dimethylaminopropyl)-*N*′-ethylcarbodiimide
EL	Emitting Layer
ETL	Electron-Transporting Layer
FEP	Fluorinated Ethylene Propylene
HATU	1-[Bis(dimethylamino)methylene]-1*H*-1,2,3-triazolo[4,5-*b*]pyridinium 3-oxide Hexafluorophosphate
HMPA	Hexamethylphosphoramide
HOAt	1-Hydroxy-7-azabenzotriazole
HOBt	1-Hydroxybenzotriazole
HOTT	*S*-(1-Oxido-2-pyridyl)-*N*,*N*,*N*′,*N*′-tetramethylthiuronium Hexafluorophosphate
HPLC	High Performance Liquid Chromatography
HRMS	High Resolution Mass Spectroscopy
HTL	Hole-Transporting Layer
IBX	2-Iodoxybenzoic Acid
IPA	Isopropyl Alcohol
JohnPhos	(2-Biphenyl)di-*tert*-butylphosphine
LCMS	Liquid Chromatography Mass Spectroscopy
LED	Light Emitting Diode
LUMO	Lowest Unoccupied Molecular Orbital

MDAP	Mass Directed Auto Purification System
MIDA	Methyliminodiacetic Acid
MO	Molecular Orbital
MOE	Molecular Operating Environment
mTOR	Mechanistic Target of Rapamycin
NBS	*N*-Bromosuccinimide
NMR	Nuclear Magnetic Resonance
Ns	2-Nitrobenzenesulfonyl, Nosyl
OLED	Organic Light Emitting Diode
OTf	Trifluoromethanesulfonate, Triflate
PBD	2-Biphenyl-4-yl-5-(4-*tert*-butylphenyl)-1,3,4-oxadiazole
PHIL	Photochemistry LED Illuminator
PI3K	Phosphatidylinositol-4,5-bisphosphate 3-kinase
PIDA	(Diacteoxyiodo)benzene
PIFA	[Bis(trifluoroacetoxy)iodo]benzene
PMB	*para*-Methoxybenzyl
PTFE	Polytetrafluoroethylene
Py	Pyridine
PyBOP®	(Benzotriazol-1-yloxy)tripyrrolidinophosphonium Hexafluorophosphate
PyBrOP®	Bromotripyrrolidinophosphonium Hexafluorophosphate
QM	Quantum Mechanical
RAE	Redox Active Ester
RT	Room Temperature
SET	Single Electron Transfer
SPhos	2-Dicyclohexylphosphino-2′,6′-dimethoxybiphenyl

T3P®	Propylphosphonic Anhydride
TADDOL	(4*R*,5*R*)-2,2-Dimethyl-*α*,*α*,*α′*,*α′*-tetraphenyldioxolane-4,5-dimethanol
TBAF	Tetrabutylammonium Fluoride
TBME	*tert*-Butyl Methyl Ether
TBS	*tert*-Butyldimethylsilyl
TBTU	2-(1*H*-Benzotriazole-1-yl)-1,1,3,3-tetramethylaminium Tetrafluoroborate
TCCA	Trichlorocyanuric Acid
TFA	Trifluoroacetic Acid
THF	Tetrahydrofuran
THP	Tetrahydropyran
TLC	Thin Layer Chromatography
Ts	Toluenesulfonyl, Tosyl
TR-FRET	Time-Resolved Fluorescence Resonance Energy Transfer
UV	Ultraviolet
XPhos	2-Dicyclohexylphosphino-2′,4′,6′-triisopropylbiphenyl

Chapter I: Conformational and synthetic studies of the novel cyclopropylpyran (CPP) moiety

1. Introduction

1.1. Bioisosteres

Bioisosterism is an important concept in drug design and is characterised by the introduction of structural changes to a molecule, which maintain or improve upon a desirable biological effect.[5-7] These changes are commonly introduced to improve a specific property of the molecule and generally relate to potency or physicochemical attributes.[5,6] By using this approach in medicinal chemistry, it is possible to overcome common issues which may otherwise lead to attrition and, therefore, loss of an otherwise promising series of molecules.

The notion of general isosterism was first presented in 1919 by Irving Langmuir who viewed atoms, groups of atoms, compounds, and radicals of identical electron counts and arrangements, as isosteres.[8] Based on the isoelectronic nature of N_2O and CO_2 and the "practically identical" properties observed between them, the concept was extended, leading to publication of a list of 21 types of isostere as shown below in Table 1.

Table 1. List of isosteres with the same electron count, as published by Langmuir.[8]

Type		Type		Type	
1	H^-, He, Li^+	**8**	N_2, CO, CN^-	**15**	ClO_3^-, SO_3^{2-}, PO_3^{3-}
2	O^{2-}, F^-, Ne, Na^+, Mg^{2+}, Al^{3+}	**9**	CH_4, NH_4^+	**16**	SO_3, PO_3^-
3	S^{2-}, Cl^-, Ar, K^+, Ca^{2+}	**10**	CO_2, N_2O, N_3^-, CNO^-	**17**	$S_2O_6^{2-}$, $P_2O_6^{4-}$
4	Cu^+, Zn^{2+}	**11**	NO_3^-, CO_3^{2-}	**18**	$S_2O_7^{2-}$, $P_2O_7^{4-}$
5	Br^-, Kr, Rb^+, Sr^{2+}	**12**	NO_2^-, O_3	**19**	SiH_4, PH_4^+
6	Ag^+, Cd^{2+}	**13**	HF, OH^-	**20**	MnO_4^-, CrO_4^{2-}
7	I^-, Xe, Cs^+, Ba^{2+}	**14**	ClO_4^-, SO_4^{2-}, PO_4^{3-}	**21**	SeO_4^{2-}, AsO_4^{3-}

The table allowed further similarities to be probed, for example if two compounds of two different types exhibited similar physical properties, then the isoelectronic groups of each type should also be similar. An example of this was given, with the similarity between argon (type 3) and methane (type 9) known. Based on this, Langmuir predicted that potassium (type 3) and ammonium (type 9) ions should also be similar due to the isoelectronic nature of these groups.[8]

In 1925, as an extension to this work, and based on experimental evidence, Grimm developed an idea known as the "hydride displacement law".[7,9,10] By adding a hydrogen atom to an element which lies up to four places before the noble gases on the "periodic system", the behaviour was predicted to mimic that of the element to the right. For example, the addition

of one hydrogen atom will cause the resulting group to become a “pseudoatom” of the atom one place to the right. This is summarised in Table 2 below in which each column represents a group of isosteres in this sense.

Table 2. Summarisation of Grimm's hydride displacement law.[7,9,10]

C	N	O	F	Ne	Na
	CH	NH	OH	FH	-
		CH_2	NH_2	OH_2	FH_2^+
			CH_3	NH_3	OH_3^+
				CH_4	NH_4^+

This model was an interesting approach based on experimental evidence but did not consider the electronics of each system. Later, in 1932, Erlenmeyer accounted for a group of atoms representing its own entity rather than acting as the combination of the individual elements.[11] Specifically, the number of valence electrons was accounted for and atoms, groups of atoms, or ions with the same valence electron count were considered to be isosteric. Further additions to the notion of isosterism were also made, including the idea that all elements within the same group of the periodic table are isosteric.[11] Additionally, groups which appeared to differ superficially but manifested similar physical properties were deemed isosteric.[12]

The work by Erlenmeyer was also one of the first examples of isosteric application in a biological system and was followed by a second publication in which this was expanded.[11,13] These experiments involved the synthesis of diazonium salts which could be attached to artificial antigens, leading to the synthesis of antibodies. The reaction was shown to be highly sensitive to substrate alterations, such as varying the regioisomer of substituted aromatic species; however, two sets of bioisosteres were found. The resulting antibodies could not differentiate between these, giving the first example of bioisosterism (Figure 3).[11,13] As predicted by both Grimm and Erlenmeyer, an oxygen atom, -NH and methine were isosteric, inducing the same effect in the biological system. Furthermore, a phenyl and thiophenyl group were also found to be isosteric, leading to the assumption that a “-CH=CH-“ group was isosteric with a sulfur atom, in this context.[13]

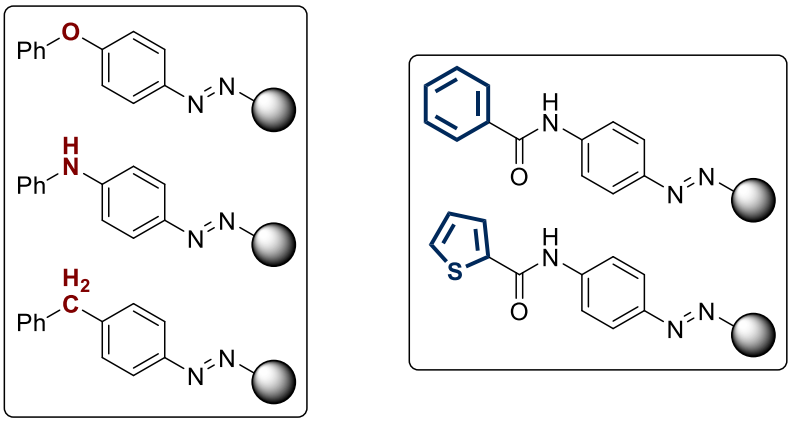

Figure 3. The two groups of isosteres found to give the same response when bound to an antigen. The compounds could not be differentiated in the biological system, giving the first example of bioisosterism.[11,13]

The first use of the term 'bioisostere' was made by Friedman in 1950, who summarised and tabulated previous data whereby bioisosteres had been used in medicinal chemistry.[14] The term was applied to compounds fitting the broadest definition of isosteres and which elicited biological activity by an identical mechanism.

In recent times, the definition has been cited as being too vague to be scientifically accurate and, as a result, Burger proposed a definition to encompass modern electronic theory and biochemical views. Bioisosteres are, therefore, described as "*compounds or groups that possess near-equal molecular shapes and volumes, approximately the same distribution of electrons, and which exhibit similar physical properties such as hydrophobicity*".[15] This definition allows coverage of all bioisosteres which are commonly grouped as "classical" and "non-classical", as will be described below (*vide infra*).

In 1979, Thornber set out eight parameters, shown in Table 3, which should be considered when modifying the structure of a molecule.[16] These parameters focus on the overall properties of the molecules, as opposed to the intrinsic electronic state of the groups being exchanged, thus fitting with a more generalised view of bioisosterism.

Table 3. The eight parameters given by Thornber which should be considered when implementing a bioisostere.

1	**Size** – molecular weight	**5**	**Water solubility**
2	**Shape** – bond angles, hybridisation	**6**	**pK_a**
3	**Electronic distribution** – polarisability, inductive effects, charge, dipoles	**7**	**Chemical Reactivity** – likelihood of metabolism
4	**Lipid solubility**	**8**	**Hydrogen bonding capacity**

In addition to consideration of these guidelines, Thornber highlighted the importance of considering the role of the moieties being substituted. Four principal roles were given and are shown below with the properties relevant to each role:

1) ***Structural*** – geometry, size, bond angles.
2) ***Receptor interactions*** – size, shape, electronic properties, pK_a, chemical reactivity, hydrogen bonding.
3) ***Pharmacokinetics*** – lipophilicity, hydrophilicity, hydrogen bonding, pK_a.
4) ***Metabolism*** – chemical reactivity.

These parameters are a cornerstone in the development of bioisosterism and represent ideas which are relevant to modern drug discovery. Frequently, the bioisosteres used in drug discovery are not structurally alike and are only mimetics in terms of their biological activity. Therefore, an accurate description also confers that a bioisostere in one system may not be applicable in another,[6] reflecting the complex nature of biology.

1.1.1. Classical Bioisosteres

Classical bioisosteres are those covered by Grimm's hydride displacement law and Erlenmeyer's broad description, factoring in the electronics of the system.[5-7,12,15] It is beyond the scope of this introduction to detail each use of these bioisosteres; however, given in Figure 4 are common "classical" bioisosteres found in the literature. A number of extensive reviews exist wherein specific uses are outlined, and the resultant effects described.[6,7,12] As expected, the effectiveness of these mimetics is dependent on the biological target and an almost infinite number of combinations have been reported.

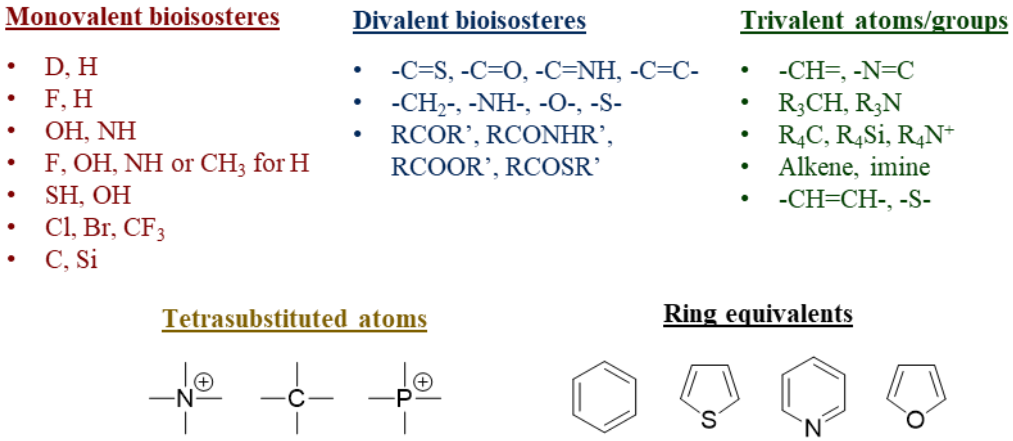

Figure 4. Summary of common "classical" bioisosteres which fall under the descriptions given by Grimm and Erlenmeyer. Figure adapted from Meanwell[6] and Brown.[12]

These set rules allow grouping, as in Figure 4, but this limits the extent to which the molecule can be altered. Furthermore, the somewhat strict grouping may restrict how bioisosterism is

considered. As a result, an alternative approach, referred to as "non-classical", relaxes these definitions and broadens the idea of bioisosterism.

1.1.2. Non-Classical Bioisosteres

The definition of non-classical bioisosteres allows the grouping of sets of compounds for which there may be no obvious likeness (structurally or electronically), but which elicit the same biological effect.[6,12,15,16] These changes may focus on one of a number of variables, affecting different properties of the molecule which can lead to subtle and non-obvious changes to the structure with a specific goal in mind.

Non-classical bioisosteres can be split into two groups, generalising the changes which may be made in addition to those classified as "classical" bioisosteres.[5,6,12]

1) Cyclic and acyclic isosteres
2) Exchangeable groups – the properties of discrete functional elements are mimicked.

As a result of the generalisation of these groups and the specificity for a given biological system, it is difficult to summarise all available bioisosteres for each common functional group. Despite this, there are some common cases in which the same group has been exemplified in several molecules. Some of these have been characterised and grouped by Thornber,[16] LaVoie[7] and Meanwell,[6] amongst others.[5,12,17,18] These reviews provide a clear overview of modern bioisosteres, and some of these are captured for common functionalities below in Figure 5. While not an exhaustive list, the majority of the bioisosteric groups do not appear to have much in common. Regardless of this, these groups can improve upon, or maintain, desirable properties of molecules in a specific biological system.

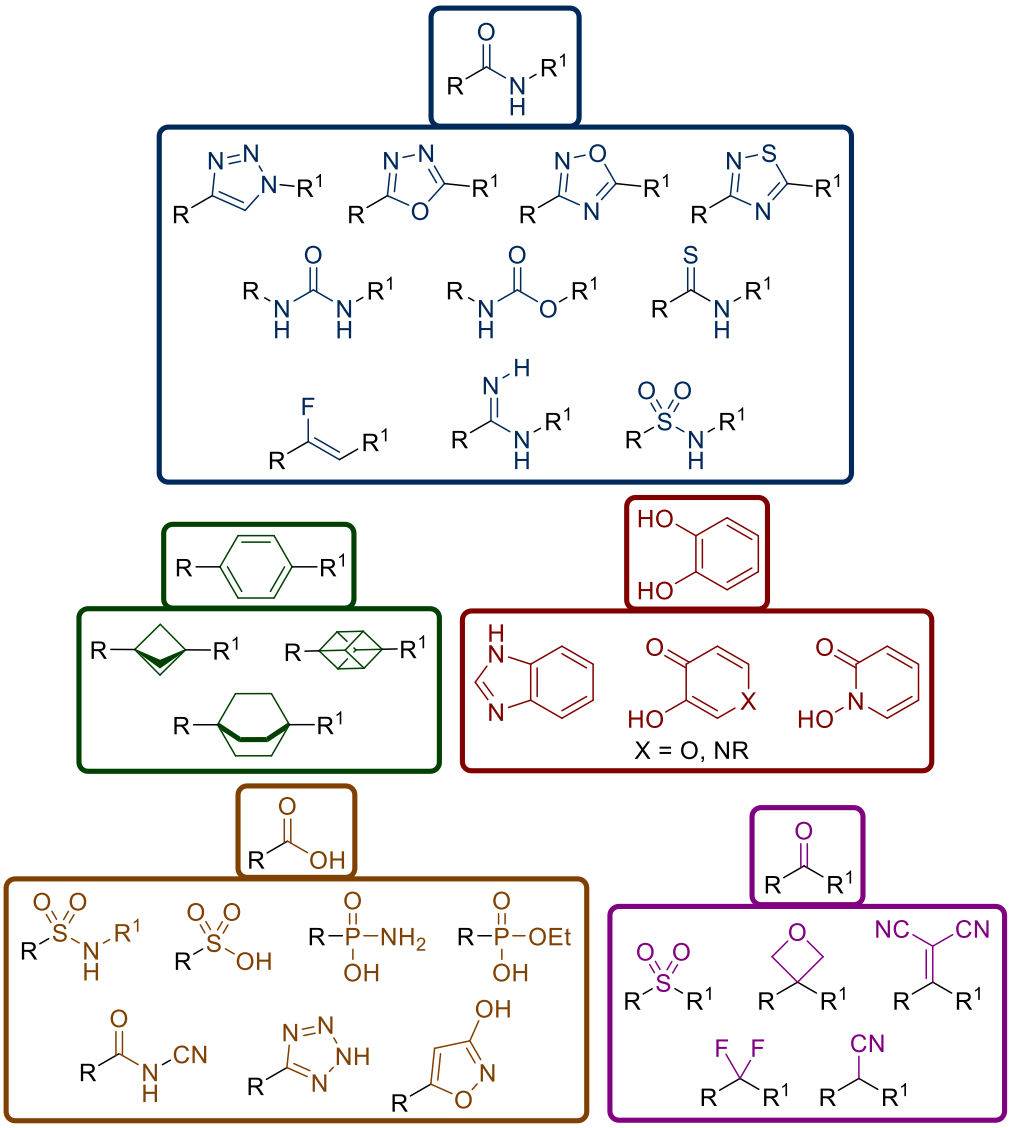

Figure 5. Non-classical bioisosteres of common groups found in medicinal chemistry.

The use of a range of moieties as bioisosteres reaffirms the position that the bioisosteric groups need not be structurally or electronically related. Additional effects may be observed upon introduction of a bioisostere, such as conformational control.[6] These effects may introduce, strengthen or weaken the control, and each of these will affect the binding of a molecule to a target of interest. An example of this is with the novel cyclopropylpyran (CPP, 3-oxabicyclo[4.1.0]heptane) bioisostere for morpholine,[2,3] shown in Figure 6. This moiety confers some conformational control in heterocyclic systems, as will be discussed (*vide infra*).

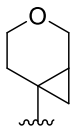

Figure 6. Structure of the cyclopropylpyran bioisostere for morpholine.

1.2. CPP Bioisostere for Morpholine

Within our own laboratory, a novel bioisostere for morpholine was recently discovered and developed.[2] The discovery emerged from the requirement to obtain a novel system which could replace morpholine as a hydrogen-bond acceptor in biological systems, specifically as a kinase inhibiting moiety. Furthermore, it was predicted that the novel moiety would adopt a stable coplanar conformation, which is required for binding to the targeted kinases (*vide infra*).

The CPP moiety was found to exhibit a similar energy profile to morpholine when using quantum mechanical (QM) modelling to undertake a dihedral angle scan.[19] The scan was conducted with a pyrimidine core due to the prevalence of the morpholine-pyrimidine system in lipid kinase inhibitors of relevance to inflammatory and fibrotic diseases which are of interest to our laboratory.[20] The scan was performed using Jaguar software and Density Functional Theory (DFT/6-31G**/B3LYP).[19,21] The dihedral angle was incrementally rotated by 10 ° and the energy minimised for each conformation and the results are summarised in Figure 7, below.

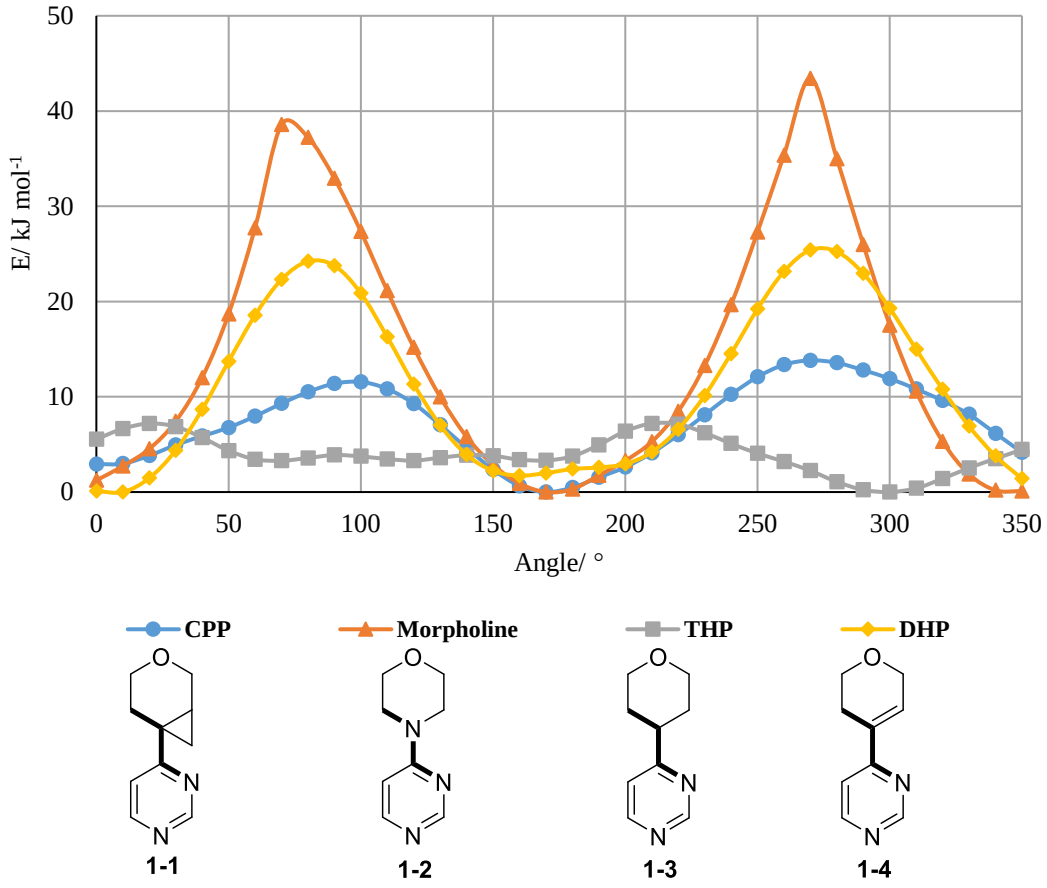

Figure 7. Dihedral angle scans of the CPP and morpholine groups alongside both tetrahydropyran (THP) and dihydropyran (DHP) rings.

Both CPP **1-1** and morpholine **1-2** favoured conformations corresponding to dihedral angles of approximately 0 ° and 180 °, as shown by the energy minima. These corresponded to conformations wherein the heteroaromatic and unsaturated rings were aligned in the same plane, and hence coplanar. Comparing this to DHP derivative **1-4**, which mimics this effect, it was proposed that coplanarity for the systems could be influenced by electronic as well as steric factors. Orbital overlap was hypothesised to occur between the pyrimidine ring and the functionality of the pyran group. Comparing this to the prediction for THP derivative **1-3**, which has a 'twisted' energy minimum at 300 °, the lack of orbital overlap and presence of only steric effects does not support coplanarity. These conformational differences are particularly important with respect to biological activity, as a low energy conformation reflecting that of the molecule in the bound state, in general, leads to increased activity.

The relative stabilisation of the coplanar conformations of molecules **1-1**, **1-2** and **1-4** was anticipated to reflect the extent of the electronic donation into the pyrimidine π-system. The electron-deficient nature of the pyrimidine ring meant that an electron-rich or electron-donating moiety would lead to considerable orbital overlap and stabilisation of the coplanar conformations. The lone-pair of electrons on the nitrogen atom of morpholine **1-2** are able to efficiently overlap with the π-orbitals electron-deficient pyrimidine (as shown in Figure 8), leading to a large stabilisation of the coplanar conformation.

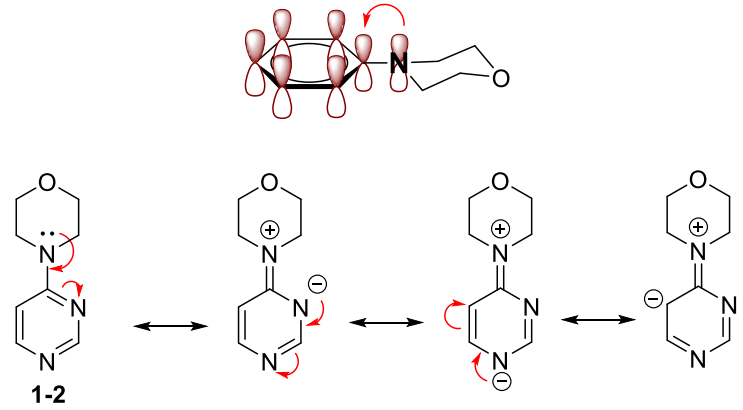

Figure 8. Orbital overlap between the lone pair of the nitrogen in the morpholine ring and the (hetero)aromatic π-system. Also shown are resonance structures for compound **1-2**.

Analysis of DHP derivative **1-4** and the respective orbital overlap shows that it is possible to form a conjugated system; however, the double bond produces a weaker mesomeric donation effect than a nitrogen lone pair (Figure 9). As such, there is less propensity for the alkene to donate electron density to the pyrimidine ring, leading to increased mismatch between the orbital energies compared to that of the morpholine. Despite this, a coplanar conformation is stabilised, albeit to a lesser extent.

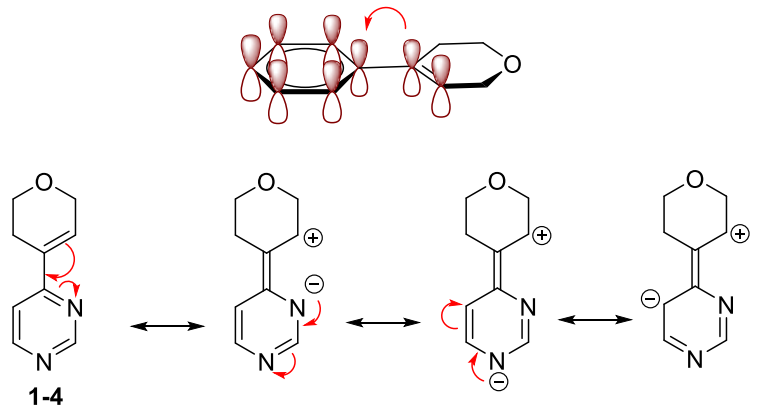

Figure 9. Orbital overlap between the alkenyl double bond in the DHP ring and the (hetero)aromatic π-system. Also shown are resonance structures for compound **1-4**.

Extending this approach to the CPP moiety, orbital overlap is possible given the electron density in the cyclopropyl ring. This may allow donation into the heteroaromatic π-system in an analogous way to the lone pair of the nitrogen atom in morpholine **1-2** (*vide supra*).[22,23] Figure 10 below shows the proposed bonding molecular orbitals (MOs) of cyclopropane which can be used to show overlap with a conjugated π-system.[24]

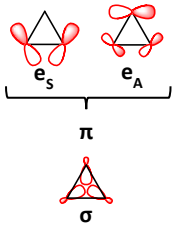

Figure 10. Walsh's molecular orbitals (MOs) of cyclopropane, derived from atomic orbitals (AOs). It is proposed that these contain a significant amount of π-character, analogous to that of a carbon-carbon double bond.

The σ-bonding MO is derived from a linear combination of three sp^2 hybrid AOs, whereas the two π-bonding MOs are derived from linear combinations of three p-orbitals in a similar fashion to that of an alkene.[24] It is postulated that the π-bonding MOs, specifically the e_A, are responsible for the observed conjugation with other π-systems;[22,23] however, this is conformation-dependent due to the directionality of the π-bonding MOs. The greatest overlap between the e_A MO and another π-system is observed when the interacting orbitals are parallel to each other or when the nodal plane of the π-system is perpendicular to the plane of the cyclopropyl ring.[22]

With respect to the CPP moiety, the cyclopropyl ring is itself part of a larger ring system and, as such, may not be able to adopt a conformation in which the orbitals have maximum overlap due to the shape of the six-membered ring and the constraints placed on this system. The term 'coplanarity' therefore refers to the conformation in which the two rings are as close to 'flat' as possible when the pucker of the saturated ring system is considered. Figure 11 below shows how the system may look and where the orbital overlap could be observed.

Figure 11. Schematic diagram showing the postulated orbital overlap from the e_A Walsh orbital of the cyclopropyl ring of the CPP into the π-system of a heteroaromatic ring.

The donation from the cyclopropyl ring into the electron-deficient π-system of the pyrimidine ring was expected to be weaker than that from morpholine **1-2** and DHP **1-4**. Nevertheless, the QM modelling shown in Figure 7 appeared to predict that this would occur to such an extent so as to favour coplanarity.

As a result of the predicted coplanarity, studies into the CPP moiety as a kinase inhibiting molecule were undertaken, giving rise to some interesting results.[2]

1.2.1. CPP as a Kinase Binding Moiety

A kinase is described as a protein which catalyses the transfer of a phosphate (PO_4^{3-}) group from adenosine triphosphate (ATP) to a specific target, causing a signalling cascade and numerous downstream effects.[25] In the human kinome there are 518 protein kinases of which 478 are grouped together into one 'superfamily' while the other 40 are referred to as 'atypical' due to differences in the domain sequences.[26] In addition, there are approximately 20 lipid kinases, including the commonly targeted phosphatidylinositol-3-kinases (PI3Ks).[27] The act of phosphorylation of various species is known to instigate a phosphorylation cascade, important to cellular messaging and responses.[26] As such, the role of kinases is highly important to biological functions,[26,28] thus making them attractive drug targets for multiple disease indications.

In order for the transfer of a phosphate group to occur, ATP must be bound in the active site, which is conserved across all kinases.[28,29] The binding site of a kinase is found in a cleft between the *C*-terminal and *N*-terminal lobes of the protein, as shown in Figure 12 for the Aurora A protein kinase.[29,30] Also shown is the structure of ATP and the key hydrogen bond formed in the active site. The binding area is also known as the 'hinge' region and is the target for the vast majority of therapeutic inhibitors.[31] It is the formation of key-hydrogen bonds in this region which lends the term 'hinge-binder' to those molecules mimicking ATP.

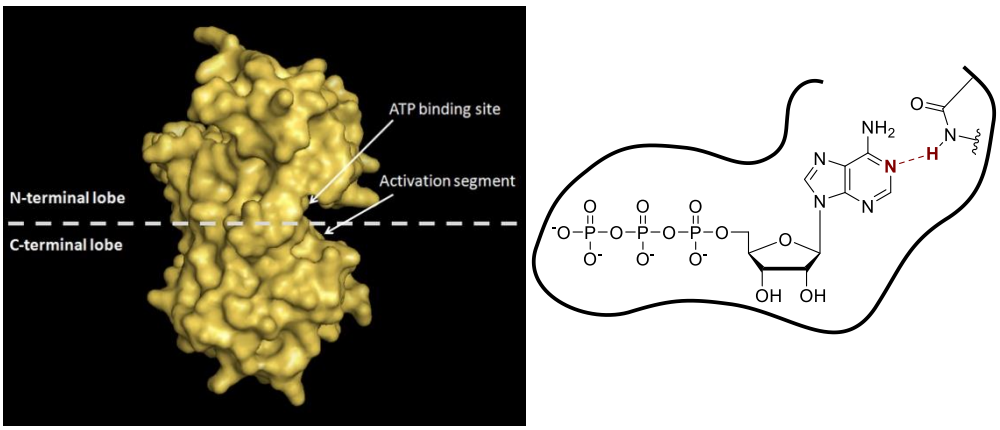

Figure 12. X-ray crystal structure of the Aurora A protein kinase showing the *N*-terminal and *C*-terminal lobes along with the binding site.[29,30] Shown alongside is a simplistic representation of ATP bound in the active site with the key hydrogen bond highlighted in red.

The CPP ring-system found use as a kinase-binding moiety in a number of lipid and lipid-like kinase inhibitors, producing comparable potencies to both the morpholine and DHP analogues.[2] The oxygen atom of the pyran ring is able to mimic the key hydrogen bond shown in Figure 12, enabling binding to the hinge region of the protein.

The source of the comparable potencies of the CPP, morpholine and DHP analogues can be related to the coplanarity of the systems. The use of DHP and THP moieties and their conformational preferences have been explored in detail by Kaplan.[32] The study found that molecular modelling predicted a low energy coplanar conformation for morpholine and DHP analogues and an orthogonal conformation for the THP analogue.[32] Furthermore, the binding conformation of the kinase inhibitors was shown to be coplanar in co-crystal biostructural data. As such, it was expected that the low energy coplanar conformation of the DHP analogue would require minimal energy input to adopt the binding conformation; however, the THP analogue would necessitate adopting a higher energy conformation in order to lie coplanar in the binding site. Therefore, an energy input is required for the THP analogue to bind to the kinase, leading to an inferior potency. This is summarised in Figure 13 below with the two conformations and potencies shown. The same rationale and approach were used for the CPP moiety with coplanar conformations shown to be lowest in energy when bound to a pyrimidine core. Very little rearrangement is required to adopt the binding conformation, leading to a comparable potency to both the DHP and morpholine analogues when tested against the mechanistic target of Rapamycin (mTOR) lipid kinase.[2]

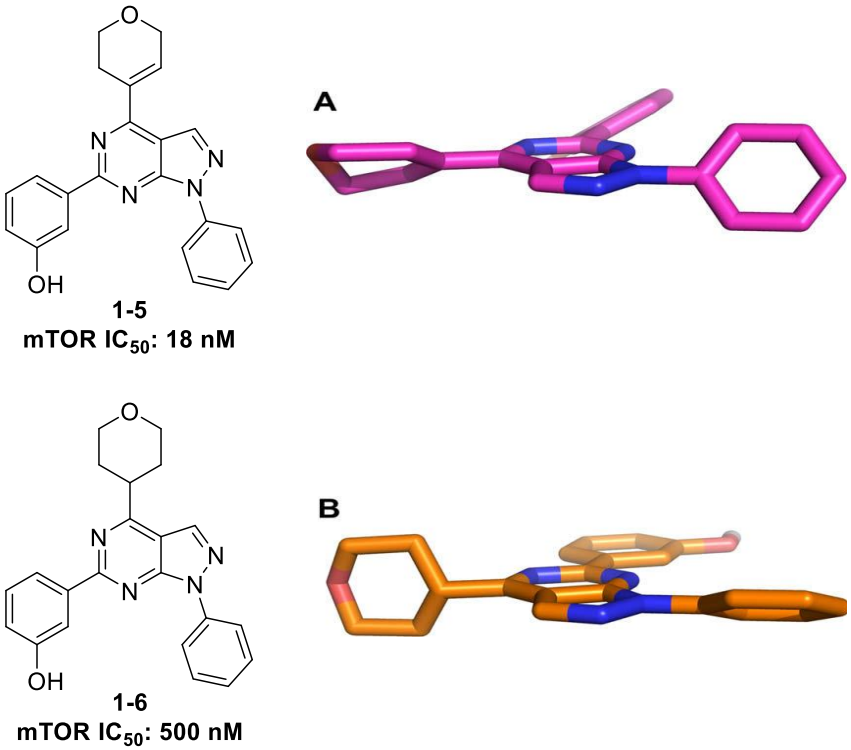

Figure 13. Kaplan's mTOR kinase inhibitors with a DHP moiety **1-5** and a THP moiety **1-6**. Shown are the corresponding lowest energy conformations and the resulting potencies.

The results reported in our laboratory concur with those described by Kaplan. The CPP moiety behaves in a similar manner to the morpholine and DHP analogues,[2] reflected in the corresponding potencies against a related series of lipid kinases (shown in Table 4).[3] The resulting coplanarity of the CPP moiety gave rise to a novel series of kinase inhibitors; however, further work was required to fully elucidate the intricacies of this group and establish the circumstances in which this would be useful.

Table 4. Summary of potency data obtained for pyrimidine-containing compounds analogous to compounds **1-4** and a *meta*-phenol group in the 2-position of the pyrimidine ring.

Core	Pyran Analogue	Isomer	PI3Kα pIC_{50}	PI3Kβ pIC_{50}	PI3Kγ pIC_{50}	PI3Kδ pIC_{50}
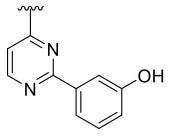	Morph.	-	6.3	6.2 (±.4)	6.1	6.6
	DHP	-	5.5 (±.6)	5.6 (±.4)	5.5 (±.7)	5.9
	CPP	1*R*, 6*S*	5.2	4.9	5.0	5.5 (±.4)
		1*S*, 6*R*	5.6	5.0	5.3 (±.5)	5.9
	THP	-	4.8	4.6	4.7	5.1

1.2.2. Challenges of the CPP Moiety

While the initial exploration of the novel CPP moiety was fruitful, yielding compounds which were equipotent with morpholine and DHP derivatives, it was necessary to explore this moiety in more detail. Variation of the core of the molecule would be important when

optimising the CPP-containing series to increasingly drug-like molecules. An experimentally confirmed set of guidelines highlighting where the CPP moiety is most likely to adopt a coplanar conformation would be a welcome addition to the overarching area. An initial study has been undertaken, probing the effect of varying the six-membered (hetero)aromatic core bound to the CPP and will be summarised below (*vide infra*).[3] Extension of this to common five-membered heterocyclic cores would provide further information with respect to the utility of this moiety.

The CPP moiety provides an additional challenge, introducing chirality to the molecules in which it is used. Furthermore, the two enantiomers exhibit different potencies *in vitro*, as highlighted in Table 4.[2] Current synthetic methods rely on separation of the two enantiomers by chiral preparative HPLC and, therefore, an enantioselective route to these compounds is desirable.

The two challenges of core variation and enantioselectivity outlined above are the focus of this chapter with an effort towards overcoming these in such a way as to allow wider use of the CPP moiety. As a result, this chapter will be composed of two principal areas of study:

1. Exploration of the CPP moiety and its conformational preference with five-membered heteroaromatic systems.
2. An enantioselective synthetic approach to an intermediate which would facilitate straightforward installation of the CPP moiety to a variety of compounds.

Section 1: Exploration of the CPP bioisostere for morpholine with five-membered heteroaromatic systems

2. Background

2.1. Dihedral Angle Scans of Six-Membered Systems

Subsequent studies of the CPP moiety investigated the variation of six-membered (hetero)aromatic cores.[3] The effect of changing the ring system on the conformational preference of these molecules was explored, leading to an improved understanding of the CPP. The variation of the six-membered core led to the dihedral angle scans shown below in Figure 14.

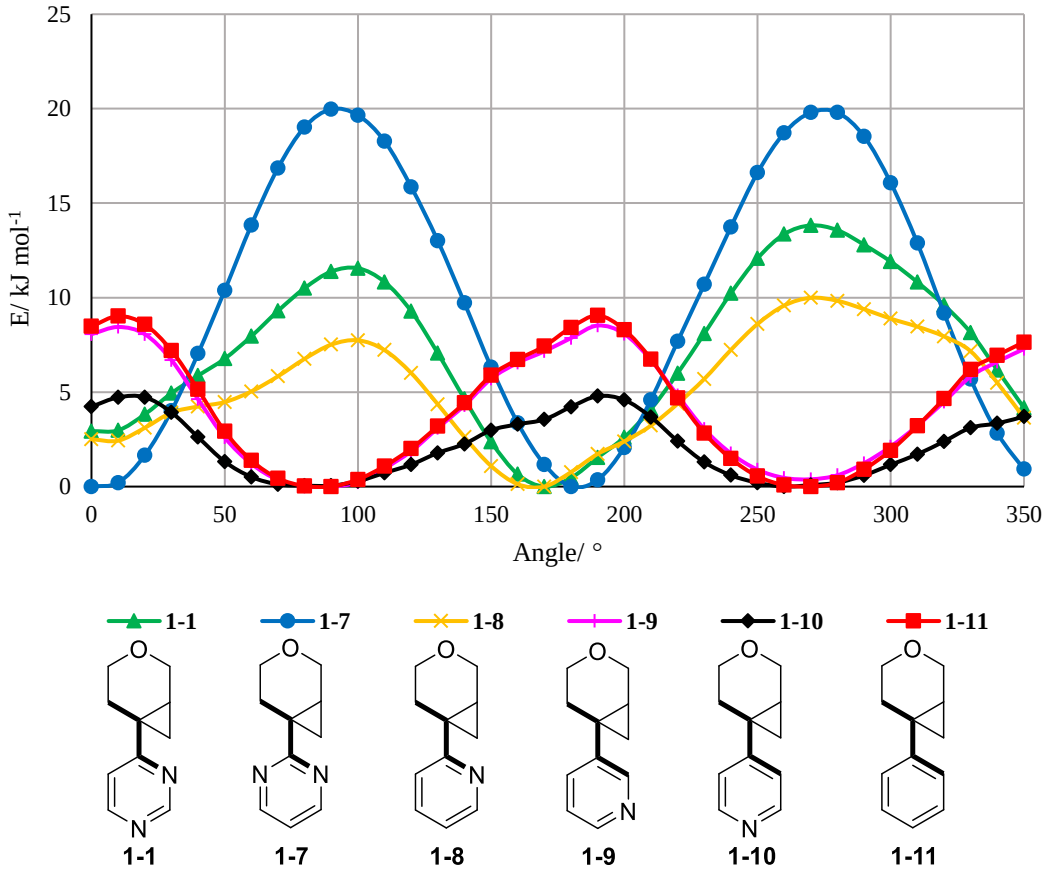

Figure 14. Dihedral angle scans of six-membered (hetero)aromatic species.

These results provided additional evidence to the proposed orbital interaction between the cyclopropyl ring and the electron-deficient heteroaromatic system, leading to low energy coplanar conformations. Both pyrimidine-containing compounds, **1-1** and **1-7** showed highly stablilised coplanar conformations, reflecting the electron-deficient nature of the ring. Replacement of the *ortho*-methine of compound **1-1** with a nitrogen atom, thereby removing steric clashes, further stabilised the coplanar conformations of pyrimidine **1-7**. This observation highlighted that the steric environment also affected the predicted conformation.

Comparison of compounds **1-1** and **1-8** suggested that increased electron-density in the heteroaromatic system led to less efficient donation from the cyclopropyl to the π-system, visible by the reduction in the relative stability of the coplanar conformation of **1-8** when compared to that of **1-1** (evidenced by the larger relative energy barriers to rotation). Furthermore, the position of the heteroatom in the pyridine analogues affected the predicted conformation and two methine groups adjacent to the CPP ring increased the steric interaction, shifting the predicted conformation from coplanar to twisted. Interestingly, there was a difference between 3-pyridyl **1-9** and 4-pyridyl **1-10**, with the latter showing less preference for a twisted conformation. This, again, intimated the presence of an electronic effect between the cyclopropyl orbitals and the heteroaromatic π-system, especially given the almost identical steric environment.

Phenyl derivative **1-11** gave an identical profile to 3-pyridyl **1-9**, indicating a lack of sufficient orbital overlap in both systems which comprise a similar steric environment. As such, both were predicted to exist in 'twisted' conformations.

2.2. Crystal Structure Analysis

The synthesis of tool compounds was undertaken, and single crystal X-ray structures obtained, enabling a comparison to the QM data. To acquire compounds which could provide both crystal structures and activity in an *in vitro* assay, a *meta*-phenol pan-lipid kinase motif was installed to the core, as with the compounds studied by Kaplan.[32]

The resulting compounds and crystal structures are shown in Table 5 along with a comparison of the predicted and observed data in addition to the angle between the average ring planes of the (hetero)aromatic ring and the CPP. Comparison of the data revealed that, overall, the modelling was predictive of the behaviour of the compounds shown. Only one deviation was observed with 4-pyridyl analogue **1-16** residing in a coplanar conformation as opposed to the predicted 'twisted' conformation. Two conclusions were made from this observation with the first being that the modelling may have underestimated the level of orbital overlap. Secondly, the calculated energy barriers of 5 kJ mol^{-1} may be sufficiently low to be overcome with intermolecular forces in the solid state.

Further computational investigations into these observations revealed that, in the absence of sufficient electronic donation from the cyclopropyl ring to the aromatic π-system, steric effects are the influencing factor.[3] A comparison of the crystal structures of 4-pyridyl analogue **1-16** and phenyl analogue **1-17**, which have identical steric environments adjacent to the CPP ring, highlighted this effect.

Table 5. Tool compounds and single crystal X-ray structures. Also shown are the predicted and observed data for comparison. More than one measured dihedral angle corresponds to the number of molecules observed in the unit cell.

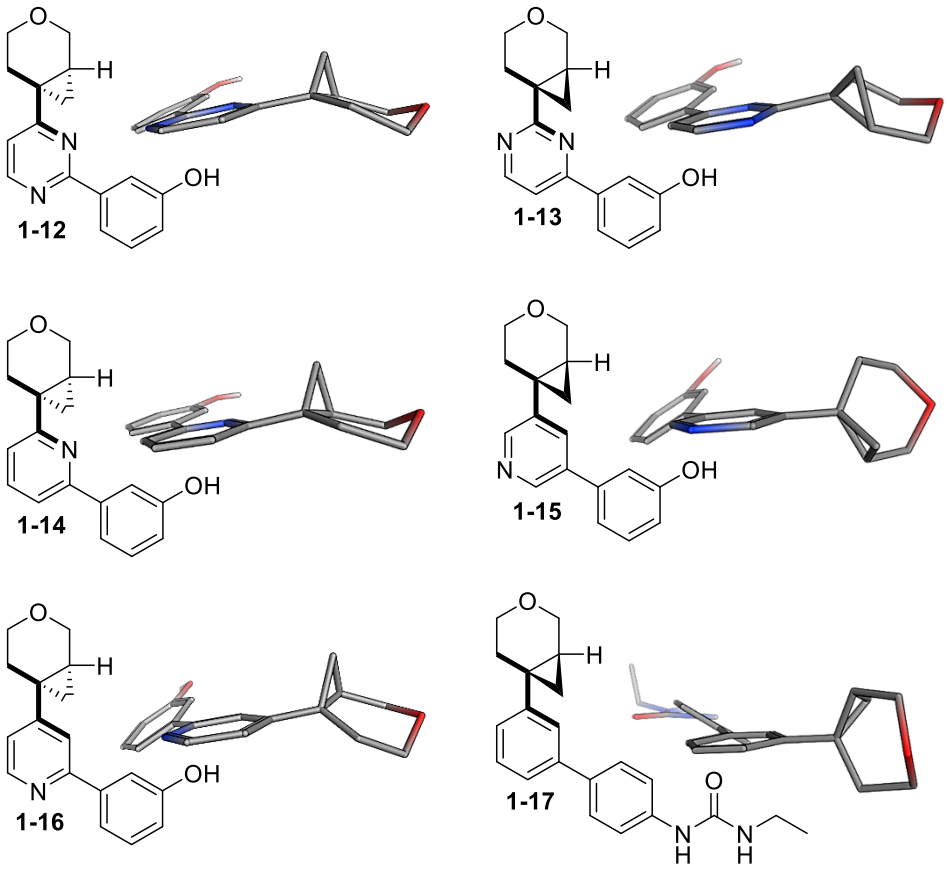

Compound	Predicted Dihedral Angle/ °	Measured Dihedral Angle/ °	Angle between average ring planes/ °
Pyrimidine **1-12**	170	15.0 180.5 184.3 192.3	34.6 35.2 36.8 26.3
Pyrimidine **1-13**	0 and 170	5.6 172.2	27.6 26.1
2-pyridine **1-14**	170	162.3 190.8	44.1 15.0
3-pyridine **1-15**	90	66.1 121.1	81.4 51.7
4-pyridine **1-16**	260	210.8 359.7	28.6 26.4
Phenyl **1-17**	270	253.9	83.8

From this work, the six-membered cores wherein the CPP would adopt a coplanar conformation could be identified. This information would be invaluable when undertaking a medicinal chemistry project, showing which analogues would likely provide low energy coplanar conformations. While six-membered cores are valuable, further uses of the CPP

moiety would be helpful to expand the uptake of this moiety in drug discovery. As such, exploration of five-membered heterocycles was undertaken to provide further insight into the conformational preferences. The reduced size and increased electron density of five-membered heteroaromatics posed an interesting challenge as to elucidating the preferred conformation of the resulting molecules. Additionally, the paucity of five-membered morpholine-derivatives in the literature (due to electron-donation into an already electron-rich system),[33] provides an interesting use for the CPP bioisostere if this is found to be both stable and coplanar.

3. Aims

The primary aim of this study was to determine if the use of the novel CPP bioisostere for morpholine could be applied to five-membered heteroaromatics. Within this, several five-membered heteroaromatic compounds could be modelled using the same approach as with the six-membered systems.[3,19] From here, selected examples could be synthesised and submitted to X-ray crystallography. These would include three different pyran analogues: DHP, THP and the novel CPP. The resulting crystal structures could then be analysed alongside the modelling to explore three key hypotheses:

1) Is the modelling, applied to six-membered systems, able to predict the conformation of five-membered heteroaromatic compounds and can this be used for molecular design?
2) Does the smaller ring size and increased electron density affect the degree to which coplanar conformations are stabilised and, therefore, the ability of the CPP to act as a bioisostere for morpholine?
3) How does the use of the CPP compare to that of the THP and DHP based on the altered characteristics of the heterocycle, and is the introduction of the CPP moiety beneficial in comparison to the THP and DHP?

The compounds for synthesis were chosen based on the perceived utility in exploring these hypotheses. Exploration of sterics, as well as the electronics of the heteroaromatic system, could be undertaken by alteration of the heteroatom as well as the introduction of a second heteroatom. The results from these experiments could then be used alongside those obtained for six-membered systems to give a complete overview of where the CPP moiety has the predicted potential to be used successfully within relevant medicinal chemistry programmes.

4. Results and Discussion

4.1. Modelling

Expanding the approach taken with six-membered to five-membered heteroaromatics was warranted to provide a more complete understanding of the applicability of the CPP moiety. Several five-membered heteroaromatic rings were chosen for modelling which aimed to cover several variables: the position of the heteroatom (2- or 3-position relative to where the CPP was bound), the size of the heteroatom (e.g. oxygen or sulfur), the presence of an additional hydrogen atom (pyrrole -NH) and the presence of two heteroatoms (oxazoles and isoxazole). A comparison of the conformations of the CPP to the THP and DHP was also made, as with the six-membered systems.

The initial iteration of compounds modelled are shown in Figure 15 with those in the blue box chosen to explore the behaviour of the three pyran analogues. Secondly, in the red box, variations in the position and size of heteroatom were probed and, finally, the compounds in the green box investigated the effect of a second heteroatom. The modelling used the approach described for the six-membered systems (*vide supra*) and was carried out by another member of our laboratories.[19]

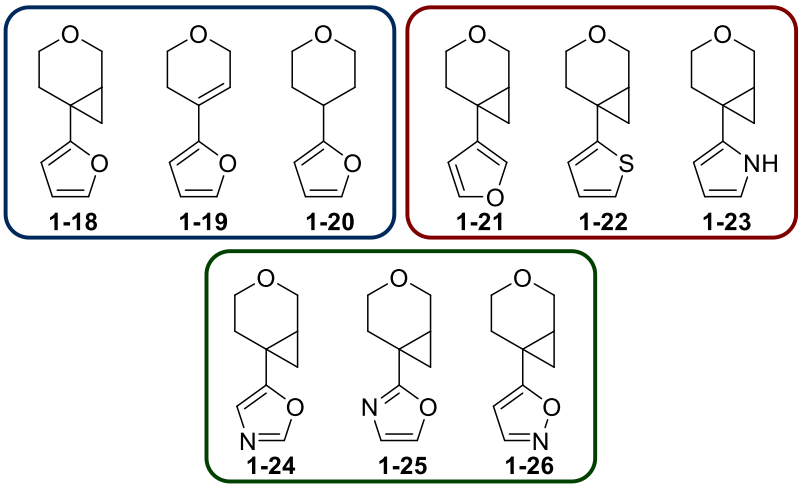

Figure 15. Five-membered heterocyclic compounds selected for DFT dihedral angle scans. Shown in the blue box are 2-furyl analogues to explore the effects of varying pyran analogues (CPP, DHP and THP). In the red box, analogues exploring both the size and position of the heteroatom are shown, and in the green box are five-membered heteroaromatic systems containing two heteroatoms.

A plot of relative energy as a function of the dihedral angle was produced for 2-furyl containing compounds **1-18** - **1-20** and is shown below in Figure 16.

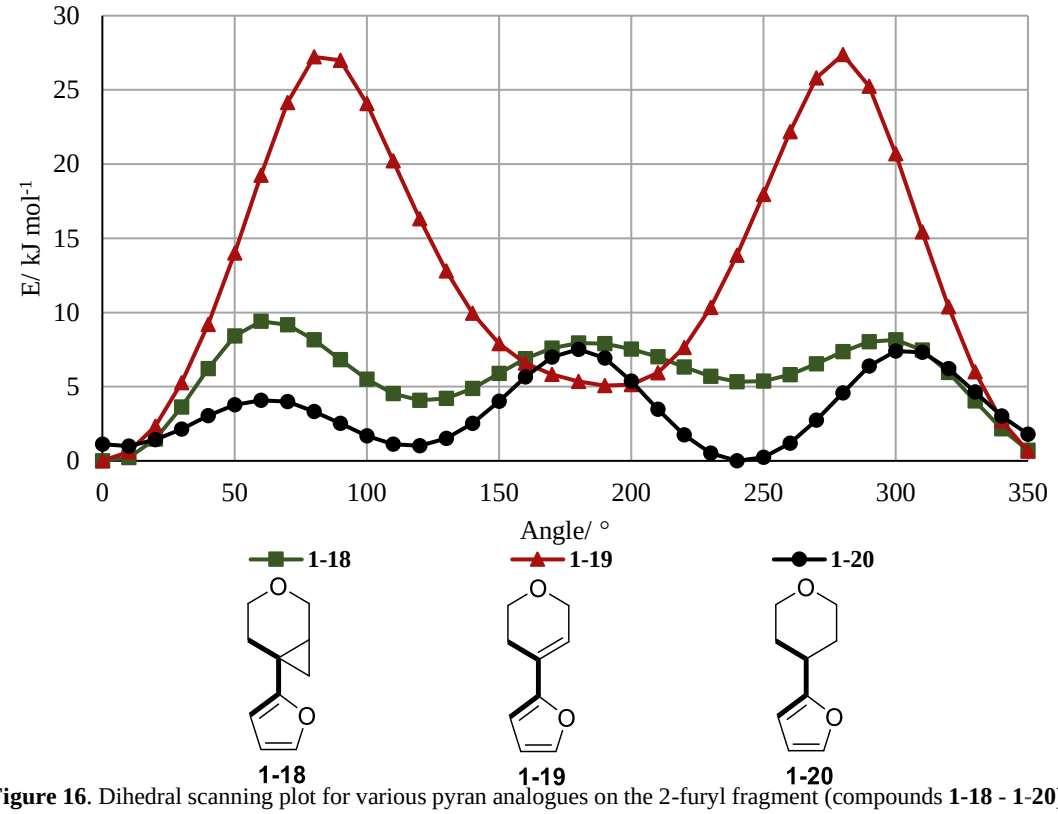

Figure 16. Dihedral scanning plot for various pyran analogues on the 2-furyl fragment (compounds **1-18** - **1-20**).

Two coplanar conformations were predicted at 0 ° and 190 ° for DHP-containing compound **1-19**, in agreement with the anticipated orbital overlap between the alkenyl double bond and the heteroaromatic π-system. Of particular note is the increased stabilisation of the minimum at 0 ° relative to that at 190 ° (5 kJ mol^{-1}) which may be due to the directionality of the protons on each ring. At 0 ° the proton on the furan ring bisects those on the DHP, whereas at 190 ° the two protons are directed at one another as shown in Figure 17.

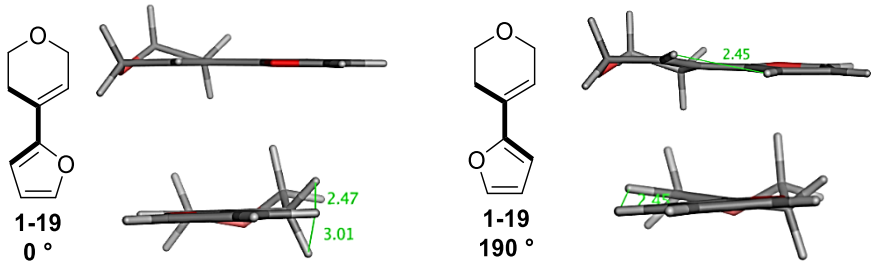

Figure 17. Two minimum energy conformations of DHP-containing compound **1-19**.

CPP-containing compound **1-18** and THP-containing compound **1-20** show much lower energy barriers to rotation than the corresponding DHP-containing compound **1-19**, indicating a decrease in the relative stabilisation of minimum energy conformations. Compounds **1-18** and **1-20** exhibit energy minima at the same three angles: 0-10 °, 120 ° and

240 °; however, the relative stabilisation of the coplanar conformation at 0 ° is larger for CPP-containing compound **1-18**, indicating that this may be favoured. THP-containing compound **1-20** is less likely to exhibit a preference due to the decreased stabilisation. Figure 18 shows the coplanar minimum for compound **1-18** and the three low energy conformations for compound **1-20**.

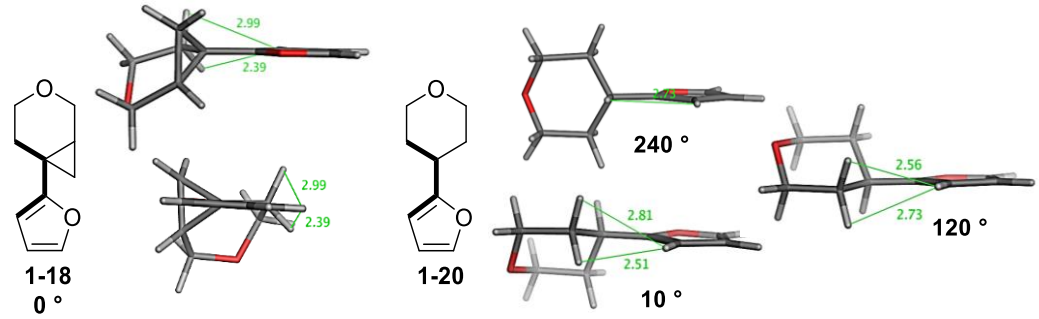

Figure 18. Energy minima for compounds **1-18** and **1-20**. **A** shows the coplanar conformation of CPP-containing compound **1-18**. **B** shows the three accessible minima for THP-containing compound **1-20**.

Compounds **1-21** – **1-23** were modelled to predict the effect of the size or position of the on the relative conformation, and the dihedral angle scans are shown below in Figure 19.

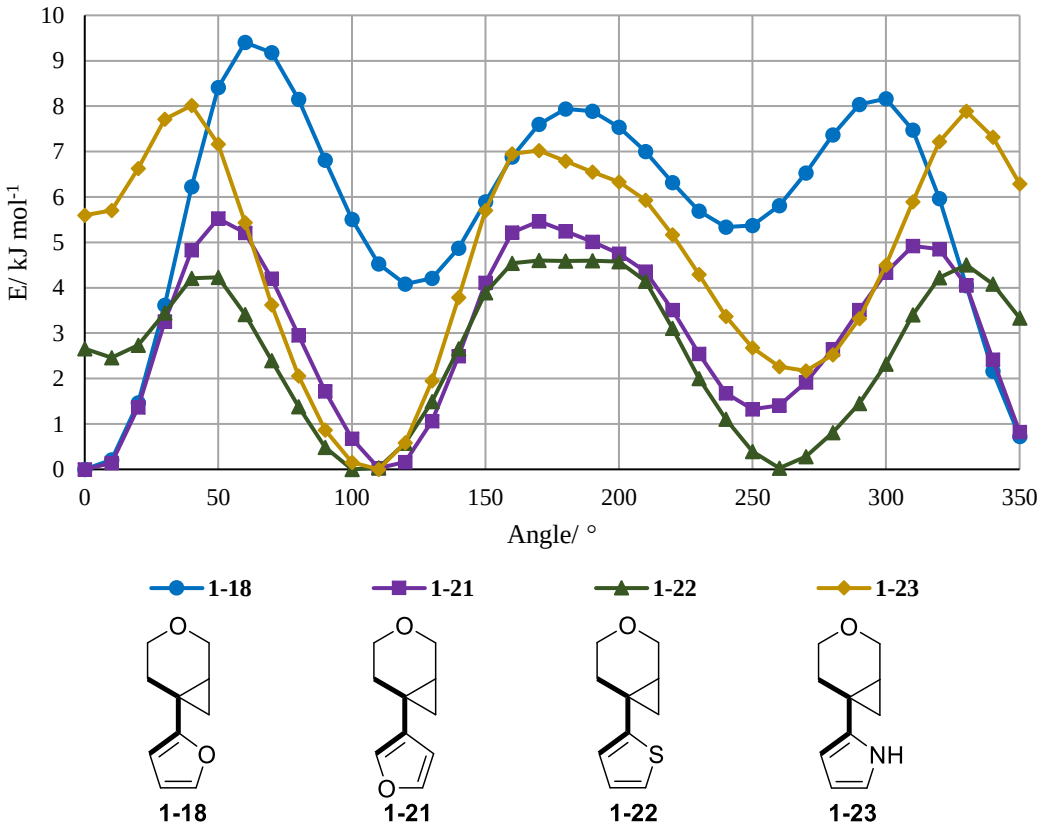

Figure 19. Dihedral angle scans of the CPP moiety with various 5-membered heterocycles (compounds **1-18**, **1-21, 1-22** and **1-23**).

3-Furyl CPP **1-21** was predicted to have a low energy coplanar conformation; however,

twisted conformations at 110 ° and 250 ° were equal in energy. The relative energy barriers between conformations are lower for 3-furyl analogue **1-21** than 2-furyl analogue **1-18**, potentially indicating reduced stabilisation of the energy minima. This may be as a result of the increase in sterics due to two protons adjacent to the CPP group (at positions 2 and 4 of the furan ring), rather than one in 2-furyl CPP **1-18**. Shown in Figure 20 below are the three minimum energy conformations, indicating the interactions between the furan protons and those in the CPP ring. The coplanar conformation at 0 ° requires the protons to be closer than in the twisted conformations (110 ° and 250 °) which may hint at some prediction of orbital overlap; however, this is unclear.

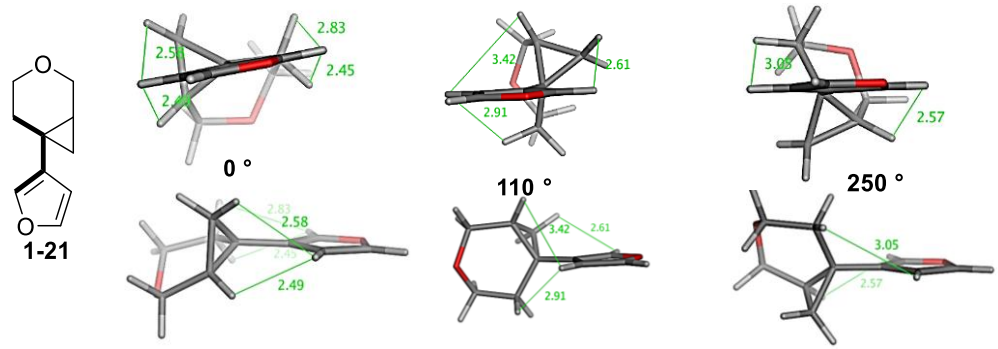

Figure 20. Minimum energy conformations of 3-furyl CPP **1-21**.

Thiophene-containing compound **1-22** and pyrrole-containing compound **1-23** have somewhat similar plots (Figure 19), which was expected given the increased size of the heteroatom. Coplanar conformations in these molecules are destabilised due to steric clashes with protons in the CPP ring, leading to a preference for twisted conformations (as shown in Figure 21).

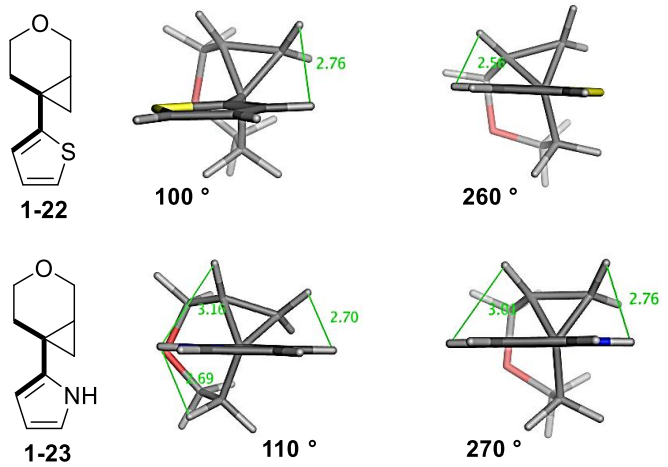

Figure 21. Minimum energy 'twisted' conformations of thiophene **1-22** and pyrroles **1-23**.

The destabilisation of the 0 ° conformation is larger for thiophene **1-22** and pyrrole **1-23** than in 3-furyl CPP **1-21**, despite the apparent similarity in steric environment. The difference in profile between 3-furyl **1-21** and pyrrole **1-23** is challenging to comprehend; however, a comparison of the bond angles and resulting changes in inter-nuclear distances may be an

influencing factor, as shown in Figure 22. Despite this, electronic differences cannot be ruled out.

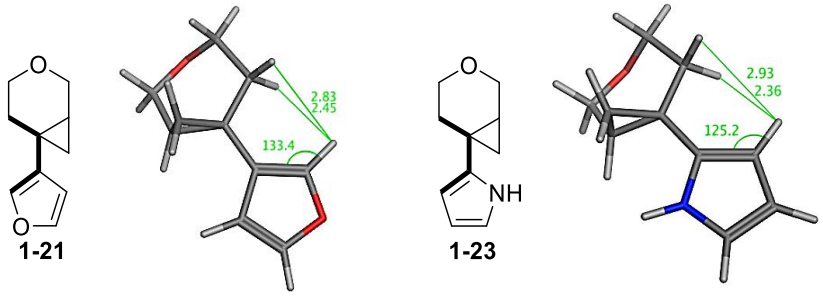

Figure 22. Conformations of compounds **1-21** and **1-23** at a dihedral angle of 0 °. The angles of protons which can clash with the CPP ring were measured as 133.4 ° for 3-furyl **1-21** and 125.2 ° for pyrrole **1-23**.

Finally, investigation of five-membered heteroaromatic species with two heteroatoms in the ring was undertaken with the second heteroatom expected to lower the relative energy of the lowest unoccupied molecular orbital (LUMO).[34] A nitrogen atom was introduced to the 2-furyl compound and moved around the ring, resulting in oxazoles **1-24** and **1-25** along with isoxazole **1-26** for which the dihedral angle scans are shown below in Figure 23.

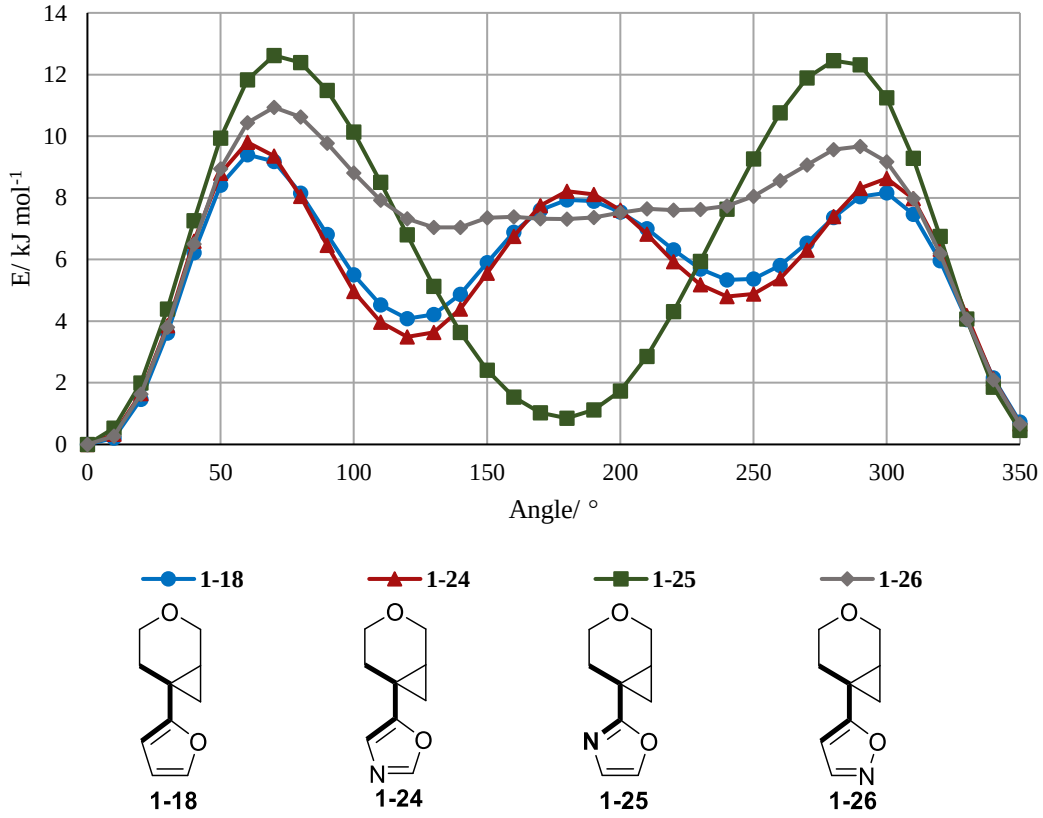

Figure 23. Dihedral angle scan of CPP hinge binder with various 5-membered heteroaromatic rings (compounds **1-18**, **1-24, 1-25** and **1-26**).

Furan-CPP **1-18** and oxazole-CPP **1-24** were predicted to have almost identical plots as the nitrogen atom introduced to the heteroaromatic ring does not reduce the size of the methine

adjacent to the CPP. Therefore, any steric clashes with the CPP ring will be almost identical for both compounds. It does not appear that the anticipated lowering of the LUMO energy has any effect on the stabilisation of the coplanar conformation in this case.

The plot of oxazole **1-25** appears to mimic that of 2-furyl DHP **1-19** (Figure 16) whereby two coplanar minima exist at 0 ° and 180 °. Replacement of the methine group in the 3-position of the furan with a nitrogen atom reduces the size and, therefore, steric interactions between the heteroaromatic system and the CPP ring. The similar energy value of both coplanar conformations is likely a reflection of the similar size of both heteroatoms.[35]

The most striking example shown in Figure 23 is the plot of isoxazole **1-26** in which a single energy minimum is predicted at 0 °. Consideration of coplanar structures, at 0 ° and 180 ° (Figure 24), highlights similar internuclear distances in both conformations. As such, it may be possible that the modelling predicts an orbital interaction when the dihedral angle is 0 ° and the cyclopropyl ring of the CPP and double bond of the heteroaromatic ring are in an antiperiplanar (*s-trans*) conformation. This has previously been reported as the most favourable conformation for cyclopropyl orbital overlap with a double bond.[36] Furthermore, the aromaticity of furan and isoxazole is reported to be approximately half that of benzene.[37] Therefore, a reduction in the aromaticity of these systems results in a larger degree of diene character than for 6-membered systems.[37] As a result, the relative conformation between the cyclopropyl and alkene-like double bond of the heteroaromatic may be more significant in these cases.

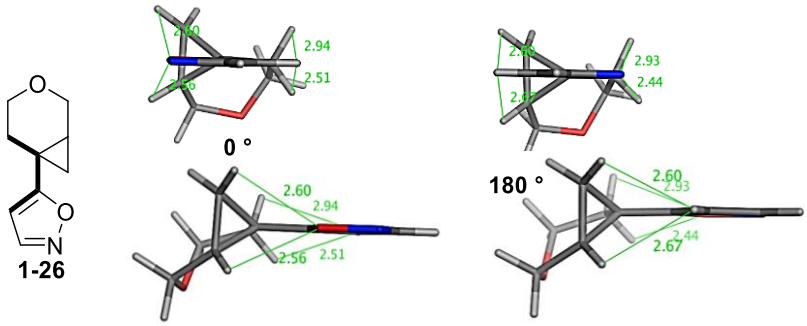

Figure 24. Predicted conformations of isoxazole **1-26** at 0 ° and 180 °. Only the coplanar conformation at 0 ° is low in energy with 180 ° representing a high energy conformation on the dihedral angle scan plot.

With the modelling in hand and detailed analysis undertaken, the corresponding heterocyclic compounds were chosen for synthesis and subsequent study of conformation using X-ray crystallography. A robust comparison could then be made between the predicted and observed conformations. 2-Furyl CPP, DHP and THP analogues **1-18** - **1-20** were chosen for synthesis, allowing verification of predictions for the CPP analogue. THP-containing

compound **1-20** was also of interest due to the presence of several energy minima, with one showing coplanarity.

Pyrrole **1-23** was chosen for synthesis due to the predicted twisted conformation with higher energy barriers than for thiophene **1-22**. Comparison of a predicted coplanar structure and a predicted twisted structure could then be carried out to determine the accuracy of the modelling with five-membered systems. The final compound chosen for synthesis was isoxazole **1-26** due to the prediction of a single, low energy, conformation which meant that it would be much easier to determine the accuracy of the modelling in this case. The THP and DHP analogues of pyrrole and isoxazole cores were subsequently modelled to allow further comparison of the modelling to the solid-state structures. The dihedral angle scan for the pyrrole analogues is shown below in Figure 25.

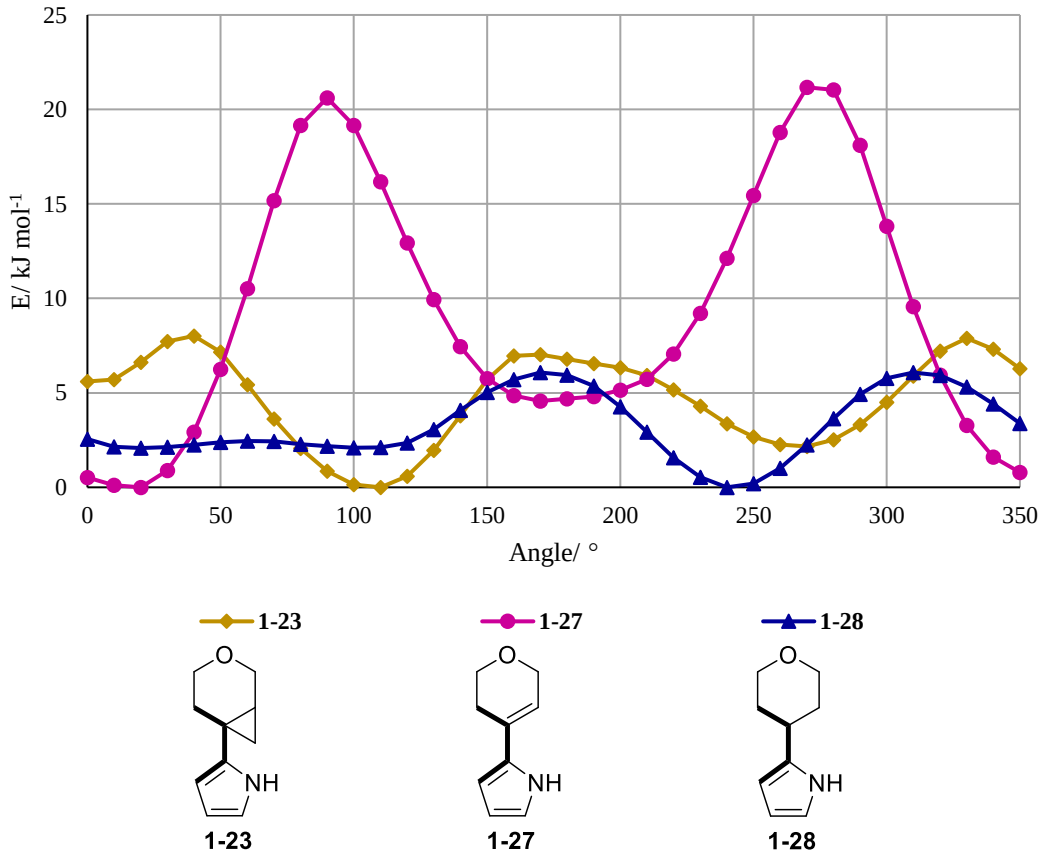

Figure 25. Dihedral angle scan of pyrrole compounds **1-23**, **1-27** and **1-28** with varying hinge binders.

As expected, pyrrole-DHP **1-27** was predicted to behave in an analogous way to the other DHP-containing compounds. The conjugation of the alkene of the DHP to the heteroaromatic system offsets the steric clashes, giving two coplanar conformations at 20 ° and 170 °. One difference is that a slight deviation from planarity is observed, causing the minimum energy conformation to exist at 20 ° rather than 0 °. This is anticipated to be due to a small clash

between the -NH proton and the alkene proton of the DHP as shown below in Figure 26. The skew of 20 ° increases the distance between the two protons, lowering the energy of this conformation relative to that at 0 °.

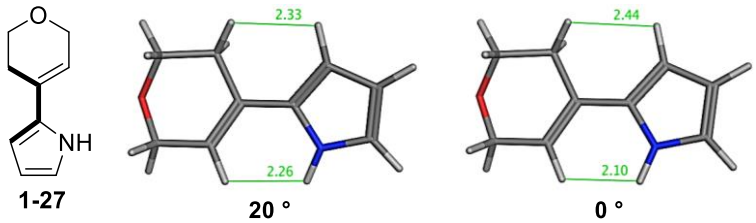

Figure 26. Conformations of pyrrole **1-27** at 20 ° and 0 °. Highlighted is the alleviation of some steric clash between the -NH and alkene proton.

Pyrrole-THP **1-28** is another interesting example with no obvious energy minimum; however, predicted low energy barriers suggest that most conformations are likely to be accessible. The energy minimum at 240 ° corresponds to the 'twisted' structure shown below in Figure 27. It is worth remembering that similar energy barriers were predicted for THP-pyrimidine **1-3** (Figure 7) which was found to crystallise in a twisted conformation.[3]

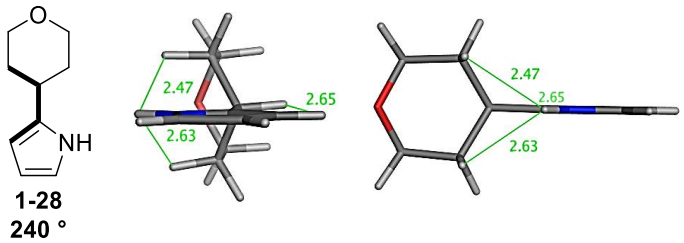

Figure 27. Minimum energy 'twisted' conformation of pyrrole **1-28** with the THP hinge binder.

Modelling for isoxazole compounds with all three hinge binders is shown in Figure 28. As with the previously described furan-DHP **1-19** and pyrrole-DHP **1-27**, the plot for isoxazole-DHP **1-29** consists of two minima at 0 ° and 190 ° and isoxazole-THP **1-30** is predicted to behave in almost exactly the same manner as the corresponding furan analogue **1-20**. The accessibility of one planar and two twisted conformations for furan **1-20** and isoxazole **1-30** mean that the synthesis and crystal structures are of high importance to determine which is preferred in the solid-state system.

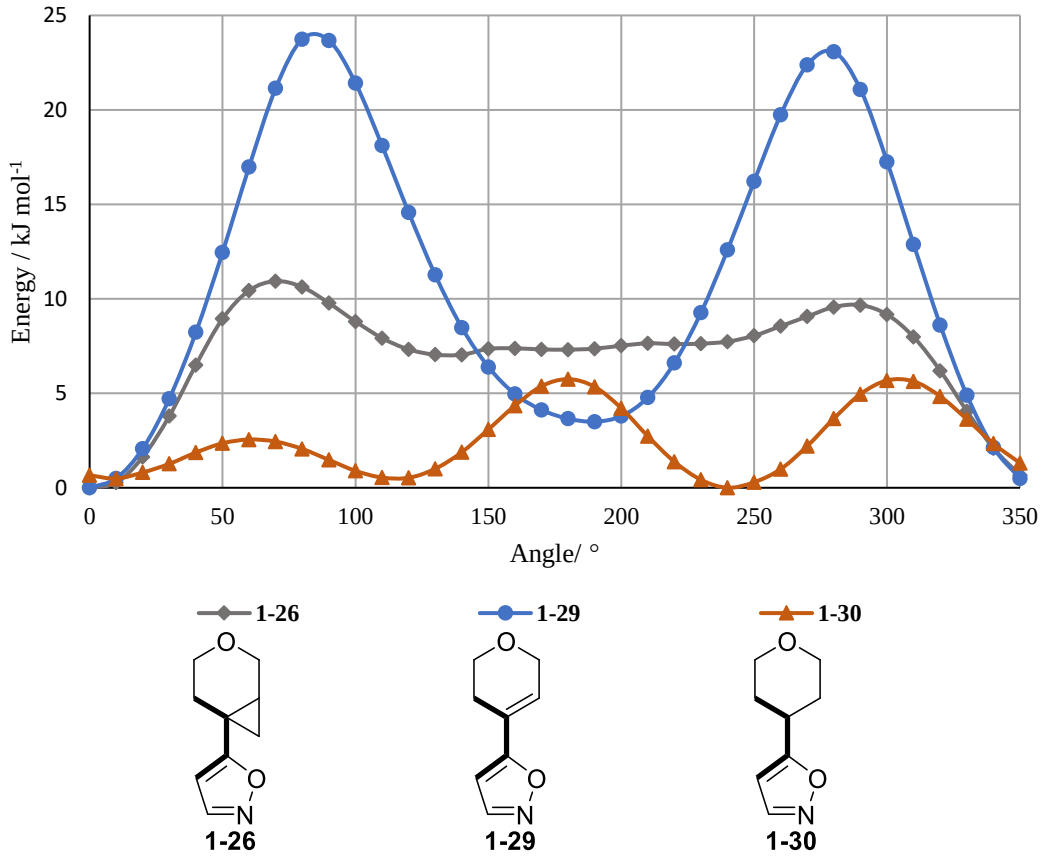

Figure 28. Dihedral angle scan of isoxazole compounds **1-26**, **1-29** and **1-30** with varying hinge binder.

Table 6, below, summarises the compounds chosen for synthesis and the justification for selection. Nine targets were selected to examine the methodology and determine the effects of the five-membered rings on the conformation of CPP-containing compounds.

Table 6. Summary of the targets chosen for synthesis along with the predicted conformations and reasons for selection.

Compound	Predicted Minimum Energy Conformation	Reason for Synthesis
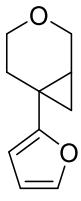 **1-18**	Coplanar	A coplanar conformation is predicted for this compound which can be compared to the DHP and THP analogues. X-ray crystallography should give a coplanar conformation which would assist in validating the QM methodology.
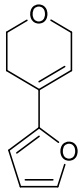 **1-19**	Coplanar	Predicted to be coplanar with electronic effects dominating.

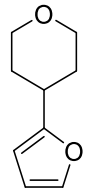 **1-20**	Twisted expected due to sterics; however, three minima are predicted with one coplanar.	Three minima are predicted with two giving twisted conformations but with low energy barriers to rotation. A twisted conformation is expected; however, coplanarity is possible.
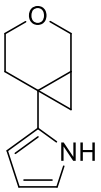 **1-23**	Twisted	Increased size at the heteroatom position gives a predicted twisted structure.
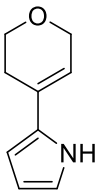 **1-27**	Coplanar	Predicted to be coplanar with electronic effects dominating.
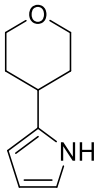 **1-28**	Twisted expected but very low energy barriers to rotation making disorder possible.	Steric factors are anticipated to affect the conformational preference. Therefore, a twisted conformation would be expected.
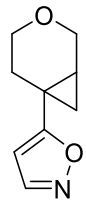 **1-26**	Coplanar	One coplanar minimum predicted for this compound. The crystal structure is expected to be a single conformer, aligned with the modelling prediction.
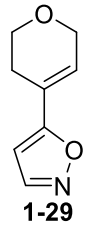 **1-29**	Coplanar	Predicted to be coplanar with electronic effects dominating.
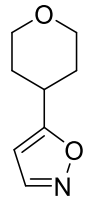 **1-30**	Twisted expected due to sterics; however, three minima predicted with one coplanar.	Similar to furan **1-20** with a twisted conformation expected but low energy barriers to rotation and three minima – coplanarity possible.

4.2. Synthesis - Targets

As with the six-membered systems, it was deemed necessary to install a *meta*-phenol group as a pan-lipid kinase binding motif in order to give compounds which could aid crystallisation and exhibit measurable biological activity, as demonstrated in previous studies in our laboratory.[3] 2,5-Disubstituted furans (**1-31** – **1-33**) and pyrroles (**1-34** – **1-36**) were chosen as targets due to the inherent reactivity of the heterocycles giving preference to electrophilic addition at the 2-position (Figure 29).

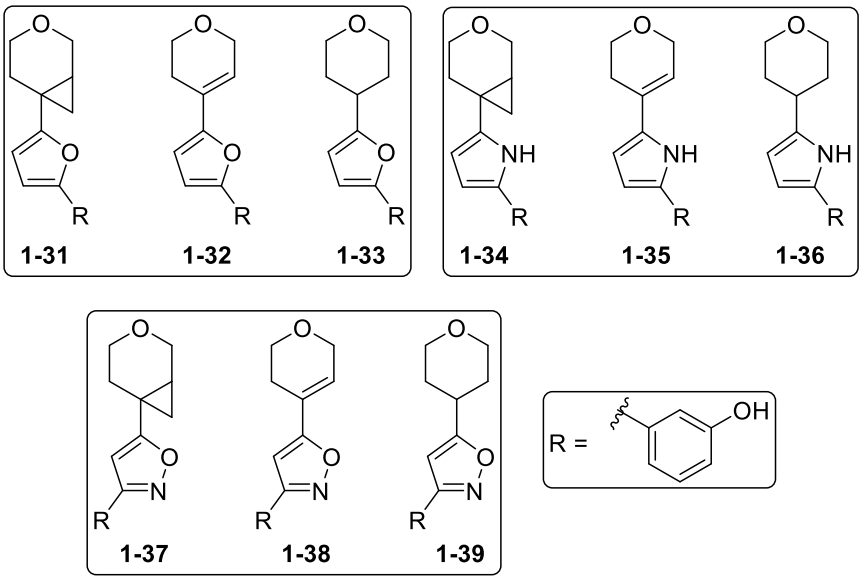

Figure 29. Initial targets for synthesis and subsequent recrystallisation and crystallography.

Synthesis of the furans and pyrroles was planned to proceed *via* a cross-coupling approach, disconnecting the groups attached to the heteroaromatic core (Scheme 2). To prevent any issues stemming from the free phenol, this would be protected using a silyl group which could be readily removed. The THP-containing compounds were considered likely to be accessible *via* the corresponding DHP derivatives through reduction of the double bond. For pyrrole compounds **1-34** – **1-36**, the nitrogen would require a protecting group to prevent unwanted by-products and side reactions with the electron-rich pyrrole ring.

Starting from the desired 2,5-disubstituted products **1-40**, either the pyran analogue or aryl unit could be disconnected first (Scheme 2). Route 1 begins with disconnection of the pyran analogue. Due to availability, both commercially and within the laboratory, of CPP and DHP boronic acid derivatives **1-42**, the disconnection to a heteroaromatic bromide **1-41** was favoured. Furthermore, bromination of the heteroaromatic ring at the 2-position was expected to be facile from compound **1-43**. In addition, the heteroaromatic bromide **1-41** would allow synthesis of all three analogues from a single intermediate. The *meta*-phenol could then be

disconnected to give either the heteroaromatic bromide **1-44** and aryl boronic acid derivative **1-45** or the heteroaromatic boronic acid derivative **1-47** and aryl bromide **1-46**.

Route 2 involved disconnection of the *meta*-phenol group first, giving a heteroaromatic bromide **1-48** and aryl boronic acid derivative **1-45 (**Scheme 2**)**. Disconnecting the bromide then gives rise to the heteroaromatic core with a pyran analogue **1-49**. Finally, the pyran could be disconnected to give heteroaromatic bromide **1-44** and a boronic acid derivative **1-42**. This route was intended to be used as a back-up due to the bespoke syntheses of each bromide, required upon installation of the pyran analogue.

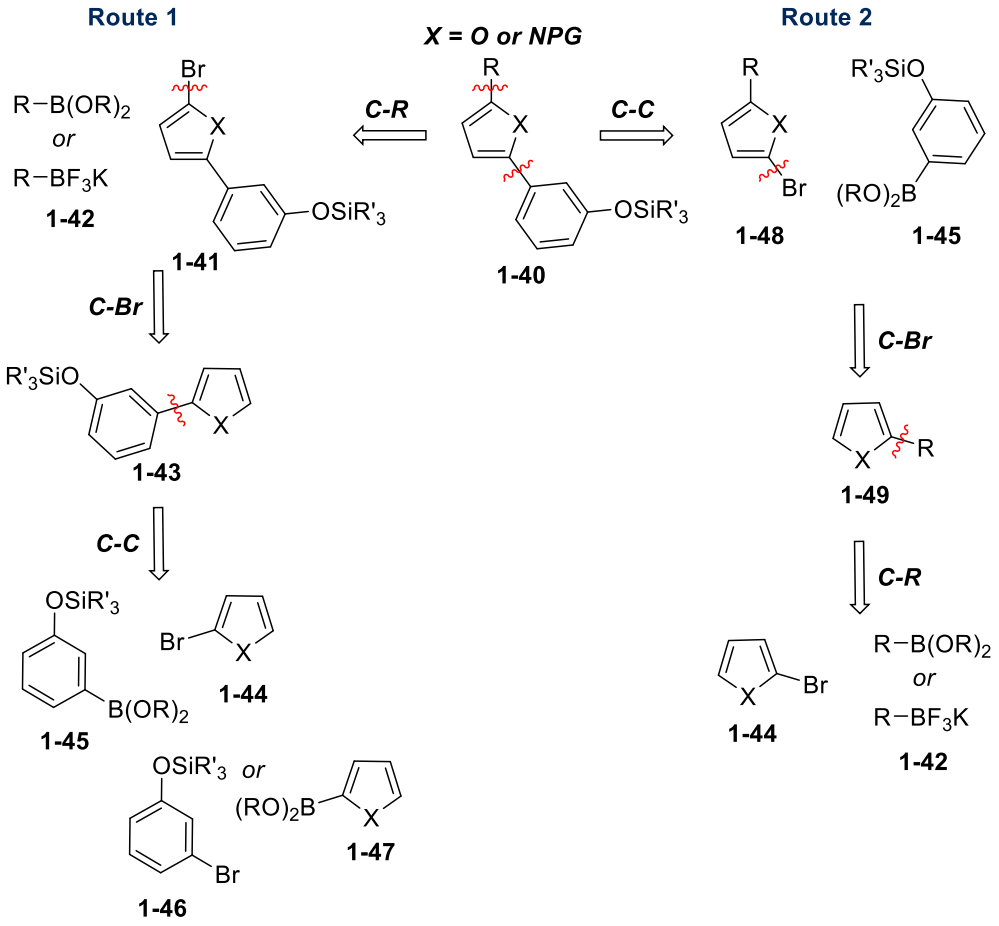

Scheme 2. Disconnection of target compounds **1-31 – 1-36** using a cross-coupling approach.

The nature of isoxazole analogues **1-37** – **1-39** and lack of commercial materials required for cross-coupling (such as those in Scheme 2) led to adoption of a ring construction approach. A dipolar cycloaddition, shown by disconnection across the ring (Scheme 3), was favoured, combining an alkyne **1-51** with a nitrile oxide **1-52**, formed *in situ* by oxidation of an oxime **1-53** with a hypervalent iodine reagent.[38]

To enable this approach, alkyne analogues of each pyran analogue would be required, with the syntheses of these expected to be straightforward with common transformations and literature precedent for the THP[39] and DHP[40-42] derivatives.

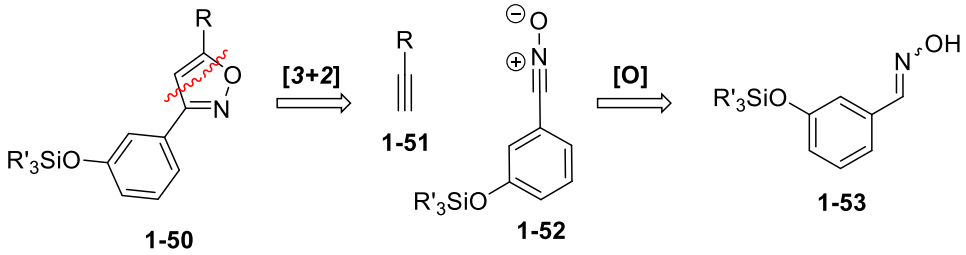

Scheme 3. Disconnection of isoxazole analogues *via* a dipolar cycloaddition approach.

4.3. Synthesis of Furans

The synthesis of the desired 2,5-disubstituted furans began with a Suzuki-Miyaura cross-coupling reaction between 2-bromofuran **1-44** and (3-((*tert*-butyldimethylsilyl)oxy)phenyl) boronic acid (Scheme 4). The *tert*-butyldimethylsilyl (TBS) ether protecting group was chosen due to the availability of the starting material and anticipated ease of removal. The cross-coupling reaction was successful, providing 2-substituted furan **1-54** was in 55% yield. Selective bromination at the 5-position with *N*-bromosuccinimide (NBS) gave brominated furan **1-55** in 83% yield. Keeping the reaction at 0 °C with a slight excess of NBS restricted the reaction to mono-bromination.

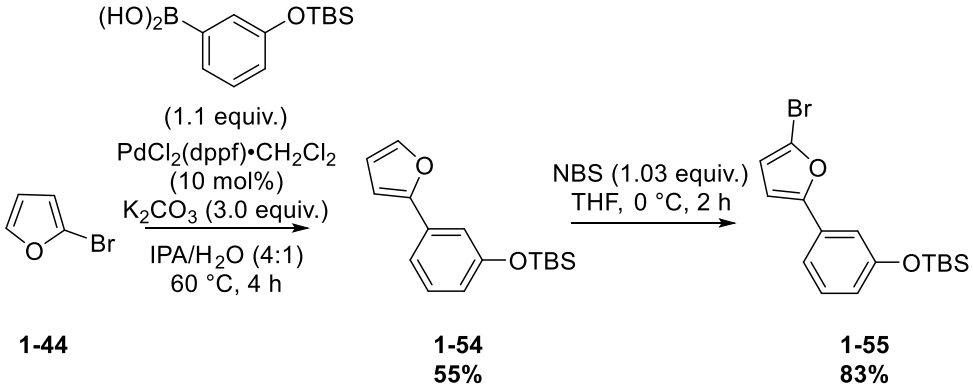

Scheme 4. Synthesis of brominated intermediate **1-55** for installation of pyran analogues.

To install the CPP moiety, the use of a tertiary potassium trifluoroborate salt was required, the synthesis of which is shown in Scheme 5 and carried out by another member of the laboratory and at a contract research organisation (CRO).[2,43] A Simmons-Smith cyclopropanation[44] of commercially available boronic acid pinacol ester **1-56** using diethylzinc[45] gave rise to CPP boronic acid pinacol ester **1-57** in 43% yield.[2] Subsequent transformation of **1-57** using non-etching conditions, gave the desired compound **1-58**.[46] This final transformation is highly reliable, consistently giving excellent yields of potassium trifluoroborate **1-58**.[43]

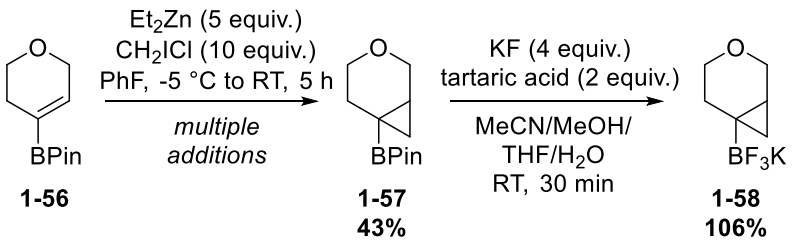

Scheme 5. Synthesis of CPP potassium trifluoroborate salt **1-58** for use in cross-coupling reactions. The 106% yield accounts for solvent and salts present in the final product; however, quantitative conversion is observed.

Potassium trifluoroborate salt **1-58** was used in favour of the corresponding boronic acid pinacol ester **1-57** as previous work had shown inferior coupling outcomes and protodeboronation.[2] Furthermore, these moieties had previously been reported to facilitate sp^2-sp^3 cross-coupling reactions between azabicyclo[4.1.0]heptanes and (hetero)aryl bromides with good yields.[47] Slow hydrolysis of the trifluoroborate salt to the corresponding boronic acid, which is able to undergo transmetallation to the palladium catalyst, is thought to be the primary reason for the reduction in by-products and side reactions; however hydrolysis rates can vary with several different parameters, including non-trivial factors such as vessel shape.[48,49] With low concentrations of the boronic acid present at any one time, side reactions such as homocoupling and protodeboronation can be reduced to enable higher yields of the desired product.

The synthesis of furan-CPP **1-31** from bromide **1-55** and CPP-trifluoroborate **1-58** was carried out using the conditions reported by Harris.[47] Pre-catalyst $Pd(OAc)_2$ and the bulky, electron-donating cataCXium A® ligand were used to facilitate the cross-coupling to give crude product **1-59** which was deprotected with *tert*-butylammonium fluoride (TBAF) giving CPP-furan **1-31** in 26% yield over two steps (Scheme 6). While this yield was somewhat lower than those reported,[47] the use of an electron-rich 5-membered heteroaromatic bromide in this work is a considerable deviation from the literature, which focused primarily on electron-deficient 6-membered heteroaromatics. Finally, the deprotection step may have contributed to a loss of product if there were any compatibility issues with the TBAF reagent and CPP or furan moieties. Racemic product **1-31** was provided to another member of our laboratories to undergo chiral preparative HPLC and obtain the two separated enantiomers,[50] which were subsequently recrystallised and submitted for X-ray crystallography.

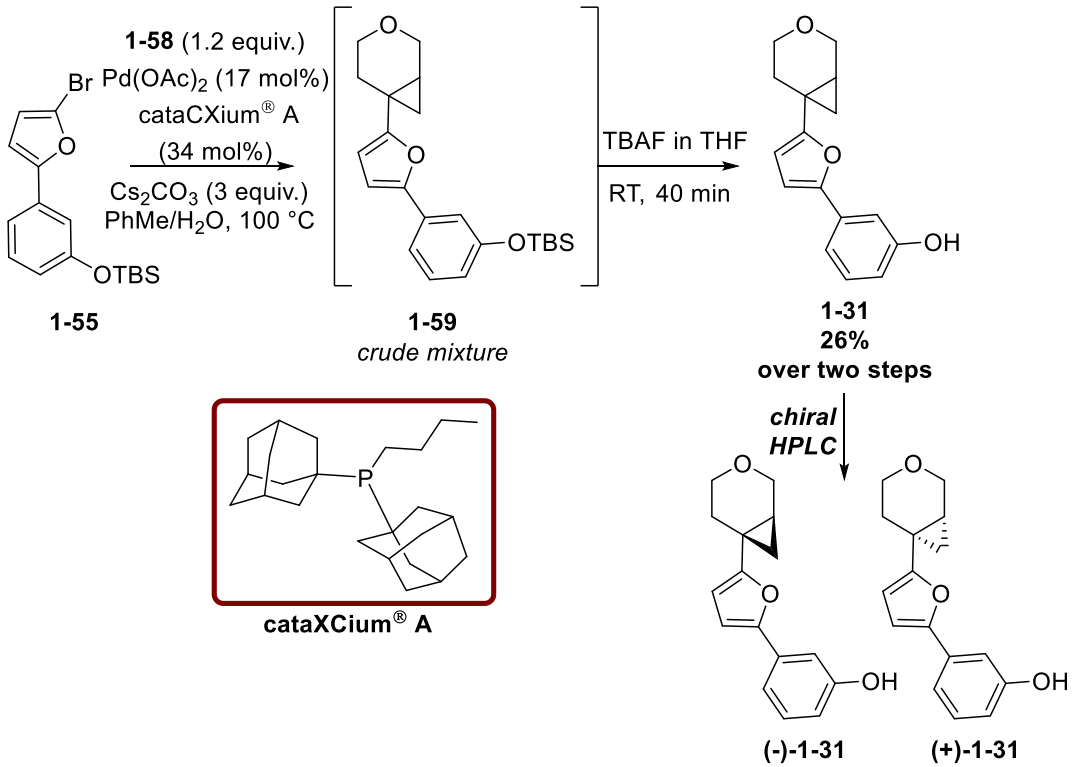

Scheme 6. Synthesis of CPP-furan **1-31** *via* a Suzuki-Miyaura cross-coupling approach and subsequent chiral preparative HPLC to obtain each enantiomer.

Installation of both the DHP and THP moieties could be achieved from the commercially available DHP boronic acid pinacol ester, **1-56**. A Suzuki-Miyaura cross-coupling would give the desired DHP-furan **1-32** and subsequent hydrogenation of some of the resulting product was anticipated provide THP analogue **1-33**. Unfortunately, the initial Suzuki-Miyaura cross-coupling reaction and subsequent silyl deprotection only gave a 30% yield of product **1-32** (Scheme 7).

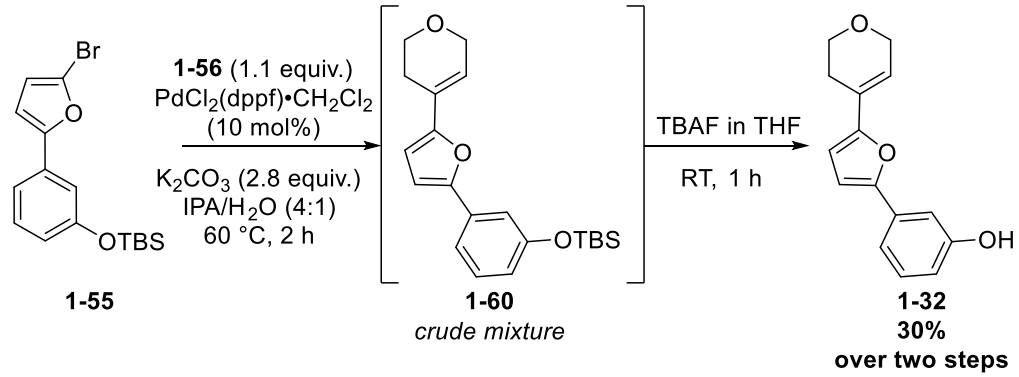

Scheme 7. Synthesis of DHP-furan **1-32** *via* Suzuki-Miyaura cross-coupling.

Given that this did not provide sufficient materials, an alternative approach to THP-analogue **1-33** was taken using methodology developed within the Jamieson laboratories.[51] A one-pot procedure combining a Suzuki-Miyaura cross-coupling reaction and hydrogenation was recently developed and showed broad utility for a palette of interesting substrates.[51] By using a highly active pre-catalyst, XPhos Pd G2, the initial cross-coupling was expected to be more efficient than in the initial attempt (Scheme 7). The pre-catalyst allows facile and almost instantaneous access to the active species [L_1Pd^0] (where L1 is XPhos), owing to the steric bulk and electron-donating ability of the ligand.[52,53] In addition, the use of this catalyst increases the rate of transmetallation with a small effect on protodeboronation, reducing by-product formation.[52] The introduction of the Pd/C catalyst at the beginning of the reaction allows a transfer-hydrogenation step to occur once the cross-coupling reaction is complete. Addition of ammonium formate in methanol initiates this step, reducing the double bond of the DHP. Despite this, initial attempts at the reaction were unsuccessful and it was found that the outcome of the reaction was dependent on the batch of DHP boronic acid pinacol ester, **1-56** which may have also affected the outcome of the initial Suzuki-Miyaura cross-coupling in Scheme 7. Some vendors supplied this as a sticky off-white solid, whereas others provided a free-flowing white solid. Analysis of these appeared identical; however, the free-flowing white solid was superior when used in the reaction. Due to this variability, the use of an alternative boron species, such as a potassium trifluoroborate salt, may prove more reliable for the installation of this group. Nevertheless, application of the one-pot procedure was successful with a subsequent deprotection of the silyl group giving THP-furan **1-33** in an excellent yield of 52% over the two steps (Scheme 8). This compound was recrystallised to give crystals suitable for X-ray crystallography.

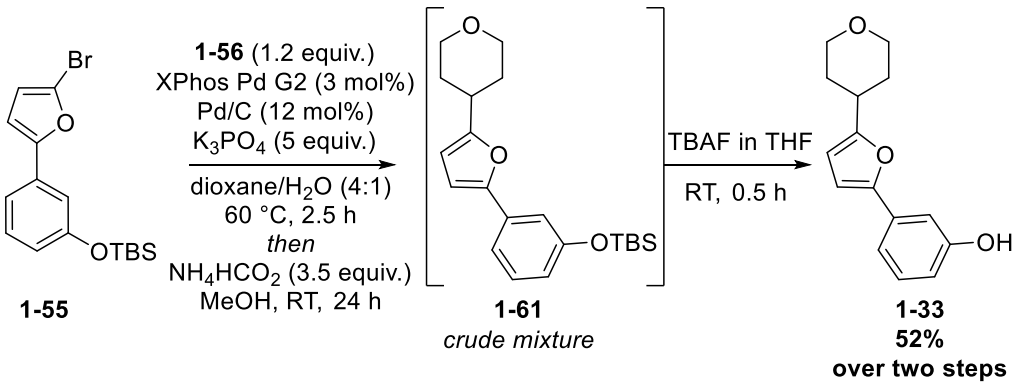

Scheme 8. Synthesis of THP-furan **1-33** using a one-pot Suzuki-Miyaura cross-coupling/hydrogenation procedure followed by TBAF deprotection.

4.4. Synthesis of Pyrroles

Pyrrole analogues **1-34** – **1-36** could by synthesised in a similar manner to furan analogues **1-31** – **1-33**; however, it was anticipated that the highly electron-rich system may be more susceptible to side-reactions. In addition, the nitrogen of the heteroaromatic ring required a protecting goup to prevent unwanted reactivity. A *tert*-butyloxycarbonyl (Boc) group was chosen for this purpose as it would reduce the the electron density of the pyrrole and be readily removed without the requirement for strongly acidic reagents.

The instability of 2-heteroaryl boronic acids, such as **1-62**, and the difficulty associated with their cross-coupling,[52,54] alongside the requirement for a Boc protecting group, led to the use of *N*-Boc-pyrrole-2-boronic acid MIDA ester **1-63** (Figure 30).

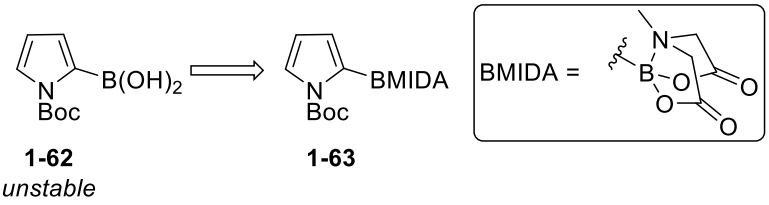

Figure 30. *N*-Boc-pyrrole-2-boronic acid MIDA ester **1-63** used in subsequent cross-coupling reactions. The structure of BMIDA is also shown.

Work by Burke *et al*. had shown that the release of the reactive boronic acid from the MIDA ester could be controlled by reaction conditions to maximise the efficiency of the Suzuki-Miyaura cross-coupling.[54] The conditions described by Burke were replicated in the reaction between MIDA ester **1-63** and (3-bromophenoxy)(*tert*-butyl)dimethylsilane to give 2-subtituted pyrrole **1-64** in 64% yield. Subsequent bromination in the 5-position with NBS at -78 °C gave intermediate **1-64** (Scheme 9).

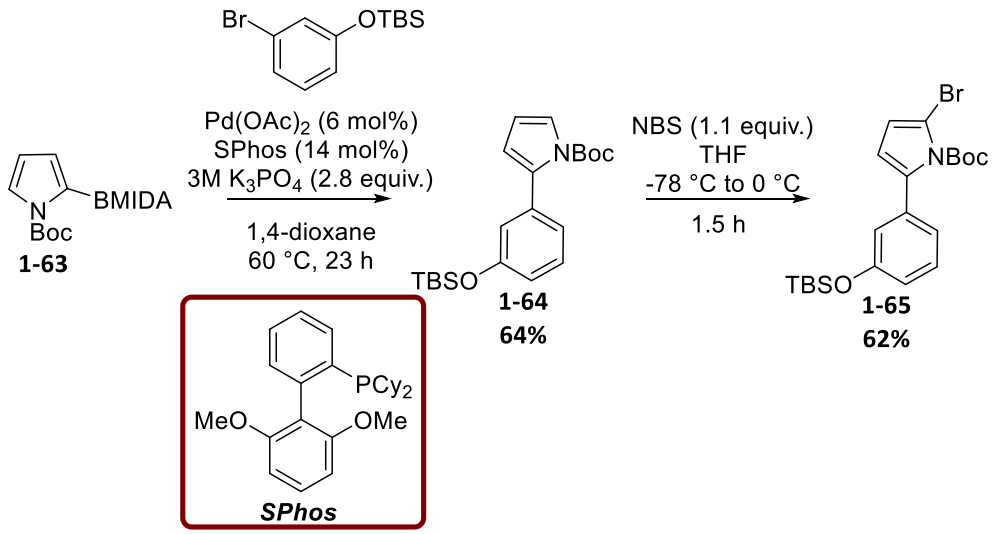

Scheme 9. Synthesis of brominated intermediate **1-65** to enable synthesis of desired pyrrole analogues.

As with the synthesis of CPP furan **1-31**, the CPP moiety was installed using potassium trifluoroborate **1-58**; however, in this case both the TBS and Boc protecting groups required removal. Due to the increased reactivity of the pyrrole in comparison to the furan, it was expected that any acidic conditions would likely lead to decomposition or polymerisation of the compound.[55] As a result, removal of both the TBS and Boc groups concurrently was not possible, leading to the telescoping of three reactions with work-ups carried out between each step. The transformations are summarised below in Scheme 10 with racemic CPP-pyrrole **1-34** separated into the two enantiomers by chiral preparative HPLC.[50]

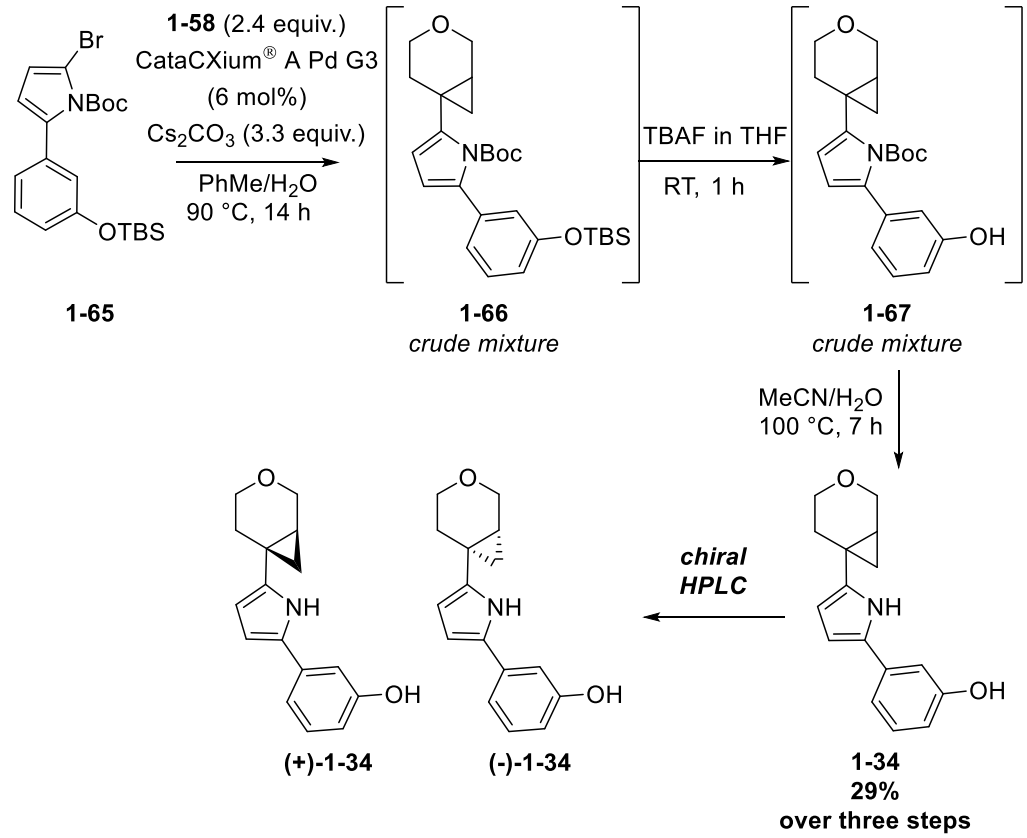

Scheme 10. Synthesis of CPP-pyrrole **1-34** *via* a Suzuki-Miyaura cross-coupling approach with two deprotection steps using crude materials. The two enantiomers were obtained by chiral preparative HPLC.

Having shown that the deprotection steps could be telescoped upon completion of the cross-coupling, this method was extended to DHP analogue **1-35** and the synthesis of this is shown below in Scheme 11**.** The deprotection steps were carried out sequentially on the product of the initial cross-coupling to give DHP-pyrrole **1-35** in 30% yield over the three steps.

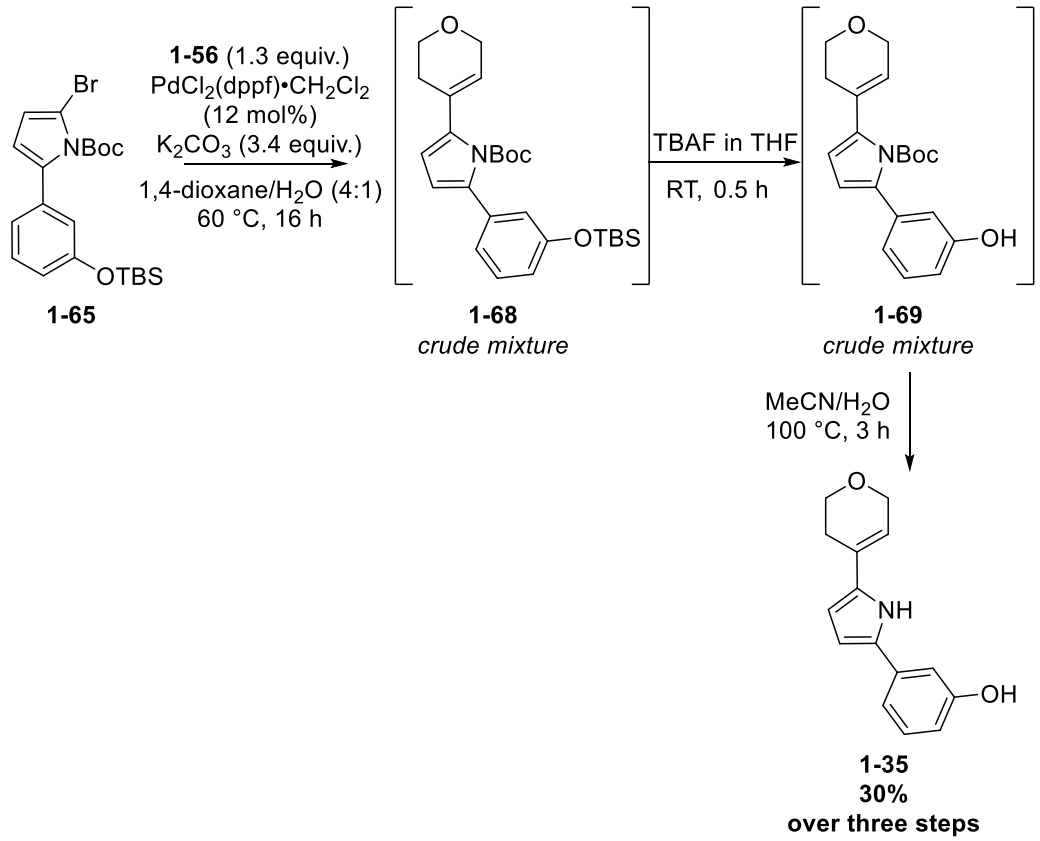

Scheme 11. Synthesis of DHP-pyrrole **1-35** *via* Suzuki-Miyaura cross-coupling reaction and two deprotection steps.

Making use of CoWare,[56] it was possible to hydrogenate DHP-pyrrole **1-35** to form the THP analogue **1-36** (Scheme 12). While this was obtained as an amorphous white solid, all attempts to recrystallise this material were unsuccessful. This was not unexpected given the limited conformational preference predicted by the modelling (Figure 25). To obtain a crystal structure of a THP-containing pyrrole, an alternative to the *meta*-phenol group was explored.

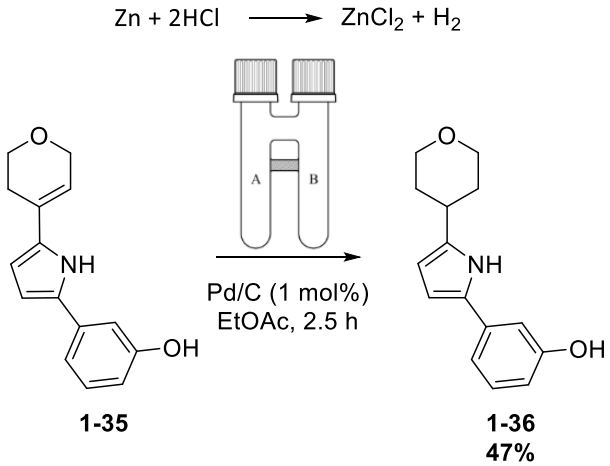

Scheme 12. Synthesis of THP-pyrrole **1-36** *via* hydrogenation of the alkene moiety in **1-35**. Compound **1-36** was unable to be recrystallised.

A *para*-phenyl ethyl urea moiety was investigated as an alternative to the *meta*-phenol moiety to increase the crystallinity of the product through increased hydrogen bonding. This group had been successfully implemented into some of the six-membered tool compounds in our previous study.[3] An initial cross-coupling using *N*-Boc-pyrrole-2-boronic acid MIDA ester **1-63** and 4-bromoaniline gave pyrrole intermediate **1-70** in 55% yield. Subsequent transformation of the aniline moiety to the *para*-phenyl ethyl urea group enabled facile access to compound **1-71** in 66% yield. Disappointingly, the bromination of urea-containing compound **1-71** was not possible with decomposition occurring upon warming of the reaction mixture to room temperature (Scheme 13).

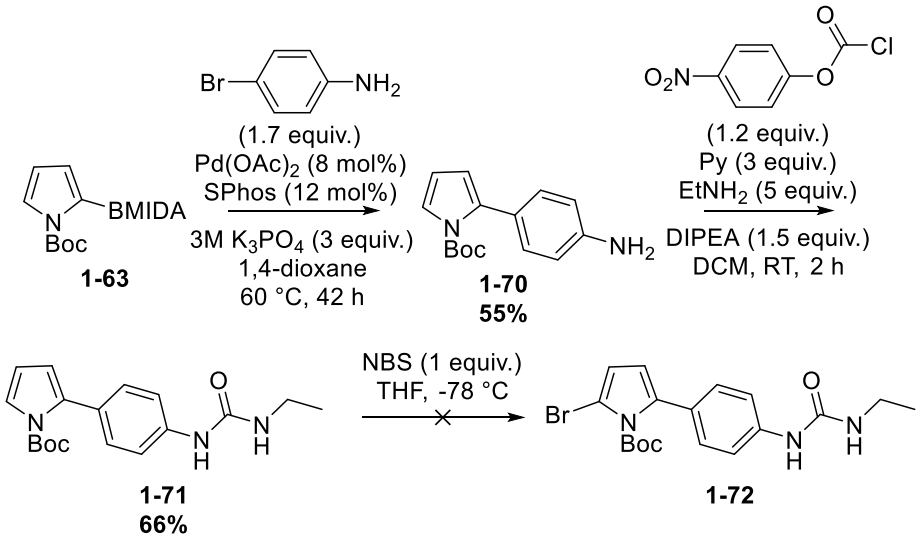

Scheme 13. Unsuccessful bromination attempt to access pyrrole **1-72** with a *para*-phenyl ethyl urea back-pocket.

These observations were used to select a *para*-nitrophenol group which would potentially reduce the electron density in the pyrrole ring, improving the stability and providing additional polarity, which was anticipated to increase the crystallinity. Using the same cross-coupling approach, access to brominated pyrrole **1-74** was possible in two steps and excellent yields (Scheme 14). The temperature of the bromination could be increased to 0 °C, presumably due to the electron-withdrawing nature of the nitrophenol group, reducing the nucleophilicity of the pyrrole.

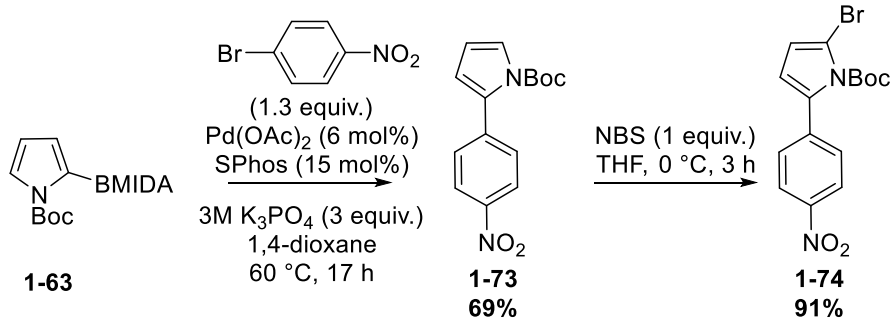

Scheme 14. Synthesis of brominated pyrrole **1-74** with a para-nitrophenol group *via* a Suzuki-Miyaura cross-coupling and bromination sequence.

The DHP moiety was installed by Suzuki-Miyaura cross-coupling to give pyrrole **1-75** in a 70% yield. Conditions to selectively reduce the DHP double bond without affecting the nitro group were explored, and an ionic reduction with trifluoroacetic acid (TFA) and Et_3SiH was found to be optimal, delivering THP-containing pyrrole **1-76** in a 48% yield. Pleasingly the use of TFA in the reaction, followed by the addition of extra equivalents, led to the concomitant removal of the Boc protecting group and, as predicted, THP-pyrrole **1-76** provided crystalline material suitable for X-ray crystallography.

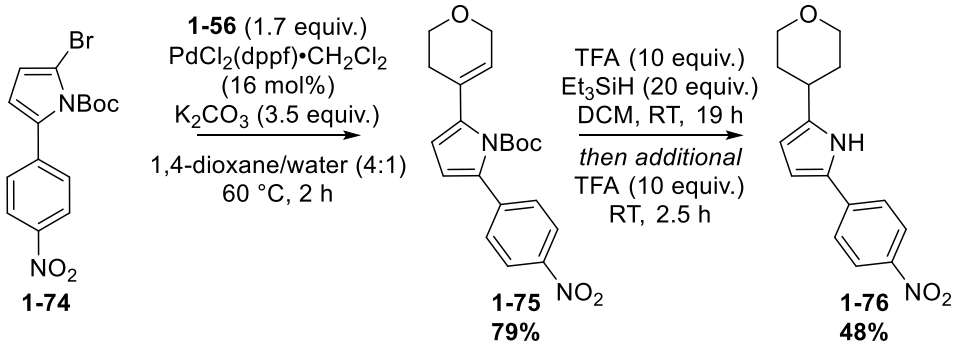

Scheme 15. Synthesis of THP-pyrrole **1-76** with a *para*-nitro group installed to facilitate recrystallisation.

4.5. Isoxazole Synthesis

The final iteration of compounds synthesised were isoxazoles **1-37** – **1-39**. The cycloaddition approach, as shown in Scheme 3, required the synthesis of the three alkynes shown in Figure 31. DHP alkyne **1-78** and THP alkyne **1-79** had been exemplified in the literature with protocols available for the syntheses.[39-42]

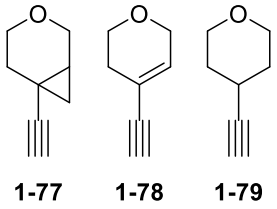

Figure 31. Structures of the alkynes required for synthesis of isoxazole analogues **1-37** – **1-39**.

THP alkyne **1-79** was obtained in one-step from commercially available THP aldehyde **1-80**, which was treated with the Bestmann-Ohira reagent **1-81**.[39,57,58] This simple and efficient method gave the desired compound in 77% crude yield (Scheme 16). The resulting alkyne was taken forward in crude form to avoid any issues caused by both instability and volatility.

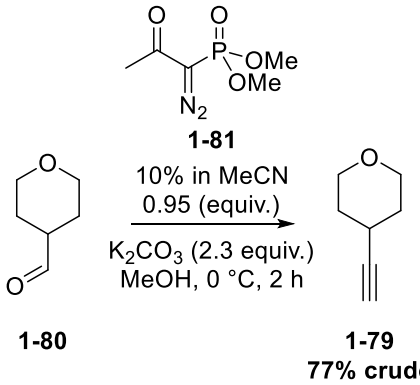

Scheme 16. Synthesis of THP alkyne **1-79** using the Bestmann-Ohira reagent **1-81**.

This approach was also applied to the synthesis of CPP alkyne **1-77**; however, the aldehyde starting material was not readily available. Therefore, starting with CPP carboxylic acid **1-82**, which was available in large quantities from a CRO,[43] a reduction and oxidation sequence gave the desired aldehyde **1-84** which was submitted to the Bestmann-Ohira conditions, providing CPP-alkyne **1-77** (Scheme 17). As with THP alkyne **1-79**, this compound was used in crude form to prevent any loss of product due to anticipated volatility.

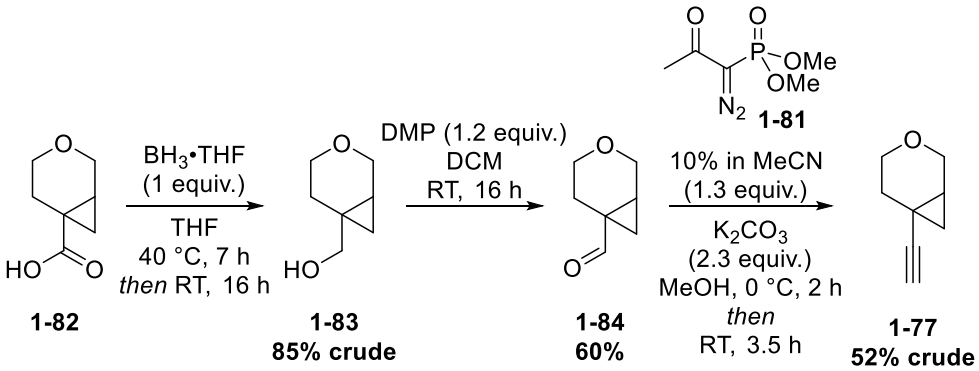

Scheme 17. Synthesis of CPP-alkyne **1-77** starting from CPP acid **1-82**. DMP = Dess-Martin Periodinane.

An alternative approach was necessary for the DHP-alkyne **1-78** as the aldehyde precursor was not commercially available. A literature survey showed that the desired compound had previously been synthesised using a Kumada-type cross-coupling between DHP-triflate **1-85** and ethynylmagnesium bromide, catalysed by $Co(acac)_3$.[40,41] A report by Hayashi had shown that $Co(acac)_3$ was the most efficient catalyst for this transformation;[42] however, a number of attempts were made with this system without success. Further exploration of the literature revealed that, contrary to the report by Hayashi, a $Pd(PPh_3)_4$ catalyst produced superior results for this transformation in the hands of another laboratory.[40] The Pd catalyst was introduced to the reaction and desired alkyne **1-78** was obtained in 47% crude yield (Scheme 18).

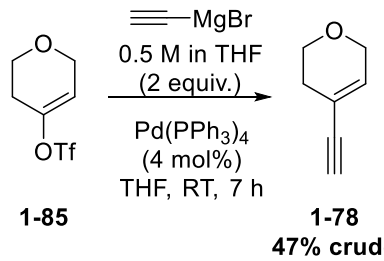

Scheme 18. Synthesis of DHP-alkyne **1-78** using a palladium-catalysed Kumada cross-coupling.

The cycloaddition partner to the alkenes required an oxime precursor, which could be oxidised to the corresponding nitrile oxide, as shown in Scheme 3. The oxime was obtained in two steps from commercially available 3-hydroxybenzaldehyde **1-86**. TBS protection of the phenolic -OH group gave quantitative conversion to compound **1-87** which was taken forward in crude form to synthesise the desired oxime **1-88** in 59% yield over the two steps (Scheme 19).

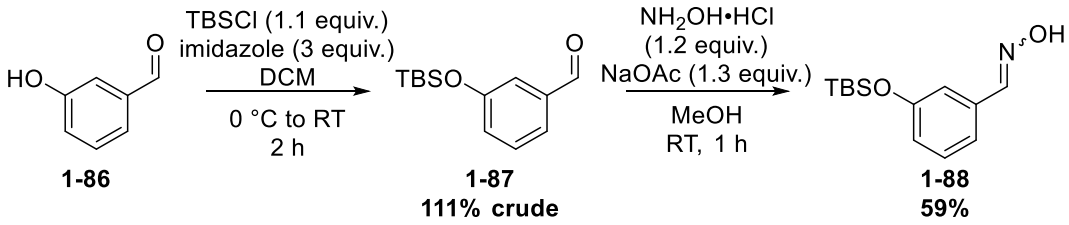

Scheme 19. Synthesis of oxime **75** for use in the cycloaddition reactions. The 111% yield is accounted for by the presence of a silanol by-product, evidenced by NMR analysis.

The synthesis of isoxazoles from alkenes and oximes is reported in the literature with *in situ* oxidation by the hypervalent iodine complex (bis(trifluoroacetoxy)iodo)benzene (PIFA).[38] The reaction is thought to proceed in a similar fashion to the Dess-Martin oxidation with the lone pair of the oxygen atom attacking the iodine atom, displacing TFA.[59,60] After the initial attack onto the iodine atom, a molecule of TFA is released and the oxime oxidised by movement of electrons from the nitrogen atom through to the iodine. An additional molecule of TFA is lost and iodobenzene formed as a by-product before subsequent loss of a proton leads to the desired nitrile oxide intermediate. This proposed mechanism reaction is shown in Scheme 20 below.

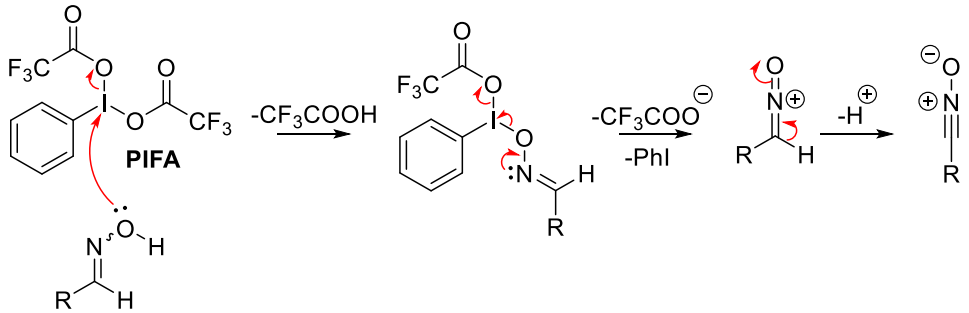

Scheme 20. Mechanism of formation of the nitrile oxide intermediate using the PIFA oxidant.

The nitrile oxide formed can then react with the alkyne reagent in a [3+2] cycloaddition, forming the desired isoxazole product. All three of the synthesised alkyne reagents were submitted to these reaction conditions, resulting in formation of three corresponding isoxazole products. Furthermore, the extrusion of two equivalents of TFA and the presence of water in the reaction mixture had the additional advantage of removing the TBS protecting group *in situ*. The reaction times were extended to allow for full removal of the protecting group. Despite the low yields obtained, no by-products were isolated; however, it appeared that hydrolysis of oxime **1-88** had occurred, with the mass of the aldehyde observed in the LCMS of the reaction mixture. The products of the three reactions are shown in Scheme 21 and the CPP-isoxazole **1-37** was given to the another member of our laboratories to undergo chiral preparative HPLC.[50]

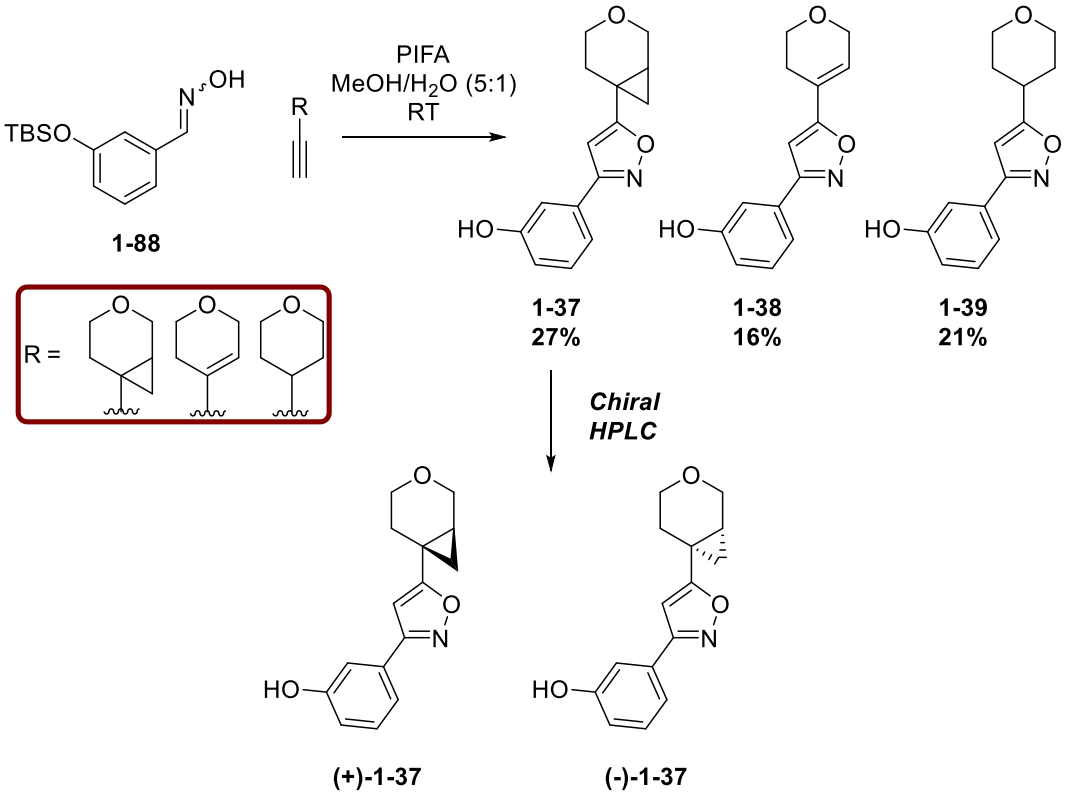

Scheme 21. Synthesis of isoxazoles **1-37**, **1-38** and **1-39** from oxime **1-88** and the corresponding alkenes, using the PIFA reagent. CPP-isoxazole **1-37** was separated into its enantiomers by chiral HPLC.

4.6. Crystal Structure Data

4.6.1. DHP analogues

All of the DHP-containing compounds were predicted to adopt coplanar conformations due to the conjugation between the double bond and the heteroaromatic ring (Figure 32); however, pyrrole analogue **1-27** was predicted to adopt a slightly skewed conformation at

20° to minimise the clash of protons on the DHP ring with the -NH proton (*vide supra*, Figure 26).

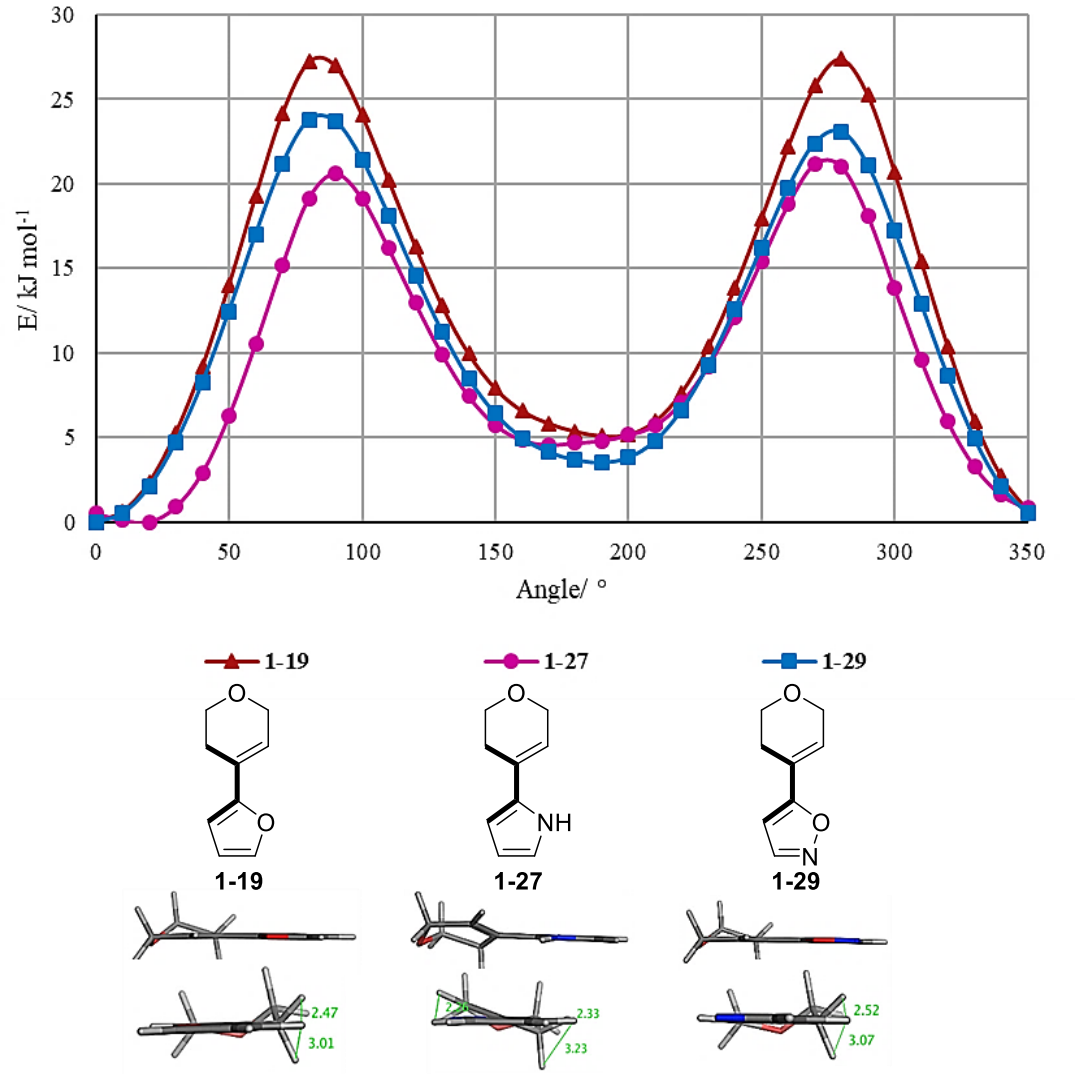

Figure 32. Dihedral angle scan of DHP analogues **1-19**, **1-27** and **1-29** showing coplanar conformations. The minimum energy conformations of each compound are also shown.

The crystal structures of the DHP-containing analogues **1-32**, **1-35** and **1-38** are shown in Figure 33 with all three analogues adopting the predicted coplanar conformations. In the case of pyrrole **1-35**, a subtle twist in the molecule exists, as predicted by the modelling. The inter-nuclear distances between protons on the heteroaromatic ring and the DHP ring are shown, with the modelling predicting these accurately for all three compounds. Comparison of the predicted dihedral angle to that of the crystal structure is shown in Table 7 along with the angle between the average ring planes. This measurement takes the average plane of the pyran analogue and the heteroaromatic ring and measured the angle between these two planes.

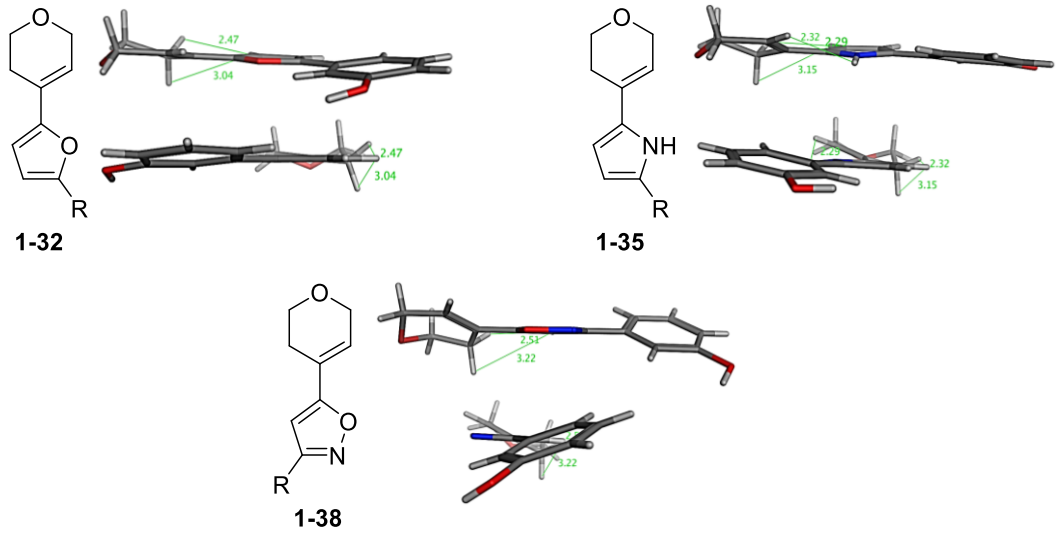

Figure 33. Single crystal X-ray crystallography structures of DHP compounds **1-32**, **1-35** and **1-38**. The structures are shown viewing from the side and along the C-C bond connecting the heteroaromatic core to the DHP moiety. R = *meta*-phenol group.

A good correlation between the predicted and measured values for these three DHP-containing compounds was observed. The main discrepancy lies with isoxazole compound **1-38** wherein the predicted dihedral angle is 0 ° but is measured as 23.9 ° in the crystal structure. The precise cause of this cannot easily be explained; however, it may be possible that the second heteroatom affects the aromaticity of the heterocycle, leading to a reduction in the conjugative effect and an increase in the effect of steric influences. Despite this, the molecule was still considered to be coplanar and, therefore, the DHP-containing compounds were well accounted for by the modelling.

Table 7. Comparison of predicted dihedral angle between the DHP moiety the heterocycle and data obtained from the crystal structures of compounds **1-32**, **1-35** and **1-38**. The angle between the average ring planes of the DHP ring and heterocycle ring is also shown, as measured from the crystal structures.

Compound	Predicted Dihedral Angle/ °	Measured Dihedral Angle/ °	Angle between average ring planes/ °
Furan **1-32**	0	6.5	1.9
Pyrrole **1-35**	20	19.0	12.0
Isoxazole **1-38**	0	23.9	21.4

4.6.2. CPP Analogues

The three CPP analogues modelled each exhibit a unique dihedral angle scan, as shown in Figure 34. CPP-furan **1-18** and CPP-isoxazole **1-26** both share a coplanar minimum energy conformation at 0 °; however, there are two, additional, local minima for CPP-furan **1-18**, both of which are twisted. This is not the case for CPP-isoxazole **1-26** with only one minimum present.

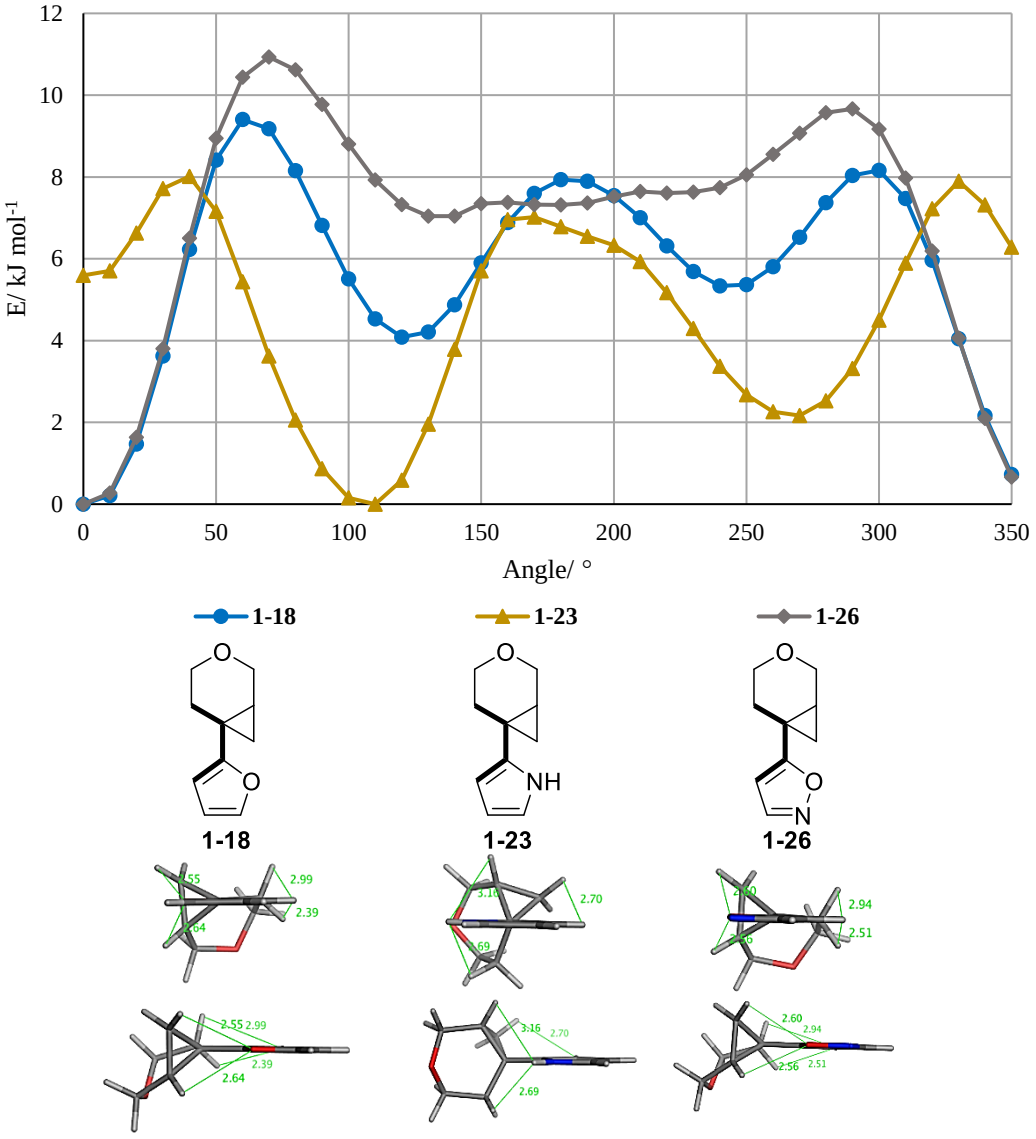

Figure 34. Dihedral angle scan of CPP analogues **1-18**, **1-23** and **1-26**. The minimum energy conformations of each compound are also shown.

Pyrrole **1-23** is predicted to exhibit a twisted conformation, presumably due to the increased steric clash upon replacement of a lone pair with a proton. Analysis of the crystal structure data allowed the accuracy of the modelling, the propensity for the CPP moiety to induce coplanarity and the effect of increasing steric bulk on the heteroatom to be explored.

The crystal structure of CPP-furan **(-)-1-31** shows that there are two molecules within the unit cell, with hydrogen bonding between them (Figure 35). Interestingly, one of these molecules adopts a coplanar conformation (molecule 1); however, it is not the predicted conformation at 0 °, but 213.8 ° which does not correlate to an energy minimum (Figure 34). The existence of this conformation highlights that the relatively small stabilisation of the energy minima may not be sufficient to restrict the conformation, as also observed with some of the six-membered systems.[3] A further interesting characteristic of **(-)-1-31** molecule 1 is that the dihedral angle between the double bond of the furan and the carbon-carbon bond in the cyclopropyl ring and pyran is 0 ° which may indicate an orbital interaction between the cyclopropyl ring and the furan π-system that was not accounted for in the modelling.

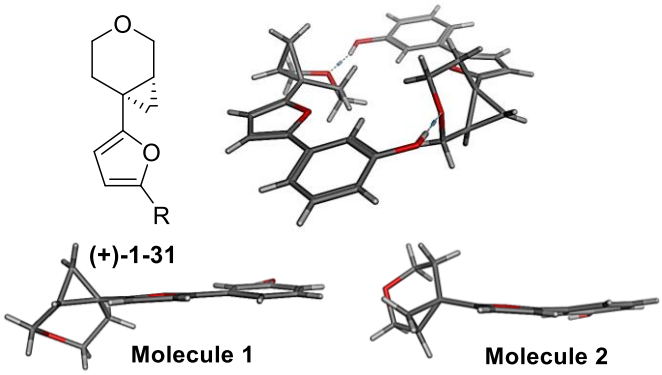

Figure 35. Crystal structure of CPP-furan **(+)-1-31**. There are two molecules shown in the unit cell with both shown individually below. R = *meta*-phenol group

(+)-1-31 Molecule 2, observed in the crystal structure, has a dihedral angle of 111.0 ° which corresponds to a predicted energy minimum (Figure 34). The presence of this conformation highlights the lack of stabilisation for a single conformation, reflected in the low energy barriers to rotation predicted by the modelling.

One final consideration with respect to the crystal structure is the presence of the hydrogen bonds between the molecules which could influence the conformation. A hydrogen bond is typically in the region of 4 kJ mol^{-1} and, given that the energy barriers to rotation are only 10 kJ mol^{-1}, it is possible that the hydrogen bonding stabilises specific conformations which are not predicted by the modelling. In any case, it is clear from the presence of both conformers and, specifically the unpredicted coplanar, that the modelling is not representative of the crystallised compound. Despite this, a coplanar conformation is accessible for CPP-furan **(+)-1-31**.

CPP-pyrrole **(+)-1-34** was predicted to be dominated by steric effects due to the increase in size around the heteroatom of the five-membered ring. As such, and as is reflected in the modelling in Figure 34, a twisted conformation was expected. The crystal structure aligns

with this prediction, with molecule **(+)-1-34** adopting a twisted conformation (Figure 36). Due to the quality of the resulting crystals, the opposite enantiomer to that modelled was chosen for crystallography. As such, the dihedral angle measured in the crystal structure is offset by 180 ° to that shown in the plot in Figure 34. Therefore, the measured dihedral angle in the crystal structure is 116.5 °, correlating to 296.5 ° (116.5 + 180) on the plot.

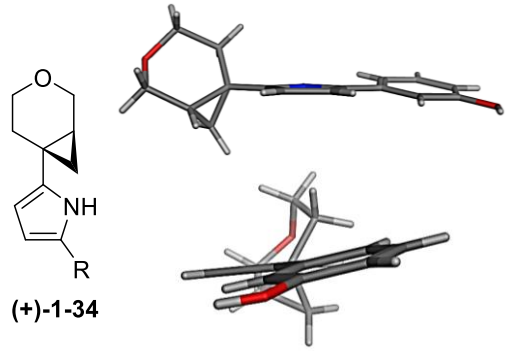

Figure 36. Crystal structure of CPP-pyrrole **(+)-1-34** viewing from the side and along the carbon-carbon bond connecting the heterocycle to the CPP moiety.

The observation of the twisted conformation of this structure agrees with both the modelling and expectation that increasing the steric demands of the system outweighs any electronic preference for coplanarity.

CPP-isoxazole **(-)-1-37** was predicted to adopt one coplanar conformation, based on the modelling. Despite this, two conformations were apparent in the crystal structure (Figure 37). Although only one of these was predicted, both exist as coplanar molecules which is the first tentative evidence of an electronic effect. The two coplanar molecules may indicate an increased orbital overlap present in the isoxazole analogue *versus* the furan, potentially due to a lowering of the LUMO of the heterocycle.[34] As a result, both coplanar conformations are lowered in energy. If this is the case, the modelling does not appear to take this into account in energy calculations.

With respect to the size of the heterocycle, it appears that coplanar conformations are readily accessible when the sterics of the systems are favourable (as with a furan and isoxazole ring). Reducing the size of the groups adjacent to the CPP ring lowers the energy of the coplanar conformation and may allow less hindered rotation around the bond without incurring an energy penalty; thus, an increased stabilisation for coplanarity is predicted.

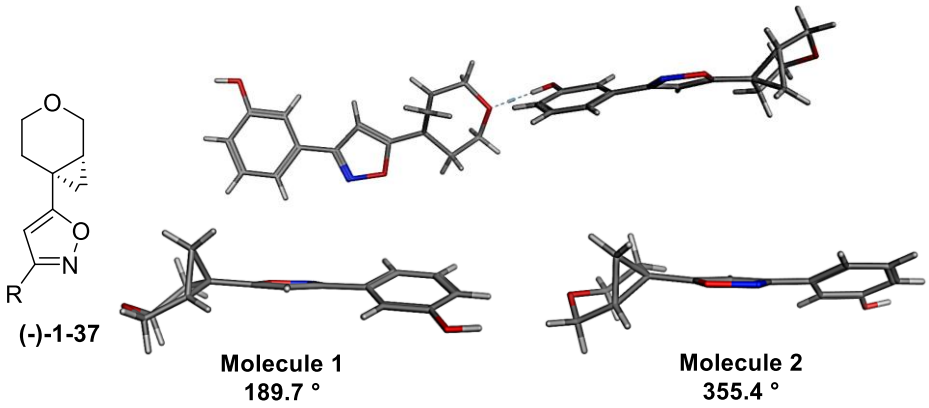

Figure 37. Crystal structure of CPP-isoxazole **(-)-1-37**. There are two molecules within the unit cell with both adopting coplanar conformations. R = *meta*-phenol.

Comparing these results to some of those obtained for six-membered rings, it appears that sterics are the dominant factor in the favoured conformation of five-membered systems. This may be due to the sub-optimal orbital overlap as a result of the higher LUMO present in the electron-rich systems. Figure 38, below, highlights two six-membered systems and their dihedral angle scans alongside CPP-furan **1-18** pyrrole **1-23** and isoxazole **1-26**.

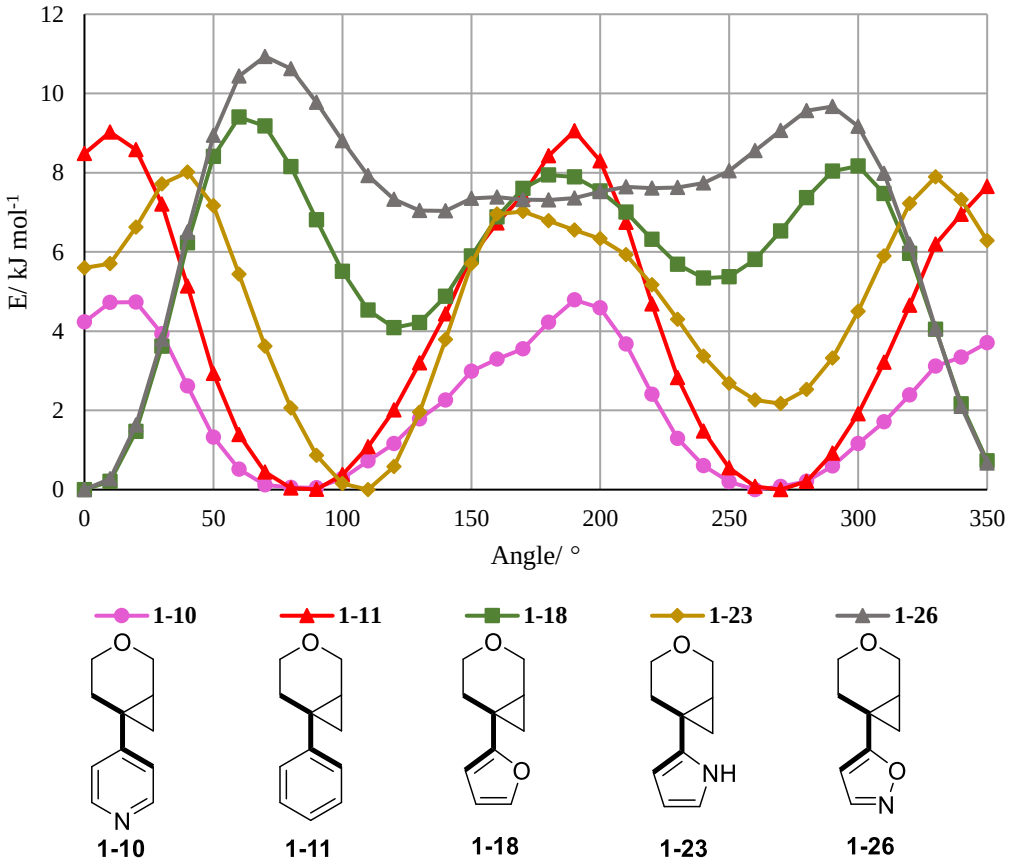

Figure 38. Dihedral angle scans of selected six- and five-membered rings with the CPP moiety.

In both 4-pyridine **1-16** and benzene **1-17**, the steric environment adjacent to the CPP is identical; however, the presence of the nitrogen atom in the pyridine was predicted to cause a lowering of the energy barriers to rotation. It is anticipated that this may be due to the model taking into account the orbital overlap with the electron-deficient pyridine. Both 4-pyridyl-CPP **1-16** and phenyl-CPP **1-17** are predicted to lie in twisted conformations as a result of the steric interactions. As described previously for 4-pyridine **1-16**, the electronic stabilisation of the coplanar conformation was not predicted to overcome this. The crystal structures of the corresponding synthesised compounds are shown in Figure 39 below. Contrary to the model, 4-pyridyl CPP **1-16** contains two coplanar conformations, whilst phenyl-CPP **1-17** exists in a twisted conformation.

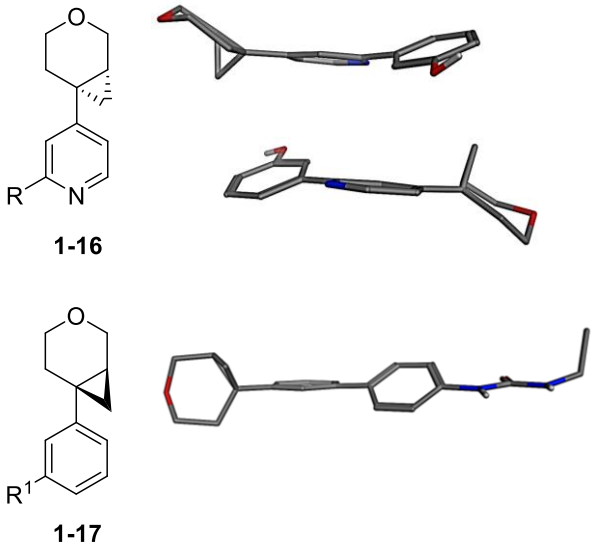

Figure 39. Crystal structures of 4-pyridyl CPP **1-16** and phenyl-CPP **1-17**. R = *meta*-phenol; R^1 = *para*-phenyl ethyl urea.

The coplanarity of 4-pyridyl CPP **1-16** is clearly an interesting deviation from the predicted outcome. This may be as a result of interactions in the solid state and crystal packing overcoming the predicted energy barrier, or as a result of electronic orbital interactions which is underestimated by the modelling.

The twisted nature of the phenyl-CPP **1-17**, which is caused almost entirely by steric interactions (evidenced by further QM studies),[3] further highlights the importance of orbital interactions in the formation of coplanar conformations in six-membered systems. Relating this to five-membered systems, it can be seen that pyrrole-CPP **1-23** and phenyl-CPP **1-17** have similar energy barriers to rotation (Figure 38). This is likely due to the similar steric environment adjacent to the CPP ring in both compounds. As such, the steric environment appears to be most significant factor in the twisted conformation for pyrrole **1-34**. Furthermore, the electron-rich nature of the pyrrole means that the orbital overlap is likely to

be very weak or non-existent and, as such, unable overcome the steric clashes to stabilise a coplanar conformation.

For CPP-furan **1-31**, the presence of the oxygen atom adjacent to the CPP, decreases the size of the heterocycle, thus reducing the influence of sterics on the conformation. The existence of both a twisted and coplanar molecule in the crystal structure (Figure 35) highlight a lack of conformational preference, probably due to this reduction in ring size. Furthermore, it is likely that there is limited orbital overlap between the cyclopropyl orbitals and the furan π-system. Therefore, it can be assumed that the observation of a coplanar structure is primarily due to the reduction in steric bulk of the heteroaromatic ring, rather than electronic stabilisation. This is further corroborated when considering CPP-isoxazole **1-9**, whereby a coplanar conformation is both predicted and observed. While the energy barriers are of similar values to the furan, the lowering of the LUMO, in comparison, may lead to some orbital overlap.

Comparison of the predicted and measured dihedral angles for these compounds, along with the angle between the average ring planes is shown below in Table 8. For the five-membered compounds, the modelling was not accurate in predicting the solid-state dihedral angle and conformation. In some cases, the conformational preference was alluded to by means of low energy barriers and lack of stabilisation, or prediction of more than one energy minimum.

Table 8. Comparison of the predicted dihedral angle between the CPP and heterocycle and the values obtained from the crystal structures of compounds **1-31**, **1-34**, **1-37**, **1-16** and **1-17**. Also shown is the angle between the average planes of the CPP ring and the heterocyclic ring.

Compound	Predicted Dihedral Angle/ °	Measured Dihedral Angle/ °	Angle between average ring planes/ °
Furan **(-)-1-31**	0	111.0 213.8	74.8 39.3
Pyrrole **(+)-1-34**	110	296.5	56.4
Isoxazole **(-)-1-37**	0	189.7 355.4	23.2 30.4
4-pyridine **1-16**	260	210.8 359.7	28.6 26.4
Phenyl **1-17**	270	253.9	83.8

4.6.3. THP Analogues

Modelling of the THP analogues revealed three energy minima for the furan and isoxazole analogues, representing both coplanar and twisted conformations. In these models, coplanar was considered to be a conformation wherein a carbon-carbon bond of the pyran ring is in the same plane as the heteroaromatic, specifically at 0 ° and 120 °. Pyrrole analogue **1-28**

was only predicted to occupy one energy minimum, corresponding to a twisted conformation and hence not predicted to be stable in a coplanar conformation. Furthermore, comparatively low energy barriers to rotation were predicted for all three systems, indicating little preference for the stabilisation of one conformation. The dihedral angle scans for the three THP-containing compounds are shown below in Figure 40.

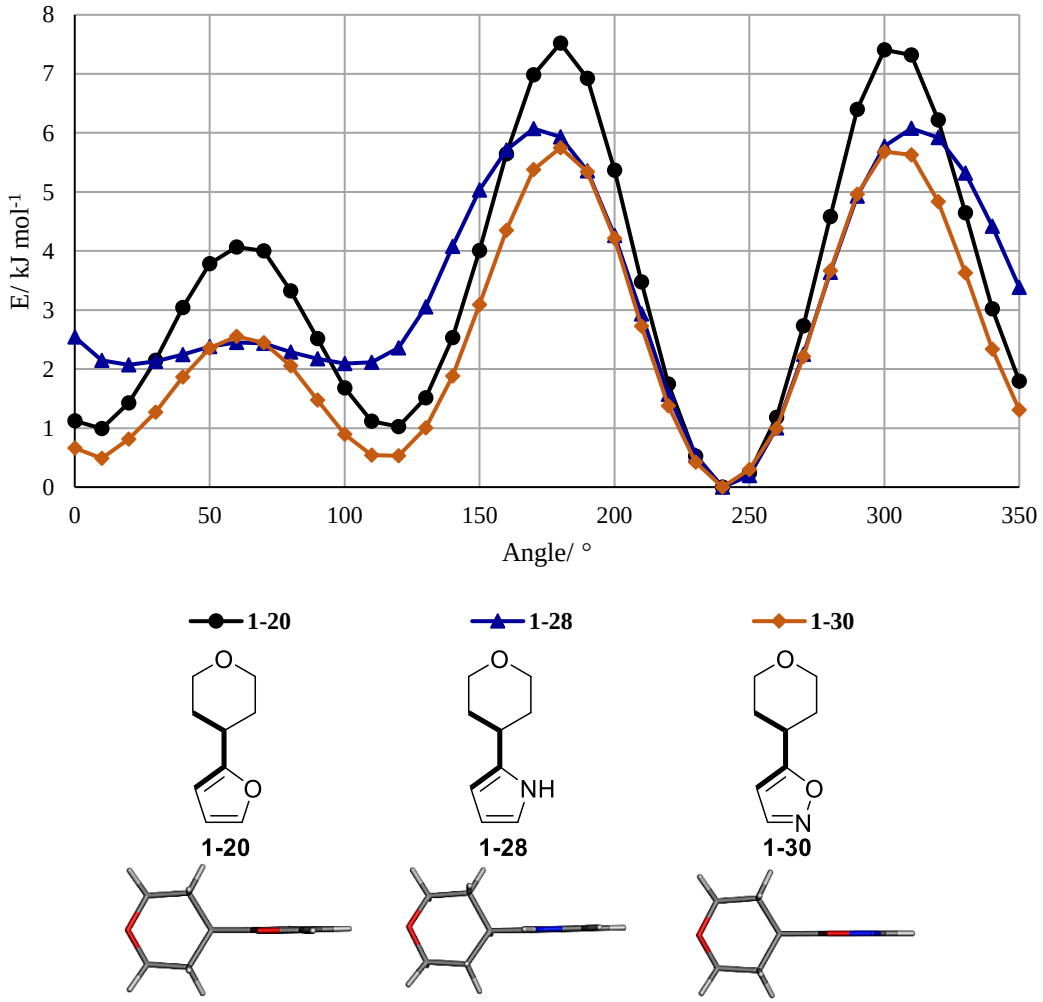

Figure 40. Dihedral angle scan of THP analogues **1-20**, **1-28** and **1-30**. The predicted minimum energy conformations of each compound are also shown.

The THP moiety cannot form meaningful electronic overlap with the π-system of the heteroaromatic rings, with the conformation decided entirely upon steric influence. As such, the impact of sterics could be carefully evaluated by using these compounds. Combined with the results obtained for the CPP compounds, analysis of the crystal structures would allow inference of the possibility of obtaining coplanar conformations without electronic effects. The crystal structures obtained for compounds **1-33**, **1-36** and **1-39** are shown in Figure 41.

From consideration of the X-ray data, THP-furan **1-33** adopts a conformation with a dihedral angle of 358.3 °, placing the carbon-carbon bond of the pyran ring coplanar with the furan

moiety. While not the lowest energy conformation predicted by the modelling, it is not an unexpected result given that a local minimum is present at 10 ° (Figure 40). A similar result is observed for THP-isoxazole **1-39**; however, two molecules are present in the unit cell with dihedral angles of 115.6 ° and 3.5 °. Both conformations can be seen to be coplanar and correspond to two of the minima in the dihedral angle scan plot (Figure 40). In addition, the isoxazole molecules are present with an unusual interaction between them, indicated by the dashed line in Figure 41. In this case, as reported by the crystallographer, 'twinning' of the crystals used to obtain the structure may have occurred. This effect is observed when two crystals of the same structure are 'inter-grown', which may affect the unit cell; however, it does not affect the conformation of the pyran analogue with respect to the heteroaromatic core.[61]

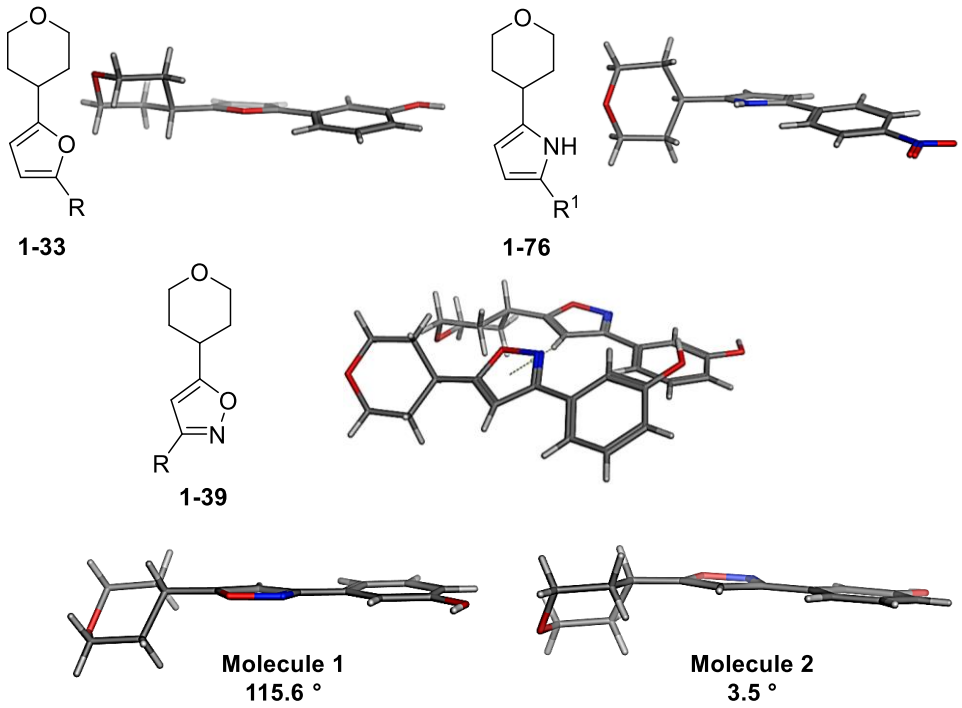

Figure 41. Crystal structures of THP-containing compounds **1-33**, **1-76** and **1-39**. R = *meta*-phenol. R^1 = *para*-nitrophenol.

As predicted, THP-pyrrole **1-76** occupies a twisted conformation in the solid state with a dihedral angle of 244.3 °, agreeing with the modelling in Figure 40. This is presumed to be as a result of the increased size of the -NH *versus* an oxygen atom (as in furan **1-33** and isoxazole **1-39**) destabilising the coplanar conformations observed in the furan and isoxazole analogues.

Despite the common energy minimum predicted for all three analogues at 240 °, only the pyrrole adopts this conformation in the solid-state. It is likely that, due to the smaller size of the heterocycles, the furan and isoxazoles can access coplanar conformations which are lower

in energy than that for the pyrrole. In addition to this, the presence of crystal packing may help to stabilise the coplanar conformations in these analogues; however, this effect is not sufficient for the pyrrole. Therefore, THP-pyrrole **1-76** is akin to a 6-membered THP-containing system with respect to the size and twisted solid-state conformation.

Observation of coplanar conformations for THP-furan **1-33** and THP-isoxazole **1-39** clearly indicates that the conformation of five-membered heteroaromatic systems are governed almost entirely by size of the heterocycle. This is confirmed when considering the three CPP-containing compounds **1-31**, **1-34** and **1-37** and their respective solid-state conformations. Coplanarity is observed; however, CPP-furan **1-31** highlights that it is possible to adopt 'twisted' conformations as well. It is apparent that there is no real conformational preference, with most of the predicted low energy conformations accessible.

Analysis of the dihedral angles and angle between the average ring planes is given below in Table 9. As is reflected in the crystal structures, the angle between the average ring planes is almost identical for THP-furan **1-33** and the two molecules of CPP-isoxazole **1-39**. The ring planes between the THP moiety and the pyrrole ring in **1-76** is 85.1 °, giving a perpendicular conformation. These data further emphasise the effect that a small increase in size has on the system, moving it from coplanar to twisted by replacement of a lone pair with a proton in the position adjacent to the pyran analogue.

Table 9. Comparison of predicted dihedral angle between the CPP and heterocycle and the values obtained from the crystal structures of compounds **1-33**, **1-76** and **1-39**. Also shown is the angle between the average planes of the THP ring and the heterocyclic ring.

Compound	Predicted Dihedral Angle/ °	Measured Dihedral Angle/ °	Angle between average ring planes/ °
Furan **1-33**	240	358.3	32.2
Pyrrole **1-76**	240	244.3	85.1
Isoxazole **1-39**	240	3.5 115.6	39.0 39.3

The data obtained for the five-membered heteroaromatic series has demonstrated that there appears to be little influence on the conformation by electronic effects, such as orbital overlap between the Walsh orbitals of the cyclopropyl ring and the π-system of the heteroaromatic. The size of the heterocycle is also important and the introduction of a second proton adjacent to the pyran analogue appears to favour twisted conformations, with little or no electronic stabilisation to counteract this. This is evident from the 'twisted' nature of CPP-pyrrole **1-34** and THP-pyrrole **1-76** whereby the replacement of a lone-pair with a proton results in a twist.

A further interesting finding is the coplanarity of THP-furan **1-33** and THP-isoxazole **1-39**. Given that these molecules adopt the same conformation as with the CPP moiety, the additional molecular complexity and lower-yielding synthesis, alongside the requirement for chiral HPLC separation to furnish single enantiomers, renders the use of the CPP in these systems less useful with respect to conformational control.

4.7. Medicinal Chemistry

The coplanar nature of the furan and isoxazole analogues with all three pyran analogues prompted an exploration into the biological activity. The presence of the *meta*-phenol group meant that the compounds synthesised were expected to show affinity for lipid kinases.[32,62] Furans **1-31** – **1-33** and isoxazole **1-37** - **1-39** were submitted to *in vitro* time-resolved fluorescence resonance energy transfer (TR-FRET) assays measuring potency values against four isoforms of the PI3K kinases. The results are summarised below in Table 10.

Table 10. Potency data obtained for furans **1-31** – **1-33** and isoxazoles **1-37** – **1-39** in the *in vitro* TR-FRET assay**.**

Compound	Core	Hinge	Isomer	PI3Kα pIC_{50}	PI3Kβ pIC_{50}	PI3Kγ pIC_{50}	PI3Kδ pIC_{50}
(+)-1-31	Furan	CPP	1*R*, 6*S*	5.0[a]	<4.5[a]	4.6[b]	4.7[a]
(-)-1-31			1*S*, 6*R*	<4.5[a]	<4.5[a]	4.8[a]	4.9[a]
1-32		DHP		5.1[c]	5.3[c]	5.1[d]	5.8[c]
1-33		THP		4.7[a]	4.9[a]	4.7[a]	5.2[a]
(-)-1-37	Isoxazole	CPP	1*R*, 6*S*	<4.5[c]	<4.5[c]	<4.5[c]	4.7[c]
(+)-1-37			1*S*, 6*R*	<4.5[c]	<4.5[c]	<4.5[c]	<4.5[c]
1-38		DHP		<4.5[a]	4.7[a]	4.8[a]	4.8[a]
1-39		THP		<4.5[a]	<4.5[a]	<4.5[a]	<4.5[a]

[a]N=2; [b]N=1; [c]N=4; [d]N=3

In general, the furan-containing analogues were more active, giving potency values above the minimum readout for the assay (pIC_{50} value of of 4.5). DHP-isoxazole **1-38** was the most active of the isoxazole-containing compounds; however, CPP-isoxazole **(-)-1-37** did give a similar potency against PI3Kδ. Overall, these compounds were not active enough to deduce any meaningful conclusions, and it is likely that a more active group than the *meta*-phenol may be required to boost the potencies above the threshold for detection in the biological assay.

With the furan-analogues showing slightly increased activity, it was possible to infer more information from these results. For example, DHP-furan **1-32** was the most active compound, specifically in PI3Kδ, giving a surprisingly high pIC_{50} value of 5.8 likely due to the rigid coplanarity of the system, driven by electronics. THP-furan **1-33** and CPP-furan **1-31** showed somewhat similar activities in all four isoforms with a small difference visible between the

two isomers of the CPP analogue, agreeing with previous studies.[2,3] From these results, the propensity for the THP analogue to adopt a coplanar conformation in the five-membered systems is confirmed to some extent, agreeing with the crystal structure data.

Comparisons to the six-membered pyrimidine systems were made, and the binding efficiency index (BEI) calculated (BEI = 1000 × (pIC_{50}/MW)) for PI3Kδ (Figure 42). The BEI is a simple measure of the binding efficiency of a molecule, taking into account the molecular weight and is commonly used to rank fragments during drug-discovery processes.[63] The results from this highlight the efficiency with which DHP-furan **1-32** can bind to this isoform. Comparing this to the DHP-pyrimidine **1-89** and morpholine-pyrimidine **1-91**, the BEI value lies between those calculated for the two six-membered systems. This is clearly a significant result and would be an intriguing starting point for a small exploratory study evaluating the DHP-furan fragment as a PI3Kδ inhibitor. This is particularly pertinent given the novel vectors introduced by the five-membered heterocycle *versus* those for the common six-membered system. Of additional interest is the increase in BEI value for THP-furan **1-33** in comparison to the six-membered THP-pyrimidine **1-90**. While a similar pIC_{50} value is observed, the smaller size of the molecule leads to an increase in BEI for the furan. This is another unusual and interesting observation which may warrant further studies into the use of this moiety as a PI3Kδ inhibitor.

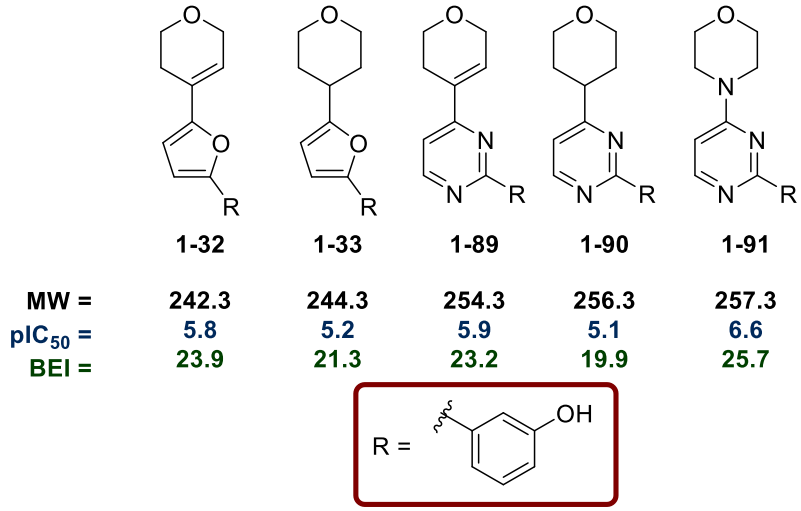

Figure 42. Comparison of the binding efficiency index (BEI) of selected five- and six-membered heterocyclic compounds to PI3Kδ. A larger BEI value indicates more efficient binding.

5. Summary and Conclusions

The aim of this part of the thesis was to determine if the CPP moiety could access coplanar conformations with five-membered heteroaromatic systems, and if it could be expanded in its use as a bioisostere for morpholine. To enable this, QM modelling was used, and the predicted low energy conformations compared to those observed in crystal structures.

Dihedral angle scans of several five-membered heteroaromatic compounds were analysed to determine the most appropriate scaffolds for synthesis. Comparison of the resultant data with that obtained for the six-membered rings revealed more complex energy plots with additional energy minima. These were interpreted as resulting from a decrease in size of the heteroaromatic ring for the five-membered analogues, leading to reduced stabilisation of specific conformations. Increased electron-density on the five-membered heterocycles was also expected to reduce electronic stabilisation from the cyclopropyl orbitals; however, this did not affect the outcome of the DHP-containing analogues, all of which were predicted to be coplanar. While the furan-containing CPP and THP compounds did not appear to exhibit a strong conformational preference, the pyrrole analogues were predicted to adopt twisted conformations, presumably due to the introduction of a proton on the heteroatom adjacent to the pyran. CPP-isoxazole was predicted to favour only one coplanar conformation, making it an interesting compound for synthesis.

A cross-coupling approach was successfully implemented to install the pyran analogues and *meta*-phenol group to furan and pyrrole cores. While the pyrrole analogues required additional deprotection steps, these compounds were obtained in sufficient quantity and quality to obtain crystalline material. The only deviation from this method was in the synthesis of THP-pyrrole **1-76** which required a *para*-nitro group in order to provide access to suitable crystalline material. Isoxazole analogues were obtained *via* a [3+2] cycloaddition approach with the use of alkyne-derivatives of each pyran analogue in combination with a common oxime intermediate.

A summary of both the modelled data and that obtained from the resulting crystal structures is provided below in Table 11. The key points are also included, highlighting where the modelling was both accurate and inaccurate; however, it should be noted that the modelling was conducted in the gas phase and, therefore, the X-Ray crystal structures are likely to be influenced by the presence on intermolecular interactions which are not predicted by the QM modelling. As such, comparisons should be examined carefully and these differing scenarios considered in the outputs of this study.

Table 11. Summary of the key modelling data alongside that obtained from the crystal structures.

Compound	Dihedral Angle/ ° (predicted)	Angle between average ring planes/ °	Modelling Accuracy
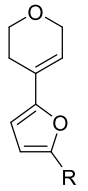 **1-32**	6.5 (0)	1.9	Modelling successfully predicted coplanar conformations.
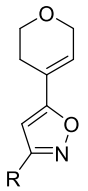 **1-38**	23.9 (0)	21.4	
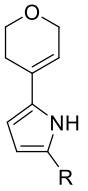 **1-35**	19.0 (20)	12.0	
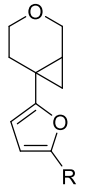 **1-31**	111.0 213.8 (0)	74.8 39.3	Modelling and crystal data do not fully align.
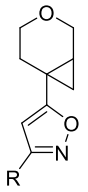 **1-37**	189.7 355.4 (0)	23.2 30.4	Modelling failed to predict second structure observed.
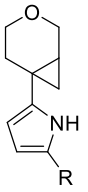 **1-34**	296.5 (110)	56.4	Modelling successfully predicted twisted conformation.

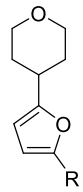 **1-33**	358.3 (240)	32.2	Modelling predicted accessibility of the coplanar conformations observed.
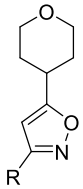 **1-39**	3.5 115.6 (240)	39.0 39.3	
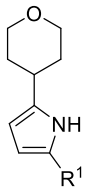 **1-76**	244.3 (240)	85.1	Modelling successfully predicted twisted conformation.

R = *meta*-phenol; R^1 = *para*-nitro.

Given the aims of this study (*vide infra*), a number of conclusions could be drawn pertaining to the use of the CPP moiety with five-membered systems:

1) The modelling does not generally align with the specific conformations observed in the crystal structures, likely due to the presence of intermolecular interactions and crystal packing which were not present in the model. Despite this, the overall dihedral angle scans do provide a useful insight into conformations which may be accessible. The implementation of a modelling approach which is more closely aligned with the system in question would likely provide more accurate predictions.
2) The reduced ring size of five-membered systems decreases the steric interaction between the heteroaromatic system and the pyran analogue. A consequence of this is that furan and isoxazole THP derivatives can access coplanar conformations.
3) Electronic overlap appears to be insufficient to induce a preference for coplanar conformations. The exception to this is isoxazole-CPP **1-37** for which a twisted conformation is, tentatively, disfavoured.

The outcomes from this project were clear, with the five membered rings reducing the steric bulk, thus allowing the THP moiety to lie coplanar. The CPP provides novelty; however, the molecular complexity and introduction of chirality outweigh the benefit. Despite this, there were some surprising results obtained when the tool compounds were submitted to the lipid

kinase assay wherein the use of a THP ring appears to provide a much simpler bioisostere for morpholine in this context.

6. Future Work

Furan-DHP **1-32** showed surprising potency against PI3Kδ with a pIC_{50} value of 5.8 and comparable BEI to pyrimidine-morpholine **1-91**. With the relatively small molecular weight associated with the compound, this value provides an excellent starting point for future studies and optimisation. To our knowledge, there are no examples of lipid kinase inhibitors with a DHP-furan moiety within the literature. Therefore, maintaining the DHP moiety, it may be possible to optimise substitution around the furan core to access more potent molecules for this purpose. Pan- or selective-lipid kinase inhibitors could conceivably be accessed *via* this fragment. Typically, for PI3Kδ selectivity, unique interactions in the 'specificity region' of the kinase active site are required.[64] These are often substituted aromatic groups and there is an abundance of literature which would enable thorough exploration of this approach to a potentially novel series of PI3Kδ inhibitors.[20] Furthermore, the *meta*-phenol group could be replaced with groups such as benzimidazoles which have previously been shown to aid with increasing the potency.[65,66] A proposed structure of this type is shown below in Figure 43.

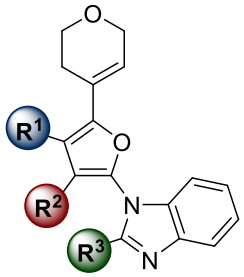

Figure 43. Potential structure of a compound making use of a benzimidazole group as a replacement of the meta-phenol originally used.

As an extension to lead optimisation, exploration of the use of the THP group in kinase-binders could be undertaken. Molecules with increased potencies would allow a more accurate comparison of the both DHP and THP with five-membered cores. It would be possible to determine whether potency is maintained at various levels upon replacement of the DHP with the THP. This would add further weight to the hypothesis of steric encumbrance being the most important aspect of coplanarity in five-membered systems. In addition, the use of a THP moiety would represent another degree of novelty in terms of lipid kinase inhibition as there are no reports of proficient use of this moiety within the literature. Figure 44 below shows the furan core and pyran analogues along with the position on the furan which could be substituted in order to increase the potency of the molecules. For THP-

containing compounds, it is likely that substitution at the 'R^1' position would lead to steric clashes, resulting in a twisted structure and reducing the potency.

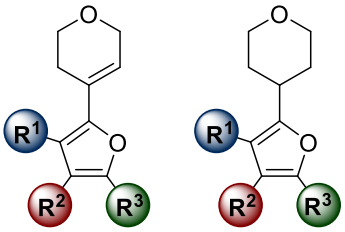

Figure 44. Structures of furan-DHP and furan-THP containing molecules with the three positions of substitution shown.

If more potent molecules could be obtained with the THP moiety, the opportunity to introduce a pyrrole core could be taken to provide further evidence for the steric argument outlined in this project. It would be expected that the presence of the -NH group would destabilise the coplanar conformation, reducing the potency of the compound.

By studying the factors affecting the conformation of various pyran analogues in five-membered systems, it may be possible to enable the synthesis of a novel series of lipid kinase inhibitors. This project has clearly identified advantages of studying the conformation of molecules, especially with the view to application in medicinal chemistry. While the CPP was not found to be advantageous in these systems, it remains an interesting and useful tool in six-membered systems.

Section 2: Studies towards an enantioselective synthesis of a cyclopropylpiperidine (CPPip) derivative

7. Background

7.1. Current Synthetic Methods to Install the CPP Moiety

Current methods towards installation of the CPP moiety result in the formation of a racemic mixture of products wherein the resulting enantiomers have been shown to exhibit different lipid kinase potencies when used in biologically active molecules.[2] Two general approaches are used with the products from both requiring the separation of enantiomers by chiral HPLC.[2,3]

The first of these approaches can be utilised with electron-deficient heterocycles and has been exemplified with pyrimidine cores as shown in Scheme 22. The route towards these analogues involves Suzuki-Miyaura cross-coupling of DHP boronic acid pinacol ester **1-56** before a Corey-Chaykovsky cyclopropanation[67] gives rise to the CPP moiety. As discussed in the synthesis of five-membered DHP-containing compounds, the quality of DHP boronic acid pinacol ester **1-56** has a direct impact on the outcome of the Suzuki-Miyaura cross-coupling (*vide supra*, Chapter 1, Section 1, part 4.3). As a result of this, the first step of this sequence can be unreliable, resulting in mixed yields. Furthermore, the cyclopropanation step is low yielding and leads to a racemic mixture.[2]

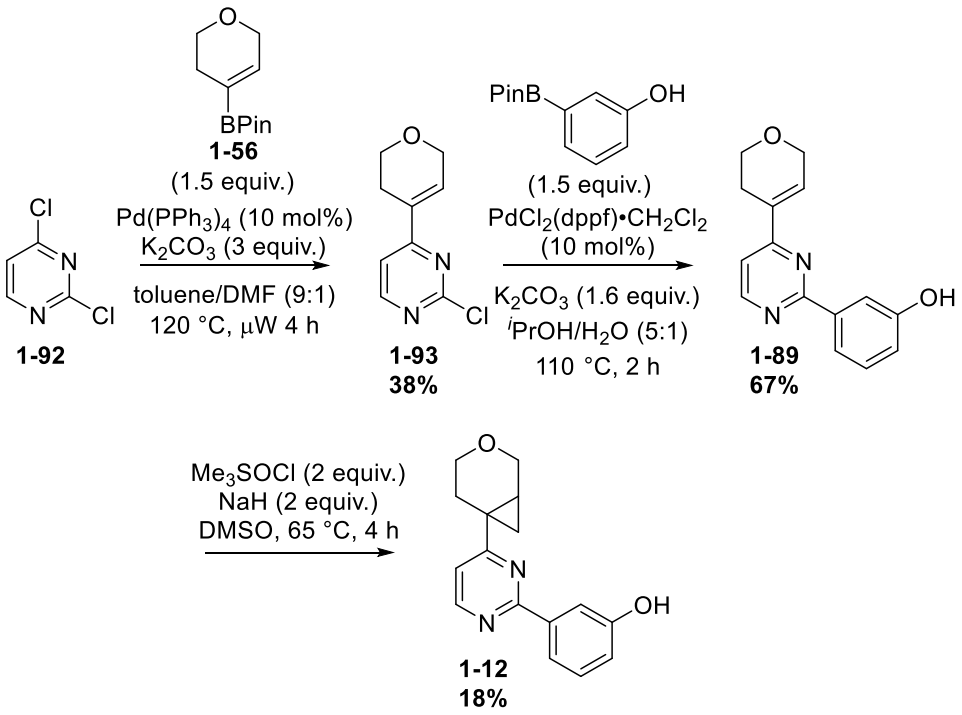

Scheme 22. Synthesis of racemic CPP-pyrimidine **1-12** *via* a Corey-Chaykovsky cyclopropanation.

A further disadvantage to this approach is the restriction to pyrimidine cores, as emphasised by the inability to cyclopropanate the corresponding pyridine analogue **1-94**, shown below. No desired product was observed in this reaction, instead leading to methylation of the phenolic -OH group to give unwanted by-product **1-95** (Scheme 23).[3]

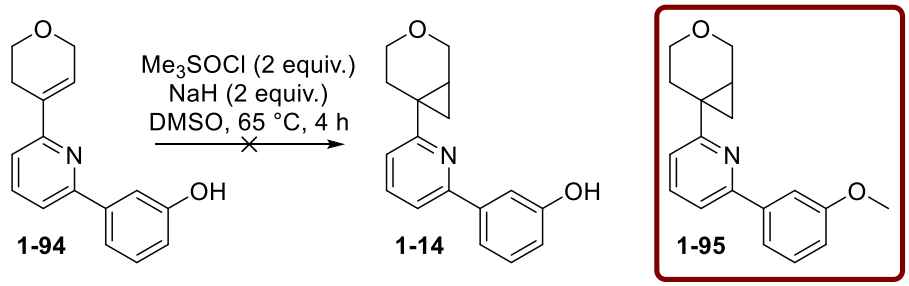

Scheme 23. Unsuccessful Corey-Chaykovsky cyclopropanation of DHP-pyridine **1-95**. Only methylated product **1-95** was obtained.

Consideration of the mechanism of this reaction highlights the importance of the electron-withdrawing nature of the pyrimidine ring. Scheme 24 shows that this moiety can delocalise the negative charge, increasing the susceptibility of nucleophilic attack at the alkenyl group. On moving to a pyridine core, the delocalisation is not possible to the same extent, disfavouring attack onto the alkene. Consequently, no product is observed in this reaction, limiting the use of this method.

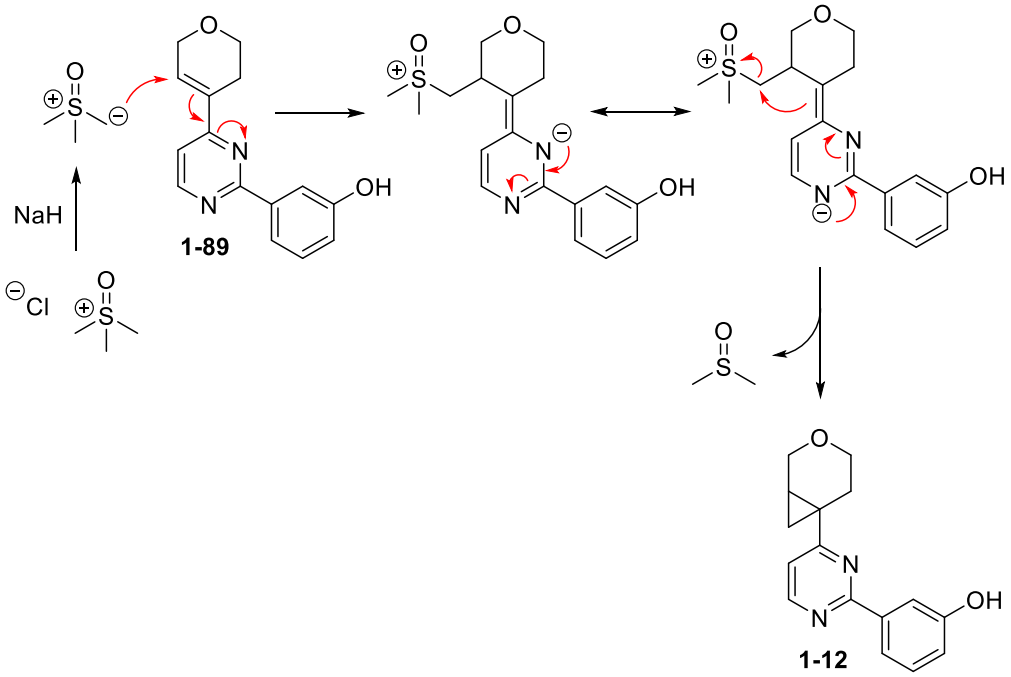

Scheme 24. Proposed mechanism for the Corey-Chaykovsky cyclopropanation of DHP-pyrimidine **1-89** to form CPP-pyrimidine **1-12**. Resonance stabilisation of the negative charge can take place within the pyrimidine ring, favouring attack of the sulfoxonium ylide onto the alkenyl group.

The alternative method for installation of the CPP moiety relies on the synthesis of racemic potassium trifluoroborate salt **1-58**. As shown in Scheme 5 for use in the synthesis of five-membered compounds, the formation of this intermediate requires a Simmons-Smith cyclopropanation of DHP boronic acid pinacol ester **1-56**.[2] Following this, conversion to the potassium trifluoroborate salt under non-etching conditions gives the desired product.[46] The yield of the initial cyclopropanation step determines the overall outcome of the two steps given the consistently high yields observed for formation of potassium trifluoroborate **1-58**.[43]

It was found that conditions optimised by Harris *et al*. were optimal for the use of potassium trifluoroborate **1-58**;[3,47] however, the outcomes appeared to be substrate-dependent. Yields obtained in the synthesis of furan and pyrrole analogues (*vide supra*) were 19% and 29%, respectively; however, the effect of the protecting group removal steps on the overall outcome is not known. When used to synthesise simple six-membered compounds, the yields were found to be somewhat improved and in the range of 21-41%.[2,3] Finally, systems with increased molecular complexity (e.g. **1-98**), synthesised as part of a lead-optimisation project, were found to undergo cross-coupling slightly more efficiently, giving yields of up to 69%.[3] Scheme 25 summarises these results with the corresponding product structures.

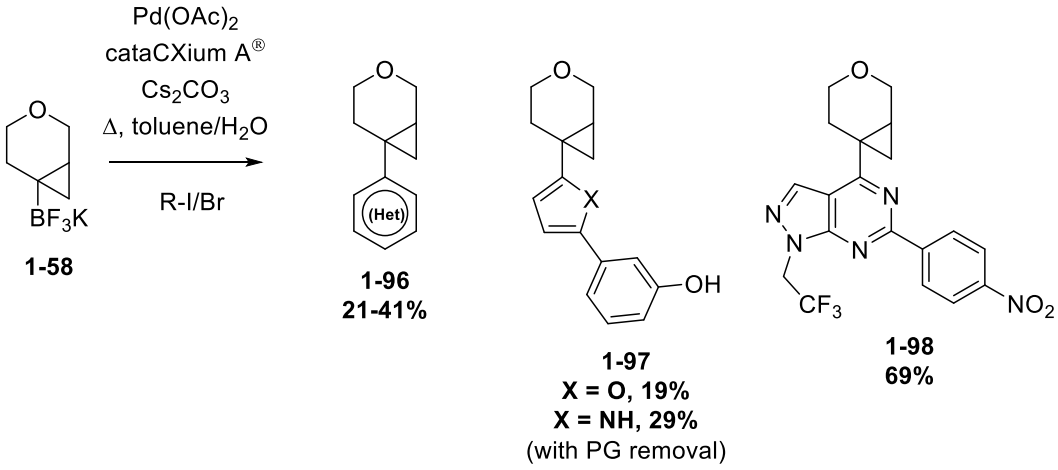

Scheme 25. Overview of yields obtained when using potassium trifluoroborate salt **1-58** in Suzuki-Miyaura cross-coupling reactions. A clear variation in yields can be seen with those observed appearing substrate dependent.

The variability in reaction outcome, coupled with the formation of racemic compounds provides a disadvantage to this method, but the general approach is a facile way of installing the desired CPP moiety. The unique nature of the CPP ring may require further optimisation of reaction conditions to elevate the yields for all substrates; however, racemate formation still represents a challenge.

7.2. Initial Exploration of an Enantioselective Route

As part of a wider series of studies into the novel CPP moiety, an initial attempt to enable an enantioselective approach was made by another member of our laboratories.[68] This route is discussed below, and was proposed to use an enantioselective Simmons-Smith cyclopropanation of an allylic alcohol as the asymmetric induction step. Facial selectivity was expected to be induced by use of a chiral boron-containing ligand, optimised by Charette (Scheme 26).[69] High enantioselectivities were reported alongside recovery of the chiral ligand.

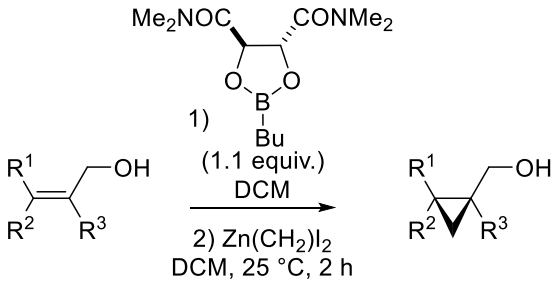

Scheme 26. Enantioselective Simmons-Smith cyclopropanation of allylic alcohols using a chiral ligand.[69]

Application of this methodology to the formation of the CPP moiety required the synthesis of the pyran ring. The planned disconnection of the pyran moiety is shown below in Scheme 27 along with the incorporation of the key asymmetric step. While this approach appears straightforward, the necessary intermediates required a somewhat protracted synthesis.

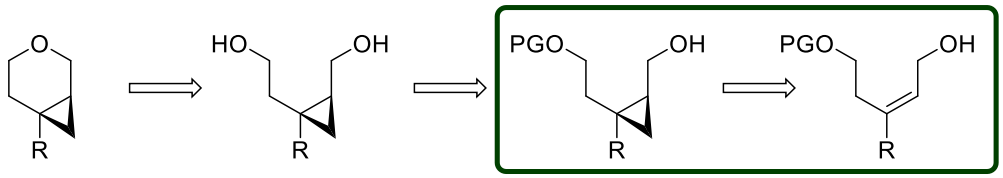

Scheme 27. Proposed retrosynthesis of the CPP incorporating the enantioselective Simmons-Smith reaction.

Initially, this methodology targeted the synthesis of 2-pyridyl analogue **1-14** (Table 5). In order to obtain the Simmons-Smith precursor, the synthetic route shown in Scheme 28 was used.[68] An initial *para*-methoxybenzyl (PMB) protection of 3-butyn-1-ol **1-99** to give **1-100**, followed by formation of the corresponding acetylide anion, and trapping with ethyl chloroformate gave intermediate **1-101** in excellent yield. The *β*-borylation of acetylenic ester **1-101** was successful, using conditions reported by Santos *et al.*[70] to give BPin **1-102** in 82% yield. This was carried into a subsequent Suzuki-Miyaura cross-coupling reaction

with chloropyridine **1-104** to give 2,6-disubstituted pyridine **1-105** which could be subjected to reduction, forming the desired allylic alcohol.

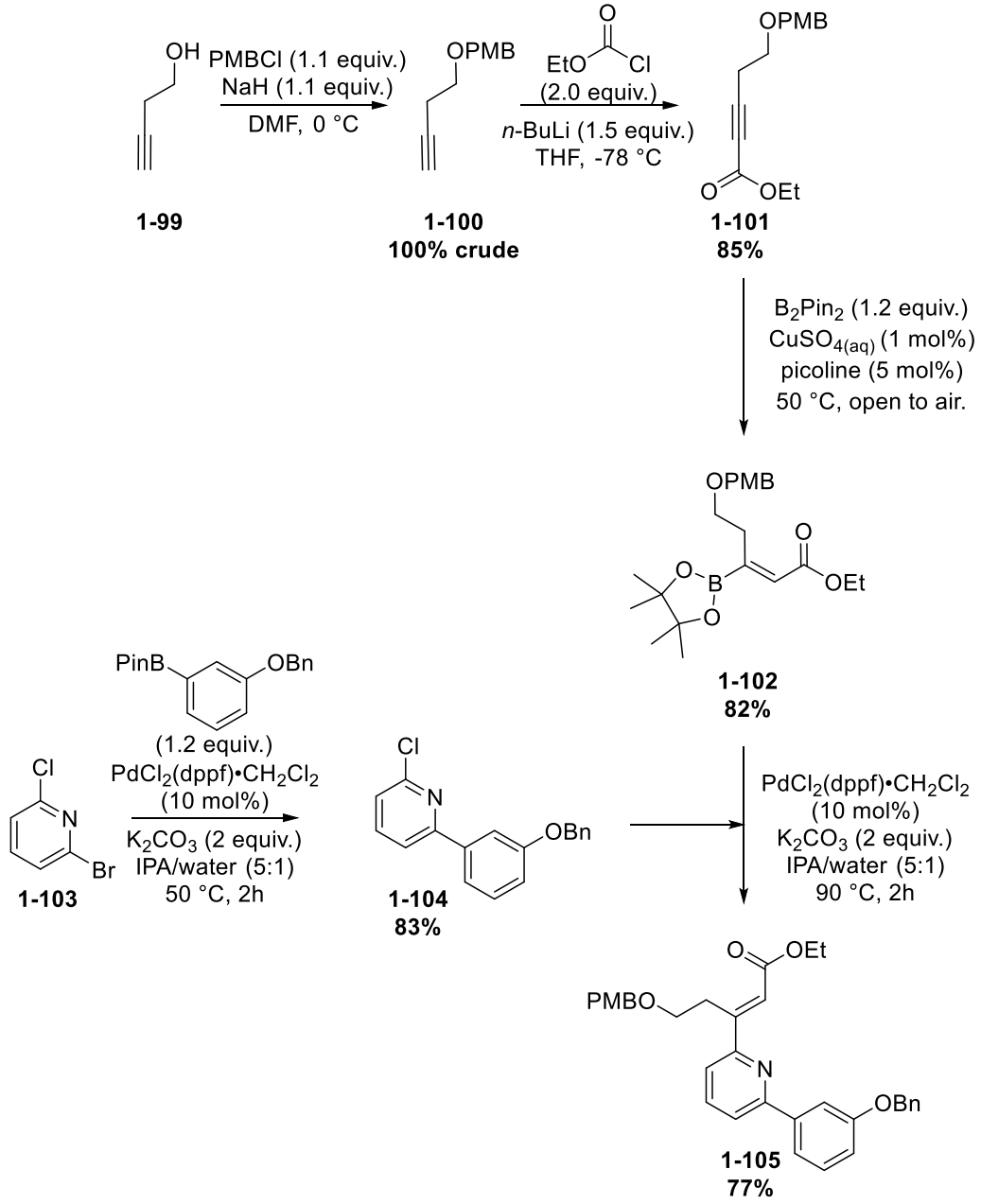

Scheme 28. Optimised synthetic route towards the desired Simmons-Smith precursor for the enantioselective synthesis of 2-pyridyl analogue **1-14**.[68]

Pyridine **1-105** provided the framework upon which construction of the pyran could begin. As shown in Scheme 29, it was found that a DIBAL-H reduction of the ester moiety in intermediate **1-105** provided allylic alcohol **1-106** in 67% yield. Implementation of the boron catalyst in the enantioselective Simmons-Smith cyclopropanation gave an enantiomeric excess (*ee*) of 94% for cyclopropane **1-107**.[68] Disappointingly, the yield for this key step was a moderate 36%, and this was not optimised further.

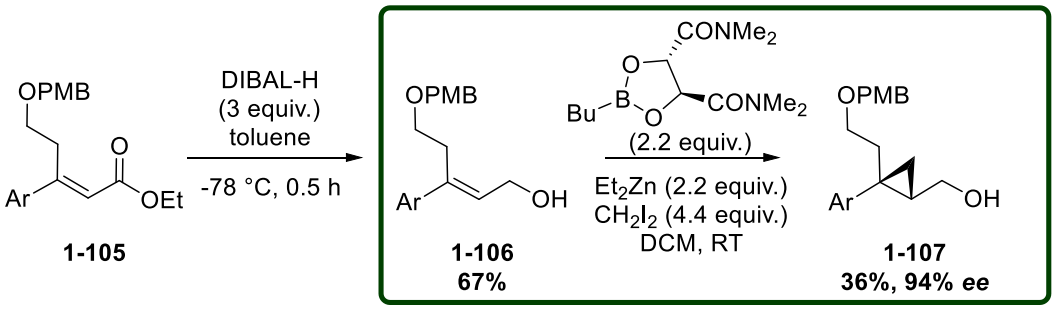

Scheme 29. Synthesis of cyclopropane **1-107** using Charette's enantioselective Simmons-Smith cyclopropanation reaction. The *ee* value was measured to be 94%.[68]

One attempt at forming the pyran ring was made from cyclopropanated intermediate **1-107**, as shown in Scheme 30.[68] Removal of the PMB protecting group was possible using ceric ammonium nitrate (CAN) giving diol **1-108** in 74% yield and pyran formation was attempted using tosyl chloride to initiate the ring closing step. The desired product was isolated; however, only a 6% yield was possible due to the small scale and unoptimised conditions.

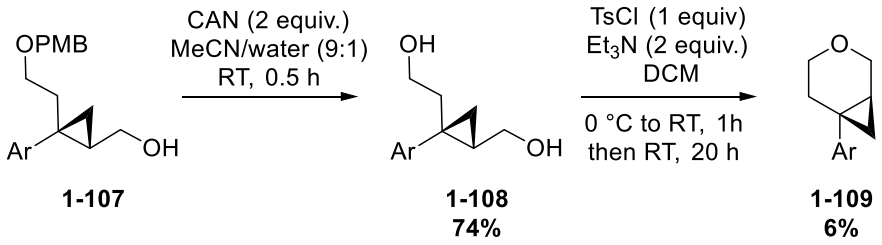

Scheme 30. PMB deprotection and ring-closing steps in the synthesis of CPP-pyridine **1-109**.[68]

Optimisation of this method is clearly desirable; however, there are some evident disadvantages for use in a lead optimisation setting. Firstly, the linear sequence consists of eight individual steps from the 3-butyn-1-ol **1-99** starting material, with the key enantioselective step generating the desired product in a moderate 36% yield. In addition, installation of the desired (hetero)aromatic core is required early in the synthesis. As a result, it is likely that each analogue would require a bespoke synthesis of at least five steps from intermediate **1-102**. Arising from this, it is possible that the enantioselective cyclopropanation step is substrate-dependent, further disadvantaging this route and causing difficulties when varying the core. Despite the evident disadvantages in lead optimisation, this route may find use when aimed at a specific enantiopure molecule such as a drug candidate, for which a large amount of enantiopure material would be required.

7.3. Alternative Approaches to an Enantioenriched Product

An alternative approach to enantioselective cyclopropanation was desirable with the aim of synthesising an enantiopure or enantioenriched intermediate, enabling facile installation of the CPP moiety. The ideal outcome was an intermediate similar to potassium trifluoroborate **1-58**. Methods aimed at accessing the generic scaffold shown in Figure 45 were explored in the literature; however, it was clear that direct access to a saturated ring was limited to low-yielding, racemic cyclopropanation reactions of unsaturated boronic acid pinacol esters.[2,47,71]

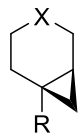

X = O, NR^1
R = $B(OR)_2$, I, Br, OTf...

Figure 45. Structure of the CPP scaffold used for literature search of preparations. R and R^1 = any group except hydrogen.

7.3.1. Cycloisomerisation of 1,6-Enynes

Direct access to this scaffold did not appear to be a viable approach; however, it was found that a closely related unsaturated derivative could be readily accessed *via* transition metal cycloisomerisation of oxygen- or nitrogen-tethered 1,6-enynes as shown in Scheme 31.[72]

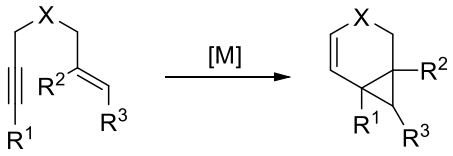

X = O, NR X = O, NR

Scheme 31. General scheme of the metal-catalysed cyclosiomerisation of 1,6-enynes into 3-azabicyclo[4.1.0]hept-4-enes and 3-oxa-bicyclo[4.1.0]hept-4-enes.

This approach builds up the desired molecular complexity, required for the CPP moiety, in one step from readily accessible 1,6-enyne starting materials. This simple method was highly desirable; however, there was evidence for several isomeric products such as those shown in Figure 46.[72-74]

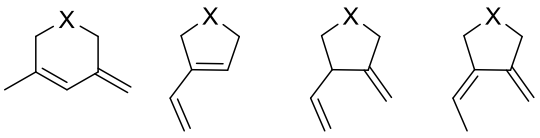

Figure 46. The basic scaffolds of possible isomers which may form in cycloisomerisation reactions.

Avoiding the formation of these isomers would be imperative to the success of the reaction, if this approach were to be implemented. Further exploration of the relevant literature demonstrated that the choice of catalyst and substrate would enable some control over the

reaction outcome.[75,76] In addition, the use of oxygen and nitrogen tethers has been shown to favour the desired bicylco[4.1.0]hept-4-enes, as will be discussed (*vide infra*).[76-78]

The formation of the bicyclo[4.1.0]hept-4-ene moiety has successfully been catalysed by platinum,[72,79,80] gold,[75,77,78] manganese,[81] iridium,[82] rhodium,[83] palladium[84] and ruthenium.[85] Gold and platinum catalysed cycloisomerisations are by far the most prevalent within the literature; however, gold catalysts are active at room temperature, as opposed to the higher temperatures seen when employing platinum.[74,77,86] Additionally, there are several examples of asymmetric syntheses of bicyclo[4.1.0]hept-4-enes. As a result, gold-catalysis was chosen as the focus of this study, aimed at the optimisation of a system in which the CPP moiety could be accessed in an enantioenriched fashion.

7.3.2. Properties of Gold and Mechanistic Data

The inherent properties of gold contribute towards the effectiveness of this metal in the cycloisomerisation of 1,6-enynes to bicyclo[4.1.0]hept-4-enes. Studies of the reaction and mechanism have shown that it proceeds *via* catalysis using a ligated gold(I) cation as highlighted below in Scheme 32. This catalytically active cation is formed by removal of the chloride from the species [LAuCl] and replacement with a non-coordinating ligand using silver salts, leading to the precipitation of AgCl. Initial binding of the gold cation to the alkyne group of the 1,6-enyne facilitates attack of the alkene onto the alkyne. Cyclopropanation occurs *via* a "push-pull" mechanism to form intermediate **A**.[74,75,87] A 1,2-hydride shift then occurs to give intermediate **B**, with stabilisation of the resulting cation by the lone pair on the heteroatom tether favouring this pathway for oxygen- and nitrogen-tethered enynes.[76-78]

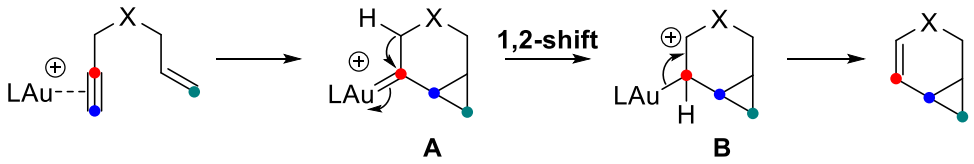

Scheme 32. Proposed mechanism for the gold-catalysed cycloisomerisation of 1,6-enynes.

Binding to the alkyne can be attributed to the unique properties of gold, resulting from relativistic effects wherein the large positive charge in the nucleus of the gold atom causes the electrons in the *s* orbitals to move at velocities approaching the speed of light.[88] As a consequence, the electrons are treated with a mass larger than that for those with non-relativistic effects.[89] The electronic structure of the gold atom is affected, with the 6*s* and 6*p* orbitals pulled closer to the nucleus and the 5*d* and 5*f* orbitals expanded due to the resulting increase in shielding.[88,89] This leads to a lower energy LUMO in the gold(I) cation which, in combination with the large electronegativity value, leads to stronger than anticipated covalent

bonding to the ligand (such as a phosphine) *via* the *s* orbital.[74,88] The positive charge of the gold(I) cation can be delocalised to the phosphine ligand, acting as one large, diffuse cation.[89] The spread of the charge results in a "soft" cation in which orbital interactions are the predominant force, favouring binding to the π-system of the alkyne (due to lower energy MOs than the alkene).[89] Back-donation from the metal to the antibonding orbitals of the alkyne is weak due to the energy difference and, as such, electron density is withdrawn from the π-system. Furthermore, the cationic nature of the Au(I) system provides an electrostatic interaction which contributes an additional effect to the binding.[86] As a result, the alkyne is susceptible to nucleophilic attack by the alkene, initiating the cycloisomerisation reaction.[74]

The enablement of this reaction under mild temperatures is clearly an advantage to the gold-catalysed method. Furthermore, the use of a ligated gold(I) cation introduces a vector from which chirality can be introduced, resulting in enantioselectivity. The disadvantage of this approach is the linearity of two-coordinate gold(I) complexes,[86,88] as a result of the orbital effects discussed (*vide supra*), which may reduce the influence of the ligand. Despite this, there are numerous examples of enantioselective gold-catalysed cycloisomerisation reactions of 1,6-enynes.

7.3.3. Enantioselective Gold-Catalysed Cycloisomerisations of 1,6-Enynes

Since the observation of bicyclo[4.1.0]hept-4-ene formation in the gold-catalysed cycloisomerisation of 1,6-enynes by Echavarren in 2004,[77] research in this area has grown. Within this expansion has been the focus on asymmetric cycloisomerisation, the first example of which was published in 2009 by Michelet and focused predominantly on oxygen-tethered enynes.[90] As shown in Figure 47 below, a biaryl-diphosphine ligand was used to induce the required asymmetry with generally good yields and excellent enantioselectivities. It is noteworthy that the resulting cyclopropyl ring is decorated with two large aromatic groups, which may be important for induction of chirality. Replacement of one of these with a small alkyl group was detrimental to the yield, but not the enantioselectivity (Figure 47B). Further to the oxygen-tethered enynes, there was one example of a nitrogen-tethered enyne (with a tosyl protecting group). Interestingly, increasing the temperature in this case improved both the yield and enantioselectivity (Figure 47C).

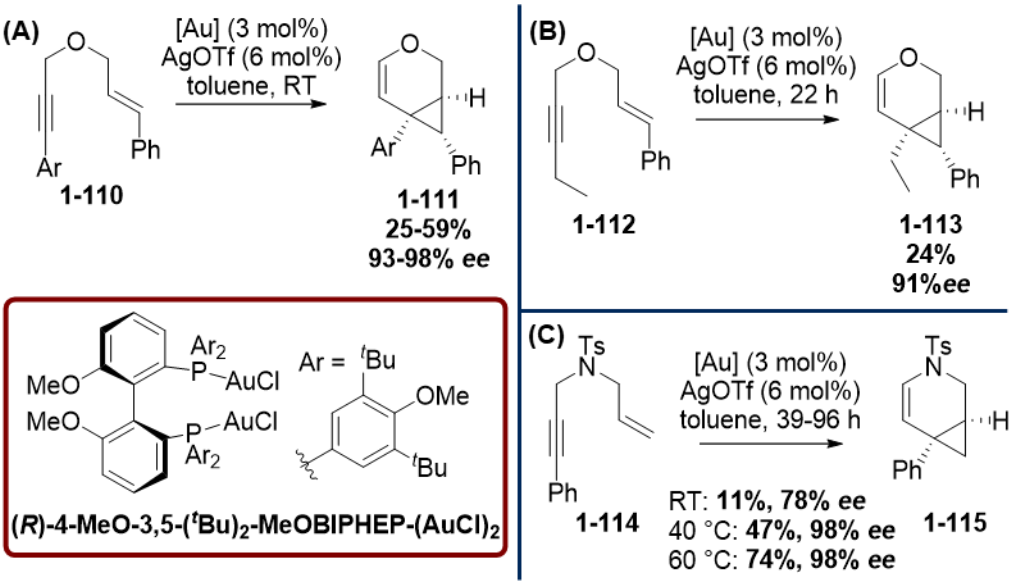

Figure 47. Summary of the work carried out by Michelet.[90] (**A**) Enantioselective synthesis of 3-oxa-bicyclo[4.1.0]hept-4-enes and structure of the pre-catalyst used. (**B**) Reaction carried out with removal of one aromatic group resulting in a lower yield. (**C**) Reaction with nitrogen-tethered enyne to give 3-azabicyclo[4.1.0]hept-4-enes. Increasing the temperature gave a shorter reaction time and increased enantioselectivity.

As a follow-up to this initial work, the substrate scope was broadened and included additional nitrogen-tethered enynes.[91] Disappointingly, the yields of these were generally poor, with a mixture of enantioselectivities observed (Scheme 33).

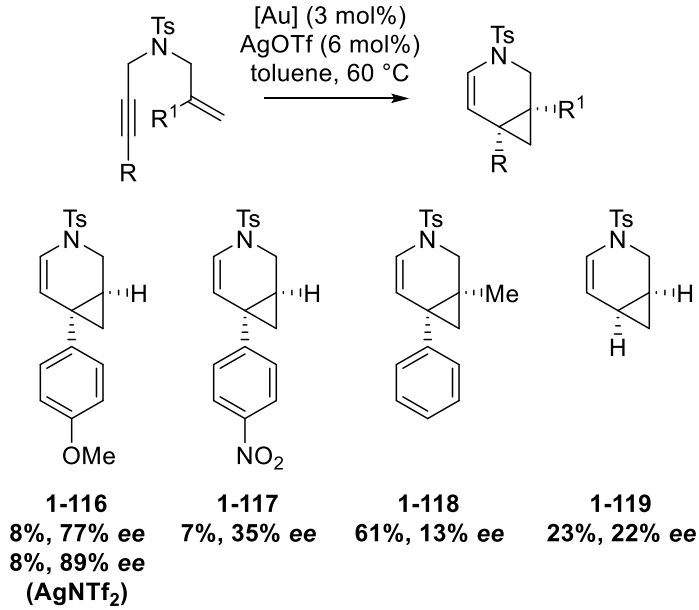

Scheme 33. Results of Michelet's follow-up work with nitrogen-tethered enynes.

It is interesting that in these systems, the cyclopropyl carbon is not substituted with a phenyl group, as with the oxygen-tethered species which may be a reason for the reduction in *ee* values. Therefore, this is not a direct comparison and may have influenced the outcome.

Another significant advancement in this field was made by the Fürstner group at the same time as the work reported by Michelet.[92] In this instance, the ligands used were significantly different and were based on (4*R*,5*R*)-2,2-dimethyl-*α*,*α*,*α*′,*α*′-tetraphenyldioxolane-4,5-dimethanol (TADDOL) scaffolds, as shown below in Figure 48. In the crystal structure of the catalyst, it can be seen that surrounding the gold atom is a chiral cavity which is extended beyond the metal centre by the naphthyl groups, favouring chiral induction.

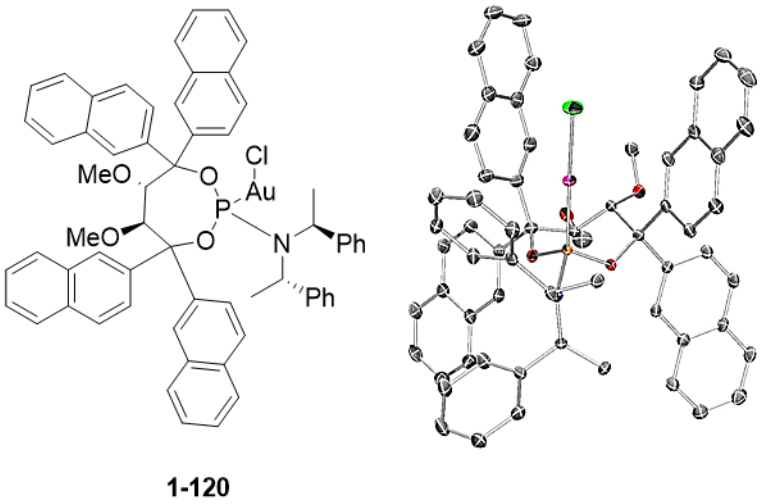

1-120

Figure 48. Structure of the TADDOL-related catalyst **1-120** used by Fürstner in the asymmetric cycloisomerisation of enynes. Also shown is the crystal structure of the catalyst, emphasising the size of the chiral cavity which is extended beynd the gold atom (in green). X-ray structure reprinted with permission from H. Teller, M. Corbet, L. Mantilli, G. Gopakumar, R. Goddard, W. Thiel and A. Fürstner, *J. Am. Chem. Soc*., 2012, **134**, 15331-15342. Copyright 2021 American Chemical Society.

Application of **1-120** to nitrogen-tethered enynes with various protecting groups gave the desired cycloisomerisation products in high yields and excellent enantioselectivities. In this instance, it was found that while the protecting groups did not appear to affect the outcome, it was necessary for an aromatic group to be present on the alkyne of the starting material to enable good enantioselectivity. Evidence for this was given when replacement of a phenyl group with a methyl (**1-120** *vs* **1-126**) resulted in a drop of enantioselectivity from 98% *ee* to 38% *ee* with the yield remaining constant. Scheme 34 below summarises the results reported. Oxygen-tethered enynes were also explored; however, these were highly functionalised with phenyl groups alpha to the tether in order to achieve useable yields and enantioselectivities.

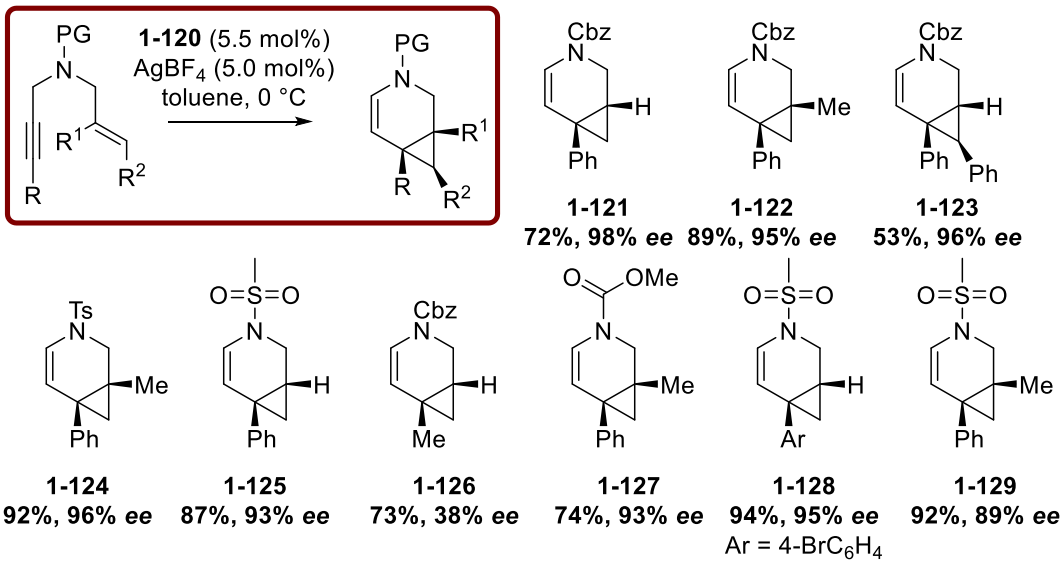

Scheme 34. Application of Fürstner's catalyst **1-120** to the cycloisomerisation of nitrogen-tethered enynes.[92]

Fürstner's conditions were then applied to a cycloisomerisation approach in the synthesis of GSK1360707, developed for the treatment of major depressive disorder (Scheme 35A).[92-94]

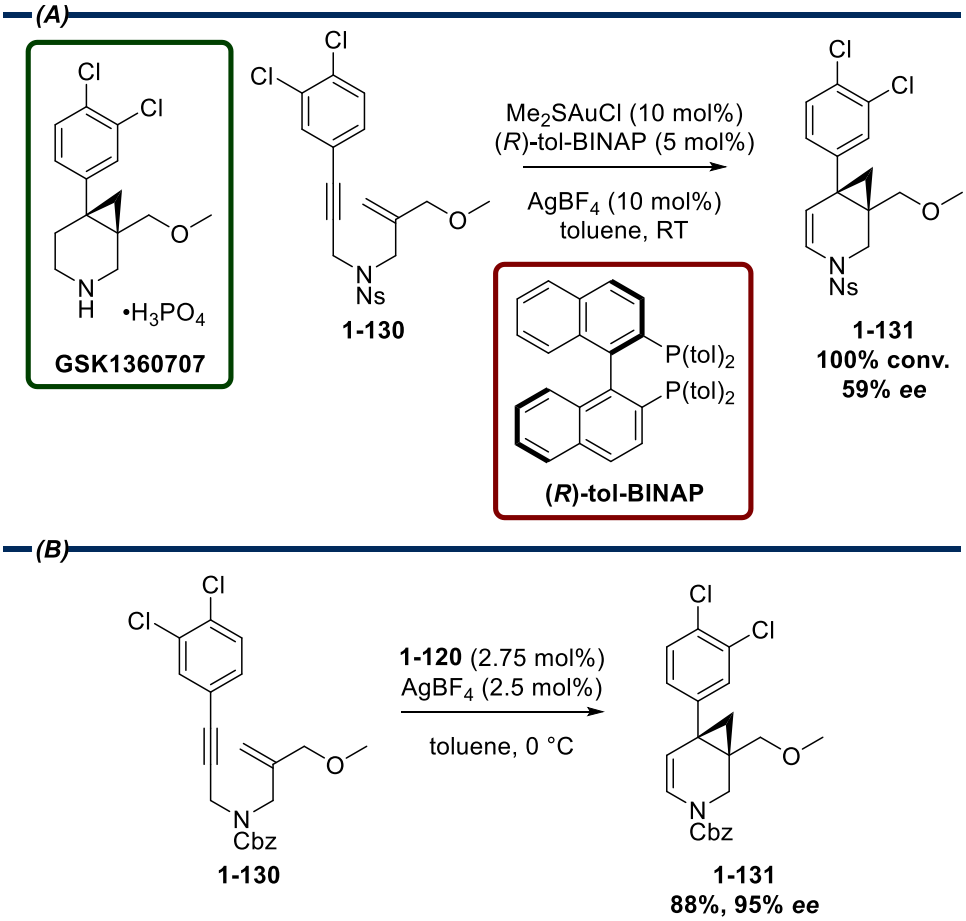

Scheme 35. (**A**) Original cycloisomerisation conditions reported for the synthesis of GSK1360707.[94] (**B**) Improved conditions in the cycloisomerisation step using catalyst **1-120**.[92,93]

Following the disclosure of a large-scale synthesis of this compound, it was found that the application of a cycloisomerisation would be beneficial to the manufacturing process for this molecule.[94] As such, a large reaction screen was undertaken, leading to the conditions shown in Scheme 35A. The use of chloro(dimethylsulfide)gold(I) chloride in combination with (*R*)-tol-BINAP ligand and silver trifluoroborate gave the desired compound with 100% conversion and an *ee* of 59%.[94] Fürstner was able to improve upon this by introducing catalyst **1-120** alongside silver trifluoroborate at 0 °C (Scheme 35B). Furthermore, having observed a limited effect upon changing the nitrogen protecting group, the 2-nitrobenzenesulfonyl (nosyl, Ns) used in the original approach, could be replaced by a carboxybenzyl (Cbz) group.[92,93] This replacement was beneficial to the downstream chemistry required to obtain the final compound. The outcome of these changes to the cycloisomerisation step meant that the 3-azabicyclo[4.1.0]hept-4-ene product **1-131** was obtained in a yield of 88% with an excellent *ee* of 95%.[92,93]

The introduction of novel ligands to the gold-catalysed cycloisomerisation to form bicyclo[4.1.0]hept-4-enes has been somewhat limited since these publications. An interesting approach was reported by Marinetti with the use of helicenes (Scheme 36A) as ligands for the transformation; however, this work was a proof-of-concept with only two substrates presented.[95,96] Despite this, *ee* values of up to 89% were observed with good to excellent yields for some of the helicene derivatives used. Similarly, Barbazanges reported on the use of a HELIXOL ligand in the cycloisomerisation reaction (Scheme 36B).[97] Applying the principle of using a helical structure to induce chirality, this report was able to broaden the substrate scope somewhat; however, the *ee* values reported were poor and a value of 11% was the best result obtained with the reaction cooled to -25 °C.

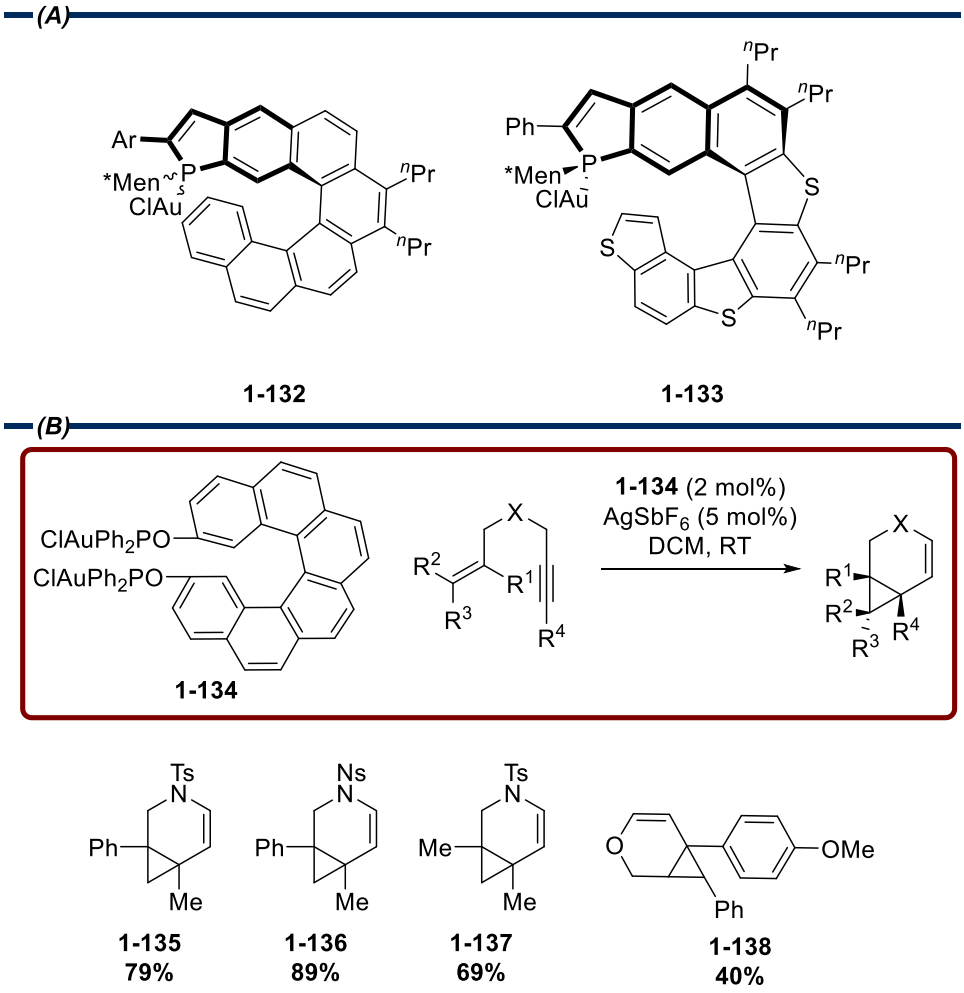

Scheme 36. (**A**) The structures of helicene ligands reported by Marinetti.[95,96] *Men = menthol. (**B**) The structure of HELIXOL ligand **1-134** and its use in cycloisomerisation reactions.[97] The substrate scope and yields are shown - *ee* values were obtained for **1-135** with enantiopure catalyst **1-134** with a maximum value of 11% (at -25 °C).

Clearly, more work would be required for these systems to become useful and expand the limited substrate scope. Furthermore, the requirement for complex syntheses and separation of enantiomers presents a large barrier towards general use.[95-97]

Other examples of unique catalytic systems have been reported, again with limited substrate scope. The two catalysts, bis-phosphine allene **1-139**[98] and phosphoramidite **1-140**,[99] are shown in Scheme 37. These systems are further examples in which the catalyst requires a bespoke synthesis and the separation of different isomers or enantiomers. As a result, the implementation of these systems may be of limited use but are nonetheless interesting examples, highlighting the ongoing development in this field.

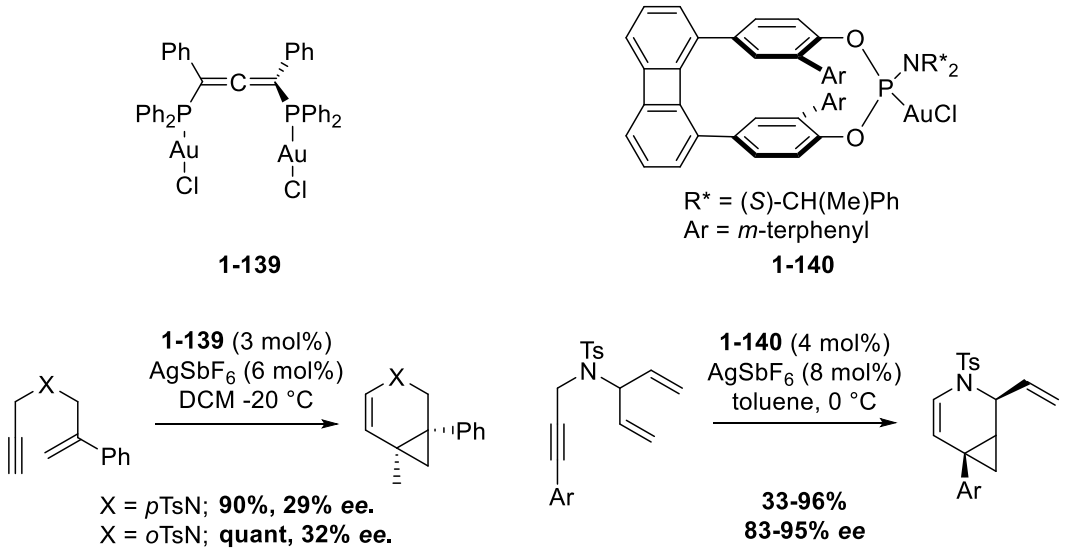

Scheme 37. Novel gold catalysts **1-139**[98] and **1-140**[99] and the corresponding reactions in the enantioselective gold-catalysed cycloisomerisation of 1,6-enynes.

An exploration of atropisomeric (diphosphine)Au_2Cl_2 catalysts (Figure 49) was undertaken by Hii wherein the properties of the ligands were analysed, alongside the outcome of the reaction.[100] These included the distance between the two gold atoms, the Au-Cl bond length, and the torsional angle between aryl rings, as measured from the available crystal structures. It was found that, in general, both the torsional angle and distance between gold atoms were affected by the size and electron-donating ability of the groups on the phosphorous atoms. Increasing the electron-donating ability of the groups on the phosphorous atom resulted in a larger distance, while the BINAP series of ligands remained rigid despite the variation of the phosphorous groups, likely due to the large barrier to rotation.

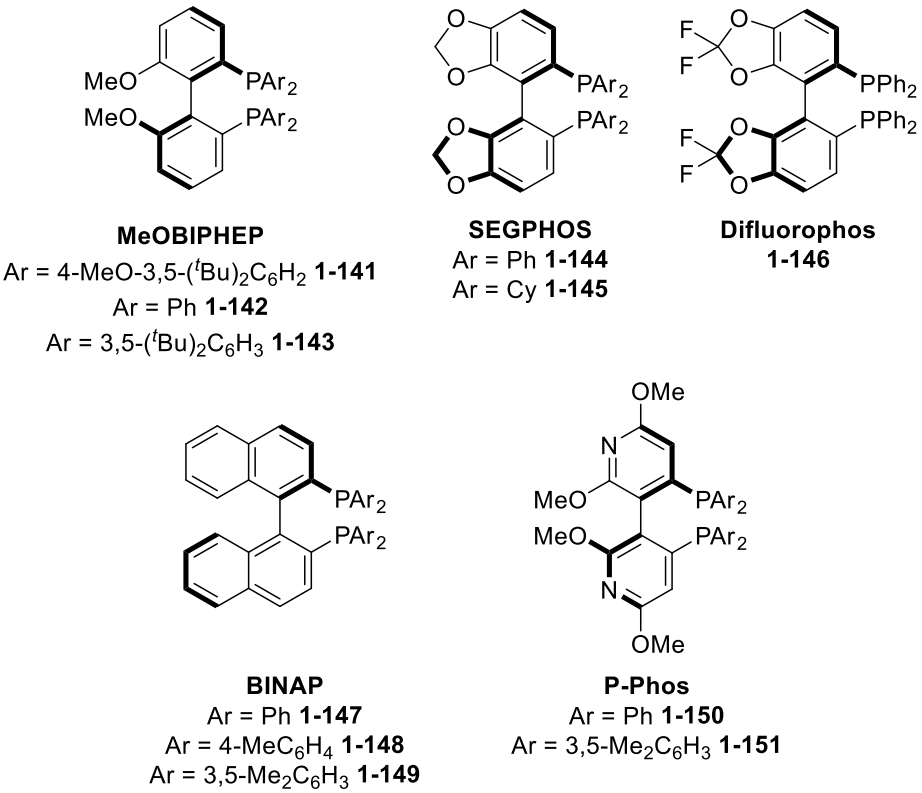

Figure 49. Gold catalysts investigated by Hii *et al.*[100]

After analysis of the catalyst properties, a cycloisomerisation reaction was performed to evaluate the effect of these on the outcome, with the initial reaction analogous to that reported by Michelet.[90,91] It is noteworthy that the yield appears to be directly affected by the silver salt used, while enantioselectivity was generally maintained. The results of these experiments are shown below in Table 12, entries 1-3**.** Some of the catalysts analysed were used in this reaction and gave comparable yields; however, the enantioselectivities could not match that obtained with the MeOBIPHEP ligand **1-141**. The BINAP derivatives **1-147** and **1-148** were introduced as they had similar distances between the Au atoms as in MeOBIPHEP. BINAP **1-148** gave a higher *ee* value of 75%, justified by the addition of electron-donating methyl groups. Additionally, P-Phos catalysts **1-150** and **1-151** were evaluated as they were measured to have a similar torsional angle to **1-141**. Catalyst **1-151** with electron-rich groups on the phosphorous atom gave an improved enantioselectivity, as expected. These results are also shown in Table 12

Table 12. Comparison of results obtained for the cycloisomerisation reaction of **1-141**.

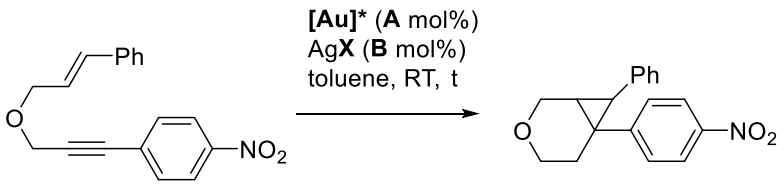

1-152 **1-153**

Entry	[Au]*	A	B	X	*t* (h)	Yield (%)	*ee*[a] (%)	Ref.
1	**1-141**	3	6	OTf	15	32	96 (−)	90,91
2	**1-141**	3	6	NTf_2	15	63	98 (−)	91
3	**1-141**	5	10	BF_4	24	87	99 (+)	100
4	**1-147**	5	10	BF_4	24	70	46 (−)	100
5	**1-148**	5	10	BF_4	24	85	75 (−)	100
6	**1-150**	5	10	BF_4	24	96	38 (−)	100
7	**1-151**	5	10	BF_4	24	92	60 (−)	100

[a]The optical rotation values of the products are given in the relevant publications; however, the specific enantiomer corresponding to these values remains ambiguous.

This study was the first to analyse the properties of the gold catalysts used in enyne cycloisomerisation reactions for bicyclo[4.1.0]hept-4-ene formation. The authors were able to define parameters for improved enantioselectivity with electron-donating groups on the phosphorous atoms providing a boost in *ee* values. In addition, a small number of substrates were synthesised using catalyst **1-151** and are shown in Figure 50.[100]

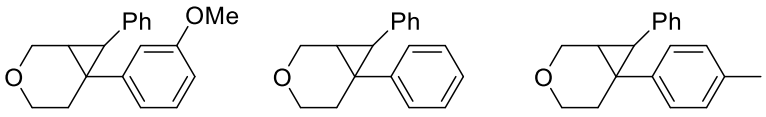

1-154 **1-155** **1-156**
86%, 66% *ee* **76%, 78% *ee*** **54%, 72% *ee***

Figure 50. Substrates synthesised in the reaction conditions shown in Table 12 using catalyst **1-151**.

Finally, Hii showed that activation of both gold centres with 2 molar equivalents of silver salt led to an improved yield in comparison to an Au/Ag ratio of 2:1.[100] It is proposed that each gold centre acts as its own catalytic moiety; however, little evidence was given to prove this. Nevertheless, this observation is useful for future work.

The most recent endeavour in this field comes from Echavarren wherein a catalyst was designed with a remote C_2-2,5-diarylpyrrolidine to create a chiral cavity.[101] By using an aromatic group on the alkyne of the enyne starting material, enantioselectivity can be induced in the cycloisomerisation. The focus of this report was not primarily aimed at the synthesis

of bicyclo[4.1.0]hept-4-ene and, therefore, only a limited number of examples are given (Scheme 38). Both the yields and *ee* values were high enough to highlight the efficacy of this system and prove the authors' hypothesis.

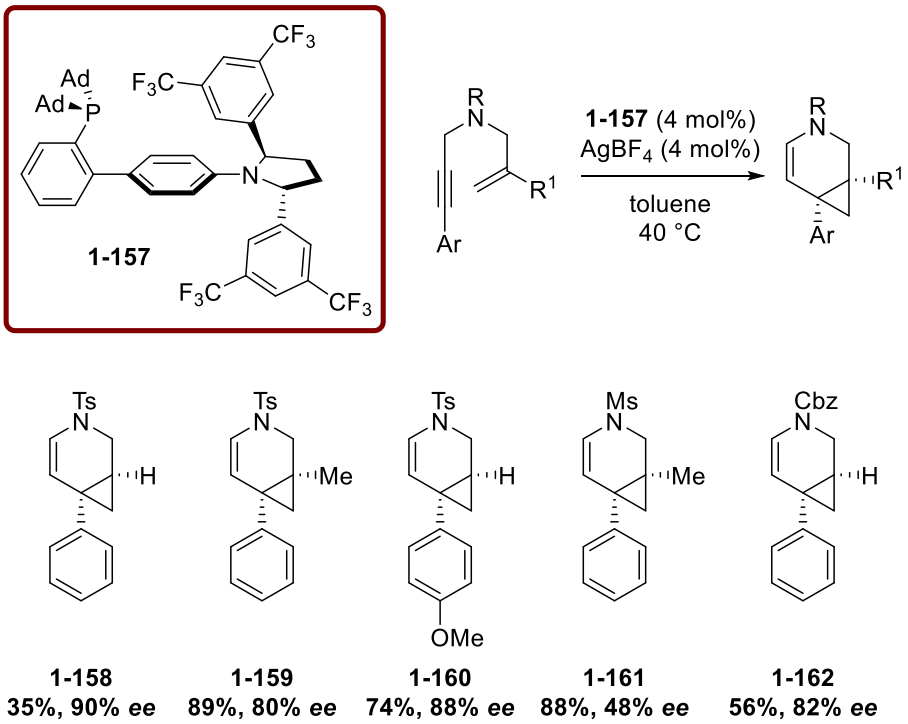

Scheme 38. 1,6-enyne cycloisomerisation using Echavarren's catalyst **1-157** to form 3-azabicyclo[4.1.0]hept-4-enes.

With all of the reports highlighted, it is clear that this area of chemistry is still evolving and at the time of writing, not fully understood. The nature of asymmetric induction in the enantioselective 1,6-enyne cycloisomerisation reaction has not been fully elucidated;[101] however, computational studies have helped to deconvolute the process.[92]

Despite the array of catalytic systems, some common features of the substrates can be found. In general, large aromatic groups are required around the cyclopropyl ring formed in the reaction to aid both the yield and enantioselectivity outcomes. In particular, it appears imperative to substitute the alkyne of the starting 1,6-enyne with an aromatic group. Furthermore, there are no examples with heteroaromatic systems which may be assumed to be due to a lack of activity in this process.

7.3.4. Application of Gold-Catalysed Cycloisomerisation to the Synthesis of a Desirable Intermediate

Literature reports highlight the efficacy of gold catalysis in the enantioselective cycloisomerisation of 1,6-enynes. To this end, it was anticipated that this may be applicable to the synthesis of an intermediate for use as a tool to install the CPP moiety of interest to the

current study. While almost all of the reported products of this reaction contain aromatic substitution at the 6-position (*vide supra*), it was anticipated that a readily functionalised group could be placed here.

Examination of previously synthesised bicyclo[4.1.0]hept-4-enes found that the Yu group had synthesised a number of compounds with a vinyl group at the 6-position (**1-164**, Scheme 39).[102] These compounds were subsequently subjected to a rhodium-catalysed [5+1] cycloaddition to yield tetrahydroisoquinolinones **1-165** as shown in Scheme 39.

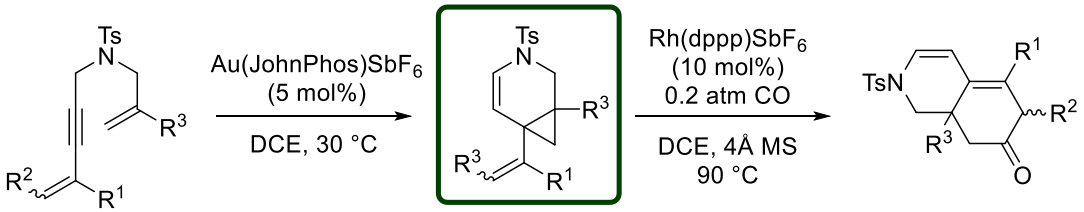

1-163 42-97%

1-164 42-97%

1-165 26-84%

Scheme 39. Synthesis of tetrahydroisoquinolinones via 3-azabicyclo[4.1.0]hept-4-enes.[102]

The isolation and use of the vinylic 3-azabicyclo[4.1.0]hept-4-enes **1-164** was promising and showed that these moieties could be readily accessed. Disappointingly, this approach did not focus on an enantioselective synthesis, instead using the achiral Au(JohnPhos)SbF_6 catalyst developed by Echavarren.[103] This can be made *in situ* from Au(JohnPhos)Cl or purchased as an acetonitrile-stabilised complex, both of which are shown below in Figure 51 and gave comparable results in the cycloisomerisation optimisation studies.[102]

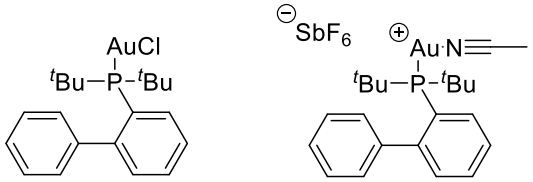

Au(JohnPhos)Cl **MeCNAu(JohnPhos)SbF_6**

Figure 51. the structure of gold catalysts containing the JohnPhos ligand, developed by Echavarren.[103]

Given the expected utility of the vinyl group for downstream transformation, the current study therefore aimed to develop methodology enabling access to vinylic 3-azabicyclo[4.1.0]hept-4-enes with an enantioselective gold catalyst. In doing so, it would be possible to determine if a non-aryl group on the alkyne of the 1,6-enyne could induce enantioselectivity under optimised conditions. This would be a significant addition to the literature with few examples of enynes containing small alkyl groups, all with poor *ee* values.[91,92]

8. Aims

As intimated above, the aim of this project was to enable the synthesis of an enantiopure or enantioenriched intermediate, which would allow facile installation of the CPP moiety in a modular fashion. This would predominantly be required for heteroaromatic systems in which the CPP has been shown to exhibit bioisosterism (*vide supra*).[2,3] To facilitate this, the initial focus was on the optimisation of a gold-catalysed cycloisomerisation step. As shown in Scheme 40, the introduction of a chiral catalyst to nitrogen-tethered enyne **1-166** was to be investigated, with the aim of synthesising a 3-azabicyclo[4.1.0]hept-4-ene. Upon reduction of the enamine double bond, the 3-azabicyclo[4.1.0]heptane (cyclopropylpiperidine, CPPip) moiety would be expected to be a bioisostere for a piperazine ring. This hypothesis is based on the analogous manner in which the oxygen-tethered CPP derivative is able to replicate the behaviour of a morpholine ring with some six-membered heteroaromatic systems. As such, this molecule would be of use in medicinal chemistry, providing a further addition to the CPP-family of bioisosteres. In addition, the presence of a chromophore on the nitrogen protecting group would provide an opportunity to follow the reactions and any by-product formation by LCMS and TLC more readily than for an oxygen-tethered derivative. Reported instabilities for oxygen-tethered products may also lead to unnecessary complications in the initial optimisation studies.[100]

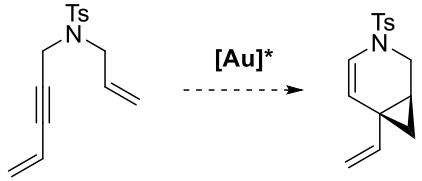

1-166 **1-167**

Scheme 40. Proposed enantioselective gold-catalysed cycloisomerisation of 1,6-enyne **1-166** to give the desired 3-azabicyclo[4.1.0]hept-4-ene **1-167**.

After the initial optimisation of the enantioselective step, a route towards a useful intermediate, such as an organoboron species or halide **1-170** was planned (Scheme 41). Selective reduction of the double bond in the ring was expected to provide the CPPip scaffold **1-168**. From here, functionalisation of the vinyl group could be undertaken, and it was envisaged that oxidative cleavage would lead to an aldehyde and, subsequently, a carboxylic acid **1-169**. The acid was viewed to be a key intermediate as it would allow several subsequent methods to be explored. The use of redox-active esters (RAEs), Barton esters, or the construction of heteroaromatic rings were all approaches which could be implemented to obtain a useful intermediate. Ultimately, the use of this intermediate to install an enantioenriched CPPip group was the desired conclusion. As such, exploration of the use of these intermediates would also be undertaken.

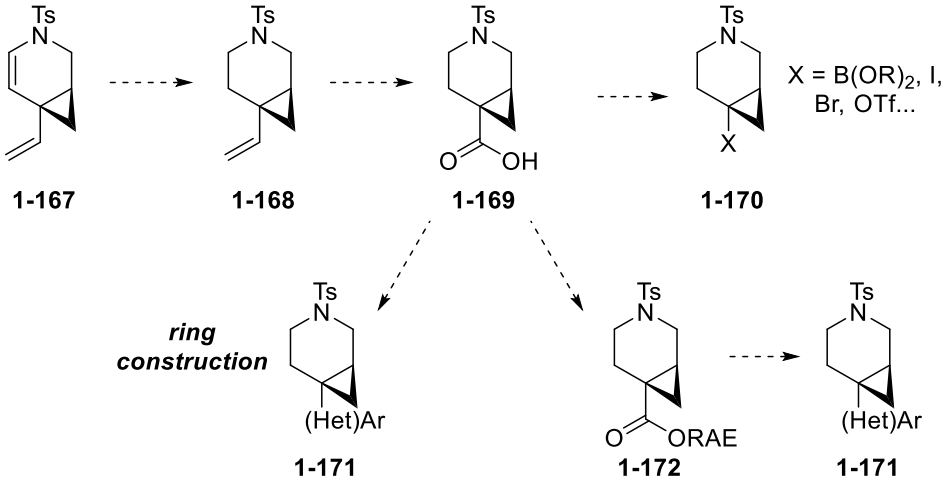

Scheme 41. Planned use of enantioenriched intermediate **1-167** in the synthesis of a useful intermediate of the structure **1-170** or direct use of the acid to access the desired compounds **1-171**.

Finally, an attempt to expedite the synthesis of the desired intermediates was planned to determine if functionalisation of the alkyne on the enyne starting material would allow cycloisomerisation with the desired group pre-installed (Scheme 42). No reports suggesting any attempts at such an approach have been disclosed. Accordingly, this strategy data would also be a valuable addition to current state-of-the-art in the preparation of the bicyclo[4.1.0]heptane template.

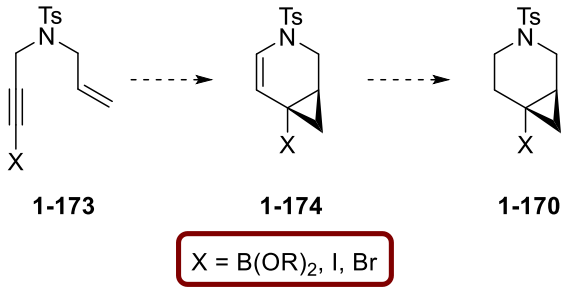

Scheme 42. Cycloisomerisation of 1,6-enyne with desired functionality installed onto starting material.

9. Results and Discussion

9.1. Exploration of Literature Precedent

Confirmation of the result reported in the literature (Scheme 43) was necessary;[102] however, the use of dichloroethane (DCE) was not a viable solvent for further studies. The associated toxicity and carcinogenicity of DCE required alternative solvents to be considered, especially as European law classes this as a substance of very high concern.[104]

Scheme 43. Reported literature transformation for the formation of 3-tosyl-6-vinyl-3-azabicyclo[4.1.0]hept-4-ene **1-166** with an achiral catalyst.[101]

Analysis of the optimisation studies carried out by Yu showed that the desired transformation was possible in both THF and DCM; albeit with a catalyst loading of 10 mol% and slightly diminished yields of 56% and 43%, respectively.[102] THF was initially chosen as the solvent for the cycloisomerisation reaction due to the higher reported yield. 1,6-Enyne **1-166** was synthesised in three steps from propargylamine following the sequence shown in Scheme 44.

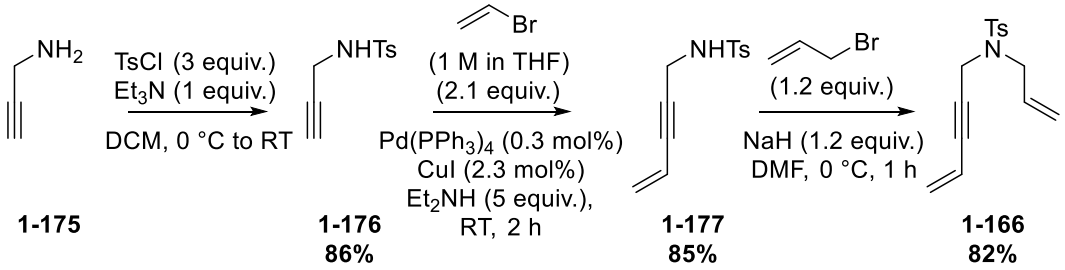

Scheme 44. Synthetic sequence to 1,6-enyne **1-166**.

1,6-Enyne **1-166** was subjected to the cycloisomerisation conditions, giving a comparable result to that reported by Yu (Scheme 45).[102] Following this, studies into the replacement of the vinyl group with a halide or boron-containing species were initiated to determine if an expedited approach would be viable.

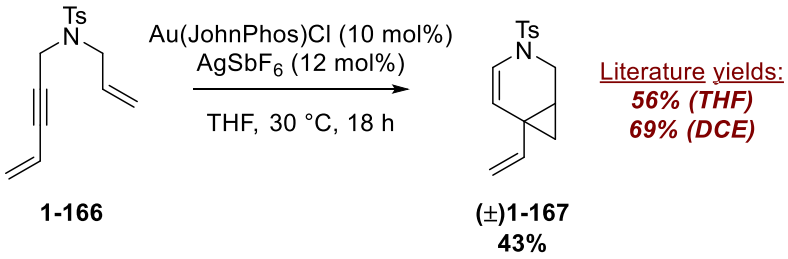

Scheme 45. Repeat of gold-catalysed cycloisomerisation of 1,6-enyne **1-166** in THF and comparison of the resulting yield to those reported in the literature.

9.2. Installation of a Cross-Coupling Handle to the 1,6-Enyne

As shown in Scheme 42 (*vide supra*) installation of the chosen functionality before the cycloisomerisation would be desirable, reducing the number of synthetic steps to the desired intermediate. Functionalisation of the terminal alkyne moiety of the 1,6-enyne with a boronic acid or ester, an iodide or a bromide would enable examination of this approach.

Bromide and iodide analogues were obtained using established reactions of the terminal alkyne moiety, highlighted in Scheme 46.[105,106] The two halides were installed at different stages, with the iodide installed pre-alkylation and the bromide post-alkylation. Bromide **1-179** was obtained in 74% yield from enyne **1-178** using a silver nitrate/NBS system wherein a silver acetylide is likely formed, before electrophilic bromination occurs.[107] Iodinated enyne **1-181** was accessed *via* initial iodination of tosyl-protected compound **1-176**. Use of KOH and iodine gave the desired iodinated alkyne **1-180** in a yield of 69% before alkylation with allyl bromide produced iodinated enyne **1-181**, which was used in crude form due to purification difficulties reported in the literature.[105] Several attempts were made to synthesise an enyne with a boronic acid or ester substituted on the alkyne moiety; however, this approach was unsuccessful with boronated products appearing to be unstable.

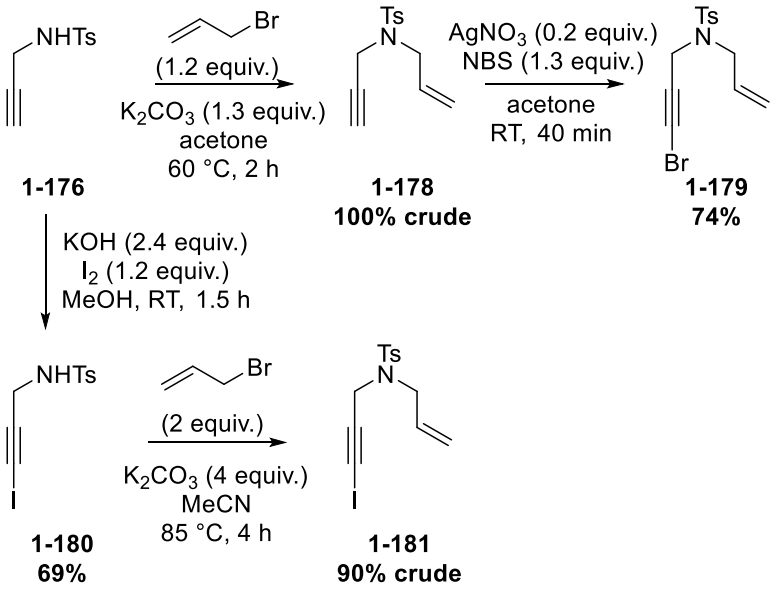

Scheme 46. Synthesis of bromo- and iodo-substituted enynes **1-179** and **1-181**.

Both halogenated enynes, **1-179** and **1-180**, were submitted to Yu's gold-catalysed cycloisomerisation conditions (Scheme 47); however, no cycloisomerisation products were observed for either substrate and spectroscopic analysis of the reactions indicated that decomposition had occurred.

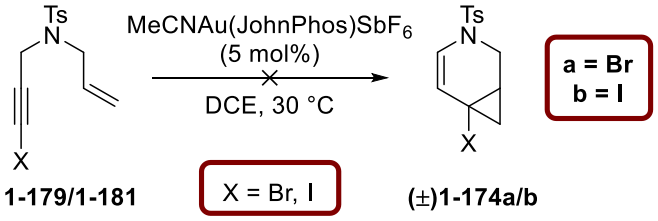

Scheme 47. Attempted gold-catalysed cycloisomerisation of halogenated enynes **1-179** and **1-181**.

These results were disappointing; however, the findings in Scheme 47 highlighted the requirement for the vinyl group in order to undergo cycloisomerisation under these conditions. Therefore, subsequent studies focused on the optimisation of an enantioselective gold-catalysed cycloisomerisation of enyne **1-166**, as shown in Scheme 40 (*vide supra*).

9.3. Investigation into Asymmetric Catalysis

9.3.1. Exploration of Ligands

The choice of ligand was carefully considered for this work and one of the key aspects was the commercial availability. With the aim of making this chemistry accessible to enable wider implementation of the CPP and CPPip, the bespoke synthesis of a chiral ligand was undesirable. Therefore, the JosiPhos family of ligands, of which the general structure is given below in Figure 52, were examined. While not specifically utilised for cycloisomerisation reactions of nitrogen-tethered 1,6-enynes, it was found that these phosphines were amenable

to ligation with gold and had been shown to induce moderate enantioselectivity.[108,109] Furthermore, several commercial analogues were available, allowing investigation of the effects of the R and R' groups on the yield and enantioselectivity.

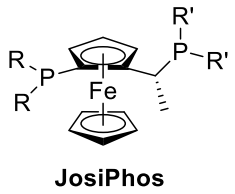

JosiPhos

Figure 52. The general structure of a JosiPhos ligand.

Several of these ligands were available within our laboratory, allowing an expedient evaluation of their effect on the cycloisomerisation reaction. To synthesise the catalysts, a simple preparation using chloro(dimethylsulfide)gold(I) chloride in DCM was used,[108] providing the desired compounds in yields of 86-100% (Scheme 48).

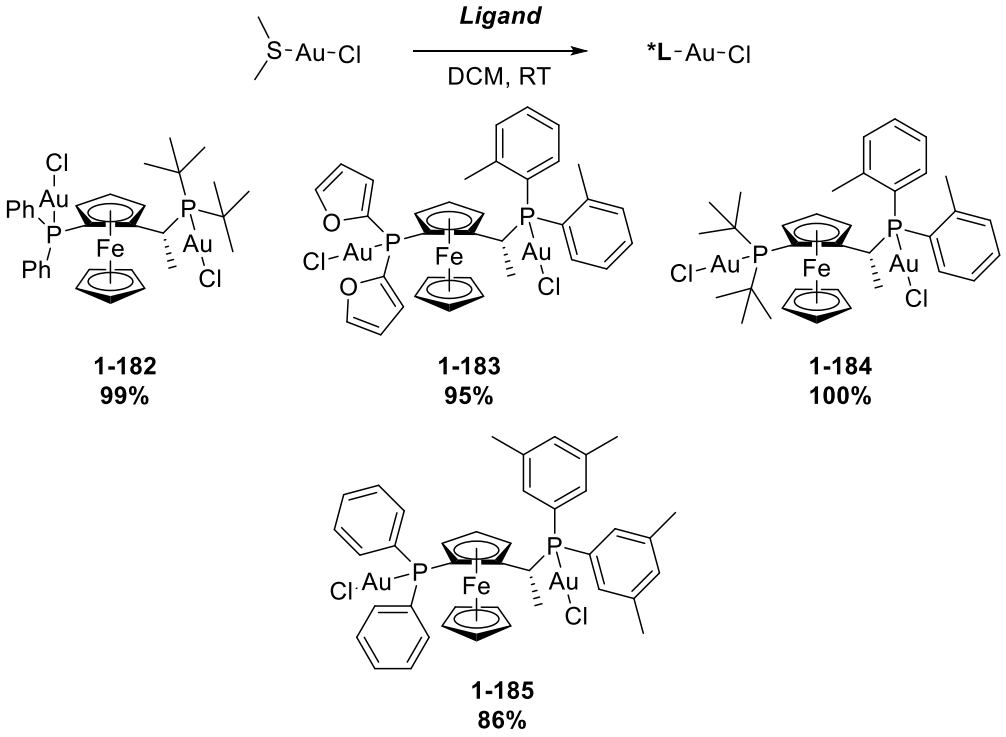

1-182
99%

1-183
95%

1-184
100%

1-185
86%

Scheme 48. Synthesis and structure of JosiPhos gold pre-catalysts for initial screening reactions.

Formation of the catalytically active gold cationic species was enabled by stirring the [L-Au-Cl] species with a slight excess of a silver salt (such as $AgSbF_6$) in the chosen solvent. This mixture was then left for the AgCl to precipitate from the solvent before the supernatant, containing the gold cation, was transferred to a separate vial containing 1,6-enyne **1-166.**

The initial cycloisomerisation of **1-166** using JosiPhos analogue **1-182** was carried out in both DCM and THF, as these gave very similar outcomes in the reported asymmetric reaction.[102] As shown below in Table 13, enantioselectivity was observed when using pre-

catalyst **1-182** in both solvents. Interestingly, the reaction in THF gave a lower yield but higher *ee* value, while DCM improved the yield but diminished the enantioselectivity. The *ee* value of 49.4% obtained in THF represented an excellent initial finding, with current literature predominantly focused on the reaction with large aromatic groups tethered to the alkyne. This *ee* value, corresponding to an approximate enantiomeric ratio of 3:1, was a highly promising result and provided evidence for the vinyl group being suitable for both stereoinduction and further functionalisation.

Despite these outcomes, it was noted that the relative conversion values did not correlate to the isolated yields, suggesting decomposition. It was unclear if this process was occurring during the reaction, upon concentration of the reaction mixture, or during the purification. Furthermore, starting material **1-166** or product **1-167** could be susceptible to decomposition; however, the enamine moiety of the product was suspected to be sensitive to the cationic catalyst upon concentration of the reaction mixture.

Table 13. Comparison of outcomes for the cycloisomerisation of 1,6-enyne **1-166** with pre-catalyst **1-182** in THF and DCM.

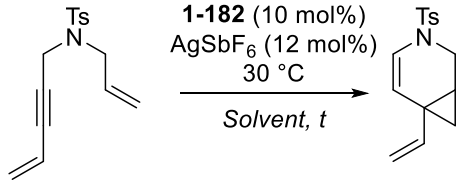

1-166 **1-167**

Entry	Solvent	*t* / hours	Relative Conversion / %	Yield / %	*ee* / %
1	THF	15	73	18	49.4
2	DCM	15.5	95	31	23.2

Reactions on 50-52 mg (0.182-0.189 mmol) scale of **1-166** .

Exploration of pre-catalysts **1-183**, **1-184** and **1-185** was undertaken in DCM in an attempt to maintain or improve the yield and increase the enantioselectivity. The results, summarised in Table 14, show that the initial pre-catalyst **1-182** gave the best overall outcome, despite pre-catalyst **1-184** displaying a comparable *ee* values. Both pre-catalysts **1-183** and **1-185** gave disappointing results with respect to conversions, yields and *ee* values. Furthermore, reaction monitoring by LCMS suggested by-product formation in the reactions with catalysts **1-183**, **1-184** and **1-185** which may have been due to decomposition or side-reactions of an unknown origin.

Table 14. Comparison of JosiPhos ligands in the cycloisomerisation reaction of 1,6-enyne **1-166**.

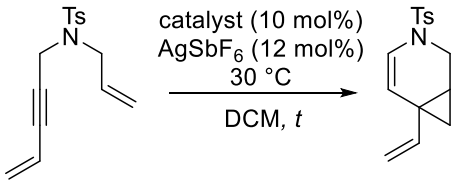

1-166 **1-167**

Entry	Catalyst	*t* / h	Relative Conversion / %	Yield / %	*ee* / %
1	**1-182**	15.5	95	31	23.2
2	**1-183**	16.5	69	9	4.2
3	**1-184**	18	94	25	24.8
4[a]	**1-185**	18	50	4	6.2

Reactions on 50-57 mg (0.182-0.207 mmol) scale of **1-166**.

While the mechanism for chiral induction is somewhat ambiguous and not fully elucidated, especially as these ligands have not been used to form azabicyclo[4.1.0]hept-4-enes, there exists some evidence as to the activation mode of the catalysts. Shown below in Figure 53 are crystal structures of **1-182** and a naphthyl analogue **1-186**, studied by Echavarren.[108] The two gold environments exist in an antiparallel arrangement, with no interaction between them.

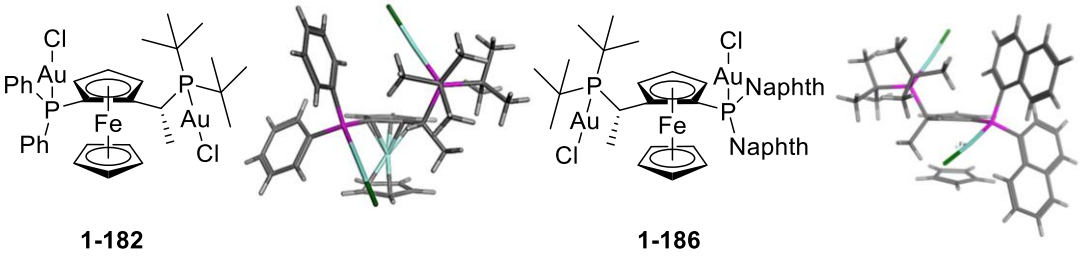

1-182 **1-186**

Figure 53. Structure of gold pre-catalysts **1-182** and **1-186** studied by Echavarren *et al*.[108] Crystal structures are available in the Cambridge Crystallographic Data Centre with the codes **1-182**: PEPZAO; **1-186**: PEPZUI.

Studies on the naphthyl analogue of this catalyst showed that, upon activation, it was the gold atom ligated to the trialkylphosphine moiety which formed the catalytically active cation, stabilised by a large π-cloud of electron density from the aromatic groups.[108] While the phenyl groups in pre-catalyst **1-182** have a reduced electron density in comparison to the naphthyl groups in **1-186**, this effect is likely to remain, albeit to a lesser extent. Furthermore, in the intramolecular [2+2] transformation in which the naphthyl analogue was found to be optimal, selectivity was thought to occur due to both steric and electronic effects from the aromatic groups.[108] Steric clashes between the substrate and the naphthyl groups, as well as π-stacking interactions, led to transition states with differing energies, thus giving selectivity. It was also found that pre-catalyst **1-186** improved both the yield and enantioselectivity in comparison to the opposite enantiomer of **1-182** used in the study.

Considering substrate **1-166**, the lack of an aromatic group on the alkyne may remove any potential π-stacking interactions with the catalyst, reducing the facial selectivity of attack from the alkene. Additionally, the reduced size of the vinyl group, compared to an aromatic substrate, and the phenyl group on the catalyst (relative to the naphthyl group) may have been factors in the moderate enantioselectivity observed. The combination of these effects, or lack thereof, may lead to a flexible transition state and reduced preference for one enantiomer. This would align with observations made by Fürstner in which a methyl group on the alkyne in the starting material produced lower enantioselectivities due to a lack of steric influence.[92] It is currently unclear if the same activation occurs for pre-catalysts such as **1-183** and **1-185** in which both phosphines contain aromatic groups; however, the lack of activity and enantioselectivity suggests that these JosiPhos systems may be unsuitable for the desired transformation.

The effectiveness of pre-catalyst **1-184** is also of interest given the similar results to pre-catalyst **1-182**. It is unclear if the gold atom on the phosphine containing the *tert*-butyl groups forms the cation, given that it is not the same environment to that in **1-182**. Despite the similar results, pre-catalyst **1-182** was chosen for further study due to the improved yield, as shown in Table 14.

9.3.2. Exploration of Solvent and Counterion

The difference in outcome of the reaction in THF and DCM led to the investigation of alternative solvents. Table 15, below, highlights those explored and the corresponding outcomes. Solvents commonly used in gold-catalysed transformations were tested, with aprotic solvents necessary in order to avoid the formation of by-products observed upon nucleophilic addition to cationic intermediates.[74,75,86]

Disappointingly, no improvement in yield over DCM or improved enantioselectivity over THF was found. The use of DMF appeared to cause co-elution of the starting material and product peaks, evidenced by the isolation of cycloisomerised product; however, further investigations to determine the conversion value were not warranted due to the inferior yield when compared to DCM. As a result of these studies, DCM remained the preferred solvent as the yield was deemed most appropriate for practical utility.

Table 15. Analysis of solvent effect on the gold-catalysed cycloisomerisation reaction of 1,6-enyne **1-166**.

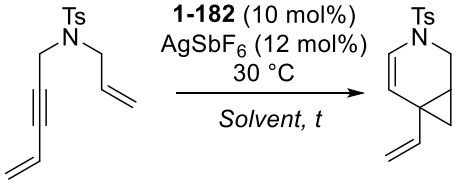

1-166 **1-167**

Entry	Solvent	*t* / h	Relative Conversion / %	Yield / %	*ee* / %
1	DCM	15.5	95	31	23.1
2	THF	15.5	73	18	49.4
3	MeCN	15.5	0	0	-[a]
4	2-MeTHF	21	7	8	-[a]
5	Toluene	21	0	2	-[a]
6	TBME	22	0	0	-[a]
7	DMF	22	0	33[b]	16.6

Reactions on 49-53 mg (0.178-0.203 mmol) scale of **1-166**. [a]Insufficient material to obtain *ee* value. [b]88% product purity due to an unknown impurity upon purification.

Variation of the counterion has been shown to be of high importance when optimising a gold-catalysed reaction and, as such, was investigated as part of the optimisation.[110] Table 16 summarises those implemented in the cycloisomerisation of **1-166** with pre-catalyst **1-182**.

Table 16. Analysis of counterion effect on the gold-catalysed cycloisomerisation reaction of 1,6-enyne **1-166**. The structure of the BArF counterion is also shown.

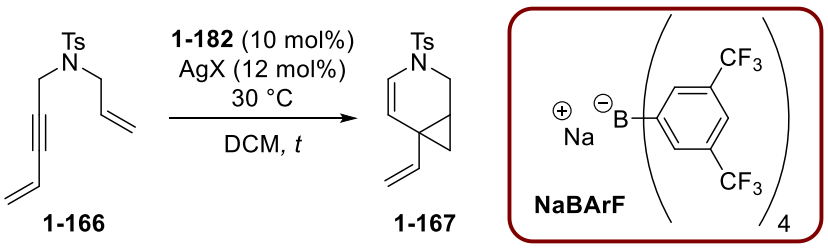

1-166 **1-167**

Entry	X	*t* / h	Relative Conversion / %	Yield / %	*ee* / %
1	SbF_6	15.5	95	31	23.1
2	BArF[a]	18	11	-[b]	-
3	PF_6	8	84	22	8.4
4	BF_4[c]	17	100	16	20.2
5	BF_4[d]	17	43	24	16.4

Reactions on 50-100 mg (0.182-0.363 mmol) scale of **1-166**. [a]NaBArF used. [b]Insufficient purity to obtain accurate yield. [c]0.2 equiv. of **1-182** and 0.3 equiv. of $AgBF_4$ added which may have given a misrepresentative conversion value and affected the isolated yield. [d]In THF.

Replacement of the counterion was not conducive to the reaction outcome, but did concur with reports that these reactions are sensitive to counterion variation.[94,110] Only the use of boron tetrafluoride (BF_4) gave compound **1-167** with a similar enantioselectivity to the hexafluoroantimonate (SbF_6) counterion. This reaction was repeated in THF to determine if the enantioselectivity would increase, as with the SbF_6 counterion (Table 13); however, the opposite effect was observed. The increased coordination of the BF_4 counterion to the catalyst, combined with coordinating THF, may reduce the activity of the catalyst, as reflected in the conversion value.

The data obtained in Table 14 and Table 16, further confirmed the discrepancy between the conversion and isolated yield, with this effect appearing to be inherent to the reaction. It was postulated that a combination of factors were responsible for this including an interaction between the catalyst and substrate or product causing decomposition, or the stability of the enamine product upon concentration and purification.

An initial investigation of the origin of the discrepancy led to the repetition of three different reactions on 100 mg scale with a normal phase purification. The larger scale allowed a more detailed analysis of where the discrepancy may have originated, and normal-phase purification explored the possibility of reverse-phase purification being detrimental to the stability of the enamine product. The results of these experiments are shown below in Table 17 with a significant discrepancy still apparent.

Table 17. Cycloisomerisation reactions on 100 mg scale of **1-166** with normal phase purification.

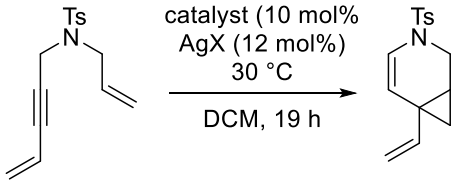

1-166 **1-167**

Entry	Catalyst	X	Relative Conversion / %	Yield / %
1	**1-182**	SbF_6	86	4
2	**1-185**	SbF_6	64	6
3	**1-182**	BF_4	100	13

Reactions on 99-103 mg (0.360-0.374 mmol) scale of **1-166** with normal phase purification.

Analysis of these reactions provided some evidence for the origin of the discrepancy; however, a single cause could not be definitively assigned. The reaction in Table 17, Entry 1 suggested that decomposition occurred upon concentration of the reaction mixture, with several by-products appearing in the NMR of the crude reaction mixture which could not be

accounted for during the reaction. Table 17, Entry 2 produced an analogous result to that on the small-scale, with by-products observed in both the reaction mixture and subsequent NMR of the concentrated crude mixture, suggesting that this catalyst caused decomposition during the reaction. It is unclear if this decomposition was exacerbated upon concentration of the reaction mixture; however, given the results from the reaction in Entry 1, this appeared likely. Finally, Table 17, Entry 3 provided some conflicting evidence with little evidence of by-product formation upon concentration of the reaction mixture. Despite this, the ratio of product peaks to those attributed to the JosiPhos system was relatively low, indicating that the loss of product may have occurred during the reaction or upon concentration.

The combination of this evidence, and the apparent instability of the product led to the conclusion that that this methodology was not amenable to further optimisation. No results of practical use were obtained, and an alternative process was investigated.

9.4. Introduction of the Nosyl Protecting Group

The poor results obtained with the tosyl protecting group presented the opportunity to explore alternatives. Yu had reported that replacement of the tosyl group with *tert*-butyloxycarbonbyl (Boc), benzyl (Bn) and nosyl (Ns) groups was unsuccessful in the cycloisomerisation reaction;[102] however, these transformations had been carried out in DCE and, as such, were repeated in DCM. The syntheses of the requisite enynes **1-189**, **1-192** and **1-195** are shown below in Scheme 49.

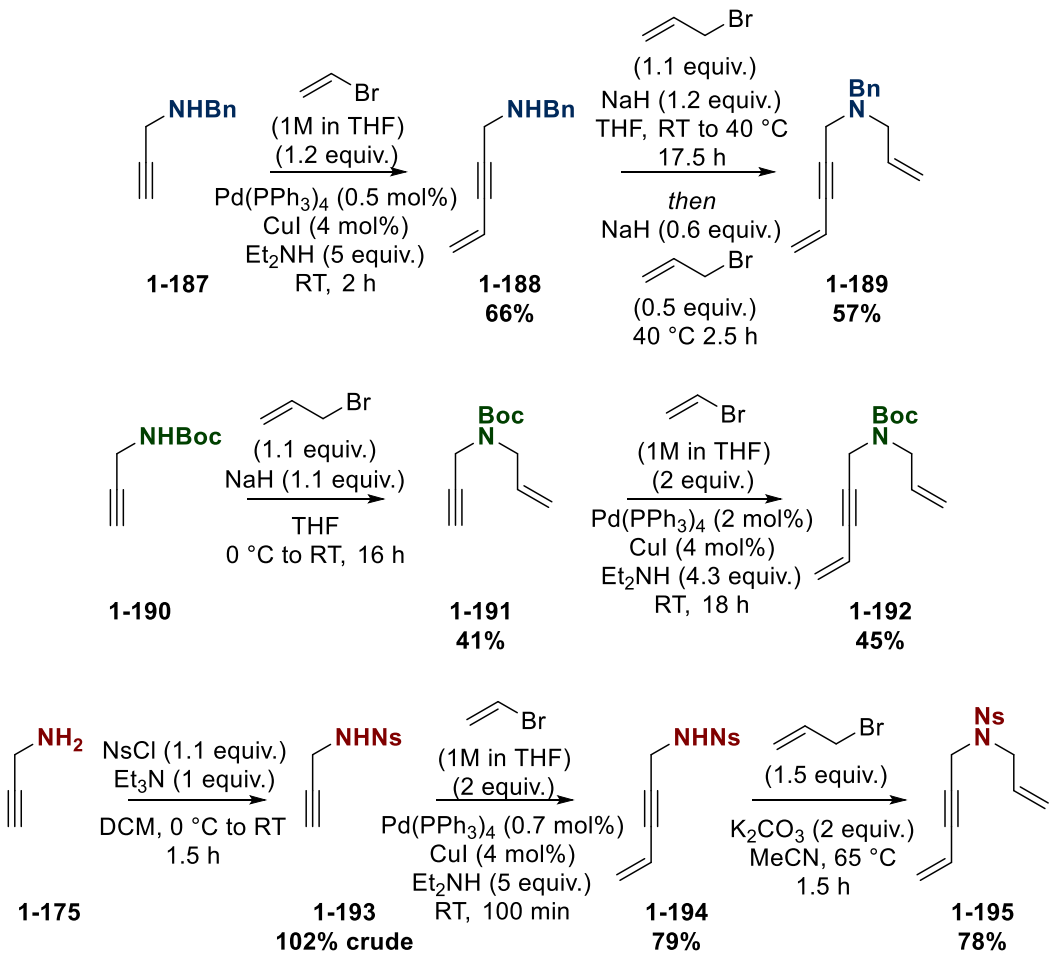

Scheme 49. Synthesis of enyne starting materials with various protecting groups.

Subjecting Bn- and Boc-protected enynes **1-189** and **1-192** to the cycloisomerisation conditions in DCM gave results in agreement with those reported by Yu.[102] No reaction was observed for Bn-protected enyne **1-189**, while Boc-protected enyne **1-192** gave full conversion to an oxazolidinone **1-197**, of which a small amount was isolated (Scheme 50).

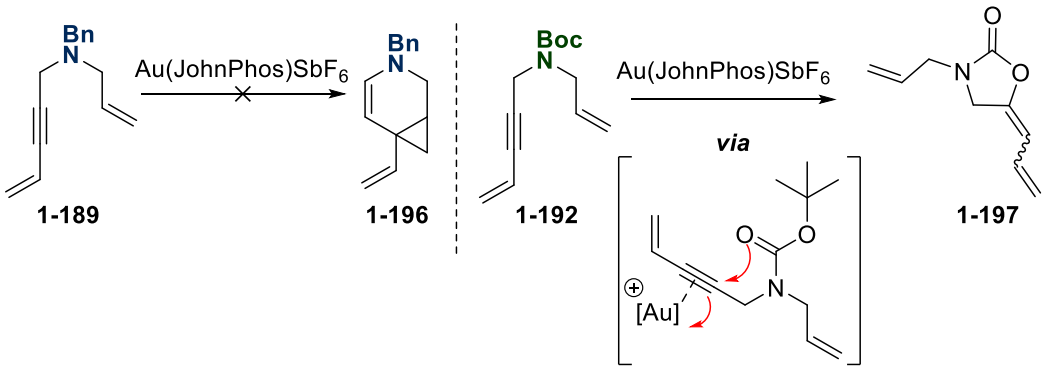

Scheme 50. Reactions attempted with Bn- and Boc-protected enynes **1-189** and **1-192**.

Nosyl-protected enyne **1-195** gave the desired product in 34% yield, contrary to the earlier literature report (Scheme 51), providing evidence that nosyl derivative **1-195** may be suitable for the enantioselective conditions. Furthermore, the nosyl protecting group provided the advantage of being more easily removed than the tosyl group. The reported synthesis of GSK1360707 corroborated this and showed that, while chemoselective removal of the tosyl group was difficult, replacement with a nosyl protecting group alleviated these issues.[94] In addition, the electron-deficient protecting group was anticipated to alter the electronics of the enamine-containing product **1-198** with the aim of sufficiently improving the stability.

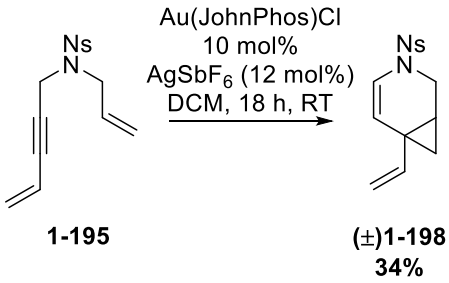

Scheme 51. Successful cycloisomerisation reaction of Ns-protected enyne **1-195** to give desired product **1-198** in 34% yield.

As with the tosyl-protected analogue **1-166**, nosyl-protected enyne **1-195** was subjected to the enantioselective reaction conditions in both DCM and THF. Disappointingly, these preliminary studies were not able to improve upon the initial results with the tosyl-protected analogue. Despite the improved enantioselectivity observed in DCM, the isolated yields of both reactions were poor. Furthermore, the initial conversion when using THF was 28% after 25 h and did not increase above 45%, even with heating which highlights the incompatibility of this solvent with substrate **1-195**. In addition, the previously discussed discrepancy between relative conversion and yield was still observed, providing some evidence that the nosyl protecting group was not able to alleviate this issue.

Table 18. Comparison of the cycloisomerisation of nosyl-protected enyne **1-195** to tosyl-protected analogue **1-166**.

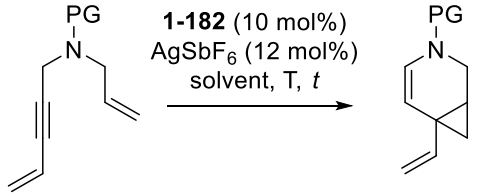

1-166 *or* **1-195** **1-167** *or* **1-198**

Entry	PG	Solvent	T	*t* / h	Relative Conversion / %	Yield / %	*ee* / %
1	Ns[a]	DCM	RT	19	99	7	28.0
2	Ns[a]	THF	RT	49[c]	45	8	35.4
3	Ts[b]	DCM	30 °C	15.5	95	31	23.2
4	Ts[b]	THF	30 °C	15	73	18	49.4

[b]Reactions on 53-56 mg (0.173-0.183 mmol) scale of **1-195**. [b]Reactions on 50-52 mg (0.182-0.189 mmol) scale of **1-166**. [c]25 h at RT then 24 h at 50 °C, 28% conversion observed after 25 h.

9.5. Implementation of the OTf Counterion

Having explored common optimisation parameters for this type of transformation, a thorough review of the literature was conducted to identify any areas which would merit further investigation. It was found that, while SbF_6 and BF_4 are the most common counterions used for the enantioselective cycloisomerisation of 1,6-enynes to bicyclo[4.1.0]hept-4-enes (*vide infra*, section 7.3.3), the seminal work reported by Michelet made use of a weakly-coordinating triflate (OTf) counterion.[90,91] This finding prompted an investigation into the effect of this counterion on the cycloisomerisation of nosyl-protected enyne **1-195**, particularly as this has been shown to affect the reaction outcome for other gold-catalysed transformations.[111] The results of these reactions are shown in Scheme 52, below.

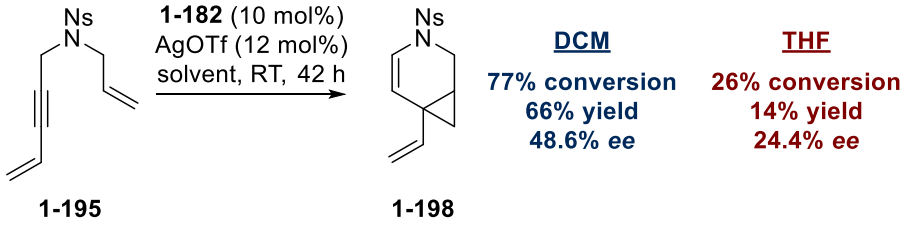

1-195 **1-198**

Scheme 52. 1,6-Enyne cycloisomerisation of **1-195** using the OTf counterion in both DCM and THF. Reactions on 53 mg (0.173 mmol) scale of **1-195**.

The outcome of these reactions was somewhat unexpected, showing substantial improvements in yields over those employing the SbF_6 counterion (Table 18) and producing results which would be of significant practical use for exploration of downstream chemistry. The improved correlation between conversion and yield also suggested that the OTf

counterion may coordinate to the catalyst to a larger extent than SbF_6,[112] reducing the activity sufficiently to prevent subsequent decomposition of the product. This catalytic system was also applied to the tosyl-protected analogue (Scheme 53), confirming that, under these conditions, the nosyl protecting group was superior.

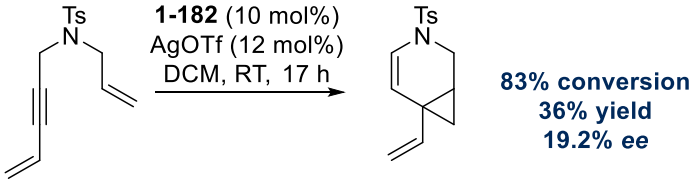

Scheme 53. Application of pre-catalyst **1-182** and AgOTf to tosyl-protected enyne **1-166**.

Use of the OTf counterion with pre-catalyst **1-182** improved the yield and enantioenrichment of product **1-198** in DCM. As a result, this method was expanded to include the other JosiPhos derivatives, initially investigated with the tosyl-protected analogue. The results of these reactions are given below in Table 19; however, no improvement over pre-catalyst **1-182** could be obtained.

Table 19. Investigation of JosiPhos pre-catalysts on the cycloisomerisation of nosyl-protected enyne **1-195**.

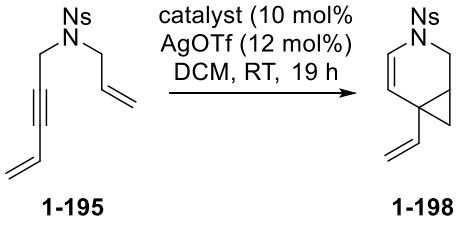

Entry	Catalyst	Relative Conversion / %	Yield / %	*ee* / %
1	**1-183**	70	16	44.8
2	**1-184**	87	19	25.8
3	**1-185**	42	29	17.6

Reactions on 59-104 mg (0.193-0.339 mmol) of **1-196**.

Pre-catalyst **1-182** and the OTf counterion gave a superior outcome and were optimal for this transformation; however, reproducibility of the initial result varied and further discrepancies between conversion and yield were observed once more, such as shown in Scheme 54.

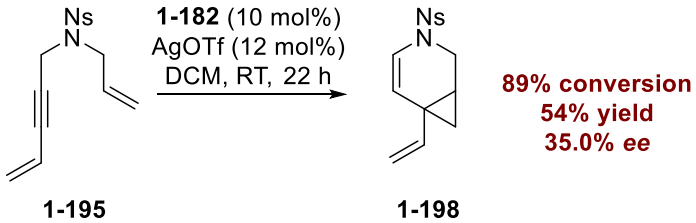

Scheme 54. 1,6-Enyne cycloisomerisation of **1-195** using OTf counterion on a 117 mg (0.382 mmol) scale with a work-up and normal-phase purification.

This disappointing result further highlighted the problematic isolation of enamine-containing product **1-198**. As a result, modifications were explored in order to remove the requirement for concentration of the reaction mixture and purification, which were thought to be detrimental to the yield. An *in situ* reduction of the potentially unstable enamine was reasoned to be an efficient way to overcome this and a preliminary investigation was carried out to determine suitability of reaction conditions.

9.6. *In Situ* Reduction of Cycloisomerised Product

Chemoselective reduction of the enamine was required given the presence of the vinyl and aromatic nitro groups. The reported synthesis of GSK1360707 made use of the nosyl protecting group and identified that an ionic reduction using TFA and Et_3SiH was highly effective for selective reduction of the carbon-carbon double bond of the enamine.[94] These conditions were implemented in the reduction of racemic **1-198** to give the desired saturated ring system (Scheme 55). As a result, subsequent studies on a one-pot cycloisomerisation-reduction process were undertaken.

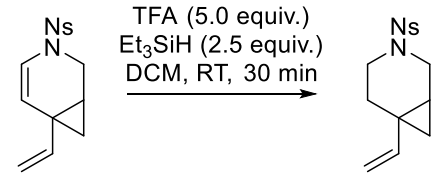

(±)1-198 **(±)1-199** **65%**

Scheme 55. Chemoselective reduction of racemic cycloisomerised product **1-198** to give the desired saturated ring

Use of the optimised conditions with pre-catalyst **1-182** and AgOTf facilitated the cycloisomerisation reaction, before the introduction of TFA and Et_3SiH to the reaction mixture (Scheme 56). The reaction was stirred for an additional 1.5 h to allow the reduction to take place; however, despite the formation of the desired product **1-199**, several issues were identified with this initial process. Firstly, a small amount of unreduced enamine **1-198** remained in the reaction mixture, making the purification of reduced compound **1-199** difficult. Secondly, by-product formation was visible upon introduction of TFA and Et_3SiH with the most significant of these co-eluting with desired product **1-199** during purification. The result of this was the isolation of a product of approximately 90% purity based on assessment of NMR and LCMS.

Despite these problems, the *ee* of the isolated product was measured to be 48.4%, showing that the *in situ* reduction did not affect the enantioselectivity of the reaction (Scheme 56). Therefore, identifying the source of the decomposition and enabling complete reduction of enamine **1-198** were expected to be beneficial to the outcome.

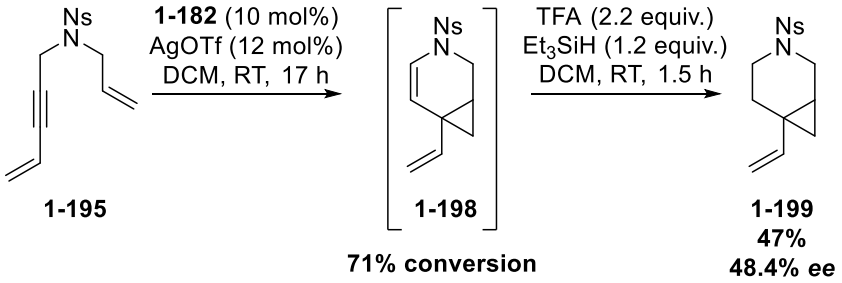

Scheme 56. Implementation of the *in situ* reduction of cycloisomerised product **1-198** to give reduced compound **1-199** which was obtained with a maximum purity of 93%.

9.6.1. Impact of TFA on the Reaction Outcome

Complete reduction of enamine intermediate **1-198** was necessary to improve the isolation of the reduced product **1-199**. In order to facilitate this, a repeat of the reaction shown, above, in Scheme 56 was investigated with a second aliquot of the reducing agents added. Complete reduction was observed; however, this was at the expense of the desired product, with the mixture containing only 72% of the desired product isolated (*vide infra*, Table 20). As shown below in Figure 54, exposure of the NMR sample of this mixture to a small amount of TFA at RT showed further decomposition of compound **1-199**.

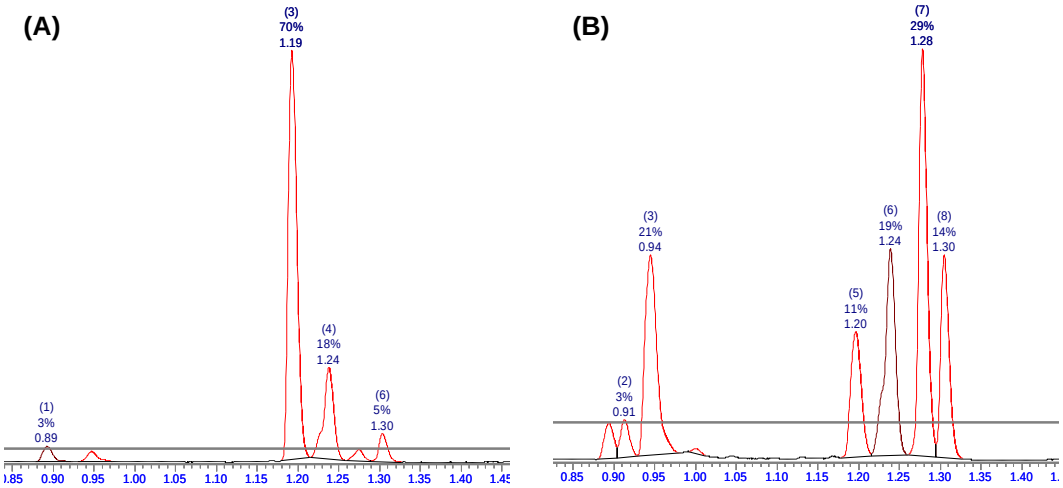

Figure 54. LCMS of mixture isolated containing reduced product **1-199**. (**A**) Isolated mixture before exposure to TFA (in $CDCl_3$). (**B**) After exposure with TFA (in $CDCl_3$). **1.19**/**1.20** min = desired product.

The presence of the by-product at 1.24 min in the LCMS was visible in both cycloisomerisation-reduction experiments and was the main impurity in the isolated material, formed upon introduction of the reducing agents. As such, this was isolated from a failed reaction on a larger scale and the structure confirmed elsewhere within our laboratories.[113] The structure is shown in Scheme 57; however, the mechanism of formation is currently unknown and may be due to the presence of a reactive gold species, formed upon the introduction of TFA and Et_3SiH. It may also be possible that the highly acidic conditions

facilitate the opening of the cyclopropyl ring. Furthermore, it is possible that diene **1-200** may go on to further react under the acidic conditions; however, the structures of other by-products could not be elucidated.

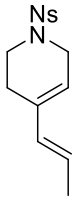

1-200

Scheme 57. The structure of by-product **1-200** at 1.24 min and a proposed mechanism of formation under acidic conditions.

Evidence of decomposition with excess TFA led to the implementation of an alternative protocol in which the reaction mixture was cooled to 0 °C before addition of 1.1 equiv. of TFA and Et_3SiH. LCMS analysis of the reaction was used to identify when the reduction had stalled and, at this point, additional equivalents of reducing agents could be introduced. A comparison of the three reactions is shown in Table 20 below.

Entry 3 gives the results obtained with the optimised procedure, resulting in an improved yield, reduction of decomposition as well as maintaining the *ee* value of the desired product. To our knowledge, this is the first example of an *in situ* reduction and represented a significant advancement to this methodology.

Table 20. Optimisation of the reduction step in the one-pot cycloisomerisation-reduction reaction.

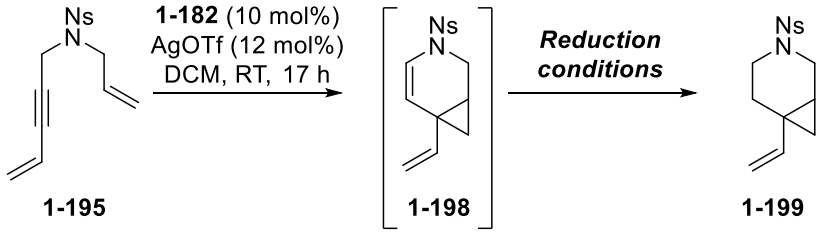

Entry	Relative Conversion of 1-195 to 1-198 / %	Reduction Conditions	Yield / %	*ee* / %
1	71	TFA (2.2 equiv.) Et_3SiH (1.2 equiv.) RT, 1.5 h	47[b]	48.4
2	74	TFA (2.2 equiv.) Et_3SiH (1.2 equiv.) RT, 3 h *Then* TFA (2.2 equiv.) Et_3SiH (1.2 equiv.) RT, 1.5 h	Mixture isolated with 72% desired product.	-
3	79	TFA (1.1 equiv.) Et_3SiH (1.1 equiv.) 0 °C, 4.5 h *then* TFA (1.1 equiv.) Et_3SiH (1.1 equiv.) 0 °C , 1.5 h	52	43.4

Reactions on 100 mg (0.326 mmol) scale. [b]Significant by-product formation observed.

9.7. Scale-up of the Gold-Catalysed Cycloisomerisation-Reduction Protocol

To showcase the practical use of the one-pot cycloisomerisation-reduction protocol, a scaled-up reaction using 2.4 g of **1-195** was carried out. With an extended reaction time for the cycloisomerisation step, full conversion was observed, before introduction of the reducing agents at 0 °C (Scheme 58). Product **1-199** was isolated in a much-improved yield of 78%, with the *ee* value maintained.

Despite *ee* values of just under 50% (correlating to approximately a 3:1 ratio of enantiomers), the improvement upon a racemic approach can clearly be seen. Furthermore, this enantioenrichment represents an excellent result given the small size of the vinyl group. Previous reports have focused on large aromatic groups and, when conditions have been applied to smaller groups, such as a methyl, the reported *ee* values did not exceed 38%.[92] Having demonstrated an efficient, enantioenriching gold-catalysed synthesis of **1-199**,

functionalisation of the vinyl group was investigated with the aim of synthesising an intermediate allowing access to (hetero)aromatic-containing compounds.

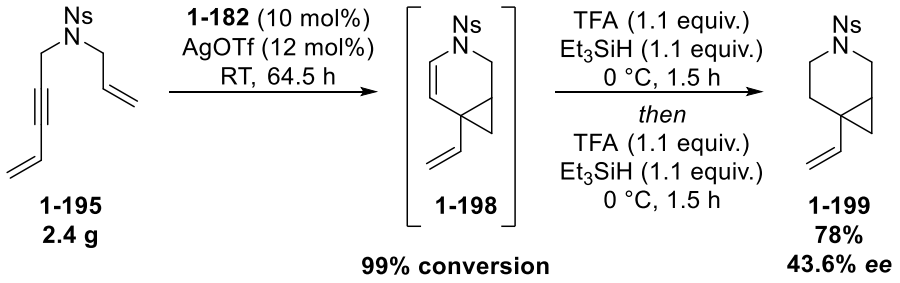

Scheme 58. Scale-up of one-pot cycloisomerisation-reduction process on 2.4 g (7.83 mmol) of **1-195**.

9.8. Functionalisation of the Vinyl Group

As described in Scheme 41 (page 98), an oxidative cleavage approach was planned to transform the vinyl group to an aldehyde. A subsequent oxidation was then expected to provide the corresponding acid, as shown in Scheme 59.

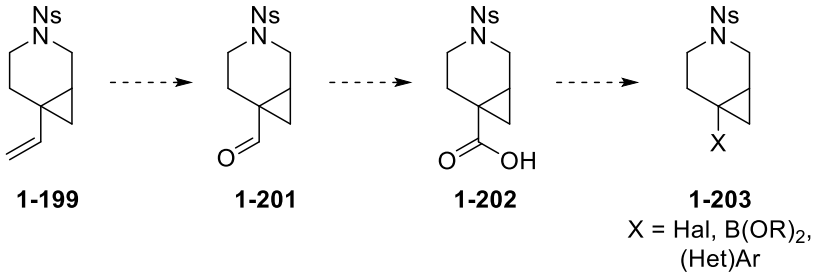

Scheme 59. Proposed oxidative route towards acid intermediate **1-202** which could be used for access compounds of the type **1-203**.

Oxidative cleavage could be facilitated in more than one way, for example, with the use of osmium tetroxide (OsO_4) and sodium periodate ($NaIO_4$), or ozonolysis; however, these approaches were deemed inappropriate. There exist several issues with the use of osmium tetroxide including the handling, safety and cost. Within our laboratory, the use of osmium tetroxide was permitted only if other options had been exhausted and were unsuccessful. Ozonolysis was not deemed a viable option as access to an ozonolyser was limited within our laboratory and this may be the case in other laboratories, which represented a barrier to use, if implemented.

A thorough assessment of the literature in the search for alternatives revealed the use of ruthenium tetroxide (RuO_4) which could be formed *in situ* from cheap and readily available ruthenium chloride ($RuCl_3 \bullet 3H_2O$).[114-117] Along with a stoichiometric oxidant, such as $NaIO_4$, dihydroxylation of alkene systems was possible, along with oxidative cleavage.[114-117] Furthermore, RuO_4 is less toxic than OsO_4 and the $RuCl_3 \bullet 3H_2O$ precursor less costly.[114]

Early work in this area used CCl_4 as a solvent,[114,115] and, therefore, a more appropriate preparation was sought from the literature. It has been reported that a 3:3:1 mixture of EtOAc/MeCN/H_2O facilitated the dihydroxylation of alkenes in 30 min.[117] Application of these conditions to compound **1-199** led to complete consumption of this material. The crude mixture obtained after work-up was shown by LCMS to contain the corresponding diol **1-204** with a peak area of 53%, and the aldehyde with a peak area of 25% (including co-elution with an unknown compound). An attempt to implement oxidative cleavage of the diol using additional $NaIO_4$ gave no change and the diol and aldehyde were isolated in 52% and 8% yields, respectively (Scheme 60).

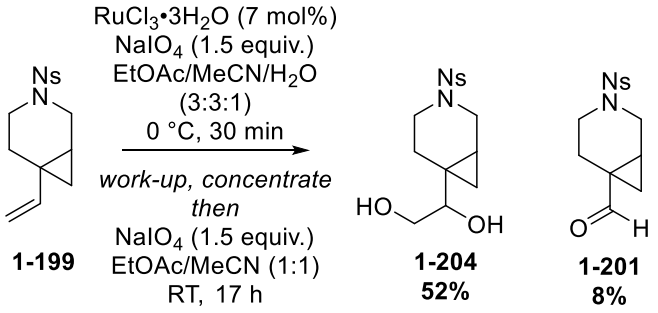

Scheme 60. Attempted dihydroxylation and oxidative cleavage of the vinyl group on compound **1-199**. The major product was diol **1-204**.

Diol **1-204** was subsequently subjected to a separate oxidative cleavage reaction using sodium periodate ($NaIO_4$) in a 4:1 THF/H_2O solvent system, frequently implemented in this type of transformation. This reaction proceeded rapidly, providing access to aldehyde **1-201** in crude yield of 84% after 45 min at RT, shown below in Scheme 61. The improved outcome of this reaction was presumed to be a result of the increased solubility of the diol and $NaIO_4$ in the THF/water solvent system. Furthermore, the increased miscibility of the two solvents could also improve the interaction between the diol and the $NaIO_4$, thus facilitating oxidative cleavage. Aldehyde **1-201** was taken through to the desired acid **1-202** by way of a Pinnick oxidation,[118,119] resulting in an 85% yield (Scheme 61).

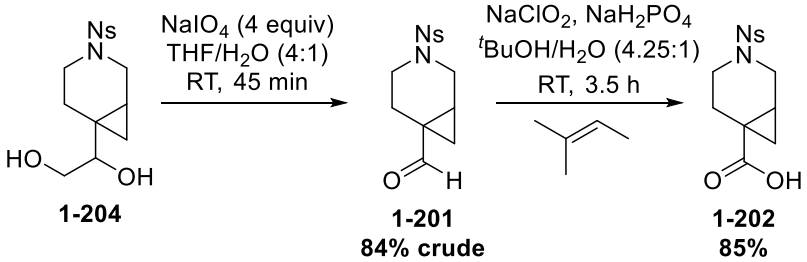

Scheme 61. Use of diol **1-204** in the synthesis of acid **1-202**. An efficient oxidative cleavage reaction in 4:1 THF/water gave aldehyde **1-201** which could be further oxidised to the acid using a Pinnick oxidation.

The success of the oxidative cleavage reaction in the THF/water solvent system prompted an exploration into the use of this with the RuO_4 dihydroxylation reaction. It was predicted that conversion of the vinyl group in **1-199** to aldehyde **1-201** would be observed. Initial investigations found that implementation of this solvent system behaved as expected, forming the desired aldehyde **1-201**; however, formation of a small amount of the desired acid **1-202** was also observed. Addition of further equivalents of $NaIO_4$ to this reaction mixture facilitated full conversion to acid **1-202**. Refinement of this procedure led to the conditions shown in Scheme 62, below.

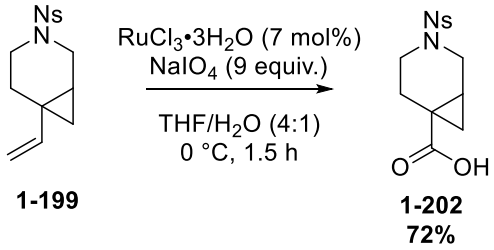

Scheme 62. Summary of optimised conditions for the formation of acid **1-202** in one step from vinyl-substituted compound **1-199**. The use of enantioenriched **1-199** (*ee* 47.0%) gave enantioenriched acid **1-202** (*ee* 49.0%).

$NaIO_4$ is required for oxidation of $RuCl_3.3H_2O$ to the active RuO_4 species as well as maintaining the oxidative cycle, as shown below in Figure 55, adapted from Schäfer.[120] Oxidation of the ruthenium(III) species gives access to the highly oxidising RuO_4 which, mechanistically, is thought to form diol **1-204** in a similar manner to the analogous reaction with OsO_4.[121] The oxidative cleavage step may then be facilitated by $NaIO_4$ which would be present in larger concentrations in the organic solvent due to the presence of water in THF. Furthermore, the presence of water in the reaction allows an equilibrium between the aldehyde and the respective hydrate to exist. From the hydrate, oxidation with RuO_4 can take place, forming the desired carboxylic acid and, presumably, formic acid from the formaldehyde formed during the oxidative cleavage step (Scheme 63).

The ability to transform the vinyl group of compound **1-199** to acid **1-202** was an exciting result, expediting the synthesis of the key acid intermediate. In addition, the use of vinyl compound **1-199** with an *ee* of 47.0% formed the acid with an *ee* measured as 49.0%. The conservation of enantioselectivity in this step provides a further advantage to this approach, which cannot be understated.

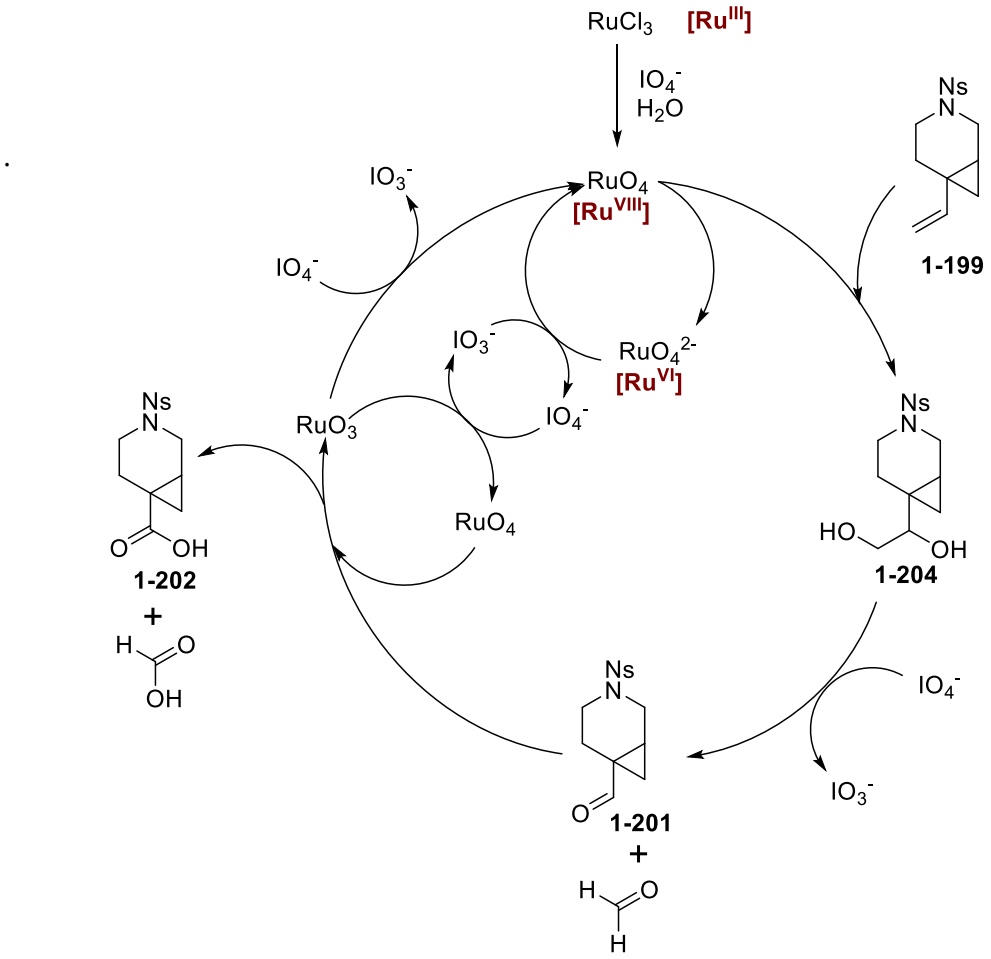

Figure 55. The proposed catalytic cycle for the oxidation of vinyl compound **1-199** to acid **1-202** using RuO_4 and $NaIO_4$.

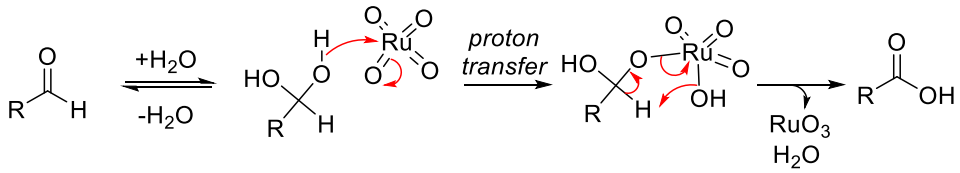

Scheme 63. Oxidation of aldehydes to acids by RuO_4 *via* a hydrate intermediate, formed in the presence of water.

9.9. Use of the Acid Intermediate

To access an intermediate of maximum utility from acid **1-202**, two approaches were considered (as shown in Scheme 64, below). Firstly, the acid could be functionalised as a redox-active ester (RAE) **1-206** which could be coupled directly or used to make a boron-containing intermediate **1-208**. Secondly, the use of a Barton ester **1-205** was anticipated to allow the synthesis of alkyl halides **1-203**. Upon synthesis of these intermediates, their use for installing an aromatic or heteroaromatic moiety could then be explored.

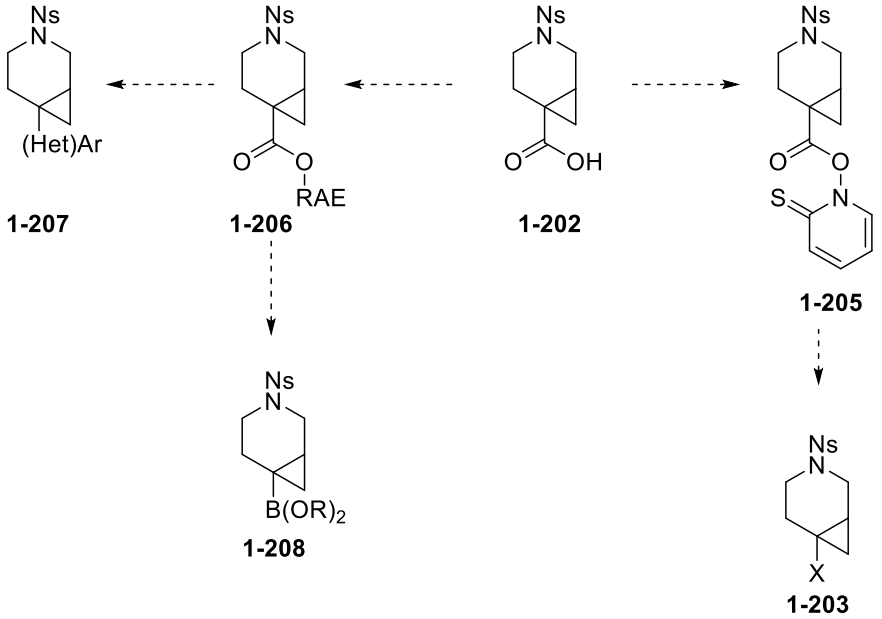

Scheme 64. Proposed use of acid **1-202** in the synthesis of both RAEs and Barton esters as means of accessing the desired boron- or halogen-containing intermediates. The direct cross-coupling of RAEs was also planned.

9.9.1. Synthesis of Halogenated Intermediates – The Barton Ester Approach

The application of Barton esters as radical precursors has been well-established since its inception in 1983.[122] This approach makes use of the acyloxypyridine-2-thione moiety which can be reduced to an alkyl radical in the presence of an external initiator, which may either be heat or light (Scheme 65).[122,123]

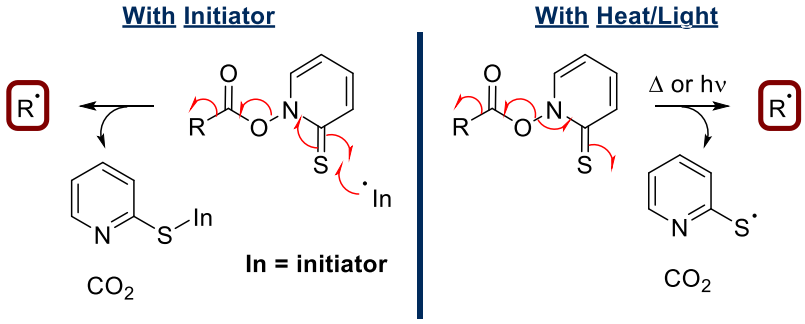

Scheme 65. The initiation of acyloxypyridine-2-thiones (Barton esters) with an initiator or with heat/light.

The resulting alkyl radical can be trapped with various species; however, most relevant to the current study is the formation of alkyl halides. The trapping of an alkyl radical with iodoform was expected to give access to the desired iodide, as in previous studies with cyclopropyl acids.[124,125] Two reports selected from the literature used differing methods of formation of the Barton ester as well as the subsequent activation, as shown in Scheme 66. Both were reported to be highly efficient processes and, as such, were applied to acid **1-202**.

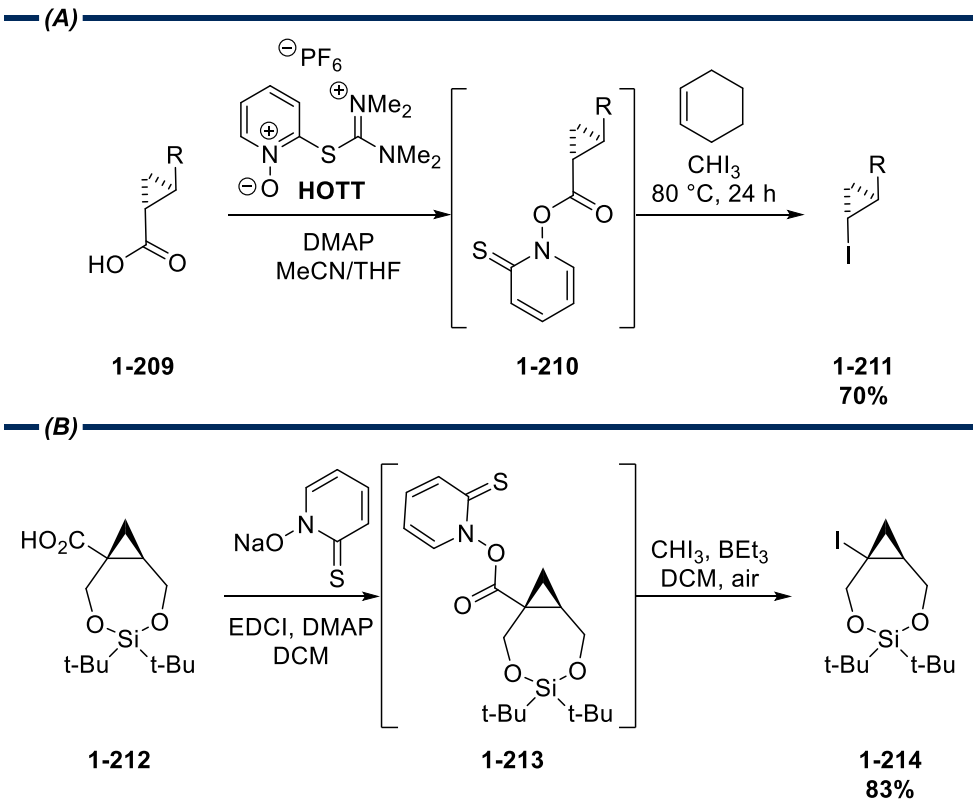

Scheme 66. Literature reports of cyclopropyl iodide preparation using the Barton ester approach. (**A**) makes use of the HOTT reagent, followed by thermal initiation of ester **1-210**.[125] (**B**) uses a standard approach to form Barton ester **1-213** which is reduced after initiation with BEt_3 and air.[124]

Carboxylic acid **1-202** was submitted to the conditions shown in Scheme 66A.[125] Full conversion to Barton ester **1-205** was observed by LCMS; however, heating this in cyclohexene, as reported in the literature,[125] did not produce the desired iodide (Scheme 67).

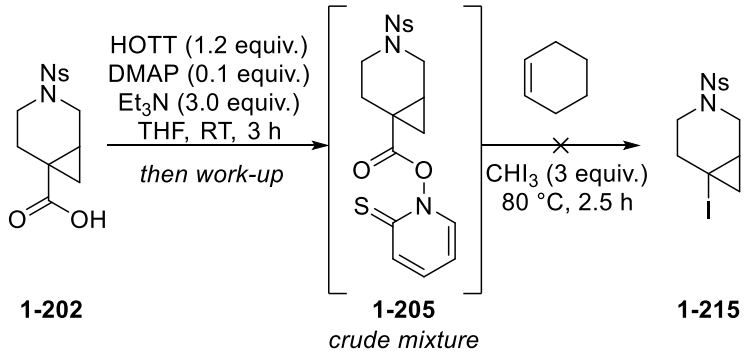

Scheme 67. Initial exploration towards the synthesis of iodide **1-215**.

As a result, BEt_3 initiation was explored, as shown in Scheme 66B. Due to the efficient conversion of acid **1-202** to Barton ester **1-205** observed with the *S*-(1-oxido-2-pyridyl)-*N*,*N*,*N*′,*N*′-tetramethylthiuronium hexafluorophosphate (HOTT) reagent, this was maintained, with subsequent BEt_3 activation replicated from the literature.[124] The formation of the ethyl radical, originating from BEt_3, was postulated to react with the thiocarbonyl

moiety on Barton ester **1-205**, as shown in Scheme 68, leading to the desired iodide in 21% yield.[126]

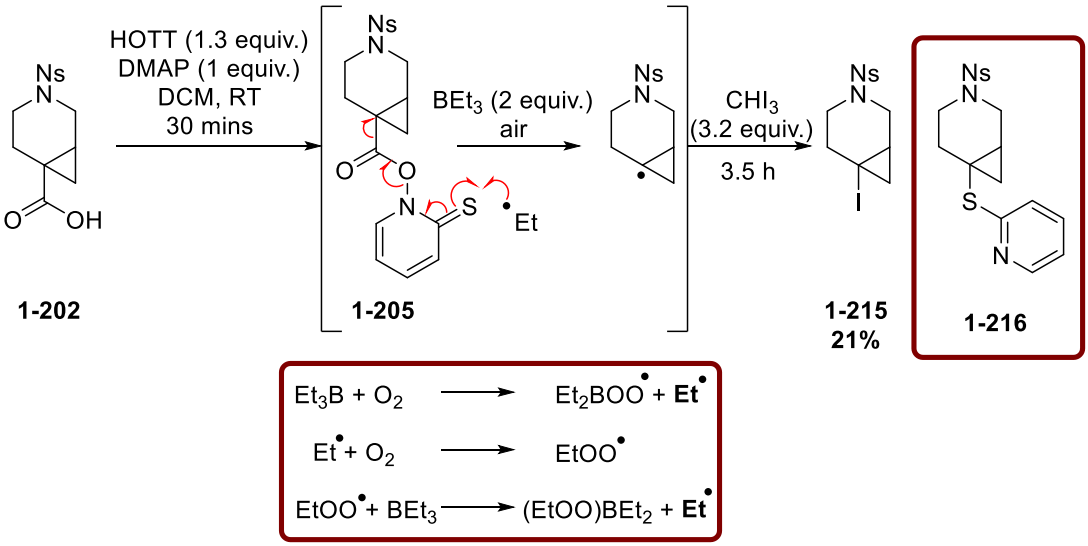

Scheme 68. Reaction using BEt_3/air as a radical initiator. The desired iodide **1-215** was formed in 21% yield. The autooxidation/propagation steps are shown in the red box.

The poor yield was postulated to be due to the reactivity of the iodide product, with several species present the reaction mixture. By-product **1-216** was tentatively identified in a crude reaction mixture and the formation of this species may be considered to be from iodine atom transfer, as shown in Scheme 69.[126] The tertiary radical formed upon loss of the iodine atom is more stable than the secondary ethyl radical, acting as a driving force for this reaction. The resulting cyclopropyl radical may then react with a molecule of Barton ester **1-205** forming by-product **1-216** and a further tertiary radical (Scheme 69).

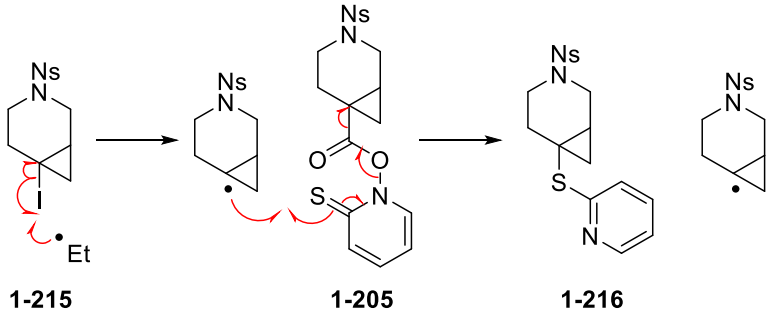

Scheme 69. Proposed formation of by-product **1-216** after an iodine atom transfer reaction with an ethyl radical resulting from the relative radical stabilities.

The resulting poor yield and cross-reactivity of the iodine product **1-215** was a clear deficiency in this approach. Therefore, the analogous formation of the bromide was investigated as this was expected to be less susceptible to atom transfer.[126] CHI_3 was replaced with $CHBr_3$ and, as shown below in Scheme 70, the outcome was improved and bromide **1-217** isolated in 60% yield, albeit with a lower purity (82%) than desired; however by-product

1-216 was not observed in this reaction. The lower purity was found to be as a result of co-elution of reduced by-product **1-218** which was difficult to remove with normal-phase purification. Further optimisation of this process was not warranted at this stage as preliminary investigations into the use of bromide **1-217** in downstream chemistry was of higher priority. Measurement of the *ee* after use of enantioenriched carboxylic acid **1-202** gave a value of 46.8% for bromide **1-217** and provided evidence for conservation of the enantioselectivity in this procedure.

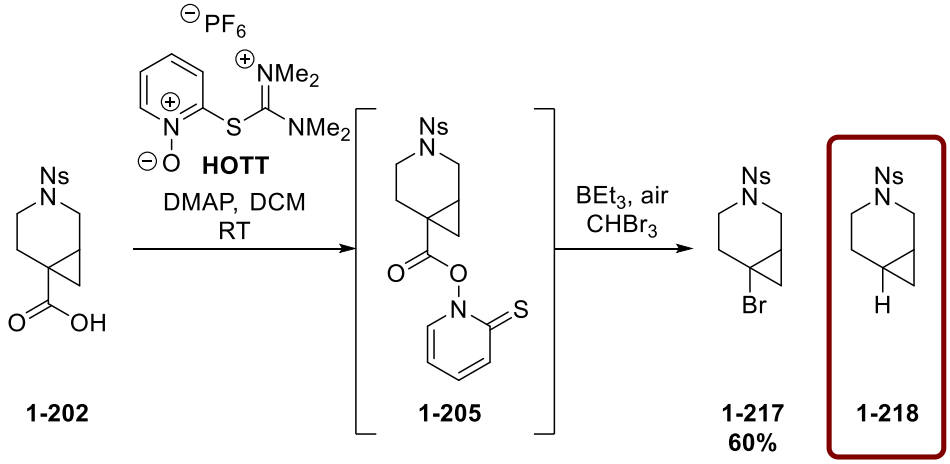

Scheme 70. Formation of bromide **1-217** via Barton ester **1-205** using bromoform as the bromide source and BEt_3/air as the radical initiator. **1-217** was obtained in 82% yield which is reflected in the reported yield. The use of enantioenriched acid **1-202** gave enantioenriched bromide **1-217** (*ee* 46.8%).

The synthesis of bromide **1-217** represented a deviation from the intended iodide target; however, bromide **1-217** provided an intermediate for which use could still be used to access the desired (hetero)aromatic species (*vide infra*).

9.9.2. Use of Redox-Active Esters as Coupling Agents

Studies into the use of RAEs as cross-coupling reagents were also initiated to evaluate the use of the acid intermediate. RAEs represent a modern adaptation of the chemistry surrounding Barton esters, offering a bench-stable alternative to esters such as **1-205**. The reactivity of these species has been explored in great depth over the last five years[127] and, more specifically, their use in sp^3-sp^2 cross-coupling reactions with (hetero)aromatic species has been an area of interest since a seminal report by Baran in 2016.[128] In this report, several redox-active species were disclosed, with all of these thought to be activated by single-electron transfer (SET) from a catalyst, as shown below in Scheme 71. The resulting radical can then be coordinated to the catalyst, leading to reductive elimination of the desired cross-coupled product.

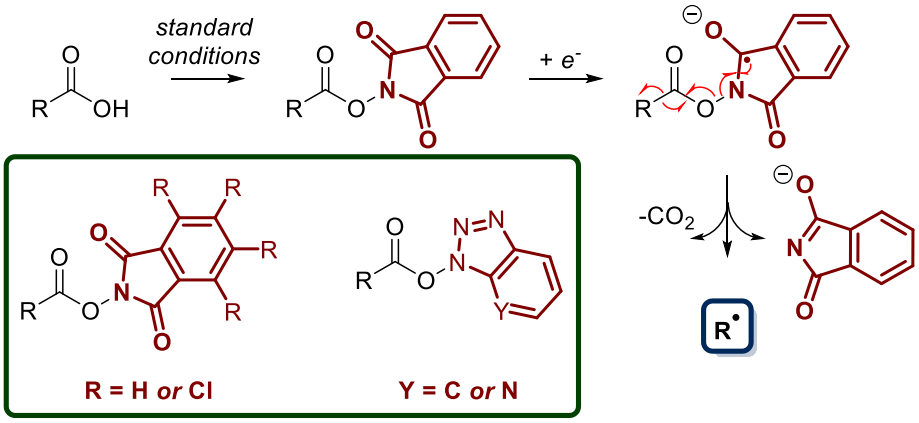

Scheme 71. Activation and structure of redox-active esters (RAEs).

While this initial report was published at the same time as a similar transformation disclosed by Weix,[129] the Baran group refined this methodology and extended the substrate scope. By using both nickel- and iron-catalysis, this cross-coupling approach included boronic acids, Grignard and organozinc reagents as coupling partners.[128,130-133]

These reports provided a promising avenue for exploration into a suitable method for installation of a (hetero)aromatic system to the CPPip scaffold. Initial studies focused on an iron-catalysed Negishi reaction due to the superior catalytic activity, non-toxic metal and inclusion of several tertiary RAEs in the substrate scope.[131] The conditions reported for use with tertiary RAEs were applied to CPPip RAEs, shown in Scheme 72.

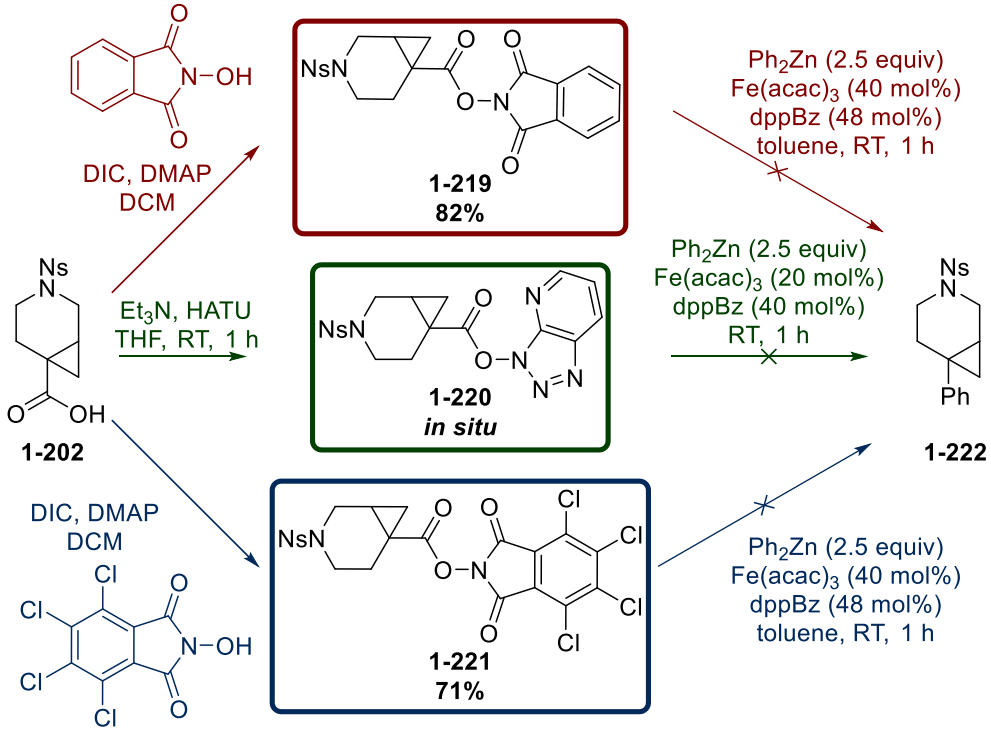

Scheme 72. Attempted synthesis of phenyl CPPip derivative **1-222** using iron-catalysed RAE cross-coupling. **1-221** was obtained in 86% purity, reflected in the yield.

The reactions of RAEs **1-219**, **1-220** and **1-221** were unable to produce any desired product with several unidentified by-products observed in the reactions. The majority of these could not be isolated; however, by-product **1-223** was identified by LCMS, ^{1}H and ^{13}C NMR from the reaction using RAE **1-219** (Scheme 73). Apparent reaction *via* the acyloxy radical indicated rapid reaction and no loss of CO_2 from the RAE, as shown in Scheme 73. The nitro group was also reduced to the corresponding aniline; however, it is unclear by which mechanism this occurred. While only isolated in a 7% yield, this product suggests that the reaction conditions are likely unsuitable for nitro-containing compounds.

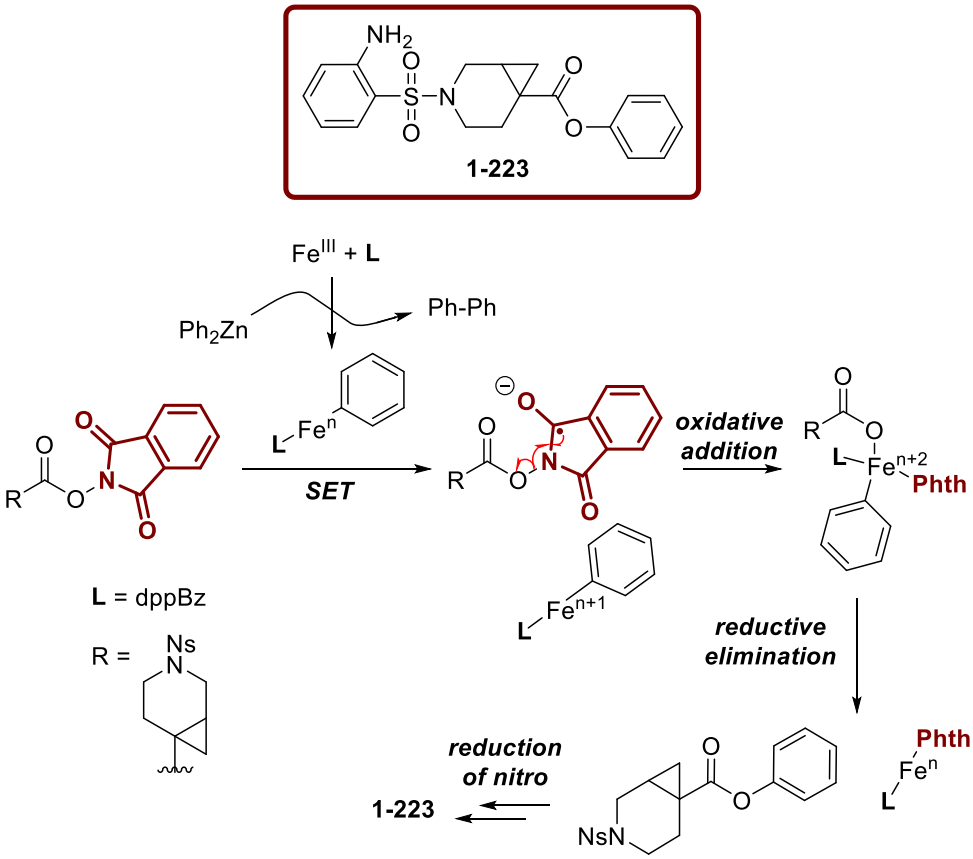

Scheme 73. Structure of isolated by-product **1-223** and the proposed mechanism of formation via reaction of the acyloxy radical. Reduction of the nitro group occurs; however, it is unclear if this is due to the acidic work-up in the presence of iron, or from a radical process. The proposed mechanism is adapted from that reported by Baran.[131]

Preliminary explorations using alternative conditions were undertaken to explore the possibility of nickel-catalysed RAE cross-couplings. Both the Suzuki-Miyaura[130] and Negishi[128] reactions were investigated to determine the viability of both approaches; however, the use of boronic acids would not be suitable for the synthesis of 2-pyridyl derivatives due to the nature of 2-pyridylboronic acids.[134] Despite this, the implementation of this methodology would have clear benefits for this study, fulfilling one of the initial aims of an intermediate which could enable cross-coupling. Phenylboronic acid was chosen as the

initial coupling partner for these reactions, giving excellent results in the literature.[128] The scope of this reaction was limited to secondary RAEs; however, it was reasoned that the presence of the cyclopropyl moiety on the CPPip may be reminiscent of a system somewhere between a secondary and tertiary system.

Application of the reported conditions to RAE **1-221** gave desired product **1-222** in a yield of 11% (Scheme 74). Reverse-phase purification was required as **1-222** appeared to be unstable on silica. During the reaction, hydrolysis and the formation of unidentified by-products were observed which may have contributed to the low yield. Furthermore, it was noted in the supplementary information of the literature report that tetrachlorophthalimide esters of tosyl-protected piperidines may be less stable due to the electron-withdrawing nature of the two groups.[130] Decarboxylation may also have occurred, with the mass of reduced compound **1-218** observed by LCMS, matching the retention time previously observed in the formation of bromide **1-217** (Scheme 70).

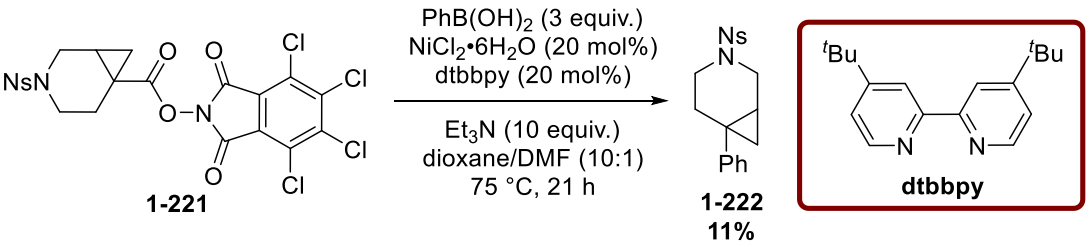

Scheme 74. Synthesis of phenyl CPPip **1-222** using Ni-catalysed RAE cross-coupling with phenylboronic acid.

The Negishi-type coupling was also attempted with RAE **1-221** to synthesise phenyl-substituted compound **1-222**. Two nickel catalysts are exemplified in the literature report with both $NiCl_2$•glyme and $NiCl_2$•$6H_2O$ finding use with different substrates.[128] As such, both were applied to the reaction of RAE **1-221** (Scheme 75).

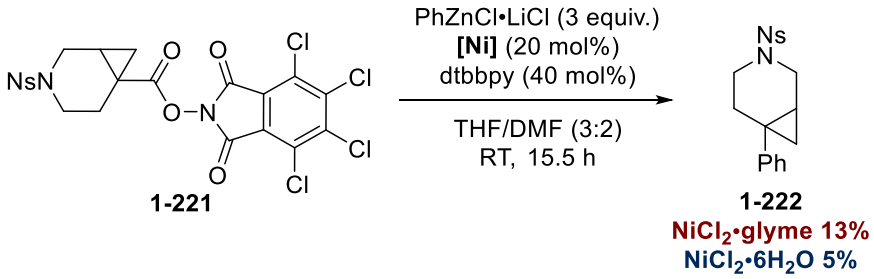

Scheme 75. Negishi-type cross-coupling reaction of RAE **1-221** with two different nickel catalysts giving different results.

Pleasingly, the use of $NiCl_2$.glyme provided the desired product **1-222** in a yield of 13% with the major by-products appearing to originate from decarboxylation and hydrolysis of the RAE. The hydrolytic liability was further exemplified by the lower yield obtained when using

the hydrated nickel catalyst, $NiCl_2.6H_2O$, agreeing with the reported instability of sulfonamide-protected tetrachlorophthalimide RAEs (*vide supra*).[130]

This preliminary investigation of the direct cross-coupling of RAEs gave promising results; however, further optimisation was not undertaken for either approach. Given additional time, a thorough investigation could be undertaken, exploring the various reaction parameters reported in the literature optimisations.[128,130] Despite this, these proof-of-concept reactions are an excellent basis for future studies and may enable access to enantioenriched (hetero)aromatic CPPip analogues which could find use in medicinal chemistry as piperazine bioisosteres.

9.10. Use of the Bromide Intermediate in Cross-Coupling Reactions

The synthesis of enantioenriched bromide **1-217** provided an additional opportunity to explore routes to (hetero)aromatic-substituted CPPip compounds. A vast number of reports have been published with the use of alkyl bromides, both activated and unactivated, as coupling partners.[135-142] Those determined to be most useful for bromide **1-217** could be split into two categories: reductive coupling and nickel-catalysed Suzuki-Miyaura cross-couplings (as shown in Scheme 76). These reactions differ in the coupling partner used, with reductive couplings combining two brominated species and the Suzuki-Miyaura cross-coupling reactions making use of (hetero)aromatic boronic acids or esters.

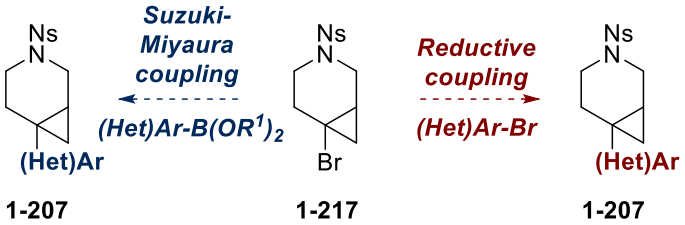

Scheme 76. The two categories of reactions in which bromide **1-217** could be used: reductive and Suzuki-Miyaura couplings.

With limited time, two reactions from each category were chosen for preliminary investigations. As with the reactions of RAEs, the nitro group on the nosyl system was monitored closely, with previous results suggesting that this may be a liability. This was particularly pertinent for reductive couplings in which the nitro group may be reduced.

Firstly, the reductive coupling approach was explored using conditions reported by O'Neill[138] and Gong,[137] as both reported use of nitrogen-protected piperidines. While these examples were limited to secondary bromides, the presence of the cyclopropyl ring was anticipated to display reactivity reminiscent of a system between secondary and tertiary (as with the RAEs). The two initial reactions are shown below in Scheme 77, with no desired product formed in either. Starting material was recovered from both in varying amounts and by-product **1-225** was recovered from reaction 1, confirming the anticipated liability of the nitro group.

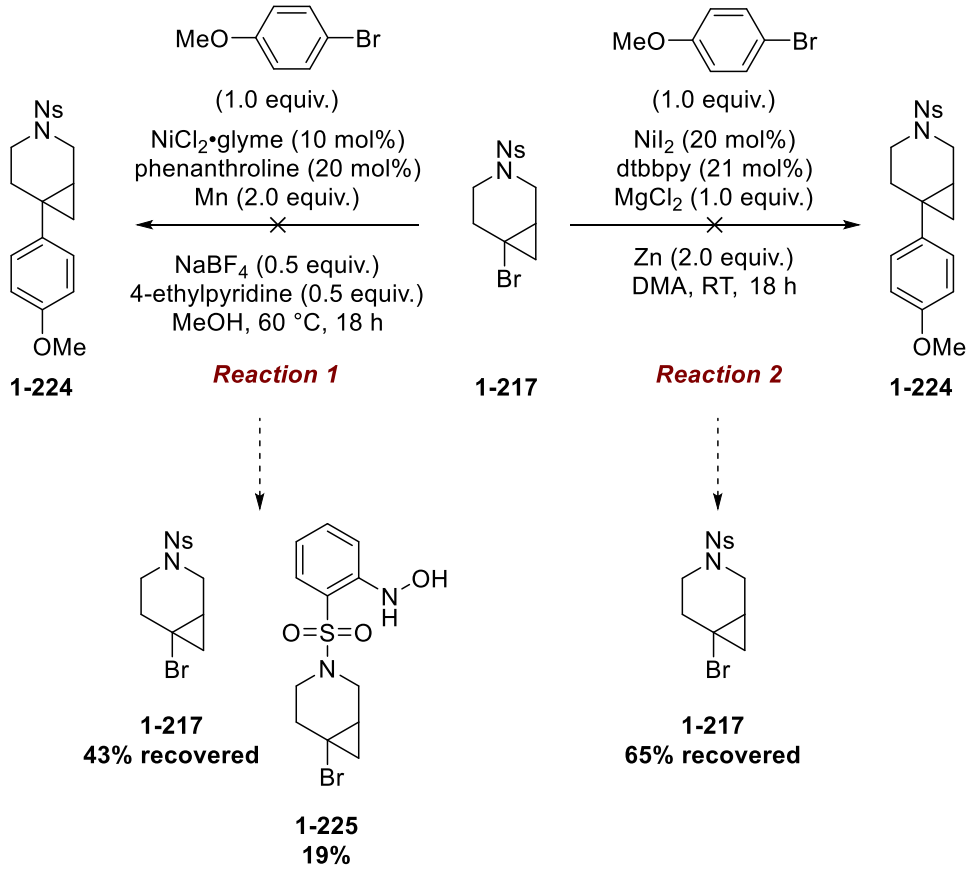

Scheme 77. Summary of the outcomes of the reductive coupling reactions using bromide **1-217**. No desired product was formed and starting material was recovered. By-product **1-225** was also isolated from Reaction 1.

Tentative analysis of the reaction mixture LCMS traces suggested that small amounts of other by-products may have formed, including aniline **1-226** (Figure 56), although these were not isolated. The lack of desired reactivity provided evidence that this approach was unlikely to be productive due to the nitro group and no further exploration was undertaken.

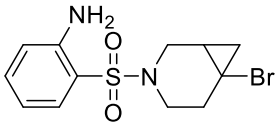

1-226

Figure 56. Proposed structure of a by-product in the reactions of bromide **1-226**.

Investigation of the Suzuki-Miyaura cross-coupling approach involved two sets of conditions, with the first being optimised for secondary bromides.[139] While protocols exist for tertiary bromides, the conditions were found to use benzene as a solvent and 9-borabicyclo[3.3.1]nonane derivatives which did not align with the aims of optimising an accessible route.[135] The second set of conditions chosen were those used in the cross-coupling of tertiary iodocyclopropane **1-214**.[124] Despite the difference in reactivity between bromides and iodides, the formation of some product was anticipated. Shown in Scheme 78 are the two reactions carried out, with no desired product observed in either. As in the reductive couplings, starting material remained present, alongside several by-products, of which only aniline **1-226** could be isolated as an impure sample from reaction 1.

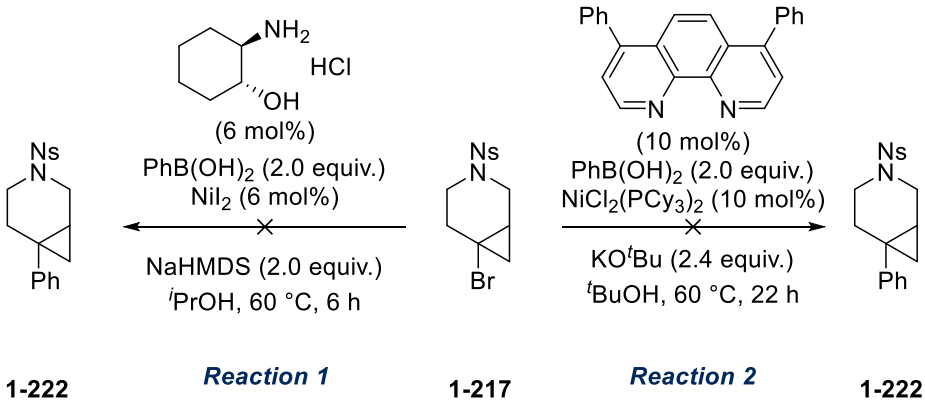

Scheme 78. Test reactions exploring the possibility of nickel-catalysed Suzuki-Miyaura cross-coupling reactions with bromide **1-217**. No desired product was observed from either reaction.

These exploratory reactions provided evidence to suggest that the presence of the nitro group likely hinders any of the desired reactivity of the bromide with no cross-coupled products observed. While not an exhaustive exploration of bromide cross-coupling, the outcomes provided some support for the discontinuation of these methods.

9.11. Synthesis of Boron-Containing Intermediates

The synthesis of boron-containing intermediates was explored as an alternative pathway in the use of RAEs and four reports for this approach were found in the literature, with two using photochemical methods.[143-146] Up until this point of the study, photoinduced transformations had been avoided due to the known excitation of the nitro functionality, often leading to reactivity from the triplet state,[147,148] resulting in reduction and formation of products such as hydroxylamines.[149,150] Nevertheless, attempts were made to implement each methodology to RAE **1-219** and Scheme 79, below, summarises the outcomes of each reaction.

The non-photoinduced reactions (1 and 2, Scheme 79) reported by Baran[144,145] were both unsuccessful. Hydrolysis of the RAE and reduction of the nitro group were the only transformations observed with both reactions stalling when acids **1-202** and **1-226** had formed. The lack of decarboxylation in these reactions is also interesting and may suggest poor reactivity of the phthalimide RAE **1-219** under non-photoinduced conditions.

Photoinduced reaction 3 gave interesting results with only decarboxylation and reduction of the nitro group observed. The reduction of the nitro group was expected but, in contrast to reactions 1 and 2, the presence of decarboxylated products suggested that activation of the RAE had taken place. Unfortunately, no evidence of borylated products could be found and only small amounts of protodecarboxylated compounds **1-218** and **1-228** were obtained as impure samples and the low recovery indicated significant decomposition in the reaction.

Having shown that photoinduction may be able to activate RAE **1-219**, reaction 4 was carried out, making use of an iridium catalyst.[146] As with the previous photoinduced reaction, it was expected that nitro reduction would occur; however, a broader excitation wavelength from compact fluorescent lamps (CFLs) was predicted to activate the RAE to a larger extent than the narrowband blue LEDs used in reaction 3. The products isolated from reaction 4 all showed nitro reduction; however, the isolation of boronic acid **1-230** represented the first example of desired reactivity. The yield of **1-230** was only 14% but warranted a comparison experiment in which the tosyl protected analogue could be used, removing nitro functionality.

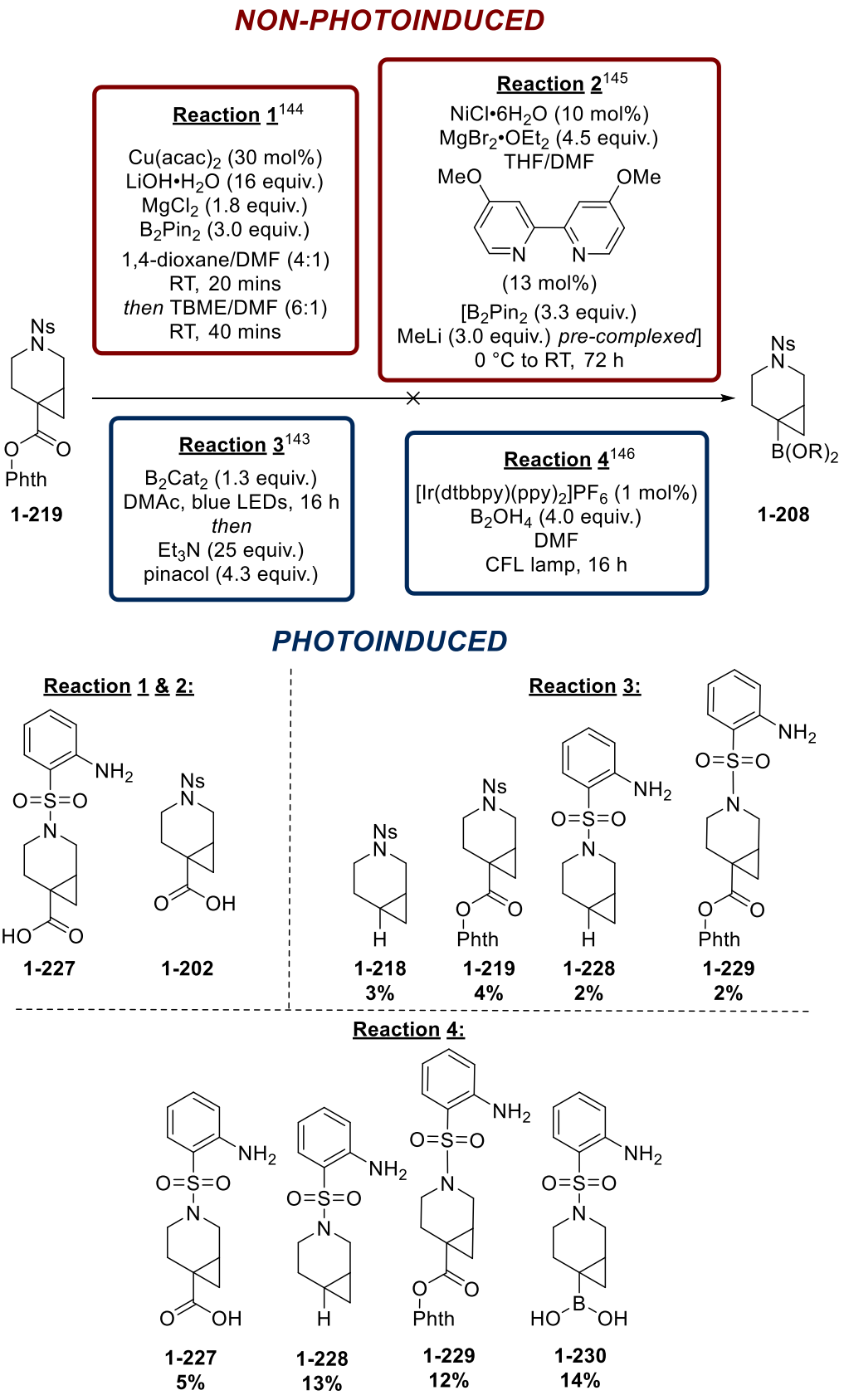

Scheme 79. Summary of reactions aimed at the synthesis of a boron-containing intermediate. No desired products were formed, and the by-products shown were observed or isolated. Isolated material is indicated by the relative yield obtained upon purification. **Reaction 2** used 4.5 equiv. of $MgBr_2$•OEt_2 instead of 1.5 equiv. but this was not expected to have changed the outcome. **Phth** = phthalimide.

9.11.1. Use of the Tosyl-Protected Analogue

Tosyl-protected CPPip RAE **1-231** was synthesised following the sequence optimised for the nosyl analogues with the enantioselective gold-catalysed cycloisomerisation-reduction implemented to give cyclised product **1-168** in 48% yield. The ruthenium-catalysed oxidation was also successful, providing acid **1-169** in 72% yield before the formation of RAE **1-231**. The *ee* values were not obtained for these reactions; however, given the conservation of the enantioselectivity observed with the nosyl-protected analogue, it was anticipated that this would be close to the value of 19.2% obtained without the *in situ* reduction (Scheme 53).

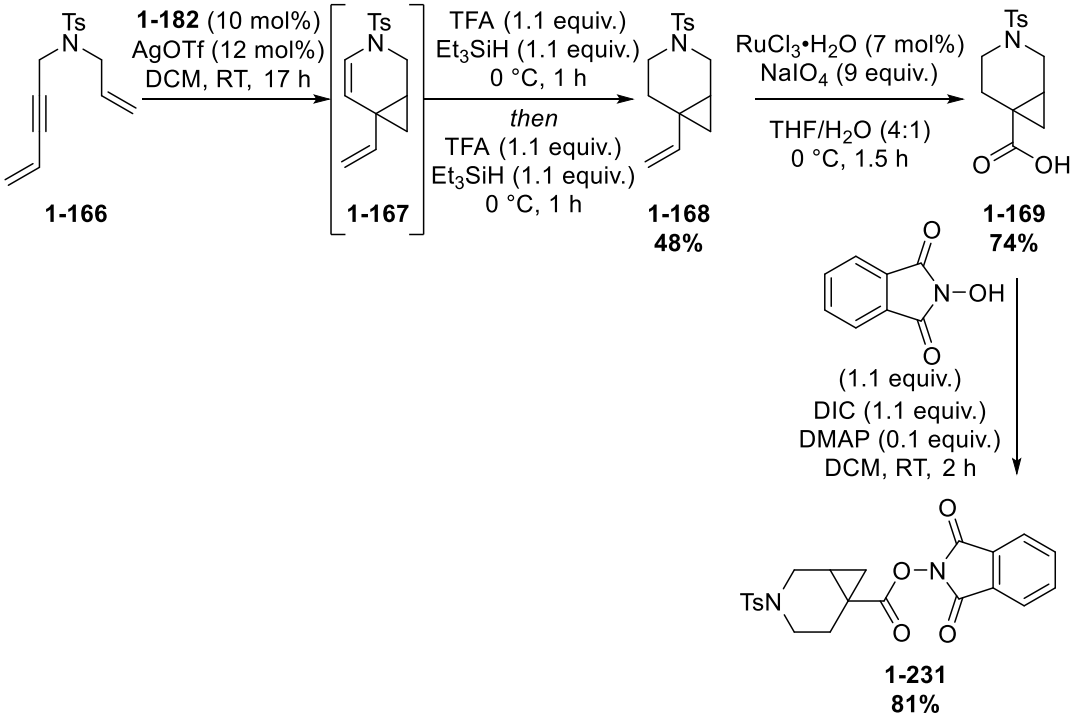

Scheme 80. Synthesis of tosyl-protected RAE **1-231** from enyne **1-166** following the same sequence as for the nosyl-protected analogues.

Removal of the nitro group from the starting material and subjection to the photochemical conditions using the iridium catalyst $[Ir(dtbbpy)(ppy)_2]PF_6$ substantially improved the outcome of the reaction and the desired boronic acid **1-232** was obtained in 66% yield (Scheme 81). Despite a small amount of hydrolysis, fewer by-products were observed, and no starting material remained. Boronic acid **1-232** was then taken through to potassium trifluoroborate **1-233** in excellent yield using non-etching conditions, as implemented previously (Scheme 81).[46]

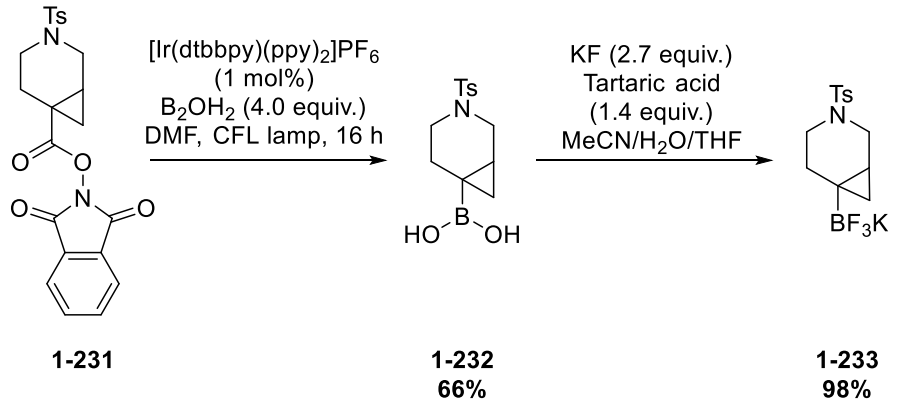

1-231 **1-232** **66%** **1-233** **98%**

Scheme 81. Synthesis of potassium trifluoroborate salt **1-233** from RAE **1-231** using photochemistry.

With the success of this reaction, it was confirmed that the presence of the nitro moiety in the nosyl protecting group was hindering the photochemical decarboxylative borylation. While no other comparisons of reactions were made with tosyl-protected compounds, it is anticipated that this is effect may be common throughout those utilising RAEs.

To conclude this study, small-scale reactions of potassium trifluoroborate **1-233** were undertaken to determine if this could be used in cross-coupling reactions.

9.11.2. Suzuki-Miyaura Cross-Coupling Reactions with Potassium Trifluoroborate 1-233

Accessing heteroaromatic species was a key aim of this project and, as such, the cross-coupling of potassium trifluoroborate **1-232** to 2-bromopyridine was explored. With very little time and limited material, only three reactions could be carried out. Given that the use of CPP potassium trifluoroborate **1-58** had been somewhat successful using conditions reported by Harris,[47] these were implemented for the initial reaction. Unfortunately, trifluoroborate **1-233** was sparingly soluble in toluene, leading to precipitation in the reaction mixture. As such, dioxane was introduced as a solvent, based on similar optimisations with cyclopropyl-containing trifluoroborate reagents.[151] Table 21 below shows the outcomes of the three reactions carried out. Clearly, a 20% yield is not of significant practical use; however, with limited changes to the conditions, this was improved from 7%. Therefore, it is likely that additional studies would enable efficient cross-coupling of potassium trifluoroborate **1-233** with a palette of (hetero)aromatic bromides or iodides.

Table 21. Initial optimisation reactions in the Suzuki-Miyaura cross-coupling reaction of potassium trifluoroborate **1-233** and 2-bromopyridine.

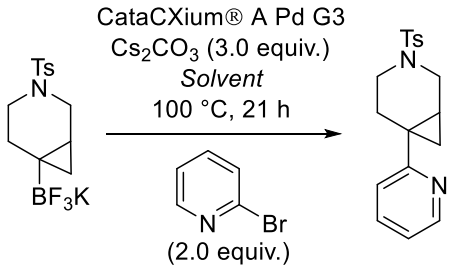

1-233 **1-234**

Entry	Pd mol %	Solvent	Yield / %
1	5	toluene/H_2O (10:1)	7
2	5	1,4-dioxane/H_2O (10:1)	11
3	20	1,4-dioxane/H_2O (10:1)	20

Despite the issues encountered with the nosyl protecting group, these results concluded the study with a desirable outcome. The synthesis and cross-coupling of an enantioenriched intermediate allowed installation of the CPPip scaffold, highlighting the potential for this approach to be highly useful in expanding the use of the CPP in medicinal chemistry applications.

10. Conclusions

An achiral gold-catalysed cycloisomerisation of enyne **1-166**, reported by Yu, was chosen as the basis for synthetic studies.[102] The introduction of a JosiPhos gold pre-catalyst to this transformation was found to induce enantioselectivity, despite the small size of the vinyl group tethered to the alkyne. Throughout the initial optimisation studies, the isolated yields of the cyclised product **1-167** were disappointingly low (≤31%) and did not correlate well to the relative conversion seen by LCMS, suggesting instability of the enamine product.

The combination of possible instability of the product and the known difficulty of tosyl-protecting group removal[94] prompted the introduction of the nosyl protecting group as a readily removable, electron-deficient alternative. Despite this, initial reactions gave similar outcomes to the tosyl analogue until the implementation of the weakly coordinating OTf was found to improve the yield of the cycloisomerisation to 66% with an *ee* value of 48.6%. Unfortunately, reproducibility was found to be an issue and, as a result, a novel one-pot cycloisomerisation-reduction procedure was optimised. This was found to maintain the *ee* (52% yield, 43.4% *ee*) and could be increased in scale to 2.4 g of starting enyne **1-195** resulting in formation of product **1-199** in an excellent yield of 78% and with an *ee* of 43.6%. Oxidation of the vinyl group using RuO_4, formed *in situ*, was optimised to give carboxylic acid **1-202** in one step with a 72% yield and no loss of *ee*, as shown below in Scheme 82.

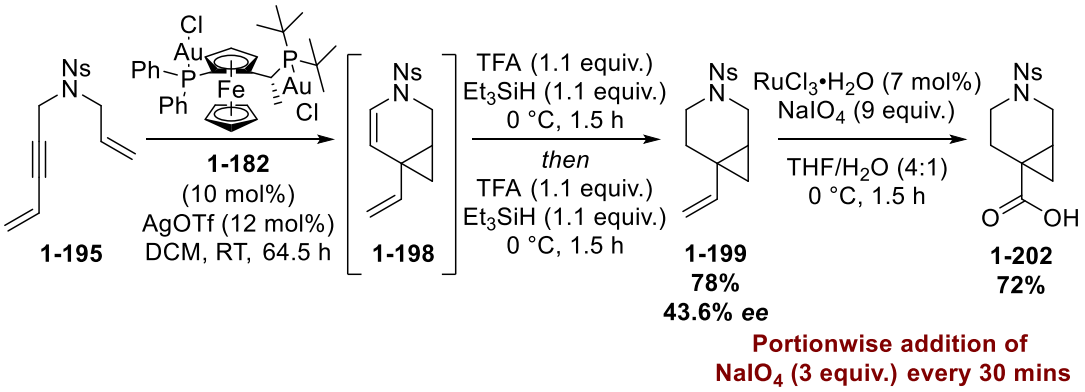

Scheme 82. Summary of optimised steps to give acid **1-202** from enyne **1-195**.

Acid **1-202** was used in further reactions aimed at synthesising intermediates for use in cross-coupling reagents, specifically RAEs and alkyl halides. Use of a Barton ester allowed access to bromide **1-217**; however, the nitro functionality of the nosyl protecting group proved to be a liability in the attempted reactions of this intermediate. An alternative approach using RAEs gave promising initial results, but further optimisation would be required for these to be of practical use (Scheme 83).

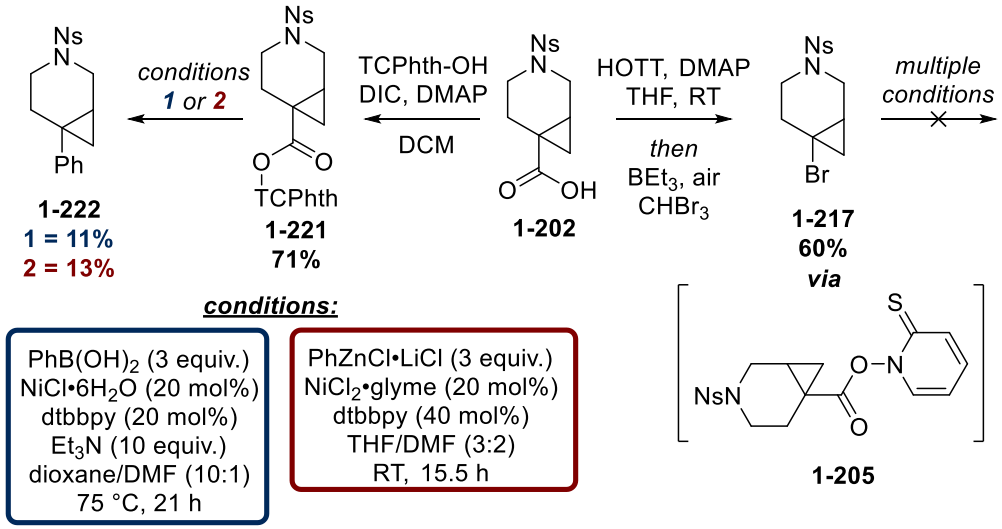

Scheme 83. Summary of the use of acid **1-202**. **TCPhth** = tetrachlorophthalimide.

The synthesis of an organoboron intermediate was investigated; however, no desired product from RAE **1-219** was observed, and the nitro group was identified as a cause of by-product formation. A comparison reaction with tosyl-protected analogue **1-231** led to the formation of boronic acid **1-232** in 66% yield. Further functionalisation to potassium trifluoroborate salt **1-233** in quantitative yield provided an intermediate enabling a Suzuki-Miyaura cross-coupling to 2-bromopyridine (Scheme 84). This result signified an important step towards fulfilling the aim of obtaining an enantioenriched intermediate to enable cross-coupling.

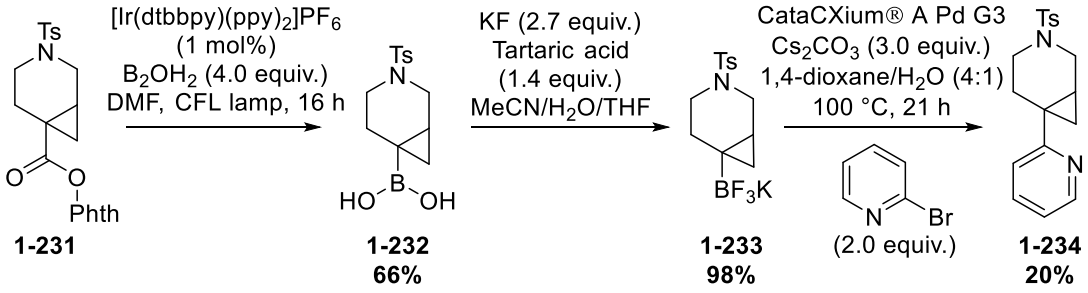

Scheme 84. The use of tosyl-protected RAE **1-231** as a means of accessing potassium trifluoroborate **1-233** for subsequent Suzuki-Miyaura cross-coupling.

Although the nosyl protecting group is superior for the cycloisomerisation step, it does not appear to be amenable to the downstream functionalisation attempted. The use of an alternative protecting group to both tosyl and nosyl protecting groups, which facilitates both the cycloisomerisation and downstream functionalisation, is desirable.

Stereoinduction using a gold pre-catalyst **1-182** and AgOTf was surprisingly effective given the moderate enantioselectivities reported for non-aromatic groups tethered to the alkyne of the enyne starting material. The formation of an enantioenriched intermediate which can be used in the syntheses of several heteroaromatic analogues provides the benefit of a single optimisation. This is highly advantageous for medicinal chemists, allowing libraries of

enantioenriched compounds to be obtained from one intermediate which can be prepared on multi-gram scales. Overall, this approach provides a promising entry point for which additional optimisation would likely lead to the efficient formation of enantioenriched (hetero)aromatic-substituted bicyclo[4.1.0]heptane derivatives.

11. Future Work

11.1. Gold-Catalysed Cycloisomerisation Optimisation

Within this study, several areas for further exploration were identified and would go some way to improving the utility of the route. An obvious starting point is to expand the optimisation of the gold-catalysed cycloisomerisation reaction. Only the JosiPhos family of ligands were explored in detail, and these have not previously been used in the formation of azabicyclo[4.1.0]hept-4-enes. Therefore, the use of more established ligands, such as those outlined in the literature (section 7.3.3), could be investigated. Furthermore, the naphthyl-substituted JosiPhos ligand discussed in section 9.3.1 may also be of interest given the effects discussed, wherein the larger groups with increased π-electron density may offer greater stereoinduction. A high-throughput approach may be implemented; however, the two-step protocol may be problematic on a smaller scale, with activation of the catalyst required before the transfer of the supernatant to solvated enyne.

The introduction of any new catalytic system should also consider the requirement for an alternative protecting group to both nosyl and tosyl. Both groups have been shown to be disadvantageous at different stages of the route and, as such, should be replaced. It was shown that both benzyl and Boc groups were unsuitable for this reaction (Scheme 50);[102,152] however, the use of a Cbz group is precedented in the literature,[92,93] with products reported to be high yielding. Therefore, this may be a suitable alternative which would not be subjected to side-reactions as with the nitro-containing nosyl group. While the use with a methyl group and Furstner's catalyst produced only a moderate *ee* of 38% (Scheme 34), it may be possible that an exploration of alternative catalytic systems may improve this outcome for Cbz-protected enyne **1-235** (Figure 57).

An additional protecting group which may find use is the benzothioazolesulfonamide (Bts) (Figure 57) group which maintains the sulfonamide moiety, shown to be effective in the cycloisomerisation reaction. This can be removed with the use of thiols under mild conditions, analogously to the nosyl group,[153] and is another option which removes the nitro moiety; however, there are no reports in which this is used for this purpose.

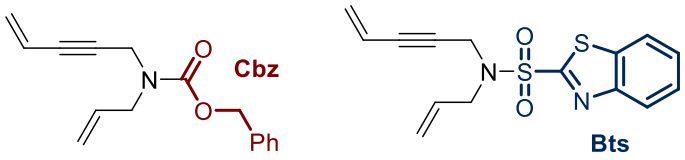

1-235 **1-236**

Figure 57. Structure of enynes with Cbz and Bts protecting groups which could be used in the gold-catalysed cycloisomerisation-reduction reaction.

If no other protecting groups are found to be suitable, it is likely that removal and replacement of the nosyl group would be required. While this would not be advantageous in terms of the number of steps required, it may be possible to do this in one-pot and with high-yields.

Finally, the gold-catalysed cycloisomerisation should be extended to include oxygen-tethered enynes, giving access to the CPP bioisostere. The conditions optimised for nitrogen-tethered enynes may be transferable; however, previous reports have noted a difference in both reactivity and stereochemical outcomes meaning that a separate optimisation may be required. Despite this, the downstream chemistry is expected to remain applicable, and without the issues of protecting group compatibility. Furthermore, the use of tetrahydropyran derivatives in the RAE approaches is well-precedented with good outcomes reported.[128,130,131]

11.2. Optimisation of Downstream Chemistry

The initial results obtained in the cross-couplings of RAE **1-221** (Scheme 83) showed that isolation of the desired cross-coupled product was possible, even in the presence of the nitro group, albeit in low yields. Therefore, it would be of high importance to determine if this reaction could be optimised, alleviating the need for protecting group variation. Both of the approaches reported by Baran were subject to extensive optimisation studies[128,130] and, therefore, exploration of the alternative catalysts, ligands and solvents reported may lead to more useful results. As with gold catalyst exploration (*vide supra*), a high-throughput approach could be implemented to achieve this in a relatively short timeframe. Unfortunately, this was not able to be carried out within this study but would be an area of immediate attention, given additional time.

12. Experimental

12.1. General Experimental

Chemicals were used as received from commercial sources (Sigma Aldrich, Fluorochem, Alfa Aesar, Fisher Scientific) without purification, unless otherwise stated. NMR spectra were recorded on a Bruker AV 700, Bruker AV 500 or a Bruker AV 400. Chemical shifts (δ) are reported in ppm and coupling constants (*J*) are in Hz. The following abbreviations are used for multiplicities: s = singlet; br s = broad singlet; d = doublet; t = triplet; q = quartet; m = multiplet; dd = doublet of doublets; dt = doublet of triplets. Liquid Chromatography Mass Spectrometry (LCMS) methods used for reaction monitoring and final purity analysis are referred to by the modifier used (formic acid, high pH or TFA). The formic acid and high pH analyses were conducted on an Acquity UPLC CSH C18 column (50 mm × 2.1 mm i.d. 1.7 µm packing diameter) at 40 °C using a 2-minute method (see section 12.2 for gradients and solvents). The TFA analysis was conducted on Acquity UPLC BEH C18 column (100 mm × 2.1 mm i.d.1.7 µm packing diameter) at 50 °C using a 10-minute method (see section 12.2 for gradient and solvents). Mass spectra were recorded using a Waters QDA with an alternate-scan positive and negative electrospray ionization with a range of 100-1500 AMU and a frequency of 5 Hz. The UV detection was a summed signal from 210 nm to 350 nm. High Resolution Mass Spectrometry (HRMS) was obtained using a UPLC-HRMS system. The chromatography was conducted on an Acquity UPLC BEH or UPLC CSH C18 column (100mm × 2.1mm i.d. 1.7µm packing diameter) at 50 °C in either a formic acid or high pH modifier (see section 12.2 for gradients and solvents). The UV detection was a summed signal from 210 nm to 500 nm. The HRMS were recorded using a Waters XEVO G2-XS Qtof with positive electrospray ionization mode with a scan range of 100 to 1200 AMU. IR spectra were obtained on a Perkin Elmer Spectrum One spectrometer. Absorption frequencies (ν_{max}) are reported in wavenumbers (cm^{-1}). Mass Directed Auto Purification System (MDAP) was carried out using a Waters ZQ MS using alternate scan positive and negative electrospray and a summed UV wavelength of 210–350 nm. The formic acid method used a Sunfire C18 column (100 mm × 19 mm, 5 µm packing diameter, 20 mL/min flow rate) or Sunfire C18 column (150 mm × 30 mm, 5 µm packing diameter, 40 mL/min flow rate), using a gradient elution at ambient temperature with the mobile phases as (A) H_2O containing 0.1% volume/volume (v/v) formic acid and (B) acetonitrile containing 0.1% (v/v) formic acid. The high pH method used an Xbridge C18 column (100 mm × 19 mm, 5 µm packing diameter, 20 mL/min flow rate) or Xbridge C18 column (150 mm × 30 mm, 5 µm packing diameter, 40 mL/min flow rate), using a gradient elution at ambient temperature with the mobile phases as (A) 10 mM aqueous ammonium bicarbonate solution, adjusted to pH 10 with 0.88 M

aqueous ammonia and (B) acetonitrile. Chiral purification was undertaken using a Chiralpak AD-H column (250 mm × 30 mm) with a flow rate of 30 mL/min for CPP-containing compounds. The solvent was varied and based on initial screening conditions and is specified for each compound. Chiral analysis of cycloisomerised products was carried out using either a Chiralpak AS-H column (50 mm × 4.6 mm, 5 micron) at 25 °C with a flow rate of 1 mL/min and a heptane/ethanol (95:5) eluent over 20 min or using a Chiralpak IG column (250 mm × 4.6 mm, 5 micron) at 25 °C with a flow rate of 1 mL/min and a heptane (+0.1% v/v isopropylamine)/ethanol eluent over 15 min. Detection used a UV diode array at 220 nm and *ee* values were obtained by comparison of the chromatograms obtained for the enantioenriched compound, the racemate and a 1:1 mixture of both with the areas under peaks measured.

The amounts of gold pre-catalysts and silver salts in cycloisomerisation reactions were intended to be used at 10 mol% and 12 mol%, respectively. Due to the small scales employed, the equivalencies may have varied from these values; however, the effect on the reaction outcomes was anticipated to be minimal, unless otherwise indicated. The actual masses of reagents used in the reactions are recorded in the relevant protocols for clarity. The precise amounts are based on those given by the balance used.

QM modelling: dihedral angle scans were obtained using Jaguar software (Schrödinger) with default settings applied.[20,21] DFT with the 6-31G** basis set and B3LYP dispersion correction were used to calculated the relative energies of each conformation.[19-21] Sandeep Pal and Giampaolo Bravi are acknowledged for their input into this work and for running the relevant computations.[19]

TR-FRET assay: inhibition of PI3K enzyme activity was determined using an HTRF assay kit based on the method reported by Gray *et al*.[154] Reactions were performed in an assay buffer containing 50 mM 4-(2-hydroxyethyl)-1-piperazineethanesulfonic acid (HEPES) at pH 7.0, 150 mM NaCl, 10 mM $MgCl_2$, 2.3 mM sodium cholate, 10 μM 3-[(3-Cholamidopropyl)-dimethylammonio]-propane- sulfonate (CHAPS), and 1 mM dithiothreitol. Enzymes were preincubated with compound, serially diluted 4-fold in 100% DMSO, for 15 min prior to initiation of the reaction upon addition of substrate solution containing ATP at the Michaelis constant (K_M) for the specific isoform tested (PI3Kα at 250 μM, PI3Kβ at 400 μM, PI3Kδ at 80 μM, and PI3Kγ at 15 μM), phosphatidylinositol 4,5-bisphosphate (PIP2) at either 5 μM (PI3Kδ) or 8 μM (PI3Kα, β, and γ) and 10 nM biotin-phosphatidylinositol (3,4,5)-trisphosphate (PIP3). Assays were quenched after 60 min by addition of a quench/detection solution prepared in 50 mM HEPES at pH 7.0, 150 mM NaCl,

2.3 mM sodium cholate, 10 μM CHAPS, 30 mM ethylenediaminetetraacetic acid (EDTA), 40 mM potassium fluoride, and 1 mM DTT containing 16.5 nM GRP-1 PH domain, 8.3 nM streptavidin-APC, and 2 nM europium-anti-GST and were left for a further 60 min in the dark to equilibrate prior to reading using a Perkin Elmer EnVision plate reader. These assays were carried out by James Rowedder and Kira Weis.[155]

12.2. LCMS and HRMS Parameters

2 minute UPLC-MS solvents and gradients

For formic acid runs, the solvents employed were:

A. 0.1% v/v solution of formic acid in water
B. 0.1% v/v solution of formic acid in acetonitrile

The gradient was as follows:

Time (min)	Flow rate (mL/min)	% A	% B
0.0	1	97	3
1.5	1	3	97
1.9	1	3	97
2.0	1	98	2

For high pH runs, the solvents employed were:

A. 10 mM ammonium bicarbonate in water adjusted to pH 10 with ammonia solution
B. Acetonitrile

The gradient was as follows:

Time (min)	Flow rate (mL/min)	% A	% B
0.0	1	100	100
0.05	1	100	0
1.5	1	3	97
1.9	1	3	97
2.0	1	100	0

10 minute UPLC-MS solvents and gradients

For TFA runs, the solvents employed were:

A. 0.1% v/v solution of TFA in water
B. 0.1% v/v solution of TFA in acetonitrile

The gradient was as follows:

Time (min)	Flow rate (mL/min)	% A	% B
0.0	0.8	97	3
8.5	0.8	0.1	99.9
9.0	0.8	0.1	99.9
9.5	0.8	97	3
10.0	0.8	97	3

UPLC-HRMS solvents and gradients

For 10 minute formic acid runs, the solvents employed were:

A. 0.1% v/v solution of formic acid in water
B. 0.1% v/v solution of formic acid in acetonitrile

The gradient was as follows:

Time (min)	Flow rate (mL/min)	% A	% B
0.0	0.8	95	5
8.5	0.8	7	93
9.0	0.8	7	93
9.5	0.8	95	5
10.0	0.8	95	5

For 20 minute high pH runs, the solvents employed were:

A. 10 mM ammonium bicarbonate in water adjusted to pH 10 with ammonia solution
B. Acetonitrile

The gradient was as follows:

Time (min)	Flow rate (mL/min)	% A	% B
0.0	0.8	99	1
0.5	0.8	99	1
17.0	0.8	10	90
18.5	0.8	10	90
19.0	0.8	99	1
20.0	0.8	99	1

12.3. Tool Compounds for Conformational Studies

tert-Butyl(3-(furan-2-yl)phenoxy)dimethylsilane (1-54)

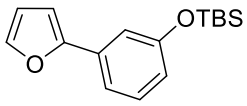

(3-((*tert*-Butyldimethylsilyl)oxy)phenyl)boronic acid (1.05 g, 4.16 mmol), 2-bromofuran **1-44** (559 mg, 3.80 mmol), $PdCl_2(dppf)\cdot CH_2Cl_2$ (296 mg, 0.362 mmol) and K_2CO_3 (1.56 g, 11.3 mmol) were dissolved in ^{i}PrOH (10 mL) and water (2.5 mL). This was degassed for 10 min and purged with nitrogen before being stirred at 60 °C for 4 h. The reaction mixture was then cooled to RT and filtered through celite, which was washed with DCM (30 mL). The filtrate was collected and washed with saturated aqueous sodium bicarbonate (30 mL), water (50 mL) and brine (30 mL). The organic layer was collected, filtered through a hydrophobic frit and concentrated *in vacuo* yielding a black residue. This was purified using a C18 column (water + 0.1% formic acid / MeCN + 0.1% formic acid 70-95%) to give **1-54** as a brown oil (577 mg, 2.10 mmol, 55%). ^{1}H NMR (400 MHz, DMSO-d_6) δ = 7.73 (dd, *J* = 0.7, 1.7 Hz, 1H), 7.32 - 7.29 (m, 2H), 7.13 (m, 1H), 6.94 (dd, *J* = 0.7, 3.4 Hz, 1H), 6.77 (ddd, *J* = 2.7, 2.7, 6.1 Hz, 1H), 6.58 (dd, *J* = 2.0, 3.4 Hz, 1H), 0.97 (s, 9H), 0.21 (s, 6H); ^{13}C NMR (101 MHz, DMSO-d_6) δ = 155.5, 152.5, 142.9, 131.7, 130.1, 118.9, 116.8, 114.6, 112.0, 106.1, 25.5, 17.9, -4.6; LCMS (formic acid) t_R = 1.65 min, [M+H$^+$] mass ion not observed (100% purity); HRMS [M+H$^+$] calculated for $C_{16}H_{23}O_2Si$ 275.1462, found [M+H$^+$] 275.1461; IR (neat) ν_{max} = 2930, 2859, 1486, 1294, 779 cm^{-1}.

(3-(5-Bromofuran-2-yl)phenoxy)(*tert*-butyl)dimethylsilane (1-55)

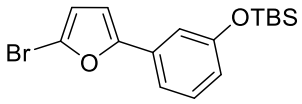

tert-Butyl(3-(furan-2-yl)phenoxy)dimethylsilane **1-54** (1.42 g, 5.17 mmol) was dissolved in THF (30 mL) and cooled to 0 °C. To this was added NBS (952 mg, 5.35 mmol) and the reaction stirred at 0 °C for 2 h. The reaction was quenched with saturated sodium bicarbonate (30 mL). This was then washed with EtOAc (3 × 70 mL). The organics were combined, dried using a hydrophobic frit and concentrated *in vacuo* yielding a brown oil. This was purified by flash column chromatography (cyclohexane 100%) to give **1-55** as a yellow oil (1.52 g, 4.30 mmol, 83%). ^{1}H NMR (400 MHz, DMSO-d_6) δ = 7.32 (dd, *J* = 7.8, 7.8 Hz, 1H), 7.28 (ddd, *J* = 1.5, 1.5, 7.8 Hz, 1H), 7.09 (dd, *J* = 2.0, 2.0 Hz, 1H), 7.03 (d, *J* = 3.7 Hz, 1H), 6.81 (ddd, *J* = 1.3, 2.4, 7.8 Hz, 1H), 6.70 (d, *J* = 3.4 Hz, 1H), 0.99 - 0.95 (m, 9H), 0.23 - 0.21 (m, 6H); ^{13}C NMR (101 MHz, DMSO-d_6) δ = 156.1, 155.3, 131.2, 130.8, 121.8, 119.9, 117.0, 114.9, 114.5, 109.4, 26.0, 18.4, -4.0; LCMS (formic acid) t_R = 1.74 min, [M+H$^+$] mass ion not seen (100% purity); HRMS [M+H$^+$] calculated for $C_{16}H_{22}{}^{79}BrO_2Si$ 353.0567, found [M+H$^+$] 353.0567; IR (neat) ν_{max} = 2929, 2853, 1471, 1213, 775 cm^{-1}.

2-(3-oxabicyclo[4.1.0]heptan-6-yl)-4,4,5,5-tetramethyl-1,3,2-dioxaborolane (1-57)

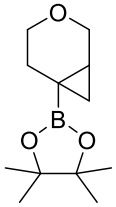

Preparation reported in Hobbs *et al*.[2]

A solution of 2-(3,6-dihydro-2*H*-pyran-4-yl)-4,4,5,5-tetramethyl-1,3,2-dioxaborolane **1-56** (1.10 g, 5 mmol) in fluorobenzene (10 mL) was cooled to -5 °C and was treated slowly with diethylzinc in hexanes (1 M, 25.0 mL, 25.0 mmol) over 2 min. The mixture was stirred at -5 °C for 5 min prior to treating with a solution of chloroiodomethane (8.82 g, 50.0 mmol) in fluorobenzene (5.0 mL) dropwise over 5 min. The mixture was stirred at -5 °C for 10 min prior to three subsequent additions of diethylzinc and chloroiodomethane in the same manner. The reaction mixture was allowed to warm to RT and stirred for 16 h. The suspension was partitioned between aqueous ammonium chloride (75 mL) and diethyl ether (2 × 50 mL) and then dried over $MgSO_4$. The extract was purified by flash column chromatography to give **1-57** (485 mg, 2.164 mmol, 43%). ^{1}H NMR (400 MHz, $CDCl_3$) δ = 3.99 (d, *J* = 11.2 Hz, 1H),

3.82 (dd, *J* = 3.5, 11.4 Hz, 1H), 3.58 (ddd, *J* = 2.6, 6.4, 11.4 Hz, 1H), 3.14 (ddd, *J* = 4.6, 11.2, 11.2 Hz, 1H), 2.02 (m, 1H), 1.65 (m, 1H), 1.21 (s, 12H), 1.07 (m, 1H), 0.94 (dd, *J* = 3.2, 8.3 Hz, 1H), 0.64 (dd, *J* = 3.3, 5.7 Hz, 1H); ^{13}C NMR (101 MHz, $CDCl_3$) δ = 83.2, 65.5, 64.7, 24.7, 24.7, 17.2, 16.2 ***1C not observed***.

Potassium (3-oxabicyclo[4.1.0]heptan-6-yl)trifluoroborate (1-58)

Preparation as in Hobbs *et al* with consistent values reported.[2]

2-(3-Oxabicyclo[4.1.0]heptan-6-yl)-4,4,5,5-tetramethyl-1,3,2-dioxaborolane **1-57** (5.04 g, 22.3 mmol) was dissolved in MeCN (55 mL) and MeOH (55 mL) under a nitrogen atmosphere. Aqueous potassium fluoride (5.23 g, 90.0 mmol) in water (20 mL) was added, and the suspension stirred at RT for 10 min. (2*R*,3*R*)-2,3-dihydroxysuccinic acid (6.69 g, 44.6 mmol) was added followed by THF (2.5 mL). The reaction mixture was stirred for 1.25 h and left standing overnight, after which the precipitate was filtered off and washed with MeCN. The filtrate was concentrated *in vacuo* and azeotroped with toluene (3 × 50 mL) and triturated with diethyl ether (3 × 30 mL) to give **1-58** (4.83 g, 23.7 mmol, 106%). ^{1}H NMR (400 MHz, DMSO-d_6) δ = 3.73 (d, *J* = 11.5 Hz, 1H), 3.66 (dd, *J* = 4.2, 10.8 Hz, 1H), 3.29 (m, 1H), 2.98 (ddd, *J* = 4.9, 10.4, 10.4 Hz, 1H), 1.70 (ddd, *J* = 4.2, 4.2, 13.8 Hz, 1H), 1.31 (ddd, *J* = 5.7, 9.8, 13.8 Hz, 1H), 0.49 (m, 1H), 0.28 (br d, *J* = 7.3 Hz, 1H), -0.13 (br s, 1H); ^{13}C NMR (101 MHz, DMSO-d_6) δ = 66.9, 64.6, 26.9, 25.4, 14.7, 13.1.

3-(5-(3-Oxabicyclo[4.1.0]heptan-6-yl)furan-2-yl)phenol (1-31)

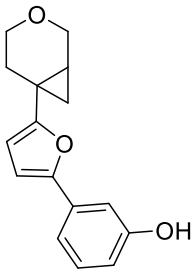

(3-(5-Bromofuran-2-yl)phenoxy)(*tert*-butyl)dimethylsilane **1-55** (85.0 mg, 0.241 mmol), (3-potassium 3-oxabicyclo[4.1.0]heptan-6-yltrifluoroborate **1-58** (61.0 mg, 0.299 mmol), $Pd(OAc)_2$ (9.0 mg, 0.04 mmol), cataCXium® A (29.0 mg, 0.081 mmol) and Cs_2CO_3 (240 mg, 0.737 mmol) were added to a microwave vial and dissolved in toluene (1.1 mL) and water (0.11 mL). This was degassed for 10 min before being heated to 100 °C for 2 h. The reaction mixture was cooled and partitioned between water (10 mL) and DCM (10 mL). The layers

were separated and the aqueous phase washed with further potions of DCM (2 × 10 mL). The organics were combined, filtered through a hydrophobic frit and concentrated *in vacuo* yielding an orange oil. The oil was dissolved in THF (3.0 mL) and to this was added TBAF (1 M in THF, 0.241 mL, 0.241 mmol). This was stirred at RT for 40 min before water (15 mL) and DCM (50 mL) were added to the reaction mixture and the layers were separated. The aqueous phase was washed with DCM (2 × 10 mL) and the organics were combined, filtered through a hydrophobic frit and concentrated *in vacuo* yielding a yellow residue. This was purified using a C18 column (water + 0.1% formic acid / MeCN + 0.1% formic acid 30-85%) giving **1-31** as a yellow solid (16.0 mg, 0.062 mmol, 26%). This was recrystallised from hot toluene to give a product suitable for X-ray crystallography. M.pt. 120-122 °C; ^{1}H NMR (400 MHz, $CDCl_3$) δ = 7.24 (t, *J* = 7.8 Hz, 1H), 7.18 (ddd, *J* = 1.2, 1.2, 7.6 Hz, 1H), 7.10 (dd, *J* = 1.6, 2.6 Hz, 1H), 6.71 (ddd, *J* = 1.1, 2.6, 7.8 Hz, 1H), 6.56 (d, *J* = 3.4 Hz, 1H), 6.08 (d, *J* = 3.4 Hz, 1H), 5.04 - 4.95 (m, 1H), 4.03 - 3.96 (m, 2H), 3.74 - 3.67 (m, 1H), 3.48 - 3.40 (m, 1H), 2.29 (ddd, *J* = 4.4, 4.4, 14.2 Hz, 1H), 2.13 (ddd, *J* = 5.9, 9.8, 14.2 Hz, 1H), 1.56 - 1.50 (m, 1H), 1.36 (dd, *J* = 4.3, 9.2 Hz, 1H), 1.04 (dd, *J* = 4.4, 6.1 Hz, 1H); ^{13}C NMR (101 MHz, $CDCl_3$) δ = 159.3, 155.8, 151.4, 132.5, 129.9, 116.0, 113.8, 110.1, 106.3, 105.2, 65.4, 64.0, 26.8, 19.8, 18.8, 16.6; LCMS (formic acid) t_R = 1.09 min, [M+H$^+$] 257.1 (100% purity); HRMS [M+H$^+$] calculated for $C_{16}H_{17}O_3$ 257.1172, found [M+H$^+$] 257.1172; IR (neat) ν_{max} = 3219, 2862, 1446, 771 cm^{-1}.

The enantiomers of this compound were separated to enable crystal structures to be obtained of each. The conditions used were 20% EtOH (+0.2% isopropylamine)/heptane (+0.2% isopropylamine), f = 30 mL/min. Column 30 mm × 25 cm Chiralpak AD-H.[50]

Enantiomer 1, (+)-1-31 (1*R*, 6*S*) $[\alpha_D]^{20}$ (0.190 g/100 mL, MeOH) = +84.2 °. t_R = 9.95 min.

Enantiomer 2, (-)-1-31 (1*S*, 6*R*) $[\alpha_D]^{20}$ (0.150 g/100 mL, MeOH) = -80.0 °. t_R = 12.04 min.

Enantiomer structures confirmed by X-ray crystallography.

3-(5-(3,6-Dihydro-2*H*-pyran-4-yl)furan-2-yl)phenol (1-32)

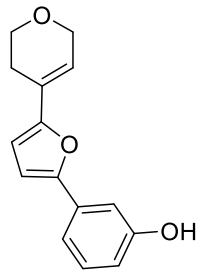

$PdCl_2(dppf)\cdot CH_2Cl_2$ (76.0 mg, 0.093 mmol), 2-(3,6-dihydro-*2H*-pyran-4-yl)-4,4,5,5-tetramethyl-1,3,2-dioxaborolane **1-56** (211 mg, 1.00 mmol), (3-(5-bromofuran-2-yl)phenoxy)(tert-butyl)dimethylsilane **1-55** (322 mg, 0.911 mmol) and K_2CO_3 (355 mg, 2.57 mmol) were dissolved in water (0.85 mL) and ^{i}PrOH (3.4 mL). The solution was degassed for 10 min before being put under an inert atmosphere and heated to 60 °C for 2 h. The reaction mixture was cooled to RT and filtered through celite which was washed with DCM (20 mL). The filtrate was collected and washed with water (20 mL). The layers were separated, and the aqueous phase washed with DCM (2 × 20 mL). The organics were combined, dried using a hydrophobic frit and concentrated *in vacuo* yielding a black oil. The oil was dissolved in THF (5.0 mL) and TBAF (1 M in THF, 1.00 mL, 1.00 mmol) added before being stirred for 1 h at RT. Water (10 mL) and DCM (10 mL) were added and the layers separated. The aqueous phase was washed with DCM (2 × 10 mL) and the organics were combined, dried using a hydrophobic frit and concentrated *in vacuo* yielding a black oil which was purified by reverse-phase purification on a C18 column (water + 0.1% formic acid / MeCN + 0.1% formic acid 35-85%) yielding a brown solid which was further purified using flash chromatography (cyclohexane/EtOAc 0-100%). **1-32** was obtained as a white solid (67.0 mg, 0.277 mmol, 30%). This was recrystallised from hot toluene to give a product suitable for X-ray crystallography. M.pt. 167-170 °C; ^{1}H NMR (400 MHz, $CDCl_3$) δ = 7.26 - 7.24 (m, 2H), 7.18 - 7.16 (m, 1H), 6.73 (m, 1H), 6.64 (d, *J* = 3.4 Hz, 1H), 6.35 (m, 1H), 6.30 (d, *J* = 3.7 Hz, 1H), 4.75 (s, 1H), 4.39 (appt. q, *J* = 2.7 Hz, 2H), 3.93 (appt. t, *J* = 5.5 Hz, 2H), 2.50 – 2.45 (m, 2H); ^{13}C NMR (151 MHz, $CDCl_3$) δ = 155.8, 153.4, 152.4, 132.3, 130.0, 124.9, 120.2, 116.5, 114.3, 110.5, 107.0, 106.8, 65.4, 64.0, 25.0; LCMS (formic acid) t_R = 1.03 min, [M+H$^+$] 243.1 (100% purity); HRMS [M+H$^+$] calculated for $C_{15}H_{15}O_3$ 243.1016, found [M+H$^+$] 243.1025; IR (neat) ν_{max} = 3311, 2824, 1219, 1117, 792 cm^{-1}.

3-(5-(Tetrahydro-2*H*-pyran-4-yl)furan-2-yl)phenol (1-33)

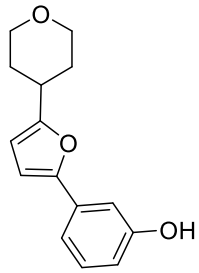

To an oven-dried microwave vial was added 2-(3,6-dihydro-2*H*-pyran-4-yl)-4,4,5,5-tetramethyl-1,3,2-dioxaborolane **1-56** (179 mg, 0.85 mmol), XPhos Pd G2 (15.0 mg, 0.019 mmol), Pd/C (89.0 mg, 0.084 mmol), K_3PO_4 (753 mg, 3.55 mmol) and (3-(5-bromofuran-2-yl)phenoxy)(*tert*-butyl)dimethylsilane **1-55** (253 mg, 0.716 mmol). The vial was capped and purged with nitrogen before 1,4-dioxane (2.2 mL) and water (0.55 mL) were added. The reaction mixture was stirred at 60 °C for 2.5 h before being cooled to RT. Ammonium formate (158 mg, 2.51 mmol) in MeOH (2.0 mL) was added and the reaction stirred at RT for 24 h. The reaction was diluted in EtOAc and filtered through celite which was rinsed with further EtOAc. The filtrate and washings were collected, dried using a hydrophobic frit and concentrated *in vacuo* yielding a pale-yellow residue. This was dissolved in THF (2.0 mL) and TBAF (1 M in THF, 1.40 mL, 1.40 mmol) added. The reaction was stirred for 30 min before being diluted with EtOAc (20 mL) and water (20 mL). The layers were separated, and the aqueous phase washed with EtOAc (2 × 20 mL). The organics were combined, dried using a hydrophobic frit and concentrated *in vacuo* yielding a brown oil, which was purified using flash chromatography (cyclohexane/EtOAc 0-100%) yielding **1-33** as a white solid (91.0 mg, 0.373 mmol, 52%). This was recrystallised from hot toluene to give a product suitable for X-ray crystallography. M.pt. 148-150 °C; ^{1}H NMR (400 MHz, DMSO-d_6) δ = 9.46 (s, 1H), 7.19 (t, *J* = 7.8 Hz, 1H), 7.08 (m, 1H), 7.04 (m, 1H), 6.74 (d, *J* = 3.4 Hz, 1H), 6.66 (ddd, *J* = 1.0, 2.4, 8.1 Hz, 1H), 6.21 (dd, *J* = 1.0, 3.2 Hz, 1H), 3.94 – 3.88 (m, 2H), 3.46 (td, *J* = 2.2, 11.5, 11.5 Hz, 2H), 2.96 (tt, *J* = 3.7, 3.7, 11.3, 11.3 Hz, 1H), 1.94 - 1.85 (m, 2H), 1.72 - 1.57 (m, 2H); ^{13}C NMR (101 MHz, DMSO-d_6) δ = 158.9, 158.1, 151.9, 132.2, 130.3, 114.7, 114.6, 110.2, 106.7, 106.3, 66.9, 34.2, 31.4; LCMS (formic acid) t_R = 1.01 min, [M+H$^+$] 245.2 (100% purity); HRMS [M+H$^+$] calculated for $C_{15}H_{17}O_3$ 245.1172, found [M+H$^+$] 245.1181; IR (neat) ν_{max} = 3201, 2937, 784 cm^{-1}.

tert-Butyl 2-(3-((tert-butyldimethylsilyl)oxy)phenyl)-1*H*-pyrrole-1-carboxylate (1-64)

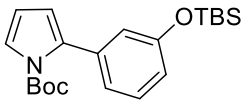

(3-Bromophenoxy)(*tert*-butyl)dimethylsilane **1-63** (2.22 g, 7.73 mmol), *N*-Boc-pyrrole-2-boronic acid MIDA ester **1-63** (2.12 g, 6.58 mmol), SPhos (390 mg, 0.950 mmol) and $Pd(OAc)_2$ (92.0 mg, 0.410 mmol) were added to a microwave vial. This was sealed and put under an inert atmosphere. 1,4-Dioxane (40 mL) was added and the reaction mixture stirred at RT for 10 min. A degassed solution of K_3PO_4 (3 M aqueous, 6.20 mL, 18.6 mmol) was added and the reaction mixture warmed to 60 °C. This was stirred for 23 h before being cooled to RT and filtered through celite, which was washed with DCM (50 mL). The filtrate was collected and washed with water (100 mL). The layers were separated, and the aqueous phase washed with DCM (2 × 100 mL). The organics were combined, dried using a hydrophobic frit and concentrated *in vacuo* yielding a brown oil which was purified using flash column chromatography (cyclohexane/EtOAc 0% then 0-10%) giving **1-64** as a colourless oil (1.56 g, 4.18 mmol, 64%). ^{1}H NMR (400 MHz, DMSO-d_6) δ = 7.33 (dd, *J* = 2.0, 3.2 Hz, 1H), 7.25 (dd, *J* = 7.8, 7.8 Hz, 1H), 6.92 (m, 1H), 6.81 (ddd, *J* = 1.0, 2.4, 8.1 Hz, 1H), 6.76 (m, 1H), 6.28 - 6.24 (m, 2H), 1.34 (s, 9H), 0.96 (s, 9H), 0.20 (s, 6H); ^{13}C NMR (101 MHz, DMSO-d_6) δ = 154.9, 149.2, 135.5, 134.5, 129.3, 123.2, 122.5, 120.7, 118.9, 114.8, 111.2, 84.0, 27.6, 26.0, 18.4, -4.1; LCMS (formic acid) t_R = 1.74 min, [M+H$^+$] 374.3 (97% purity); HRMS [M+H$^+$] calculated for $C_{21}H_{32}NO_3Si$ 374.2146, found [M+H$^+$] 374.2150; IR (neat) ν_{max} = 2930, 2859, 1738, 1310, 1141 cm^{-1}.

tert-Butyl 2-bromo-5-(3-((*tert*-butyldimethylsilyl)oxy)phenyl)-1*H*-pyrrole-1-carboxylate (1-65)

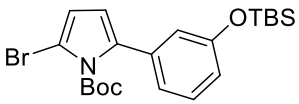

tert-Butyl 2-(3-((*tert*-butyldimethylsilyl)oxy)phenyl)-1*H*-pyrrole-1-carboxylate **1-64** (696 mg, 1.86 mmol) was dissolved in THF and cooled to -78 °C. To this was added NBS (348 mg, 1.96 mmol) in portions of 116 mg every 30 min. The reaction mixture was stirred for 1 h after the final addition before being warmed to 0 °C and stirred for an extra 1 h. Additional NBS (100 mg, 0.563 mmol) was added and the reaction mixture stirred for 30 min. The reaction mixture was then quenched with saturated aqueous sodium bicarbonate (10 mL) and warmed to RT. This was diluted with water (20 mL) and EtOAc (40 mL). The layers were

separated, and the aqueous phase washed with EtOAc (2 × 40 mL). The organic layers were combined, dried using a hydrophobic frit and concentrated in vacuo yielding a brown residue which was purified by flash column chromatography (cyclohexane/EtOAc 0-10%). **1-65** was obtained as a yellow oil (525 mg, 1.16 mmol, 62%). ^{1}H NMR (400 MHz, $CDCl_3$) δ = 7.25 - 7.20 (m, 1H), 6.90 (ddd, *J* = 1.2, 1.2, 7.9 Hz, 1H), 6.83 - 6.79 (m, 2H), 6.32 (d, *J* = 3.4 Hz, 1H), 6.18 (d, *J* = 3.4 Hz, 1H), 1.37 (s, 9H), 1.02 - 1.00 (m, 9H), 0.23 - 0.21 (m, 6H); ^{13}C NMR (101 MHz, $CDCl_3$) δ = 155.4, 148.6, 136.5, 135.3, 128.9, 121.2, 119.9, 118.9, 114.8, 112.6, 102.0, 85.0, 27.3, 25.6, 18.2, -4.4; LCMS (formic acid) t_R = 1.79 min, [M+H$^+$] 452.3 and 454.3 (89% purity); HRMS [M+H$^+$] calculated for $C_{21}H_{31}{}^{79}BrNO_3Si$ 452.1251, found [M+H$^+$] 452.1256; IR (neat) ν_{max} = 2931, 2857, 1755, 1297 cm^{-1}.

3-(5-(3-oxabicyclo[4.1.0]heptan-6-yl)-1*H*-pyrrol-2-yl)phenol (1-34)

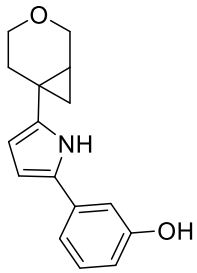

tert-Butyl 2-bromo-5-(3-((*tert*-butyldimethylsilyl)oxy)phenyl)-1*H*-pyrrole-1-carboxylate **1-65** (370 mg, 0.818 mmol), potassium 3-oxabicyclo[4.1.0]heptan-6-yltrifluoroborate **1-58** (399 mg, 1.96 mmol), cataCXium® A Pd G3 (37.0 mg, 0.051 mmol) and Cs_2CO_3 (884 mg, 2.71 mmol) were added to a microwave vial and dissolved in toluene (16 mL) and water (1.6 mL). This was degassed for 10 min before being purged with nitrogen and heated to 90 °C for 14 h. The reaction was cooled and filtered through celite, which was washed with EtOAc (20 mL). This filtrate was diluted with water (20 mL) and the layers separated. The aqueous phase was washed with EtOAc (2 × 20 mL) and the organics combined, dried using a hydrophobic frit and concentrated *in vacuo* yielding a yellow oil. This was dissolved in TBAF (1 M in THF, 5.00 mL, 5.00 mmol) and stirred at RT for 1 h before water (20 mL) and EtOAc (20 mL) were added to the reaction mixture and the layers separated. The aqueous phase was washed with a further portion of EtOAc (20 mL). The organics were combined, dried using a hydrophobic frit and concentrated *in vacuo* to give a brown oil which was purified using a C18 column (water/MeCN + 0.1% ammonium bicarbonate 30-85%) yielding a brown residue. To this was added water (15 mL) and the reaction heated to 100 °C for 2 h before MeCN (5.0 mL) was added to the reaction and this stirred at 100 °C for 5 h. The reaction mixture was then concentrated *in vacuo* yielding **1-34** as an off-white solid (61.0 mg, 0.239 mmol, 29%). This was recrystallised using vapour diffusion of toluene into MeCN to give

crystals suitable for X-ray crystallography. M.pt. 178-180 °C; ^{1}H NMR (600 MHz, CD_3CN) δ = 9.18 (br s, 1H), 7.19 (dd, *J* = 7.9, 7.9 Hz, 1H), 7.07 (m, 1H), 7.00 (t, *J* = 2.0 Hz, 1H), 6.86 (s, 1H), 6.64 (m, 1H), 6.32 (m, 1H), 5.92 (dd, *J* = 2.6, 3.3 Hz, 1H), 3.99 (dd, *J* = 4.0, 11.4 Hz, 1H), 3.86 (dd, *J* = 0.7, 11.4 Hz, 1H), 3.55 (m, 1H), 3.44 (ddd, *J* = 5.7, 8.7, 11.6 Hz, 1H), 2.12 - 2.09 (m, 2H), 1.34 (m, 1H), 1.11 (dd, *J* = 4.2, 9.0 Hz, 1H), 0.87 (dd, *J* = 4.4, 5.9 Hz, 1H); ^{13}C NMR (151 MHz, CD_3CN) δ = 158.6, 141.3, 136.1, 132.1, 131.2, 116.8, 113.8, 111.7, 107.1, 107.0, 66.5, 64.8, 30.7, 20.5, 19.3, 17.3; LCMS (high pH) t_R = 0.99 min, [M+H$^+$] 256.2 (100% purity); HRMS [M+H$^+$] calculated for $C_{16}H_{18}NO_2$ 256.1332, found [M+H$^+$] 256.1342; IR (neat) ν_{max} = 3340, 3284, 2852, 776 cm^{-1}.

The enantiomers of this compound were separated to enable crystal structures to be obtained of each. The conditions used were 20% EtOH (+0.2% isopropylamine)/heptane, f = 30 mL/min, column 30 mm × 25 cm Chiralpak AD-H.[50]

Enantiomer 1, (-)-1-34, (1*R*, 6*S*) $[\alpha_D]^{20}$ (1.00 g/100 mL, MeOH) = -16.0 °; t_R = 20.10 min

Enantiomer 2, (+)-1-34, (1*S*, 6*R*) $[\alpha_D]^{20}$ (1.00 g/100 mL, MeOH) = +16.0 °; t_R = 23.43 min

3-(5-(3,6-Dihydro-2*H*-pyran-4-yl)-1*H*-pyrrol-2-yl)phenol (1-35)

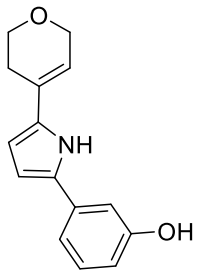

$PdCl_2$(dppf)·CH_2Cl_2 (96.0 mg, 0.118 mmol), *tert*-butyl 2-bromo-5-(3-((*tert*-butyldimethylsilyl)oxy)phenyl)-1*H*-pyrrole-1-carboxylate **1-65** (443 mg, 0.979 mmol), 2-(3,6-dihydro-2*H*-pyran-4-yl)-4,4,5,5-tetramethyl-1,3,2-dioxaborolane **1-56** (275 mg, 1.31 mmol) and K_2CO_3 (465 mg, 3.36 mmol) were dissolved in 1,4-dioxane (4.0 mL) and water (1.0 mL). This was degassed for 10 min before being purged with nitrogen and heated to 60 °C for 16 h. The reaction mixture was cooled to RT before being filtered through celite, which was washed with DCM. The filtrate and washings were collected and washed with water (20 mL). The layers were separated, and the aqueous phase washed with DCM (2 × 20 mL). The organics were combined, dried using a hydrophobic frit and concentrated *in vacuo* yielding a brown oil which was dissolved in TBAF (1 M in THF, 10.0 mL, 10.0 mmol) and stirred at RT for 30 min. Water (20 mL) and DCM (20 mL) were added to the reaction and the layers separated. The aqueous phase was washed with DCM (2 × 20 mL) and the organics were

combined, dried using a hydrophobic frit and concentrated *in vacuo* yielding a yellow oil which was purified using a KP-NH flash column (cyclohexane/EtOAc 0-100%) to give a yellow oil. This was dissolved in water (8 mL) and acetonitrile (3 mL) and heated to 100 °C for 3 h before being cooled to RT and concentrated *in vacuo* yielding a brown solid. This was purified using Combiflash EZ Prep with a XSelect® CSH™ Prep C18 5 µm OBD™ column (MeCN / Water + 0.1% ammonium bicarbonate 15-75%) to give **1-35** as a yellow solid (71.0 mg, 0.293 mmol, 30%). The solid was recrystallised by vapour diffusion using DCM and toluene for 4 days to give pale yellow crystals suitable for X-ray crystallography. M.pt. 146-149 °C ^{1}H NMR (400 MHz, CD_3CN) δ = 9.34 (m, 1H), 7.22 (t, *J* = 7.6 Hz, 1H), 7.14 (m, 1H), 7.07 (m, 1H), 6.91 (s, 1H), 6.69 (ddd, *J* = 1.0, 2.4, 7.8 Hz, 1H), 6.46 (dd, *J* = 2.6, 3.6 Hz, 1H), 6.22 (m, 1H), 6.09 (m, 1H), 4.28 (appt. q, *J* = 2.7 Hz, 2H), 3.87 (dd, *J* = 5.5, 5.5 Hz, 2H), 2.49 – 2.43 (m, 2H); ^{13}C NMR ***weak sample, only 12 Cs visible and most quaternary Cs not observed*** (101 MHz, CD_3CN) δ = 134.1, 133.6, 129.8, 126.3, 115.9, 113.0, 110.8, 106.9, 106.8, 65.0, 63.8, 25.9; LCMS (high pH) t_R = 0.94 min, [M+H$^+$] 242.3 (100% purity); HRMS [M+H$^+$] calculated for $C_{15}H_{16}NO_2$ 242.1176, found [M+H$^+$] 242.1180; IR (neat) ν_{max} = 3426, 3278, 2820, 1594, 1459, 774 cm^{-1}.

3-(5-(tetrahydro-2*H*-pyran-4-yl)-1*H*-pyrrol-2-yl)phenol (1-36)

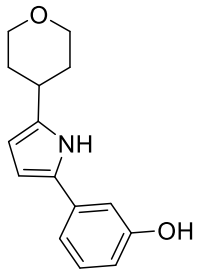

Pd/C (14 mg, 0.013 mmol) and 3-(5-(3,6-dihydro-2*H*-pyran-4-yl)-1*H*-pyrrol-2-yl)phenol **1-35** (32.0 mg, 0.133 mmol) in EtOAc (5.0 mL) were added to one chamber of the CoWare. To the other chamber was added zinc (454 mg, 6.94 mmol). The apparatus was put under a nitrogen atmosphere before 2 M aqueous HCl solution 7.00 mL, 14.0 mmol) was added to the chamber containing zinc. This was stirred at RT for 2.5 h before the reaction mixture was filtered through celite, which was washed with EtOAc. The washings were collected and concentrated *in vacuo* yielding a brown residue which was purified using MDAP (high pH) on Xselect CSH C18 column (water + 0.1% ammonium bicarbonate / MeCN 15-55%). The solvent was removed *in vacuo* to give **1-36** as a white solid (15.1 mg, 0.062 mmol, 47%). ^{1}H NMR (400 MHz, CD_3CN) δ = 9.27 (br s, 1H), 7.19 (t, *J* = 7.8 Hz, 1H), 7.05 (ddd, *J* = 1.0, 1.7, 7.8 Hz, 1H), 6.99 (m, 1H), 6.64 (ddd, *J* = 1.0, 2.4, 8.1 Hz, 1H), 6.37 (m, 1H), 5.93 (m, 1H), 4.02-3.95 (m, 2H), 3.49 (dt, *J* = 2.2, 11.7 Hz, 2H), 2.88 (tt, *J* = 3.7, 11.8 Hz, 1H), 1.93-

1.85 (m, 2H), 1.79 - 1.66 (m, 2H) ***1 exchangeable proton not observed***; ^{13}C NMR (101 MHz, CD_3CN) δ = 158.7, 139.9, 136.1, 131.8, 131.2, 116.6, 113.8, 111.6, 107.1, 106.2, 68.8, 35.5, 34.3; LCMS (high pH) t_R = 0.92 min, [M+H$^+$] 244.2 (100% purity); HRMS [M+H$^+$] calculated for $C_{15}H_{18}NO_2$ 244.1332, found [M+H$^+$] 244.1343; IR (neat) ν_{max} = 3293, 2941, 2847, 761 cm^{-1}.

tert-butyl 2-(4-aminophenyl)-1*H*-pyrrole-1-carboxylate (1-70)

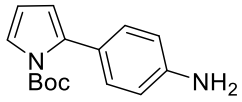

4-Bromoaniline (481 mg, 2.80 mmol), *N*-Boc-pyrrole-2-boronic acid MIDA ester **1-63** (519 mg, 1.611 mmol), SPhos (77.0 mg, 0.188 mmol) and $Pd(OAc)_2$ (27.0 mg, 0.120 mmol) were added to a microwave vial. This was sealed and put under a nitrogen atmosphere. 1,4-Dioxane (9.4 mL) was added and the reaction stirred at RT for 10 min. A degassed solution of K_3PO_4 (3 M aqueous, 1.60 mL, 4.80 mmol) was added and the reaction mixture warmed to 60 °C. This was stirred for 42 h before being cooled to RT and filtered through celite, which was washed with DCM. The filtrate was collected and washed with water (30 mL) and the layers separated. The aqueous phase washed with DCM (2 × 30 mL) and the organics were combined, dried using a hydrophobic frit and concentrated *in vacuo* yielding a brown oil. This was purified by flash column chromatography (cyclohexane/EtOAc 0-80%) to give **1-70** as a yellow oil containing impurities. The oil was then purified using a reverse phase column (KP-C18, acetonitrile/water + 0.1% ammonium carbonate 30-85%) to give **1-70** as a white amorphous solid (229 mg, 0.886 mmol, 55%). ^{1}H NMR (400 MHz, $CDCl_3$) δ = 7.32 (dd, *J* = 1.8, 3.3 Hz, 1H), 7.19 - 7.14 (m, 2H), 6.72 - 6.67 (m, 2H), 6.21 (dd, *J* = 3.3, 3.3 Hz, 1H), 6.13 (dd, *J* = 1.8, 3.3 Hz, 1H), 3.75 (br s, 2H), 1.42 (s, 9H); ^{13}C NMR (101 MHz, $CDCl_3$) δ = 145.5, 135.4, 130.3, 124.8, 121.9, 114.3, 113.6, 110.4, 83.3, 27.7; LCMS (high pH) t_R = 1.19 min, [M+H$^+$] 259.2 (purity 100%); HRMS [M+H$^+$] calculated for $C_{15}H_{19}N_2O_2$ 259.1441, found [M+H$^+$] 259.1445; IR (neat) ν_{max} = 3456, 3368, 2979, 1737, 1334, 1146 cm^{-1}.

tert-Butyl 2-(4-(3-ethylureido)phenyl)-1*H*-pyrrole-1-carboxylate (1-71)

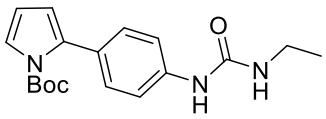

tert-Butyl 2-(4-aminophenyl)-1*H*-pyrrole-1-carboxylate **1-70** (229 mg, 0.886 mmol) was dissolved in DCM (5.0 ml). To this was added pyridine (0.220 mL, 2.72 mmol) and 4-nitrophenyl carbonochloridate (213 mg, 1.06 mmol) and the reaction put under a nitrogen

atmosphere and stirred at RT for 30 min. DIPEA (0.230 mL, 1.317 mmol) and ethanamine (2 M in THF, 2.20 mL, 4.44 mmol) were then added to the reaction mixture which was stirred at RT for a further 1.5 h. The reaction mixture was then diluted with DCM (30 mL) and washed with saturated aqueous sodium bicarbonate (4 × 50 mL). The aqueous layers were combined and washed with DCM (100 mL). The organics were then combined, dried using a hydrophobic frit and concentrated *in vacuo* to yield a yellow oil. This was dissolved in the minimum amount of DCM and pentane added until a precipitate had formed, giving both a yellow oil and off-white solid. This was dried under a flow of nitrogen at RT before being triturated with diethyl ether until no yellow colour remained in the solid to give **1-71** as an amorphous white solid (193 mg, 0.586 mmol, 66%). ^{1}H NMR (400 MHz, DMSO-d_6) δ = 8.45 (s, 1H), 7.38 (d, *J* = 8.8 Hz, 2H), 7.29 (dd, *J* = 1.7, 3.4 Hz, 1H), 7.18 - 7.14 (m, 2H), 6.24 (dd, *J* = 3.3, 3.3 Hz, 1H), 6.16 (dd, *J* = 1.8, 3.3 Hz, 1H), 6.09 (t, *J* = 5.6 Hz, 1H), 3.12 (dq, *J* = 5.6, 7.2 Hz, 2H), 1.34 (s, 9H), 1.06 (t, *J* = 7.2 Hz, 3H); ^{13}C NMR (101 MHz, DMSO-d_6) δ = 155.0, 148.8, 139.7, 134.6, 129.1, 126.2, 122.0, 116.6, 113.5, 110.6, 83.3, 33.9, 27.1, 15.4; LCMS (high pH) t_R = 1.16 min, [M+H$^+$] 330.2 (purity 100%); HRMS [2M+H$^+$] calculated for $C_{36}H_{47}N_6O_6$ 659.3552, found [2M+H$^+$] 659.3551; IR (neat) ν_{max} = 3329, 2978, 1310, 1144, 727 cm^{-1}.

tert-Butyl 2-bromo-5-(4-(3-ethylureido)phenyl)-1*H*-pyrrole-1-carboxylate (1-72)

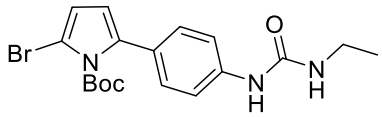

tert-Butyl 2-(4-(3-ethylureido)phenyl)-1*H*-pyrrole-1-carboxylate **1-71** (176 mg, 0.534 mmol) was dissolved in THF (5.5 mL) and the mixture cooled to -78 °C. To this was added NBS (99.0mg, 0.556 mmol) in 3 portions of 33 mg (one portion every 30 min). After the final addition, the reaction mixture was stirred for 1 h at -78 °C before being warmed to RT and concentrated *in vacuo* to yield a dark blue residue. LCMS of this residue indicated decomposition when compared to that of the reaction mixture at -78 °C.

tert-Butyl 2-(4-nitrophenyl)-1*H*-pyrrole-1-carboxylate (1-73)

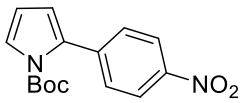

1-Bromo-4-nitrobenzene (438 mg, 2.17 mmol), *N*-Boc-pyrrole-2-boronic acid MIDA ester **1-63** (543 mg, 1.686 mmol), SPhos (102 mg, 0.248 mmol) and $Pd(OAc)_2$ (24.0 mg, 0.107 mmol) were added to a microwave vial. This was sealed and put under a nitrogen atmosphere.

1,4-Dioxane (8.0 mL) was added and the reaction stirred at RT for 10 min. A degassed solution of K_3PO_4 (3 M aqueous, 1.70 mL, 5.10 mmol) was added and the reaction mixture warmed to 60 °C. This was stirred for 17 h before being cooled to RT and filtered through celite, which was washed with DCM. The filtrate was collected and washed with water (30 mL). The layers were separated, and the aqueous phase washed with DCM (2 × 30 mL). The organics were combined, dried using a hydrophobic frit and concentrated *in vacuo* yielding a brown residue and this was purified by flash column chromatography (cyclohexane/EtOAc 0-50%). **1-73** was obtained as an off-white amorphous solid (336 mg, 1.17 mmol, 69%). ^{1}H NMR (400 MHz, $CDCl_3$) δ = 8.26 - 8.21 (m, 2H), 7.56 - 7.51 (m, 2H), 7.43 (dd, *J* = 1.7, 3.2 Hz, 1H), 6.35 (dd, *J* = 1.8, 3.3 Hz, 1H), 6.30 (t, *J* = 3.4 Hz, 1H), 1.46 (s, 9H); ^{13}C NMR (101 MHz, $CDCl_3$) δ = 148.9, 146.7, 140.7, 132.8, 129.6, 124.3, 122.9, 116.5, 111.1, 84.5, 27.7; LCMS (high pH) t_R = 1.37 min, [M+H$^+$] mass ion not observed; HRMS [M+H$^+$] calculated for $C_{15}H_{17}N_2O_4$ 289.1183, no mass ion observed; IR (neat) ν_{max} = 1743, 1508, 1341, 1307, 1145 cm^{-1}.

1-73 is a known compound and data are consistent with reported literature.[156]

***tert*-Butyl 2-bromo-5-(4-nitrophenyl)-1*H*-pyrrole-1-carboxylate (1-74)**

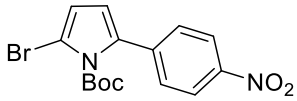

tert-Butyl 2-(4-nitrophenyl)-1*H*-pyrrole-1-carboxylate **1-73** (336 mg, 1.17 mmol) was dissolved in THF (12 mL) and this was cooled to 0 °C. To this was added NBS (207 mg, 1.17 mmol) and the reaction mixture stirred for 3 h at 0 °C. This was diluted with EtOAc (20 mL) and washed with water (20 mL). The aqueous phase was then washed with EtOAc (2 × 20 mL). The organics were combined, dried using a hydrophobic frit and concentrated *in vacuo* yielding a yellow gum which was purified by flash column chromatography (cyclohexane/TBME 0-40%). **1-74** was obtained as a yellow oil which solidified at RT (390 mg, 1.06 mmol, 91%). ^{1}H NMR (400 MHz, $CDCl_3$) δ = 8.27 - 8.23 (m, 2H), 7.48 - 7.44 (m, 2H), 6.38 (d, *J* = 3.7 Hz, 1H), 6.34 (d, *J* = 3.7 Hz, 1H), 1.45 - 1.43 (m, 9H); ^{13}C NMR (101 MHz, $CDCl_3$) δ = 148.2, 146.7, 140.1, 134.4, 128.2, 123.5, 115.6, 115.0, 104.7, 86.1, 27.5; LCMS (high pH) t_R = 1.43 min, [M-H]$^-$ 365.2 and 367.2; HRMS [M+H$^+$] calculated for $C_{15}H_{16}{}^{79}BrN_2O_4$ 367.0288, no mass ion observed; IR (neat) ν_{max} = 2981, 1748, 1507, 1296 cm^{-1}.

1-74 is a known compound and data are consistent with reported literature.[156]

***tert*-Butyl 2-(3,6-dihydro-2*H*-pyran-4-yl)-5-(4-nitrophenyl)-1*H*-pyrrole-1-carboxylate (1-75)**

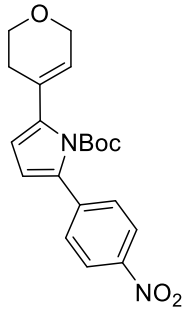

2-(3,6-Dihydro-2*H*-pyran-4-yl)-4,4,5,5-tetramethyl-1,3,2-dioxaborolane **1-56** (39.0 mg, 0.186 mmol), $PdCl_2(dppf)\cdot CH_2Cl_2$ (14.0 mg, 0.017 mmol), K_2CO_3 (52.0 mg, 0.376 mmol) and *tert*-butyl 2-bromo-5-(4-nitrophenyl)-1*H*-pyrrole-1-carboxylate **1-74** (40.0 mg, 0.109 mmol) were dissolved in 1,4-dioxane (0.70 mL) and water (0.18 mL). This was degassed for 10 min before being put under a nitrogen atmosphere and heated to 60 °C for 2 h. The reaction mixture was then filtered through celite, which was washed with DCM (10 mL). The DCM was then washed with water (10 mL) and the layers separated. The aqueous phase was washed with DCM (2 × 10 mL) and the organics combined, dried using a hydrophobic frit and concentrated *in vacuo* yielding a brown residue. This was purified using the Combiflash EZ Prep with a XSelect® CSH™ Prep C18 5 µm OBD™ column (water + 0.1% ammonium bicarbonate / MeCN 50-99%) to give **1-75** as a yellow oil which solidified slowly at RT (32.2 mg, 0.086 mmol, 79%). ^{1}H NMR (400 MHz, CD_3CN) δ = 8.26 - 8.22 (m, 2H), 7.59 - 7.55 (m, 2H), 6.41 (d, *J* = 3.4 Hz, 1H), 6.20 (d, *J* = 3.7 Hz, 1H), 5.84 (m, 1H), 4.23 (appt q, *J* = 2.7 Hz, 2H), 3.86 (appt. t, *J* = 5.5 Hz, 2H), 2.43 – 2.38 (m, 2H), 1.38 (s, 9H); ^{13}C NMR (101 MHz, CD_3CN) δ = 151.1, 148.0, 141.8, 140.6, 134.8, 130.2, 130.2, 127.3, 124.7, 115.7, 112.5, 86.5, 66.4, 65.3, 30.6, 28.1; LCMS (high pH) t_R = 1.38 min, [M-($CO_2{}^tBu$)+H^+] 271.1; HRMS [M+NH_4^+] calculated for $C_{20}H_{26}N_3O_5$ 388.1867, found [M+NH_4^+] 388.1868; IR (neat) ν_{max} = 1733, 1509, 1305 cm^{-1}.

2-(4-nitrophenyl)-5-(tetrahydro-2*H*-pyran-4-yl)-1*H*-pyrrole (1-76)

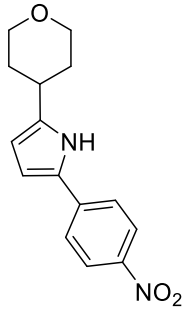

tert-Butyl 2-(3,6-dihydro-2*H*-pyran-4-yl)-5-(4-nitrophenyl)-1*H*-pyrrole-1-carboxylate **1-75** (166 mg, 0.448 mmol) was dissolved in DCM (6.0 mL) and degassed for 10 min before

Et_3SiH (1.40 mL, 8.77 mmol) and TFA (0.350 mL, 4.54 mmol) were added. This was stirred for 19 h, after which additional TFA (0.180 mL, 2.77 mmol) was added and the reaction stirred at RT for a further 2.5 h. Et_3SiH (0.700 mL, 4.38 mmol) was added and the reaction mixture stirred for 2 h before being slowly added to saturated aqueous sodium bicarbonate (10 mL). This was then washed with DCM (3 × 20 mL) and the organics combined, dried using a hydrophobic frit and concentrated *in vacuo* yielding an orange solid. This was dissolved in DCM (5 mL) and washed with saturated aqueous sodium bicarbonate (3 × 10 mL). The organic layer was then concentrated *in vacuo* yielding **1-76** as an amorphous orange solid (59.0 mg, 0.217 mmol, 48%). This was recrystallised from hot MeCN to give crystals suitable for X-ray crystallography. ^{1}H NMR (400 MHz, DMSO-d_6) δ = 11.28 (br s, 1H), 8.19 - 8.15 (m, 2H), 7.85 - 7.80 (m, 2H), 6.73 (dd, *J* = 2.7, 3.4 Hz, 1H), 5.98 (m, 1H), 3.97 - 3.89 (m, 2H), 3.43 (dt, *J* = 2.1, 11.7 Hz, 2H), 2.87 (tt, *J* = 3.8, 11.7 Hz, 1H), 1.88 - 1.81 (m, 2H), 1.75 - 1.61 (m, 2H); ^{13}C NMR (101 MHz, DMSO-d_6) δ = 143.7, 141.8, 139.3, 128.1, 124.3, 122.9, 110.1, 106.2, 66.9, 33.7, 32.4; LCMS (high pH) t_R = 1.15 min, [M+H$^+$] 273.1 (97% purity); HRMS [M+H$^+$] calculated for $C_{15}H_{17}N_2O_3$ 273.1234, found [M+H$^+$] 273.1231; IR (neat) ν_{max} = 3279, 2959, 2868, 1595, 1501, 1312, 750 cm^{-1}.

4-Ethynyltetrahydro-2*H*-pyran (1-79)

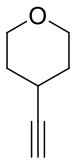

Tetrahydro-2*H*-pyran-4-carbaldehyde **1-80** (250 mg, 2.19 mmol) was dissolved in MeOH (4.2 mL) and cooled to 0 °C. To this was added dimethyl (1-diazo-2-oxopropyl)phosphonate **1-81** (10% in MeCN, 5.00 mL, 2.08 mmol) followed by K_2CO_3 (696 mg, 5.04 mmol). This was stirred for 2 h at 0 °C. The reaction mixture was then poured into diethyl ether (10 mL). This was washed with water (2 × 15 mL) followed by brine (15 mL). The combined aqueous layers were then washed with diethyl ether (20 mL) and the organics combined, dried using a hydrophobic frit and concentrated *in vacuo* yielding **1-79** as a pale-yellow oil (185 mg, 1.68 mmol, 77%). This was used in subsequent reactions without further purification. ^{1}H NMR (400 MHz, $CDCl_3$) δ = 3.91 (ddd, *J* = 3.7, 5.7, 11.6 Hz, 2H), 3.54 - 3.47 (m, 2H), 2.64 (dtt, *J* = 2.4, 4.2, 8.6 Hz, 1H), 2.11 (d, *J* = 2.4 Hz, 1H), 1.89 - 1.80 (m, 2H), 1.73 - 1.64 (m, 2H); TLC R_f = 0.42 (30% EtOAc/cyclohexane - visualised using permanganate stain).

1-79 is a known compound and NMR data are consistent with reported literature.[157]

(3-Oxabicyclo[4.1.0]heptan-6-yl)methanol (1-83)

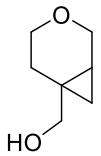

3-Oxabicyclo[4.1.0]heptane-6-carboxylic acid **1-82** (2.05 g, 14.4 mmol) was dissolved in THF (20 mL). This was cooled to 0 °C and BH_3·THF (1 M in THF, 14.5 mL, 14.5 mmol) added. The reaction mixture was stirred for 30 min before being heated to 40 °C for 7 h. After this time, the reaction mixture was cooled and additional BH_3·THF (7.30 mL, 7.30 mmol) was added and the reaction mixture stirred for 16 h. NaOH (1 M aqueous, 15 mL) was added and the solution stirred for 5 min before being extracted with DCM (70 mL) with brine (20 mL) added to aid separation. The aqueous layer was separated and washed with a further portion of DCM (50 mL). The organics were combined, dried using a hydrophobic frit and concentrated *in vacuo* yielding **1-83** as a colourless oil (1.57 g, 12.3 mmol, 85%). This was used without further purification. ^{1}H NMR (400 MHz, $CDCl_3$) δ = 3.89 - 3.86 (m, 2H), 3.59 (ddd, *J* = 3.9, 5.9, 11.4 Hz, 1H), 3.48 (d, *J* = 10.8 Hz, 1H), 3.38 (d, *J* = 12.2 Hz, 1H), 3.28 (ddd, *J* = 5.4, 9.6, 11.4 Hz, 1H), 1.97 - 1.90 (m, 1H), 1.85 (m, 1H), 1.45 (s, 1H), 0.91 (tdd, *J* = 2.7, 5.8, 8.7 Hz, 1H), 0.65 (dd, *J* = 4.4, 8.8 Hz, 1H), 0.59 (dd, *J* = 5.4 Hz, 5.4 Hz, 1H); ^{13}C NMR (101 MHz, $CDCl_3$) δ = 71.3, 65.9, 64.3, 26.1, 20.0, 15.3, 14.7.

3-Oxabicyclo[4.1.0]heptane-6-carbaldehyde (1-84)

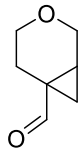

(3-Oxabicyclo[4.1.0]heptan-6-yl)methanol **1-83** (302 mg, 2.36 mmol) was dissolved in DCM (12 mL). Dess-Martin periodinane (1.23 g, 2.90 mmol) was added slowly and the reaction mixture stirred for 16 h. The reaction mixture was quenched with an aqueous solution of sodium thiosulfate (28% w/v, 10 mL). The layers were separated and the aqueous washed with DCM (3 × 10 mL). The organics were combined and washed with NaOH (1 M aqueous, 20 mL). The layers were again separated and the organic dried using a hydrophobic frit before being concentrated *in vacuo* at RT, giving an oil which formed a waxy white solid when left at RT. This was dissolved in diethyl ether (5.0 mL) and filtered through a hydrophobic frit. The solvent was then removed *in vacuo* to yield a colourless oil and white solid. This mixture

was purified using flash chromatography (cyclohexane/EtOAc 0-60%). **1-84** was obtained as a colourless oil (199 mg, 1.58 mmol, 60%). ^{1}H NMR (400 MHz, $CDCl_3$) δ = 8.67 (s, 1H), 4.10 (d, *J* = 11.5 Hz, 1H), 3.80 (dd, *J* = 3.4, 11.5 Hz, 1H), 3.77 (ddd, *J* = 2.0, 6.8, 11.7 Hz, 1H), 3.10 (dt, *J* = 4.6, 11.6 Hz, 1H), 2.62 (ddd, *J* = 1.7, 4.8, 14.5 Hz, 1H), 1.73 (ddd, *J* = 6.8, 11.9, 14.5 Hz, 1H), 1.54 (m, 1H), 1.45 (dd, *J* = 4.4, 9.5 Hz, 1H), 1.23 (dd, *J* = 4.6, 6.8 Hz, 1H); ^{13}C NMR (101 MHz, $CDCl_3$) δ = 200.2, 64.5, 64.3, 29.4, 21.1, 19.1, 18.3; IR (neat) ν_{max} = 2942, 2853, 2712, 1702 cm^{-1}; TLC R_f = 0.26 (30% EtOAc/cyclohexane - visualised using permanganate stain).

6-Ethynyl-3-oxabicyclo[4.1.0]heptane (1-77)

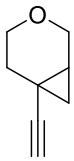

3-Oxabicyclo[4.1.0]heptane-6-carbaldehyde **1-84** (180 mg, 1.43 mmol) was dissolved in MeOH (3.2 mL) and cooled to 0 °C. To this was added dimethyl (1-diazo-2-oxopropyl)phosphonate **1-81** (10% in MeCN, 4.50 mL, 1.87 mmol) followed by K_2CO_3 (454 mg, 3.28 mmol). This was stirred for 1 h at 0 °C before being warmed to RT and stirred for 3.5 h. The reaction mixture was then poured into diethyl ether (10 mL) which was washed with water (2 × 10 mL) and brine (10 mL). The organic layer was then dried using a hydrophobic frit and concentrated under a flow of nitrogen at RT to give **1-77** as a yellow oil (97.0 mg, 0.745 mmol, 52%). This was used in subsequent reactions without further purification. ^{1}H NMR (400 MHz, $CDCl_3$) δ = 3.93 - 3.85 (m, 2H), 3.58 (ddd, *J* = 3.8, 5.6, 11.7 Hz, 1H), 3.30 (ddd, *J* = 6.1, 9.4, 11.6 Hz, 1H), 2.10 - 1.98 (m, 2H), 1.95 (s, 1H), 1.34 (m, 1H), 1.15 (dd, *J* = 4.4, 9.0 Hz, 1H), 0.87 (dd, *J* = 4.4, 6.4 Hz, 1H); TLC R_f = 0.43 (30% cyclohexane/EtOAc – visualised using permanganate stain).

4-Ethynyl-3,6-dihydro-2*H*-pyran (1-78)

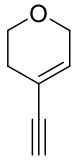

To an oven dried round bottom flask (100 mL) was added 3,6-dihydro-2*H*-pyran-4-yl trifluoromethanesulfonate **1-85** (630 mg, 2.71 mmol) and $Pd(PPh_3)_4$ (123 mg, 0.106 mmol). These were dissolved in THF (6.0 mL) and placed under a nitrogen atmosphere. This was stirred at RT for 5 min before ethynylmagnesium bromide (0.5 M in THF, 11.0 mL, 5.50 mmol) was added dropwise. This was then stirred at RT for 7 h before being quenched with 2 M aqueous HCl (10 mL) and diluted with diethyl ether (30 mL). The layers were separated

and the aqueous phase washed with diethyl ether (30 mL). The organics were combined, washed with brine (50 mL) and dried using a hydrophobic frit before being concentrated *in vacuo* yielding a brown oil. The brown oil was dissolved in diethyl ether (30 mL) and washed with water (3 × 50 mL). The organic was dried using a hydrophobic frit and concentrated *in vacuo* (550 mbar) yielding **1-78** as a brown oil (137 mg, 1.27 mmol, 47%). The product was used in subsequent reactions without further purification. ^{1}H NMR (400 MHz, $CDCl_3$) δ = 6.19 (m, 1H), 4.22 – 4.17 (m, 2H), 3.81 (t, *J* = 5.5 Hz, 2H), 2.91 (s, 1H), 2.28 (m, 2H).

1-78 is a known compound and the NMR data agrees with reported literature.[40,41]

3-((*tert*-Butyldimethylsilyl)oxy)benzaldehyde (1-87)

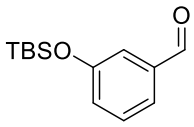

3-Hydroxybenzaldehyde **1-86** (2.11 g, 17.3 mmol) was dissolved in DCM (40 mL) and cooled to 0 °C. TBS-Cl (2.86 g, 19.0 mmol) and imidazole (3.53 g, 51.8 mmol) were added and the reaction mixture warmed to RT slowly. This was stirred for 2 h at RT before water (40 mL) was added and the layers separated. The aqueous phase was then washed with DCM (2 × 40 mL) and the organics combined, dried using a hydrophobic frit and concentrated *in vacuo*. This gave **1-87** as a pale yellow oil (4.52 g, 19.1 mmol, 111%). This was used in subsequent reactions without further purification with a silanol by-product present by NMR accounting for the 111% yield. ^{1}H NMR (400 MHz, $CDCl_3$) δ = 9.96 (s, 1H), 7.48 (m, 1H), 7.41 (t, *J* = 7.3 Hz, 1H), 7.33 (m, 1H), 7.11 (ddd, *J* = 1.2, 2.6, 7.9 Hz, 1H), 1.01 (s, 9H), 0.24 (s, 6H); LCMS (formic acid) t_R = 1.46 min, [M+H$^+$] 237.2 (100% purity).

74 is a known compound and the NMR data agree with reported literature.[158]

3-((*tert*-Butyldimethylsilyl)oxy)benzaldehyde oxime (1-88)

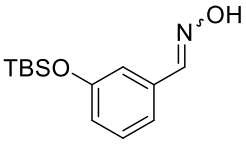

3-((*tert*-Butyldimethylsilyl)oxy)benzaldehyde **1-87** (1.08 g, 4.57 mmol) was dissolved in MeOH (10 mL). To this was added $NH_2OH{\cdot}HCl$ (378 mg, 5.44 mmol) and NaOAc (473 mg, 5.77 mmol) and the reaction mixture stirred at RT for 1 h. This was then concentrated *in vacuo* and the residue dissolved in EtOAc (10 mL). This was washed with water (2 × 10 mL). The aqueous layers were combined and washed with EtOAc (20 mL). The organics were then

combined and concentrated *in vacuo* yielding a colourless oil. This was purified by flash chromatography (cyclohexane/EtOAc 0-20%) yielding **1-88** as a colourless oil (680 mg, 2.70 mmol, 59%). ^{1}H NMR (400 MHz, $CDCl_3$) δ = 8.09 (s, 1H), 7.25 (t, *J* = 8.0 Hz, 1H), 7.15 (m, 1H), 7.09 (m, 1H), 6.88 (ddd, *J* = 1.1, 2.6, 8.1 Hz, 1H), 1.01 - 1.00 (m, 9H), 0.22 - 0.21 (m, 6H) ***exchangeable -OH not observed***; ^{13}C NMR (101 MHz, $CDCl_3$) δ = 156.0, 150.3, 133.3, 129.7, 121.9, 120.5, 118.1, 25.7, 18.2, -4.4; LCMS (formic acid) t_R = 1.36 min, [M+H$^+$] 252.2 (100% purity); HRMS [M+H$^+$] calculated for $C_{13}H_{22}NO_2Si$ 252.1414, found [M+H$^+$] 252.1416; IR (neat) ν_{max} = 2958, 2930, 2859, 1252, 837, 780 cm^{-1}.

3-(5-(3-Oxabicyclo[4.1.0]heptan-6-yl)isoxazol-3-yl)phenol (1-37)

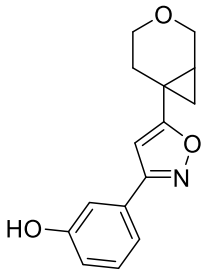

6-Ethynyl-3-oxabicyclo[4.1.0]heptane **1-77** (315 mg, 2.58 mmol) and 3-((*tert*-butyldimethylsilyl)oxy)benzaldehyde oxime **1-88** (974 mg, 3.87 mmol) were dissolved in MeOH (5.4 mL) and water (1.1 mL). To this was added 555 mg, every 2 h, of bis(trifluoroacetoxy)iodobenzene (PIFA) (1.67 g, 3.87 mmol). The reaction mixture was stirred at RT for 16 h before being diluted with saturated aqueous sodium bicarbonate (10 mL) and this washed with EtOAc (3 × 20 mL). The combined organics were then washed with water (50 mL), dried using a hydrophobic frit and concentrated *in vacuo* giving a brown oil which was purified by flash chromatography (cyclohexane/EtOAc 0-70%). The product from the first purification was further purified using reverse phase chromatography on a C18 column (water + 0.1% formic acid / MeCN + 0.1% formic acid 35-75%). This gave **1-37** as a colourless oil which solidified slowly at RT (181 mg, 0.703 mmol, 27%). The product was recrystallised from hot toluene to give crystals suitable for X-ray crystallography. M.pt. 116-119 °C; ^{1}H NMR (400 MHz, $CDCl_3$) δ = 7.34 - 7.29 (m, 2H), 7.27 (m, 1H), 6.93 (m, 1H), 6.19 (s, 1H), 3.97 (d, *J* = 2.4 Hz, 2H), 3.70 (ddd, *J* = 3.7, 6.0, 11.6 Hz, 1H), 3.42 (ddd, *J* = 5.0, 10.0, 11.6 Hz, 1H), 2.31 (m, 1H), 2.18 (m, 1H), 1.66 (m, 1H), 1.48 (dd, *J* = 4.6, 9.3 Hz, 1H), 1.17 (dd, *J* = 4.6, 6.6 Hz, 1H) ***exchangeable -OH not observed***; ^{13}C NMR (101 MHz, $CDCl_3$) δ = 177.4, 162.5, 156.6, 130.2, 130.2, 119.0, 117.4, 113.6, 97.2, 65.0, 63.8, 26.3, 20.9, 20.1, 15.9; LCMS (formic acid) t_R = 0.92 min, [M+H$^+$] 258.1 (100% purity); HRMS [M+H$^+$] calculated for $C_{15}H_{16}NO_3$ 258.1125, found [M+H$^+$] 258.1125; IR (neat) ν_{max} = 3266, 2869, 1121, 790 cm^{-1}.

The enantiomers of this compound were separated to give less disorder in the crystal structures. The conditions used were 40% EtOH/heptane, f = 30 mL/min, Column 30 mm × 25 cm Chiralpak AD-H.

Enantiomer 1, **(+)-1-37**, **(1*S*, 6*R*)** $[\alpha_D]^{20}$ (0.180 g/100 mL, MeOH): +44.4 °. t_R = 9.16 min.

Enantiomer 2, **(-)-1-37**, **(1*R*, 6*S*)** $[\alpha_D]^{20}$ (0.160 g/100 mL, MeOH): -50.0 °. t_R = 12.95 min.

Enantiomer structures confirmed by X-ray crystallography.

3-(5-(3,6-Dihydro-2*H*-pyran-4-yl)isoxazol-3-yl)phenol (1-38)

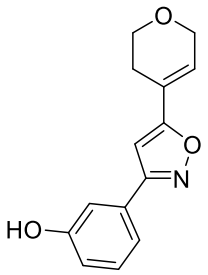

4-Ethynyl-3,6-dihydro-2*H*-pyran **1-78** (137 mg, 1.27 mmol) and 3-((*tert*-butyldimethylsilyl)oxy)benzaldehyde oxime **1-88** (480 mg, 1.91 mmol) were dissolved in MeOH (3.5 mL) and water (0.70 mL). To this was added 160 mg, every 2 h, of bis(trifluoroacetoxy)iodobenzene (PIFA) (820 mg, 1.91 mmol). The reaction mixture was stirred at RT for 3 h before additional bis(trifluoroacetoxy)iodobenzene (PIFA) (340 mg, 0.791 mmol) was added. The reaction was then stirred at RT for 16 h before being diluted with saturated aqueous sodium bicarbonate (10 mL). This was then washed with EtOAc (3 × 10 mL) and the organic layers combined and washed with water (20 mL). The organic phase was collected, dried using a hydrophobic frit and concentrated *in vacuo* giving a brown oil which was purified by flash chromatography (cyclohexane/EtOAc 20-100%) yielding a pale yellow solid. This was further purified by reverse phase C18 column (MeCN + 0.1% formic acid / water + 0.1 % formic acid 20-85%) yielding a yellow solid. Further purification was performed using flash column chromatography on silica gel (cyclohexane/EtOAc 0-80%) giving **1-38** as a white solid (48.5 mg, 0.20 mmol, 16%). This was recrystallised from hot toluene/MeCN giving colourless needle-like crystals suitable for X-ray crystallography. M.pt. 179-180 °C; ^{1}H NMR (400 MHz, DMSO-d_6) δ = 9.76 (s, 1H), 7.33 - 7.26 (m, 3H), 7.01 (s, 1H), 6.92 (m, 1H), 6.62 (m, 1H), 4.27 (appt q, *J* = 2.9 Hz, 2H), 3.83 (appt. t, *J* = 5.4 Hz, 2H), 2.48 - 2.43 (m, 2H); ^{13}C NMR (101 MHz, DMSO-d_6) δ = 169.8, 162.6, 158.3, 130.6, 130.2, 128.5, 123.1, 117.9, 117.7, 113.5, 98.4, 65.0, 63.4, 25.2; LCMS (formic acid) t_R = 0.89

min, [M+H$^+$] 244.3 (95% purity); HRMS [M+H$^+$] calculated for $C_{14}H_{14}NO_3$ 244.0968, found [M+H$^+$] 244.0971; IR (neat) ν_{max} = 3302, 2877, 1467 cm^{-1}.

3-(5-(Tetrahydro-2*H*-pyran-4-yl)isoxazol-3-yl)phenol (1-39)

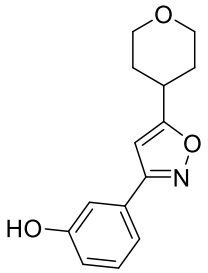

4-Ethynyltetrahydro-2*H*-pyran **1-79** (185 mg, 1.68 mmol) and 3-((*tert*-butyldimethylsilyl)oxy)benzaldehyde oxime **1-88** (633 mg, 2.52 mmol) were dissolved in methanol (3.5 mL) and water (0.70 mL). To this was added 361 mg, every 2 h, of bis(trifluoroacetoxy)iodobenzene (PIFA) (1.08 g, 2.52 mmol) and the reaction stirred at RT for 16 h. The reaction mixture was then diluted with saturated aqueous sodium bicarbonate (10 mL). This was then washed with EtOAc (3 × 10 mL) and the organic layers combined and washed with water (20 mL) before being dried using a hydrophobic frit and concentrated *in vacuo*. This gave a brown oil which was purified by flash chromatography (cyclohexane/EtOAc 0-100%) yielding a pale brown solid. This was further purified by MDAP (formic acid) on Xselect CSH C18 column (water + 0.1% formic acid / MeCN + 0.1% formic acid 15-55%) yielding **1-39** as a white solid (85.0 mg, 0.350 mmol, 21%). This was recrystallised from hot toluene yielding colourless crystals suitable for X-ray crystallography. M.pt. 157-160 °C; ^{1}H NMR (400 MHz, DMSO-d_6) δ = 9.67 (s, 1H), 7.30 (dd, *J* = 8.1, 8.1 1H), 7.27 - 7.23 (m, 2H), 6.88 (ddd, *J* = 1.3, 2.3, 7.8 Hz, 1H), 6.77 (d, *J* = 1.0 Hz, 1H), 3.95 – 3.88 (m, 2H), 3.48 (dt, *J* = 2.2, 11.5 Hz, 2H), 3.14 (tt, *J* = 3.8, 11.2 Hz, 1H), 1.98 - 1.90 (m, 2H), 1.76 - 1.65 (m, 2H); ^{13}C NMR (101 MHz, DMSO-d6) δ = 177.0, 162.2, 158.2, 130.4, 117.9, 117.6, 113.5, 98.6, 66.7, 40.7, 33.3, 30.9; LCMS (formic acid) t_R = 0.88 min, [M+H$^+$] 246.1 (100% purity); HRMS [M+H$^+$] calculated for $C_{14}H_{16}NO_3$ 246.1125, found [M+H$^+$] 246.1136; IR (neat) ν_{max} = 3316, 2965, 2931, 2853, 1603, 1471 cm^{-1}.

12.4. Protocols for Synthetic Studies

12.4.1. Literature Preparation of Tosyl-Protected Enyne and Cycloisomerisation

4-Methyl-*N*-(prop-2-yn-1-yl)benzenesulfonamide (1-176)

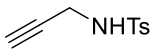

Propargylamine **1-175** (1.50 mL, 23.4 mmol) and Et_3N (3.30 mL, 23.7 mmol) were dissolved in DCM (14 mL) and degassed for 10 min before being cooled to 0 °C. In a separate vessel, *p*-toluenesulfonyl chloride (13.5 g, 70.6 mmol) was dissolved in DCM (44 mL) and degassed for 10 min before being added dropwise to the propargylamine-containing round-bottom flask. The reaction mixture was warmed to RT and stirred for 4 h before being concentrated *in vacuo*. The resulting residue was dissolved in the minimum amount of MeOH and added to an aminopropyl cartridge (50 g) which was eluted with MeOH. The eluent was collected and concentrated *in vacuo* yielding a brown oil. The oil was dissolved in DCM (50 mL) and washed with water (50 mL) saturated aqueous ammonium chloride (50 mL) and brine (50 mL). The combined aqueous layers were then combined and washed with DCM (2 × 50 mL). The organics were combined, dried using a hydrophobic frit and concentrated *in vacuo* yielding a brown residue. This was purified by flash chromatography (cyclohexane/EtOAc 0-40%) yielding **1-176** as an amorphous white solid (4.19 g, 20.0 mmol, 86%). ^{1}H NMR (400 MHz, $CDCl_3$) δ = 7.81 - 7.76 (m, 2H), 7.33 (dd, *J* = 0.7, 8.6 Hz, 2H), 4.54 (br t, *J* = 5.3 Hz, 1H), 3.84 (dd, *J* = 2.6, 6.0 Hz, 2H), 2.45 (s, 3H), 2.12 (t, *J* = 2.4 Hz, 1H); LCMS (high pH) t_R = 0.87 min, $[M-H]^-$ 208.1 (purity 100%).

1-176 is a known compound and the NMR data agree with reported literature.[159]

4-Methyl-*N*-(pent-4-en-2-yn-1-yl)benzenesulfonamide (1-177)

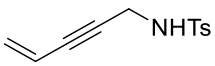

1-177 was prepared using a literature procedure.[160]

CuI (21.0 mg, 0.110 mmol) and $Pd(PPh_3)_4$ (18.0 mg, 0.016 mmol) were dissolved in Et_2NH (2.50 mL, 23.9 mmol) under an inert atmosphere. **1-176** (1.00 g, 4.78 mmol) was added followed by vinyl bromide (1 M in THF, 10.0 mL, 10.0 mmol) and the reaction mixture allowed to stir at RT for 2 h before being poured into ice-cold water (40 mL). This was extracted with diethyl ether (3 × 20 mL). The organics were combined, dried using a hydrophobic frit and concentrated *in vacuo* yielding a brown oil. This was purified by flash chromatography (cyclohexane/EtOAc 0-60%) to give **1-177** as an amorphous off-white solid (952 mg, 4.05 mmol, 85%). ^{1}H NMR (400 MHz, $CDCl_3$) δ = 7.81 - 7.77 (m, 2H), 7.32 (d, *J*

= 8.6 Hz, 2H), 5.56 (m, 1H), 5.45 - 5.38 (m, 2H), 4.54 (br t, *J* = 5.5 Hz, 1H), 3.96 (dd, *J* = 1.8, 6.0 Hz, 2H), 2.43 (s, 3H); ^{13}C NMR (101 MHz, $CDCl_3$) δ = 143.7, 136.8, 129.7, 127.7, 127.5, 116.2, 83.8, 83.4, 33.7, 21.5; LCMS (high pH) t_R = 1.02 min, $[M-H]^-$ 234.2 (100% purity); HRMS $[M+H^+]$ calculated for $C_{12}H_{14}NO_2S$ 236.0740, found $[M+H^+]$ 236.0741; IR (neat) ν_{max} = 3269, 1320, 1153 cm^{-1}.

1-177 is a known compound and the ^{1}H NMR data agree with reported literature.[160]

***N*-Allyl-4-methyl-*N*-(pent-4-en-2-yn-1-yl)benzenesulfonamide (1-166)**

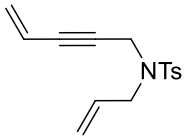

1-166 was prepared using a literature procedure.[102]

1-177 (2.34 g, 9.94 mmol) was dissolved in DMF (50 mL) and the solution degassed for 10 min before being put under a nitrogen atmosphere. This was then cooled to 0 °C before NaH (477 mg, 11.9 mmol) was added. The reaction mixture was stirred for 30 min before allyl bromide (1.00 mL, 11.6 mmol) was added slowly and the reaction mixture stirred for 1 h before saturated aqueous ammonium chloride (20 mL) was added. This was then diluted with water (30 mL) and diethyl ether (100 mL). The layers were separated and the aqueous washed with diethyl ether (2 × 200 mL). The organics were combined and washed with LiCl solution (10% aqueous, 3 × 50 mL). The organic layer was then dried using a hydrophobic frit and concentrated *in vacuo* to yield a yellow oil which was purified by flash chromatography (cyclohexane/EtOAc 0-60%) to give **1-166** as a pale yellow oil (2.24 g, 8.13 mmol, 82%). ^{1}H NMR (400 MHz, $CDCl_3$) δ = 7.75 (d, *J* = 8.4 Hz, 2H), 7.30 (d, *J* = 7.9 Hz, 2H), 5.76 (m, 1H), 5.52 (tdd, *J* = 2.0, 11.3, 17.2 Hz, 1H), 5.40 - 5.22 (m, 4H), 4.21 (d, *J* = 1.5 Hz, 2H), 3.82 (d, *J* = 6.4 Hz, 2H), 2.42 (s, 3H); ^{13}C NMR (101 MHz, $CDCl_3$) δ = 143.4, 136.1, 132.1, 129.4, 127.8, 127.2, 119.8, 116.3, 84.2, 82.5, 49.2, 36.6, 21.5; LCMS (high pH) t_R = 1.27 min, $[M+H^+]$ 276.1 (purity 100%); HRMS $[M+H^+]$ calculated for $C_{15}H_{18}NO_2S$ 276.1053, found $[M+H^+]$ 276.1060; IR (neat) ν_{max} = 2920, 1348, 1161 cm^{-1}.

1-166 is a known compound and the ^{1}H NMR data agree with reported literature.[102]

3-Tosyl-6-vinyl-3-azabicyclo[4.1.0]hept-4-ene (1-167)

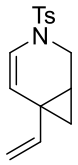

1-167 was prepared using a literature procedure.[102]

To an oven-dried microwave vial was added Au(JohnPhos)Cl (72.0 mg, 0.136 mmol) and $AgSbF_6$ (53.0 mg, 0.154 mmol) which were dissolved in THF (6.0 mL) under an inert atmosphere. This was stirred at RT for 30 min and left to stand until the formed AgCl had precipitated. The supernatant was then used as the catalyst in the cyclisation reaction. The supernatant containing catalyst was added to an oven-dried microwave vial containing **1-166** (353 mg, 1.28 mmol) in THF (7.0 mL) and this stirred for 18 h at 30 °C. The reaction mixture was then filtered through a hydrophobic frit and concentrated *in vacuo* yielding a grey/brown residue. This was purified by flash chromatography (cyclohexane/EtOAc 0-60%) to give **1-167** as a colourless oil (153 mg, 0.556 mmol, 43%). ^{1}H NMR (400 MHz, $CDCl_3$) δ = 7.70 - 7.66 (m, 2H), 7.36 - 7.31 (m, 2H), 6.44 (d, *J* = 8.1 Hz, 1H), 5.51 - 5.42 (m, 2H), 5.02 (dd, *J* = 0.9, 17.2 Hz, 1H), 4.96 (dd, *J* = 1.0, 10.5 Hz, 1H), 3.95 (m, 1H), 3.07 (dd, *J* = 2.7, 11.7 Hz, 1H), 2.45 (s, 3H), 1.59 (m, 1H), 0.99 (ddd, *J* = 0.7, 4.5, 8.7 Hz, 1H), 0.85 (dd, *J* = 4.6, 6.1 Hz, 1H); ^{13}C NMR (101 MHz, $CDCl_3$) δ = 143.8, 141.6, 134.8, 129.8, 127.1, 121.3, 111.4, 111.3, 40.5, 27.6, 22.7, 21.5, 19.5; LCMS (high pH) t_R = 1.29 min, [M+H$^+$] 276.2 (purity 98%); HRMS [M+H$^+$] calculated for $C_{15}H_{18}NO_2S$ 276.1053, found [M+H$^+$] 276.1057; IR (neat) ν_{max} = 1632, 1347, 1163 cm^{-1}.

1-167 is a known compound and the data agree with reported literature.[102]

12.4.2. Synthesis of Halogenated Enynes

***N*-Allyl-4-methyl-*N*-(prop-2-yn-1-yl)benzenesulfonamide (1-178)**

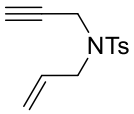

1-178 was prepared using a literature procedure.[161]

1-176 (1.05 g, 5.02 mmol), K_2CO_3 (923 mg, 6.68 mmol) and allyl bromide (0.500 mL, 5.78 mmol) were dissolved in acetone (10 mL). The reaction mixture was heated to 60 °C and stirred for 2 h before being cooled to RT. The residue was diluted with EtOAc (10 mL) and

water (10 mL). The layers were separated and the aqueous washed with EtOAc (2 × 20 mL). The organics were combined, dried using a hydrophobic frit and concentrated *in vacuo* yielding **1-178** as a yellow solid (1.25 g, 5.01 mmol, 100%) which was used without further purification. ^{1}H NMR (400 MHz, $CDCl_3$) δ = 7.75 (d, *J* = 8.3 Hz, 2H), 7.31 (d, *J* = 8.1 Hz, 2H), 5.75 (tdd, *J* = 6.5, 10.2, 16.9 Hz, 1H), 5.34 - 5.22 (m, 2H), 4.11 (d, *J* = 2.4 Hz, 2H), 3.84 (d, *J* = 6.6 Hz, 2H), 2.44 (s, 3H), 2.02 (t, *J* = 2.4 Hz, 1H); LCMS (high pH) t_R = 1.15 min, [M+H$^+$] 250.1 (purity 100%).

1-178 is a known compound and the NMR data agree with reported literature.[161]

***N*-Allyl-*N*-(3-bromoprop-2-yn-1-yl)-4-methylbenzenesulfonamide (1-179)**

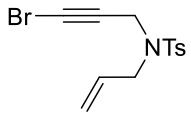

1-179 was prepared using a literature procedure.[106]

1-178 (254 mg, 1.02 mmol) was dissolved in acetone, placed under an inert atmosphere and cooled to 0 °C. To this was added NBS (238 mg, 1.34 mmol) and $AgNO_3$ (31.0 mg, 0.182 mmol) and the reaction mixture warmed to RT and stirred for 40 min before being diluted with water (10 mL). This was washed with EtOAc (2 × 10 mL) and the organics combined, washed with brine (10 mL). The organics were then dried using a hydrophobic frit and concentrated *in vacuo* yielding a colourless oil which was purified by flash chromatography (cyclohexane/EtOAc 0-80%) to give **1-179** as a colourless oil which solidified over time (246 mg, 0.749 mmol, 74%). ^{1}H NMR (400 MHz, $CDCl_3$) δ = 7.76 - 7.71 (m, 2H), 7.35 - 7.31 (m, 2H), 5.74 (tdd, *J* = 6.4, 10.2, 16.9 Hz, 1H), 5.33 - 5.23 (m, 2H), 4.10 (s, 2H), 3.82 - 3.78 (m, 2H), 2.45 (s, 3H); ^{13}C NMR (101 MHz, $CDCl_3$) δ = 143.7, 135.7, 131.9, 129.5, 127.8, 120.0, 72.9, 49.4, 44.9, 36.9, 21.6; LCMS (high pH) t_R = 1.26 min, [M+H$^+$] 328.0 (purity 95%); HRMS [M+H$^+$] calculated for $C_{13}H_{15}{}^{79}BrNO_2S$ 328.0001, found [M+H$^+$] 328.0009; IR (neat) ν_{max} = 1423, 1331, 1161 cm^{-1}.

***N*-(3-Iodoprop-2-yn-1-yl)-4-methylbenzenesulfonamide (1-180)**

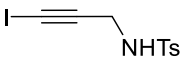

1-180 was prepared using a literature procedure.[162]

1-176 (308 mg, 1.47 mmol), I_2 (437 mg, 1.72 mmol) and KOH (0.430 mL, 3.58 mmol) were dissolved in MeOH (1.8 mL), put under an inert atmosphere and stirred at RT for 1.5 h. The reaction mixture was then diluted with water (5 mL). This was extracted with EtOAc (3 × 10

mL) and the organics combined, washed with sodium thiosulfate (28% aqueous 20 mL) and brine (20 mL) before being dried using a hydrophobic frit and concentrated *in vacuo* yielding a white solid. This was purified on the Reveleris reverse-phase purification system (Sunfire Formic column 30-85% MeCN + 0.1% formic acid/Water +0.1% formic acid) yielding **1-180** as an off-white amorphous solid (342 mg, 1.02 mmol, 69%). 1H NMR (400 MHz, $CDCl_3$) δ = 7.80 - 7.75 (m, 2H), 7.37 - 7.32 (m, 2H), 4.52 (br t, *J* = 5.9 Hz, 1H), 4.00 (d, *J* = 6.1 Hz, 2H), 2.45 (s, 3H); LCMS (high pH) t_R = 1.02 min, $[M-H]^-$ 334.0 (purity 95%).

1-180 is a known compound and the NMR data agree with reported literature.[105]

***N*-Allyl-*N*-(3-iodoprop-2-yn-1-yl)-4-methylbenzenesulfonamide (1-181)**

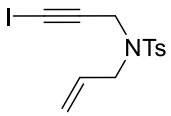

1-181 was prepared using a literature procedure.[105]

1-180 (86 mg, 0.257 mmol) and K_2CO_3 (142 mg, 1.03 mmol) were dissolved in MeCN (2.6 mL). To this was added allyl bromide (44.0 µL, 0.513 mmol) before the reaction was heated to 85 °C and stirred for 4 h before being cooled to RT and diluted with saturated bicarb (5 mL). This was extracted with DCM (3 × 10 mL) and the organics were combined, dried using a hydrophobic frit and concentrated *in vacuo* yielding **1-181** as a brown oil (87.0 mg, 0.232 mmol, 90%) which was used without further purification. ^{1}H NMR (400 MHz, $CDCl_3$) δ = 7.75 - 7.71 (m, 2H), 7.36 - 7.32 (m, 2H), 5.74 (tdd, *J* = 6.5, 10.2, 17.0 Hz, 1H), 5.32 - 5.23 (m, 3H), 4.22 (s, 2H), 3.82 - 3.78 (m, 2H), 2.46 (s, 3H); LCMS (high pH) t_R = 1.27 min, $[M-H]^-$ 374.1 (purity 86%).

1-181 is a known compound and the NMR data agree with reported literature.[105]

Attempted Cycloisomerisations to 1-174a and 1-174b:

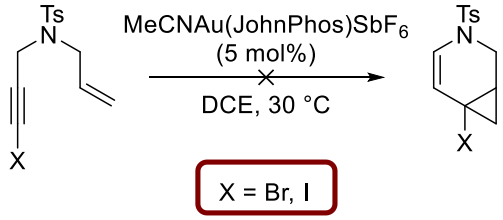

*With bromide **1-179**:*

To a heat-gun dried 10-20 mL microwave vial was added **1-179** (125 mg, 0.381 mmol) and MeCNAu(JohnPhos)SbF_6 (18.0 mg, 0.023 mmol). These were dissolved in DCE (7.6 mL) and the reaction mixture heated to 30 °C for 4 h before being cooled to RT and concentrated

in vacuo yielding a brown residue. This was dissolved in DCM and purified by flash chromatography (cyclohexane/TBME 0-50%). No identifiable products were isolated.

*With iodide **1-181**:*

To a heat-gun dried 10-20 mL microwave vial was added **1-181** (136 mg, 0.362 mmol) and MeCNAu(JohnPhos)SbF_6 (14.0 mg, 0.018 mmol). These were dissolved in DCE (7.6 mL) and the reaction mixture heated to 30 °C for 29 h before being cooled to RT and concentrated *in vacuo* yielding a brown residue. This was dissolved in DCM and purified by flash chromatography (cyclohexane/TBME 0-50%). No identifiable products were isolated.

12.4.3. Synthesis of Gold Pre-catalysts

General Procedure A

The general procedure was adapted from the literature.[108]

(Me_2S)AuCl was added to a solution of the corresponding phosphine in dry DCM (0.1 M) at RT. The solution was left stirring for 1-3 h and then concentrated under vacuum or a flow of nitrogen. The crude was dissolved in the minimum amount of DCM and precipitated by addition of pentane or hexane. The precipitate was allowed to settle before the solvent was removed by pipette. The solid was then dried under vacuum.

1-182

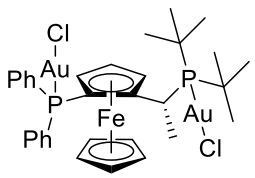

Following General Procedure A using (Me_2S)AuCl (548 mg, 1.86 mmol) and phosphine (500 mg, 0.922 mmol) in DCM (9.2 mL) stirred for 2 h to give **1-182** as an orange solid (921 mg, 0.914 mmol, 99%). ^{1}H NMR (700 MHz, $CDCl_3$) δ = 7.85 (br dd, *J* = 7.2, 13.6 Hz, 2H), 7.75 (br dd, *J* = 7.6, 13.6 Hz, 2H), 7.57 (br d, *J* = 6.4 Hz, 1H), 7.56 - 7.49 (m, 4H), 7.44 (m, 1H), 4.84 (br s, 1H), 4.69 (br s, 1H), 4.32 (m, 1H), 4.19 (br s, 1H), 4.15 (s, 5H), 2.16 (br dd, *J* = 8.1, 10.2 Hz, 3H), 1.58 - 1.54 (m, 14H ***due to overlap with water peak***), 1.02 (br d, *J* = 14.8 Hz, 9H); ^{13}C NMR (176 MHz, $CDCl_3$) δ = 135.3 (d, *J* = 14.6 Hz), 133.7 (d, *J* = 14.0 Hz), 132.2 (d, *J* = 2.5 Hz), 131.7 (d, *J* = 2.5 Hz), 130.2 (d, *J* = 61.7 Hz), 129.8 (d, *J* = 12.1 Hz), 129.6 (br d, *J* = 68.7 Hz), 128.9 (d, *J* = 12.7 Hz), 102.0 (br dd, *J* = 8.9, 16.5 Hz), 73.9-73.8 (m), 72.4 (d, *J* = 5.7 Hz), 71.9 (d, *J* = 8.3 Hz), 70.8, 65.3 (dd, *J* = 2.5, 73.1 Hz), 38.5 (d, *J* = 17.8 Hz), 37.7 (d, *J* = 23.5 Hz), 32.0 (d, *J* = 5.1 Hz), 31.2 (dd, *J* = 5.1, 20.3 Hz), 29.4 (d, *J* =

4.5 Hz), 24.0 (d, *J* = 2.5 Hz); ^{31}P NMR (162 MHz, $CDCl_3$) δ = 86.8, 20.7; MALDI (α-cyano-4-hydroxycinnamic acid matrix) $[M]^+$ calculated for $C_{32}H_{40}Au_2Cl_2FeP_2$ 1006.066, found 1006.048 & $[M\text{-}Cl]^+$ $C_{32}H_{40}Au_2ClFeP_2$ 971.097, found 971.078.

1-182 is an enantiomer of a published compound and agreed with the literature for this.[108]

1-183

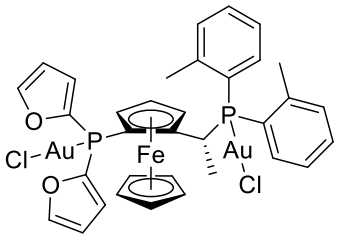

Following General Procedure A using $(Me_2S)AuCl$ (103 mg, 0.350 mmol) and phosphine (102 mg, 0.173 mmol) in DCM (3.4 mL) stirred for 2.5 h to give **1-183** as an orange solid (173 mg, 0.164 mmol, 95%). ^{1}H NMR (700 MHz, $CDCl_3$) δ = 7.84 (m, 1H), 7.77 (s, 1H), 7.54 (s, 1H), 7.50 (br dd, *J* = 7.6, 7.6 Hz, 1H), 7.46 - 7.39 (m, 2H), 7.21 (dd, *J* = 3.4, 3.4 Hz, 1H), 7.18 (m, 1H), 7.01 (dd, *J* = 7.4, 7.4 Hz, 1H), 6.89 (dd, *J* = 7.4, 7.4 Hz, 1H), 6.64 (m, 1H), 6.55 (m, 1H), 6.34 (dd, *J* = 2.5, 2.5 Hz, 1H), 6.29 (m, 1H), 5.26 (br s, 2H), 4.79 (s, 1H), 4.68 (br s, 1H), 4.08 (s, 5H), 2.29 (s, 3H), 2.07 - 2.00 (m, 6H); ^{13}C NMR (176 MHz, $CDCl_3$) δ = 148.6 (dd, *J* = 6.0, 11.8 Hz), 145.9 (d, *J* = 92.2 Hz), 143.3 (d, *J* = 92.8 Hz), 142.0 (d, *J* = 8.9 Hz), 141.7 (d, *J* = 10.8 Hz), 135.9 (d, *J* = 14.0 Hz), 132.5 (br d, *J* = 8.3 Hz), 132.2 (d, *J* = 8.3 Hz), 131.8 (d, *J* = 8.9 Hz), 131.6 (d, *J* = 1.9 Hz), 131.3 (d, *J* = 2.5 Hz), 127.0 (d, *J* = 8.9 Hz), 126.8 (d, *J* = 54.0 Hz), 126.1 (d, *J* = 11.4 Hz), 125.2 (d, *J* = 54.0 Hz), 124.0 (d, *J* = 29.2 Hz), 122.7 (d, *J* = 22.3 Hz), 111.4 (dd, *J* = 9.2, 14.3 Hz), 95.3 (d, *J* = 6.4 Hz), 95.2 (d, *J* = 6.4 Hz), 73.6 (d, *J* = 5.7 Hz), 72.8 (appt. t, *J* = 8.3 Hz), 72.0 (d, *J* = 8.9 Hz), 70.8, 64.3 (br d, *J* = 83.9 Hz), 29.8 (d, *J* = 5.1 Hz), 29.7 (d, *J* = 5.1 Hz), 24.5 (d, *J* = 8.3 Hz), 23.2 (d, *J* = 8.9 Hz), 22.7 (d, *J* = 11.4 Hz); ^{31}P NMR (162 MHz, $CDCl_3$) δ = 32.3, -23.6; MALDI (α-cyano-4-hydroxycinnamic acid matrix) $[M\text{-}Cl]^+$ calculated for $C_{34}H_{32}Au_2ClFeO_2P_2$ 1019.025, found 1019.039; IR (neat) ν_{max} = 1448, 1008, 750 cm^{-1}.

1-184

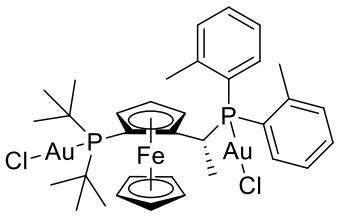

Following General Procedure A using $(Me_2S)AuCl$ (108 mg, 0.368 mmol) and phosphine (100 mg, 0.175 mmol) in DCM (2.9 mL) stirred for 1 h to give **1-184** as an orange solid (182

mg, 0.176 mmol, 100%). ^{1}H NMR (700 MHz, $CDCl_3$) δ = 8.22 (br s, 1H), 7.43 (m, 1H), 7.39 (m, 1H), 7.37 - 7.28 (m, 2H), 7.22 (m, 1H), 7.16 (br s, 1H), 6.96 (br s, 1H), 5.68 (br s, 1H), 4.92 (m, 1H), 4.68 - 4.44 (m, 7H), 2.50 - 2.37 (m, 6H), 1.80 (br d, *J* = 19.1 Hz, 3H), 1.73 (br d, *J* = 15.7 Hz, 9H), 1.29 (br d, *J* = 15.7 Hz, 9H); ^{13}C NMR (176 MHz, $CDCl_3$) δ = 142.3 (d, *J* = 6.4 Hz), 142.1 (d, *J* = 10.8 Hz), 132.8 (br d, *J* = 8.3 Hz), 132.3, 127.2, 126.9, 126.6 (br d, *J* = 12.7 Hz), 125.5 (d, *J* = 60.4 Hz), 125.1 (d, *J* = 9.5 Hz), 74.6-74.3 (m), 73.6-73.3 (m), 72.3 (br s), 70.2-70.0 (m), 69.2 (br dd, *J* = 7.9, 45.5 Hz), 39.0 (d, *J* = 28.6 Hz), 37.5 (d, *J* = 29.9 Hz), 30.6 (br d, *J* = 5.7 Hz), 30.4 (br s), 28.3-28.1 (m), 22.7, 22.6 ***2 Cs not observed and broad peaks due to weak sample***. ^{31}P NMR (162 MHz, $CDCl_3$) δ = 56.7, 28.8; MALDI (α-cyano-4-hydroxycinnamic acid matrix) $[M]^+$ calculated for $C_{34}H_{44}Au_2Cl_2FeP_2$ 1034.098, found 1034.110 & $[M\text{-}Cl]^+$ $C_{34}H_{44}Au_2ClFeP_2$ 999.129, found 999.139; IR (neat) ν_{max} = 2971, 1448 cm^{-1}.

1-184 is a known compound and the NMR data agree with reported literature.[108]

1-185

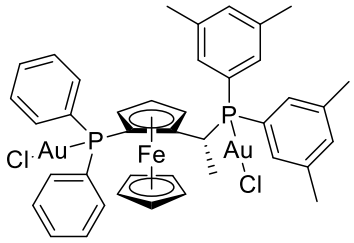

Following General Procedure A using (Me_2S)AuCl (92.0 mg, 0.313 mmol) and phosphine (100 mg, 0.175 mmol) in DCM (3.4 mL) stirred for 3 h to give **1-185** as an orange solid (149 mg, 0.135 mmol, 86%). ^{1}H NMR (700 MHz, $CDCl_3$) δ = 7.73 (br dd, *J* = 7.6, 13.6 Hz, 2H), 7.53 (m, 1H), 7.50 - 7.45 (m, 4H), 7.33 (m, 1H), 7.20 - 7.15 (m, 4H), 7.12 (s, 1H), 7.03 (br dd, *J* = 7.4, 13.4 Hz, 2H), 6.48 (br s, 1H), 5.27 - 5.20 (m, 2H), 4.73 (br s, 1H), 4.21 (br s, 1H), 3.98 (s, 5H), 2.40 (s, 6H), 2.05 (s, 6H), 1.77 (dd, *J* = 7.0, 18.0 Hz, 3H); ^{13}C NMR (176 MHz, $CDCl_3$) δ = 139.2 (d, *J* = 12.1 Hz), 138.3 (d, *J* = 12.1 Hz), 135.0 (d, *J* = 14.6 Hz), 134.0-133.8 (m, 2C), 132.2 (d, *J* = 13.4 Hz), 132.0 (d, *J* = 2.5 Hz), 132.0 (br d, *J* = 68.0 Hz), 131.8 (d, *J* = 7.6 Hz), 131.7 (d, *J* = 7.6 Hz), 130.8 (d, *J* = 62.9 Hz), 130.5 (d, *J* = 2.5 Hz), 128.8 (d, *J* = 12.1 Hz), 128.6 (d, *J* = 12.1 Hz), 128.7 (br d, *J* = 54.7 Hz), 127.4 (d, *J* = 55.3 Hz), 96.8 (br dd, *J* = 8.3, 17.2 Hz), 73.1 (appt. br t, *J* = 7.9 Hz), 72.2 (d, *J* = 5.1 Hz), 72.0 (br d, *J* = 7.6 Hz), 70.8, 66.1 (dd, *J* = 1.9, 70.6 Hz), 30.9 (dd, *J* = 4.5, 32.4 Hz), 23.0 (d, *J* = 7.0 Hz), 21.4, 21.3; ^{31}P NMR (162 MHz, $CDCl_3$) δ = 53.1, 19.7; MALDI (α-cyano-4-hydroxycinnamic acid matrix) $[M\text{-}Cl]^+$ calculated for $C_{40}H_{40}Au_2ClFeP_2$ 1067.097, found 1067.089; IR (neat) ν_{max} = 2916, 1435, 899 cm^{-1}.

12.4.4. Tosyl-Protected Enyne Reactions

General Procedure B

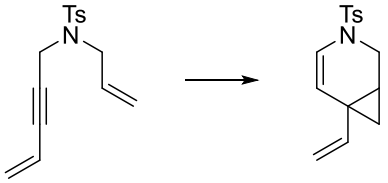

1-166 **1-167**

General Procedure B was adapted from a literature preparation.[102]

In an oven or heat-gun dried microwave vial, the gold pre-catalyst and silver salt were dissolved in the reaction solvent (1.0 mL) and stirred for 30 min at RT under an inert atmosphere. This was then left to stand until the AgCl had precipitated. The supernatant was used as the catalyst for the reaction and was transferred to a second oven or heat-gun dried microwave vial containing *N*-allyl-4-methyl-*N*-(pent-4-en-2-yn-1-yl)benzenesulfonamide **1-166** in reaction solvent (2.0 mL). The reaction mixture was stirred at 30 °C. Upon completion of the reaction, the reaction mixture was concentrated *in vacuo* before being purified using either the MDAP High pH system (water + 0.1% ammonium bicarbonate / MeCN 30-99%) or using the Combiflash EZ Prep with a XSelect® CSH™ Prep C18 5 µm OBD™ column (water + 0.1% ammonium bicarbonate / MeCN 30-85%). **1-167** was obtained as a colourless oil. For spectroscopic data, see literature preparation of **1-167** (*vide supra*).

Chiral Analysis

Chiral analysis was carried out using a Chiralpak AS-H (50 mm x 4.6 mm, 5 micron, 25 °C) column with a flow rate of 1 mL/ min and a heptane/ethanol (95:5) eluent over 20 min. Detection used a UV diode array at 220 nm. *Ee* values were obtained by measuring the area under each peak.

The experiments carried out using this general procedure are combined in Table 22 below.

Table 22. Reported experiments using General Procedure B and the amounts of reagents used.

Experiment	Amount of 1-166	Catalyst	Amount of Catalyst	AgX	Amount of AgX	Solvent	Time / h	Rel. Conv. / %	Yield / %	ee / %	Purification
Table 13, Entry 1 **Table 15, Entry 2** **Table 18, Entry 4**	50 mg (0.182 mmol)	**1-182**	22 mg (0.022 mmol)	$AgSbF_6$	10 mg (0.029 mmol)	THF	15	73	18	49.4	EZ Prep then MDAP
Table 13, Entry 2 **Table 14, Entry 1** **Table 15, Entry 1** **Table 16, Entry 1** **Table 18, Entry 3**	52 mg (0.189 mmol)	**1-182**	18 mg (0.018 mmol)	$AgSbF_6$	8 mg (0.023 mmol)	DCM	15.5	95	31	23.2	MDAP
Table 14, Entry 2	57 mg (0.207 mmol)	**1-183**	21 mg (0.020 mmol)	$AgSbF_6$	8 mg (0.023 mmol)	DCM	16.5	69	9	4.2	MDAP
Table 14, Entry 3	57 mg (0.207 mmol)	**1-184**	25 mg (0.024 mmol)	$AgSbF_6$	9 mg (0.026 mmol)	DCM	18	94	25	24.8	EZ Prep
Table 14, Entry 4	54 mg (0.196 mmol)	**1-185**	24 mg (0.022 mmol)	$AgSbF_6$	13 mg (0.038 mmol)	DCM	18	50	4	6.2	EZ Prep
Table 15, Entry 3	52 mg (0.189 mmol)	**1-182**	22 mg (0.022 mmol)	$AgSbF_6$	8 mg (0.023 mmol)	MeCN	15.5	0	0	N/A	N/A
Table 15, Entry 4	50 mg (0.182 mmol)	**1-182**	19 mg (0.019 mmol)	$AgSbF_6$	12 mg (0.035 mmol)	2-MeTHF	21	7	8	N/A	MDAP
Table 15, Entry 5	50 mg (0.182 mmol)	**1-182**	21 mg (0.021 mmol)	$AgSbF_6$	13 mg (0.038 mmol)	Toluene	21	0	2	N/A	MDAP
Table 15, Entry 6	53 mg (0.192 mmol)	**1-182**	18 mg (0.018 mmol)	$AgSbF_6$	10 mg (0.029 mmol)	TBME	22	0	0	N/A	MDAP
Table 15, Entry 7	49 mg (0.178 mmol)	**1-182**	17 mg (0.017 mmol)	$AgSbF_6$	10 mg (0.029 mmol)	DMF	22	0	33[a]	16.6	MDAP
Table 16, Entry 2	52 mg (0.189 mmol)	**1-182**	17 mg (0.017 mmol)	$NaBArF^b$	21 mg (0.024 mmol)	DCM	18	11	21[c]	N/A	MDAP
Table 16. Entry 3	56 mg (0.203 mmol)	**1-182**	24 mg (0.024 mmol)	$AgPF_6$	9 mg (0.036 mmol)	DCM	8	84	22	8.4	MDAP
Table 16, Entry 4	50 mg (0.182 mmol)	**1-182**	29 mg (0.029 mmol)	$AgBF_4$	9 mg (0.046 mmol)	DCM	17	100	16	20.2	MDAP
Table 16, Entry 5	49 mg (0.178 mmol)	**1-182**	22 mg (0.022 mmol)	$AgBF_4$	8 mg (0.041 mmol)	THF	18	43	24	16.4	EZ Prep

[a]88% purity; [b]NaBArF used with NaCl precipitating in catalyst formation. [c]35% purity by LCMS.

General Procedure C

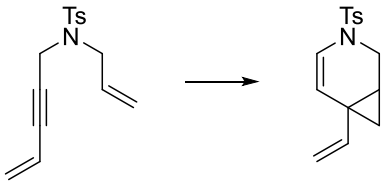

1-166 **1-167**

This procedure was adapted from a literature preparation.[102]

In an oven or heat-gun dried microwave vial, the gold pre-catalyst and silver salt were dissolved in DCM (2.0 mL) and stirred for 30 min at RT under an inert atmosphere. This was then left to stand until the AgCl had precipitated. The supernatant was used as the catalyst for the reaction and was transferred to a second oven or heat-gun dried microwave vial containing *N*-allyl-4-methyl-*N*-(pent-4-en-2-yn-1-yl)benzenesulfonamide **1-166** in DCM (4.0 mL). The reaction mixture was stirred at 30 °C for 19 h . Upon completion, the reaction mixture was concentrated *in vacuo* to give a brown residue. This was purified by normal phase chromatography, with the eluent system shown in Table 23**,** to give **1-167** as a colourless oil. For spectroscopic data, see literature preparation of **1-167** (*vide supra*).

The experiments carried out using General Procedure C are combined in Table 23 below.

Table 23. Reported experiments using General Procedure C and the amounts of reagents used.

Experiment	Amount of 1-166	Catalyst	Amount of Catalyst	AgX	Amount of AgX	Rel. Conv. / %	Yield / %	Purification
Table 17, Entry 1	102 mg (0.370 mmol)	**1-182**	35 mg (0.035 mmol)	$AgSbF_6$	16 mg (0.047 mmol)	86	4	cyclohexane/TBME (0-10% then 10%)
Table 17, Entry 2	99 mg (0.360 mmol)	**1-185**	47 mg (0.043 mmol)	$AgSbF_6$	15 mg (0.044 mmol)	64	6	cyclohexane/TBME (0-10% then 10%)
Table 17, Entry 3	103 mg (0.374 mmol)	**1-182**	37 mg (0.037 mmol)	$AgBF_4$	11 mg (0.057 mmol)	100	13	cyclohexane/toluene (0-80%)

12.4.5. Synthesis of Nitrogen-Protected Enynes

_N_-Benzylpent-4-en-2-yn-1-amine (1-188)

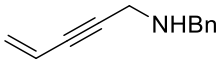

$Pd(PPh_3)_4$ (20.0 mg, 0.017 mmol), *N*-benzylprop-2-yn-1-amine **1-187** (473 mg, 3.26 mmol) and CuI (23.0 mg, 0.121 mmol) were dissolved in Et_2NH (1.70 mL, 16.3 mmol) and THF (5.0 mL). To this was added vinyl bromide (1 M in THF) (4.00 mL, 4.00 mmol) and the reaction mixture stirred at RT for 2 h before being diluted with water (20 mL) and diethyl ether (20 mL). The layers were separated and the aqueous washed with diethyl ether (2 × 20 mL). The organics were combined, dried using a hydrophobic frit and concentrated *in vacuo* yielding a brown oil which was purified by flash chromatography (cyclohexane/EtOAc 0-50%). **1-188** was obtained as a brown oil (370 mg, 2.16 mmol, 66%). ^{1}H NMR (400 MHz, $CDCl_3$) δ = 7.39 - 7.32 (m, 4H), 7.27 (m, 1H), 5.85 (m, 1H), 5.65 (m, 1H), 5.47 (dd, *J* = 2.2, 11.2 Hz, 1H), 3.91 (br s, 2H), 3.57 (br s, 2H); ^{13}C NMR (101 MHz, $CDCl_3$) δ = 139.5, 128.4, 128.4, 127.1, 126.6, 117.1, 88.3, 82.4, 52.4, 38.1; LCMS (high pH) t_R = 1.04 min, [M+H$^+$] 172.0 (purity 100%); HRMS [M+H$^+$] calculated for $C_{12}H_{14}N$ 172.1121, found [M+H$^+$] 172.1128; IR (neat) ν_{max} = 3027, 1453, 734, 697 cm^{-1}.

_N_-Allyl-_N_-benzylpent-4-en-2-yn-1-amine (1-189)

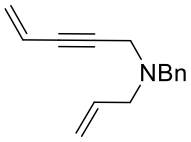

N-Benzylpent-4-en-2-yn-1-amine (691 mg, 4.04 mmol) was dissolved in THF (20 mL) and cooled to 0 °C before NaH (186 mg, 4.65 mmol) was added and the resulting mixture stirred for 15 min. Allyl bromide (0.38 mL, 4.39 mmol) was then added slowly and the reaction warmed to RT and stirred for 17.5 h before being heated to 40 °C for 2.5 h before being cooled to RT and additional NaH (90.0 mg, 2.32 mmol) and allyl bromide (0.19 mL, 2.20 mmol) were added. The reaction mixture was heated to 40 °C and stirred for an additional 1.5 h before being cooled to RT. Saturated aqueous ammonium chloride (10 mL) was added and then diluted with water (20 mL) and EtOAc (30 mL). The layers were separated and the aqueous washed with further EtOAc (2 × 30 mL). The organics were combined, dried using a hydrophobic frit and concentrated *in vacuo* yielding a brown oil which was purified by flash chromatography (cyclohexane/EtOAc 0-50%). **1-189** was obtained as a pale yellow oil (488 mg, 2.31 mol, 57%). ^{1}H NMR (400 MHz, $CDCl_4$) δ = 7.42 - 7.25 (m, 5H), 5.98 - 5.84 (m, 2H), 5.68 (m, 1H), 5.50 (dd, *J* = 2.2, 11.1 Hz, 1H), 5.31 (ddd, *J* = 1.6, 1.6, 17.2 Hz, 1H), 5.20 (m, 1H), 3.68 (s, 2H), 3.46 (d, *J* = 2.0 Hz, 2H), 3.22 (d, *J* = 6.4 Hz, 2H); ^{13}C NMR (101

MHz, $CDCl_3$) δ = 138.7, 135.7, 129.2, 128.3, 127.1, 126.5, 117.9, 117.1, 85.3, 84.3, 57.4, 56.7, 42.2; LCMS (high pH) t_R = 1.39 min, [M+H$^+$] 212.1 (purity 195%); HRMS [M+H$^+$] calculated for $C_{15}H_{18}N$ 212.1434, found [M+H$^+$] 212.1443; IR (neat) ν_{max} = 2814, 918, 738, 697 cm^{-1}.

1-189 is a known compound and the data agree with those reported.[102]

***tert*-Butyl allyl(prop-2-yn-1-yl)carbamate (1-191)**

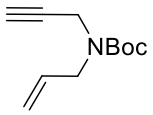

tert-Butyl prop-2-yn-1-ylcarbamate **1-190** (999 mg, 6.44 mmol) was dissolved in THF (32 ml) and the solution degassed for 10 min before being put under a nitrogen atmosphere. This was then cooled to 0 °C before NaH (283 mg, 7.09 mmol) was added. The reaction mixture was stirred for 30 min before allyl bromide (0.613 mL, 7.09 mmol) was added slowly and the mixture warmed to RT. This was stirred for 16 h and saturated aqueous ammonium chloride (20 mL) was added to the reaction mixture which was washed with diethyl ether (50 mL). The layers were separated and the aqueous washed with diethyl ether (50 mL). The organics were combined and dried using a hydrophobic frit before being concentrated *in vacuo* to give a yellow oil which was purified by flash chromatography (cyclohexane/EtOAc 0-30%). **1-191** was obtained as a colourless oil (511 mg, 2.62 mmol, 41%). ^{1}H NMR (400 MHz, $CDCl_3$) δ = 5.78 (tdd, *J* = 5.9, 10.3, 17.1 Hz, 1H), 5.22 - 5.12 (m, 2H), 4.13 - 3.97 (m, 2H), 3.96 - 3.87 (m, 2H), 2.18 (t, *J* = 2.4 Hz, 1H), 1.47 (s, 9H); ^{13}C NMR (101 MHz, $CDCl_3$) δ = 154.8, 133.3, 117.1, 80.3, 79.6, 71.2, 48.5, 35.4, 28.3; TLC R_f = 0.51 (cyclohexane/EtOAc 30%); IR (neat) ν_{max} = 3302, 2978, 1693, 1403, 1244, 1166, 1144 cm^{-1}.

1-191 is a known compound and the data agree with those reported.[163]

***tert*-Butyl allyl(pent-4-en-2-yn-1-yl)carbamate (1-192)**

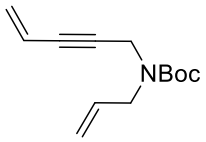

CuI (31.0 mg, 0.164 mmol) and $Pd(PPh_3)_4$ (70.0 mg, 0.061 mmol) were dissolved in Et_2NH (1.82 mL, 17.4 mmol). To this was added a solution of *tert*-butyl allyl(prop-2-yn-1-yl)carbamate **1-191** (800 mg, 4.10 mmol) in THF (6.1 mL). The reaction was cooled to 0 °C and vinyl bromide (1 M in THF) (8.19 mL, 8.19 mmol) bromide was added. The reaction was warmed to RT slowly and stirred for 18 h before being cooled to 0 °C. Water (20 mL)

was then added and the resulting solution was extracted with diethyl ether (3 × 20 mL). The organics were combined, dried using a hydrophobic frit and concentrated *in vacuo* to give a brown oil which was purified by flash chromatography (cyclohexane/EtOAc 2%). The isolated material from the initial purification was contaminated and submitted to further flash chromatography (cyclohexane/EtOAc 0-1%). **1-192** was isolated as a dark yellow oil (411 mg, 1.86 mmol, 45%). ^{1}H NMR (400 MHz, CD_2Cl_2) δ = 5.85 - 5.74 (m, 2H), 5.64 - 5.58 (m, 1H), 5.47 (dd, *J* = 2.2, 11.0 Hz, 1H), 5.20 - 5.12 (m, 2H), 4.21 - 4.02 (m, 2H), 3.91 (d, *J* = 5.9 Hz, 2H), 1.45 (s, 9H); ^{13}C NMR (101 MHz, CD_2Cl_2) δ = 134.3, 127.4, 117.4, 117.1, 86.5, 82.3, 80.5, 49.2, 36.6, 28.6 ***peak for carbonyl not observed***; LCMS (formic acid) t_R = 1.30 min, [M-^{t}Bu+2H^{+}] 166.0 (purity 100%).

1-192 is a known compound and the data agree with those reported.[102]

2-Nitro-*N*-(prop-2-yn-1-yl)benzenesulfonamide (1-193)

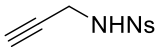

174 was prepared using a literature procedure.[94]

Propargylamine **1-175** (11.0 mL, 172 mmol) and Et_3N (24.0 mL, 172 mmol) were dissolved in DCM (172 mL) and cooled to 0 °C. 2-Nitrobenzenesulfonyl chloride (40.2 g, 181 mmol) was added portionwise over 15 min. The reaction was then warmed to RT and stirred for 1.5 h before being quenched with 2 M aqueous HCl (20 mL). The layers were separated and the organic washed with water (100 mL) and saturated aqueous bicarb (50 mL). The organic layer was dried using a hydrophobic frit and concentrated *in vacuo* to yield a brown oil which solidified at RT. This was transferred to a smaller vial in DCM and concentrated *in vacuo* to yield **1-193** as a brown grainy solid (42.2 g, 176 mmol, 102%). This was used without further purification. ^{1}H NMR (400 MHz, $CDCl_3$) δ = 8.22 (m, 1H), 7.93 (m, 1H), 7.80 - 7.74 (m, 2H), 5.69 (br s, 1H), 4.03 (dd, *J* = 2.6, 6.2 Hz, 2H), 1.99 (t, *J* = 2.6 Hz, 1H); ^{13}C NMR (101 MHz, $CDCl_3$) δ = 148.0, 134.1, 133.8, 132.9, 131.6, 125.5, 77.4, 73.3, 33.4; LCMS (high pH) t_R = 0.77 min, [M-H]$^{-}$ 239.1 (purity 97%); HRMS [M+H^{+}] calculated for $C_9H_9N_2O_4S$ 241.0278, found [M+H^{+}] 241.0283; IR (neat) ν_{max} = 3296, 1536, 1331 cm^{-1}.

174 is a known compound and the data agree with reported literature.[94]

2-Nitro-*N*-(pent-4-en-2-yn-1-yl)benzenesulfonamide (1-194)

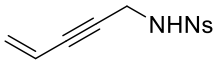

CuI (99.0 mg, 0.520 mmol) and $Pd(PPh_3)_4$ (102 mg, 0.088 mmol) were dissolved in diethylamine (6.90 mL, 66.0 mmol) under an inert atmosphere. **1-193** (3.17 g, 13.2 mmol) was dissolved in vinyl bromide (1 M in THF) (26.4 mL, 26.4 mmol) and added to the reaction mixture. This was stirred at RT for 1 h 40 min before being diluted with water (30 mL) and diethyl ether (50 mL). The layers were separated and the aqueous washed with diethyl ether (2 × 50 mL). The organics were combined, dried using a hydrophobic frit and concentrated *in vacuo* yielding a brown oil which was purified by flash chromatography (cyclohexane/EtOAc 0-60%) yielding **1-194** as a brown oil which solidified slowly at RT (2.79 g, 10.5 mmol, 79%). ^{1}H NMR (400 MHz, $CDCl_3$) δ = 8.24 (m, 1H), 7.93 (m, 1H), 7.81 - 7.72 (m, 2H), 5.69 (br t, *J* = 5.9 Hz, 1H), 5.44 (m, 1H), 5.37 - 5.27 (m, 2H), 4.17 - 4.13 (m, 2H); ^{13}C NMR (101 MHz, $CDCl_3$) δ = 134.3, 133.6, 132.9, 131.6, 127.9, 125.4, 115.8, 83.8, 83.2, 34.2; LCMS (high pH) t_R = 0.95 min, $[M-H]^-$ 265.2 (purity 98%); HRMS $[M+H^+]$ calculated for $C_{11}H_{11}N_2O_4S$ 267.0434, found $[M+H^+]$ 267.0439; IR (neat) ν_{max} = 3317, 1533, 1329, 1156 cm^{-1}.

***N*-Allyl-2-nitro-*N*-(pent-4-en-2-yn-1-yl)benzenesulfonamide (1-195)**

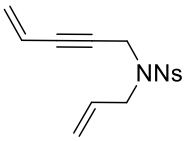

1-194 (5.12 g, 19.2 mmol) and K_2CO_3 (5.37 g, 38.9 mmol) were dissolved in MeCN (50 mL). Allyl bromide (2.50 mL, 28.9 mmol) was added and the reaction heated to 65 °C for 1.5 h before being cooled to RT. Saturated aqueous ammonium chloride (50 mL) was added followed by EtOAc (80 mL) and the layers were separated. The aqueous was washed with EtOAc (2 × 80 mL) and the organics were combined, dried using a hydrophobic frit and concentrated *in vacuo* yielding a brown residue. This was purified by flash column chromatography (cyclohexane/TBME 0-50%) to give **1-195** as a pale yellow oil (4.59 g, 15.0 mmol, 78%). ^{1}H NMR (400 MHz, $CDCl_3$) δ = 8.08 (m, 1H), 7.74 - 7.61 (m, 3H), 5.75 (tdd, *J* = 6.4, 10.2, 16.9 Hz, 1H), 5.62 (m, 1H), 5.50 - 5.40 (m, 2H), 5.36 - 5.23 (m, 2H), 4.26 (d, *J* = 2.0 Hz, 2H), 4.03 (d, *J* = 6.4 Hz, 2H); ^{13}C NMR (101 MHz, $CDCl_3$) δ = 148.3, 133.6, 133.0, 131.7, 131.5, 131.0, 127.8, 124.1, 120.2, 116.1, 84.2, 82.6, 49.6, 36.7; LCMS (high pH) t_R = 1.19 min, $[M+NH_4^+]$ 324.0 (purity 100%); HRMS $[M+H^+]$ calculated for $C_{14}H_{15}N_2O_4S$ 307.0747, found $[M+H^+]$ 307.0750; IR (neat) ν_{max} = 1541, 1355, 1163 cm^{-1}.

1-195 is a known compound and the data agree with reported literature.[102]

12.4.6. Cycloisomerisation Reactions with Nitrogen-Protected Enynes

*With Benzyl-protected enyne **1-189**:*

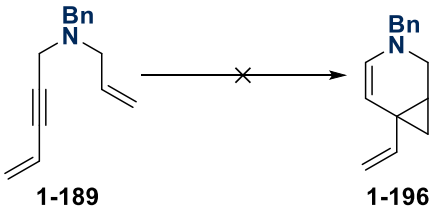

Au(JohnPhos)Cl (25.0 mg, 0.047 mmol) and $AgSbF_6$ (20.0 mg, 0.057 mmol) were added to an oven-dried microwave vial and put under a nitrogen atmosphere before DCM (3.0 mL) was added. This was stirred for 30 min and then left to stand until the AgCl had precipitated. The supernatant was used as the catalyst and was transferred to a second oven-dried microwave vial containing *N*-allyl-*N*-benzylpent-4-en-2-yn-1-amine **1-189** (100 mg, 0.473 mmol) in DCM (5.6 mL). This was stirred at RT for 17 h before being concentrated *in vacuo*. NMR of the concentrated, crude reaction mixture indicated only the presence of starting material.

*With Boc-protected enyne **1-192**:*

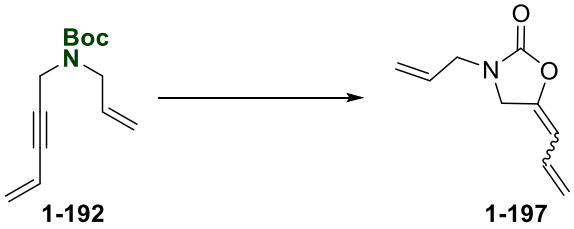

Au(JohnPhos)Cl (24.0 mg, 0.045 mmol) and $AgSbF_6$ (19.0 mg, 0.054 mmol) were added to an oven-dried microwave vial and put under a nitrogen atmosphere before DCM (2.8 mL) was added. This was stirred at RT for 30 min and left to stand until the formed AgCl had precipitated. The supernatant was then used as the catalyst and was transferred to a second oven-dried microwave vial containing *tert*-butyl allyl(pent-4-en-2-yn-1-yl)carbamate **1-192** (100 mg, 0.452 mmol) in DCM (5.4 mL). The reaction was stirred at RT for 2 h before being concentrated *in vacuo*. The resulting brown residue was purified by flash chromatography (cyclohexane/EtOAc 0-10%) to give two isomers of product **1-197.**

Isomer 1: 7.0 mg, 0.04 mmol, 9%; ^{1}H NMR (400 MHz, $CDCl_3$) δ = 6.64 (m, 1H), 5.78 (m, 1H), 5.33 - 5.28 (m, 2H), 5.26 (m, 1H), 5.14 (appt. ddq, *J* = 0.9, 1.8, 17.2 Hz, 1H), 5.04 (appt. ddq, *J* = 0.9, 1.8, 10.4 Hz, 1H), 4.16 (dd, *J* = 0.9, 1.8 Hz, 2H), 3.93 (dt, *J* = 1.3, 6.1 Hz, 2H); ^{13}C NMR (101 MHz, $CDCl_3$) δ = 155.0, 142.4, 131.2, 128.8, 119.3, 115.7, 104.1, 47.5, 46.4; LCMS (formic acid) t_R = 0.92 min, [M+H$^+$] 166.0 (purity 100%).

Isomer 2: 10.0 mg, 0.06 mmol, 13%; ^{1}H NMR (400 MHz, $CDCl_3$) δ = 6.06 (dd, *J* = 10.8, 17.1 Hz, 1H), 5.84 (m, 1H), 5.74 (m, 1H), 5.28 (m, 1H), 5.26 - 5.22 (m, 2H), 5.06 (t, *J* = 3.5 Hz, 1H), 4.01 (dt, *J* = 1.3, 6.1 Hz, 2H), 3.90 - 3.86 (m, 2H); ^{13}C NMR (101 MHz, $CDCl_3$) δ = 150.0, 147.9, 131.3, 127.9, 118.7, 116.2, 98.4, 51.2, 44.8; LCMS (formic acid) t_R = 0.80 min, [M+H$^+$] 166.0 (purity 92%).

The data for these by-products agrees with that reported in the literature.[102]

*With nosyl-protected enyne **1-195**:*

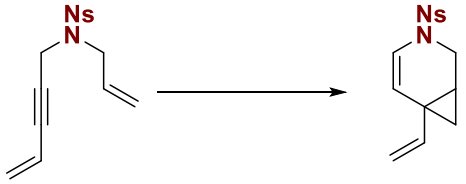

1-195 **1-198**

Au(JohnPhos)Cl (21.0 mg, 0.040 mmol) and $AgSbF_6$ (21.0 mg, 0.061 mmol) were added to an oven-dried microwave vial and put under a nitrogen atmosphere before DCM ((2.0 mL) was added. This was stirred at RT for 1 h and left to stand until the formed AgCl had precipitated. The supernatant was then used as the catalyst in the cyclisation reaction and added to a second oven-dried microwave vial containing *N*-allyl-2-nitro-*N*-(pent-4-en-2-yn-1-yl)benzenesulfonamide **1-195** (100 mg, 0.326 mmol) in DCM (3.0 mL) and this stirred at RT for 18 h. The reaction mixture was then filtered through a hydrophobic frit and concentrated *in vacuo* yielding a yellow residue which was purified using the Combiflash EZ Prep with a XSelect® CSH™ Prep C18 5 µm OBD™ column (water + 0.1% ammonium bicarbonate / MeCN 30-85%). **1-198** was obtained as a dark yellow oil (34 mg, 0.111 mmol, 34%). ^{1}H NMR (400 MHz, $CDCl_3$) δ = 7.98 (m, 1H), 7.77 - 7.69 (m, 2H), 7.66 (m, 1H), 6.42 (dd, *J* = 0.7, 8.3 Hz, 1H), 5.64 (dd, *J* = 0.5, 8.3 Hz, 1H), 5.51 (dd, *J* = 10.6, 17.2 Hz, 1H), 5.06 (dd, *J* = 0.9, 17.2 Hz, 1H), 4.99 (dd, *J* = 0.7, 10.5 Hz, 1H), 4.04 (td, *J* = 1.3, 12.2 Hz, 1H), 3.34 (dd, *J* = 2.8, 12.1 Hz, 1H), 1.71 (m, 1H), 1.08 (ddd, *J* = 0.7, 4.7, 8.7 Hz, 1H), 0.88 (dd, *J* = 4.9, 6.1 Hz, 1H); ^{13}C NMR (101 MHz, $CDCl_3$) δ = 148.1, 141.3, 133.9, 131.7, 131.4, 130.7, 124.2, 120.4, 113.3, 111.7, 41.0, 28.0, 22.9, 19.6; LCMS (high pH) t_R = 1.22 min, [M+H$^+$] 307.1 (purity 96%); HRMS [M+H$^+$] calculated for $C_{14}H_{15}N_2O_4S$ 307.0747, found [M+H$^+$] 307.0749; IR (neat) ν_{max} = 1630, 1541, 1360, 1171 cm^{-1}.

12.4.7. Nosyl-Protected Enyne Reactions

(3-((2-Nitrophenyl)sulfonyl)-6-vinyl-3-azabicyclo[4.1.0]hept-4-ene (1-198)

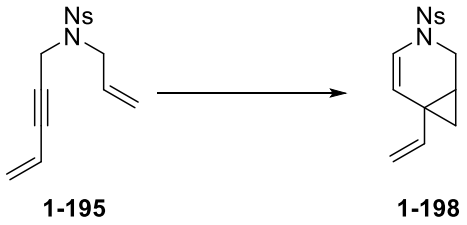

1-195 **1-198**

Chiral Analysis:

Chiral analysis was carried out using a Chiralpak IG (250 mm x 4.6 mm, 5 micron) column at 25 °C with a flow rate of 1 mL/ min and a heptane (+0.1% v/v isopropylamine)/ethanol (+0.1% v/v isopropylamine) 1:1 eluent over 15 min. Detection used a UV diode array at 220 nm. *Ee* values were obtained by measuring the area under each peak.

Table 18, Entry 1 – in DCM

To an oven-dried microwave vial was added **1-182** (18.0 mg, 0.018 mmol) and $AgSbF_6$ (11.0 mg, 0.032 mmol) which were dissolved in DCM (1.0 mL) under an inert atmosphere. This was stirred at RT for 1 h and left to stand until the formed AgCl had precipitated. The supernatant was then used as the catalyst in the cyclisation reaction and added to a second oven-dried microwave vial containing **1-195** (56.0 mg, 0.183 mmol) in DCM (2.0 mL) and this stirred at RT for 19 h before the reaction mixture was concentrated under a flow of nitrogen to give a brown residue which was purified using the MDAP High pH system (water + 0.1% ammonium bicarbonate / MeCN 30-99%) yielding **1-198** as a yellow gum (4.1 mg, 0.013 mmol, 7%). Measured *ee* value = 28.0%.

Table 18, Entry 2 – in THF

To an oven-dried microwave vial was added **1-182** (17.0 mg, 0.017 mmol) and $AgSbF_6$ (10.0 mg, 0.029 mmol) which were dissolved in THF (1.0 mL) under an inert atmosphere. This was stirred at RT for 1 h and left to stand until the formed AgCl had precipitated. The supernatant was then used as the catalyst in the cyclisation reaction and added to a second oven-dried microwave vial containing **1-195** (53.0 mg, 0.173 mmol) in THF (2.0 mL) and the reaction mixture stirred at RT for 25 h. The temperature was then increased to 50 °C and the reaction mixture stirred for an additional 24 h before being cooled to RT. The reaction mixture was then concentrated under a flow of nitrogen to yield a black residue which was purified using the MDAP High pH system (water + 0.1% ammonium bicarbonate / MeCN 30-99%) yielding **1-198** as a yellow gum (4.5 mg, 0.015 mmol, 8%). Measured *ee* value = 35.4%.

Table 18 Entries 3 and 4 reported in Table 24 (*vide supra,* Section 12.4.4)

Scheme 52 – Introduction of OTf Counterion

DCM:

To an oven-dried microwave vial was added **1-182** (20.0 mg, 0.020 mmol) and AgOTf (5.0 mg, 0.020 mmol) which were dissolved in DCM (1.0 mL) under an inert atmosphere. This was stirred at RT for 1 h and left to stand until the formed AgCl had precipitated. The supernatant was then used as the catalyst in the cyclisation reaction and added to a second oven-dried microwave vial containing **1-195** (53.0 mg, 0.173 mmol) in DCM (2.0 mL) and the reaction stirred at RT for 42 h before being concentrated under a flow of nitrogen to give a brown solid. This was purified using the MDAP High pH system (water + 0.1% ammonium bicarbonate / MeCN 30-99%) yielding **1-198** as a yellow oil (34.9 mg, 0.114 mmol, 66%). Measured *ee* value = 48.6%.

THF:

To an oven-dried microwave vial was added **1-182** (19.0 mg, 0.019 mmol) and AgOTf (7.0 mg, 0.025 mmol) which were dissolved in THF (1.0 mL) under an inert atmosphere. This was stirred at RT for 1 h and left to stand until the formed AgCl had precipitated. The supernatant was then used as the catalyst in the cyclisation reaction and added to a second oven-dried microwave vial containing **1-195** (53.0 mg, 0.173 mmol) in THF (2.0 mL) and the reaction mixture stirred at RT for 42 h before being concentrated under a flow of nitrogen to give a brown solid. This was purified using the MDAP High pH system (water + 0.1% ammonium bicarbonate / MeCN 30-99%) yielding **1-198** as a yellow oil (7.5 mg, 0.024 mmol, 14%). Measured *ee* value = 24.4%.

Scheme 53 – Introduction of AgOTf to Tosyl-Protected Enyne 1-166

To an oven-dried microwave vial was added **1-182** (37.0 mg, 0.036 mmol) and AgOTf (11.0 mg, 0.044 mmol) which were dissolved in DCM (2.7 mL) under an inert atmosphere. This was stirred at RT for 30 min and left to stand until the formed AgCl had precipitated. The supernatant was then used as the catalyst in the cyclisation reaction and added to a second oven-dried microwave vial containing **1-166** (100 mg, 0.363 mmol) in DCM (4.0 mL) and the reaction mixture stirred at RT for 17 h before being concentrated *in vacuo* to give a brown solid. This was purified using flash chromatography (cyclohexane/DCM 0-80%) yielding **1-167** as a colourless oil (36.1 mg, 0.131 mmol, 36%). Measured *ee* value = 19.2%.

Table 19, Entry 1 – Catalyst 1-183 with AgOTf

To an oven-dried microwave vial was added **1-183** (33.0 mg, 0.031 mmol) and AgOTf (10.0 mg, 0.039 mmol) which were dissolved in DCM (2.0 mL) under an inert atmosphere. This was stirred at RT for 1 h and left to stand until the formed AgCl had precipitated. The supernatant was then used as the catalyst in the cyclisation reaction and added to a second oven-dried microwave vial containing **1-195** (104 mg, 0.339 mmol) in DCM (4.0 mL) and the reaction mixture stirred at RT for 19 h before being concentrated under a flow of nitrogen to give a brown solid which was purified by flash chromatography (cyclohexane/TBME 0-50%). This gave **1-198** as a yellow oil (16.2 mg, 0.053 mmol, 16%). Measured *ee* value = 44.8%.

Table 19, Entry 2 – Catalyst 1-184 with AgOTf

To an oven-dried microwave vial was added **1-184** (16.0 mg, 0.015 mmol) and AgOTf (7.0 mg, 0.027 mmol) which were dissolved in DCM (1.0 mL) under an inert atmosphere. This was stirred at RT for 1 h and left to stand until the formed AgCl had precipitated. The supernatant was then used as the catalyst in the cyclisation reaction and added to a second oven-dried microwave vial containing **1-195** (59 mg, 0.193 mmol) in DCM (2.0 mL) and the reaction mixture stirred at RT for 19 h before being concentrated under a flow of nitrogen to give a brown solid. This was purified using the MDAP High pH system (water + 0.1% ammonium bicarbonate / MeCN 30-99%) yielding **1-198** as a yellow oil (11.0 mg, 0.036 mmol, 19%). Measured *ee* value = 25.8%.

Table 19, Entry 3 – Catalyst 1-185 with AgOTf

To an oven-dried microwave vial was added **1-185** (21.0 mg, 0.019 mmol) and AgOTf (5.0 mg, 0.020 mmol) which were dissolved in DCM (1.0 mL) under an inert atmosphere. This was stirred at RT for 1 h and left to stand until the formed AgCl had precipitated. The supernatant was then used as the catalyst in the cyclisation reaction and added to a second oven-dried microwave vial containing **1-195** (59 mg, 0.193 mmol) in DCM (2.0 mL) and the reaction mixture stirred at RT for 19 h before being concentrated under a flow of nitrogen to give a brown solid. This was purified using the MDAP High pH system (water + 0.1% ammonium bicarbonate / MeCN 30-99%) yielding **1-198** as a yellow oil (17.2 mg, 0.056 mmol, 29%). Measured *ee* value = 17.6%.

Scheme 54 – Repeat of Initial Conditions

To an oven-dried microwave vial was added **1-182** (34.0 mg, 0.034 mmol) and AgOTf (13.0 mg, 0.051 mmol) which were dissolved in DCM (2.0 mL) under an inert atmosphere. This was stirred at RT for 30 min and left to stand until the formed AgCl had precipitated. The supernatant was then used as the catalyst in the cyclisation reaction and added to a second oven-dried microwave vial containing **1-195** (117 mg, 0.382 mmol) in DCM (4.0 mL) and the reaction stirred at RT for 22 h before the reaction mixture was diluted with water (10 mL). The layers were separated and the aqueous washed with DCM (2 × 10 mL). The organics were combined, dried using a hydrophobic frit and concentrated *in vacuo* yielding a yellow oil which was purified by flash chromatography (cyclohexane/TBME 0-60%). **1-198** was obtained as a yellow oil (63.1 mg, 0.206 mmol, 54%). Measured *ee* value = 35.0%.

12.4.8. Reduction of Enamine

3-((4-Nitrophenyl)sulfonyl)-6-vinyl-3-azabicyclo[4.1.0]heptane (1-199)

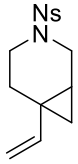

1-198 (192 mg, 0.627 mmol) was dissolved in DCM (6.3 mL) before Et_3SiH (0.25 mL, 1.57 mmol) and TFA (0.24 mL, 3.13 mmol) were added. This was stirred at RT for 30 min before being added slowly to saturated sodium bicarbonate solution (20 mL). The layers were separated and the aqueous washed with DCM (2 × 20 mL). The combined organics were dried using a hydrophobic frit and concentrated *in vacuo* yielding a brown oil which was purified by flash chromatography (cyclohexane/TBME 0-60%). **1-199** was obtained as a colourless oil (125 mg, 0.291 mmol, 65%). ^{1}H NMR (400 MHz, $CDCl_3$) δ = 7.98 (m, 1H), 7.73 - 7.59 (m, 3H), 5.48 (dd, *J* = 10.5, 17.4 Hz, 1H), 4.96 - 4.89 (m, 2H), 3.65 (m, 1H), 3.55 (m, 1H), 3.27 - 3.13 (m, 2H), 2.17 (m, 1H), 1.91 (ddd, *J* = 5.4, 7.9, 13.8 Hz, 1H), 1.20 (m, 1H), 0.86 (dd, *J* = 5.1, 8.8 Hz, 1H), 0.78 (m, 1H); ^{13}C NMR (101 MHz, $CDCl_3$) δ = 148.2, 144.4, 133.5, 132.1, 131.5, 130.8, 124.0, 110.5, 44.2, 42.1, 25.6, 20.0, 19.5, 17.4; LCMS (formic acid) t_R = 1.19 min, [M+H$^+$] 309.0 (purity 91%); HRMS [M+H$^+$] calculated for $C_{14}H_{17}N_2O_4S$ 309.0904, found [M+H$^+$] 309.0909; IR (neat) ν_{max} = 3088, 2922, 2860, 1541, 1345, 1163, 1129 cm^{-1}.

12.4.9. *In Situ* Reduction of Enamine

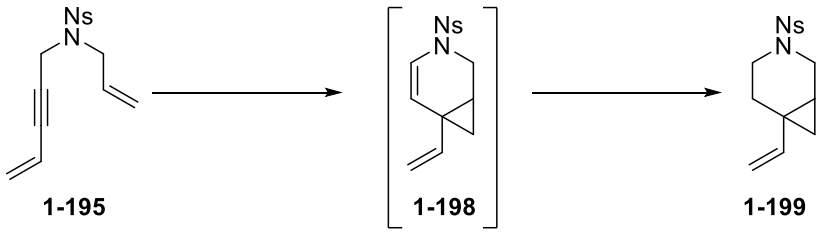

General Procedure D

To an oven-dried microwave vial was added **1-182** (33.0 mg, 0.033 mmol) and AgOTf (10.0 mg, 0.039 mmol) which were dissolved in DCM (2.0 mL) under an inert atmosphere. This was stirred at RT for 30 min and left to stand until the formed AgCl had precipitated. The supernatant was then used as the catalyst in the cyclisation reaction and added to a second vial containing **1-195** (100 mg, 0.326 mmol) in DCM (4.0 mL) and this stirred at RT for 17 h. The reaction mixture was then subjected to the reduction conditions and purification method specified for each reaction.

Chiral Analysis:

Chiral analysis was carried out using a Chiralpak IG (250 mm x 4.6 mm, 5 micron) column at 25 °C with a flow rate of 1 mL/ min and a heptane (+0.1% v/v isopropylamine)/ethanol (+0.1% v/v isopropylamine) 1:1 eluent over 20 min. Detection used a UV diode array at 250 nm. *Ee* values were obtained by measuring the area under each peak.

Table 20, Entry 1 (also shown in *Scheme 56*)

Following General Procedure D. After 17 h, TFA (55.0 µL, 0.718 mmol) and Et_3SiH (63.0 µL, 0.392 mmol) were added and the reaction stirred for 1.5 h before being added to a stirring solution of saturated aqueous sodium bicarbonate (15 mL). The layers were separated and the organic washed with water (10 mL) before being dried using a hydrophobic frit and concentrated *in vacuo* giving a brown residue. This was purified using flash chromatography (cyclohexane/TBME 0-100%) to give **1-199** as a colourless oil (46.9 mg, 0.152 mmol, 47%). The maximum purity of this sample of **1-199** was measured to be 93% by LCMS. Measured *ee* value = 48.4%.

Table 20, Entry 2

Following General Procedure D. After 17 h, TFA (55.0 µL, 0.718 mmol) and Et_3SiH (63.0 µL, 0.392 mmol) were added and the reaction stirred for 3 h. Additional TFA (55.0 µL, 0.718 mmol) and Et_3SiH (63.0 µL, 0.392 mmol) were added and the reaction stirred for an

additional 1.5 h before being added to a stirring solution of saturated aqueous sodium bicarbonate (15 mL). The layers were separated and the aqueous washed with DCM (2 × 10 mL). The organics were combined, dried using a hydrophobic frit and concentrated *in vacuo* giving a brown residue. This was purified using flash chromatography (cyclohexane/DCM 30-100%). Isolated from this was a colourless oil (42.0 mg) containing **1-199** with a purity of 72% by LCMS.

Table 20, Entry 3

Following General Procedure D. After 17 h the reaction mixture was cooled to 0 °C and TFA (28.0 µL, 0.359 mmol) and Et_3SiH (57.0 µL, 0.359 mmol) were added and the reaction stirred for 4.5 h at this temperature. Additional TFA (28.0 µL, 0.359 mmol) and Et_3SiH (57.0 µL, 0.359 mmol) were added and the reaction stirred for an additional 1.5 h before being added to a stirring solution of saturated aqueous sodium bicarbonate (10 mL). The layers were separated and the organic dried using a hydrophobic frit and concentrated *in vacuo* giving a brown residue. This was purified using flash chromatography (cyclohexane/DCM 0-80%) to give **1-199** as a colourless oil (52.1 mg, 0.169 mmol, 52%). Measured *ee* value = 43.4%.

(*E*)-1-((2-Nitrophenyl)sulfonyl)-4-(prop-1-en-1-yl)-1,2,3,6-tetrahydropyridine (1-200)

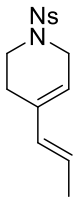

By-product **1-200** was isolated from a failed scale-up cycloisomerisation-reduction reaction (using 1.0 g of **1-195**) and isolated by another member of our laboratories.[164] The purification used an XBridge C18 30 mm × 150 mm, 5 micromolar column with a flow rate of 40 mL/ min. The solvent system consisted of: Solvent A = 10mM ammonium bicarbonate in water, adjusted to pH 10 with ammonia solution; and Solvent B = MeCN. The gradient used was 40-100% MeCN over 25 min. **1-200** was identified by NMR, showing a purity of approximately 85%. ^{1}H NMR (600 MHz, DMSO-d_6) δ = 8.02 (br d, *J* = 7.7 Hz, 1H), 7.98 (br d, *J* = 7.9 Hz, 1H), 7.90 (br t, *J* = 7.3 Hz, 1H), 7.85 (m, 1H), 6.05 (br d, *J* = 15.6 Hz, 1H), 5.61 (br s, 1H), 5.60 (m, 1H), 3.83 (br s, 2H), 3.40 (br t, *J* = 5.8 Hz, 2H), 2.23 (br s, 2H), 1.71 (br d, *J* = 6.4 Hz, 3H); ^{13}C NMR (151 MHz, DMSO-d_6) δ = 147.8, 134.7, 133.5, 132.3, 132.3, 130.2, 129.8, 124.2, 123.6, 120.5, 44.5, 42.3, 24.2, 17.9; LCMS (high pH) t_R = 1.25 min, [M+H$_+$] 309.0 (purity 100%).

HSQC-DEPT:

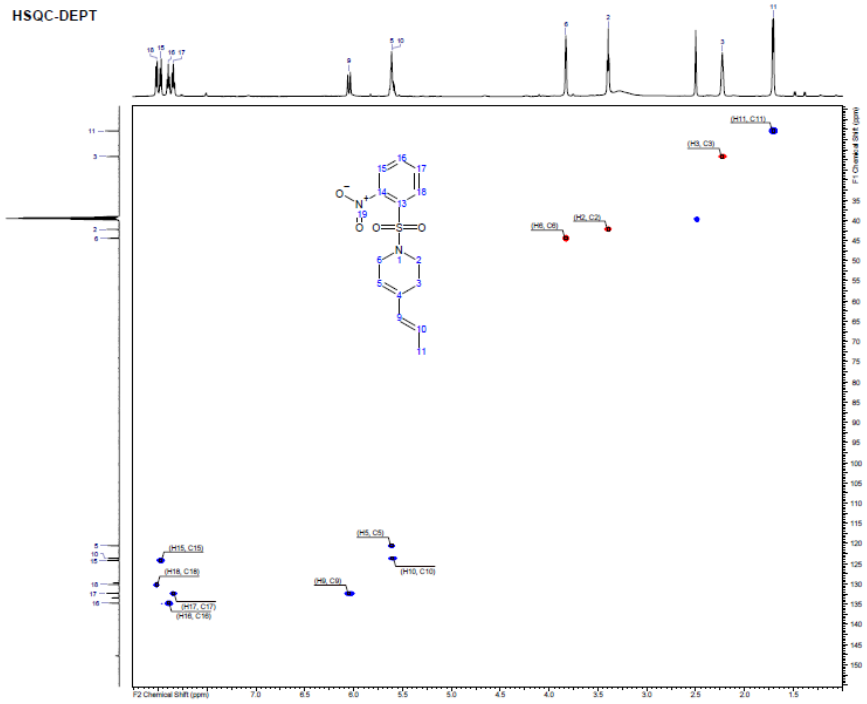

HMBC:

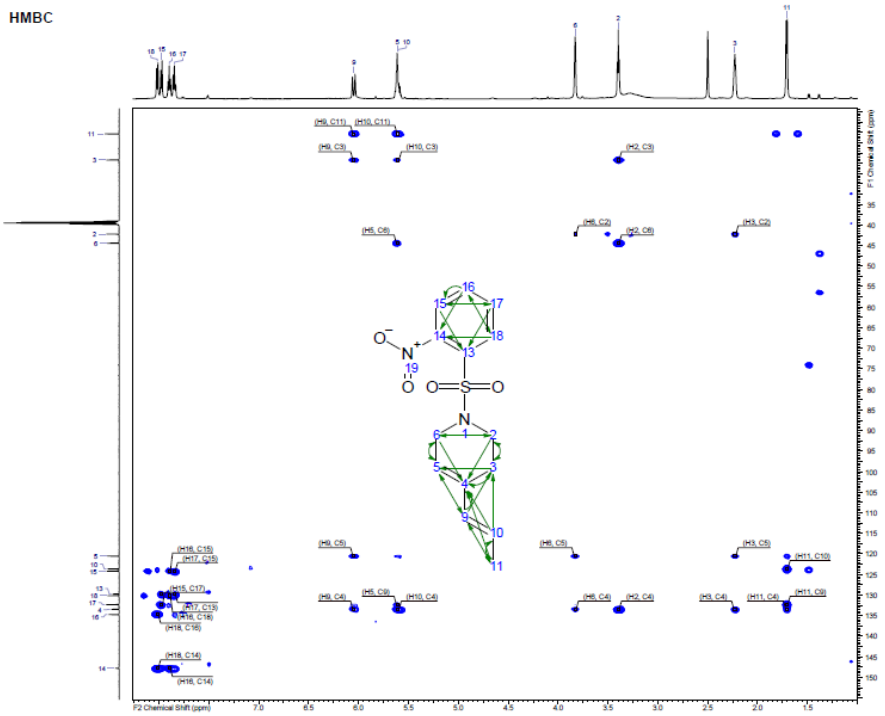

^{15}N HMBC:

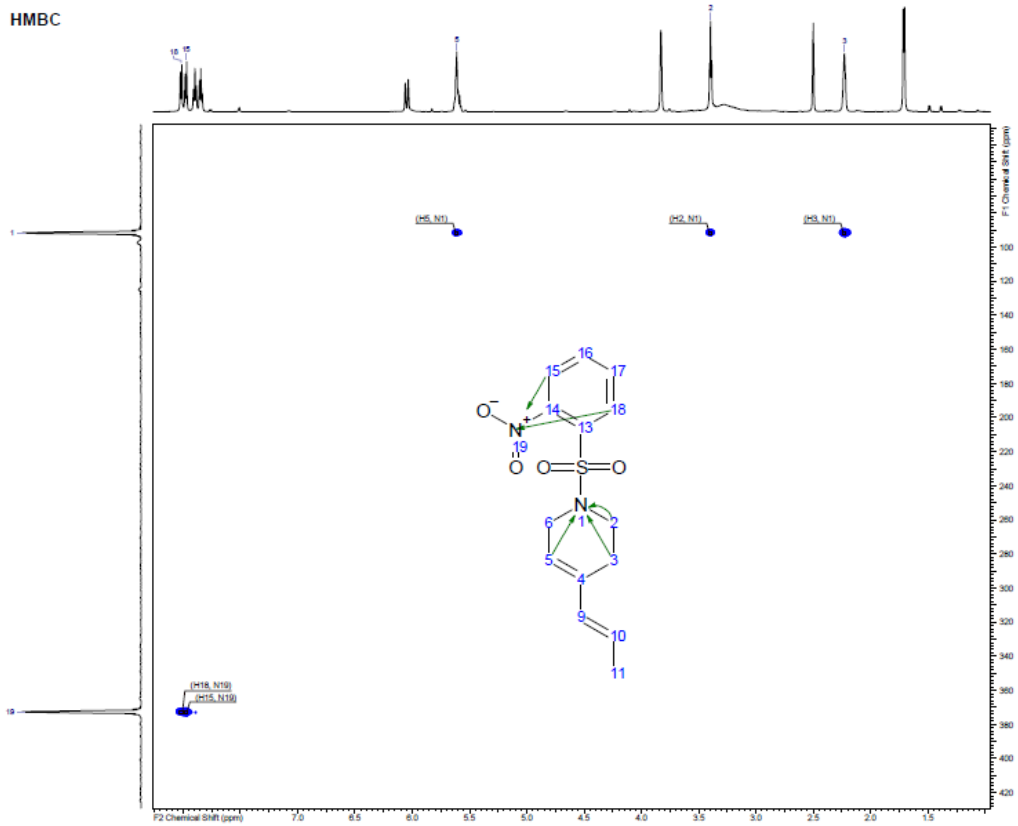

COSY:

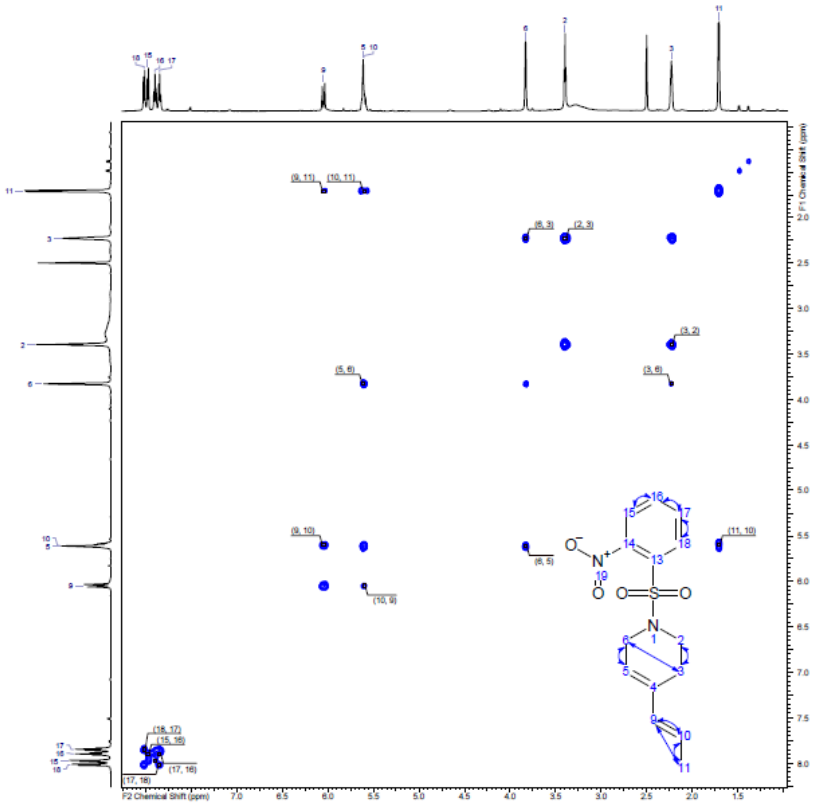

12.4.10. Scale-Up Reaction

Scheme 58 – 2.4 g Reaction

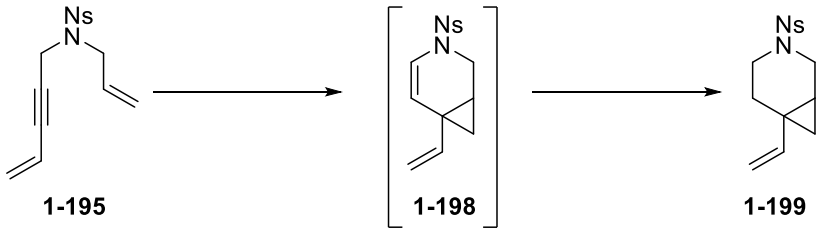

To a heat-gun dried round-bottom flask (150 mL) was added **1-182** (845 mg, 0.839 mmol, and AgOTf (242 mg, 0.940 mmol) which were dissolved in DCM (45 mL) under an inert atmosphere. This was stirred at RT for 30 min and left to stand until the formed AgCl had precipitated. The supernatant was then used as the catalyst in the cyclisation reaction. The supernatant was added to a heat-gun dried round-bottom flask (500 mL) containing **1-195** (2.40 g, 7.83 mmol) in DCM (100 mL). The reaction was stirred at RT for 64.5 h before being cooled to 0 °C. TFA (0.66 mL, 8.62 mmol) and Et_3SiH (1.38 mL, 8.62 mmol) were added and the reaction mixture stirred at this temperature for 1.5 h before additional TFA (0.66 mL, 8.62 mmol) and Et_3SiH (1.38 mL, 8.62 mmol) were added. The reaction was stirred for 1 h 15 min at 0 °C before being added to a stirring solution of saturated aqueous sodium bicarbonate (250 mL). The layers were separated and the organic dried using a hydrophobic frit and concentrated *in vacuo* to give a dark residue which was purified by flash chromatography (cyclohexane/DCM 0-80%). **1-198** was obtained as a pale yellow oil (2.04 g, 6.09 mmol, 78%). Measured *ee* value = 43.6%.

12.4.11. Synthesis of Acid 1-202

Initial Attempt Yielding 1-(3-((2-nitrophenyl)sulfonyl)-3-azabicyclo[4.1.0]heptan-6-yl)ethane-1,2-diol (1-204) and 3-((2-nitrophenyl)sulfonyl)-3-azabicyclo[4.1.0]heptane-6-carbaldehyde (1-201)

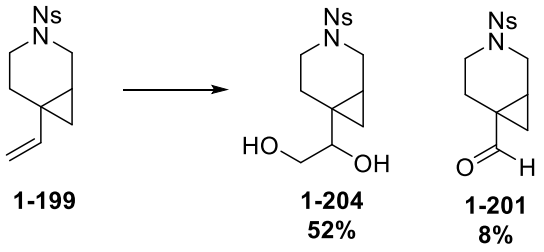

This protocol was based on a literature procedure.[117]

To a vigorously stirring solution of **1-199** in EtOAc/MeCN (1:1, 5.2 mL), cooled in an ice bath, was added a solution of $NaIO_4$ (136 mg, 0.637 mmol) and $RuCl_3•3H_2O$ (8.0 mg, 0.030 mmol) in Water (0.87 mL). The reaction mixture was stirred vigorously for 30 min before

being quenched with 28% aqueous $Na_2S_2O_3$ (5.0 mL) and diluted with water (5.0 mL) and EtOAc (10 mL). Brine (5 mL) was added to aid separation. The layers were separated and the aqueous washed with further EtOAc (2 × 10 mL). The organics were combined, dried using a hydrophobic frit and concentrated *in vacuo* yielding a dark residue. LCMS analysis confirmed the presence of diol. Therefore, the crude mixture was dissolved in EtOAc/MeCN (1:1, 5.2 mL) and sodium periodate (136 mg, 0.637 mmol) added. This was stirred at RT for 17 h before being quenched with 28% aqueous $Na_2S_2O_3$ (5.0 mL). The layers were separated and the aqueous washed with EtOAc (3 × 10 mL). The organics were combined, dried using a hydrophobic frit and concentrated *in vacuo*. The crude residue was purified by flash chromatography (cyclohexane/EtOAc 0-100% then flushed with 3:1 EtOAc/EtOH).

1-201 was obtained as a colourless oil (10.6 mg, 0.034 mmol, 8%). ^{1}H NMR (400 MHz, $CDCl_3$) δ = 8.66 (s, 1H), 8.01 - 7.98 (m, 1H), 7.75 - 7.67 (m, 2H), 7.64 (m, 1H), 4.01 (dd, *J* = 1.3, 1.3, 13.1 Hz, 1H), 3.61 (m, 1H), 3.38 (dd, *J* = 4.2, 13.0 Hz, 1H), 2.79 - 2.65 (m, 2H), 1.80 (m, 1H), 1.70 (dddd, *J* = 1.2, 4.3, 6.7, 9.4 Hz, 1H), 1.48 (dd, *J* = 5.3, 9.4 Hz, 1H), 1.23 (dd, *J* = 5.6, 6.6 Hz, 1H); ^{13}C NMR (101 MHz, $CDCl_3$) δ = 199.5, 148.1, 133.8, 132.1, 131.7, 131.0, 124.2, 43.6, 42.7, 29.4, 21.1, 19.6, 17.7; LCMS (high pH) t_R = 0.95 min, $[M+H^+]$ 310.0 purity 100%).

1-204 was obtained as a pale yellow oil after flushing the column with 3:1 EtOAc/EtOH and was isolated a mixture of diastereomers. These were not separated, and the mixtures used in further reactions (75.0 mg, 0.219 mmol, 52%). ^{1}H NMR (400 MHz, DMSO-d_6) δ = 7.99 - 7.94 (m, 4H), 7.89 (dt, *J* = 1.6, 7.6 Hz, 2H), 7.86 - 7.82 (m, 2H), 4.55 (dd, *J* = 4.2, 5.6 Hz, 2H), 4.35 (t, *J* = 5.7 Hz, 2H), 3.51 (d, *J* = 12.2 Hz, 2H), 3.38 - 3.30 (m, 4H), 3.28 - 3.18 (m, 4H), 2.93 (ddd, *J* = 4.6, 4.6, 7.0 Hz, 1H), 2.85 - 2.71 (m, 3H), 2.01 (m, 1H), 1.89 (ddd, *J* = 5.1, 5.1, 14.2 Hz, 1H), 1.65 - 1.53 (m, 2H), 1.11 (m, 1H), 0.99 (m, 1H), 0.69 - 0.58 (m, 2H), 0.28 (dd, *J* = 5.1, 5.1 Hz, 1H), 0.23 (m, 1H); LCMS (high pH) t_R = 0.77 min (split peak but treated as one), $[M-H]^-$ 341.1 (purity 95%).

3-((2-Nitrophenyl)sulfonyl)-3-azabicyclo[4.1.0]heptane-6-carbaldehyde (1-201)

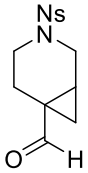

1-204 (75.0 mg, 0.219 mmol) was dissolved in THF/water (4:1 11 mL) before $NaIO_4$ (190 mg, 0.888 mmol) was added and the reaction mixture stirred at RT for 45 min. The reaction

mixture was diluted with EtOAc (20 mL) and water (20 mL). Brine (10 mL) was added to aid separation of the organic and aqueous layers. The layers were separated and the aqueous washed with EtOAc (2 × 20 mL). The organics were combined, dried using a hydrophobic frit and concentrated *in vacuo* yielding **1-201** as a pale yellow oil (57.0 mg, 0.155 mmol, 84%). This was used in subsequent reactions without further purification. For spectroscopic data, see above (*vide supra*).

3-((2-Nitrophenyl)sulfonyl)-3-azabicyclo[4.1.0]heptane-6-carboxylic acid (1-202)

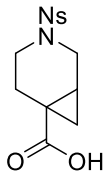

*Oxidation of aldehyde **1-201**:*

This protocol was based on a literature procedure.[119]

1-204 (57.0 mg, 0.184 mmol), 2-methylbut-2-ene (0.58 mL, 5.51 mmol) and NaH_2PO_4 (44.1 mg, 0.367 mmol) were dissolved in ^tBuOH (1.5 mL) and water (0.353 mL). To this was added $NaClO_2$ (24.9 mg, 0.276 mmol) and DCM (1.0 mL). The reaction mixture was stirred at RT for 3.5 h before being poured into 2 M HCl (aqueous, 5.0 mL). This was then extracted with DCM (3 × 10 mL). The combined organics were then washed with brine (50 mL). The layers were separated and the aqueous washed with DCM (20 mL) before being acidified with 2 M HCl (aqueous). The acidified aqueous was then washed with DCM (3 × 30 mL). The organics were combined, dried using a hydrophobic frit and concentrated *in vacuo* yielding **1-202** as an amorphous white solid (50.9 mg, 0.156 mmol, 85%).

One-Pot Oxidation:

To a vigorously stirring solution of **1-199** (500 mg, 1.62 mmol) in THF/water (4:1, 22 mL) cooled in an ice bath was added $RuCl_3•3H_2O$ (25.0 mg, 0.097 mmol). $NaIO_4$ (3.12 g, 14.6 mmol) was added in portions of 1.04 g every 30 min. The reaction mixture was diluted with water (50 mL) and this was washed with EtOAc (2 × 50 mL). The organics were combined and dried using a hydrophobic frit before being washed with saturated aqueous sodium bicarbonate (2 × 100 mL). The aqueous layers were then combined, acidified with 1 M HCl (aqueous) and this extracted with EtOAc (3 × 100 mL). The organics were combined, dried using a hydrophobic frit and concentrated *in vacuo* yielding **1-202** as an amorphous off-white solid (383 mg, 1.17 mmol, 72%).

Spectroscopic Data:

^{1}H NMR (400 MHz, DMSO-d_6) δ = 12.30 (m, 1H), 8.02 - 7.95 (m, 2H), 7.90 (dt, *J* = 1.6, 7.6 Hz, 1H), 7.85 (m, 1H), 3.58 - 3.47 (m, 2H), 3.27 (m, 1H), 2.93 (ddd, *J* = 5.3, 9.6, 13.0 Hz, 1H), 2.55 (m, 1H), 1.78 - 1.69 (m, 2H), 1.31 (dd, *J* = 4.2, 9.0 Hz, 1H), 0.78 (dd, *J* = 4.3, 6.5 Hz, 1H); ^{13}C NMR (101 MHz, DMSO-d_6) δ = 175.7, 135.1, 132.9, 130.5, 124.7, 43.9, 42.4, 24.0, 20.4, 20.3, 19.0; LCMS (formic acid) t_R = 0.90 min, [M-H]$^-$ 325.2 (purity 100%); HRMS [M-H]$^-$ calculated for $C_{13}H_{13}N_2O_6S$ 325.0500, found [M+H$^+$] 325.0497; IR (neat) ν_{max} = 2879, 1672, 1541 cm^{-1}.

12.4.12. Synthesis of Alkyl Halides from Acid 1-202

6-Iodo-3-((2-nitrophenyl)sulfonyl)-3-azabicyclo[4.1.0]heptane (1-215)

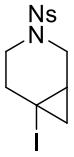

HOTT (95.0 mg, 0.257 mmol), DMAP (25.0 mg, 0.205 mmol) and **1-202** (67.0 mg, 0.205 mmol) were dissolved in DCM (1.5 mL) and stirred in the dark for 30 min before iodoform (258 mg, 0.655 mmol) was added, followed by Et_3B (1.0 M in hexanes, 0.410 mL, 0.410 mmol). The reaction was stirred for a further 3.5 h before being partitioned between EtOAc (10 mL) and 28% aqueous $Na_2S_2O_3$ (10 mL). The organic layer was then washed with brine (10 mL) before being dried using a hydrophobic frit and concentrated *in vacuo* to give a brown residue. This was purified by flash chromatography (cyclohexane/EtOAc 0-100%) to give **1-215** as a yellow oil (18.0 mg, 0.044 mmol, 21%). ^{1}H NMR (400 MHz, $CDCl_3$) δ = 8.01 - 7.95 (m, 1H), 7.75 - 7.67 (m, 2H), 7.66 - 7.62 (m, 1H), 3.78 (dd, *J* = 5.4, 13.0 Hz, 1H), 3.56 (dd, *J* = 1.8, 12.8 Hz, 1H), 3.14 (t, *J* = 6.2 Hz, 2H), 2.60 (m, 1H), 2.48 (m, 1H), 1.68 (m, 1H), 1.27 (m, 1H), 1.00 (t, *J* = 6.5 Hz, 1H); ^{13}C NMR (101 MHz, $CDCl_3$) δ = 148.2, 133.7, 132.0, 131.6, 130.9, 124.2, 43.8, 42.7, 37.6, 22.7, 21.6, -5.5; LCMS (formic acid) t_R = 1.21 min, [M+H$^+$] 409.0 (purity 97%); IR (neat) ν_{max} = 2923, 1540, 1370, 1164, 1133 cm^{-1}.

6-Bromo-3-((2-nitrophenyl)sulfonyl)-3-azabicyclo[4.1.0]heptane (1-217)

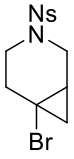

HOTT (469 mg, 1.26 mmol), DMAP (162 mg, 1.33 mmol) and **1-202** (330 mg, 1.01 mmol) were dissolved in DCM (7.2 mL) and stirred in the dark for 1 h before being exposed to air,

followed by the addition of bromoform (0.265 mL, 3.03 mmol) and Et_3B (1.0 M in hexanes, 2.02 mL, 2.02 mmol). The reaction mixture was stirred for 1 h and then diluted with EtOAc (30 mL). This was washed with 28% aqueous $Na_2S_2O_3$ (30 mL) and brine (30 mL) before being dried using a hydrophobic frit and concentrated *in vacuo* to give a brown oil which was purified by flash chromatography (cyclohexane/EtOAc 0-60%). **1-217** was obtained as a brown oil (217 mg, 0.602 mmol, 60%). ^{1}H NMR (400 MHz, $CDCl_3$) δ = 7.97 (m, 1H), 7.75 - 7.67 (m, 2H), 7.63 (m, 1H), 3.74 (dd, *J* = 5.5, 12.8 Hz, 1H), 3.52 (td, *J* = 1.5, 12.7 Hz, 1H), 3.26 - 3.12 (m, 2H), 2.55 - 2.44 (m, 2H), 1.74 (m, 1H), 1.35 (dd, *J* = 6.7, 9.9 Hz, 1H), 0.98 (dd, *J* = 6.6, 6.6 Hz, 1H); ^{13}C NMR (101 MHz, $CDCl_3$) δ = 148.1, 133.7, 132.0, 131.7, 130.9, 124.2, 44.1, 42.5, 34.6, 27.1, 21.4, 20.0; LCMS (formic acid) t_R = 1.17 min, [M+H$^+$] 360.9 (purity 82%); HRMS [M+H$^+$] calculated for $C_{12}H_{14}{}^{79}BrN_2O_4S$ 360.9852, found [M+H$^+$] 360.9852; IR (neat) ν_{max} = 2927, 2864, 1539, 1343, 1163 cm^{-1}.

12.4.13. Formation and Use of Redox Active Esters

1,3-Dioxoisoindolin-2-yl 3-((2-nitrophenyl)sulfonyl)-3-azabicyclo[4.1.0]heptane-6-carboxylate (1-219)

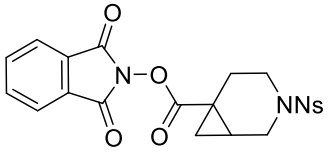

This protocol was based on a literature procedure.[128]

N-hydroxyphthalimide (50.0 mg, 0.306 mmol), **1-202** (100 mg, 0.306 mmol) and DMAP (3.74 mg, 0.031 mmol) were dissolved in DCM (3.0 mL) and the resulting mixture vigorously stirred while DIC (53.0 µL, 0.337 mmol) was added. This was stirred for 45 min before being filtered through a celite cartridge (2.5 g) which was washed with further DCM. The solvent was removed *in vacuo* to give a light brown residue which was purified by flash chromatography (cyclohexane/EtOAc 0-80%). **1-219** was obtained as an amorphous white solid (119 mg, 0.252 mmol, 82%). ^{1}H NMR (400 MHz, $CDCl_3$) δ = 8.00 (m, 1H), 7.91 - 7.86 (m, 2H), 7.82 - 7.77 (m, 2H), 7.76 - 7.69 (m, 2H), 7.66 (m, 1H), 3.97 (td, *J* = 1.4, 13.1 Hz, 1H), 3.62 (m, 1H), 3.50 (dd, *J* = 4.0, 13.1 Hz, 1H), 2.91 (ddd, *J* = 5.0, 11.1, 13.2 Hz, 1H), 2.79 (m, 1H), 2.19 (m, 1H), 2.10 (m, 1H), 1.91 (dd, *J* = 5.0, 9.4 Hz, 1H), 1.26 (m, 1H); ^{13}C NMR (101 MHz, $CDCl_3$) δ = 170.5, 161.9, 134.8, 133.8, 132.0, 131.7, 130.9, 128.9, 124.3, 124.0, 43.3, 42.4, 23.8, 22.8, 21.0, 19.2 ***1 quaternary C not observed***; LCMS (formic acid) t_R = 1.21 min, [M+NH_4^+] 489.2 (purity 92%); HRMS [M+H$^+$] calculated for $C_{21}H_{18}N_3O_8S$ 472.0809, found [M+H$^+$] 472.0816; IR (neat) ν_{max} = 1777, 1739, 1540, 1348 cm^{-1}.

4,5,6,7-Tetrachloro-1,3-dioxoisoindolin-2-yl 3-((2-nitrophenyl)sulfonyl)-3-azabicyclo[4.1.0]heptane-6-carboxylate (1-221)

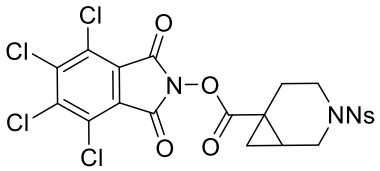

This protocol was based on a literature procedure.[128]

To a round-bottom flask was added **1-202** (100 mg, 0.306 mmol), *N*-hydroxytetrachlorophthalimide (97.0 mg, 0.322 mmol) and DMAP (4.0 mg, 0.031 mmol). DCM (1.5 mL) was added and the reaction mixture stirred vigorously before DIC (50.0 µL, 0.322 mmol) was added dropwise. The reaction mixture was kept at RT for 2 h before being filtered under vacuum. The solid was washed with DCM and the filtrate collected. This was concentrated *in vacuo* to give a yellow solid which was purified by flash chromatography (cyclohexane/EtOAc 0-50%). **1-221** was obtained as a colourless oil which solidified under vacuum (132 mg, 0.216 mmol, 71%). ^{1}H NMR (400 MHz, $CDCl_3$) δ = 8.02 (m, 1H), 7.78 - 7.69 (m, 2H), 7.66 (m, 1H), 3.97 (m, 1H), 3.63 (m, 1H), 3.49 (dd, *J* = 4.2, 13.0 Hz, 1H), 2.90 (ddd, *J* = 5.0, 11.1, 13.2 Hz, 1H), 2.75 (m, 1H), 2.18 (m, 1H), 2.10 (ddd, *J* = 6.2, 11.2, 14.5 Hz, 1H), 1.91 (dd, *J* = 5.3, 9.4 Hz, 1H), 1.29 (dd, *J* = 5.3, 7.2 Hz, 1H); ^{13}C NMR (101 MHz, $CDCl_3$) δ = 170.1, 157.5, 148.2, 141.1, 133.9, 131.9, 131.7, 130.9, 130.5, 124.7, 124.3, 43.3, 42.3, 23.7, 23.1, 21.1, 19.1; LCMS (formic acid) t_R = 1.45 min, [M+H$^+$] 624.9 (purity 86%); HRMS [M+H$^+$] calculated for $C_{21}H_{14}Cl_4N_3O_8S$ 607.9250, found [M+H$^+$] 607.9257; IR (neat) ν_{max} = 1781, 1743, 1542, 1364, 1163, 1130, 1039, 731, 576 cm^{-1}.

3-((2-Nitrophenyl)sulfonyl)-6-phenyl-3-azabicyclo[4.1.0]heptane (1-222)

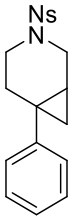

Scheme 72:

The protocols were based on literature procedures and diphenylzinc was prepared according to the literature.[131]

Preparation 1:

To a microwave vial was added $Fe(acac)_3$ (14.0 mg, 0.041 mmol) and 1,2-bis(diphenylphosphaneyl)benzene (dppBz) (22.0 mg, 0.049 mmol) and this was evacuated and backfilled with nitrogen 3 times. To this was added **1-219** (48.0 mg, 0.102 mmol) in toluene (0.5 mL) under an inert atmosphere. The mixture was stirred at RT for 5 min before diphenylzinc (0.34 M in THF, 0.750 mL, 0.255 mmol) was added in one portion. The reaction mixture was stirred for 1 h at RT before being diluted with 1 M HCl (aqueous) and washed with diethyl ether. The organic layer was collected, dried using a hydrophobic frit and concentrated *in vacuo* yielding an orange oil which was purified by flash column chromatography (cyclohexane/EtOAc 0-100%). Only one identifiable product was isolated (**1-223**):

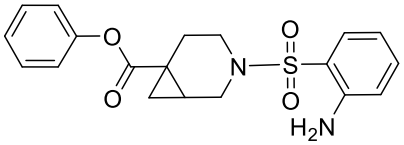

^{1}H NMR (400 MHz, $CDCl_3$) δ = 7.92 - 7.68 (m, 3H), 7.45 - 7.29 (m, 4H), 7.19 - 7.06 (m, 3H), 6.89 (m, 1H), 3.76 (m, 1H), 3.47 (m, 1H), 3.15 (m, 1H), 2.67 (m, 1H), 2.57 (ddd, *J* = 4.9, 10.9, 12.3 Hz, 1H), 1.90 - 1.77 (m, 2H), 1.51 (dd, *J* = 4.2, 9.3 Hz, 1H), 0.98 (m, 1H); ^{13}C NMR (101 MHz, $CDCl_3$) δ = 179.3, 143.3, 140.5, 134.5, 134.14, 130.8, 129.7, 123.6, 123.5, 121.9, 121.2, 121.1, 118.9, 116.4, 43.7, 42.8, 23.8, 23.4, 22.4, 20.5, 20.2; LCMS (formic acid) t_R = 1.20 min, [M+H$^+$] 373.1 (purity 78%).

Preparation 2:

1-202 (33.0 mg, 0.100 mmol) and HATU (38.0 mg, 0.100 mmol) were added to a microwave vial which was evacuated and backfilled with nitrogen 3 times. Et_3N (14.0 µL, 0.100 mmol) was added, followed by THF (0.20 mL). This was stirred for 1 h. In another vial, $Fe(acac)_3$ (7.0 mg, 0.020 mmol) and 1,2-bis(diphenylphosphaneyl)benzene (dppBz) (18.0 mg, 0.040 mmol) were added and the vial evacuated and backfilled with nitrogen 3 times. THF (0.30 mL) was added and the reaction stirred until all solids were dissolved. The acid-containing mixture was then transferred to the vial. Diphenylzinc (0.4 M in THF, 0.630 mL, 0.250 mmol) was then added and the mixture stirred for 1 h before being diluted with water (10 mL). The layers were separated and the organic collected, dried using a hydrophobic frit and concentrated *in vacuo* to give a light orange residue. This was purified by flash chromatography (cyclohexane/EtOAc 0-20%). No product was isolated.

Preparation 3:

To a microwave vial was added $Fe(acac)_3$ (13.0 mg, 0.036 mmol) and 1,2-bis(diphenylphosphaneyl)benzene (dppBz) (19.0 mg, 0.043 mmol) and this was evacuated and backfilled with nitrogen 3 times. To this was added **1-221** (55.0 mg, 0.090 mmol) in toluene (0.65 ml) under an inert atmosphere. The mixture was stirred at RT for 5 min before diphenylzinc (0.34 M in THF, 0.660 ml, 0.226 mmol) was added in one portion. The reaction mixture was stirred for 1 h at RT before being diluted with 1 M HCl (aqueous) and washed with diethyl ether. The organic layer was collected, dried using a hydrophobic frit and concentrated *in vacuo* yielding an orange residue which was purified by flash chromatography (cyclohexane/EtOAc 0-100%). No desired or identifiable products were isolated.

Scheme 74:

This protocol was based on a literature procedure.[130]

Nickel Catalyst Preparation:

To a microwave vial was added $NiCl_2 \bullet 6H_2O$ (84.0 mg, 0.353 mmol) and 4,4'-di-*tert*-butyl-2,2'-bipyridine (dtbbpy) (95.0 mg, 0.353 mmol). The vial was evacuated and backfilled with nitrogen 3 times before DMF (7.0 mL) was added and the resulting mixture stirred at RT for 3 h.

Reaction:

A round-bottom flask was charged with phenylboronic acid (37.0 mg, 0.300 mmol) and **1-221** (61.0 mg, 0.100 mmol) before being evacuated and backfilled with nitrogen 3 times. 1,4-Dioxane (4.0 mL) was added and the resulting mixture stirred for 1 minute before Et_3N (0.14 mL, 1.00 mmol) was added. This was stirred for 5 min before the nickel catalyst (0.40 mL, 0.020 mmol) was added and the vial heated immediately to 75 °C. This was stirred for 21 h before being cooled to RT and diluted with EtOAc and water. The layers were separated and the organic washed with brine before being dried using a hydrophobic frit and concentrated *in vacuo*. The resulting yellow residue was purified the Combiflash EZ Prep with a XSelect® CSH™ Prep C18 5 µm OBD™ column (MeCN / Water + 0.1% ammonium bicarbonate 35-99%). **1-222** was obtained as an amorphous colourless solid (4.1 mg, 0.011 mmol, 11%).

Scheme 75:

These protocols were based on literature procedures and PhZnCl•LiCl was prepared according to the literature.[128]

$NiCl_2$•glyme Catalyst:

To a microwave vial was added **1-221** (61.0 mg, 0.100 mmol), $NiCl_2$•glyme (4.0 mg, 0.020 mmol) and 4,4'-di-*tert*-butyl-2,2'-bipyridine (dtbbpy) (11.0 mg, 0.040 mmol). The vial was sealed and the suba seal covered with parafilm before being evacuated and backfilled with nitrogen 3 times. DMF (1.0 mL) was added and the mixture stirred for 2 min before the addition of PhZnCl•LiCl (0.2 M in THF, 1.50 mL, 0.300 mmol) . The reaction mixture was stirred for 15.5 h at RT before being diluted with EtOAc and washed with water and brine. The organic was collected, dried using a hydrophobic frit and concentrated *in vacuo* to give a yellow residue. This was dissolved in the minimum amount of DCM and added to a silica cartridge under gravity (1.0 g, pre-equilibrated with cyclohexane). Once loaded, the cartridge was flushed with cyclohexane (approximately 4 column volumes) and this was collected into a vial. The cartridge was then flushed with EtOAc (approximately 4 column volumes). This was collected separately into a 50 mL round bottom. The collected cyclohexane was passed through a 2nd silica cartridge (5.0 g, pre-equilibrated) and was washed with cyclohexane (approximately 4 column volumes) before being flushed with EtOAc (approximately 4 column volumes). The EtOAc was collected and concentrated *in vacuo* yielding a yellow gum which was purified using the Combiflash EZ Prep with a XSelect® CSH™ Prep C18 5 µm OBD™ column (MeCN / Water + 0.1% ammonium bicarbonate 35-99%). **1-222** was obtained as an amorphous colourless solid (5.0 mg, 0.013 mmol, 13%).

$NiCl_2$•$6H_2O$ Catalyst:

To a microwave vial was added **1-221** (61.0 mg, 0.10 mmol), $NiCl_2$•$6H_2O$ (5.0 mg, 0.020 mmol) and 4,4'-di-tert-butyl-2,2'-bipyridine (dtbbpy) (11.0 mg, 0.040 mmol). The vial was sealed and the suba seal covered with parafilm before being evacuated and backfilled with nitrogen 3 times. DMF (1.0 mL) was added and the mixture stirred for 2 min before the addition of aryl zinc (0.2 M in THF, 1.50 mL, 0.300 mmol). The reaction mixture was stirred for 15.5 h at RT before being diluted with EtOAc and washed with water and brine. The organic was collected, dried using a hydrophobic frit and concentrated *in vacuo* to give a yellow residue. This was dissolved in the minimum amount of DCM and added to a silica cartridge under gravity (1.0 g, pre-equilibrated with cyclohexane). Once loaded, the cartridge was flushed with cyclohexane (approximately 4 column volumes) and this was collected into

a vial. The cartridge was then flushed with EtOAc (approximately 4 column volumes). This was collected separately into a 50 mL round bottom. The collected cyclohexane was passed through a 2nd silica cartridge (5.0 g, pre-equilibrated). and was washed with cyclohexane (approximately 4 column volumes) before being flushed with EtOAc (approximately 4 column volumes). The EtOAc was collected and concentrated *in vacuo* yielding a yellow gum which was purified using the Combiflash EZ Prep with a XSelect® CSH™ Prep C18 5 µm OBD™ column (MeCN / Water + 0.1% ammonium bicarbonate 35-99%). **1-222** was obtained as an amorphous colourless solid (2.0 mg, 5.30 µmol, 5%).

*Spectroscopic Data (**1-222**):*

^{1}H NMR (400 MHz, $CDCl_3$) δ = 8.03 (m, 1H), 7.74 - 7.66 (m, 2H), 7.64 (m, 1H), 7.31 - 7.15 (m, 5H), 3.80 (dd, *J* = 5.6, 12.7 Hz, 1H), 3.64 (dd, *J* = 2.0, 12.7 Hz, 1H), 3.31 - 3.26 (m, 2H), 2.23 - 2.16 (m, 2H), 1.48 (dddd, *J* = 2.0, 5.6, 5.6, 9.1 Hz, 1H), 1.12 (dd, *J* = 5.1, 8.8 Hz, 1H), 0.88 (dd, *J* = 5.4, 5.4 Hz, 1H); ^{13}C NMR (101 MHz, $CDCl_3$) δ = 146.6, 133.5, 132.3, 131.5, 131.0, 128.5, 127.5, 126.3, 124.1, 44.5, 42.5, 30.8, 23.0, 18.2, 16.8 ***1 quaternary C not observed***; LCMS (formic acid) t_R = 1.31 min, [M+H$^+$] 359.1 (purity 94%); HRMS [M+H$^+$] calculated for $C_{18}H_{19}N_2O_4S$ 359.1060, found [M+H$^+$] 359.1064; IR (neat) ν_{max} = 2924, 1542, 1372, 1165, 1130 cm^{-1}.

12.4.14. Reactions of Bromide 1-217

6-(4-methoxyphenyl)-3-((2-nitrophenyl)sulfonyl)-3-azabicyclo[4.1.0]heptane (1-224)

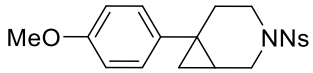

Scheme 77 – **Reaction 1**

This protocol was based on a literature procedure.[138]

To an oven dried microwave vial was added **1-217** (100 mg, 0.277 mmol), manganese (30.0 mg, 0.554 mmol), 1,10-phenanthroline (10.0 mg, 0.055 mmol), $NaBF_4$ (15.0 mg, 0.138 mmol) and $NiCl_2$•glyme (6.0 mg, 0.028 mmol). This was evacuated and backfilled with nitrogen 3 times before the addition of 4-ethylpyridine (16.0 µL, 0.138 mmol) and 1-bromo-4-methoxybenzene (35.0 µL, 0.277 mmol) by quick removal and replacement of the septum. The mixture was once again purged 3 times before being heated to 60 °C under nitrogen for 18 h. The reaction mixture was diluted with EtOAc (5.0 mL) before being filtered through celite which was washed with further EtOAc. The filtrate was collected and concentrated *in vacuo*. The resulting residue was purified by flash chromatography (cyclohexane/EtOAc 0-60%). No desired product was observed or isolated. The starting bromide **1-217** was

recovered (43.0 mg, 0.119 mmol, 43%). A by-product was also isolated in a small amount and identified by NMR and LCMS as hydroxylamine **1-225** with 84% purity:

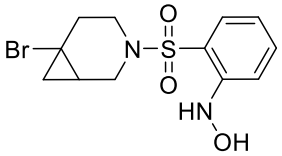

^{1}H NMR (400 MHz, DMSO-d_6) δ = 8.95 (s, 1H), 8.26 (s, 1H), 7.58 - 7.51 (m, 2H), 7.36 (m, 1H), 6.93 (m, 1H), 3.69 (ddd, *J* = 0.9, 6.4, 12.8 Hz, 1H), 3.18 - 3.08 (m, 2H), 2.85 (m, 1H), 2.39 - 2.33 (m, 2H), 1.77 (m, 1H), 1.22 (dd, *J* = 6.6, 10.0 Hz, 1H), 0.96 (dd, *J* = 6.6, 6.6 Hz, 1H); ^{13}C NMR (101 MHz, DMSO-d_6) δ = 149.2, 134.4, 129.2, 118.8, 118.8, 114.4, 43.9, 42.0, 34.0, 29.3, 20.3, 19.3; LCMS (formic acid) t_R = 1.09 min, [M+H$^+$] 346.9 (purity 84%).

Scheme 77 – **Reaction 2**

This protocol was based on a literature procedure.[137]

To a heat-gun dried microwave vial was added **1-217** (54.0 mg, 0.15 mmol), 4,4'-di-*tert*-butyl-2,2'-bipyridine (dtbbpy) (9.0 mg, 0.032 mmol), zinc (20.0 mg, 0.300 mmol), NiI_2 (9.0 mg, 0.029 mmol) and $MgCl_2$ (14.0 mg, 0.150 mmol). This was put under an inert atmosphere and dissolved in DMAc (1.0 mL) before 1-bromo-4-methoxybenzene (19.0 µL, 0.150 mmol) was added and the reaction stirred for 18 h. The reaction mixture was purified by flash chromatography (cyclohexane/EtOAc 0-60%) loaded directly onto a pre-equilibrated silica gel column (24 g) with a small amount of DCM to rinse the reaction vessel. The column was eluted with cHex/EtOAc (0-60%). Only starting bromide **1-217** was recovered (35.0 mg, 0.097 mmol, 67%).

3-((2-Nitrophenyl)sulfonyl)-6-phenyl-3-azabicyclo[4.1.0]heptane (1-222)

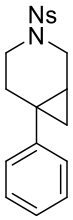

Scheme 78 – Reaction 1

This protocol was based on a literature procedure.[139]

NiI_2 (5.0 mg, 0.017 mmol), *trans*-2-aminocyclohexanol hydrochloride (3.0 mg, 0.017 mmol), phenylboronic acid (68.0 mg, 0.554 mmol) and NaHMDS (102 mg, 0.554 mmol) were weighed into a microwave vial. The vial was capped and evacuated and backfilled with nitrogen 3 times before the solids were dissolved in ^{i}PrOH (0.55 mL). The resulting solution

was stirred at RT for 5 min before **1-217** (100 mg, 0.277 mmol) was added by quick removal and replacement of the cap. The reaction mixture was again backfilled and purged with nitrogen 3 times. This was then heated to 60 °C for 6 h, after which reaction mixture was cooled to RT and filtered through a short pad of silica which was washed with 50 mL of 1:1 petroluem ether/diethyl ether. The filtrate was collected, concentrated *in vacuo* and the resulting residue purified by flash chromatography (cyclohexane/EtOAc 0-50%). Some starting material was recovered but contained several impurities. A small amount of by-product was also isolated, again containing several impurities. LCMS and proton NMR provided some evidence towards the structure **1-226**:

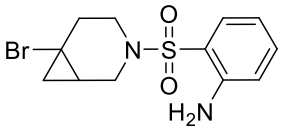

^{1}H NMR (400 MHz, $CDCl_3$) δ = 7.55 (dd, *J* = 1.5, 8.1 Hz, 1H), 7.31 (ddd, *J* = 1.7, 7.1, 8.3 Hz, 1H), 6.80 - 6.70 (m, 2H), 5.00 (br s, 2H), 3.50 (m, 1H), 3.42 (m, 1H), 3.08 (m, 1H), 2.98 (m, 1H), 2.51 - 2.45 (m, 2H), 1.69 (dddd, *J* = 1.8, 5.0, 6.6, 10.1 Hz, 1H), 1.30 (m, 1H), 0.96 (dd, *J* = 6.6, 6.6 Hz, 1H); LCMS (formic acid) t_R = 1.15 min, [M+H$^+$] 330.9 (purity 50%).

Scheme 78 – Reaction 2

This protocol was based on a literature procedure.[124]

$Ni(PCy_3)_2Cl_2$ (10.0 mg, 0.014 mmol) and 4,7-diphenyl-1,10-phenanthroline (5.0 mg, 0.014 mmol) were dissolved in ^{t}BuOH (0.70 mL) under a nitrogen atmosphere. ^{t}BuOK (37.0 mg, 0.332 mmol) and phenylboronic acid (34.0 mg, 0.277 mmol) were added and the reaction mixture stirred at 60 °C for 5 min. **1-217** (50.0 mg, 0.138 mmol) was then added and the reaction stirred at 60 °C for 22 h. This was then filtered through a silica cartridge (1.0 g) and this was washed with ether. The filtrate and washings were combined and concentrated *in vacuo*. NMR and LCMS of the resulting crude mixture indicated no formation of the desired product and the presence of several unidentified species.

12.4.15. Synthesis of Boron-Containing Intermediates

2-((6-(4,4,5,5-Tetramethyl-1,3,2-dioxaborolan-2-yl)-3-azabicyclo[4.1.0]heptan-3-yl)sulfonyl)aniline (1-208a)

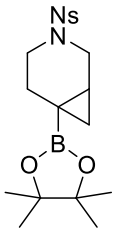

Scheme 79 – Reaction 1

This protocol was based on a literature procedure.[144]

1-219 (84.0 mg, 0.178 mmol), $Cu(acac)_2$ (14.0 mg, 0.053 mmol), $MgCl_2$ (30.0 mg, 0.315 mmol), ground $LiOH•H_2O$ (121 mg, 2.88 mmol) and B_2Pin_2 (139 mg, 0.547 mmol) were added to a vial. This was evacuated and purged with nitrogen 3 times before 1,4-dioxane/DMF (4:1, 1.25 mL) was added and the reaction mixture stirred for 20 min at RT. By this time, a gel had formed in the vial – therefore, TBME/DMF (6:1, 1.25 mL) was added and the reaction mixture stirred for a further 40 minutes before being diluted with EtOAc (20 mL) and saturated aqueous ammonium chloride (20 mL). The layers were separated and the organic washed with 10% aqueous K_2CO_3 solution (20 mL). The aqueous was washed with DCM (3 × 20 mL) and 9:1 $CHCl_3/^iPrOH$(6 × 20 mL). The aqueous was then acidified with 2 M HCl and washed with DCM (2 × 50 mL). All of the organics were combined, dried using a hydrophobic frit and concentrated *in vacuo* yielding a brown solid which was purified by flash chromatography (cyclohexane/TBME 0-100%). No identifiable products were isolated in significant quantities and LCMS of the reaction mixture provided tentative evidence of hydrolysis of the starting material **1-219**.

Scheme 79 – Reaction 2

This protocol was based on a literature procedure.[145]

Formation of Ni Catalyst:

$NiCl_2•6H_2O$ (24.0 mg, 0.1 mmol) and 4,4'-dimethoxy-2,2'-bipyridine (28.0 mg, 0.13 mmol) were added to a microwave vial and this was evacuated and backfilled with nitrogen 3 times. THF (4.0 mL) was added and the resulting mixture stirred at RT until no granular nickel was observed.

Preparation of [B2pin2Me]Li complex:

B_2Pin_2 (168 mg, 0.662 mmol) was dissolved in THF (0.6 mL) under nitrogen in a microwave vial and cooled to 0 °C before methyllithium (1.4 M in diethyl ether, 0.43 mL, 0.602 mmol) was added. This was then warmed to RT and stirred for 1 h.

Reaction:

A microwave vial was charged with **1-219** (80.0 mg, 0.170 mmol) and $MgBr_2$•OEt (200 mg, 0.774 mmol) before being evacuated and backfilled with nitrogen 3 times. This was then charged with 0.68 mL of the Ni catalyst suspension before being vigorously stirred for approximate 10 min until no granular $MgBr_2$ was observed. The suspension was cooled to 0 °C before the addition of 0.80 mL of the B_2Pin_2 mixture. The reaction mixture was stirred at this temperature for 72 h before being filtered through a celite and silica cartridge which were washed with diethyl ether. The solid at the top of the celite cartridge was collected and purified using the ACQUprep (water + 0.1% formic acid/MeCN + 0.1% formic acid 15-55%). Small amounts of two compounds were isolated as samples containing unknown impurities but were not quantified.

Scheme 79 – Reaction 3

This protocol was based on a literature procedure.[143]

1-219 (50.0 mg, 0.106 mmol) and B_2Cat_2 (32.0 mg, 0.135 mmol) were added to a dry vial before being dissolved in DMAc (1.10 mL). The headspace of the vial was purged with a stream of nitrogen for approximately 10 seconds. The vial was sealed and stirred under blue LED irradiation (PHIL PACER[165], 200 mA) for 16 h. Pinacol (54.0 mg, 0.457 mmol) dissolved in Et_3N (0.370 mL, 2.65 mmol) was added to the reaction mixture and this stirred for 2 h. The reaction mixture was then added to EtOAc (10 mL), water (3 mL) and saturated aqueous ammonium chloride (3.0 mL). The layers were separated and the aqueous was washed with further EtOAc (2 × 10 mL). The organics were combined, dried using a hydrophobic frit and concentrated *in vacuo* yielding a red/brown solution which was dissolved in EtOAc (10 mL) and washed with 5% aqueous LiCl solution (2 × 30 mL). The organic was dried using a hydrophobic frit and concentrated *in vacuo* yielding a brown residue which was purified by flash chromatography (cyclohexane/EtOAc 0-100%). No desired product was isolated from the purification. Starting material (2.0 mg, 0.005 mmol,

4%) and small amounts of three by-products were tentatively identified from impure samples as:

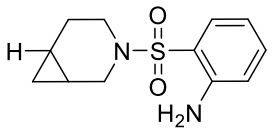

1-228 Isolated as 1.0 mg sample with unknown impurities, yield approximated from LCMS purity of 57% as 0.6 mg, 0.002 mmol, 2%. ^{1}H NMR (400 MHz, $CDCl_3$) δ = 7.56 (dd, *J* = 1.2, 8.1 Hz, 1H), 7.30 (m, 1H), 6.77 - 6.69 (m, 2H), 3.53 (m, 1H), 3.26 (dd, *J* = 5.1, 11.7 Hz, 1H), 3.18 (m, 1H), 2.70 (ddd, *J* = 5.3, 9.6, 12.0 Hz, 1H), 2.03 (m, 1H), 1.82 (m, 1H), 1.09 - 0.93 (m, 2H), 0.65 (ddd, *J* = 4.8, 8.7, 8.7 Hz, 1H), 0.30 (appt. q, *J* = 5.1 Hz, 1H); LCMS (formic acid) t_R = 1.07 min, [M+H$^+$] 253.1 (purity 57%).

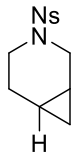

1-218 Isolated as a mixture with catechol and N-hydroxyphthalimide – 14% purity by NMR giving (1 mg, 0.004 mmol, 3%). ^{1}H NMR (400 MHz, $CDCl_3$) δ = 7.99 (m, 1H), 7.93 - 7.88 (m, 4H), 7.82 - 7.77 (m, 5H), 7.71 - 7.68 (m, 2H), 7.63 (m, 1H), 6.93 - 6.88 (m, 25H), 6.86 - 6.81 (m, 26H), 5.32 (s, 25H), 3.65 (m, 1H), 3.54 (m, 1H), 3.30 (m, 1H), 2.98 (ddd, *J* = 5.4, 9.3, 13.0 Hz, 1H), 2.06 (tdd, *J* = 5.1, 7.4, 14.2 Hz, 1H), 1.87 (m, 1H), 1.15 - 1.01 (m, 2H), 0.74 (ddd, *J* = 5.0, 8.7, 8.7 Hz, 1H), 0.34 (appt. q, *J* = 5.4 Hz, 1H); LCMS (formic acid) t_R = 1.11 min, [M+H$^+$] 283.0 (purity 5%).

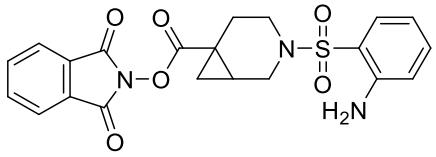

1-229 Isolated as 2.8 mg sample with unknown impurities, yield approximated from LCMS purity of 30% as 1.0 mg, 0.002 mmol, 2%. ^{1}H NMR (400 MHz, $CDCl_3$) δ = 7.92 - 7.85 (m, 2H), 7.83 - 7.76 (m, 2H), 7.58 (m, 1H), 7.32 (ddd, *J* = 1.6, 7.2, 8.4 Hz, 1H), 6.81 - 6.72 (m, 2H), 5.25 - 4.90 (m, 2H), 3.85 (d, *J* = 12.2 Hz, 1H), 3.55 (m, 1H), 3.21 (m, 1H), 2.75 (m, 1H), 2.61 (ddd, *J* = 5.0, 11.2, 12.3 Hz, 1H), 2.15 (m, 1H), 2.05 (ddd, *J* = 6.2, 11.3, 14.5 Hz, 1H), 1.84 (dd, *J* = 4.6, 9.5 Hz, 1H), 1.24 (m, 1H); LCMS (formic acid) t_R = 1.17 min, [M+H$^+$] 442.1 (purity 30%).

(3-((2-Nitrophenyl)sulfonyl)-3-azabicyclo[4.1.0]heptan-6-yl)boronic acid (1-208b)

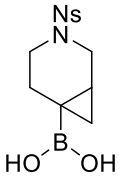

Scheme 79 – Reaction 4

This protocol was based on a literature procedure.[146]

1-219 (110 mg, 0.233 mmol), $[Ir(dtbbpy)(ppy)_2]PF_6$ (2.0 mg, 2.333 µmol) and B_2OH_2 (84.0 mg, 0.933 mmol) were weighed into a round bottom flask and put under an inert atmosphere before being the addition of DMF (0.80 mL). This was irradiated with CFL lamps for 16 h before the reaction mixture was transferred to a 50 mL flask and diluted with toluene (~5 mL). This was concentrated *in vacuo* giving a yellow solid which was purified using the ACQU prep (water+ 0.1% formic acid/ MeCN +0.1% formic acid - 15-75%). No desired product was isolated; however, several by-products were obtained:

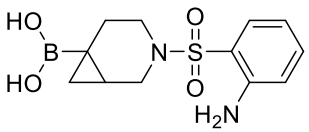

1-230 (10.0 mg, 0.033 mmol, 14%). ^{1}H NMR (400 MHz, $CDCl_3$) δ = 7.54 (m, 1H), 7.28 (m, 1H), 6.77 - 6.68 (m, 2H), 5.05 (br s, 2H), 3.68 (m, 1H), 3.33 (m, 1H), 3.14 (m, 1H), 2.46 (m, 1H), 2.24 (m, 1H), 1.57 (m, 1H), 1.25 (m, 1H), 0.94 (m, 1H), 0.68 (m, 1H); ^{13}C NMR (101 MHz, $CDCl_3$) δ = 146.1, 134.0, 130.2, 118.6, 117.6, 117.1, 44.2, 43.1, 23.7, 18.7, 18.0 ***1C not observed due to quadrupolar boron***; LCMS (formic acid) t_R = 0.79 min, $[M+H^+]$ 297.0 (purity 95%); HRMS $[M+H^+]$ calculated for $C_{12}H_{18}BN_2O_4S$ 297.1075, found $[M+H^+]$ 297.1073; IR (neat) ν_{max} = 3481, 3379, 2857, 1615, 1483, 1452, 1404, 1336, 1142 cm^{-1}.

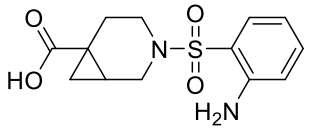

1-227 (3.3 mg, 0.011 mmol, 5%). ^{1}H NMR (400 MHz, $CDCl_3$) δ = 7.55 (dd, *J* = 1.2, 8.1 Hz, 1H), 7.29 (m, 1H), 6.75 (ddd, *J* = 1.2, 7.1, 8.1 Hz, 1H), 6.72 (m, 1H), 3.73 (ddd, *J* = 1.4, 1.4, 12.2 Hz, 1H), 3.43 (dddd, *J* = 1.3, 3.4, 6.2, 12.3 Hz, 1H), 3.12 (dd, *J* = 4.4, 12.2 Hz, 1H), 2.69 (m, 1H), 2.54 (ddd, *J* = 5.1, 11.0, 12.2 Hz, 1H), 1.89 - 1.80 (m, 2H), 1.52 (dd, *J* = 4.2, 9.3 Hz, 1H), 1.00 (dd, *J* = 4.3, 6.7 Hz, 1H); ^{13}C NMR (101 MHz, $CDCl_3$) δ = 179.8, 146.1, 134.3, 130.1, 118.3, 117.7, 117.3, 43.6, 42.7, 23.7, 22.4, 20.6, 20.2; LCMS (formic acid) t_R

= 0.86 min, [M+H$^+$] 297.0 (purity 98%); HRMS [M+H$^+$] calculated for $C_{13}H_{17}N_2O_4S$ 297.0904, found [M+H$^+$] 297.0906; IR (neat) ν_{max} = 3480, 3378, 2927, 2858, 1683, 1616, 1484, 1452, 1321, 1144 cm^{-1}.

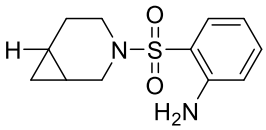

1-228 (8.0 mg, 0.030 mmol, 13%). ^{1}H NMR (400 MHz, $CDCl_3$) δ = 7.55 (dd, *J* = 1.2, 8.1 Hz, 1H), 7.29 (m, 1H), 6.77 - 6.70 (m, 2H), 5.02 (br s, 2H), 3.52 (td, *J* = 1.4, 11.8 Hz, 1H), 3.26 (dd, *J* = 5.1, 11.7 Hz, 1H), 3.18 (dddd, *J* = 1.2, 4.8, 5.8, 12.2 Hz, 1H), 2.70 (ddd, *J* = 5.1, 9.5, 12.2 Hz, 1H), 2.02 (dddd, *J* = 5.0, 5.0, 7.7, 14.0 Hz, 1H), 1.79 (dddd, *J* = 2.0, 5.7, 9.6, 14.0 Hz, 1H), 1.11 - 0.92 (m, 2H), 0.65 (ddd, *J* = 4.8, 8.7, 8.7 Hz, 1H), 0.29 (appt. q, *J* = 5.1 Hz, 1H); ^{13}C NMR (101 MHz, $CDCl_3$) δ = 146.1, 133.9, 130.2, 118.7, 117.5, 117.1, 44.8, 42.6, 23.5, 9.8, 9.7, 7.3; LCMS (formic acid) t_R = 1.08 min, [M+H$^+$] 253.1 (purity 84%); HRMS [M+H$^+$] calculated for $C_{12}H_{17}N_2O_2S$ 253.1005, found [M+H$^+$] 253.1004; IR (neat) ν_{max} = 3479, 3376, 2855, 1730, 1616, 1483, 1452, 1320, 1144 cm^{-1}.

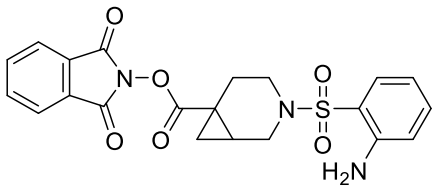

1-229 (13.0 mg, 0.029 mmol, 12%). ^{1}H NMR (400 MHz, $CDCl_3$) δ = 7.90 - 7.84 (m, 2H), 7.82 - 7.75 (m, 2H), 7.58 (m, 1H), 7.32 (m, 1H), 6.81 - 6.71 (m, 2H), 5.04 (br s, 2H), 3.85 (d, *J* = 12.2 Hz, 1H), 3.54 (dddd, *J* = 1.5, 3.1, 6.2, 12.5 Hz, 1H), 3.20 (dd, *J* = 4.2, 12.2 Hz, 1H), 2.75 (m, 1H), 2.61 (ddd, *J* = 5.0, 11.1, 12.5 Hz, 1H), 2.14 (m, 1H), 2.05 (m, 1H), 1.83 (dd, *J* = 4.8, 9.4 Hz, 1H), 1.25 (dd, *J* = 4.9, 7.1 Hz, 1H); ^{13}C NMR (101 MHz, $CDCl_3$) δ = 170.6, 161.9, 146.1, 134.8, 134.4, 130.1, 128.9, 123.9, 118.2, 117.8, 117.4, 43.4, 42.5, 23.8, 23.2, 21.2, 19.1; LCMS (formic acid) t_R = 1.17 min, [M+H$^+$] 442.1 (purity 84%); HRMS [M+H$^+$] calculated for $C_{21}H_{20}N_3O_6S$ 442.1067, found [M+H$^+$] 442.1064; IR (neat) ν_{max} = 3482, 3380, 1777, 1741, 1617, 1484, 1453, 1324 cm^{-1}.

12.4.16. Synthesis and Use of Tosyl-Protected Redox Active Ester

3-Tosyl-6-vinyl-3-azabicyclo[4.1.0]heptane (1-168)

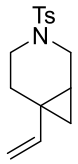

To a heat-gun dried round-bottom flask (150 mL) was added **1-182** (450 mg, 0.447 mmol) and AgOTf (138 mg, 0.536 mmol) which were dissolved in DCM (28 mL) under an inert atmosphere. This was stirred at RT for 30 min and left to stand until the formed AgCl had precipitated. The supernatant was then used as the catalyst in the cyclisation reaction. The supernatant was added to a heat-gun dried round-bottom flask (150 mL) containing **1-166** (1.23 g, 4.47 mmol) in DCM (55 mL). The reaction was stirred at RT for 17 h before being cooled to 0 °C. Et_3SiH (0.785 mL, 4.91 mmol) and TFA (0.379 mL, 4.91 mmol) were added and the reaction stirred at this temperature for 1 h before the addition of further Et_3SiH (0.785 mL, 4.91 mmol) and TFA (0.379 mL, 4.91 mmol). The reaction was stirred for 1 h before being added to a stirring solution of saturated aqueous sodium bicarbonate (50 mL). The layers were separated, and the organic collected, dried using a hydrophobic frit and concentrated *in vacuo*. The resulting black oil was purified by flash chromatography (cyclohexane/DCM 0-80%). **1-168** was obtained as a colourless oil; however, NMR showed the presence of starting enyne **1-166**. Therefore, this mixture was further purified by flash chromatography (cyclohexane/DCM 50%) to give **1-168** as a colourless oil (539 mg, 1.94 mmol, 48%). ^{1}H NMR (400 MHz, $CDCl_3$) δ = 7.66 - 7.62 (m, 2H), 7.34 - 7.29 (m, 2H), 5.44 (dd, *J* = 10.5, 17.4 Hz, 1H), 4.90 (m, 1H), 4.87 (dd, *J* = 0.9, 4.8 Hz, 1H), 3.40 (d, *J* = 11.7 Hz, 1H), 3.24 (dd, *J* = 5.4, 11.7 Hz, 1H), 3.05 (m, 1H), 2.77 (m, 1H), 2.44 (s, 3H), 2.15 (m, 1H), 1.89 (ddd, *J* = 5.4, 8.4, 13.9 Hz, 1H), 1.13 (m, 1H), 0.80 (dd, *J* = 4.9, 8.8 Hz, 1H), 0.73 (m, 1H); ^{13}C NMR (101 MHz, $CDCl_3$) δ = 144.7, 143.4, 133.8, 129.6, 127.6, 110.3, 44.5, 42.5, 25.8, 21.5, 19.9, 19.8, 17.7; LCMS (formic acid) t_R = 1.28 min, [M+H$^+$] 278.1 (purity 91%); HRMS [M+H$^+$] calculated for $C_{15}H_{20}NO_2S$ 278.1209, found [M+H$^+$] 278.1212; IR (neat) ν_{max} = 2926, 2852, 1634, 1338, 1161 cm^{-1}.

3-Tosyl-3-azabicyclo[4.1.0]heptane-6-carboxylic acid (1-169)

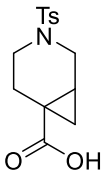

To a vigorously stirring solution of **1-168** (592 mg, 2.13 mmol) in THF/water (4:1, 31 mL), cooled in an ice bath, was added $RuCl_3.3H_2O$ (28.0 mg, 0.107 mmol). $NaIO_4$ (1.37 g, 6.40 mmol) was added in portions of 826 mg every 30 min before being stirred for a further 1 h. After this, additional $NaIO_4$ (456 mg, 2.13 mmol) was added and the reaction stirred for 1 h. Following this, the reaction mixture was diluted water (50 mL) and this was washed with EtOAc (2 × 50 mL). The organics were combined and dried using a hydrophobic frit before being washed with saturated aqueous sodium bicarbonate (3 × 100 mL). The layers were separated and the aqueous acidified using 1 M HCl (aqueous). The acidified aqueous was extracted with EtOAc (3 × 50 mL) and the organics combined, dried using a hydrophobic frit and concentrated in vacuo to give **1-169** as an amorphous off-white solid (464 mg, 1.57 mmol, 74%). ^{1}H NMR (400 MHz, DMSO-d_6) δ = 12.25 (br s, 1H), 7.65 - 7.60 (m, 2H), 7.46 - 7.41 (m, 2H), 3.38 (br d, *J* = 12.0 Hz, 1H), 3.13 (m, 1H), 3.04 (dd, *J* = 5.0, 12.1 Hz, 1H), 2.45 (m, 1H), 2.41 (s, 3H), 1.75 - 1.66 (m, 2H), 1.26 (dd, *J* = 4.0, 9.2 Hz, 1H), 0.76 (dd, *J* = 4.0, 6.5 Hz, 1H) ***1H present under DMSO peak***; ^{13}C NMR (101 MHz, DMSO-d_6) δ = 175.2, 143.4, 133.3, 129.8, 127.2, 43.7, 42.3, 23.6, 20.9, 20.1, 19.7, 18.7; LCMS (formic acid) t_R = 0.96 min, [M+H$^+$] 296.0 (purity 94%); HRMS [M+H$^+$] calculated for $C_{14}H_{18}NO_3S$ 296.0951, found [M+H$^+$] 296.0955; IR (neat) ν_{max} = 2870, 1672, 1336, 1310, 1160 cm^{-1}.

1,3-Dioxoisoindolin-2-yl 3-tosyl-3-azabicyclo[4.1.0]heptane-6-carboxylate (1-231)

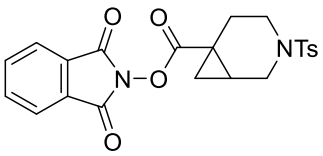

To a round bottom flask (100 mL) was added **1-169** (100 mg, 0.339 mmol), *N*-hydroxyphthalimide (58.0 mg, 0.356 mmol) and DMAP (4.0 mg, 0.034 mmol). DCM (1.7 mL) was added and the reaction mixture stirred vigorously before DIC (55 µL, 0.356 mmol) was added dropwise. The reaction mixture was kept at RT for start 2 h before being filtered under vacuum. The solid was washed with DCM and the filtrate collected and concentrated *in vacuo* to give a brown residue. This was purified by flash chromatography

(cyclohexane/EtOAc 0-50%) to give **1-231** as a white amorphous solid (121 mg, 0.275 mmol, 81%). ^{1}H NMR (400 MHz, $CDCl_3$) δ = 7.90 - 7.84 (m, 2H), 7.82 - 7.76 (m, 2H), 7.68 - 7.63 (m, 2H), 7.38 - 7.33 (m, 2H), 3.87 (m, 1H), 3.53 (m, 1H), 2.93 (dd, *J* = 4.2, 11.7 Hz, 1H), 2.78 (m, 1H), 2.46 (s, 3H), 2.37 (m, 1H), 2.18 - 2.04 (m, 2H), 1.87 (dd, *J* = 4.9, 9.5 Hz, 1H), 1.30 (dd, *J* = 4.9, 7.1 Hz, 1H); ^{13}C NMR (101 MHz, $CDCl_3$) δ = 170.5, 161.9, 143.9, 134.8, 133.3, 129.8, 128.9, 127.6, 124.0, 43.6, 42.9, 24.0, 23.3, 21.5, 21.2, 19.1; LCMS (formic acid) t_R = 1.26 min, [M+H$^+$] 441.1 (purity 95%); HRMS [M+H$^+$] calculated for $C_{22}H_{21}N_2O_6S$ 441.1115, found [M+H$^+$] 441.1113; IR (neat) ν_{max} = 2850, 1770, 1740, 1335, 1168 cm^{-1}.

(3-Tosyl-3-azabicyclo[4.1.0]heptan-6-yl)boronic acid (1-232)

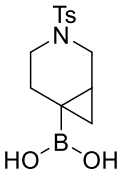

This protocol was based on a literature procedure.[146]

1-231 (547 mg, 1.24 mmol), $[Ir(dtbbpy)(ppy)_2]PF_6$ (11.0 mg, 0.012 mmol) and B_2OH_2 (445 mg, 4.97 mmol) were weighed into a round bottom flask and put under an inert atmosphere before being the addition of DMF (4.2 mL). This was irradiated with CFL lamps for 15 h. The reaction mixture was directly loaded onto the ACQUprep (2 x injections) and purified (water+ 0.1% formic acid/ MeCN +0.1% formic acid - 15-85%). **1-232** was obtained as an amorphous colourless solid (243 mg, 0.823 mmol, 66%). ^{1}H NMR (400 MHz, CD_3CN) δ = 7.60 (d, *J* = 8.4 Hz, 2H), 7.34 (d, *J* = 7.9 Hz, 2H), 3.48 (m, 1H), 3.20 (m, 1H), 3.04 (m, 1H), 2.37 (s, 3H), 2.32 (m, 1H), 2.20 (m, 1H), 1.47 (m, 1H), 1.22 (m, 1H), 0.90 (m, 1H), 0.55 (m, 1H); ^{13}C NMR (101 MHz, CD_3CN) δ = 144.8, 135.2, 130.7, 128.6, 45.6, 44.2, 26.1, 24.6, 21.6, 19.1, 18.4 ***1C not observed due to quadrupolar boron***; ^{11}B NMR (128 MHz, CD_3CN) δ = 31.7; LCMS (formic acid) t_R = 0.90 min, [M+H$^+$] 296.0 (purity 100%); HRMS [M+H$^+$] calculated for $C_{13}H_{19}BNO_4S$ 296.1122, found [M+H$^+$] 296.1120; IR (neat) ν_{max} = 2860, 1404, 1334, 1155 cm^{-1}.

Potassium trifluoro(3-tosyl-3-azabicyclo[4.1.0]heptan-6-yl)borate (1-233)

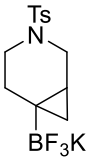

This protocol was based on a literature procedure.[46]

1-232 (243 mg, 0.823 mmol) was dissolved in MeCN (3.3 mL) and to this was KF (191 mg, 3.29 mmol) in water (0.33 mL). The mixture was stirred until complete dissolution of the boronic acid occurred. Separately, *D*-tartaric acid (254 mg, 1.69 mmol) was dissolved in THF (1.2 mL) and added dropwise to the boronic acid solution. The resulting mixture was stirred until the white precipitate had settled. When the stirring had stopped, the precipitate did not settle and therefore additional MeCN (2.5 mL) was added and this stirred for a further 5 min before being allowed to settle. The reaction mixture was then filtered under vacuum. The reaction vessel and filter cake was rinsed with acetonitrile and the filtrate concentrated *in vacuo* to give **1-233** as an amorphous white solid (289 mg, 0.809 mmol, 98%). ^{1}H NMR (400 MHz, CD_3CN) δ = 7.61 - 7.56 (m, 2H), 7.40 - 7.35 (m, 2H), 3.25 (d, *J* = 11.2 Hz, 1H), 3.04 (dd, *J* = 5.9, 11.5 Hz, 1H), 2.92 – 2.84 (m, 1H), 2.49 (ddd, *J* = 4.9, 8.9, 11.6 Hz, 1H), 2.41 (s, 3H), 1.48 (ddd, *J* = 5.1, 8.8, 13.9 Hz, 1H), 0.81 - 0.75 (m, 1H), 0.36 (dd, *J* = 2.8, 7.7 Hz, 1H), -0.13 (dd, *J* = 2.8, 2.8 Hz, 1H) ***1H not observed***; ^{13}C NMR (101 MHz, CD_3CN) δ = 144.5, 134.9, 130.6, 128.6, 46.8, 44.5, 27.2, 21.6, 14.0, 13.7 ***1C not observed due to quadrupolar boron***; ^{19}F NMR (376 MHz, CD_3CN) δ = -150.4; ^{11}B NMR (128 MHz, CD_3CN) δ = 4.2; IR (neat) ν_{max} = 1327, 1160, 939 cm^{-1}.

12.4.17. Suzuki-Miyaura Cross-Coupling with Potassium Trifluoroborate 1-233

6-(Pyridin-2-yl)-3-tosyl-3-azabicyclo[4.1.0]heptane (1-234)

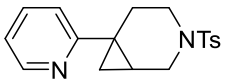

General Procedure E

To a microwave vial was added 2-bromopyridine (32.0 µL, 0.336 mmol), **1-233** (60.0 mg, 0.168 mmol), cataCXium® A Pd G3 and Cs_2CO_3 (164 mg, 0.504 mmol). These were dissolved in 1,4-Dioxane or toluene (1.5 mL) and Water (0.15 mL) and the resulting solution degassed for 10 min before being evacuated and backfilled with nitrogen 3 times. The reaction mixture was then heated to 100 °C for 21 h before being cooled to RT and diluted with EtOAc and water. The layers were separated and the organic washed with brine. The combined aqueous were washed with further EtOAc before the organics were combined and concentrated *in vacuo* to give a yellow oil which was purified by flash chromatography

(cyclohexane/EtOAc 0-40%) to give **1-234** as a light brown or off-white amorphous solid. ^{1}H NMR (400 MHz, $CDCl_3$) δ = 7.70 - 7.64 (m, 2H), 7.57 (m, 1H), 7.33 - 7.28 (m, 2H), 7.14 (m, 1H), 7.08 - 7.02 (m, 1H), 3.54 (td, *J* = 1.4, 11.6 Hz, 1H), 3.34 (dd, *J* = 5.4, 11.7 Hz, 1H), 3.19 (m, 1H), 2.89 (ddd, *J* = 5.1, 8.4, 12.1 Hz, 1H), 2.61 (m, 1H), 2.44 - 2.40 (m, 3H), 2.20 (ddd, *J* = 5.3, 8.6, 13.8 Hz, 1H), 1.77 (m, 1H), 1.30 (dd, *J* = 4.6, 9.0 Hz, 1H), 0.97 (dd, *J* = 4.8, 6.0 Hz, 1H); ^{13}C NMR (101 MHz, $CDCl_3$) δ = 163.8, 149.0, 143.4, 136.2, 133.7, 129.6, 127.6, 120.6, 119.5, 44.6, 42.9, 27.2, 23.0, 21.5, 20.6, 19.5; LCMS (high pH) t_R = 1.16 min, [M+H$^+$] 329.0 (purity 96%); HRMS [M+H$^+$] calculated for $C_{18}H_{21}N_2O_2S$ 329.1318, found [M+H$^+$] 329.1325; IR (neat) ν_{max} = 2922, 2851, 1588, 1473, 1337, 1163 cm^{-1}.

The experiments carried out using General Procedure E are combined in Table 24 below:

Table 24. Reported experiments using General Procedure C and the amounts of reagents used.

Experiment	Amount Pd	Solvent	Yield	Yield/ %
Table 21, Entry 1	5 mol% (6 mg, 8.4 µmol)	toluene	4 mg (0.012 mmol)	7
Table 21, Entry 2	5 mol% (6 mg, 8.4 µmol)	1,4-dioxane	6 mg (0.018 mmol)	11
Table 21, Entry 3	20 mol% (25 mg, 0.034 mmol)	1,4-dioxane	11 mg (0.033 mmol)	20

Chapter II: UV-induced 1,3,4-oxadiazole formation from 5-substituted tetrazoles and carboxylic acids in flow

13. Introduction

13.1. 1,3,4-Oxadiazoles

13.1.1. Properties and Use in Medicinal Chemistry

Oxadiazoles are five-membered heterocycles containing two nitrogen atoms and one oxygen atom which exist in four different regioisomeric forms (Figure 58).[166,167]

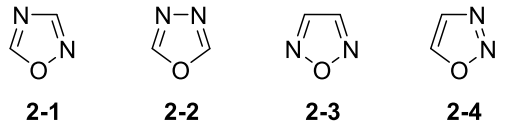

Figure 58. The structures of the four oxadiazole isomers. 1,2,4-oxadiazole **2-1**; 1,3,4-oxadiazole **2-2**; 1,2,5-oxadiazole **2-3**; 1,2,3-oxadiazole **2-4**.

Of these four isomers, the two which garner the most attention are the 1,3,4- and 1,2,4-isomers.[168] The primary reason for the extensive study of these two regioisomers is likely due to their use in medicinal chemistry as bioisosteres for carbonyl-containing groups such as esters, amides and carbamates (see section 1.1).[5,7,166,169,170] Furthermore, the substituents in both the 1,2,4- and 1,3,4-isomers can be identically orientated with the heteroatoms of the ring altered relative to each other as shown in Figure 59.

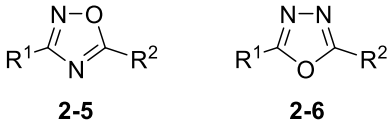

Figure 59. Comparison of orientation of the 'R' groups on both 1,2,4- and 1,3,4-oxadiazoles.

As a result of this bioisosterism and the orientation of the carbon-linked ‘R’ groups, much research has focused on the use of these compounds in medicinal chemistry programmes. It has also been the case that the variation in physicochemical properties between the two has been explored in detail.[166,171] Despite being virtually identical in terms of the molecular shape around the heteroaromatic core, there are distinct differences between the two when factors such as lipophilicity and metabolic stability are considered. Boström *et al*. highlighted that in a large number of oxadiazole matched pairs, the 1,3,4-isomers generally possessed a lower lipophilicity profile than the corresponding 1,2,4-isomers.[166] As a result of this, other physicochemical properties such as aqueous solubility and metabolic stability were more favourable for the 1,3,4-isomers and this data was consistent with further studies by MacFaul and others.[166,171] A rationale for these properties was discussed and attributed to the existence of a larger dipole for the 1,3,4-isomer due to the location of the heteroatoms and, therefore, a differentiation in the charge distributions. This dipole and the calculated hydrogen bond accepting ability of the heteroatoms are highlighted in Figure 60.

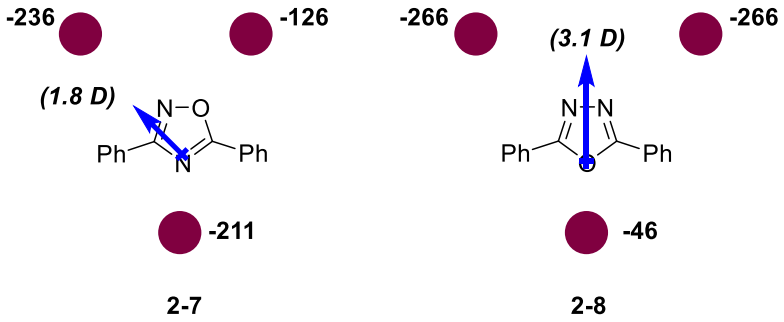

Figure 60. Comparison of the dipoles of 2,5-diphenyl-1,2,4-oxadiazole **2-7** and 2,5-diphenyl-1,3,4-oxadiazole **2-8** which are indicated by the blue arrows. Also shown are the calculated V_{min} values (kcal mol^{-1}) which indicate the strength of hydrogen bond accepting ability. A larger negative value indicates a stronger ability to hydrogen bond. Figure adapted from Boström *et al*.[166]

As can be seen, a larger dipole exists for the 1,3,4-oxadiazole isomer, along with the propensity for the nitrogen atoms to act as stronger hydrogen bond-acceptors than those in the 1,2,4-oxadiazole isomer. This effect is seen to be the biggest influence on the difference in physicochemical properties. The 1,3,4-oxadiazole isomer can clearly be seen to be the preferred choice when compared to the 1,2,4-oxadiazole isomer, especially with respect to physicochemical properties. The increased ability to accept a hydrogen-bond may also improve binding in proteins and thus improve potency when this moiety is included in bioactive compounds.

Within the medicinal chemistry literature, this moiety is used extensively and has been incorporated into compounds which are shown to exhibit antibacterial,[172] antimitotic,[173] antiviral[174] and anti-inflammatory[169] properties. A widely showcased example of the use of the 1,3,4-oxadiazole in an approved drug is Raltegravir which is used to treat HIV (Figure 61).[175] In this structure, the 1,3,4-oxadiazole provides an increase in potency against HIV-integrase when compared to other heterocycles synthesised containing three heteroatoms. This effect could be as a result of the increased dipole and hydrogen-bond accepting properties described above.

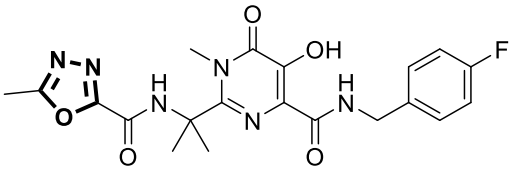

Figure 61. The structure of Raltegravir – an oxadiazole-containing drug which is used in the treatment of HIV.

Based on the large number of literature reports that exist focusing on the 1,3,4-oxadiazole heterocycle, it is unsurprising that it is considered to be a privileged structure, with the moiety finding use in numerous molecules acting against various biological targets.[174] As such, this heterocycle should be a fundamental component in any medicinal chemist's toolbox.

13.1.2. Use in OLEDs

In addition to the frequent use in medicinal chemistry, the 1,3,4-oxadiazole moiety is also prevalent in the literature pertaining to organic light-emitting diodes (OLEDs). Compounds containing the heterocycle possess attributes important to the efficient functioning of OLEDs such as a high quantum yield of luminescence, thermal stability and electron-transporting properties.[176] The quantum yield of luminescence is described as the ratio of photons emitted to those absorbed by the molecules and, as such, a higher value is desirable for a system in which light emission is the primary purpose.[177] Oxadiazole-containing compounds are primarily used in multi-layer OLEDs which are composed as shown in Figure 62.[178]

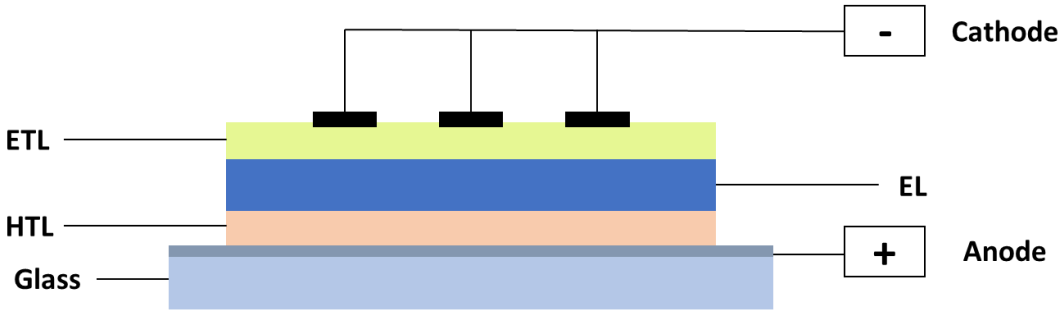

Figure 62. A schematic diagram of a multi-layer OLED highlighting the various layers. **ETL** = electron-transporting layer; **EL** = emitting layer; **HTL** = hole-transporting layer. Adapted from Mitschke and Bäuerle.[178]

OLEDs produce light through a process known as electroluminescence by which an electric field is applied across a substrate, causing a separation of electrons and electron holes. The recombination of these leads to an excited state which can decay by radiative emission of a photon.[179,180] It was discovered that the use of oxadiazole-containing compounds in the electron-transporting layer (ETL) was advantageous as they are inherently electron-deficient and, as such, have a high affinity for electrons. Furthermore, these compounds have been shown to possess high ionisation energies, thus causing them to act as hole-blockers as well.[178,179] These properties lead to recombination in the emitting layer, improving the efficiency of devices when compared to single-layer OLEDs (with no ETL or HTL).[181]

The first example of using oxadiazoles in this manner was in 1989 when Adachi *et al*. synthesised 2-biphenyl-4-yl-5-(4-*tert*-butylphenyl)-1,3,4-oxadiazole (PBD) and applied it to their multi-layer system.[182] The use of PBD was not without drawbacks with the compound being susceptible to recrystallisation after multiple uses when deposited as a thin film, thus reducing the lifetime of the device.[183] As a result, a plethora of oxadiazole-containing compounds have subsequently been described in the literature, improving upon PBD. Dimers, oligomers, polymers and oxadiazole-doped polymer systems are commonplace in

modern systems.[176,178-180,183,184] It is also possible to use oxadiazole-containing polymers as single-layer systems in which they are contained within the EL.[178,185] Some examples of 1,3,4-oxadiazoles used in OLEDs are shown in Figure 63.

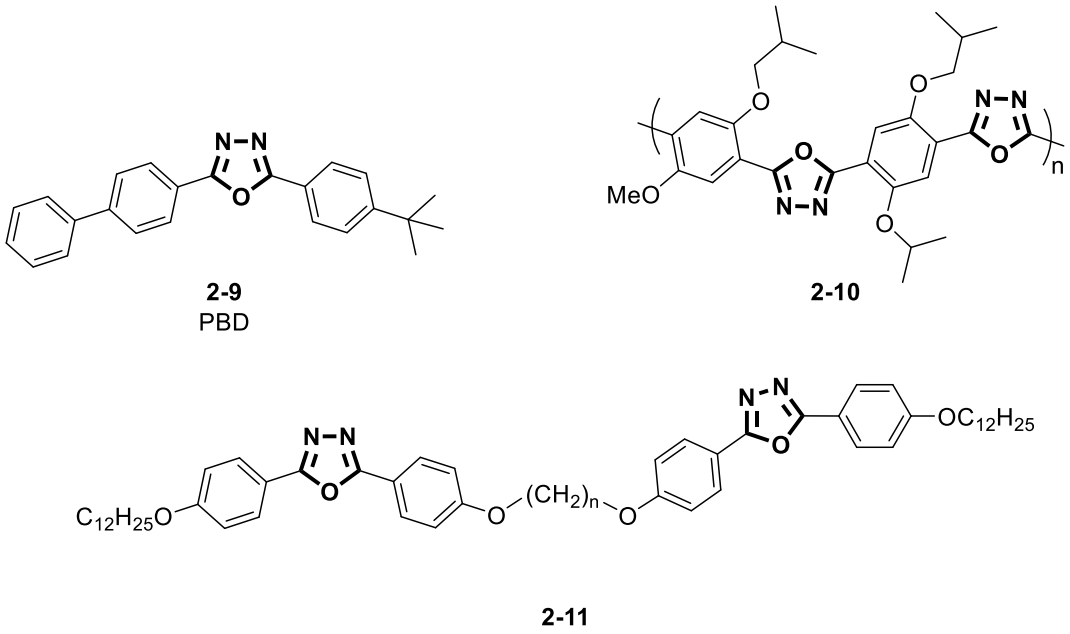

Figure 63. The structures of some oxadiazole-containing compounds used in OLEDs as electron-transporting materials.

The wide variety of oxadiazole-containing compounds allows for a range of properties to be introduced to OLED systems. Therefore, the use of this moiety cannot be understated in this application with some of these compounds still used in modern systems.

Extensive use of 1,3,4-oxadiazoles in both medicinal and materials chemistry highlights the importance of the moiety across different fields of chemistry. As a direct result of this, several synthetic methods towards the heterocyclic scaffold exist and will be explored in the following sections (*vide infra*).

13.2. Synthetic Routes Towards 1,3,4-Oxadiazoles

A variety of syntheses have been reported for the formation of 1,3,4-oxadiazoles, generally falling into five categories: cyclodehydration, cyclodesulfurisation, oxidative cyclisation, condensation, and the Huisgen reaction. These transformations and the respective starting materials are summarised in Scheme 85 below.[168,186] These all provide efficient routes to the desired compounds; however, there are of course advantages and disadvantages of each.

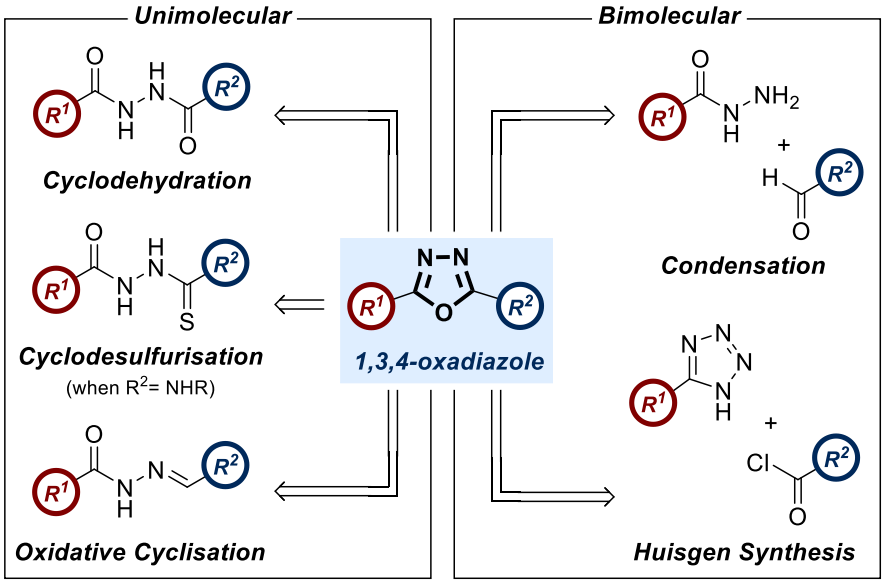

Scheme 85. Schematic diagram highlighting the five main methods of synthesising 1,3,4-oxadiazoles. These include cyclodehydration of 1,2-diacylhydrazines; cyclodesulfurisation of 1,4-disubstituted thiosemicarbazides; oxidative cyclisation of semicarbazones; condensation of acyl hydrazines and aldehydes followed by cyclisation and the Huisgen reaction between a 5-substituted tetrazole and an acylating agent such as an acid chloride or

13.2.1. Cyclodehydration of 1,2-Diacylhydrazines

The cyclodehydration of 1,2-diacylhydrazines is one of the most common methods of forming 1,3,4-oxadiazoles and several procedures exist to facilitate this transformation. The 1,2-diacylhydrazine moiety **2-15** can be constructed from an acyl hydrazine **2-12** and a carboxylic acid **2-13** or acid chloride **2-14** before undergoing cyclodehydration as shown in Scheme 86.

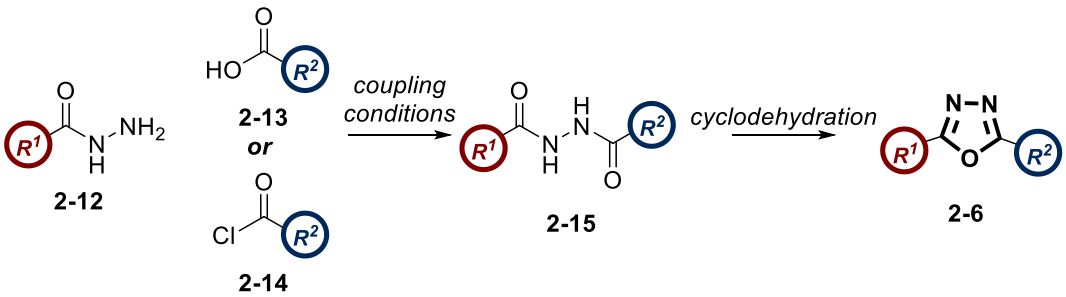

Scheme 86. The coupling of an acyl hydrazine **2-12** and a carboxylic acid **2-13** or acid chloride **2-14** to form 1,2-diacylhydrazines **2-15** before undergoing cyclodehydration to the desired 1,3,4-oxadiazole **2-6**.

Despite the general approach to 1,2-diacylhydrazines, there exists a variety of conditions for

the coupling. Table 25 highlights some examples of these syntheses and the various substrates used. The isolated 1,2-diacylhydrazines undergo cyclodehydration with an array of reagents, also shown in Table 25. A common feature of most of the reactions shown is the forcing conditions required to form the 1,3,4-oxadiazole; however, the yields are generally good, and the variety of substrates suggest the process is somewhat flexible in nature. Despite this, sensitive functional groups and certain protecting groups could be susceptible to decomposition by the generally harsh and acidic conditions.

Table 25. Selected examples of substrates and conditions used in the synthesis of 1,2-diacylhydrazines.

Acids				
R^1 (acylhydrazine)	**R^2** (acid)	**Coupling Conditions**	**Cyclodehydration conditions**	**Ref.**
Various examples 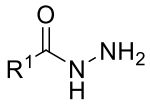	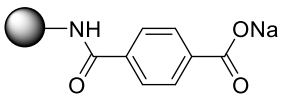	PyBOP® DIPEA DMF	DIC DCM 100 °C	187
Various examples 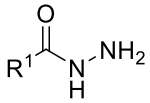	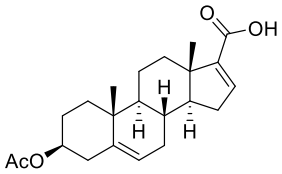	CDI DCM/DMF	$POCl_3$ 80 °C	188
Various examples 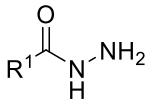	Various examples 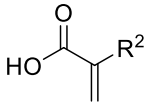	EDCI DCM	PPh_3 Cl_3CCCl_3 DIPEA MeCN RT	189
Acid chlorides				
R^1 (acylhydrazine)	**R^2** (acid chloride)	**Coupling Conditions**	**Cyclodehydration conditions**	**Ref.**
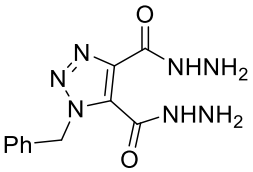	Various examples 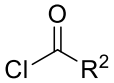	Dry pyridine	$SOCl_2$ PhH reflux	190
A 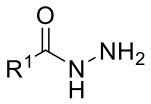 **B** 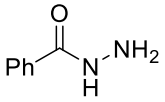	Various examples **A** 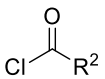 **B** 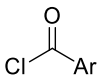	**A** Et_3N, DCM **B** Na_2CO_3, THF/H_2O	$[Et_2NSF_2]BF_4$ (XtalFluor-E) AcOH DCE 90 °C	191
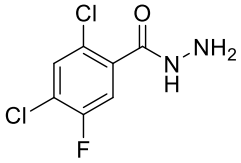	Various examples 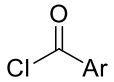	THF	$POCl_3$ reflux	192

Various examples 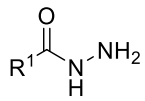	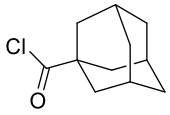	pyridine	$POCl_3$ reflux	193

Sureshbabu *et al*. have shown that it is possible to form oxadiazole products from amino acid-derived 1,2-diacylhydrazines **2-18** using *N*-(3-dimethylaminopropyl)-*N*′-ethylcarbodiimide (EDCI) as a mild cyclodehydrating agent, giving excellent yields.[194] The authors also reported the synthesis of the 1,2-diacylhydrazine precursor from an acid fluoride **2-17** under mild conditions (Scheme 87).

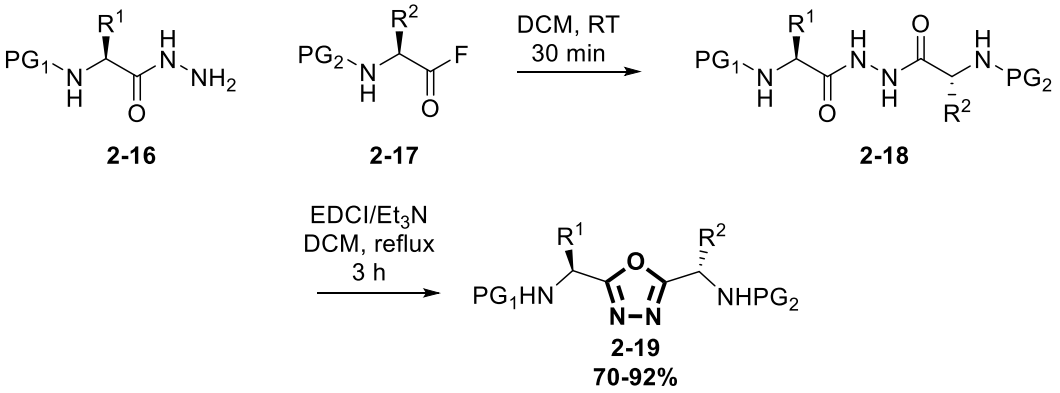

Scheme 87. Synthesis of amino-acid derived 1,2-diacylhydrazine **2-18** and cyclodehydration to corresponding oxadiazole **2-19**.

Publications in which the starting 1,2-diacylhydrazine synthesis is not reported are common, with the focus on the cyclodehydration of these molecules. A range of conditions for the transformation can be found and these methodologies use reagents such as: catalytic zirconium(IV) chloride;[195] triflic anhydride and pyridine;[196] and triflic anhydride with *N*-methylimidazole.[197] Moderate to good yields are obtained, however, the substrate scope is limited for the first two reports. The use of triflic anhydride with *N*-methylimidazole offers an approach tailored to pharmaceutically relevant compounds with the scope and cost considerations of the reagents reflecting this.

While the two-step methods highlighted are successful (*vide supra*), it has been shown that one-pot procedures, combining the 1,2-diacylhydrazine formation and cyclodehydration, are also possible. In these methods, it is common for an acylhydrazine **2-12** to be coupled to a carboxylic acid **2-13** *in situ* before undergoing cyclodehydration to give the desired product. As with the two-step procedures, several different conditions are used for these transformations. The use of $POCl_3$ to enable both the coupling and cyclodehydration in one-

pot has been successfully employed by El-Emam *et al.*[193] In doing so, a direct comparison to their two-step method, shown in Table 25, with the one-pot procedure can be seen with the latter offering slightly improved yields (Scheme 88).[193] The one-pot procedure also makes use of carboxylic acids which are, in general, more readily available and stable.

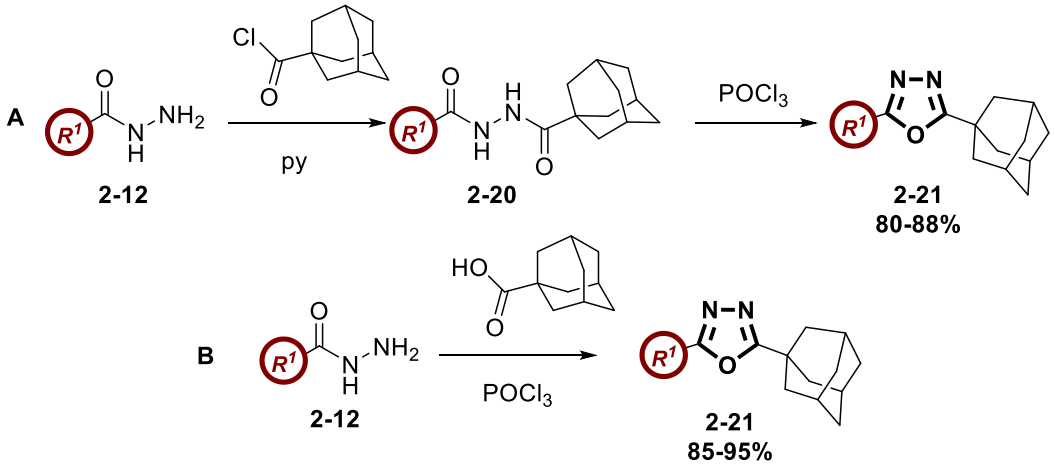

Scheme 88. Comparison of a two-step (A) and one-pot (B) cyclodehydration process.

When using carboxylic acids **2-13** as starting materials, it is common to see amide coupling reagents used to form 1,2-diacylhydrazines **2-15** *in situ* before addition of a dehydrating reagent to enable cyclisation to the 1,3,4-oxadiazole **2-6**. Examples of this are shown below in Table 26 whereby common reagents such as HATU are used. This approach and the examples given appear to use milder cyclodehydration conditions than the corresponding reactions in Table 25. Given this, and the *in situ* activation of carboxylic acids **2-13**, this method of cyclodehydration is one way in which the scope could be improved by eliminating harsh conditions and reagents such as $POCl_3$.

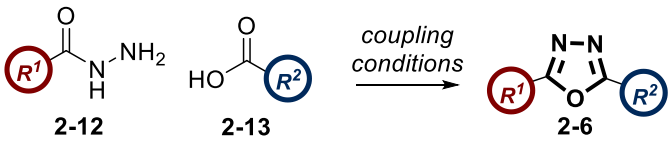

Table 26. Amide coupling reagents and cyclodehydrating agents used in one-pot syntheses of 1,3,4-oxadiazoles **2-6** from acylhydrazines **2-12** and carboxylic acids **2-13**.

Amide Coupling Reagent	Cyclodehydrating Reagent	Ref.

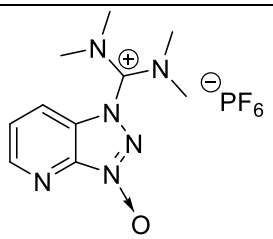 (HATU), DIPEA	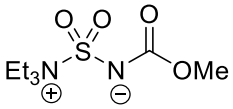 (Burgess Reagent)	198
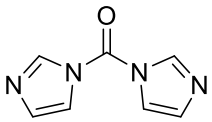 (CDI)	PPh_3, CBr_4	199
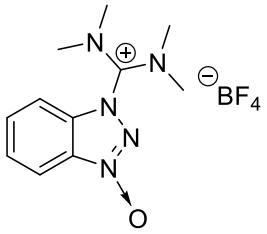 (TBTU), DIPEA	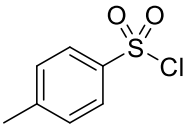 (TsCl), DIPEA	200

Further streamlining this route, an example in which the coupling reagent acts as a dehydrating agent was showcased by Augustine *et al*. with the use of 2.5 equivalents of propylphosphonic anhydride (T3P®).[201] This method produced several diverse 1,3,4-oxadiazoles **2-6** in excellent yields of 84-94% (Scheme 89).

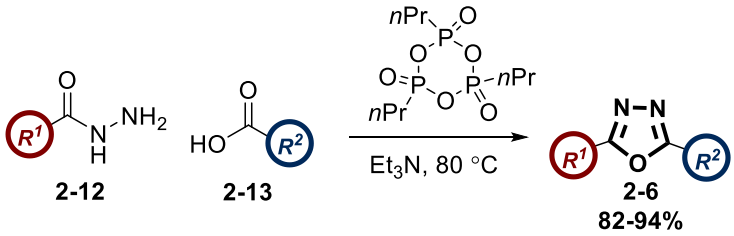

Scheme 89. The synthesis of 1,3,4-oxadiazoles **2-6** from acylhydrazines **2-12** and carboxylic acids **2-13** using T3P® as both an amide coupling and cyclodehydrating reagent.

As intimated above, this cyclisation method is one of the most common approaches to 1,3,4-oxadiazoles **2-6**. It provides a simple and efficient method to the desired products; however, some of the reagents have associated issues, such as being corrosive and/or expensive with the harsh conditions unable to be tolerated by sensitive functional groups or molecules. Additional methods can be used for cyclodehydration but these examples use highly toxic materials such as hexamethylphosphoramide (HMPA)[202] or hydrazine[203,204] and represent less viable options in a modern day laboratory.

13.2.2. Cyclodesulfurisation of 1,4-Disubstituted Thiosemicarbazides

Cyclodesulfurisation of 1,4-disubstituted thiosemicarbazides is specific to the synthesis of 5-substituted-2-amino-1,3,4-oxadiazoles **2-24** (Scheme 90). There are fewer examples within the literature when compared to those employing a cyclodehydration approach to 1,3,4-oxadiazoles **2-6**; however, those that exist generally involve the synthesis of the thiosemicarbazide **2-23** from an acylhydrazine **2-12** and an isothiocyanate **2-22** (Scheme 90). With this approach, a two-step process involving isolation of the thiosemicarbazide **2-23**, appears to be favoured compared to equivalent one-pot procedures. The synthesis of thiosemicarbazides will not be explored as part of this introduction; however, it is important

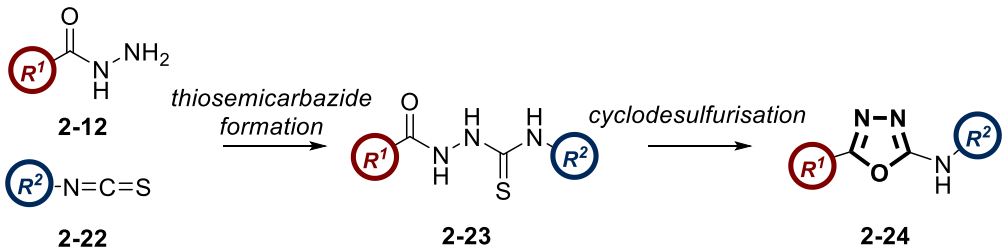

to highlight both the availability and toxicity of the isothiocyanate starting materials **2-22**. These are highly electrophilic species which are best prepared and used when required, an issue which may hinder the applicability of this approach but can be undertaken in a flow system.[205] Furthermore, these reagents exhibit toxicity and are often sensitising agents.[206]

Scheme 90. General approach to 5-substituted-2-amino-1,3,4-oxadiazoles **2-24** using cyclodesulfurisation of thiosemicarbazides **2-23**.

As with the cyclodehydration of 1,2-diacylhydrazines, a variety of conditions are reported for the cyclodesulfurisation step (Scheme 90). Table 27 below summarises several selected literature examples with the key reagents highlighted. The substrate scope and yield of these processes varies between each publication; however, the yields are generally good, and the 'R' group tolerance is sufficiently high to support very broad applicability.

Table 27. Literature conditions for the cyclodesulfurisation of thiosemicarbazides **2-23** to form 5-substituted-2-amino-1,3,4-oxadiazoles **2-24**.

Thiosemicarbazide	Cyclisation conditions	1,3,4-Oxadiazole	Ref.
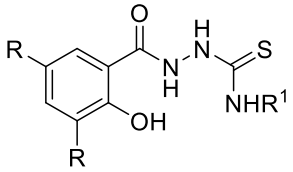	**A:** DCC, PhH **B**: HgO/EtOH	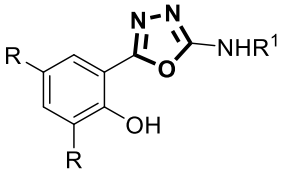	207

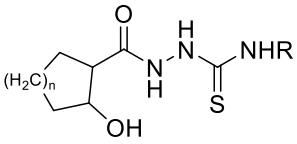	MeI then MeOH/KOH	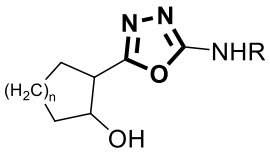	208
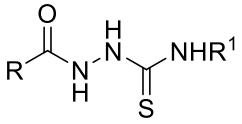	I_2/NaOH, EtOH *or* DCC, MeOH/acetone	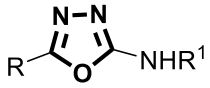	169
	TsCl, py, THF		209
	IBX, Et_3N, DCM		210
	EDCI·HCl, DMSO		211
	DIPEA, TBTU, DMF		212
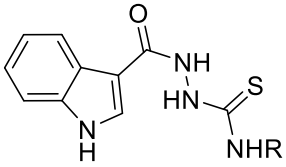	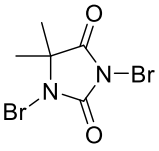 KI, ^{i}PrOH/MeCN$_{(aq)}$	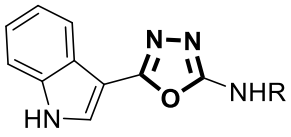	213
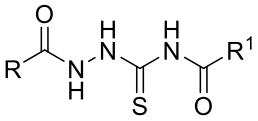	KIO_3, H_2O	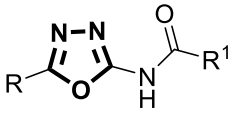	214

Of the methods reported above, those published most recently have focused their efforts on the use of greener, less expensive reagents which are easily removed to give pure oxadiazole products.[209,210,212,213] This contrasts some of the original reports which utilised mercury salts[207] or carcinogenic alkylating agents such as methyl iodide[208] and exemplifies how this approach has evolved. Furthermore, Dolman *et al*. compared the use of 1,2-diacylhydrazines and the corresponding thiosemicarbazides under their conditions and found that for the synthesis of 5-substituted-2-amino-1,3,4-oxadiazoles, cyclodesulfurisation was far superior with improved yields for each example.[209]

Cyclodesulfurisation is possible with amino acid derivatives and this was exemplified by the Sureshbabu group, as with cyclodehydration (*vide supra*, Scheme 87). Tosyl chloride and pyridine were used as the cyclisation reagents as shown below (Scheme 91).[215] The presence of the amino acid moieties and the protecting groups in this example emphasise the mild conditions which may not be possible for the corresponding cyclodehydration reactions.

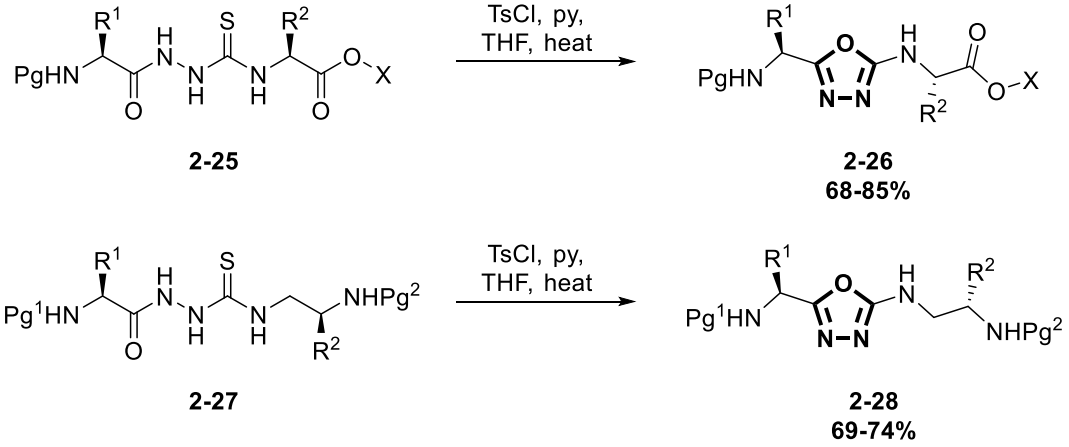

Scheme 91. The cyclodesulfurisation of thiosemicarbazide derivatives of amino acids to form peptidomimetics.

A small number of the reports outlined in Table 27 allude to one-pot procedures using their methods; however, only limited examples are given with mixed results.[207,209] Despite this, there are true one-pot procedures in which the thiosemicarbazide is both formed and cyclised in the same reaction vessel to give the desired 1,3,4-oxadiazoles, as shown in Scheme 92.[216-218]

Overall, this method is an efficient way of synthesising 5-substituted-2-amino-1,3,4-oxadiazoles **2-24** and can be undertaken with a range of conditions and reagents, some of which are more environmentally friendly and efficient than others. Generally broad substrate scopes also favour this approach which may stem from the use of less harsh conditions and reagents than for cyclodehydration; however, an obvious disadvantage is the use of isothiocyanates.

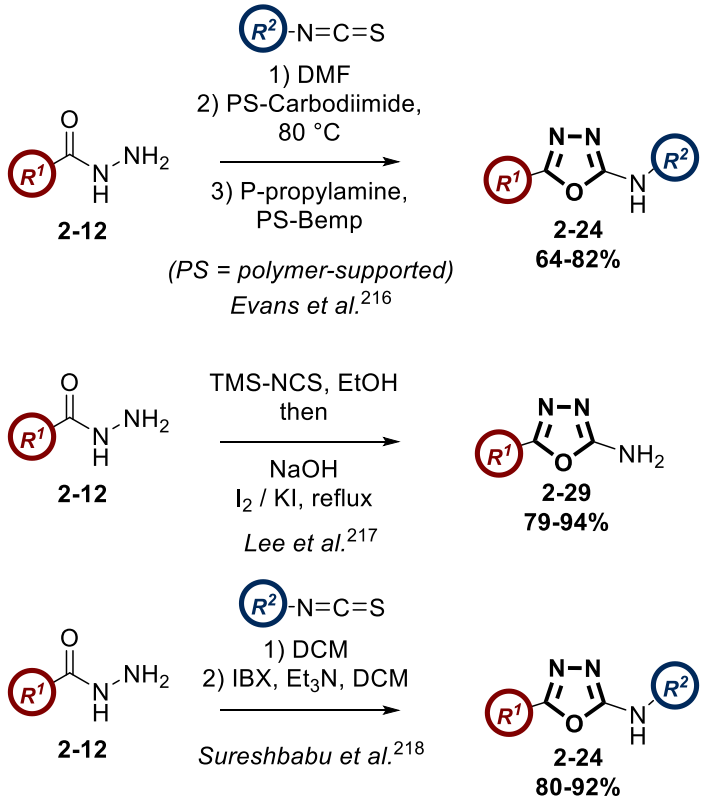

Scheme 92. One-pot synthesis of 5-substituted-2-amino-1,3,4-oxadiazoles *via* thiosemicarbazide intermediates.

13.2.3. Oxidative Cyclisation of Semicarbazones

Oxidative cyclisation of semicarbazones is another widely used approach in the synthesis of 1,3,4-oxadiazoles. This process involves the formation of a semicarbazone **2-31** from an aldehyde **2-30** and acylhydrazine **2-12** before undergoing cyclisation under oxidising conditions (Scheme 93). The condensation step is not discussed in this section; however, the overall transformation can be achieved in one pot using a condensation and oxidation sequence as will be discussed in section 13.2.4 (*vide infra*).

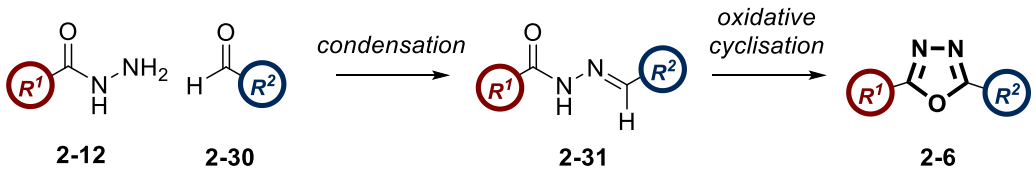

Scheme 93. General approach to 1,3,4-oxadiazoles **2-6** *via* oxidative cyclisation of semicarbazones **2-31** which are formed by the condensation of aldehydes with acylhydrazines **2-12**.

Following the trend of the previously discussed syntheses of 1,3,4-oxadiazoles, there exists a plethora of conditions within the literature for oxidative cyclisation. Table 28 below shows a selection of these conditions, which includes conventional reaction conditions as well as the use of electrochemistry. These examples collectively cover a broad substrate scope with the 2- and 5-positions of the 1,3,4-oxadiazole substituted with both alkyl and aryl substituents. The focus of modern methods is that of a catalytic approach to reduce the amount of expensive and toxic oxidants.[219,220] In doing this, oxidative cyclisation may become more scalable and environmentally friendly, increasing the likelihood of wider use.

Table 28. Examples of oxidative cyclisation conditions for the synthesis of 1,3,4-oxadiazoles **2-6** from semicarbazones **2-31**.

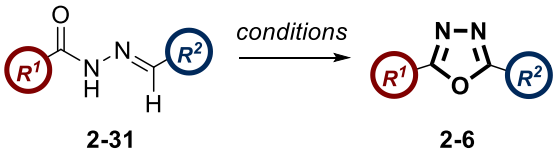

Cyclisation conditions	Ref.	Cyclisation conditions	Ref.
Electrochemical NaOAc, MeOH 0.5A, 4-5 F mol^{-1}	221	*N*-chlorosuccinimde DBU, DCM	222
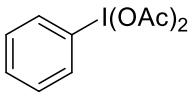 **PIDA** $NaOAc{\cdot}3H_2O$, MeOH	223	$Cu(OTf)_2$ (10 mol%) O_2 (air), Cs_2CO_3 DMF, 110 °C	220
$KMnO_4$, SiO_2 microwave heating *Or* Acetone/H_2O, $KMnO_4$ microwave heating	224	*Electrochemical* MeOH/$NaIO_4$ Pt-electrode	225
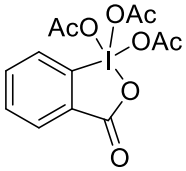 **DMP** DCM *or* DMF	226	I_2 (10 mol%) Aqueous H_2O_2, K_2CO_3 *or* Cs_2CO_3 DMSO	219

Further to the examples in Table 28, both Werber and Rajak used a mixture of bromine and sodium acetate to access 5-substituted-2-amino-1,3,4-oxadiazoles **2-24**, with the former synthesising compounds substituted on the amino moiety.[227,228] A more recent approach to these substituted heterocycles by Yadav makes use of photochemistry to initiate a radical approach to oxidative cyclisation with the use of an organic dye, eosin Y.[229] These methods are summarised below in Scheme 94 with all seeming equally effective. The use of photochemistry highlights the possibility of accessing these compounds using modern methods as well as removal of thermal energy.

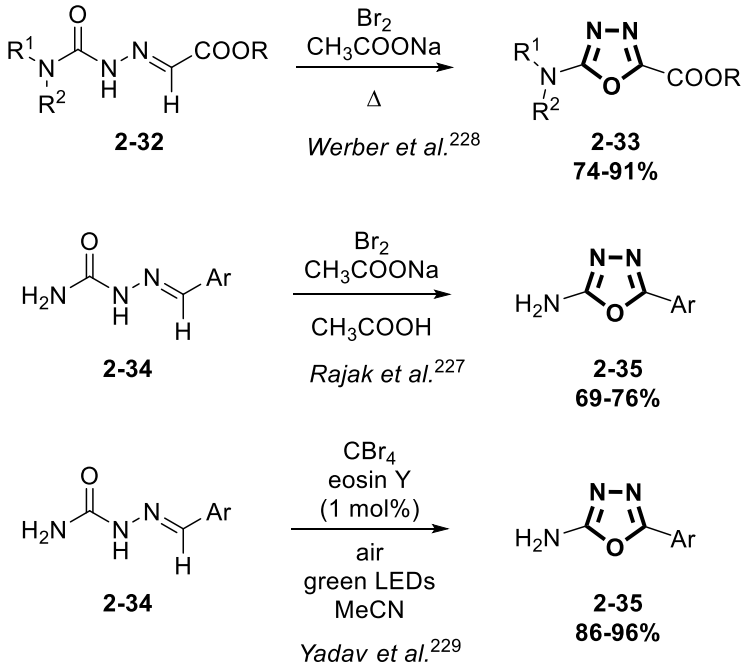

Scheme 94. Methods for the synthesis of 5-substituted-2-amino-1,3,4-oxadiazoles from semicarbazones.

One final approach in the oxidative cyclisation of semicarbazones is to use chloramine T as the oxidant to form 1,3,4-oxadiazoles from the reactive nitrile imine intermediates (see section 13.2.5). This is relatively well-precedented on several different substrates and finds use in the cyclisation of functionalised semicarbazones as highlighted by Rai *et al*. (Scheme 95).[230,231]

The oxidative cyclisation of semicarbazones provides an efficient and robust approach to 1,3,4-oxadiazoles with a good overall substrate scope; however, issues with functional group tolerability and the use of strong oxidants may limit use in functionally sensitive systems. Furthermore, some of the reagents in the selected examples can be costly and possess sub-optimal properties and hazards.

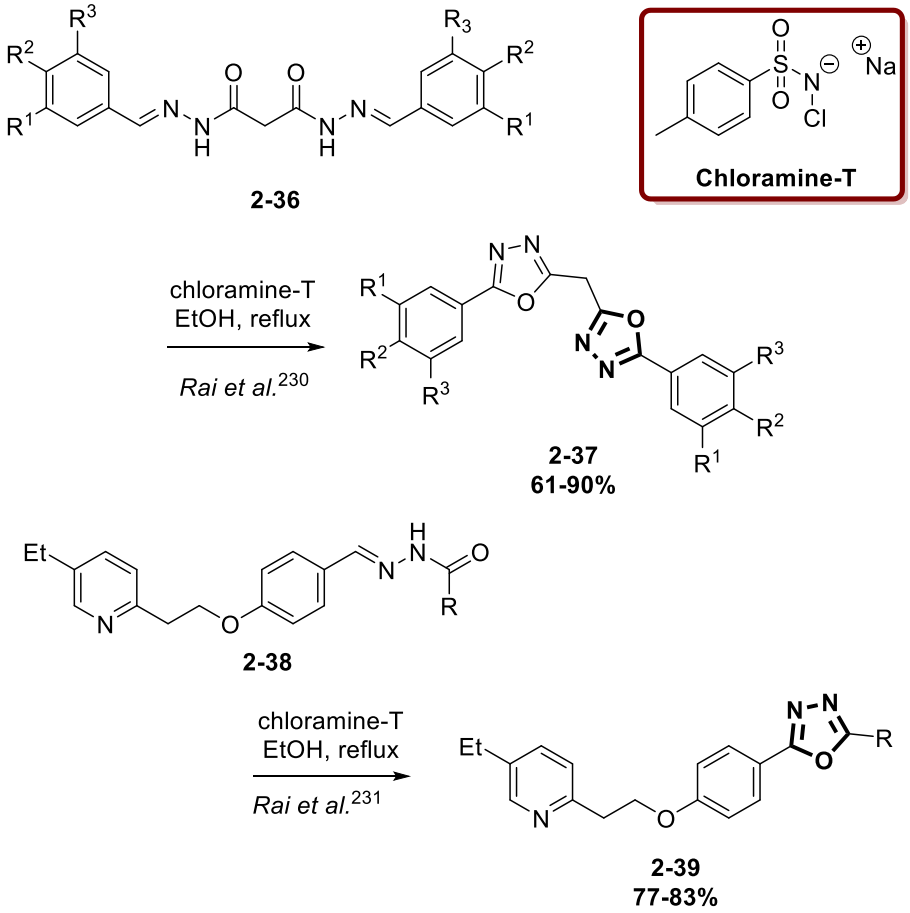

Scheme 95. The synthesis of functionalised 1,3,4-oxadiazoles from semicarbazones using chloramine-T as an oxidant.

13.2.4. Condensation of Acyl Hydrazines and Aldehydes

The condensation reaction between an acyl hydrazine **2-12** and an aldehyde **2-30** leads to the formation of a semicarbazone **2-31** as shown in Scheme 93. As such, the one-pot condensation and cyclisation approach towards 1,3,4-oxadiazoles **2-6** can be considered as an extension of the previous oxidative cyclisation method. The main difference between these two syntheses is in the use of either isolated or crude semicarbazone **2-31**. A small number of examples are found in the literature with an interesting variety of oxidation conditions. Recently, Chang and Yu have shown that this one-pot procedure can be carried out in the presence of iodine to form both 5-substituted-2-amino- and 2,5-disubstituted-1,3,4-oxadiazoles (Scheme 96).[232,233]

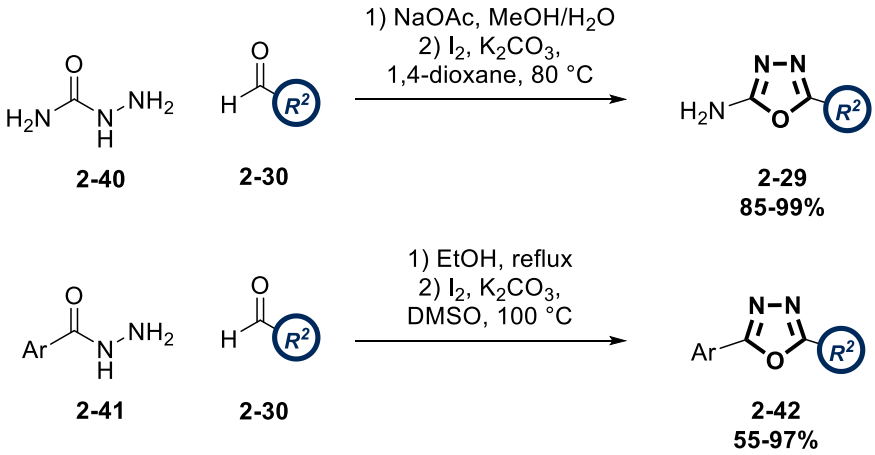

2-40 **2-30** **2-29** **85-99%**

2-41 **2-30** **2-42** **55-97%**

Scheme 96. The iodine-mediated synthesis of 1,3,4-oxadiazoles in a condensation reaction between an aldehyde **2-30** and aminourea hydrochloride **2-40**, or an acylhydrazine **2-41**.

Other reagents facilitating this transformation include trichlorocyanuric acid (TCCA),[234] CAN,[235] an acidic $ZnO\text{-}TiO_2$ solid catalyst,[236] and the organic dye eosin Y with green LEDs.[237] These approaches are highlighted in Scheme 97.

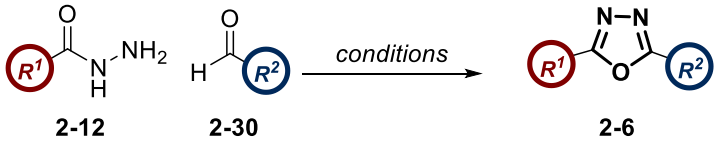

2-12 **2-30** **2-6**

Desai et al.[234]: TCCA, EtOH; **56-87%**

Dabiri et al.[235]: CAN, reflux, DCM; **25-67%**

Yadav et al.[237]: i) DMF 60 °C; ii) eosin Y (2 mol%), green LEDs, DIPEA, O_2 (air); **70-96%**

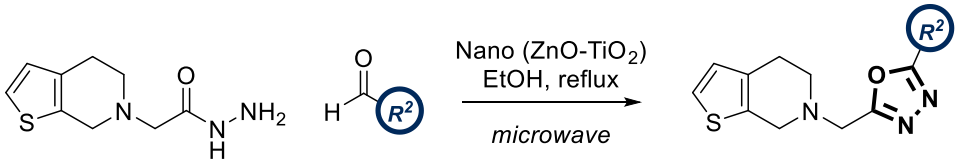

2-43 **2-30** *Sangshetti et al.*[236] **2-44**

Scheme 97. Synthesis of 1,3,4-oxadiazoles *via* a condensation and in situ cyclisation using various conditions.

The photochemical approach complements previous work by Yadav[229] and extends this to a one-pot methodology, maintaining the use of eosin Y and green LEDs with high yields obtained. The other methods shown use chemical reagents to enable the analogous transformations, albeit with lower yields.

A similar condensation approach makes use of triethyl orthoesters as replacements for aldehydes, thus obviating the requirement for oxidation. These one-pot processes are somewhat scarce within the literature; however, they are noteworthy alongside the traditional

condensation approach. Both of the following examples use acid catalysis alongside microwave heating to achieve the desired transformation;[238,239] however, the catalyst differs between the two as shown in Scheme 98 with Varma and Polshettiwar using a solid Nafion® catalyst.[238] While being a noteworthy mention, the use of orthoesters may not be widely adopted due to limitations of the 'R' group present on the orthoester with very limited scope reported for both methods.

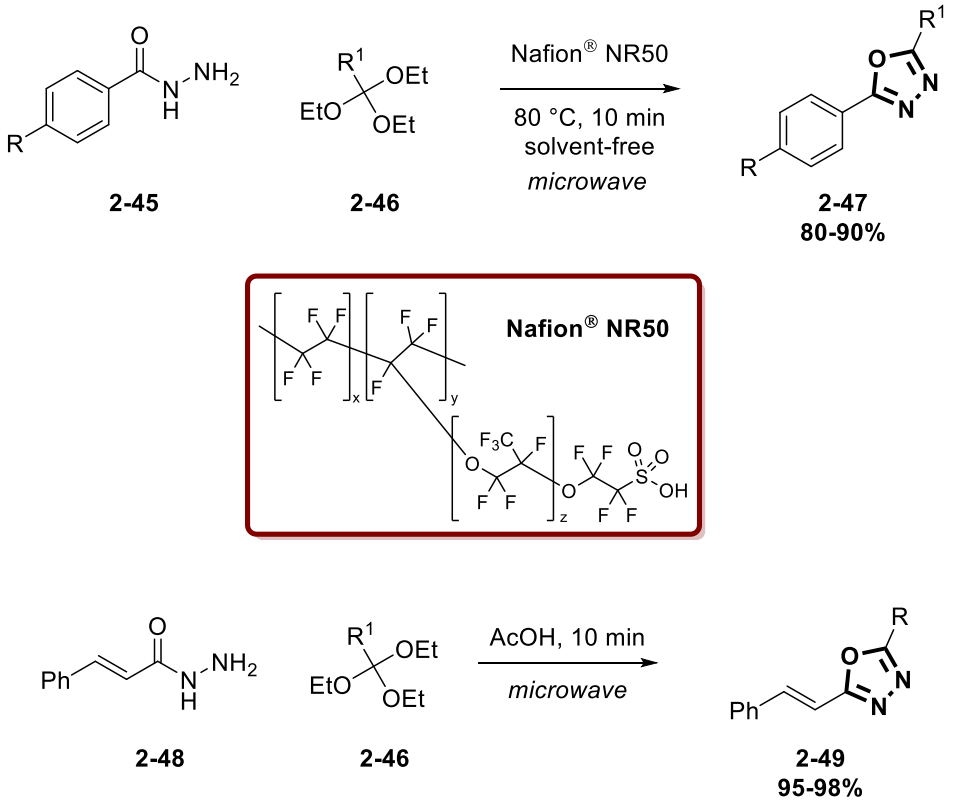

Scheme 98. The synthesis of 1,3,4-oxadiazoles from acylhydrazines and triethyl orthoesters using acid catalysts.

As previously mentioned, condensation methods offer an extension to the oxidative cyclisation approach outlined in section 13.2.3 (*vide supra*), albeit with the added efficiency of being a one-pot process. As such, this methodology is a useful part of the synthetic chemist's toolbox.

13.2.5. The Huisgen Reaction

The final method for 1,3,4-oxadiazole synthesis is the Huisgen reaction. First reported in 1958 by Professor Rolf Huisgen, it involves the combination of a 5-substituted tetrazole **2-50** and an acylating agent **2-14**/**2-51**.[240-242] The reaction is initiated by acylation of the 5-substituted tetrazole to give *N*-acyl tetrazole intermediate **2-52**, from which nitrogen is lost under the thermal conditions. A reactive nitrile imine intermediate **2-53** forms and subsequently closes in an intramolecular cyclisation to yield the desired 2,5-disubstituted 1,3,4-oxadiazole **2-6** (Scheme 99).[243] This synthesis of 1,3,4-oxadiazoles and a subsequent

adaptation of this approach was the focus of the study reported later in this chapter (*vide infra*).

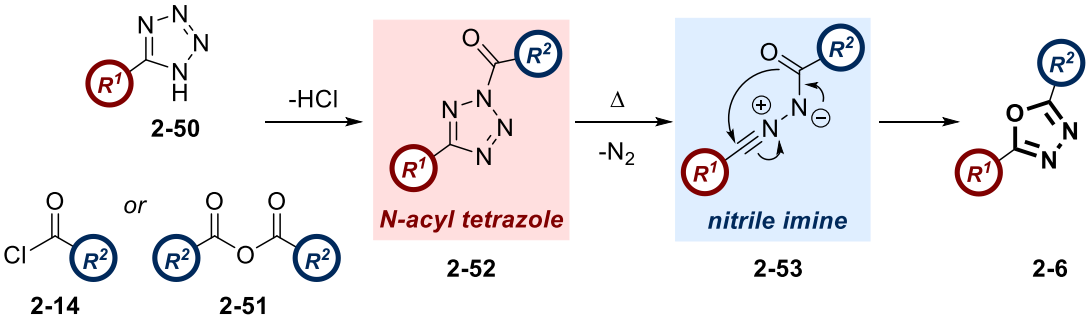

Scheme 99. The Huisgen synthesis of 2,5-disubstituted-1,3,4-oxadiazoles **2-6** from 5-substituted tetrazoles **2-50** and acid chlorides **2-14** or acid anhydrides **2-51**.

Compared to the methods previously discussed, relatively little attention has been given to this approach, potentially due to the scalability and safety issues associated with the required high temperatures and thermal instability of tetrazoles.[244,245] Despite this, there are still numerous examples in both the medicinal and materials chemistry literature wherein the Huisgen reaction is employed. The simplicity of this method may be overlooked by the wider chemistry community as most examples are found in the syntheses of materials for use in OLEDs and similar devices. In terms of the practical procedure, this often entails heating acid chlorides and tetrazoles with a base such as pyridine or using the desired anhydride as the reaction solvent.[176,244-254] In these cases the temperature almost always exceeds 100 °C in order to extrude nitrogen from the *N*-acyl tetrazole intermediate **2-52**.

An advantage of this process, which sets it aside from the other methodologies, is that there is no requirement for additional reagents, such as oxidants or dehydrating reagents, to facilitate the cyclisation. This is beneficial as two separate molecules can be combined *in situ* to form the desired heterocycle without the prior synthesis of bespoke intermediates which may be unstable or incompetent cyclisation precursors. As such, this may allow the efficient synthesis of analogues without an initial combination reaction. The approach with acid chlorides is shown in Scheme 100 below with selected examples.

Not only does this approach reduce the complexity of the reaction set-up, there are also environmental and safety benefits as highly corrosive and toxic reagents such as $POCl_3$ are not required, as with other methods. On the other hand, the high temperatures may alleviate some of this benefit. Furthermore, the release of HCl and the corrosive nature of acid chlorides may cause issues with the implementation of this method on scale.

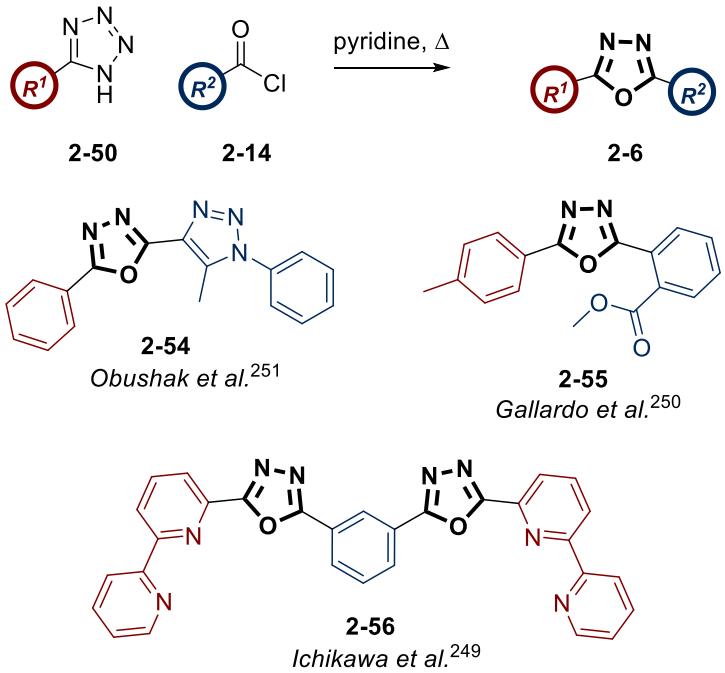

Scheme 100. Huisgen synthesis of oxadiazoles from 5-substituted tetrazoles **2-50** and acid chlorides **2-14** with some literature examples highlighted.

Despite the advantages mentioned above, there is a caveat to this method in that the required tetrazole starting materials may require assembly. Even with the commercial availability of some tetrazoles, more structurally diverse systems require synthesis, with the tetrazole moiety installed from the corresponding nitrile precursor in a [3+2] cycloaddition with sodium azide (Scheme 101a).[247,250-254] While this preparation is the most common approach to tetrazole moieties, it does not come without associated risks. Most notably, sodium azide is known to be explosive, making it undesirable for the large-scale preparation of tetrazoles. Furthermore, there are several associated hazards to health which can be found in the safety data sheet. Finally, on contact with water, hydrazoic acid can form which is only slightly less toxic than hydrogen cyanide.[255] To overcome some of these disadvantages reagents, such as trimethylsilyl azide ($TMSN_3$), have been introduced to give several variations on this approach (Scheme 101a).[256] In addition, flow systems have been introduced to the remove the necessity of handling the dangerous azide reagents, improving the safety of this method and giving high yields for a number of 5-substituted tetrazoles.[257]

Oximes can also be used as precursors, replacing the nitrile group in traditional syntheses; however, azides are still required (Scheme 101b).[258] Finally, within our laboratories a novel azide-free Suzuki-hydrogenolysis protocol has been developed which allows the synthesis of a number of 5-substituted tetrazoles from 1-benzyl-5-bromotetrazole (Scheme 101c).[259]

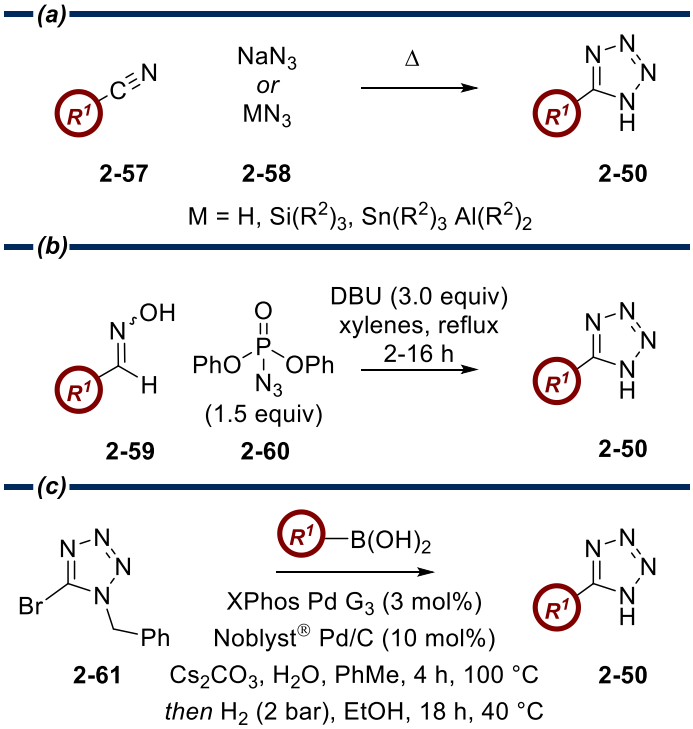

Scheme 101. ***(a)*** The synthesis of 5-substituted tetrazoles **2-50** from a nitrile **2-57** and sodium azide or azide derivative **2-58** in a [3+2] cycloaddition. ***(b)*** The synthesis of 5-substituted tetrazoles **2-50** from oximes **2-59** and diphenyl phosphoryl azide (DPPA) **2-60**. ***(c)*** The novel synthesis of 5-substituted tetrazoles **2-50** from 1-benzyl-5-bromotetrazole **2-61** in a Suzuki-hydrogenolysis protocol developed in our laboratories.

Streamlining the Huisgen approach by activating carboxylic acids as the corresponding acid chlorides in a 'one-pot' procedure is one way in which the Huisgen reaction has been adapted to facilitate more complex structures; however, this often involves the use of toxic reagents such as thionyl chloride[260-262] or oxalyl chloride.[263,264] The principal difference between this and the previous approach is the lack of purification of the resulting acid chloride, which is often isolated by removal of the excess chlorinating agent under reduced pressure. Examples of this are highlighted in Scheme 102.

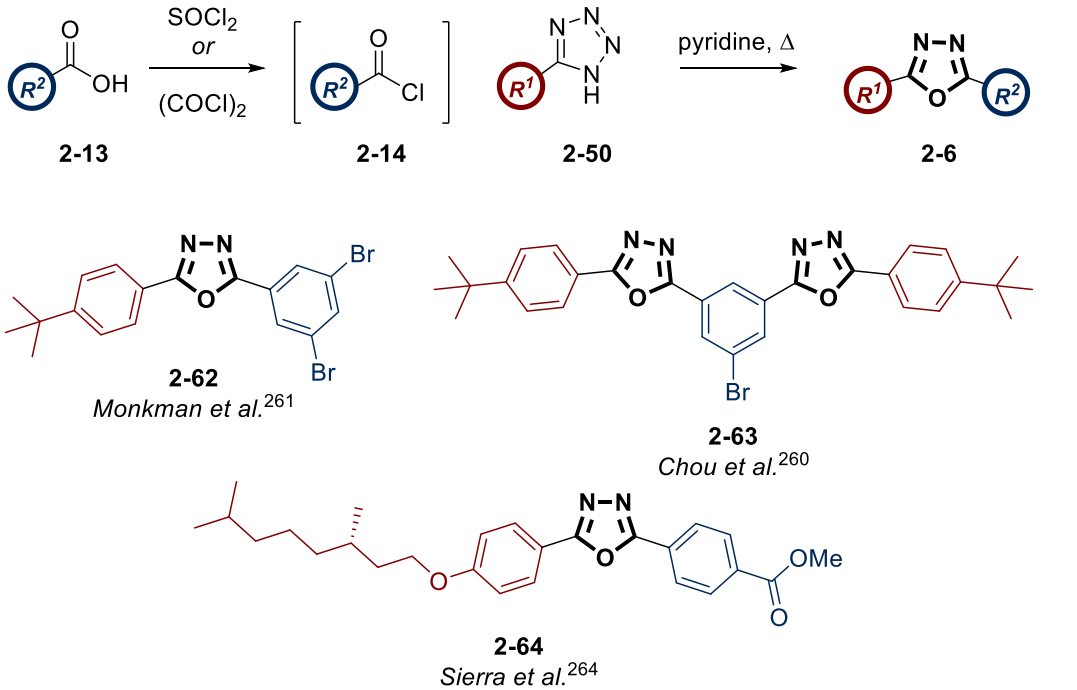

Scheme 102. *In situ* formation of acid chloride **2-14** from the corresponding carboxylic acid **2-13** using thionyl chloride or oxalyl chloride to enable the Huisgen reaction to give 1,3,4-oxadiazoles **2-6**. Also shown are literature examples synthesised using this method.

While the substrate scope when using these modifications appears broad, the use or formation of acid chlorides is necessary for the reaction to proceed. By using carboxylic acids without further functionalisation, a step would be removed, providing additional advantages. Furthermore, carboxylic acids are more ubiquitous and less hazardous than their acid chloride counterparts.

The first example of using carboxylic acids was reported in 1980 by Považanec *et al*. in which the acid could be activated with dicyclohexylcarbodiimide (DCC), enabling the formation of the *N*-acyl tetrazole intermediate **2-52**.[265] Heating to 120 °C allowed access to a wide variety of unsymmetrical 2,5-disubstituted-1,3,4-oxadiazoles. Adoption of this approach has been somewhat limited when compared to the use of acid chlorides. Nevertheless, examples exist and, as with most of the Huisgen reactions, are predominantly found in the materials chemistry literature (Scheme 103).[266-275]

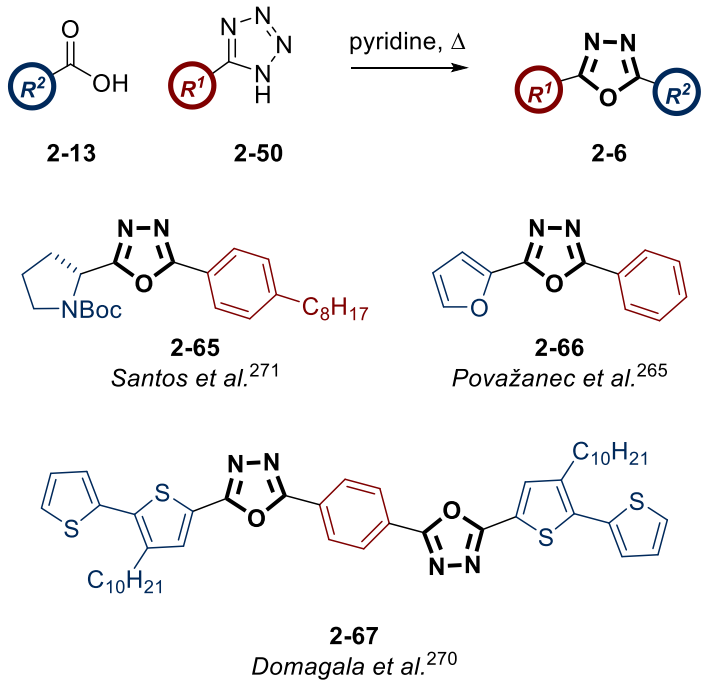

Scheme 103. Formation of 2,5-disubstituted-1,3,4-oxadiazoles **2-6** from carboxylic acids **2-13** and 5-substituted tetrazoles **2-50** by activation with DCC.

Diisopropylcarbodiimide (DIC) is the only other activating reagent reported in the literature for the formation of 1,3,4-oxadiazoles **2-6**, and only one example was noted.[276] At the time of writing, no evidence for examination of alternative amide coupling reagents could be found in the literature. Therefore, this underexplored area may generate useful data to determine if this is possible. Furthermore, there have been no reports in which anything other than thermal energy has been used to form nitrile imine **2-53**. Therefore, a further exploration into whether photochemical methods could be applied to this reaction are arguably required in an attempt to modernise this reaction.

13.3. Use of Light to Form Nitrile Imines

In the mechanism of the Huisgen reaction, the key intermediate is the nitrile imine **2-53** (Scheme 99) which undergoes intramolecular cyclisation. The loss of nitrogen from *N*-acyl tetrazole **2-52** to give this intermediate requires a significant amount of thermal energy, as highlighted by the high temperatures necessary to facilitate the transformation (*vide supra*). An alternative, and more energy efficient, approach may be to use light in order to extrude nitrogen from the tetrazole ring and form the desired nitrile imine. While this has not been utilised for the Huisgen synthesis of 1,3,4-oxadiazoles, it has been known to be an effective method for extruding nitrogen from 2,5-diaryl tetrazoles, as first reported in 1967.[277] Subsequently it was found that the quantum yield for this reaction with various 2,5-diaryl tetrazoles was relatively high, with values in the region of 0.5-0.9.[278] Given this efficiency,

the photolysis of 2,5-diaryl tetrazoles has since been implemented in a number of 1,3-dipolar cycloadditions. While initial publications used broad spectrum mercury lamps, the first example with a narrow band lamp using 302 nm light was in the synthesis of pyrazolines reported by Lin *et al.* (Scheme 104).[279]

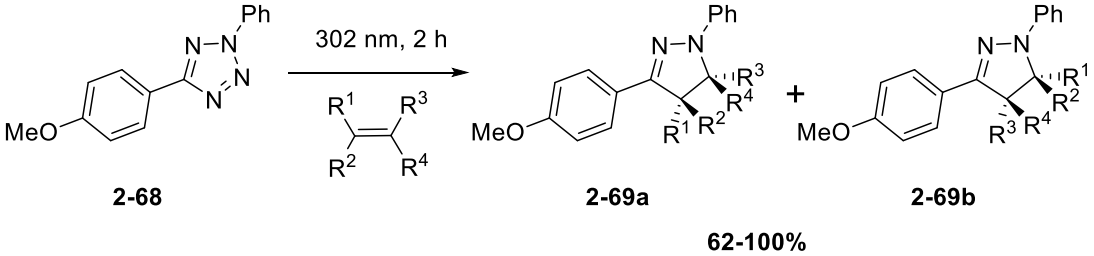

Scheme 104. The synthesis of pyrazolines **2-69a** and **2-69b** from nitrile imines formed *via* photochemical activation of 2,5-diaryl tetrazoles **2-68** using a narrow band UV lamp.

Since this report, narrow band photolysis and subsequent reaction of the nitrile imine intermediate has found several uses in both the synthesis of complex molecules and bioorthogonal chemistry.[280-283] The use of light with a more narrow emission spectrum improves the utility of this approach and allows for a broader substrate scope.[279]

Within our laboratories, nitrile imines and their use in synthesis have been a key area of research for a number of years. This has culminated in two recent publications which highlight the synthetic utility of nitrile imines in the metal-free synthesis of carbon-carbon bonds.[284,285] One of these reports focuses on the photoactivation of 2,5-diaryl tetrazoles as a way of accessing nitrile imines in order to undergo the desired synthetic transformation (Scheme 105).[285]

Given this result and knowledge within our laboratories, expanding this process to the synthesis of 1,3,4-oxadiazoles was expected to be possible with irradiation in the range reported for various 2,5-diaryl tetrazoles (250-365 nm).[260,281,286,287] The presence of the conjugated carbonyl group in the 2-position of the *N*-acyl tetrazole intermediate **2-52** was anticipated to have a similar conjugative effect as that of an aromatic ring and, therefore, the maximum absorbance should remain a similar value. This application of photochemistry as a modern and scalable approach to the Huisgen synthesis of 1,3,4-oxadiazoles will be explored in the subsequent sections of this chapter.

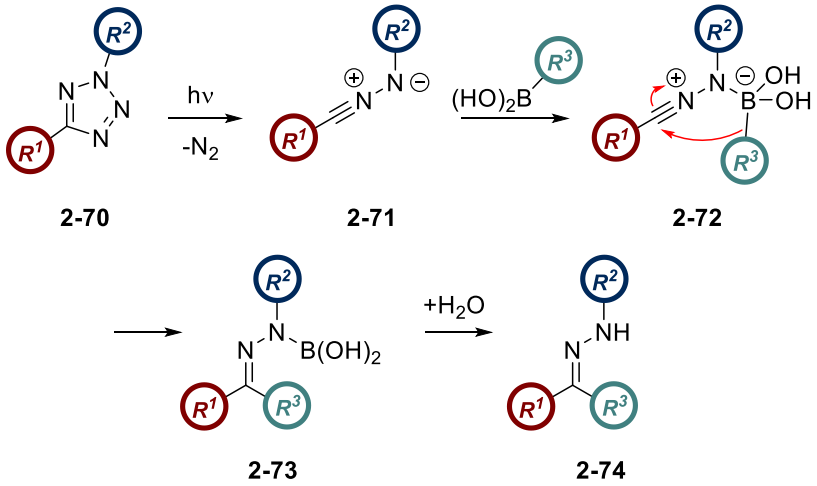

Scheme 105. Metal-free synthesis of carbon-carbon bonds starting with a 2,5-diaryl tetrazoles **2-70** as a precursor to the reactive nitrile imine intermediate **2-71** obtained by photolysis with a UV lamp.

14. Aims

The desired outcome of this study was to identify conditions in which *N*-acyl tetrazole **2-52** could be formed *in situ* from carboxylic acids **2-13** and 5-substituted tetrazoles **2-50**. Photochemical activation of the intermediate could then be used to initiate formation of the active nitrile imine **2-53**, allowing subsequent cyclisation to the desired 1,3,4-oxadiazole **2-6**. Implementation of a simple flow set-up was also planned in order to maximise the light-uptake of the reaction, with the intention of improving the yield when compared to batch reactions.[285] This concept is well-reported in the literature and was expected to be applicable to the intended system.

The use of alternative amide coupling agents for formation of *N*-acyl tetrazole **2-52** could also be explored to determine whether there are viable alternatives to the published examples of DCC or DIC. No optimisation of this kind has previously been reported and an answer to this question is desirable given that the formation of the often insoluble urea by-products can be troublesome,[288] especially in flow. Furthermore, the substrate scope could be investigated to allow identification of any advantages or limitations of this methodology. Photochemical activation, previously unreported for this reaction, may have some intrinsic differences when compared to thermal activation and these could be examined from the substrate scope, if necessary.

15. Results and Discussion

15.1. Initial Photochemical Experiments

The photochemical degradation of 2,5-diaryl tetrazoles **2-70** to nitrile imine intermediates **2-71** is well precedented in the literature and, specifically, within our laboratory.[285] It was not known whether this methodology could be applied in the same way to the Huisgen reaction to form reactive nitrile imines **2-52** from *N*-acyl tetrazoles **2-53** (Scheme 106).

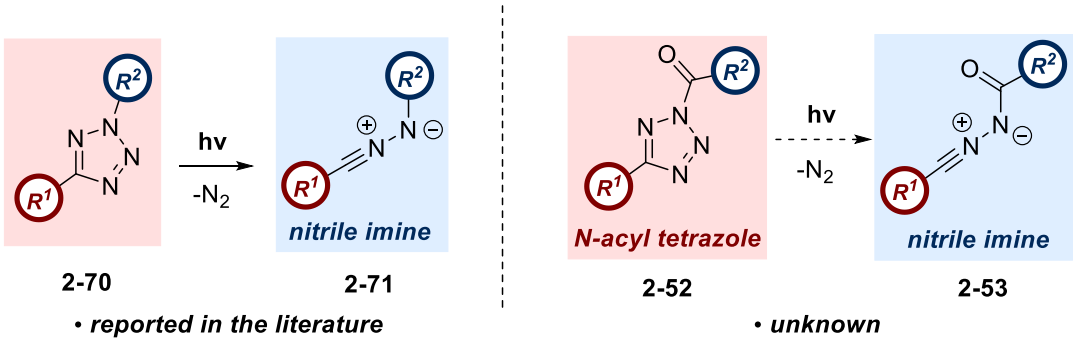

Scheme 106. The reported photochemical degradation of 2,5-diaryl tetrazoles **2-70** to form nitrile imines **2-71** and the unreported photochemical degradation of *N*-acyl tetrazoles **2-52** to form nitrile imines **2-53**.

In order to explore the possibility of a photo-induced Huisgen synthesis of oxadiazoles **2-6**, two control reactions were carried out by another member of our laboratory (Scheme 107).[289] A mixture of 5-phenyl-1*H*-tetrazole **2-75** and 4-methoxybenzoyl chloride **2-76** in toluene and pyridine was heated to 100 °C while a separate reaction was irradiated with a Philips PL-S 9W/12 UV-B lamp. These reactions allowed a direct comparison of the two approaches and showed that, in our hands, the photochemical approach was more efficient, giving a yield 14% higher than the thermal counterpart. From these results, it was rationalised that photochemical initiation of the Huisgen reaction was possible; specifically, with a UV-B lamp with wavelength of 290-315 nm.

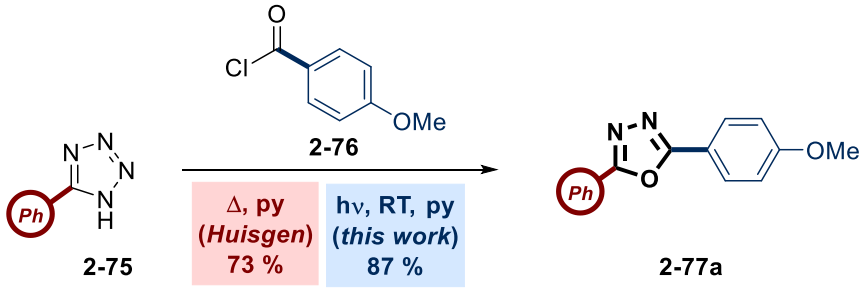

Scheme 107. The thermal and photochemical reactions of 5-phenyl-1*H*-tetrazole **2-75** and 4-methoxybenzoyl chloride **2-76** in toluene and pyridine to give 2-(4-methoxyphenyl)-5-phenyl-1,3,4-oxadiazole **2-77a**.

A UV/Vis emission spectrum of the lamp used was taken to determine the precise wavelength emitted and confirm that degradation of the *N*-acyl tetrazole **2-52** occurred due to irradiation in the expected region of 250-365 nm (Figure 64).[260,281,286,287] As can be seen, a broad emission occurs in the region of 280-360 nm with a more intense spike at approximately 310

nm. Additional peaks are also observed in the near UV and visible regions at 360, 400, 435, 540 and 580 nm, which could be due to background visible light; however, it is not uncommon for these lamps to emit outside their reported range.[290,291]

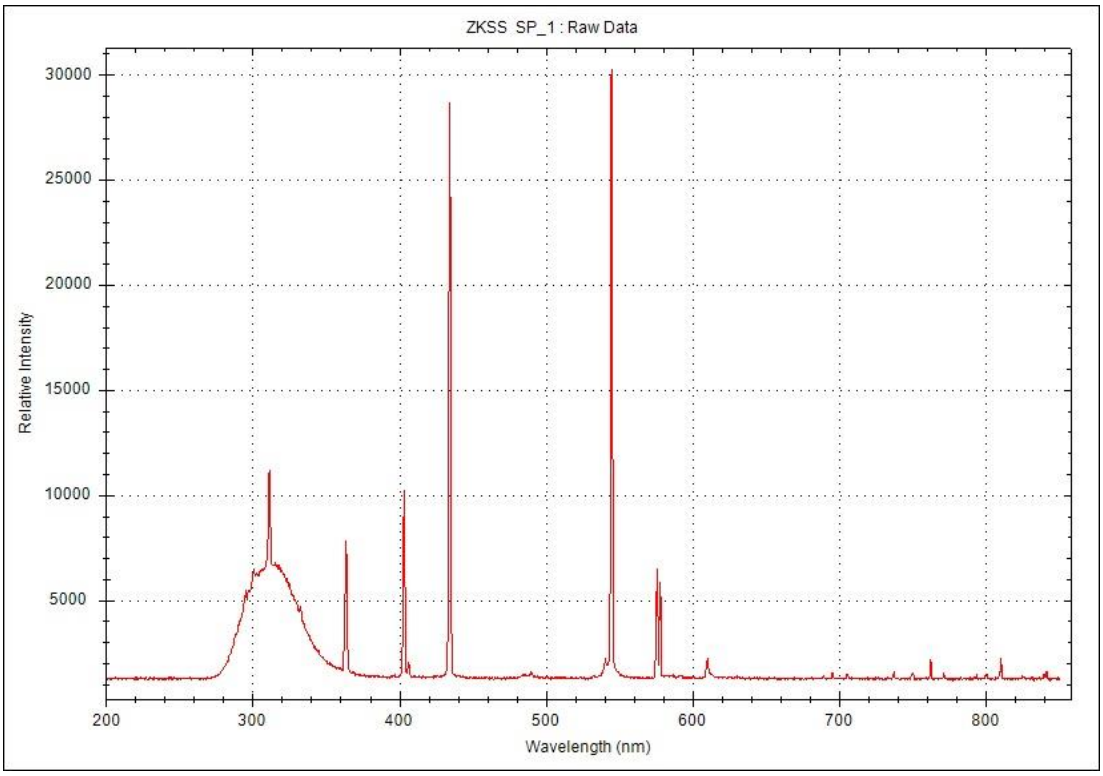

Figure 64. The emission spectrum of the Philips PL-S 9W/12 UV-B lamp used in the photochemical degradation of *N*-acyl tetrazole **2-52**.

The use of UV-B light, while clearly effective in this reaction, has associated safety issues which must be considered. UV-B is the most harmful of the UV rays, penetrating the skin, causing burns and, eventually, cancer.[292] As such, safety precautions must be taken in order to minimise exposure when working with UV-B light. Throughout this study, the necessary safety precautions were taken, allowing safe work with the lamp minimal exposure to the resulting light.

15.2. Introduction of Carboxylic Acids and Coupling Conditions

Conducting the Huisgen reaction under photochemical conditions with 4-methoxybenzoyl chloride **2-76** and obtaining a higher yield than the thermal counterpart fulfilled one of the original aims of this project. To further this methodology and improve its accessibility, replacement of acid chlorides with carboxylic acids was desirable. Alleviating the *in situ* formation of HCl and reducing the corrosive nature of the reaction mixture was one of the major advantages anticipated from this change. In addition, carboxylic acids are relatively

benign with increased molecular diversity available from commercial materials when compared to acid chlorides.

To facilitate the formation of *N*-acyl tetrazole **2-52** from a carboxylic acid **2-13** and 5-substituted tetrazole **2-50** it was necessary to introduce a coupling agent (Scheme 108). While DCC and DIC had been used to facilitate this previously,[266-276] an investigation into the use of other coupling agents has not been reported in the literature.

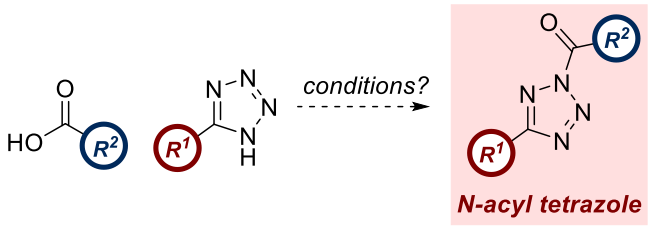

2-13 **2-50** **2-52**

Scheme 108. General scheme for formation of *N*-acyl tetrazole **2-52** from a carboxylic acid **2-13** and 5-substituted tetrazole **2-50**.

To explore this proposed transformation and examine various coupling reagents, the reaction between 4-methoxycarboxylic acid **2-78** and 5-phenyl-1*H*-tetrazole **2-75** was carried out. Several common amide coupling reagents were investigated, and the results are summarised in Table 29. DCM was found to be the optimal solvent for solubility of the starting materials with 5-phenyl-1*H*-tetrazole **2-75** appearing particularly insoluble in other solvents.

The amide coupling reagents were selected to cover the three main families; carbodiimides, phosphonium- and uronium-containing agents. Of those used, only carbodiimides DCC and DIC afforded any significant conversion (Table 29, entries 7 and 8). All the other reagents showed very little, if any, reactivity.

Table 29. Photochemical Huisgen reaction between 5-phenyl-1*H*-tetrazole **2-75** and 4-methoxybenzoic acid **2-78** with various amide coupling reagents.

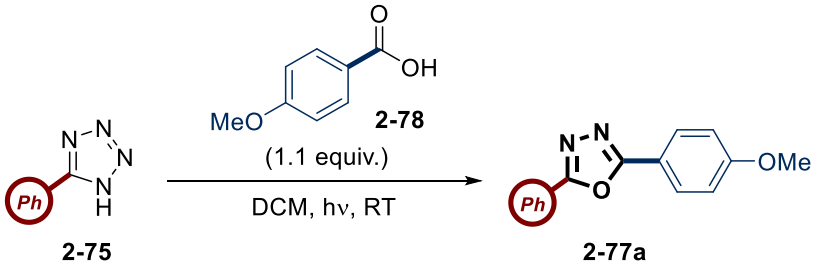

2-75 **2-77a**

Entry	Coupling Reagent	Solvent	Time (h)	Yield (%)
1[a][b]	HATU/DIPEA	DCM	8	N.R.
2[a][c]	HATU/DIPEA	DMF	21	N.R.
3[a]	PyBOP®/DIPEA	DCM	6	N.R.
4[a][d]	PyBrOP®/DIPEA	DCM	19	N.R.
5[e]	EDCI/DMAP	DCM	19	4
6[e][f]	CDI/DMAP	DCM	19	N.R.
7[g]	DCC	DCM	19	51
8	DIC	DCM	23	50
9[h]	DCC/DMAP	DCM	5	55
10[i]	DCC/HOAt	DCM	19	N.R.
11	DCC/Oxyma	DCM	19	8
12	DCC/HOBt	DCM	19	N.R.

Reactions carried out in quartz round-bottom flasks in front of a UV-B lamp with 1.1 equiv. of carboxylic acid, 1.1 equiv. of coupling reagent at a concentration of 0.12 M with respect to the tetrazole. [a] 3.0 equiv. DIPEA. [b] 1.0 equiv. HATU. [c] 1.25 equiv. HATU. [d] 1.2 equiv. PyBrOP®. [e] 1.5 equiv. DMAP. [f] irradiated for 6.5 h in presence of CDI before addition of DMAP and further irradiation for 12.5 h. [g] 1.27 equiv. carboxylic acid. [h] 0.1 equiv. DMAP. [i] 1.23 equiv. carboxylic acid.

If the mechanism of activation of the carboxylic acid is considered, the active ester which would be theoretically displaced by the tetrazole nucleophile would be the 1-hydroxy-7-azabenzotriazole (HOAt) ester **2-79** for entries 1, 2 and 10. Therefore, an equilibrium can be thought to exist between these two species as shown below in Scheme 109.

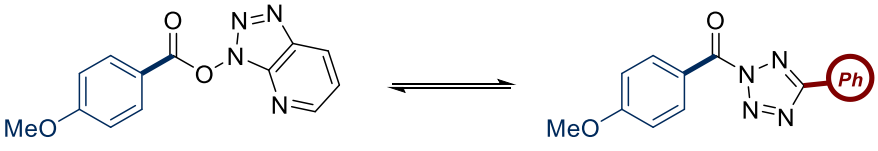

2-79 **2-80**

Scheme 109. Theoretical equilibrium between active HOAt ester **2-79** and *N*-acyl tetrazole **2-80**.

In order to form *N*-acyl tetrazole **2-80** and, subsequently, the corresponding nitrile imine, the HOAt active ester must be displaced by 5-phenyl-1*H*-tetrazole **2-75**. Clearly, as no reaction occurred in these experiments, this did not happen. Given that the pK_a values of HOAt and

5-phenyl-1*H*-tetrazole are 3.38[293] and 4.53,[294] respectively, it would be expected that both would be anionic in entries 1 and 2 in the presence of *N*,*N*-diisopropylethylamine (DIPEA; 3.0 equiv.). Furthermore, the more stable HOAt anion would appear to be a better leaving group based on this data. The lack of reaction does not support this hypothesis and therefore it is likely that the tetrazole anion is less nucleophilic than the HOAt anion. The reduced nucleophilicity is likely due to mesomeric stabilisation of the anion in the aromatic system, as shown below (Scheme 110).

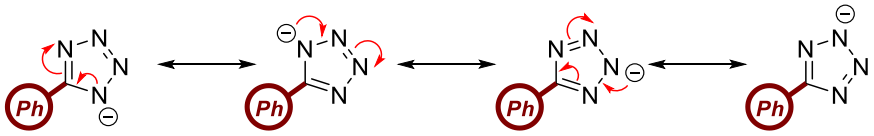

Scheme 110. Resonance of the 5-phenyl tetrazole anion onto each of the nitrogen atoms in the aromatic system providing stability and reducing the relative nucleophilicity.

Further highlighting the reluctance of the 5-phenyl-1*H*-tetrazole **2-75** to displace to HOAt ester is the isolation of active ester **2-79**, with NMR data consistent with the structure. This was obtained from the reaction with DCC and HOAt as the coupling reagents (entry 10) and shows the superior nucleophilicity of HOAt.

Additional evidence for this hypothesis can be found when looking at entries 3, 11 and 12. The use of (benzotriazol-1-yloxy)tripyrrolidinophosphonium hexafluorophosphate (PyBOP®) and 1-hydroxybenzotriazole (HOBt) would both result in the same active ester (**2-81**, Scheme 111) prior to displacement by 5-phenyl-1*H*-tetrazole. With the lack of product formed in these reactions, this displacement does not occur, and the ^{1}H NMR spectra of the crude reaction mixtures possess identical peaks, interpreted as active ester **2-81**. These were not isolated, but the spectral data provides some evidence towards this hypothesis.

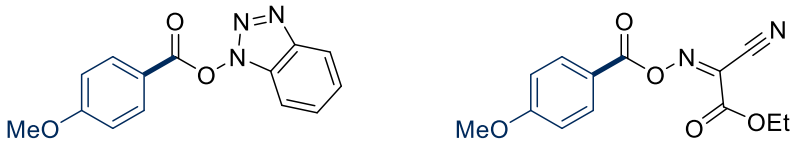

2-81 **2-82**

Scheme 111. The active esters of PyBOP® and HOBt **2-81** and oxyma **2-82**.

With Oxyma, the structure of the active ester formed in the reaction would be that of **2-82** (Scheme 111). It can be seen from Table 29 entry 11 that an 8% yield was obtained for this reaction, suggesting that 5-phenyl-1*H*-tetrazole **2-75** is a slightly more competitive nucleophile in this reaction. Considering the pK_a of Oxyma is 4.60,[295] it would be expected to be in competition with the tetrazole (pK_a 4.53).[294] This argument does not account for the low yield obtained; however, the result could be explained by relative nucleophilicity. The oxyma anion can delocalise the negative charge into both the carbonyl and cyano groups on

the molecule. The added stability allows displacement with 5-phenyl-1*H*-tetrazole **2-75** to be more favourable relative to the displacement of HOBt or HOAt anions.

Consideration of the relative stabilities of the active *esters* versus the *N*-acyl tetrazole *amide* moiety is also necessary. It is generally observed that amides exhibit a greater relative stability than esters due to donation of the nitrogen lone-pair into the π-system of the carbonyl bond. This can be attributed to the higher electronegativity value for oxygen in comparison to nitrogen.[296] Therefore, it would be expected that the *N*-acyl tetrazole would form the thermodynamically more stable carbonyl compounds; however, donation of the nitrogen lone-pair may be disrupted in the *N*-acyl tetrazole intermediate for two reasons. Firstly, there is competition for the nitrogen lone pair which will be delocalised between the tetrazole aromatic π-system as well as into the carbonyl bond, thus reducing the strength of the amide bond. Furthermore, the conformation of the two systems may also affect the relative stability. *N*-Acyl tetrazole **2-80** has a rigid structure around the tetrazole moiety which may cause the molecule to adopt a more twisted conformation to avoid steric clashes, thus decreasing the orbital overlap of the system and reducing the relative stability. In active esters **2-79** and **2-81**, the benzotriazole systems are attached to the ester moiety through a single bond, allowing rotation. As such, the ester resonance will be unaffected by the conformation of this group, contributing to a more stabilised system relative to the *N*-acyl tetrazole. Figure 65 shows the structures of active ester **2-79** and *N*-acyl tetrazole **2-80** after standard energy minimisation using MOE 2019.01.[297] It is observed that, as expected, the ester group of **2-79** is in one plane with the benzotriazole twisted and that the amide moiety of the *N*-acyl tetrazole **2-80** is slightly skewed from planarity, which may affect the relative stability.

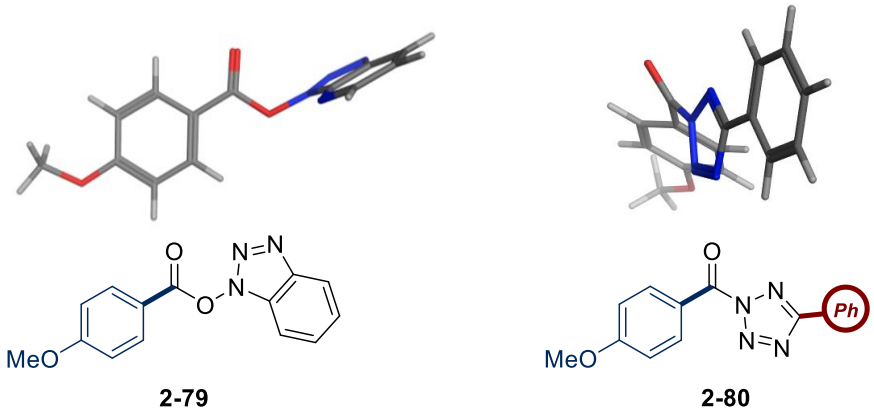

2-79 **2-80**

Figure 65. Energy minimised structures of active ester **2-79** and N-acyl tetrazole **2-80**.

The use of bromotripyrrolidinophosphonium hexafluorophosphate (PyBrOP®) and CDI (Table 29, entries 4 and 6) gave no product, with the respective NMR spectra of the crude mixtures providing no evidence for the presence of the active ester, or bromide in the case of

PyBrOP®. This may be due to instability or decomposition of the intermediates, thus explaining the lack of product. The use of EDCI (Table 29, entry 5) gave a small amount of product but no spectral evidence for the active ester could be found.

DCC and DIC both gave equally respectable yields without additional additives (Table 29, entries 7 and 8). To account for this observation, it is likely that the formation of the insoluble urea by-products drives the irreversible reaction upon displacement with 5-phenyl-1*H*-tetrazole **2-75**. Without additives such as HOBt or HOAt, there is no competition for nucleophilic attack of the tetrazole and therefore the *N*-acyl tetrazole **2-52** can readily form; driven by the urea formation and subsequent formation and cyclisation of the nitrile imine to the aromatic 1,3,4-oxadiazole product. The addition of a catalytic amount of 4-(dimethylamino)pyridine (DMAP) to the reaction increased the rate of reaction and improved the yield slightly; however, the improvement was not so significant as to warrant these conditions optimal.

Confirmation that DCC and DIC were the most efficient reagents for this transformation was obtained upon scaling the reactions from 50 mg to 200 mg of 5-phenyl-1*H*-tetrazole **2-75**. The oxadiazole product was isolated in 50% yield from both reactions, indicating equal efficiency for both. The two reactions differed in the solubility of the urea by-products which was an important consideration with the aim of putting this reaction into a flow system. As can be noted in Figure 66, an appreciable difference in precipitate is observed between the two reactions on a 200 mg scale, with DIC producing the more soluble diisopropylurea.[288] Therefore, DIC was chosen as the coupling agent to take forward into a flow system.

Figure 66. Photograph of the two larger-scale reactions between 5-phenyl-1*H*-tetrazole **2-75** and 4-methoxybenzoic acid **2-78**. The flask on the left-hand side contains DIC as the coupling reagent and the flask on the right-hand side contains DCC. A difference in the amount of precipitate present can be seen with the diisopropylurea by-product being more soluble in organic solvent.

15.3. Implementation of Flow

Photochemistry in flow has been shown to improve the outcome of reactions within our laboratory, specifically when forming nitrile imines.[285] In addition, it is well-known that by reducing the optical path to the reaction vessel, the absorbance can increase, providing more efficient irradiation of the reaction mixture.[298] With this in mind, it was anticipated that by introducing the optimal batch conditions into a flow system, the yield should be improved.

To enable this methodology to be as widely accessible and practical as possible, the flow system was designed to be simple and readily assembled. The photoreactor was analogous to that reported by Booker-Milburn and Berry,[299] consisting of PTFE tubing wrapped around a quartz chamber placed over the UV-B lamp. A peristaltic pump was used to enable the reaction mixture to circulate through the system from a round-bottom flask, as shown in Figure 68, below.

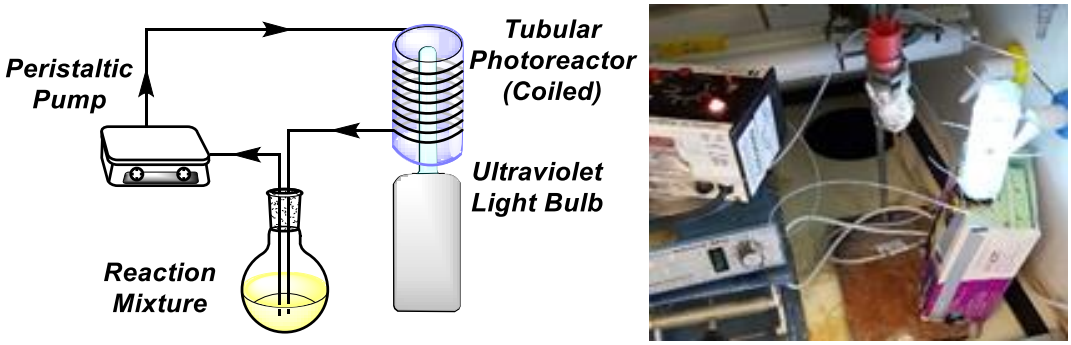

Figure 67. A schematic diagram of the flow apparatus alongside a photograph of the system used.

To prevent the occurrence of blockages due to the diisopropylurea by-product (**2-86**, Scheme 113), the concentration of the reaction was reduced from 0.12 M (in the batch reactions) to 0.04 M. By solubilising the reaction mixture and preventing precipitate formation, the UV light could penetrate the reaction mixture, unhindered by solid. Despite the 3-fold dilution, precipitate was still observed on the first run. Therefore, the solvent system required adjustment to enable complete dilution and a 9:1 DCM/DMF mixture was tested, with DMF expected to efficiently solubilise diisopropylurea. Pleasingly, there were no issues with this system and the reaction mixture was pumped around the system for 1 hour. The results of this are summarised below in Scheme 112.

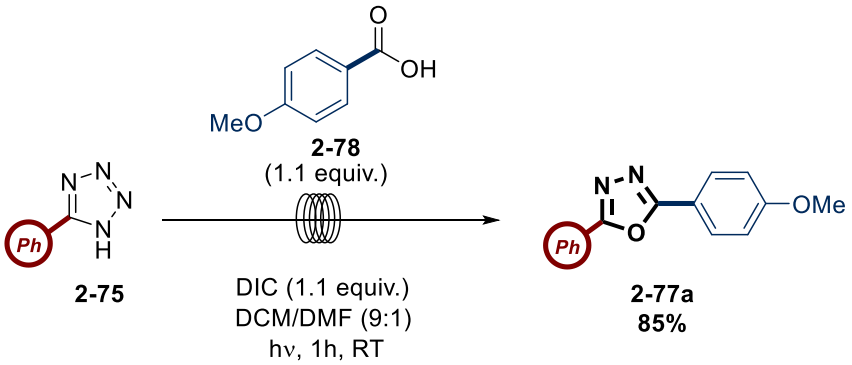

Scheme 112. Optimised flow conditions for the photochemical Huisgen reaction between 5-phenyl-1*H*-tetrazole **2-75** and 4-methoxybenzoic acid **2-78**. 1.1 equiv. of DIC was used and the reaction mixture was at a concentration of 0.04 M with respect to the tetrazole. 1,3,4-oxadiazole **2-77a** was formed in 85% yield.

As predicted, more efficient irradiation of the reaction mixture, in addition to the absence of precipitate, led to an improved yield of 85%. With this result in hand, two control experiments were undertaken; one without DIC and one without UV-B irradiation. As expected, no reaction occurred in the absence of DIC. In the absence of light, a very small amount of impure product was obtained (4% yield) with predominantly starting materials remaining. These results confirmed that both light and the activating agent are essential for a successful reaction. Following this, an investigation into the wavelength of activation and substrate scope was undertaken.

15.4. Wavelength Screen

With optimised conditions in hand, it was necessary to confirm that the outlying peaks on the emission spectrum of the lamp (Figure 64) were not responsible for the degradation of *N*-acyl tetrazole **2-52**. To do this, test reactions were carried out at six visible light wavelengths (365, 385, 405, 420, 450, 525 nm) as well as a control without light. These reactions were carried out in HPLC vials using the Pacer Photochemistry LED Illuminator (PHIL).[165] The LCMS traces of the visible light reactions are shown below in Figure 68 below.

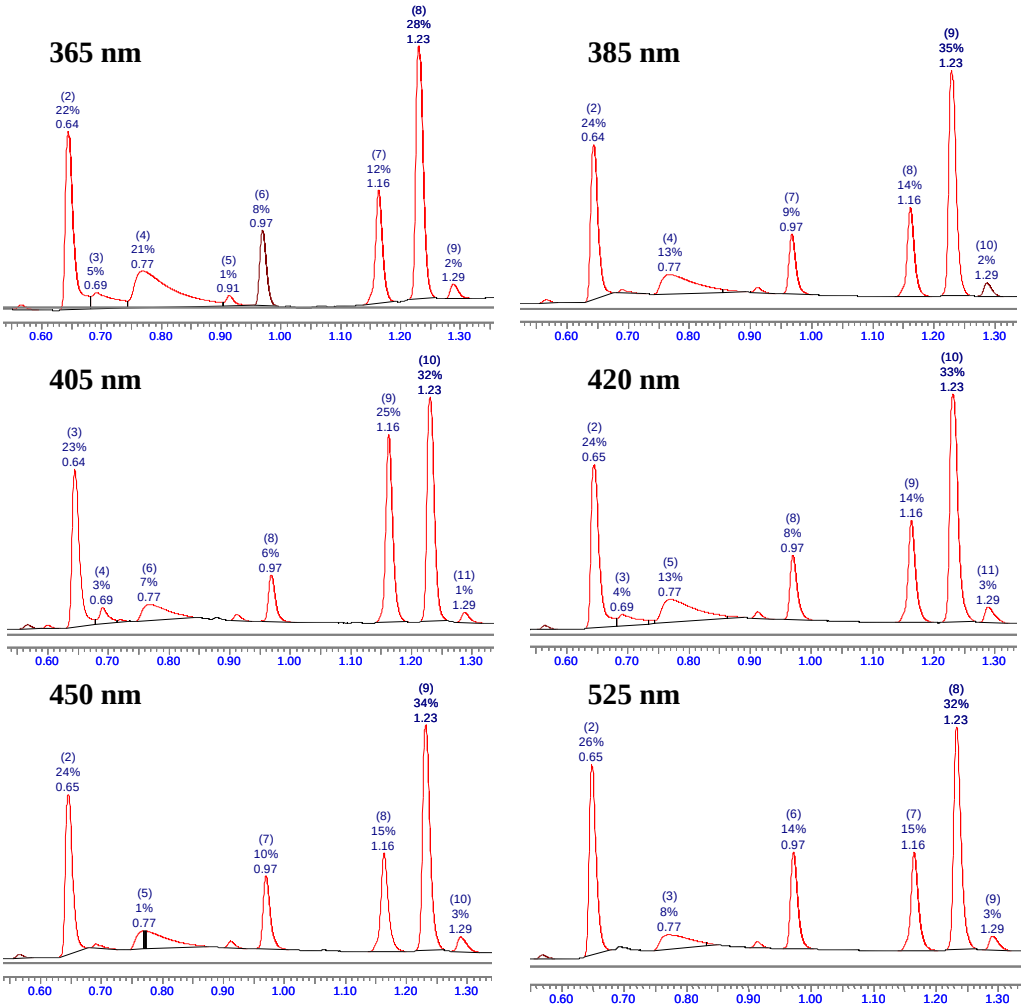

Figure 68. LCMS UV traces for test reactions between 5-phenyl-1*H*-tetrazole **2-75** and 4-methoxybenzoic acid **2-78** at various wavelengths with irradiation for 24 h. Peak identifiers: **0.64/0.65 min** = 5-phenyl-1*H*-tetrazole; **0.77 min** (**br**) = 4-methoxybenzoic acid; **1.16 min** = 2-(4-methoxyphenyl)-5-phenyl-1,3,4-oxadiazole; **1.23 min** = 4-methoxybenzoic anhydride.

In the reaction profiles shown, the 5-phenyl-1*H*-tetrazole **2-75** and 4-methoxybenzoic acid **2-78** starting materials are still present, albeit in differing amounts. It can be inferred, by comparing to the reaction using the optimum wavelength (Figure 69), that the outlying wavelengths do not promote the formation of the 1,3,4-oxadiazole.

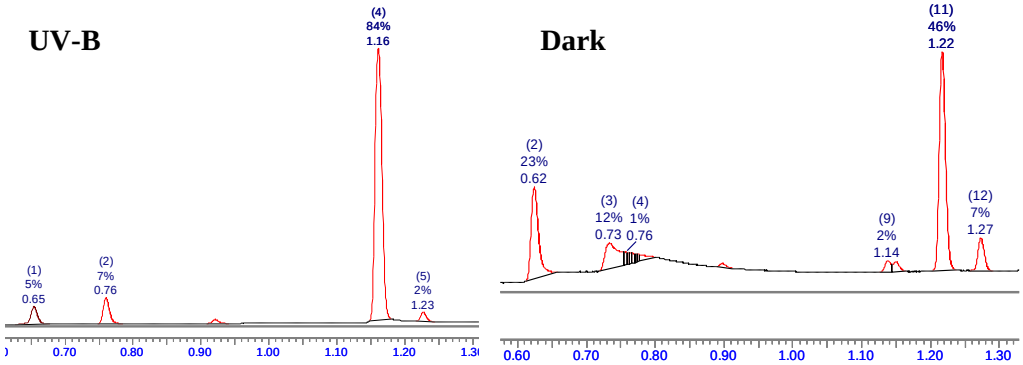

Figure 69. LCMS trace of the reaction between 5-phenyl-1*H*-tetrazole **2-75** and 4-methoxybenzoic acid **2-78** using the optimal UV-B lamp and in the absence of irradiation. Observed is the majority formation of the desired oxadiazole (**1.16 min**) when using the UV-B lamp and mostly acid anhydride in the dark.

It is apparent from the wavelength screen (Figure 68) that a significant amount of 4-methoxybenzoic anhydride **2-85** is formed, as shown in Scheme 113. This results from attack of the carboxylate anion **2-84** onto the *O*-acylisourea intermediate **2-83**; however, it may also be possible that *N*-acyl tetrazole **2-52** is a precursor to the acid anhydride given its relative instability and the leaving group propensity of the tetrazole. This could explain the increased presence of acid anhydride **2-85** when wavelengths other than UV-B are used to irradiate the reaction mixture as very little, if any, nitrile imine **2-53** is formed from the photolysis of *N*-acyl tetrazole **2-52.** Further evidence for this can be taken from the control reaction in the absence of light (Figure 69) wherein the LCMS trace highlights the lack of product in addition to formation of acid anhydride **2-85**.

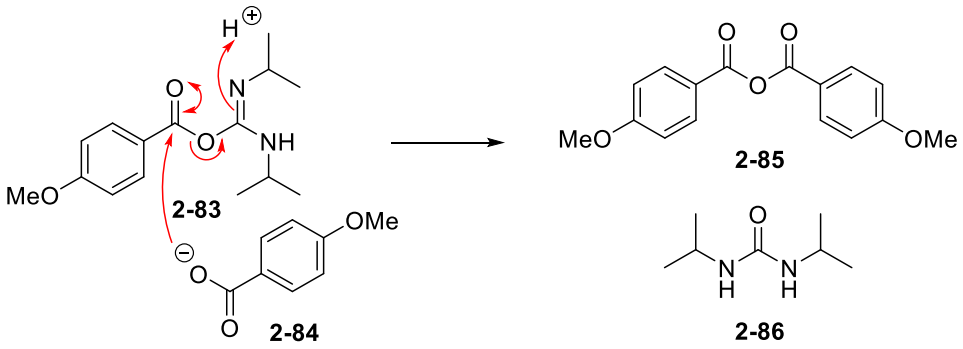

Scheme 113. Mechanism of formation of 4-methoxybenzoic acid anhydride **2-85** from *O*-acylisourea **2-83**.

An additional possibility could be that the acid anhydride is a reactive species, akin to *O*-acylisourea **2-83**. Previous experiments have highlighted the reactivity of acid anhydrides in the Huisgen reaction and,[244,245,247] as such, it is sensible to assume that this species may lead to *N*-acyl tetrazole intermediate **2-80** by way of reaction with the 5-phenyl-1*H*-tetrazole **2-75**. In the absence of the optimum irradiation wavelength, this is not a productive pathway and very little nitrile imine intermediate would be formed, Therefore, the *N*-acyl tetrazole is susceptible to attack by the carboxylate species, re-forming the anhydride.

A summary of the wavelength screen is provided in Table 30 and these experiments provide confirmation that the use of the UV-B lamp was justified, giving superior conversion and reaction profiles compared to visible wavelengths.

Table 30. Table summarising LCMS data of reactions at various wavelengths (shown in Figure 68 and Figure 69). Reaction at 310 nm is that using the UV-B lamp

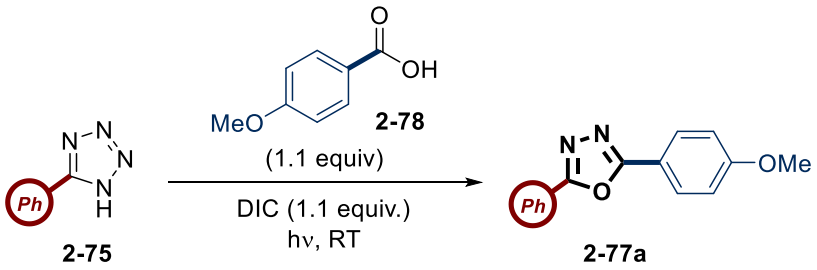

Wavelength (nm)	Peak Area (%)			
	Tetrazole	Acid	Oxadiazole	Anhydride
Dark[a]	23	13	2	46
365[a]	22	21	12	28
385[a]	24	13	14	35
405[a]	23	7	25	32
420[a]	24	13	14	33
450[a]	24	4	15	34
525[a]	26	8	15	32
310[b]	5	7	**84**	2

[a]Reaction run on 0.088 mmol scale of 5-phenyl-1*H*-tetrazole **2-75** with irradiation/in the dark for 24 hours; [b]Reaction run on 0.684 mmol of 5-phenyl-1*H*-tetrazole **2-75** irradiated for 1 hour.

15.5. Carboxylic Acid Scope

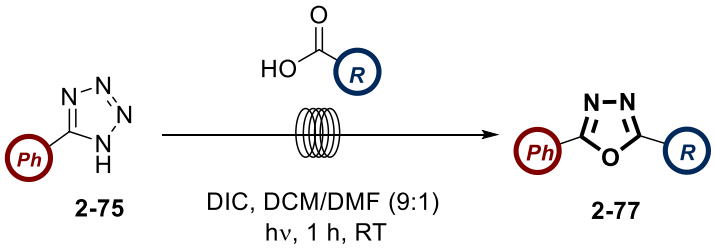

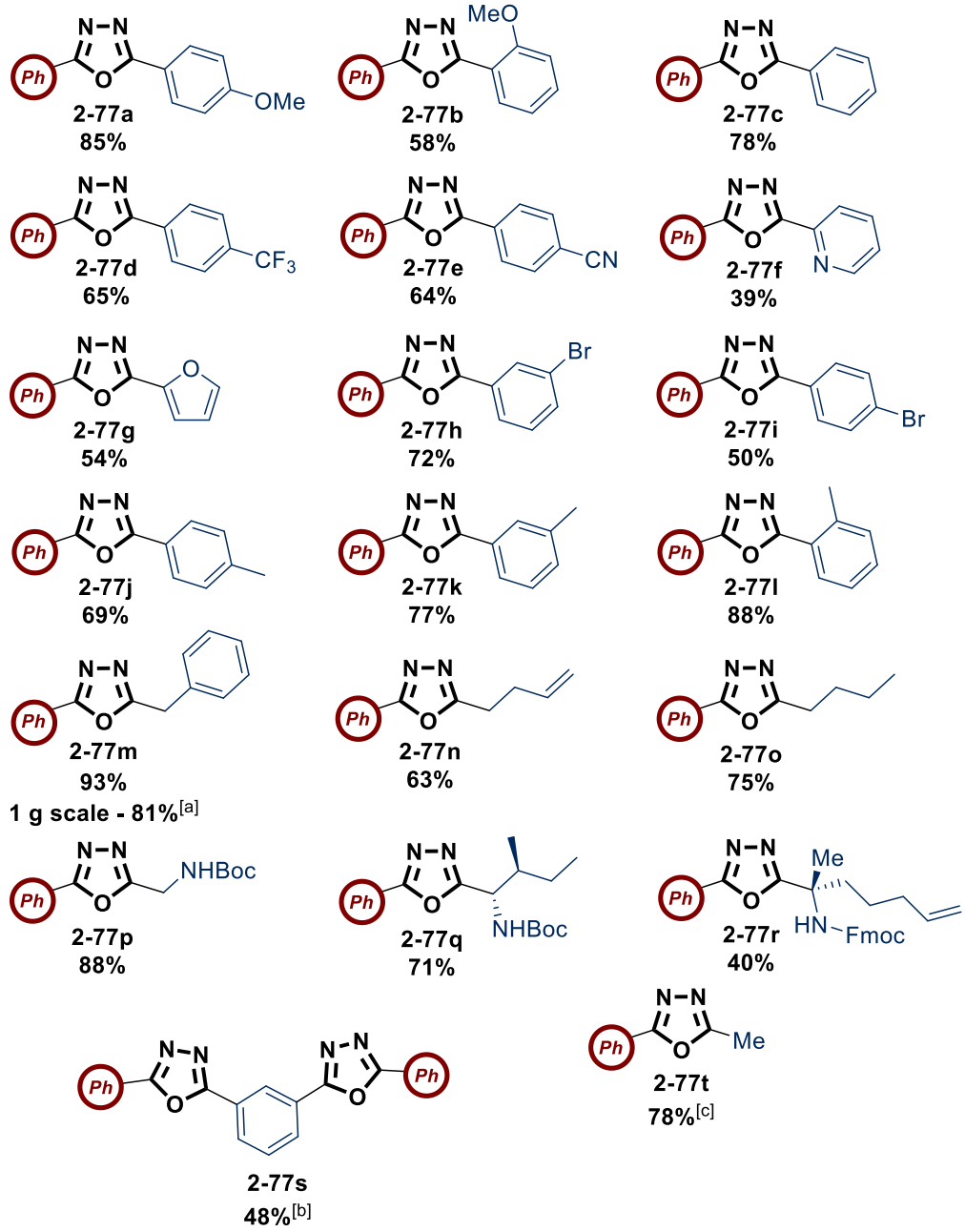

Scheme 114. Reaction of 5-phenyl-1*H*-tetrazole **2-75** (0.342 mmol) with carboxylic acids (1.1 equiv.) and DIC (1.1 equiv.). [a] 4.5 h reaction time. [b] 2 h reaction time, with the acid as the limiting reagent using 2.2 equiv. of 5-phenyl-1*H*-tetrazole **2-75** and DIC. [c] Ac_2O (2.0 equiv. in place of the carboxylic acid) in dimethoxyethane (replacing DCM/DMF).

The use of the optimised conditions led to the exploration of several carboxylic acid derivatives in the reaction. Scheme 114 shows the oxadiazoles successfully prepared with isolated yields of up to 93% obtained for a broad range of substrates, including electron-rich (**2-77a**, **2-77b**), electron-neutral (**2-77c**) and electron-poor aromatic carboxylic acids (**2-77d**, **2-77e**). *Ortho*-, *meta*- and *para*-methyl substituted benzoic acids **2-77j**, **2-77k** and **2-77l** all furnished highly acceptable yields. Surprisingly, the *ortho*-methyl benzoic acid derived product **2-77l** was obtained in the highest yield (88%) with the *para*- derivative showing the lowest yield of the three. These results suggest that increasing the inductive electronic effect towards the carboxylic acid group may improve the reaction outcome. The reason for this is unclear; however, it may be possible that the carboxylate anion becomes more reactive towards the DIC additive. Further evidence for this can be seen from electron-donating groups, such as **2-77a**, being obtained in higher yield than those containing strong electron-withdrawing groups, as in **2-77d** and **2-77e**.

Further consideration of the mechanism of formation of the reactive nitrile imine intermediate **2-52** may also provide a rationale for this observation. In the analogous thermal reaction of diaryl tetrazoles, the formation of the nitrile imine intermediate was found to be dependent on the electronics of the groups at both the carbon and nitrogen termini of the tetrazole ring.[300,301] Specifically, electron-withdrawing substituents on the nitrogen atom were found to increase the rate of formation of nitrogen, and therefore the nitrile imine. As a result, a degree of charge separation was proposed in the diaryl tetrazole as shown below in Figure 70. While this is not an exact structure of the intermediate, it does represent a possible build-up of charge, which is key to the loss of nitrogen in a non-concerted fashion.

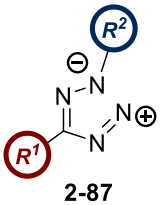

2-87

Figure 70. Hypothetical charge separation for diaryl tetrazoles based on Hammett plots produced by Baldwin *et al*.[297,298]

More recent studies into the photolysis of diaryl tetrazoles have shown that a similar mechanism exists for this method of activation. Initial work by Tomaschewski *et al*. gave further evidence that electron-withdrawing groups increased the quantum yield of the reaction.[278] This was analogous to the aforementioned work by Baldwin for thermolytic activation in which a charge separation between N2 and N3 may be present in the rate-determining step. Building on this study, two papers published by Barner-Kowollik *et al*. elucidated a potential mechanism which is shown below in Figure 71.[302-304] The mechanism

involves excitation of an electron of the diaryl tetrazole to the LUMO in a (π→π*) transition. The resulting singlet undergoes an intersystem crossing to a triplet state, which must be close in energy. Decomposition of the tetrazole occurs *via* a diradical intermediate, as shown below, which occurs in a non-concerted fashion, agreeing with the thermolytic mechanism. A conical intersection, by which two potential energy curves intersect, allows a crossover to the resulting nitrile imine dipole.

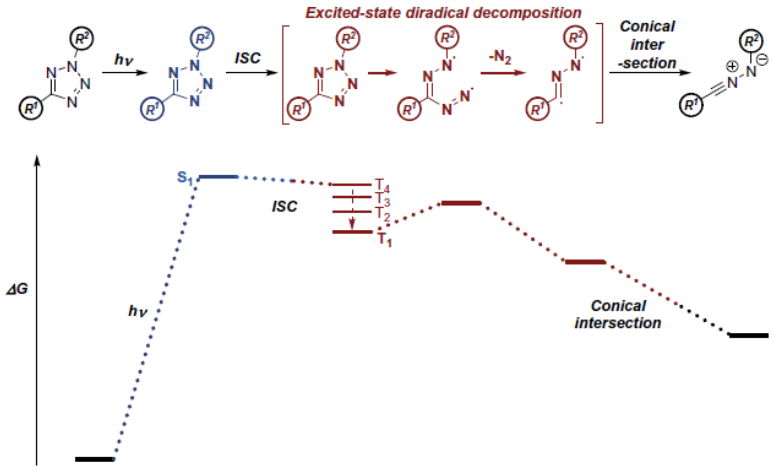

Figure 71. Elucidated mechanism of the photolysis of diaryl tetrazoles. Photolysis excites an electron into the LUMO of the molecule before and intersystem crossing takes place to access the triplet state. From here nitrogen is lost from the diradical species shown before a conical intersection gives access to the nitrile imine dipole. Diagram reproduced with permission from Livingstone and Jamieson.[300]

Extending these approaches to the *N*-acyl tetrazole intermediate **2-52,** it can be seen below in Scheme 115 that the negative charge or radical on the N3 atom could be delocalised into the carbonyl group, thus providing some stability in a similar way to an electron-withdrawing group in the diaryl tetrazole. Withdrawing groups, such as in **2-77d** and **2-77e**, would provide additional stability to this charge separation and lead to a more stable nitrile imine **2-53** while reducing the nucleophilicity of the carbonyl for the subsequent cyclisation. The increased stability and reduced nucleophilicity may correlate with a lower yield if the resulting nitrile imine is sufficiently long-lived to decompose or enable formation of by-products. While there were no obvious by-products isolated from the reactions, these may have formed in such a small amount as to not be noticed on the scale the reaction was conducted. It is possible that decomposition or rearrangement of the nitrile imine occurred due to additional irradiation as a result of the longer lifetime.[305] On the other hand, electron-donating groups such as **2-77a**

may lead to a more reactive nitrile imine which cyclises more rapidly. This could lead to an increase in desired product and reduction in by-products or decomposition.

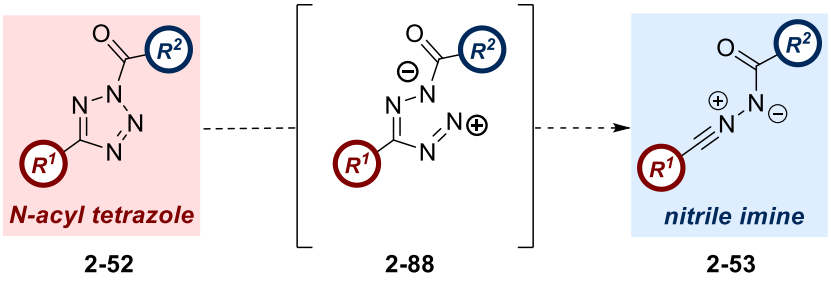

Scheme 115. Possible charge separation on the *N*-acyl tetrazole intermediate before the loss of nitrogen occurs. This may be affected by the electronic nature of the R^2 group.

2-(2-Methoxyphenyl)-5-phenyl-1,3,4-oxadiazole **2-77b** was obtained in a lower yield despite containing an electron-donating group in the *ortho*-position of the aromatic ring. This is potentially due to the steric bulk of this group which may preclude the intramolecular cyclisation. It may also affect the intersystem crossing from the excited singlet state to the triplet if the *ortho*-substituent causes a difference in conformation between the two. As such, alternative relaxation pathways may dominate and inhibit nitrile imine formation.[303]

Five- and six-membered heteroaromatic carboxylic acids, such as furan-containing oxadiazole **2-77g** and pyridine-containing oxadiazole **2-77f**, were also tolerated in yields of 54% and 39%, respectively. It may be possible that the furan heterocycle is not particularly amenable to a photochemical approach using UV light owing to its stability. The lower yield obtained for **2-77f** could be a direct result of the basic nitrogen in the pyridine ring, causing the molecule to exist as a zwitterion,[306] stabilised by hydrogen bonding from both DMF and 5-phenyl-1*H*-tetrazole **2-75** (Figure 72). The increased stabilisation of the zwitterion may reduce the activity towards DIC and therefore give smaller amounts of the reactive *O*-acylisourea. Furthermore, the pyridyl moiety is electron-deficient and this may have a similar effect as discussed above (*vide supra*).

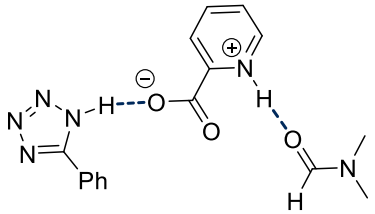

Figure 72. Theoretical hydrogen bonding between 5-phenyl-1*H*-tetrazole **2-75**, DMF and the zwitterion of picolinic acid.

Bromide-containing aromatics **2-77h** and **2-77i** were accessed in good yields, allowing the introduction of a handle to install further functionality and extend the molecules. The

discrepancy between the two yields is interesting as the *para*-substituted regioisomer was obtained in a lower yield (50%) than the *meta*-substituted (72%). Currently, there is no clear explanation for this observation, but it may be possible to elucidate in future studies.

Three aliphatic acids generated oxadiazoles **2-77m**, **2-77n**, and **2-77o** in yields ranging from 63% to 93%, highlighting the broad utility of this method. In the case of **2-77n** no cycloaddition by-products between the alkene of pentenoic acid and the intermediate nitrile imine were observed, indicating the favourability and selectivity of the intramolecular 1,5-rearrangement to deliver the 1,3,4-oxadiazole unit. Also of note was the gram-scale synthesis of **2-77m**, with only modest reduction of yield. Given the simplicity of the flow system, this result cannot be understated as it showcases the potential scalability of this method.

Importantly, nitrogen-protected amino acids (**2-77p**, **2-77q**, **2-77r**) were also compatible with these conditions, giving the desired oxadiazoles in yields of 40-88%, with increasing substitution at the *α*-position resulting in lower yields, consistent with increased steric demands. Again, no by-products from the pendant alkene of (*S*)-*N*-Fmoc-*α*-4-n-pentenylalanine were observed. Furthermore, no evidence of epimerization was noted when using Boc-Ile-OH as a substrate to deliver product **2-77q**. The resulting compounds would be otherwise difficult to access with the mild conditions in this system allowing for use of both Fmoc and Boc protecting groups which may be sensitive to high temperatures or acidic conditions. These compounds and their analogues may find use as peptidomimetics; something which has been previously reported for 1,3,4-oxadiazole species.[194,215]

Additionally, isophthalic acid could be subjected to the flow conditions with altered stoichiometry and reaction time to yield *bis*-oxadiazole **2-77s.** Related to this outcome, the formation of the highly conjugated system containing two oxadiazoles in conjugation with the same aromatic ring has found application in the synthesis of electron transporting materials in OLEDs.[307]

Finally, a direct comparison to a thermally-initiated flow reaction was desired. To this end, a publication by Kappe and Reichart in which acid chlorides and anhydrides are used as acylating agents in flow at high temperatures, was used as the basis for the final experiment.[245] By retaining the authors' optimised conditions but replacing thermolysis with photolysis, oxadiazole **2-77t** was obtained in 78% yield, comparable to the 84% reported. This result gave assurance that the photochemical approach could be widely applied to carboxylic acids, acid chlorides and acid anhydrides.

Whilst the substrate scope exemplified in Scheme 114 covers a broad range of acids, there were some examples of the reaction being unsuccessful. The acids for which sub-optimal results were obtained are shown in Figure 73.

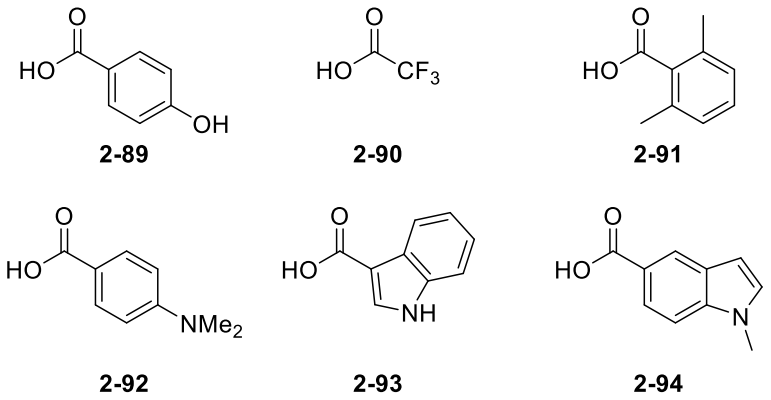

Figure 73. The structures of carboxylic acids which provided sub-optimal results in the flow photochemistry Huisgen reaction.

Several hypotheses for the mixed results obtained with these acids are proposed. 4-Hydroxybenzoic acid **2-89** is very likely to have undergone esterification in the presence of DIC which has the potential to form a number of products. This was reflected by a large number of spots on the TLC plate of the crude reaction mixture. Given that 4-methoxybenzoic acid could be submitted to the reaction and give 85% yield of the corresponding 1,3,4-oxadiazole, it can be assumed that the free hydroxy group is the primary reason for the failure of this reaction.

The use of TFA **2-90** did not form the desired oxadiazole, with the isolated product resembling tetrazole starting material. Therefore, it is likely that the highly acidic nature of TFA (pK_a 0.23) caused protonation of the 5-phenyl-1*H*-tetrazole starting material **2-75**,[308] rendering it unreactive. In addition, it has previously been shown by Kizhnyaev *et al*. that introduction of trifluoroacetic anhydride to 5-substituted tetrazoles at room temperature is able to produce several trifluoromethyl-substituted 1,3,4-oxadiazoles.[309] The use of the anhydride presumably negates any protonation of the tetrazole and the strong electronegativity of the trifluoromethyl group allows for decomposition of the intermediate *N*-acyl tetrazole at room temperature.

Carboxylic acid **2-91** was able to form the desired 1,3,4-oxadiazole product; however, this was limited to a 12% yield which contained significant impurities. While some *ortho*-substituents can be tolerated (Scheme 114), it would appear that the additional steric hindrance in this example led to a poor yield, in agreement with the lower yields reported with increasing steric bulk when amino acids are used (**2-77p**, **2-77q**, **2-77r**).

Aniline **2-92** and indoles **2-93** and **2-94** are known to absorb UV light before undergoing reactions in their excited states.[310-312] Therefore, it is unsurprising that only 13% of impure 1,3,4-oxadiazole product was obtained from the reaction of **2-92**; probably due to the presence of side reactions and subsequent formation of by-products as dimethylaniline is known to react with acids upon irradiation.[313] Both indoles **2-93** and **2-94** did not appear to yield desired product in any capacity which is likely due to side reactions or decomposition from the excited states, reflected by the large number of spots observed on the TLC plates.

From these results it can be concluded that strong acids, large steric bulk in close proximity to the reactive centre of the acid and functional groups which can interact with DIC, such as free alcohols, are detrimental to the formation of the desired 1,3,4-oxadiazoles. Furthermore, functionality which can be excited by irradiation from UV-B light appears to be unsuitable in these reaction conditions and may be more successful in the thermal Huisgen reaction. In order to circumvent any potential issues with starting material absorption, it may be possible to obtain a UV/Vis absorption spectrum to determine if any occurs within the excitation range of the UV-B lamp.

15.6. 5-Substituted Tetrazole Scope

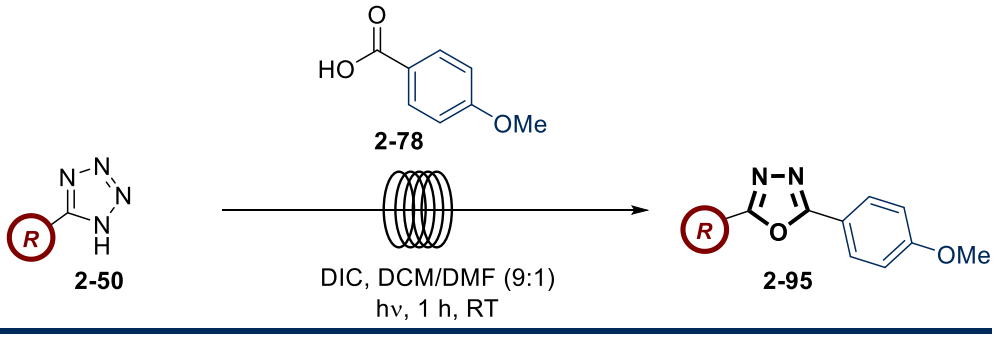

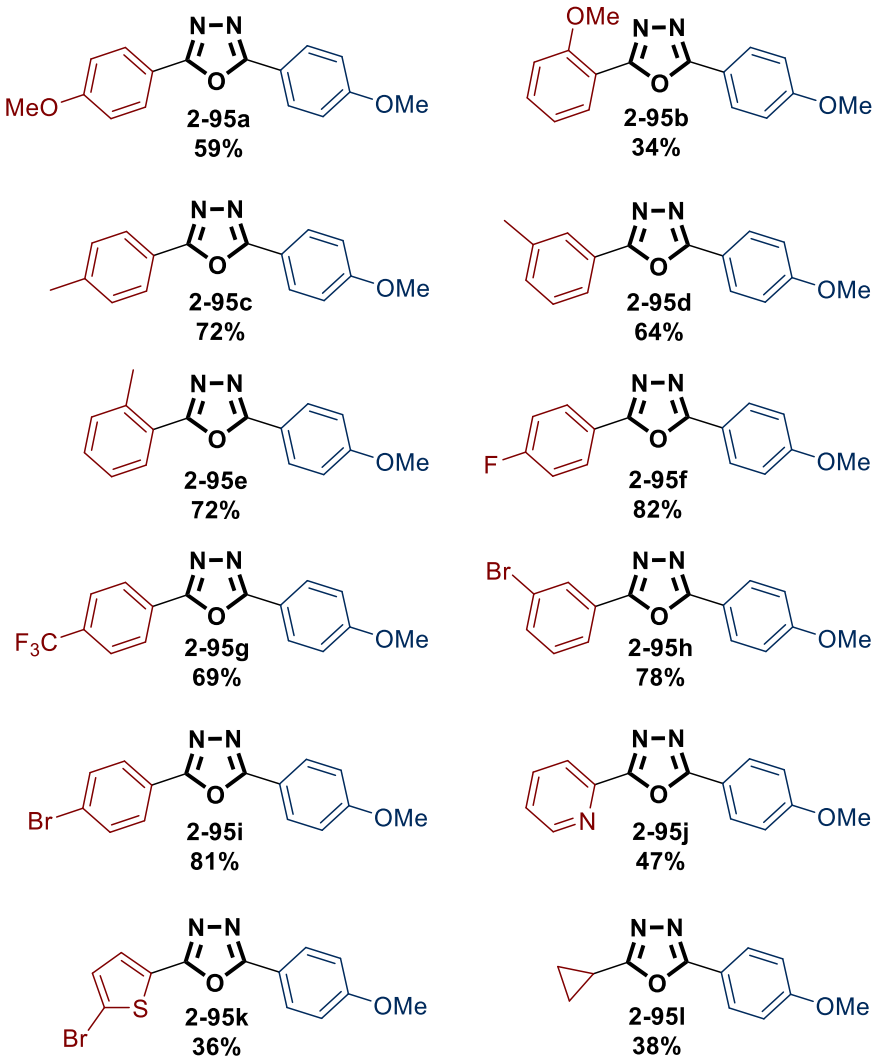

Scheme 116. Reaction of 4-methoxybenzoic acid **2-78** (1.1 equiv.) with tetrazoles (1.0 equiv.) and DIC (1.1 equiv.) on scales of between 0.148-0.342 mmol of tetrazole.

Several tetrazoles were subjected to the reaction with 4-methoxybenzoic acid and Scheme 116 shows the results obtained. Both electron-rich (**2-95a**) and electron-poor aromatics (**2-**

95f, **2-95g**) performed well, giving yields in the range of 59-82%. As with the carboxylic acid scope, the electronics of the system appeared to affect the yield somewhat. Strong electron donating groups on the tetrazole starting material diminish the yields slightly; however, this effect appears less pronounced than that observed for the carboxylic acid scope. This concurs with the results published by Baldwin as the gradient of the Hammett plot relating to the *C*-terminus is shallower than that for the *N*-terminus.[300,301] In addition, the electronic effects on the *C*-terminus of the *N*-acyl tetrazole **2-52** oppose those for the *N*-terminus, again agreeing with Baldwin's analysis.[300,301]

Electron-donating groups may reduce the electrophilicity of the adjacent carbon of the nitrile imine. As a result, the nitrile imine may be stabilised, diminishing the efficiency of the cyclisation process and resulting in a longer-lived reactive species which may undergo decomposition or rearrangement (*vide supra*). It should be noted here that direct resonance of the groups with the nitrile imine intermediate will likely influence the yield of the oxadiazole products. For example, both *para*- and *ortho*-methoxy derivatives **2-95a** and **2-95b** have electron-donating groups in direct resonance with the positive charge of the electrophilic carbon of the nitrile imine as shown below in Figure 74. Stabilisation of the nitrile imine appears to result in a decreased yield.

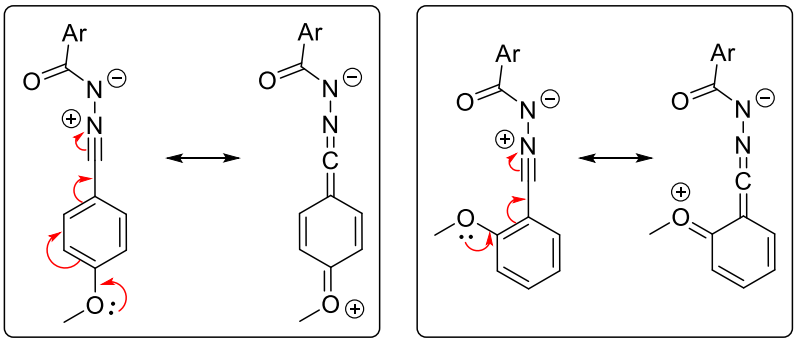

Figure 74. Hypothetical resonance stabilisation of the electrophilic carbon of the nitrile imine intermediate with both *para*- and *ortho*-methoxy groups on the *C*-aryl ring.

Ortho-methoxy substituted aryl tetrazole **2-95b** generated the corresponding oxadiazole in a yield of 34%. The close proximity of the methoxy group to the reactive centre may have an additional effect, thus diminishing the efficiency of the cyclisation further. The yields of **2-95c-i** are all somewhat similar (within 20%) despite containing both inductively donating and withdrawing groups, thus highlighting that inductive effects do not have as strong an effect when on the *C*-terminus of the *N*-acyl tetrazole **2-52** or corresponding nitrile imine **2-53**.

Pyridine-containing oxadiazole **2-95j** was obtained in a moderate yield which may be due to its electron-withdrawing nature. As with the methoxy groups, it is possible to stabilise the *N*-

acyl nitrile imine **2-53** by resonance, shown below in Figure 75. Furthermore, in an analogous reaction under thermal conditions using 4-methoxybenzoyl chloride **2-76** and on a much larger scale (1.5 g), the reported yield was 62%,[314] which is somewhat comparable to the 47% yield obtained in the current study. This may point towards some inherent instability in either the intermediates or product itself. Furthermore, a recrystallisation was necessary after chromatography which can lead to some loss of product in the procedure itself, especially on such a small scale.

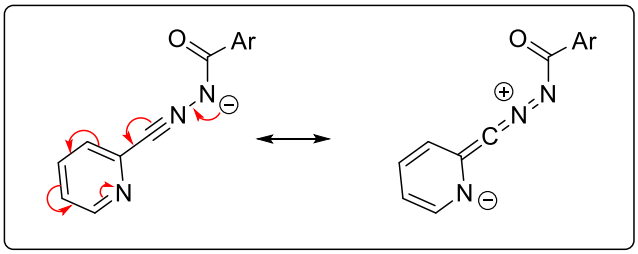

2-95j

Figure 75. Hypothetical resonance stabilisation of the negative charge of the nitrile imine intermediate by the pyridyl moiety on the *C*-terminus of the intermediate.

Thiophene-containing oxadiazole **2-95k** is a further example of a moderate yield in this reaction. As with the previous examples, resonance stabilisation is again possible with donation from the lone pair of the thiophene reducing the electrophilicity of the nitrile imine (*cf*. **2-95a** Figure 74).

Recycling the reaction mixture through the flow system can also affect the yield if the product formed is able to absorb light from the lamp. Given that the effective emission of the UV-B lamp is approximately 310 nm, any absorption at this wavelength may cause attrition of the incident light, affecting the formation of the nitrile imine **2-53**. Relating this to the Beer-Lambert law, as the concentration of the product increases, so does the absorption of the light ($A = \varepsilon cl$).[298,304] By taking the UV/Vis absorption of the compounds obtained alongside the respective LCMS traces, it can be seen that for oxadiazoles **2-95a**, **2-95b**, **2-95j** and **2-95k**, the λ_{max} values lie close to the emission wavelength of the lamp (Figure 76). Therefore, it can be inferred that any product in the reaction mixture can absorb this light, reducing the quantum yield for the photolysis of *N*-acyl tetrazole **2-52**.

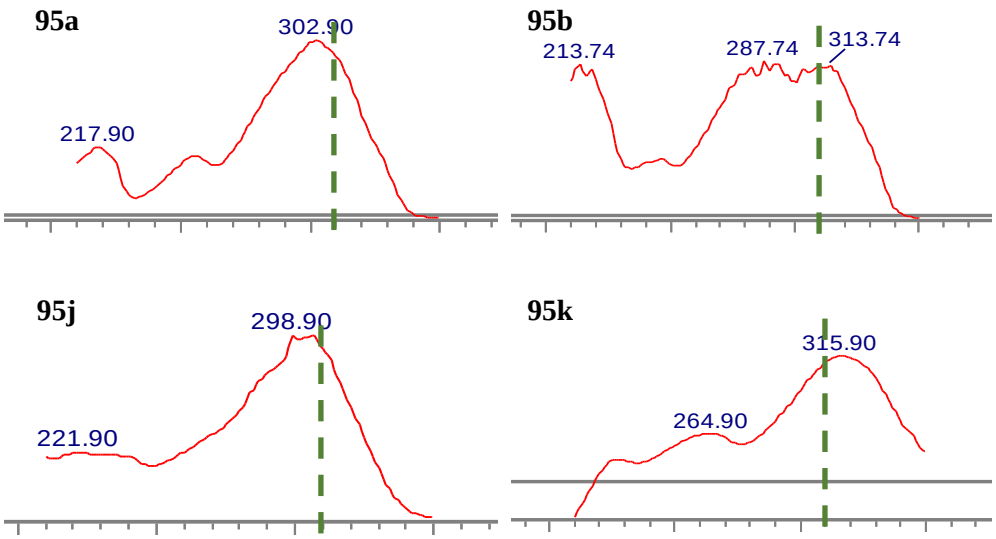

Figure 76. UV absorption spectra obtained with the LCMS of oxadiazoles **2-95a**, **2-95b**, **2-95j** and **2-95k**. Shown is the overlap of the absorption with the 310 nm emission of the UV-B lamp (highlighted by green line).

The effect of the tetrazole substituent on the wavelength of absorption (λ_{max}) should also be considered as these groups form part of the conjugated system. As such, changes to the electronics and sterics can influence λ_{max} values which may impact the efficiency of the reaction. In the case of carboxylic acid substrate scope, the carbonyl group on the *N*-terminus is always present despite the changing structure of the rest of the substrate. Therefore, the shift in the absorption may be more noticeable with a change of the *C*-terminus substituent. The most obvious consequence of this may be reflected in the low yield obtained for oxadiazole **2-95b**. Due to the *ortho*-methoxy group, the aromatic system may lie outside of the plane of the tetrazole ring. The result of this is a loss of conjugation and, therefore, a blueshift in the λ_{max} which may be significant the absorption shifts to a value outside of the emission range of the UV-B lamp. Further confirmation of this could be found by obtaining a UV/Vis spectrum of the *N*-acyl tetrazole; however, these are highly unstable and reactive species.

Electron-donating and electron-withdrawing substituents will also affect the λ_{max} value; however, this is likely to be a relatively small effect in comparison to the loss of conjugation and appears to be reflected in the corresponding yields of oxadiazoles **2-95c-i** which are all of similar value. As such, the main influence of the yield is likely to be the stabilising effects on the reactive intermediates (*vide supra*).

Compound **2-95l** contains a non-aromatic, cyclopropyl group at the *C*-terminus of the tetrazole. The effect of this must be considered alongside the lack of reaction of the substrates shown below in Figure 77. These all contain aliphatic groups or atoms with low propensity

for conjugation, thus reducing the size of the conjugated π-system in the reactive *N*-acyl tetrazole intermediate **2-52**. The absence of oxadiazole formation when using tetrazoles **2-196 - 2-98** is consistent with the understanding that increased conjugation lowers the energy of the electron excitation in a molecule. As such, and according to Equation 1, this would lead to a larger λ_{max} value. In the context of this reaction it is proposed that the reduction in conjugation in comparison to the tetrazoles surveyed in Scheme 116 would offer the reverse scenario in which the λ_{max} value would decrease. Therefore, a mismatch would be present with the emission of the UV-B lamp not sufficiently high in energy to excite the resulting *N*-acyl tetrazoles **2-52**.

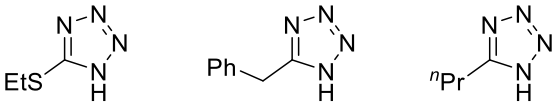

2-96 **2-97** **2-98**

Figure 77. Structures of the tetrazoles which did not yield any of the corresponding oxadiazole products.

Equation 1 $$E = \frac{hc}{\lambda}$$

Another example which was subjected to the reaction conditions but did not yield a significant amount of product is tetrazole **2-99** (Figure 78). Initially, it did not appear that the reaction had produced any product. LCMS analysis obtained after initial purification showed that there was a very small amount of the desired product; however, this equated to an approximate 5% yield showing that this substrate is likely not amenable to the photochemical Huisgen reaction. Despite the presence of the carbonyl at the *C*-terminus, the λ_{max} of the *N*-acyl tetrazole **2-52** appears to be outside of the range of the UV-B lamp.

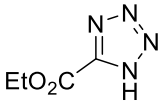

2-99

Figure 78. Ethyl 1*H*-tetrazole-5-carboxylate **2-99** which was submitted to the reaction conditions but only gave an approximate 5% yield.

Given these results, the successful formation of oxadiazole **2-95l**, albeit in moderate yield, must be attributed to an alternative interaction which allows excitation by the UV-B lamp. The interaction is likely due to the π-like orbitals of the cyclopropyl ring[36] interacting with those of the tetrazole, thus lowering the λ_{max} in an analogous manner to an aromatic substituent.

Exploration of tetrazole substrates gives an excellent insight into the factors influencing the outcome of this reaction. The only disadvantage of this work lies with the use of alkyl tetrazoles and those containing atoms with low ability to conjugate, which do not appear to be amenable with the UV-B lamp used here. This would be problematic if a 2,5-dialkyl substituted 1,3,4-oxadiazole is required; however, if only one alkyl group is necessary, this could be introduced with the use of an alkyl carboxylic acid which is shown to be highly efficient (Scheme 114). Aside from this, the majority of other tetrazoles performed well, giving high yielding oxadiazole products.

15.7. Application of Conditions

Finally, in order to further exemplify this method, the cyclooxygenase 2 (COX-2) inhibitor **2-101**[315] was synthesized from the corresponding carboxylic acid **2-100** and tetrazole **2-50** (Scheme 117). This compound was obtained in an excellent yield of 85%, which compares favourably to other reported preparations.[172,315] The additional complexity introduced to the carboxylic acid showcases that this methodology is able to reach much further than for simple 2,5-disubstituted 1,3,4-oxadiazoles.

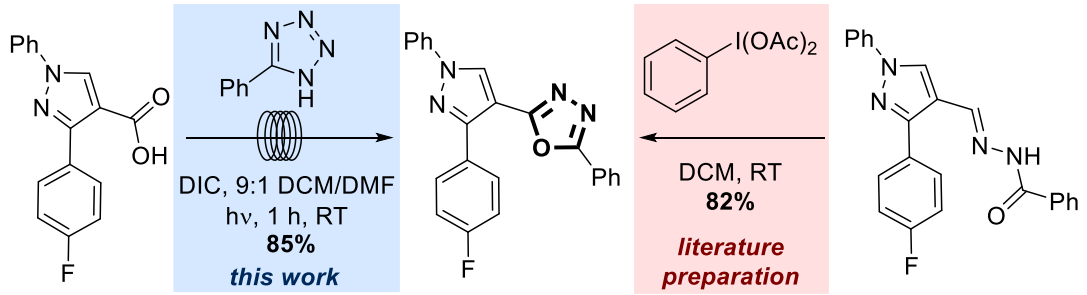

2-100 **2-101** **2-102**

Scheme 117. The synthesis of COX-2 inhibitor **2-101** using the novel photochemical Huisgen formation of 1,3,4-oxadiazoles from 5-phenyl-1*H*-tetrazole **2-50** and carboxylic acid **2-100**. Also shown is the literature preparation from semicarbazone **2-102** in an oxidative cyclisation approach.

16. Summary and Conclusions

16.1. Summary of Work

A summary of the work carried out in this project is shown below in Scheme 118. The use of photochemistry has allowed the modernisation of an under-utilised approach to pharmaceutically relevant 1,3,4-oxadiazoles. UV-promotion of the Huisgen reaction for the synthesis of 1,3,4-oxadiazoles is a valuable direct alternative for the traditional thermolytic process. When incorporated into a simple flow chemistry manifold, this method is amenable to scale up, and enables the synthesis of a broad palette of valuable oxadiazole analogues from readily available precursors in a highly efficient manner. This represents a significant advancement in the light-mediated synthesis of this fundamentally important heterocyclic template.

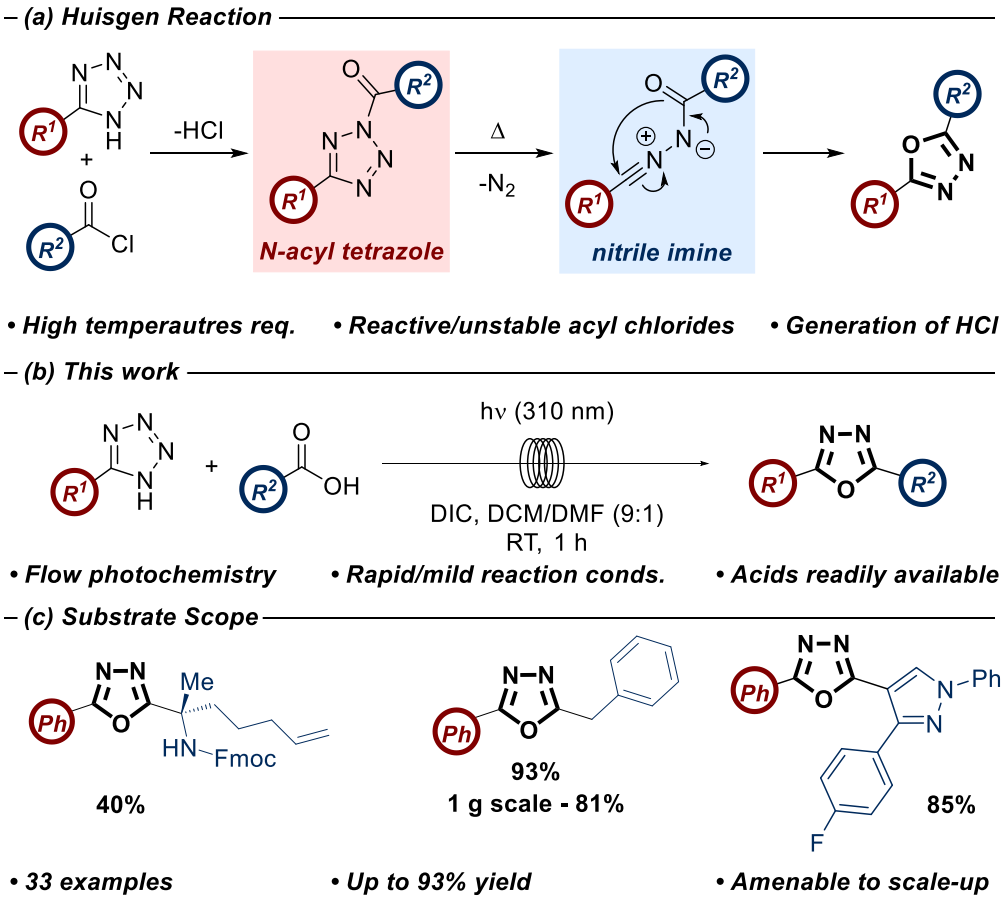

Scheme 118. Summary of work carried out in this project. (a) The traditional Huisgen reaction making use of acid chlorides and thermal activation. (b) The novel approach discussed here with optimised conditions shown. (c) Selected substrates and their corresponding yields.

16.2. Conclusions

Initial studies in our laboratory confirmed that it would be possible to replace the high temperatures often required in the Huisgen reaction with irradiation of the reaction mixture by a Philips PL-S 9W/12 UV-B lamp. The reaction between 5-phenyl-1*H*-tetrazole **2-75** and 4-methoxybenzoyl chloride **2-76** was carried out under both thermal and photochemical conditions in toluene and pyridine (Scheme 107). The results showed that, in our hands, the light activated Huisgen process was superior in yield to the thermally activated counterpart. As such, this reaction was explored in detail with a view to improving both the efficiency and usability. To do this, replacement of the commonly used acid chlorides with carboxylic acids was explored using *in situ* activation.

Exploration of the reaction between 5-phenyl-1*H*-tetrazole **2-75** and 4-methoxycarboxylic acid **2-78** (Table 29) was undertaken with amide coupling reagents from the three most common families (carbodiimides, phosphonium and uronium). In agreement with literature precedent, only carbodiimides DCC and DIC produced a significant amount of the desired 1,3,4-oxadiazole **2-77a**. Furthermore, it was observed that the use of DIC incurred less precipitate formation, owing to the higher solubility of the diisopropylurea by-product **2-86** in DCM compared to dicyclohexylurea.[288] Aiming to move the reaction into a flow setting, this was an important observation, leading to DIC being the reagent of choice.

A functionally simple flow system was constructed using a peristaltic pump, PTFE tubing and a quartz chamber which was placed over the UV-B lamp, based on those used by Booker-Milburn and Berry.[299] It was necessary to introduce DMF into the solvent mixture (9:1 DCM/DMF), solubilising the reagents, product, and urea by-product thus providing a yield of 85%; an improvement of 35% compared to the batch reaction.

Several carboxylic acids were subjected to the conditions with generally high yields obtained for all (39-93%). These included aromatic, alkyl and amino acid moieties with electron-donating groups generally more efficient at forming the desired oxadiazoles. Furthermore, the scale of the reaction could be increased to 1 g of 5-benzyl-1*H*-tetrazole to form oxadiazole **2-77m** in only a slightly decreased yield (81% *vs* 93%) compared to the 50 mg preparation examined initially. A direct comparison to a thermally initiated Huisgen reaction in flow was also possible using conditions published by Kappe and a comparable yield to that reported was obtained.[245] Furthermore, acetic anhydride was used as the acylating agent giving another variable which could be introduced to the photochemical reaction.

The scope of the tetrazole substituents was investigated in a similar fashion to the acids. Again, the yields obtained for the oxadiazole products was generally very good; however, substituents which could stabilise the charges of the nitrile imine intermediate by resonance (**2-95a**, **2-95b**, **2-95j**, **2-95k**) reduced the yield, likely due to an increased lifetime of the nitrile imine **2-53**. The tetrazole substituent could affect the value of λ_{max} of the molecule, giving the potential for a mismatch with the emission of the UV-B lamp.

Finally, the methodology was applied to a pharmaceutically relevant molecule of increased complexity. COX-2 inhibitor **2-101** could be obtained in 85% yield, a slight improvement on the reported literature approach. Moreover, the Huisgen method removes the necessity of using an acyl hydrazine to form the semicarbazone intermediate **2-102**. The synthesis of analogues becomes facile by simply changing the tetrazole starting material within the limitations discussed (*vide supra*).

Overall, the UV-B initiation of the Huisgen synthesis of 1,3,4-oxadiazoles is a novel and impactful method which has been shown to be highly efficient. The use of readily available carboxylic acids in conjunction with flow chemistry represents a significant step in the modernisation of this approach. Replacing high temperatures with light further increases the accessibility of this methodology in a modern laboratory setting. Having demonstrated a broad substrate scope and use of a simple flow system with components found in most laboratories, the bar to accessing this reaction has been lowered. It is anticipated that having addressed the common drawbacks there will be an uptake in the use of this under-utilised transformation.

17. Future Work

17.1. Reproducibility and UV/Vis Studies

The adaptation of the Huisgen synthesis of 1,3,4-oxadiazoles to allow photochemical activation is a substantial improvement upon the traditional approach. The results reported here have shown that this new method provides almost all of the desired compounds in good to excellent yields. While it is anticipated that the use of this activation method will become widespread, the issue of reproducibility is inherent to many new photochemical reactions.[165,316] As such, the application of this method in a separate system to that in which the optimisation and scope was carried out is of utmost importance. By applying this methodology in a different laboratory and using a different lamp with the same emission spectrum, confidence in the reproducibility of the reaction would be obtained. This would also show that it is not necessarily a specific lamp which is required but the wavelength of emission at approximately 310 nm.

Thermal activation of the unsuccessful carboxylic acid and tetrazole starting materials should also be carried out. If these are successful, it provides evidence to the proposal of alternative pathways from electronic excitation of the corresponding *N*-acyl tetrazoles. If alkyl tetrazoles **2-96 - 2-98** also produce the desired 1,3,4-oxadiazoles under thermal conditions, it would point towards a shift of the λ_{max} values due to the loss of conjugation and UV/Vis spectra of the reaction mixtures could provide further evidence. By using the acid chloride and 5-phenyl-1*H*-tetrazole **2-75** it may be possible to add an excess of pyridine to initiate the reaction and form *N*-acyl tetrazole **2-52** which may be detected. The resultant spectra could be compared to that obtained for the individual starting materials as well as the mixture before addition of pyridine (Figure 79). Finally, UV/Vis spectra of the corresponding oxadiazole products should be obtained to determine if any absorbance may be due to their formation. From the resulting spectra, the alkyl and aryl *N*-acyl tetrazole peaks (if observed) could be compared to determine if this agrees with the hypotheses discussed (*vide supra*).

If it is found that the λ_{max} values for alkyl tetrazoles are indeed lower than for aryl tetrazoles, it may be possible to facilitate the formation of 1,3,4-oxadiazoles by using a higher energy UV lamp. This could be attempted, possible with a lamp commonly used for visualising TLC plates at either 254 or 280 nm as was effective for Lin *et al*.[279] The risk with this method is that the high energy irradiation may cause several reactions and may decompose the starting materials if they are able to be excited, especially given that 5-phenyl-1*H*-tetrazole has a λ_{max} value of 241 nm.[317]

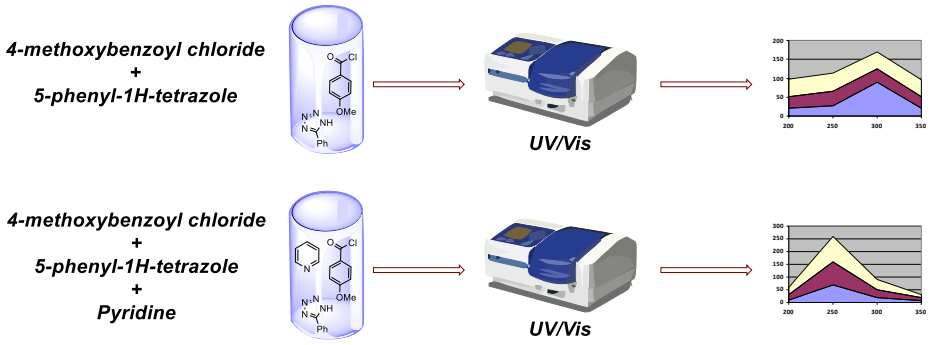

Figure 79. Possible UV/Vis experiments to determine if the *N*-acyl tetrazole intermediate **2-52** can be detected. The wavelength of absorption could be compared between alkyl and aryl tetrazoles.

17.2. Reactor Set-up

While the use of a simple flow system in this project was a key aim, there was no exploration of the physical parameters of the set-up. As is well-documented, there are several variables which can lead to an increase in both yield and productivity of photochemical reactions in flow.[318,319] To this end, variables such as: replacing the tubing material (for example, PTFE with FEP); layering of coils around the lamp and the flow rate are all factors which can affect the outcome of the reaction.[299,320] A desirable outcome of this exploration would be a first-pass reaction in which complete conversion to the 1,3,4-oxadiazole products is observed upon one pass around the lamp. As a result, any attenuation of the UV-B light from absorption by the products would be removed and may increase the yields of the specific examples highlighted in Figure 76 (*vide supra*, section 15.6). A schematic of how an alternative system might look is shown below in Figure 80.

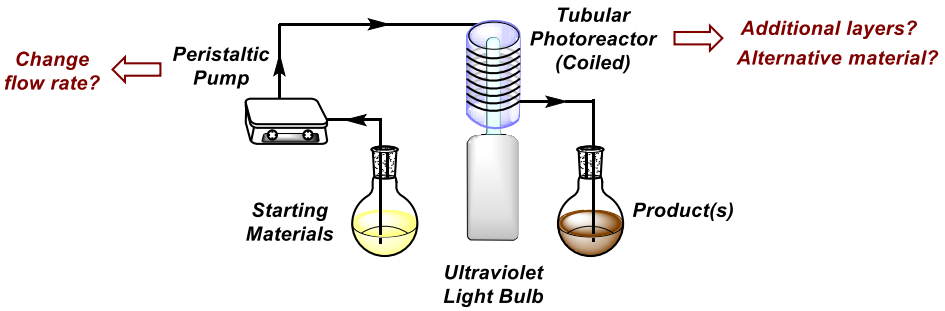

Figure 80. A schematic diagram showing how a first-pass reaction might be assembled. Also shown are other variables related to the coil around the UV-B lamp and the flow rate.

17.3. Alternative Starting Materials

The Huisgen reaction has been shown to be successful with three main types of acylating agents: acid chlorides, acid anhydrides and carboxylic acids. These are commonly found throughout the literature (*cf.* section 13.2.5). Despite the focus on carboxylic acids as readily available starting materials, it has been shown here that all of these substrates are amenable to the photochemical Huisgen reaction. In addition to these, Huisgen was able to show that by using isocyanates, it was possible to access a small number of 5-substituted-2-amino-1,3,4-oxadiazoles **2-24**.[321] This methodology was later expanded by Koldobskii *et al*. with the use of microwave heating;[322] however, there has been little exploration beyond this and only limited use.[323] The presence of an intermediate *N*-acyl tetrazole in the reaction should make this approach amenable to excitation by the UV-B lamp used in this project. As such, an exploration of isocyanates as substrates in this reaction would be a useful expansion of this body of work (Scheme 119). An advantage of this approach is the lack of requirement of a base or activating agent in order to form the *N*-acyl tetrazole intermediate **2-105**.

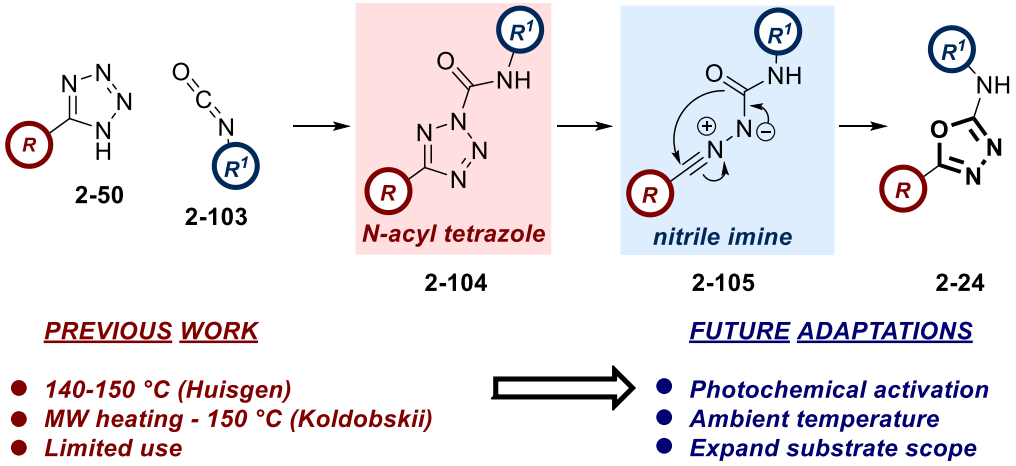

Scheme 119. The Huisgen synthesis of 5-substituted-2-amino-1,3,4-oxadiazoles **2-24** using tetrazoles **2-50** and isocyanates **2-103** as starting materials.

A disadvantage of this approach is the limited accessibility of isocyanates compared to acids and, as a result, the substrate scope may not cover as wide a range. While these compounds are accessible *via* a Curtius rearrangement,[324] it does require the use of azides with the issues previously discussed in section 13.2.5. Furthermore, there are associated health risks as some isocyanates can act as sensitisers. Despite this, their use in a controlled environment should allow facile access to several 5-substituted-2-amino-1,3,4-oxadiazoles **2-24**.

Huisgen had also shown that when the isocyanate was replaced by phenyl-isothiocyanate, the corresponding 2-phenyl-5-phenyl-1,3,4-thiadiazole could be formed in 64% yield.[321] Again, Koldobskii *et al*. expanded the substrate scope of the reaction by using microwave heating

(Scheme 120).[325] With these reactions, as with isocyanates, no additional reagents were required; however, temperatures in the region of 170 °C were necessary. Furthermore, the reaction required the uses of isothiocyanates which, as previously detailed, are toxic. Nevertheless, it would be of interest to determine if this is a further approach amenable to photochemical activation.

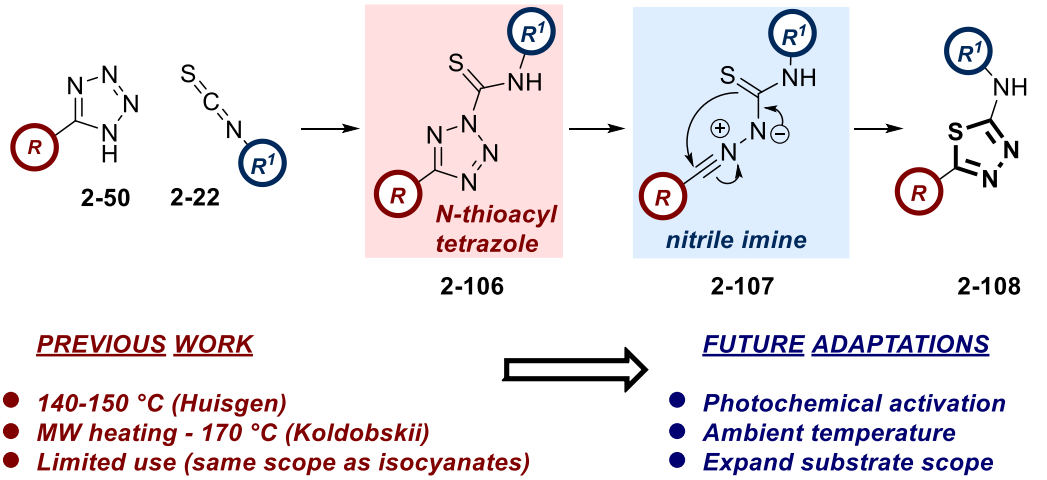

Scheme 120. Synthesis of 5-substituted-2-amino-1,3,4-thiadiazoles **2-108** from tetrazoles **2-50** isothiocyanates **2-22**.

While it is expected that the use of isothiocyanates in the reaction will work under photochemical conditions, it will almost certainly require an alternative wavelength for activation of the *N*-thioacyl tetrazole **2-106**. This is a result of a weaker carbon-sulfur double bond in comparison to the corresponding carbon-oxygen double bond. Furthermore, the excited states have been found to exist at a lower energy and, referring to Equation 1, this means that the absorption wavelength will be higher.[326,327] As a result, a screen of an initial reaction would be the best course of action. As in section 15.4, the PHIL Pacer system could be used to identify if visible wavelengths would be optimal for the reaction alongside the use of the original UV-B lamp and a control reaction in the dark. Once this result had been obtained, further optimisation and substrate scope could be explored.

The addition of isocyanates and isothiocyanates to the photochemical Huisgen reaction broadens the utility of this approach to heterocycle synthesis. If positive results can be obtained in the simple flow system described, there is no reason that this work could not be repeated in several different laboratories. The limiting factor in this may be the procurement of the UV-B lamp; however, with the increased uptake in modern photochemistry, it is highly likely that a supplier could be found. As a result, this underexplored area of chemistry has the potential to be of high impact in heterocyclic assembly.

18. Experimental

18.1. General Information

Chemicals were used as received from commercial sources (Sigma Aldrich, Fluorochem, Alfa Aesar) without purification, unless otherwise stated. NMR spectra were recorded on a Bruker AV 500 or a Bruker AV 400. Chemical shifts (δ) are reported in ppm and coupling constants (*J*) are in Hz. The following abbreviations are used for multiplicities: s = singlet; br s = broad singlet; d = doublet; t = triplet; q = quartet; m = multiplet; dd = doublet of doublets; dt = doublet of triplets; spt = septet. Liquid Chromatography Mass Spectrometry (LCMS) methods used for reaction monitoring and final purity analysis are referred to by the modifier used (formic acid or high pH). The analysis was conducted on an Acquity UPLC CSH C18 column (50 mm x 2.1 mm i.d. 1.7µm packing diameter) at 40 °C using a 2-minute method. Mass spectra were recorded using a Waters QDA with an alternate-scan positive and negative electrospray ionization with a range of 100-1500 AMU and a frequency of 5 Hz. The UV detection was a summed signal from 210 nm to 350 nm. High Resolution Mass Spectrometry (HRMS) was obtained using a UPLC-HRMS system. The chromatography was conducted on an Acquity UPLC BEH or UPLC CSH C18 column (100mm x 2.1mm i.d. 1.7µm packing diameter) at 50 °C in either a formic acid or high pH modifier. The UV detection was a summed signal from 210 nm to 500 nm. The HRMS were recorded using a Waters XEVO G2-XS Qtof with positive electrospray ionization mode with a scan range of 100 to 1200 AMU. IR spectra were obtained on a Perkin Elmer Spectrum One spectrometer. Absorption frequencies (ν_{max}) are reported in wavenumbers (cm^{-1}). Photochemical flow reactions were carried out in PTFE tubing (0.7 x 1.6 mm, sourced from ADTECH) wrapped around a quartz tube with diameter of 3.5 cm. The bulb used was a Philips PL-S 9W/12 with a range of 290-315 nm. A Pharmacia Fine Chemicals peristaltic pump was used to pump the reaction mixture through the tubing at a flow rate of 2 mL min^{-1}. The reactor volume was measured to be 3.5 mL.

18.2. Initial Experiments

2-(4-Methoxyphenyl)-5-phenyl-1,3,4-oxadiazole (2-77a) – *initial reaction with acid chloride*

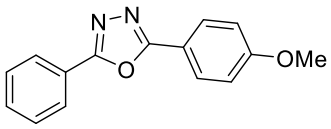

5-Phenyl-1*H*-tetrazole (37.0 mg, 0.250 mmol), 4-methoxybenzoyl chloride (68.0 µL, 0.500 mmol) and pyridine (60.0 µL, 0.750 mmol) were dissolved in toluene (1 mL) and either heated to 100 °C or irradiated with UV-B light until the starting material was consumed. The reaction mixture was purified by flash column chromatography (0-25% EtOAc/petroleum ether) to give the product as a white solid.

Heating: 45.9 mg, 0.182 mmol, 73%.

UV light: 55.0 mg, 0.218 mmol, 87%.

18.3. Optimisation Experiments

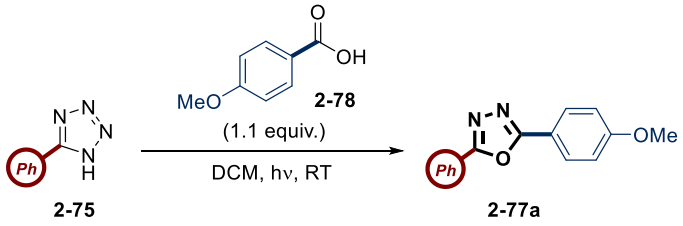

Entry	Coupling Reagent	Solvent	Time (h)	Yield (%)
1[a][b]	HATU/DIPEA	DCM	8	N.R.
2[a][c]	HATU/DIPEA	DMF	21	N.R.
3[a]	PyBOP®/DIPEA	DCM	6	N.R.
4[a][d]	PyBrOP®/DIPEA	DCM	19	N.R.
5[e]	EDCI/DMAP	DCM	19	4
6[e][f]	CDI/DMAP	DCM	19	N.R.
7[g]	DCC	DCM	19	51
8	DIC	DCM	23	50
9[h]	DCC/DMAP	DCM	5	55
10[i]	DCC/HOAt	DCM	19	N.R.
11	DCC/Oxyma	DCM	19	8
12	DCC/HOBt	DCM	19	N.R.

Reactions carried out in quartz round-bottom flasks in front of a UV-B lamp with 1.1 equiv. of carboxylic acid, 1.1 equiv. of coupling reagent at a concentration of 0.12 M with respect to the tetrazole. [a] 3.0 equiv. DIPEA. [b] 1.0 equiv. HATU. [c] 1.25 equiv. HATU. [d] 1.2 equiv. PyBrOP®. [e] 1.5 equiv. DMAP. [f] irradiated for 6.5 h in presence of CDI before addition of DMAP and further irradiation for 12.5 h. [g] 1.27 equiv. carboxylic acid. [h] 0.1 equiv. DMAP. [i] 1.23 equiv. carboxylic acid.

Entry 1.

4-Methoxybenzoic acid (60.0 mg, 0.394 mmol) and HATU (143 mg, 0.376 mmol) were dissolved in DCM (1.4 mL). DIPEA (179 µL, 1.03 mmol) was added and the reaction mixture stirred for 15 min at RT. 5-Phenyl-1*H*-tetrazole (55.0 mg, 0.376 mmol) was added and the reaction mixture irradiated for 8 h. Only starting materials were observed by TLC with no product visible when compared to an authentic sample.

Entry 2.

4-Methoxybenzoic acid (60.0 mg, 0.394 mmol) and HATU (162 mg, 0.426 mmol) were dissolved in DMF (1.4 mL) before DIPEA (179 µL, 1.03 mmol) was added and the reaction mixture stirred for 15 min at RT. 5-Phenyl-1*H*-tetrazole (50.0 mg, 0.342 mmol) was added and the reaction mixture irradiated for 21 h before being diluted with EtOAc (10 mL) and 1 M aqueous NaOH (10 mL). The layers were separated and the organic washed with water (10 mL) and 5% aqueous LiCl solution (2 × 10 mL). The organic was collected, dried using a hydrophobic frit and concentrated *in vacuo* to give an orange residue. NMR and TLC of the crude mixture showed no desired product when compared to an authentic sample.

Entry 3.

5-Phenyl-1*H*-tetrazole (50.0 mg, 0.342 mmol), 4-methoxybenzoic acid (60.0 mg, 0.394 mmol) and PyBOP® (196 mg, 0.376 mmol) were dissolved in DCM (1.4 mL). DIPEA (179 µL, 1.03 mmol) was added and the reaction mixture irradiated for 6 h before being concentrated *in vacuo* giving a brown oil which was dissolved in EtOAc (10 mL). This was washed with water (10 mL) and saturated aqueous ammonium chloride solution (10 mL) before being concentrated *in vacuo* to give a brown residue. TLC of this showed no desired product when compared to an authentic sample.

Entry 4.

5-Phenyl-1*H*-tetrazole (52.0 mg, 0.356 mmol), 4-methoxybenzoic acid (62.0 mg, 0.407 mmol) and PyBrOP® (201 mg, 0.431 mmol) were dissolved in DCM (1.4 mL). DIPEA (179 µL, 1.03 mmol) was added and the reaction stirred for 15 min at RT before being irradiated for 19 h. The reaction mixture was concentrated *in vacuo* to give a yellow oil. This was dissolved in EtOAc (10 mL) and washed with water (10 mL) and saturated aqueous ammonium chloride (10 mL). The organic was collected, dried using a hydrophobic frit and concentrated *in vacuo* to give a yellow oil with some solid present. TLC and NMR of this did not show any desired product when compared to an authentic sample.

Entry 5. ***Reaction diluted due to solubility of EDCI***

5-Phenyl-1*H*-tetrazole (50.0 mg, 0.342 mmol), 4-methoxybenzoic acid (60.0 mg, 0.394 mmol), EDCI (72.0 mg, 0.376 mmol) and DMAP (63.0 mg, 0.513 mmol) were dissolved in DCM (2.8 mL) and the reaction mixture irradiated for 19 h. This was diluted with DCM (10 mL) and washed with water (10 mL) and brine (10 mL). The organic was collected, dried using a hydrophobic frit and concentrated *in vacuo* to give an off-white residue which was purified by flash column chromatography (0-0.5% MeOH/DCM). **2-77a** was obtained as an off-white solid (3.2 mg, 0.013 mmol, 4%).

Entry 6. ***Reaction diluted due to solubility of CDI***

5-Phenyl-1*H*-tetrazole (53.0 mg, 0.363 mmol), 4-methoxybenzoic acid (60.0 mg, 0.394 mmol) and CDI (65.0 mg, 0.401 mmol) were dissolved in DCM (2.8 mL) and the reaction mixture irradiated for 6.5 h. TLC showed no desired product had formed when compared to an authentic sample. DMAP (70.0 mg, 0.572 mmol) was added and the reaction mixture irradiated for a further 12.5 h before being diluted with DCM (10 mL). This was washed with water (10 mL) and 1 M aqueous HCl (10 mL). The organic was collected, dried using a hydrophobic frit and concentrated *in vacuo* giving a pale yellow oil. TLC and NMR of this showed no desired product had formed when compared to an authentic sample.

Entry 7. ***Reaction diluted due to solubility of DCC***

5-Phenyl-1*H*-tetrazole (50.0 mg, 0.342 mmol), 4-methoxybenzoic acid (66.0 mg, 0.434 mmol) and DCC (78.0 mg, 0.376 mmol) were dissolved in DCM (2.8 mL). The reaction mixture was stirred at RT for 15 min before being irradiated for 19 h. TLC indicated that the desired product had formed when compared to an authentic sample. Therefore, the reaction mixture was concentrated *in vacuo* giving a white solid which was suspended in EtOAc (5.0 mL) and filtered. The collected solid was washed with further EtOAc. The filtrate was concentrated *in vacuo* giving a white solid which was purified by flash column chromatography (0-0.5% MeOH/DCM) to give the desired product **2-77a** as a white solid (44.1 mg, 0.175 mmol, 51%).

Entry 8. ***Reaction diluted as a direct comparison to DCC reaction***

5-Phenyl-1*H*-tetrazole (53.0 mg, 0.363 mmol) and 4-methoxybenzoic acid (63.0 mg, 0.414 mmol) were dissolved in DCM (2.8 mL) and DIC (59 µL, 0.376 mmol) was added. The reaction mixture irradiated for 23 h before being diluted with DCM (10 mL). This was washed with water (10 mL) and 1 M aqueous NaOH (10 mL). The organic was collected, dried using a hydrophobic frit and concentrated *in vacuo* to give a white solid which was

purified by flash column chromatography (0-0.5% MeOH/DCM) to give **2-77a** as an off-white solid (45.9 mg, 0.182 mmol, 50%).

Entry 9.

5-Phenyl-1*H*-tetrazole (67.0 mg, 0.458 mmol), 4-methoxybenzoic acid (77.0 mg, 0.504 mmol), DCC (104 mg, 0.504 mmol) and DMAP (6.0 mg, 0.049 mmol) were dissolved in DCM (3.7 mL) and the reaction mixture irradiated for 5 h before being concentrated *in vacuo*. The remaining white solid was suspended in EtOAc (5.0 mL) and filtered. The solid was washed with further EtOAc and the filtrate collected and concentrated *in vacuo* to give a white solid which was purified by flash column chromatography (0-0.5% MeOH/DCM) to give **2-77a** as a white solid (64.1 mg, 0.254 mmol, 55%).

Entry 10.

5-Phenyl-1*H*-tetrazole (50.0 mg, 0.342 mmol), 4-methoxybenzoic acid (64.0 mg, 0.421 mmol), DCC (78.0 mg, 0.376 mmol) and HOAt (51.0 mg, 0.376 mmol) were dissolved in DCM (2.8 mL) and the reaction mixture irradiated for 19 h before being concentrated *in vacuo*. The remaining white solid was suspended in EtOAc (5.0 mL) and filtered. The solid was washed with further EtOAc and the filtrate collected and concentrated *in vacuo* to give an off-white residue which was purified by flash column chromatography (0-0.5% MeOH/DCM). No desired product was isolated; however, the active HOAt ester was isolated and NMR data obtained. ^{1}H NMR (400 MHz, $CDCl_3$) δ = 8.75 (d, *J* = 4.5 Hz, 1H), 8.47 (d, *J* = 8.5 Hz, 1H), 8.27 (d, *J* = 8.5 Hz, 2H), 7.47 (dd, *J* = 4.5, 8.5 Hz, 1H), 7.07 (d, *J* = 8.5 Hz, 2H), 3.95 (s, 3H); ^{13}C NMR (126 MHz, $CDCl_3$) δ = 165.4, 162.2, 151.8, 140.9, 135.2, 133.3, 129.6, 120.8, 116.6, 114.6, 55.7.

Entry 11.

5-Phenyl-1*H*-tetrazole (59.0 mg, 0.404 mmol), 4-methoxybenzoic acid (70.0 mg, 0.460 mmol), DCC (89.0 mg, 0.431 mmol) and oxyma (55.0 mg, 0.387 mmol) were dissolved in DCM (2.8 mL) and the reaction mixture irradiated for 19 h before being concentrated *in vacuo*. The remaining white solid was suspended in EtOAc (5.0 mL) and filtered. The solid was washed with further EtOAc and the filtrate collected and concentrated *in vacuo* to give an off-white residue which was purified by flash column chromatography (0-0.5% MeOH/DCM) to give **2-81a** as a white solid (7.7 mg, 0.031 mmol, 8%).

Entry 12.

5-Phenyl-1*H*-tetrazole (50.0 mg, 0.342 mmol), 4-methoxybenzoic acid (60.0 mg, 0.376 mmol), DCC (78.0 mg, 0.376 mmol) and HOBt (54.0 mg, 0.400 mmol) were dissolved in DCM (2.8 mL) and the reaction mixture irradiated for 19 h before being concentrated *in*

vacuo. The remaining white solid was suspended in EtOAc (5.0 mL) and filtered. The solid was washed with further EtOAc and the filtrate collected and concentrated *in vacuo* to give an off-white residue. TLC and NMR of this showed no desired product had formed when compared to an authentic sample.

Scale-up of DCC reaction

5-Phenyl-1*H*-tetrazole (200 mg, 1.37 mmol), 4-methoxybenzoic acid (229 mg, 1.51 mmol) and DCC (311 mg, 1.51 mmol) were dissolved in DCM (11.2 mL) and the reaction mixture irradiated for 19 h before being concentrated *in vacuo*. The remaining white solid was suspended in EtOAc (10 mL) and filtered. The solid was washed with further EtOAc and the filtrate collected and concentrated *in vacuo* to give a white solid which was purified by flash column chromatography (0-0.5% MeOH/DCM) to give **2-77a** as an off-white solid (171 mg, 0.678 mmol, 50%).

Scale-up of DIC reaction

5-Phenyl-1*H*-tetrazole (200 mg, 1.37 mmol), 4-methoxybenzoic acid (229 mg, 1.51 mmol) and DIC (0.235 µL, 1.51 mmol) were dissolved in DCM (11.2 mL) and the reaction mixture irradiated for 19 h before being concentrated *in vacuo*. The remaining white solid was suspended in EtOAc (10 mL) and filtered. The solid was washed with further EtOAc and the filtrate collected and concentrated *in vacuo* to give a white solid which was purified by flash column chromatography (0-0.5% MeOH/DCM) to give **2-77a** as an off-white solid (171 mg, 0.678 mmol, 50%).

18.4. Flow Experiments

Initial run – DCM solvent

5-Phenyl-1*H*-tetrazole (50.0 mg, 0.342 mmol) and 4-methoxybenzoic acid (60.0 mg, 0.376 mmol) were dissolved in DCM (8.4 mL). DIC (59.0 µL, 0.376 mmol) was added and the reaction mixture pumped through the flow system. A blockage formed within 1 h and caused the system to leak. The reaction was abandoned.

Introduction of DMF (9:1 DCM/DMF)

5-Phenyl-1*H*-tetrazole (57.0 mg, 0.390 mmol) and 4-methoxybenzoic acid (62.0 mg, 0.407 mmol) were dissolved in DCM/DMF (9:1, 8.4 mL). DIC (64.0 µL, 0.429 mmol) was added and the reaction mixture pumped through the flow system for 1 h. The reaction mixture was then collected and concentrated *in vacuo* before being dissolved in EtOAc (20 mL). This was washed with water (10 mL) and 5% aqueous LiCl solution (2 × 20 mL). The organic layer was collected, dried using a hydrophobic frit and concentrated *in vacuo*. The resulting residue

was purified by flash column chromatography (0-0.5% MeOH/DCM) to give **2-77a** as a white solid (84.0 mg, 0.333 mmol, 85%).

18.5. Control Reactions

Without DIC

5-Phenyl-1*H*-tetrazole (50.0 mg, 0.342 mmol) and 4-methoxybenzoic acid (57.0 mg, 0.376 mmol) were dissolved in DCM/DMF (9:1, 8.4 mL) and the reaction mixture pumped through the flow system for 1 h. The reaction mixture was then collected and concentrated *in vacuo* before being dissolved in EtOAc (20 mL). This was washed with water (10 mL) and 5% aqueous LiCl solution (2 × 20 mL). The organic layer was collected, dried using a hydrophobic frit and concentrated *in vacuo*. NMR and TLC of the crude material showed no desired product when compared to an authentic sample.

Reaction in the dark

5-Phenyl-1*H*-tetrazole (50.0 mg, 0.342 mmol) and 4-methoxybenzoic acid (57.0 mg, 0.376 mmol) were dissolved in DCM/DMF (9:1, 8.4 mL). DIC (64.0 µL, 0.429 mmol) was added and the reaction mixture pumped through the flow system for 1 h in the dark. The reaction mixture was then collected and concentrated *in vacuo* before being dissolved in EtOAc (20 mL). This was washed with water (10 mL) and 5% aqueous LiCl solution (2 × 20 mL). The organic layer was collected, dried using a hydrophobic frit and concentrated *in vacuo*. The resulting residue was purified by flash column chromatography (0-0.5% MeOH/DCM) to give **2-77a** as an off-white solid (3.4 mg, 0.013 mmol, 4%). The NMR of the product showed that impurities were also present.

18.6. Wavelength Screen

Visible light screen

5-Phenyl-1*H*-tetrazole (90.0 mg, 0.615 mmol) and 4-methoxybenzoic acid (103 mg, 0.677 mmol) were dissolved in DCM/DMF (9:1, 15.0 mL) (13.5 mL) as a stock solution. 1.5 mL of this was added to 7 HPLC vials. To each vial was added DIC (10.5 µL). 6 of the vials were irradiated using the PHIL pacer photoreactor[165] for 24 hours at various wavelengths (365nm, 385 nm, 405 nm, 420 nm, 450 nm and 525 nm) with shaking. One vial was left in the dark for 24 h with shaking. LCMS of each reaction mixture was taken, as shown in Table 30, section 15.4.

Reaction with UV-B to obtain LCMS

Using a Philips PL-S 9W/12 lamp but in a UV cabinet. 5-Phenyl-1*H*-tetrazole (100 mg, 0.684 mmol) and 4-methoxybenzoic acid (115 mg, 0.753 mmol) were dissolved in DCM/DMF (9:1, 16.7 mL). DIC (0.120 ml, 0.753 mmol) was then added and this was irradiated with UV-B light for 1 h. LCMS of the reaction mixture was taken.

18.7. Substrate Scope

General Flow Procedure.

Tetrazole (1 equiv) and carboxylic acid (1.1 equiv) were dissolved in DCM/DMF (9:1, 0.04 M). DIC (1.1 equiv) was added and the reaction mixture pumped through the flow system for 1 h. The reaction mixture was then collected and concentrated *in vacuo* before being dissolved in EtOAc (20 mL). This was washed with water (10 mL) and 5% aqueous LiCl solution (2 × 20 mL). The organic layer was collected, dried using a hydrophobic frit and concentrated *in vacuo*. The resulting residue was purified by flash column chromatography on silica gel.

18.7.1. Acid Substrate Scope

2-(4-Methoxyphenyl)-5-phenyl-1,3,4-oxadiazole (2-77a)

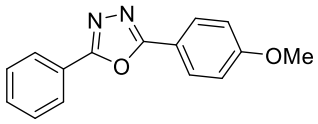

Following the General Flow Procedure using 5-phenyl-1*H*-tetrazole (57.0 mg, 0.390 mmol), 4-methoxybenzoic acid (62.0 mg, 0.407 mmol), DIC (64.0 µL, 0.429 mmol) and 9:1 DCM/DMF (8.4 mL). Elution with 0-0.5% MeOH/DCM afforded **2-77a** as a white solid (84.0 mg, 0.333 mmol, 85%). ^{1}H NMR (400 MHz, $CDCl_3$): δ 8.17 - 8.12 (m, 2H), 8.11 - 8.07 (m, 2H), 7.57 - 7.50 (m, 3H), 7.07 - 7.02 (m, 2H), 3.90 (s, 3H); ^{13}C NMR (101 MHz, $CDCl_3$) δ 164.5, 164.1, 162.3, 131.5, 129.0, 128.7, 126.8, 124.1, 116.5, 114.5, 55.5; LCMS (High pH) t_R = 1.17 min, [M+H$^+$] 253.0 (99% purity).

2-77a is a known compound and the NMR data are consistent with reported literature.[241,328]

2-(2-Methoxyphenyl)-5-phenyl-1,3,4-oxadiazole (2-77b)

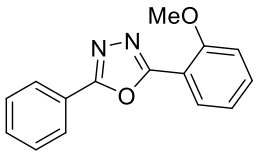

Following the General Flow Procedure using 5-phenyl-1*H*-tetrazole (50.0 mg, 0.342 mmol), 2-methoxybenzoic acid (57.0 mg, 0.376 mmol), DIC (59.0 µL, 0.376 mmol) and 9:1 DCM/DMF (8.4 mL). Elution with 0-0.5% MeOH/DCM afforded a white solid which was impure. A second purification using 20% EtOAc/40-60 °C petroleum ether afforded **2-77b** as a white solid (50.0 mg, 0.198 mmol, 58%). ^{1}H NMR (400 MHz, $CDCl_3$) δ = 8.18 - 8.11 (m, 2H), 8.03 (dd, *J* = 1.5, 7.5 Hz, 1H), 7.57 - 7.49 (m, 4H), 7.14 - 7.06 (m, 2H), 4.00 (s, 3H); ^{13}C NMR (101 MHz, $CDCl_3$) δ = 164.3, 163.3, 157.9, 133.0, 131.5, 130.5, 129.0, 126.9, 124.2, 120.7, 113.1, 112.0, 56.0; LCMS (High pH) t_R = 1.10 min, [M+H$^+$] 253.0 (purity 100%).

2-77b is a known compound and the NMR data are consistent with reported literature.[329]

2,5-Diphenyl-1,3,4-oxadiazole (2-77c)

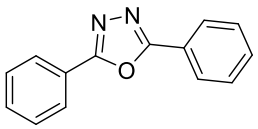

Following the General Flow Procedure using 5-phenyl-1*H*-tetrazole (50.0 mg, 0.342 mmol), benzoic acid (47.0 mg, 0.376 mmol), DIC (59.0 µL, 0.376 mmol) and 9:1 DCM/DMF (8.4 mL). Elution with 0-0.5% MeOH/DCM afforded **2-77c** as a white solid (59.1 mg, 0.266 mmol, 78%). ^{1}H NMR (400 MHz, $CDCl_3$) δ = 8.19 - 8.11 (m, 4H), 7.61 - 7.50 (m, 6H); ^{13}C NMR (101 MHz, $CDCl_3$) δ = 164.6, 131.7, 129.1, 126.9, 124.0; LCMS (High pH) t_R = 1.17 min, [M+H$^+$] 223.0 (purity 100%).

2-77c is a known compound and the NMR data are consistent with reported literature.[328]

2-Phenyl-5-(4-(trifluoromethyl)phenyl)-1,3,4-oxadiazole (2-77d)

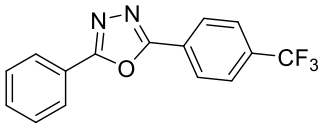

Following the General Flow Procedure using 5-phenyl-1*H*-tetrazole (52 mg, 0.356 mmol), 4-(trifluoromethyl)benzoic acid (72.0 mg, 0.379 mmol), DIC (59.0 µL, 0.376 mmol) and 9:1 DCM/DMF (8.4 mL). Elution with 0-0.5% MeOH/DCM afforded **2-77d** as a white solid

(64.0 mg, 0.221 mmol, 65%). ^{1}H NMR (400 MHz, $CDCl_3$) δ = 8.28 (d, *J* = 8.0 Hz, 2H), 8.20 - 8.12 (m, 2H), 7.82 (d, *J* = 8.5 Hz, 2H), 7.63 - 7.52 (m, 3H); ^{19}F NMR (376 MHz, $CDCl_3$) δ = -63.08 (s); ^{13}C NMR (101 MHz, $CDCl_3$) δ = 165.2, 163.4, 133.3 (q, $^{2}J_{CF}$ = 31.9 Hz), 132.1, 129.2, 127.4, 127.2, 127.1, 126.1 (q, $^{3}J_{CF}$ = 3.9 Hz), 123.6, 123.6 (q, $^{1}J_{CF}$ = 272.6 Hz); LCMS (formic acid) t_R = 1.32 min, [M+H$^+$] 291.0 (purity 95%).

2-77d is a known compound and the NMR data are consistent with reported literature.[329]

4-(5-Phenyl-1,3,4-oxadiazol-2-yl)benzonitrile (2-77e)

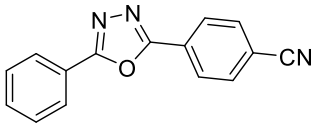

Following the General Flow Procedure using 5-phenyl-1*H*-tetrazole (50.0 mg, 0.342 mmol), 4-cyanobenzoic acid (55.0 mg, 0.376 mmol), DIC (59.0 µL, 0.376 mmol) and 9:1 DCM/DMF (8.4 mL). Elution with 0-0.5% MeOH/DCM afforded **2-77e** as an off-white solid (54.1 mg, 0.219 mmol, 64%). ^{1}H NMR (400 MHz, $CDCl_3$) δ = 8.26 (d, *J* = 8.0 Hz, 2H), 8.14 (dd, *J* = 1.3, 7.8 Hz, 2H), 7.84 (d, *J* = 8.5 Hz, 2H), 7.64 - 7.52 (m, 3H); ^{13}C NMR (101 MHz, $CDCl_3$) δ = 165.3, 163.0, 132.8, 132.2, 129.2, 127.7, 127.3, 127.0, 123.3, 117.8, 115.1; LCMS (formic acid) t_R = 1.09 min, [M+H$^+$] 248.0 (purity 99%).

2-77e is a known compound and the NMR data are consistent with reported literature.[328]

2-Phenyl-5-(pyridin-2-yl)-1,3,4-oxadiazole (2-77f)

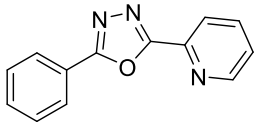

Following the General Flow Procedure using 5-phenyl-1*H*-tetrazole (50.0 mg, 0.342 mmol), 2-picolinic acid (46.0 mg, 0.376 mmol), DIC (59.0 µL, 0.376 mmol) and 9:1 DCM/DMF (8.4 mL). Elution with 0-0.5% MeOH/DCM afforded **2-77f** as a white solid (29.9 mg, 0.134 mmol, 39%). ^{1}H NMR (400 MHz, $CDCl_3$) δ = 8.83 (d, *J* = 4.5 Hz, 1H), 8.33 (d, *J* = 8.0 Hz, 1H), 8.23 (dd, *J* = 1.8, 7.8 Hz, 2H), 7.92 (ddd, *J* = 1.8, 1.8, 7.8 Hz, 1H), 7.60 - 7.51 (m, 3H), 7.49 (ddd, *J* = 1.0, 5.0, 7.5 Hz, 1H); ^{13}C NMR (101 MHz, $CDCl_3$) δ = 165.6, 163.8, 150.3, 143.6, 137.3, 132.0, 129.0, 127.3, 125.8, 123.6, 123.3; LCMS (High pH) t_R = 0.90 min, [M+H$^+$] 224.0 (purity 100%).

2-77f is a known compound and the NMR data are consistent with reported literature.[200,220]

2-(Furan-2-yl)-5-phenyl-1,3,4-oxadiazole (2-77g)

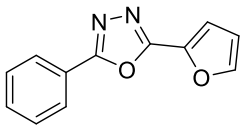

Following the General Flow Procedure using 5-phenyl-1*H*-tetrazole (50.0 mg, 0.342 mmol), furan-2-carboxylic acid (42.0 mg, 0.376 mmol), DIC (59.0 µL, 0.376 mmol) and 9:1 DCM/DMF (8.4 mL). Elution with 0-0.5% MeOH/DCM afforded **2-77g** as a yellow solid (39.0 mg, 0.184 mmol, 54%). ^{1}H NMR (400 MHz, $CDCl_3$) δ = 8.13 (dd, *J* = 1.8, 7.8 Hz, 2H), 7.68 (m, 1H), 7.59 - 7.50 (m, 3H), 7.24 (d, *J* = 3.5 Hz, 1H), 6.63 (dd, *J* = 1.5, 3.5 Hz, 1H); ^{13}C NMR (101 MHz, $CDCl_3$) δ = 163.9, 157.4, 145.7, 139.5, 131.8, 129.1, 127.0, 123.5, 114.1, 112.2; LCMS (High pH) t_R = 1.02 min, [M+H$^+$] 213.0 (purity 100%).

2-77g is a known compound and the NMR data are consistent with reported literature.[220]

2-(3-Bromophenyl)-5-phenyl-1,3,4-oxadiazole (2-77h)

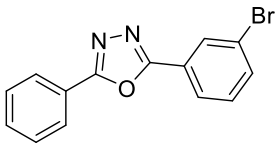

Following the General Flow Procedure using 5-phenyl-1*H*-tetrazole (50.0 mg, 0.342 mmol), 3-bromobenzoic acid (76.0 mg, 0.376 mmol), DIC (59.0 µL, 0.376 mmol) and 9:1 DCM/DMF (8.4 mL). Elution with 5% EtOAc/40-60 °C petroleum ether afforded **2-77h** as a white solid (74.1 mg, 0.246 mmol, 72%). ^{1}H NMR (400 MHz, $CDCl_3$) δ = 8.28 (app. t, *J* = 1.8 Hz, 1H), 8.17 - 8.12 (m, 2H), 8.09 (m, 1H), 7.68 (m, 1H), 7.60 - 7.52 (m, 3H), 7.42 (app. t, *J* = 7.8 Hz, 1H); ^{13}C NMR (101 MHz, $CDCl_3$) δ = 164.9, 163.2, 134.6, 131.9, 130.6, 129.7, 129.1, 127.0, 125.7, 125.4, 123.6, 123.1; LCMS (High pH) t_R = 1.32 min, [M+H$^+$] = 300.9 and 302.9 (purity 100%).

2-77h is a known compound and the NMR data are consistent with reported literature.[330]

2-(4-Bromophenyl)-5-phenyl-1,3,4-oxadiazole (2-77i)

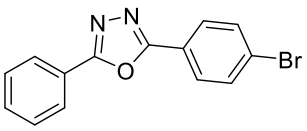

Following the General Flow Procedure using 5-phenyl-1*H*-tetrazole (50.0 mg, 0.342 mmol), 4-bromobenzoic acid (76.0 mg, 0.376 mmol), DIC (59.0 µL, 0.376 mmol) and 9:1 DCM/DMF (8.4 mL). Elution with 0-0.5% MeOH/DCM afforded **2-77i** as a white solid (52.1

mg, 0.173 mmol, 50%). ^{1}H NMR (400 MHz, $CDCl_3$) δ = 8.13 (dd, *J* = 1.8, 7.8 Hz, 2H), 8.04 - 7.98 (m, 2H), 7.71 - 7.65 (m, 2H), 7.59 - 7.49 (m, 3H); ^{13}C NMR (101 MHz, $CDCl_3$) δ = 164.7, 163.8, 132.4, 131.8, 129.1, 128.3, 126.9, 126.4, 123.7, 122.8; LCMS (High pH) t_R = 1.31 min, [M+H$^+$] 300.9 and 302.9 (purity 98%).

2-77i is a known compound and the NMR data are consistent with reported literature.[328]

2-Phenyl-5-(*p*-tolyl)-1,3,4-oxadiazole (2-77j)

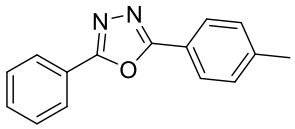

Following the General Flow Procedure using 5-phenyl-1*H*-tetrazole (50.0 mg, 0.342 mmol), 4-methylbenzoic acid (51.0 mg, 0.376 mmol), DIC (59.0 µL, 0.376 mmol) and 9:1 DCM/DMF (8.4 mL). Elution with 0-0.5% MeOH/DCM afforded **2-77j** as a white solid (56.0 mg, 0.237 mmol, 69%). ^{1}H NMR (400 MHz, $CDCl_3$) δ 8.17 - 8.13 (m, 2H), 8.04 (dd, *J* = 2.0, 8.5 Hz, 2H), 7.58 - 7.50 (m, 3H), 7.35 (dd, *J* = 1.8, 8.3 Hz, 2H), 2.45 (d, *J* = 2.5 Hz, 3H); ^{13}C NMR (101 MHz, $CDCl_3$) δ = 164.7, 164.3, 142.2, 131.6, 129.7, 129.0, 126.9, 124.0, 121.2, 21.6 1C not observed; LCMS (High pH) t_R = 1.25 min, [M+H$^+$] 237.0 (97% purity).

2-77j is a known compound and the NMR data are consistent with reported literature.[220]

2-Phenyl-5-(*m*-tolyl)-1,3,4-oxadiazole (2-77k)

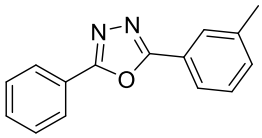

Following the General Flow Procedure using 5-phenyl-1*H*-tetrazole (50.0 mg, 0.342 mmol), 3-methylbenzoic acid (51.0 mg, 0.376 mmol), DIC (59.0 µL, 0.376 mmol) and 9:1 DCM/DMF (8.4 mL). Elution with 2% EtOAc/40-60 °C petroleum ether afforded **2-77k** as a white solid (62.1 mg, 0.263 mmol, 77%). ^{1}H NMR (400 MHz, $CDCl_3$) δ = 8.19 - 8.11 (m, 2H), 7.97 (s, 1H), 7.94 (d, *J* = 7.5 Hz, 1H), 7.59 - 7.51 (m, 3H), 7.42 (app. t, *J* = 7.5 Hz, 1H), 7.36 (d, *J* = 7.5 Hz, 1H), 2.46 (s, 3H); ^{13}C NMR (101 MHz, $CDCl_3$) δ = 164.7, 164.5, 138.9, 132.5, 131.6, 129.0, 128.9, 127.4, 126.9, 124.1, 124.0, 123.8, 21.3; LCMS (High pH) t_R = 1.26 min, [M+H$^+$] 237.0 (purity 100%).

2-77k is a known compound and the NMR data are consistent with reported literature.[329]

2-Phenyl-5-(*o*-tolyl)-1,3,4-oxadiazole (2-77l)

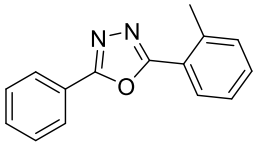

Following the General Flow Procedure using 5-phenyl-1*H*-tetrazole (50.0 mg, 0.342 mmol), 2-methylbenzoic acid (51.0 mg, 0.376 mmol), DIC (59.0 µL, 0.376 mmol) and 9:1 DCM/DMF (8.4 mL). Elution with 0-0.5% MeOH/DCM afforded **2-77l** as a white solid (70.9 mg, 0.300 mmol, 88%). ^{1}H NMR (500 MHz, $CDCl_3$) δ = 8.17 - 8.13 (m, 2H), 8.06 - 8.04 (m, 1H), 7.58 - 7.52 (m, 3H), 7.44 (m, 1H), 7.39 - 7.34 (m, 2H), 2.78 (s, 3H); ^{13}C NMR (101 MHz, $CDCl_3$) δ = 164.8, 164.1, 138.4, 131.8, 131.6, 131.2, 129.1, 128.9, 126.9, 126.1, 124.0, 123.0, 22.1; LCMS (High pH) t_R = 1.26 min, [M+H$^+$] 237.0 (purity 100%).

2-77l is a known compound and the NMR data are consistent with reported literature.[200]

2-Benzyl-5-phenyl-1,3,4-oxadiazole (2-77m)

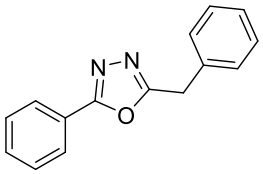

Following the General Flow Procedure using 5-phenyl-1*H*-tetrazole (57.0 mg, 0.390 mmol), 2-phenylacetic acid (59.0 mg, 0.433 mmol), DIC (67.0 µL, 0.433 mmol) and 9:1 DCM/DMF (9.6 mL). Elution with 0-0.5% MeOH/DCM afforded **2-77m** as a white solid (74.9 mg, 0.317 mmol, 93%). ^{1}H NMR (400 MHz, $CDCl_3$) δ = 8.05-7.99 (m, 2H), 7.57 - 7.46 (m, 3H), 7.41 - 7.29 (m, 5H), 4.31 (s, 2H); ^{13}C NMR (101 MHz, $CDCl_3$) δ = 165.2, 165.2, 133.9, 131.6, 128.9, 128.9, 128.8, 127.5, 126.8, 123.9, 31.9; LCMS (High pH) t_R = 1.12 min, [M+H$^+$] 237.0 (purity 100%).

Gram-scale synthesis of 2-77m. 5-Phenyl-1*H*-tetrazole (1.00 g, 6.84 mmol) and phenylacetic acid (1.02 g, 7.52 mmol) were dissolved in DCM/DMF (9:1, 167 mL). DIC (1.16 mL, 7.52 mmol) was then added and the reaction mixture irradiated in flow for 4.5 h. The reaction mixture was concentrated *in vacuo* before being dissolved in EtOAc (50 mL). This was washed with water (50 mL) and 5% aqueous LiCl solution (2 × 100 mL) before being dried using a hydrophobic frit and concentrated *in vacuo*. The crude solid was dissolved in DCM (20 mL) and filtered. The filtrate was concentrated *in vacuo* and the resulting solid purified by flash column chromatography. Elution with 0-0.5% MeOH/DCM afforded **2-77m** as an off-white solid (1.31 g, 5.52 mmol, 81%).

2-77m is a known compound and the NMR data are consistent with reported literature.[200]

2-(But-3-en-1-yl)-5-phenyl-1,3,4-oxadiazole (2-77n)

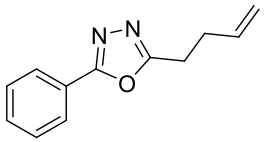

Following the General Flow Procedure using 5-phenyl-1*H*-tetrazole (50.0 mg, 0.342 mmol), pent-4-enoic acid (38.0 µL, 0.376 mmol), DIC (59.0 µL, 0.376 mmol) and 9:1 DCM/DMF (8.4 mL). Elution with 5% EtOAc/40-60 °C petroleum ether afforded **2-77n** as a pale yellow oil (43.2 mg, 0.215 mmol, 63%). ^{1}H NMR (500 MHz, $CDCl_3$) δ = 8.07 - 8.02 (m, 2H), 7.56 - 7.48 (m, 3H), 5.91 (tdd, *J* = 6.4, 10.3, 17.1 Hz, 1H), 5.15 (tdd, *J* = 1.6, 1.6, 17.2 Hz, 1H), 5.09 (tdd, *J* = 1.4, 1.4, 10.3 Hz, 1H), 3.05 (t, *J* = 7.6 Hz, 2H), 2.65 - 2.60 (m, 2H); ^{13}C NMR (101 MHz, $CDCl_3$) δ = 166.3, 164.8, 135.7, 131.5, 129.0, 126.8, 124.0, 116.6, 30.4, 25.0; LCMS (High pH) t_R = 1.05 min, [M+H$^+$] 201.0 (purity 100%); HRMS (High pH) t_R = 7.72 min, [M+H$^+$] calculated for $C_{12}H_{13}N_2O$ 201.1022, found 201.1029; IR (neat) ν_{max} = 1572, 1553, 707, 689 cm^{-1}.

2-Butyl-5-phenyl-1,3,4-oxadiazole (2-77o)

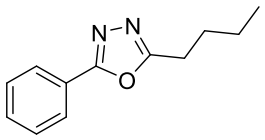

Following the general procedure using 5-phenyl-1*H*-tetrazole (50.0 mg, 0.342 mmol), pentanoic acid (41.0 µL, 0.376 mmol), DIC (59.0 µL, 0.376 mmol) and 9:1 DCM/DMF (8.4 mL). Elution with 0-0.5% MeOH/DCM afforded **2-77o** as a yellow oil (52.2 mg, 0.257 mmol, 75%). ^{1}H NMR (400 MHz, $CDCl_3$) δ = 8.07 - 8.00 (m, 2H), 7.57 - 7.46 (m, 3H), 2.93 (t, *J* = 8.0 Hz, 2H), 1.84 (quin., *J* = 7.5 Hz, 2H), 1.52 – 1.43 (m, 2H), 0.98 (t, *J* = 7.5 Hz, 3H); ^{13}C NMR (101 MHz, $CDCl_3$) δ = 167.0, 164.7, 131.4, 129.0, 126.7, 124.1, 28.6, 25.1, 22.1, 13.6; LCMS (High pH) t_R = 1.13 min, [M+H$^+$] 203.0 (purity 98%).

2-77o is a known compound and the NMR data are consistent with reported literature.[200]

***tert*-Butyl ((5-phenyl-1,3,4-oxadiazol-2-yl)methyl)carbamate (2-77p)**

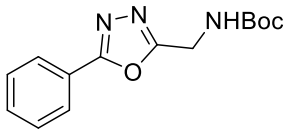

Following the General Flow Procedure using 5-phenyl-1*H*-tetrazole (50.0 mg, 0.342 mmol), (*tert*-butoxycarbonyl)glycine (66.0 mg, 0.376 mmol), DIC (59.0 µL, 0.376 mmol) and 9:1 DCM/DMF (8.4 mL). Elution with 10% EtOAc/DCM afforded **2-77p** as a colourless oil which solidified at RT (83.1 mg, 0.301 mmol, 88%). ^{1}H NMR (400 MHz, $CDCl_3$) δ = 8.05 - 8.00 (m, 2H), 7.56 - 7.45 (m, 3H), 5.37 (br s, 1H), 4.63 (br d, *J* = 5.5 Hz, 2H), 1.47 (s, 9H); ^{13}C NMR (101 MHz, $CDCl_3$) δ = 165.2, 163.9, 155.4, 131.8, 129.0, 126.9, 123.6, 80.5, 35.9, 28.2; LCMS (High pH) t_R = 0.98 min, [M+H$^+$] 276.1 (purity 100%); HRMS (High pH) t_R = 7.38 min, [M+2H]$^+$-*t*Bu calculated for $C_{10}H_{10}N_3O_3$ 220.0717, found 220.0719; IR (neat) ν_{max} = 3352, 2972, 1710, 1510, 1248, 1160 cm^{-1}.

***tert*-Butyl ((1*S*,2*S*)-2-methyl-1-(5-phenyl-1,3,4-oxadiazol-2-yl)butyl)carbamate (2-77q)**

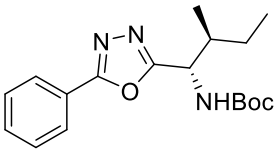

Following the General Flow Procedure using 5-phenyl-1*H*-tetrazole (50.0 mg, 0.342 mmol), (*tert*-butoxycarbonyl)-*L*-isoleucine (87.0 mg, 0.376 mmol), DIC (59.0 µL, 0.376 mmol) and 9:1 DCM/DMF (8.4 mL). Elution with 2.5% EtOAc/DCM afforded **2-77q** as a pale yellow oil (81.0 mg, 0.244 mmol, 71%). ^{1}H NMR (400 MHz, DMSO-*d*$_6$) δ = 8.01 - 7.94 (m, 2H), 7.71 (br d, *J* = 8.3 Hz, 1H), 7.66 - 7.57 (m, 3H), 4.75 (br t, *J* = 7.9 Hz, 1H), 1.98 (m, 1H), 1.52 (m, 1H), 1.38 (s, 8H), 1.30 - 1.21 (m, 2H), 0.88 (t, *J* = 7.4 Hz, 3H), 0.83 (d, *J* = 6.8 Hz, 3H); ^{13}C NMR (101 MHz, DMSO-*d*$_6$) δ = 166.3, 163.9, 155.3, 132.0, 129.4, 126.4, 123.3, 78.6, 51.4, 37.0, 28.1, 24.9, 15.2, 10.8; LCMS (High pH) t_R = 1.27 min, [M+H$^+$] 332.1 (purity 100%); HRMS (High pH) t_R = 10.24 min, [M+2H]$^+$-^{t}Bu calculated for $C_{14}H_{18}N_3O_3$ 276.1343, found 276.1342; IR (neat) ν_{max} = 3242, 2969, 1706, 1250, 1163 cm^{-1}.

(9*H*-Fluoren-9-yl)methyl (*S*)-(2-(5-phenyl-1,3,4-oxadiazol-2-yl)hept-6-en-2-yl)carbamate (2-77r)

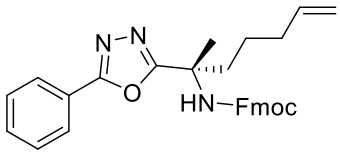

Following the General Flow Procedure using 5-phenyl-1*H*-tetrazole (55.0 mg, 0.375 mmol), (*S*)-2-((((9*H*-fluoren-9-yl)methoxy)carbonyl)amino)-2-methylhept-6-enoic acid (157 mg, 0.413 mmol), DIC (64.0 µL, 0.413 mmol) and 9:1 DCM/DMF (9.2 mL). Elution with 0-5% EtOAc/DCM afforded **2-77r** as a yellow oil (72.0 mg, 0.150 mmol, 40%). ^{1}H NMR (400 MHz, DMSO-d_6) δ = 8.17 - 8.00 (br s, 1H), 7.94 - 7.82 (m, 4H), 7.69 (br d, *J* = 6.1 Hz, 2H), 7.64 - 7.51 (m, 3H), 7.44 - 7.24 (m, 4H), 5.76 (tdd, *J* = 6.6, 10.3, 17.1 Hz, 1H), 5.03 - 4.90 (m, 2H), 4.35 - 4.13 (m, 3H), 2.14 - 1.88 (m, 4H), 1.64 (br s, 3H), 1.47 - 1.27 (m, 2H); ^{13}C NMR (101 MHz, DMSO-d_6) δ = 169.6, 163.5, 154.8, 143.7 (m, 1C), 140.7, 138.3, 131.9, 129.4, 127.6, 127.0, 126.3, 125.1, 123.4, 120.1, 115.0, 65.3, 53.5, 46.6, 37.6, 33.0, 23.5, 22.1; LCMS (High pH) t_R = 1.47 min, [M+H$^+$] 480.2 (purity 100%); HRMS (formic acid) t_R = 6.96 min, [M+H$^+$] calculated for $C_{30}H_{30}N_3O_3$ 480.2282, found 480.2291; IR (neat) ν_{max} = 3317, 2941, 1448, 1247 cm^{-1}.

1,3-Bis(5-phenyl-1,3,4-oxadiazol-2-yl)benzene (2-77s)

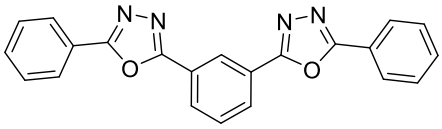

5-phenyl-1*H*-tetrazole (50.0 mg, 0.342 mmol) and isophthalic acid (26.0 mg, 0.155 mmol) were dissolved in DCM/DMF (8:2, 8.4 mL). DIC (53.0 µL, 0.342 mmol) was added and the reaction mixture irradiated in flow for 2 h. The reaction mixture was then collected and concentrated in vacuo before being dissolved in EtOAc (20 mL). This was washed with water (10 mL) and 5% aqueous LiCl solution (2 × 20 mL). DCM (10 mL) was added to the collected organics to dissolve the precipitate before this was dried using a hydrophobic frit and concentrated in vacuo. The crude product was purified by flash column chromatography (0-0.5% MeOH/DCM) to afford **2-77s** as an off-white solid (27.2 mg, 0.074 mmol, 48%). ^{1}H NMR (400 MHz, $CDCl_3$) δ = 8.88 (t, *J* = 1.5 Hz, 1H), 8.35 (dd, *J* = 1.8, 7.8 Hz, 2H), 8.23 - 8.17 (m, 4H), 7.74 (t, *J* = 7.8 Hz, 1H), 7.63-7.54 (m, 6H); ^{13}C NMR (101 MHz, $CDCl_3$) δ = 165.1, 163.6, 132.0, 130.0, 129.8, 129.2, 127.1, 125.1, 125.0, 123.6; LCMS (High pH) t_R = 1.32 min, [M+H$^+$] 367.0 (purity 99%).

2-77s is a known compound and the NMR data are consistent with reported literature.[307]

2-Methyl-5-phenyl-1,3,4-oxadiazole (2-77t) – *Conditions adapted from Kappe and Reichart*

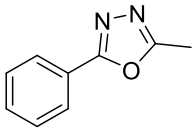

5-Phenyl-1*H*-tetrazole (100 mg, 0.684 mmol) and acetic anhydride (130 µL, 1.37 mmol) were dissolved in DME (8.6 mL). The reaction mixture was pumped through the flow system for 1 h. Water (2 mL) was added and this stirred for 1 h before being concentrated to dryness. The resulting solid was washed with 2 M aqueous NaOH and filtered. The collected solid was washed with 2 M aqueous NaOH and water several times before being left over vacuum to give **2-77t** as an off-white solid (86.4 mg, 0.537 mmol, 78%). ^{1}H NMR (400 MHz, $CDCl_3$) δ = 8.04 - 8.00 (m, 2H), 7.54 - 7.46 (m, 3H), 2.61 (s, 3H); ^{13}C NMR (101 MHz, $CDCl_3$) δ = 164.8, 163.6, 131.5, 129.0, 126.7, 123.9, 11.0; LCMS (High pH) t_R = 0.79 min, [M+H$^+$] 161.0 (purity 100%).

2-77t is a known compound and the NMR data are consistent with reported literature.[245]

18.7.2. Unsuccessful Carboxylic Acid Substrates

4-Hydroxybenzoic acid (2-89)

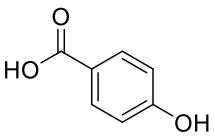

Following the General Flow Procedure using 5-phenyl-1*H*-tetrazole (50.0 mg, 0.342 mmol), 4-hydroxybenzoic acid (52.0 mg, 0.376 mmol), DIC (59.0 µL, 0.376 mmol) and 9:1 DCM/DMF (8.4 mL). Several spots present by crude TLC and attempted purification by flash column chromatography (20% EtOAc/40-60 °C petroleum ether) gave none of the desired product.

Trifluoroacetic acid (2-90)

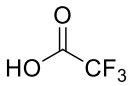

Following the General Flow Procedure using 5-phenyl-1*H*-tetrazole (50.0 mg, 0.342 mmol), trifluoroacetic acid (29.0 µL, 0.376 mmol), DIC (59.0 µL, 0.376 mmol) and 9:1 DCM/DMF (8.4 mL). Elution with 5% DCM/MeOH gave none of the desired product.

2,6-Dimethylbenzoic acid (2-91)

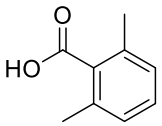

Following the General Flow Procedure using 5-phenyl-1*H*-tetrazole (59.0 mg, 0.404 mmol), 2,6-dimethylbenzoic acid (67.0 mg, 0.444 mmol), DIC (68.0 µL, 0.444 mmol) and 9:1 DCM/DMF (8.4 mL). Purification by flash column chromatography (0-0.4% DCM/MeOH) gave 2-(2,6-dimethylphenyl)-5-phenyl-1,3,4-oxadiazole as a colourless oil (10.0 mg, 0.040 mmol, 12%). ^{1}H NMR (400 MHz, $CDCl_3$) δ = 8.15 - 8.10 (m, 2H), 7.60 - 7.51 (m, 3H), 7.35 (m, 1H), 7.19 (d, *J* = 7.53 Hz 2H), 2.38 - 2.34 (s, 6H); ^{13}C NMR (101 MHz, $CDCl_3$) δ = 165.0, 163.7, 138.9, 131.8, 130.9, 129.1, 128.0, 126.9, 124.1, 124.0, 20.5; LCMS (High pH) t_R = 1.28 min, [M+H$^+$] 251.1 (purity 78%).

2-(2,6-dimethylphenyl)-5-phenyl-1,3,4-oxadiazole is a known compound and the NMR data are consistent with reported literature.[331]

4-(Dimethylamino)benzoic acid (2-92)

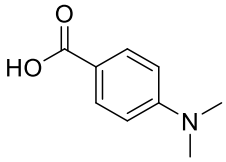

Following the General Flow Procedure using 5-phenyl-1*H*-tetrazole (50.0 mg, 0.342 mmol), 4-(dimethylamine)benzoic acid (62.0 mg, 0.376 mmol), DIC (59.0 µL, 0.376 mmol) and 9:1 DCM/DMF (8.4 mL). Elution with 0-1% MeOH/DCM gave *N*,*N*-dimethyl-4-(5-phenyl-1,3,4-oxadiazol-2-yl)aniline as a yellow oil (12.0 mg, 0.045 mmol, 13%). ^{1}H NMR contained several impurities. ^{1}H NMR (500 MHz, DMSO-d_6) δ = 8.22 - 8.16 (m, 2H), 8.07 - 8.01 (m, 2H), 7.64 - 7.60 (m, 3H), 6.90 - 6.85 (m, 2H), 3.12 (s, 6H).

N,*N*-dimethyl-4-(5-phenyl-1,3,4-oxadiazol-2-yl)aniline is a known compound and the proton NMR data agrees with reported literature but also contains impurities.[332]

1*H*-indole-3-carboxylic acid (2-93)

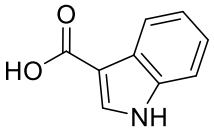

Following the General Flow Procedure using 5-phenyl-1*H*-tetrazole (50.0 mg, 0.342 mmol), 1*H*-indole-3-carboxylic acid (61.0 mg, 0.376 mmol), DIC (59.0 µL, 0.376 mmol) and 9:1 DCM/DMF (8.4 mL). Several spots present by crude TLC and attempted purification by flash column chromatography (20-25% EtOAc/40-60 °C petroleum ether) gave none of the desired product.

1-methyl-1*H*-indole-5-carboxylic acid (2-94)

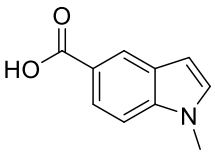

Following the General Flow Procedure using 5-phenyl-1*H*-tetrazole (50.0 mg, 0.342 mmol), 1-methyl-1*H*-indole-5-carboxylic acid (66.0 mg, 0.376 mmol), DIC (59.0 µL, 0.376 mmol) and 9:1 DCM/DMF (8.4 mL). Several spots present by crude TLC and attempted purification by flash column chromatography (25% EtOAc/40-60 °C petroleum ether) gave none of the desired product and caused decomposition of the crude mixture.

18.7.3. Tetrazole Substrate Scope

2,5-Bis(4-methoxyphenyl)-1,3,4-oxadiazole (2-95a)

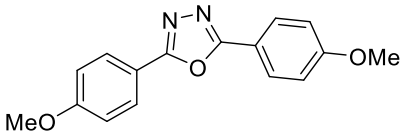

Following the General Flow Procedure using 5-(4-methoxyphenyl)-1*H*-tetrazole (26 mg, 0.148 mmol), 4-methoxybenzoic acid (25 mg, 0.162 mmol), DIC (25 µL, 0.162 mmol) and 9:1 DCM/DMF (3.6 mL). Elution with 0-0.5% MeOH/DCM afforded **2-95a** as a white solid (19 mg, 0.067 mmol, 59%). ^{1}H NMR (400 MHz, $CDCl_3$) δ = 8.08 - 8.02 (m, 4H), 7.05 - 7.00 (m, 4H), 3.89 (s, 6H); ^{13}C NMR (101 MHz, $CDCl_3$) δ = 164.1, 162.2, 128.5, 116.6, 114.4, 55.4; LCMS (High pH) t_R = 1.17 min, [M+H$^+$] 283.0 (purity 97%).

2-95a is a known compound and the NMR data is consistent with reported literature.[328]

2-(2-Methoxyphenyl)-5-(4-methoxyphenyl)-1,3,4-oxadiazole (2-95b)

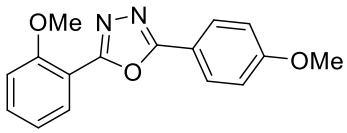

Following the General Flow Procedure using 5-(2-methoxyphenyl)-1*H*-tetrazole (38.0 mg, 0.342 mmol), 4-methoxybenzoic acid (57.0 mg, 0.376 mmol), DIC (59.0 µL, 0.376 mmol) and 9:1 DCM/DMF (8.4 mL). Reverse phase chromatography was undertaken using a Combiflash EZ Prep with a XSelect® CSH™ Prep C18 5 µm OBD™ column and elution with 20-85% MeCN/H_2O + 0.1% ammonium bicarbonate. The fractions containing product were combined and the acetonitrile removed *in vacuo*. The remaining water was washed with DCM (3 × 20 mL) and the organics were combined, dried using a hydrophobic frit and concentrated *in vacuo* to give **2-95b** as a pale yellow oil (33.1 mg, 0.117 mmol, 34%). ^{1}H NMR (400 MHz, $CDCl_3$) δ = 8.09 - 8.04 (m, 2H), 7.99 (dd, *J* = 1.7, 7.6 Hz, 1H), 7.53 - 7.47 (m, 1H), 7.11 - 7.05 (m, 2H), 7.04 - 6.99 (m, 2H), 3.98 (s, 3H), 3.87 (s, 3H); ^{13}C NMR (101 MHz, $CDCl_3$) δ = 164.3, 162.8, 162.1, 157.8, 132.8, 130.3, 128.6, 120.7, 116.7, 114.4, 113.3, 112.0, 56.0, 55.4; LCMS (High pH) t_R = 1.10 min, [M+H$^+$] 283.0 (purity 100%); HRMS (High pH) t_R = 8.52 min, [M+H$^+$] calculated for $C_{16}H_{15}N_2O_3$ 283.1077, found 283.1080; IR (neat) ν_{max} = 2836, 1603, 1498, 1249 cm^{-1}.

2-(4-Methoxyphenyl)-5-(*p*-tolyl)-1,3,4-oxadiazole (2-95c)

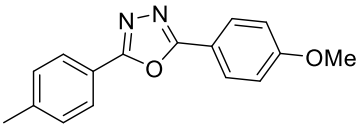

Following the General Flow Procedure using 5-(*p*-tolyl)-1*H*-tetrazole (31.0 mg, 0.194 mmol), 4-methoxybenzoic acid (32.0 mg, 0.213 mmol), DIC (33.0 µL, 0.213 mmol) and 9:1 DCM/DMF (4.7 mL). Elution with 0-0.5% MeOH/DCM afforded **2-95c** as a white solid (37.1 mg, 0.139 mmol, 72%). ^{1}H NMR (400 MHz, $CDCl_3$) δ = 8.09 - 8.04 (m, 2H), 8.00 (d, *J* = 8.5 Hz, 2H), 7.32 (d, *J* = 8.0 Hz, 2H), 7.05 - 6.99 (m, 2H), 3.88 (s, 3H), 2.43 (s, 3H); ^{13}C NMR (101 MHz, $CDCl_3$) δ = 164.2, 162.2, 142.0, 129.7, 128.6, 126.7, 121.3, 116.5, 114.4, 55.4, 21.6 1C not observed; LCMS (High pH) t_R = 1.25 min, [M+H$^+$] 267.0 (purity 100%).

2-95c is a known compound and the NMR data are consistent with reported literature.[220]

2-(4-Methoxyphenyl)-5-(*m*-tolyl)-1,3,4-oxadiazole (2-95d)

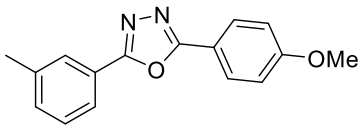

Following the General Flow Procedure using 5-(*m*-tolyl)-1*H*-tetrazole (31.0 mg, 0.194 mmol), 4-methoxybenzoic acid (32.0 mg, 0.213 mmol), DIC (33.0 µL, 0.213 mmol) and 9:1 DCM/DMF (4.7 mL). Elution with 0-0.5% MeOH/DCM gave an impure off-white solid. A second purification using 0.25% MeOH in DCM afforded **2-95d** as a white solid (33.1 mg, 0.124 mmol, 64%). ^{1}H NMR (500 MHz, $CDCl_3$) δ = 8.09 - 8.05 (m, 2H), 7.94 (s, 1H), 7.91 (d, *J* = 7.6 Hz, 1H), 7.40 (app. t, *J* = 7.9 Hz, 1H), 7.34 (d, *J* = 7.9 Hz, 1H), 7.04 - 7.00 (m, 2H), 3.88 (s, 3H), 2.45 (s, 3H); ^{13}C NMR (101 MHz, $CDCl_3$) δ = 164.4, 164.3, 162.3, 138.9, 132.3, 128.9, 128.7, 127.3, 123.9, 123.9, 116.5, 114.5, 55.4, 21.3; LCMS (High pH) t_R = 1.26 min, [M+H$^+$] 267.0 (purity 100%); HRMS (High pH) t_R = 9.89 min, [M+H$^+$] calculated for $C_{16}H_{15}N_2O_2$ 267.1128, found 267.1136; IR (neat) ν_{max} = 1614, 1497, 1254 cm^{-1}.

95d is a known compound and the NMR data are consistent with reported literature.[333]

2-(4-Methoxyphenyl)-5-(*o*-tolyl)-1,3,4-oxadiazole (2-95e)

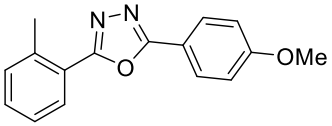

Following the General Flow Procedure using 5-(*o*-tolyl)-1*H*-tetrazole (31.0 mg, 0.194 mmol), 4-methoxybenzoic acid (32.0 mg, 0.213 mmol), DIC (33.0 µL, 0.213 mmol) and 9:1 DCM/DMF (4.7 mL). Elution with 0-0.5% MeOH/DCM afforded **2-95e** as a white solid (37.1 mg, 0.139 mmol, 72%). ^{1}H NMR (500 MHz, $CDCl_3$) δ = 8.10 - 8.05 (m, 2H), 8.02 (d, *J* = 7.9 Hz, 1H), 7.44 - 7.40 (m, 1H), 7.38 - 7.33 (m, 2H), 7.05 - 7.01 (m, 2H), 3.89 (s, 3H), 2.77 (s, 3H); ^{13}C NMR (101 MHz, $CDCl_3$) δ = 164.3, 164.0, 162.3, 138.3, 131.7, 131.0, 128.8, 128.6, 126.1, 123.1, 116.4, 114.5, 55.4, 22.1; LCMS (High pH) t_R = 1.26 min, [M+H$^+$] 267.0 (purity 100%).

2-95e is a known compound and the NMR data are consistent with reported literature.[334]

2-(4-Fluorophenyl)-5-(4-methoxyphenyl)-1,3,4-oxadiazole (2-95f)

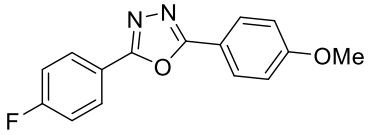

Following the General Flow Procedure using 5-(4-fluorophenyl)-1*H*-tetrazole (31.0 mg, 0.189 mmol), 4-methoxybenzoic acid (32.0 mg, 0.208 mmol), DIC (32.0 µL, 0.208 mmol) and 9:1 DCM/DMF (4.6 mL). Elution with 0-0.5% MeOH/DCM afforded **2-95f** as a white solid (42.0 mg, 0.155 mmol, 82%). ^{1}H NMR (500 MHz, $CDCl_3$) δ = 8.16 - 8.11 (m, 2H), 8.09 - 8.05 (m, 2H), 7.25 - 7.20 (m, 2H), 7.06 - 7.01 (m, 2H), 3.90 (s, 3H); ^{19}F NMR (376 MHz, $CDCl_3$) δ = -107.15 - -107.24 (m); ^{13}C NMR (101 MHz, $CDCl_3$) δ = 164.6, 164.7 (d, $^{1}J_{CF}$ = 253.5 Hz), 163.3, 162.4, 129.1 (d, $^{3}J_{CF}$ = 8.5 Hz), 128.7, 120.4 (d, $^{4}J_{CF}$ = 3.9 Hz), 116.3, 116.4 (d, $^{2}J_{CF}$ = 22.3 Hz), 114.5, 55.5; LCMS (High pH) t_R = 1.19 min. [M+H$^+$] 271.0 (purity 97%).

2-95f is a known compound and the NMR data are consistent with reported literature.[328]

2-(4-Methoxyphenyl)-5-(4-(trifluoromethyl)phenyl)-1,3,4-oxadiazole (2-95g)

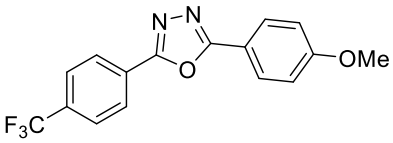

Following the General Flow Procedure 5-(4-(trifluoromethyl)phenyl)-1*H*-tetrazole (31.0 mg, 0.145 mmol), 4-methoxybenzoic acid (24.0 mg, 0.160 mmol), DIC (25.0 µL, 0.160 mmol) and 9:1 DCM/DMF (3.5 mL). Elution with 0-0.5% MeOH/DCM afforded **2-95g** as a white solid (32.1 mg, 0.100 mmol, 69%). ^{1}H NMR (400 MHz, $CDCl_3$) δ = 8.25 (d, *J* = 8.5 Hz, 2H), 8.11 - 8.06 (m, 2H), 7.80 (d, *J* = 8.0 Hz, 2H), 7.07 - 7.02 (m, 2H), 3.90 (s, 3H); ^{19}F NMR (376 MHz, $CDCl_3$) δ = -63.06 (s); ^{13}C NMR (101 MHz, $CDCl_3$) δ = 165.1, 163.0, 162.6, 133.1 (q, $^{2}J_{CF}$ = 32.9 Hz), 128.9, 127.3, 127.1, 126.1 (q, $^{3}J_{CF}$ = 3.9 Hz), 123.6 (q, $^{1}J_{CF}$ = 272.8 Hz), 116.0, 114.6, 55.5; LCMS (High pH) t_R = 1.32 min, [M+H$^+$] 321.0 (purity 98%); HRMS (High pH) t_R = 10.66 min, [M+H$^+$] calculated for $C_{16}H_{12}F_3N_2O_2$ 321.0845, found 321.0850; IR (neat) ν_{max} = 1611, 1495, 1324, 1118 cm^{-1}.

2-(3-Bromophenyl)-5-(4-methoxyphenyl)-1,3,4-oxadiazole (2-95h)

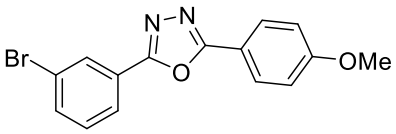

Following the general procedure using from 5-(3-bromophenyl)-1*H*-tetrazole (77.0 mg, 0.342 mmol), 4-methoxybenzoic acid (57.0 mg, 0.376 mmol), DIC (59.0 µL, 0.376 mmol) and 9:1 DCM/DMF (8.4 mL). Following the general procedure. Elution with 0-0.5% MeOH/DCM gave **2-9h** as a white solid (88.0 mg, 0.266 mmol, 78%). ^{1}H NMR (400 MHz, $CDCl_3$) δ = 8.27 (appt. t, *J* = 1.8 Hz, 1H), 8.11 - 8.05 (m, 3H), 7.68 (ddd, *J* = 1.1, 1.9, 8.0 Hz, 1H), 7.41 (appt. t, *J* = 7.9 Hz, 1H), 7.07 - 7.02 (m, 2H), 3.91 (s, 3H); ^{13}C NMR (101 MHz, $CDCl_3$) δ = 164.9, 162.8, 162.5, 134.5, 130.6, 129.6, 128.8, 125.9, 125.3, 123.1, 116.1, 114.6, 55.5; LCMS (High pH) t_R = 1.31 min, [M+H$^+$] 330.9 & 332.9 (purity 100%); HRMS (Formic acid) t_R = 5.84 min, [M+H$^+$] calculated for $C_{15}H_{12}BrN_2O_2$ 331.0077, found 331.0080; IR (neat) ν_{max} = 1616, 1503, 1268 cm^{-1}.

2-(4-Bromophenyl)-5-(4-methoxyphenyl)-1,3,4-oxadiazole (2-95i)

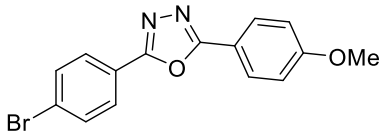

Following the General Flow Procedure 5-(4-bromophenyl)-1*H*-tetrazole (77.0 mg, 0.342 mmol), 4-methoxybenzoic acid (57.0 mg, 0.376 mmol), DIC (59.0 µL, 0.376 mmol) and 9:1 DCM/DMF (8.4 mL). Elution with 0-0.5% MeOH/DCM afforded **2-95i** as a white solid (92.0 mg, 0.278 mmol, 81%). ^{1}H NMR (500 MHz, $CDCl_3$) δ = 8.09 - 8.04 (m, 2H), 8.01 - 7.97 (m, 2H), 7.69 - 7.65 (m, 2H), 7.05 - 7.01 (m, 2H), 3.89 (s, 3H); ^{13}C NMR (101 MHz, $CDCl_3$) δ = 164.6, 163.3, 162.4, 132.3, 128.7, 128.1, 126.1, 122.9, 116.1, 114.5, 55.4; LCMS (High pH) t_R = 1.31 min, [M+H$^+$] 330.9 and 332.8 (purity 98%).

2-95i is a known compound and the NMR data are consistent with reported literature.[328]

2-(4-Methoxyphenyl)-5-(pyridin-2-yl)-1,3,4-oxadiazole (2-95j)

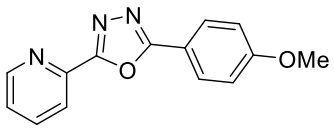

Following the General Flow Procedure using 2-(1*H*-tetrazol-5-yl)pyridine (50.0 mg, 0.340 mmol), 4-methoxybenzoic acid (57.0 mg, 0.376 mmol), DIC (59.0 µL, 0.376 mmol) and 9:1

DCM/DMF (8.4 mL). Elution with 2% MeOH/DCM gave a white solid which was impure. This was recrystallized from hot methanol to afford **2-95j** as a white solid (41.1 mg, 0.162 mmol, 47%). MPt: 154.6-157.3 °C; ^{1}H NMR (500 MHz, $CDCl_3$) δ = 8.79 (br d, *J* = 4.6 Hz, 1H), 8.28 (d, *J* = 7.9 Hz, 1H), 8.16 - 8.11 (m, 2H), 7.88 (ddd, *J* = 1.5, 7.8, 7.8 Hz, 1H), 7.45 (ddd, *J* = 1.1, 4.8, 7.6 Hz, 1H), 7.03 - 6.99 (m, 2H), 3.87 (s, 3H); ^{13}C NMR (101 MHz, $CDCl_3$) δ = 165.5, 163.3, 162.5, 150.1, 143.7, 137.2, 129.1, 125.6, 123.1, 116.0, 114.4, 55.4; LCMS (High pH) t_R = 0.92 min, [M+H$^+$] 254.0 (purity 100%).

2-95j is a known compound and the NMR data are consistent with reported literature.[314]

2-(5-Bromothiophen-2-yl)-5-(4-methoxyphenyl)-1,3,4-oxadiazole (2-95k)

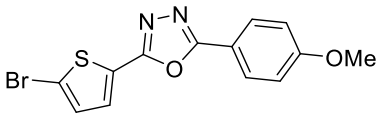

Following the General Flow Procedure using 5-(5-bromothiophen-2-yl)-1*H*-tetrazole (79.0 mg, 0.342 mmol), 4-methoxybenzoic acid (57.0 mg, 0.376 mmol), DIC (59.0 µL, 0.376 mmol) and 9:1 DCM/DMF (8.4 mL). Elution with 0-0.2% MeOH/DCM gave an impure off-white solid. This was further purified eluting with 0-50% TBME/cyclohexane to afford **2-95k** as a white solid (40.0 mg, 0.119 mmol, 36%). ^{1}H NMR (400 MHz, $CDCl_3$) δ = 8.06 - 7.95 (m, 2H), 7.52 (d, *J* = 3.9 Hz, 1H), 7.13 (d, *J* = 3.9 Hz, 1H), 7.04 - 6.98 (m, 2H), 3.88 (s, 3H); ^{13}C NMR (101 MHz, $CDCl_3$) δ = 164.1, 162.5, 159.3, 131.1, 129.5, 128.7, 126.8, 117.7, 116.0, 114.6, 55.5; LCMS (High pH) t_R = 1.31 min, [M+H$^+$] 336.8 and 338.8 (purity 100%); HRMS (High pH) t_R = 10.33 min, [M+H$^+$] calculated for $C_{13}H_{10}BrN_2O_2S$ 336.9641, found 336.9646; IR (neat) ν_{max} = 1614, 1582, 1491, 1265, 1018 cm^{-1}.

2-Cyclopropyl-5-(4-methoxyphenyl)-1,3,4-oxadiazole (2-95l)

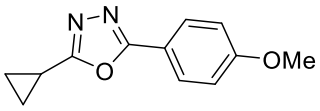

Following the General Flow Procedure using 5-cyclopropyl-1*H*-tetrazole (38.0 mg, 0.342 mmol), 4-methoxybenzoic acid (57.0 mg, 0.376 mmol), DIC (59.0 µL, 0.376 mmol) and 9:1 DCM/DMF (8.4 mL). Reverse phase chromatography was undertaken using a Combiflash EZ Prep with a XSelect® CSH™ Prep C18 5 µm OBD™ column and elution with 20-85% MeCN/H_2O + 0.1% ammonium bicarbonate. The fractions containing product were combined and the acetonitrile removed *in vacuo*. The remaining water was washed with DCM (3 × 20 mL) before being neutralized with ammonium chloride. The aqueous was washed with further DCM (3 × 10 mL). The organics were combined, dried using a

hydrophobic frit and concentrated *in vacuo* to give **2-95l** as a colorless oil (28.0 mg, 0.129 mmol, 38%). ^{1}H NMR (400 MHz, $CDCl_3$) δ = 7.97 - 7.88 (m, 2H), 7.02 - 6.94 (m, 2H), 3.82 (s, 3H), 2.20 (m, 1H), 1.23 - 1.12 (m, 4H); ^{13}C NMR (101 MHz, $CDCl_3$) δ = 167.8, 163.8, 162.0, 128.3, 116.7, 114.4, 55.4, 8.2, 6.4; LCMS (High pH) t_R = 0.95 min, [M+H$^+$] 217.1 (purity 100%); HRMS (High pH) t_R = 6.88 min, [M+H$^+$] calculated for $C_{12}H_{13}N_2O_2$ 217.0972, found 217.0973; IR (neat) ν_{max} = 1614, 1575, 1499, 1252 cm^{-1}.

18.7.4. Unsuccessful Tetrazole Substrates

5-(Ethylthio)-1*H*-tetrazole (2-96)

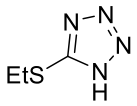

Following the General Flow Procedure using 5-(ethylthio)-1*H*-tetrazole (45.0 mg, 0.342 mmol), 4-methoxybenzoic acid (57.0 mg, 0.376 mmol), DIC (59.0 µL, 0.376 mmol) and 9:1 DCM/DMF (8.4 mL). Attempted purification by flash column chromatography (0-0.2% MeOH/DCM) gave none of the desired product.

5-Benzyl-1*H*-tetrazole (2-97)

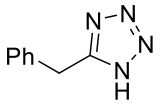

Following the General Flow Procedure using 5-benzyl-1*H*-tetrazole (55.0 mg, 0.342 mmol), 4-methoxybenzoic acid (57.0 mg, 0.376 mmol), DIC (59.0 µL, 0.376 mmol) and 9:1 DCM/DMF (8.4 mL). TLC of the crude mixture showed no evidence of reaction or formation of the desired product.

5-Propyl-1*H*-tetrazole (2-98)

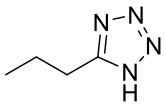

Following the General Flow Procedure using 5-propyl-1*H*-tetrazole (38.0 mg, 0.342 mmol), 4-methoxybenzoic acid (57.0 mg, 0.376 mmol), DIC (59.0 µL, 0.376 mmol) and 9:1 DCM/DMF (8.4 mL). Attempted purification by flash column chromatography (0-0.5% MeOH/DCM) did not give any significant amount of the desired product.

Ethyl 1*H*-tetrazole-5-carboxylate (2-99)

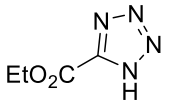

Following the General Flow Procedure using ethyl 1*H*-tetrazole-5-carboxylate (49.0 mg, 0.342 mmol), 4-methoxybenzoic acid (57.0 mg, 0.376 mmol), DIC (59.0 µL, 0.376 mmol) and 9:1 DCM/DMF (8.4 mL). Attempted purification by flash column chromatography (0-0.4% MeOH/DCM) gave 10.0 mg of contaminated product, ethyl 5-(4-methoxyphenyl)-1,3,4-oxadiazole-2-carboxylate. LCMS of this showed 58% purity, meaning very little of the desired product had formed.

18.8. COX-2 Inhibitor

2-(3-(4-Fluorophenyl)-1-phenyl-1*H*-pyrazol-4-yl)-5-phenyl-1,3,4-oxadiazole (2-101)

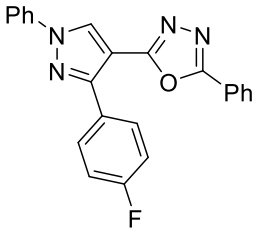

Following the General Flow Procedure using 5-phenyl-1*H*-tetrazole (50.0 mg, 0.342 mmol), 3-(4-fluorophenyl)-1-phenyl-1*H*-pyrazole-4-carboxylic acid (106 mg, 0.376 mmol), DIC (59.0 µL, 0.376 mmol) and 9:1 DCM/DMF (8.4 mL). Elution with 0-0.1% MeOH/DCM afforded **2-101** as a white solid (111 mg, 0.291 mmol, 85%). ^{1}H NMR (400 MHz, $CDCl_3$) δ = 8.68 (s, 1H), 8.02 - 7.96 (m, 4H), 7.86 - 7.82 (m, 2H), 7.58 - 7.48 (m, 5H), 7.43 - 7.38 (m, 1H), 7.24 - 7.17 (m, 2H); ^{19}F NMR (376 MHz, $CDCl_3$) δ = -112.31 - -112.39 (m, 1F); ^{13}C NMR (101 MHz, $CDCl_3$) δ = 164.6, 163.9, 160.9 (d, $^{1}J_{CF}$ = 242.0 Hz), 150.9, 139.1, 131.7, 131.0 (d, $^{3}J_{CF}$ = 8.5 Hz), 129.7, 129.4, 129.1, 127.9 (br d, J = 3.1 Hz), 127.7, 126.7, 123.7, 119.5, 115.3 (br d, $^{2}J_{CF}$ = 21.6 Hz), 106.4; LCMS (High pH) t_R = 1.46 min, [M+H$^+$] 383.1 (purity 99%); HRMS (High pH) t_R = 12.18 min, [M+H$^+$] calculated for $C_{23}H_{16}FN_4O$ 383.1303, found 383.1307; IR (neat) ν_{max} = 3384, 1592, 1510, 1221 cm^{-1}.

2-101 is a known compound and the NMR data are consistent with reported literature.[172,315]

Appendix

X-Ray Crystal Structure Data

Table 31. Selected crystal structure data for furan-containing compounds **1-31**, **1-32** and **1-33**.

Structure	**1-31**	**1-32**	**1-33**
Mol. Formula	$C_{16}H_{16}O_3$	$C_{15}H_{14}O_3$	$C_{15}H_{16}O_3$
Temperature (K)	123(2)	123(2)	123(2)
Wavelength (Å)	1.54184	1.54184	1.54184
Crystal system	Monoclinic	Orthorhombic	Monoclinic
Space group	$P2_1$	$P2_12_12_1$	$P2_{1/c}$
***a* (Å)**	10.9557(5)	6.5942(8)	10.0770(5)
***b* (Å)**	10.1277(6)	8.0249(5)	9.2932(4)
***c* (Å)**	11.7216(7)	22.5968(16)	13.8960(7)
***β* (°)**	98.486(6)	90	100.941(5)
Volume (Å^3)	1286.34(12)	1195.77(18)	1277.67(11)
Z	4	4	4
Theta range (°)	6.766 to 73.171	3.912 to 74.688	4.469 to 69.970
Reflections collected	11882	4029	4600
Independent reflections	5021 [R(int) = 0.0364]	2339 [R(int) = 0.0409]	2418 [R(int) = 0.0442]
No. of parameters	351	167	167
Goodness-of-fit	1.071	1.161	1.034
Final R [I>2σ(I)]	0.0553	0.0495	0.0595
wR2 (all data)	0.1609	0.1727	0.1797
Largest difference peak (eÅ^{-3})	0.290	0.335	0.320
Deepest hole (eÅ^{-3})	-0.203	-0.382	-0.298

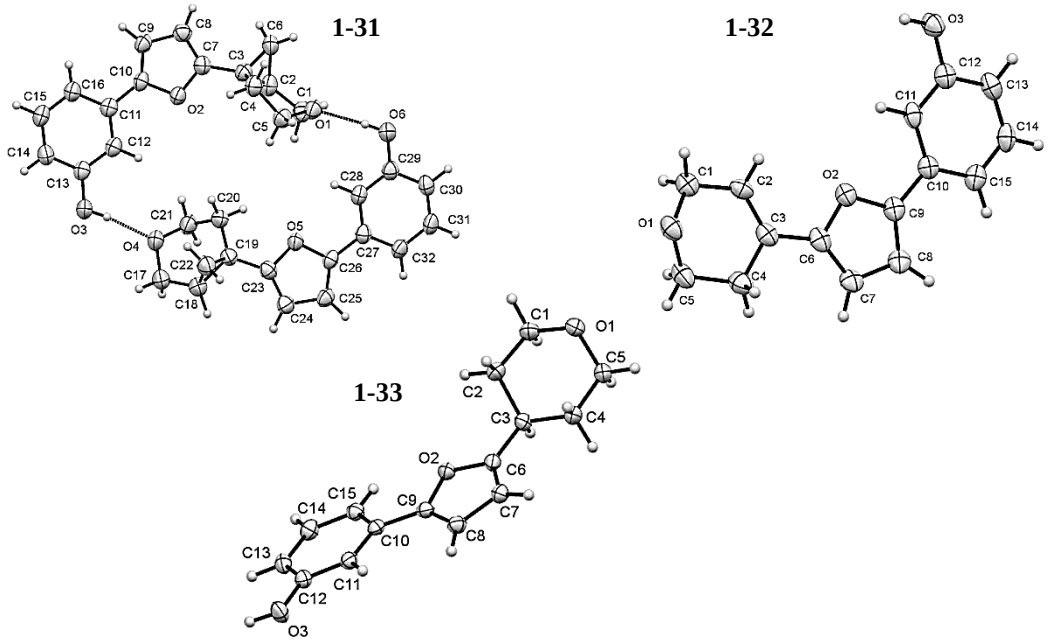

Table 32. Selected crystal structure data for furan-containing compounds **1-34**, **1-35** and **1-76**.

Structure	**1-34**	**1-35**	**1-76**
Mol. Formula	$C_{16}H_{17}NO_2$	$C_{15}H_{15}NO_2$	$C_{15}H_{16}N_2O_3$
Temperature (K)	123(2)	123(2)	123(2)
Wavelength (Å)	1.54184	1.54184	1.54184
Crystal system	Orthorhombic	Monoclinic	Triclinic
Space group	$P2_12_12_1$	$C2/c$	P-1
***a* (Å)**	6.6306(18)	16.8276(4)	7.2367(7)
***b* (Å)**	11.1504(3)	6.2467(2)	8.3700(7)
***c* (Å)**	18.1702(5)	23.2573(5)	10.8552(9)
***β* (°)**	90	102.390(2)	99.631(7)
Volume (Å^3)	1343.4(4)	2387.80(11)	644.55(10)
Z	4	8	2
Theta range (°)	4.653 to 72.975	3.892 to 73.062	5.315 to 73.215
Reflections collected	4513	8007	5799
Independent reflections	2627 [R(int) = 0.0233]	2361 [R(int) = 0.0219]	2527 [R(int) = 0.0156]
No. of parameters	193	172	186
Goodness-of-fit	1.046	1.076	1.063
Final R [I>2σ(I)]	0.0400	0.0387	0.0400
wR2 (all data)	0.1095	0.1054	0.1116
Largest difference peak (eÅ^{-3})	0.195	0.269	0.273
Deepest hole (eÅ^{-3})	-0.203	-0.199	-0.219

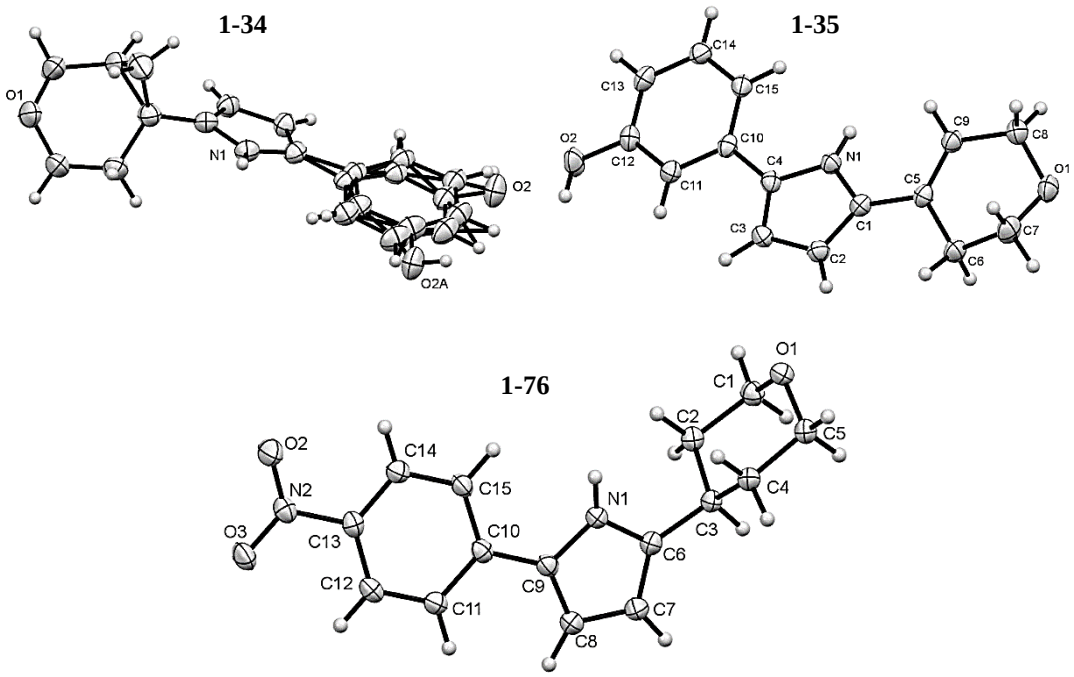

Table 33. Selected crystal structure data for furan-containing compounds **1-37**, **1-38** and **1-39**.

Structure	**1-37**	**1-38**	**1-39**
Mol. Formula	$C_{15}H_{15}NO_3$	$C_{14}H_{13}NO_3$	$C_{14}H_{15}NO_3$
Temperature (K)	123(2)	123(2)	123(2)
Wavelength (Å)	1.54184	1.54184	1.54184
Crystal system	Monoclinic	Monoclinic	Monoclinic
Space group	$P2_1$	$P2_{1/c}$	$P2_1$
***a* (Å)**	10.6195(10)	7.5380(3)	8.5893(8)
***b* (Å)**	10.5061(8)	5.8523(2)	10.3571(7)
***c* (Å)**	11.658(8)	25.4362(12)	13.5731(14)
***β* (°)**	95.043(8)	95.197(4)	95.483(9)
Volume (Å^3)	1294.95(18)	1117.50(8)	1201.94(19)
Z	4	4	4
Theta range (°)	3.808 to 69.942	3.490 to 72.869	5.854 to 69.948
Reflections collected	7825	3771	3753
Independent reflections	4748 [R(int) = 0.0304]	2177 [R(int) = 0.0158]	3753 [R(int) = ?]
No. of parameters	352	167	328
Goodness-of-fit	1.123	1.041	1.005
Final R [I>2σ(I)]	0.0543	0.0435	0.0768
wR2 (all data)	0.1916	0.1262	0.2211
Largest difference peak (eÅ^{-3})	0.438	0.322	0.451
Deepest hole (eÅ^{-3})	-0.305	-0.284	-0.310

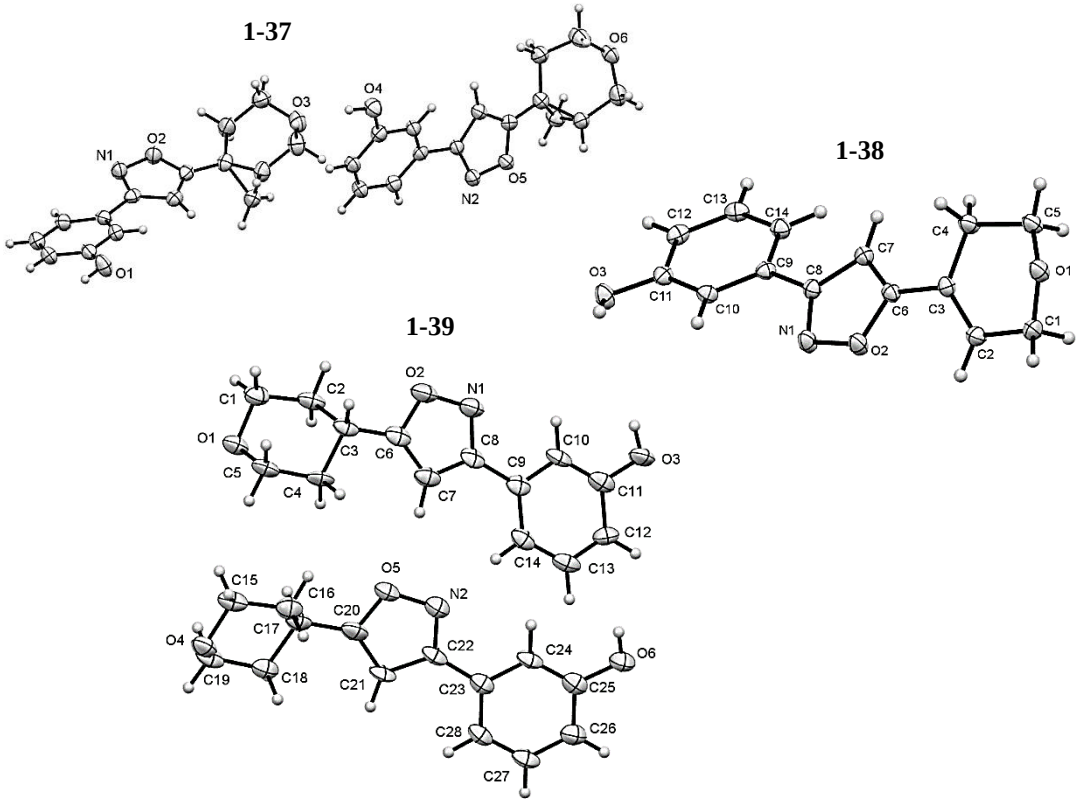

References

1. J. Jampilek, *Molecules*, 2019, **24**, 3839.
2. H. Hobbs, G. Bravi, I. Campbell, M. Convery, H. Davies, G. Inglis, S. Pal, S. Peace, J. Redmond and D. Summers, *J. Med. Chem.*, 2019, **62**, 6972-6984.
3. D. Summers, PhD Thesis, University of Strathclyde, 2019.
4. L. Green, K. Livingstone, S. Bertrand, S. Peace and C. Jamieson, *Chem. Eur. J.*, 2020, **26**, 14866-14870.
5. S. Kumari, A. V. Carmona, A. K. Tiwari and P. C. Trippier, *J. Med. Chem.*, 2020, **63**, 12290-12358.
6. N. A. Meanwell, *J. Med. Chem.*, 2011, **54**, 2529-2591.
7. G. A. Patani and E. J. LaVoie, *Chem. Rev.*, 1996, **96**, 3147-3176.
8. I. Langmuir, *J. Am. Chem. Soc.*, 1919, **41**, 1543-1559.
9. H. Grimm, *Z. Electrochem*, 1925, **31**, 474-480.
10. H. Grimm, *Naturwissenschaften*, 1929, **17**, 557-564.
11. H. Erlenmeyer and M. Leo, *Helv. Chim. Acta*, 1932, **15**, 1171-1186.
12. N. Brown, in *Bioisosteres in Medicinal Chemistry*, 2012, DOI: https://doi.org/10.1002/9783527654307.ch1.
13. H. Erlenmeyer, E. Berger and M. Leo, *Helv. Chim. Acta*, 1933, **16**, 733-738.
14. H. L. Friedman, *NASNRS*, 1951, **206**, 295-358.
15. A. Burger, in *Progress in Drug Research / Fortschritte der Arzneimittelforschung / Progrès des recherches pharmaceutiques*, ed. E. Jucker, Birkhäuser Basel, Basel, 1991, DOI: 10.1007/978-3-0348-7139-6_7, pp. 287-371.
16. C. W. Thornber, *Chem. Soc. Rev.*, 1979, **8**, 563-580.
17. P. K. Mykhailiuk, *Org. Biomol. Chem.*, 2019, **17**, 2839-2849.
18. A. F. Stepan, C. Subramanyam, I. V. Efremov, J. K. Dutra, T. J. O'Sullivan, K. J. DiRico, W. S. McDonald, A. Won, P. H. Dorff, C. E. Nolan, S. L. Becker, L. R. Pustilnik, D. R. Riddell, G. W. Kauffman, B. L. Kormos, L. Zhang, Y. Lu, S. H. Capetta, M. E. Green, K. Karki, E. Sibley, K. P. Atchison, A. J. Hallgren, C. E. Oborski, A. E. Robshaw, B. Sneed and C. J. O'Donnell, *J. Med. Chem.*, 2012, **55**, 3414-3424.
19. S. Pal and G. Bravi, *Unpublished work*.
20. M. W. D. Perry, R. Abdulai, M. Mogemark, J. Petersen, M. J. Thomas, B. Valastro and A. Westin Eriksson, *J. Med. Chem.*, 2019, **62**, 4783-4814.
21. A. D. Bochevarov, E. Harder, T. F. Hughes, J. R. Greenwood, D. A. Braden, D. M. Philipp, D. Rinaldo, M. D. Halls, J. Zhang and R. A. Friesner, *Int. J. Quantum Chem*, 2013, **113**, 2110-2142.
22. A. L. Goodman and R. H. Eastman, *J. Am. Chem. Soc.*, 1964, **86**, 908-911.
23. S. W. Staley, *J. Am. Chem. Soc.*, 1967, **89**, 1532-1533.
24. A. D. Walsh, *Trans. Faraday Soc.*, 1949, **45**, 179-190.
25. S. K. Hanks and T. Hunter, *FASEB J.*, 1995, **9**, 576-596.
26. G. Manning, D. B. Whyte, R. Martinez, T. Hunter and S. Sudarsanam, *Science*, 2002, **298**, 1912.
27. K. C. Duong-Ly and J. R. Peterson, *Curr. Protoc. Pharmacol.*, 2013, **60**, 2.9.1-2.9.14.
28. M. E. M. Noble, J. A. Endicott and L. N. Johnson, *Science*, 2004, **303**, 1800.
29. S. W. Cowan-Jacob, H. Möbitz and D. Fabbro, *Curr. Opin. Cell Biol.*, 2009, **21**, 280-287.
30. S. Cheek, H. Zhang and N. V. Grishin, *J. Mol. Biol.*, 2002, **320**, 855-881.
31. D. Fabbro, *Mol. Pharmacol.*, 2015, **87**, 766-775.
32. J. Kaplan, J. C. Verheijen, N. Brooijmans, L. Toral-Barza, I. Hollander, K. Yu and A. Zask, *Bioorg. Med. Chem. Lett.*, 2010, **20**, 640-643.

33. C. A. Ramsden and V. Milata, in *Adv. Heterocycl. Chem.*, ed. A. R. Katritzky, Academic Press, 2006, vol. 92, pp. 1-54.
34. A. Modelli and P. D. Burrow, *J. Phys. Chem. A*, 2004, **108**, 5721-5726.
35. S. S. Batsanov, *Inorg. Mater.*, 2001, **37**, 871-885.
36. A. de Meijere, *Angew. Chem. Int. Ed.*, 1979, **18**, 809-826.
37. N. A. Meanwell, in *Adv. Heterocycl. Chem.*, eds. E. F. V. Scriven and C. A. Ramsden, Academic Press, 2017, vol. 123, pp. 245-361.
38. A. M. Jawalekar, E. Reubsaet, F. P. J. T. Rutjes and F. L. van Delft, *Chem. Commun.*, 2011, **47**, 3198-3200.
39. A. P. Degnan, D. Maxwell, M. D. Hill, H. Fang, M. F. Parker, F. Yang, J. J. Bronson and J. E. Macor, *US20120283264, 2015*
40. J. S. Alford, J. E. Spangler and H. M. L. Davies, *J. Am. Chem. Soc.*, 2013, **135**, 11712-11715.
41. B. T. Parr and H. M. L. Davies, *Angew. Chem. Int. Ed.*, 2013, **52**, 10044-10047.
42. E. Shirakawa, T. Sato, Y. Imazaki, T. Kimura and T. Hayashi, *Chem. Commun.*, 2007, 4513-4515.
43. GVK-BIO, *Unpublished work*, 2017.
44. H. E. Simmons and R. D. Smith, *J. Am. Chem. Soc.*, 1958, **80**, 5323-5324.
45. J. Furukawa, N. Kawabata and J. Nishimura, *Tetrahedron*, 1968, **24**, 53-58.
46. A. J. J. Lennox and G. C. Lloyd-Jones, *Angew. Chem. Int. Ed.*, 2012, **51**, 9385-9388.
47. M. R. Harris, Q. Li, Y. Lian, J. Xiao and A. T. Londregan, *Org. Lett.*, 2017, **19**, 2450-2453.
48. A. J. J. Lennox and G. C. Lloyd-Jones, *J. Am. Chem. Soc.*, 2012, **134**, 7431-7441.
49. D. Leonori and V. K. Aggarwal, *Angew. Chem. Int. Ed.*, 2015, **54**, 1082-1096.
50. E. Hortense, S. Jackson, R. Briers and E. Clarke, *Unpublished work*.
51. P. S. Campbell, C. Jamieson, I. Simpson and A. J. B. Watson, *Chem. Commun.*, 2018, **54**, 46-49.
52. T. Kinzel, Y. Zhang and S. L. Buchwald, *J. Am. Chem. Soc.*, 2010, **132**, 14073-14075.
53. D. S. Surry and S. L. Buchwald, *Angew. Chem. Int. Ed.*, 2008, **47**, 6338-6361.
54. D. M. Knapp, E. P. Gillis and M. D. Burke, *J. Am. Chem. Soc.*, 2009, **131**, 6961-6963.
55. B. S. Lamb and P. Kovacic, *J. Polym. Sci., Polym. Chem. Ed.*, 1980, **18**, 1759-1770.
56. A. Modvig, T. L. Andersen, R. H. Taaning, A. T. Lindhardt and T. Skrydstrup, *J. Org. Chem.*, 2014, **79**, 5861-5868.
57. S. Müller, B. Liepold, G. J. Roth and H. J. Bestmann, *Synlett*, 1996, **6**, 521-522.
58. S. Ohira, *Synth. Commun.*, 1989, **19**, 561-564.
59. X. Ban, Y. Pan, Y. Lin, S. Wang, Y. Du and K. Zhao, *Org. Biomol. Chem.*, 2012, **10**, 3606-3609.
60. K. Wang, X. Fu, J. Liu, Y. Liang and D. Dong, *Org. Lett.*, 2009, **11**, 1015-1018.
61. A. Kennedy, *Unpublished work*, 2018.
62. D. Niu, R. C. Petter, J. Singh, A. F. Kluge, H. Mazdiyasni, Z. Zhu, L. Qiao and K. Kuntz, *WO2011031896A2, 2011*
63. C. Abad-Zapatero, O. Perišić, J. Wass, A. P. Bento, J. Overington, B. Al-Lazikani and M. E. Johnson, *Drug Discov. Today*, 2010, **15**, 804-811.
64. M. S. Miller, P. E. Thompson and S. B. Gabelli, *Biomolecules*, 2019, **9**, 82.
65. J. M. Murray, Z. K. Sweeney, B. K. Chan, M. Balazs, E. Bradley, G. Castanedo, C. Chabot, D. Chantry, M. Flagella, D. M. Goldstein, R. Kondru, J. Lesnick, J. Li, M. C. Lucas, J. Nonomiya, J. Pang, S. Price, L. Salphati, B. Safina, P. P. A. Savy, E. M. Seward, M. Ultsch and D. P. Sutherlin, *J. Med. Chem.*, 2012, **55**, 7686-7695.
66. B. S. Safina, S. Baker, M. Baumgardner, P. M. Blaney, B. K. Chan, Y.-H. Chen, M. W. Cartwright, G. Castanedo, C. Chabot, A. J. Cheguillaume, P. Goldsmith, D. M. Goldstein, B. Goyal, T. Hancox, R. K. Handa, P. S. Iyer, J. Kaur, R. Kondru, J. R.

Kenny, S. L. Krintel, J. Li, J. Lesnick, M. C. Lucas, C. Lewis, S. Mukadam, J. Murray, A. J. Nadin, J. Nonomiya, F. Padilla, W. S. Palmer, J. Pang, N. Pegg, S. Price, K. Reif, L. Salphati, P. A. Savy, E. M. Seward, S. Shuttleworth, S. Sohal, Z. K. Sweeney, S. Tay, P. Tivitmahaisoon, B. Waszkowycz, B. Wei, Q. Yue, C. Zhang and D. P. Sutherlin, *J. Med. Chem.*, 2012, **55**, 5887-5900.

67. E. J. Corey and M. Chaykovsky, *J. Am. Chem. Soc.*, 1965, **87**, 1353-1364.
68. D. Summers, *Unpublished Work* 2016.
69. A. B. Charette and H. Juteau, *J. Am. Chem. Soc.*, 1994, **116**, 2651-2652.
70. C. L. Peck, J. A. Calderone and W. L. Santos, *Synthesis*, 2015, **47**, 2242-2248.
71. M. Rujian, Y. Hongbin and Z. Minglang, *Chinese patent, CN102070526B, 2013*
72. A. Fürstner, F. Stelzer and H. Szillat, *J. Am. Chem. Soc.*, 2001, **123**, 11863-11869.
73. I. D. G. Watson and F. D. Toste, *Chem. Sci.*, 2012, **3**, 2899-2919.
74. L. Zhang, J. Sun and S. A. Kozmin, *Adv. Synth. Catal.*, 2006, **348**, 2271-2296.
75. C. Nieto-Oberhuber, M. P. Muñoz, S. López, E. Jiménez-Núñez, C. Nevado, E. Herrero-Gómez, M. Raducan and A. M. Echavarren, *Chem. Eur. J.*, 2006, **12**, 1677-1693.
76. G. C. Lloyd-Jones, *Org. Biomol. Chem.*, 2003, **1**, 215-236.
77. C. Nieto-Oberhuber, M. P. Muñoz, E. Buñuel, C. Nevado, D. J. Cárdenas and A. M. Echavarren, *Angew. Chem. Int. Ed.*, 2004, **43**, 2402-2406.
78. C. Ferrer, M. Raducan, C. Nevado, C. K. Claverie and A. M. Echavarren, *Tetrahedron*, 2007, **63**, 6306-6316.
79. J. Blum, H. Beer-Kraft and Y. Badrieh, *J. Org. Chem.*, 1995, **60**, 5567-5569.
80. L. Ye, Q. Chen, J. Zhang and V. Michelet, *J. Org. Chem.*, 2009, **74**, 9550-9553.
81. T. Ozawa, T. Kurahashi and S. Matsubara, *Org. Lett.*, 2012, **14**, 3008-3011.
82. E. Benedetti, A. Simonneau, A. Hours, H. Amouri, A. Penoni, G. Palmisano, M. Malacria, J.-P. Goddard and L. Fensterbank, *Adv. Synth. Catal.*, 2011, **353**, 1908-1912.
83. S. Y. Kim and Y. K. Chung, *J. Org. Chem.*, 2010, **75**, 1281-1284.
84. H. M. Oh, J. E. Park, J. Kim, J. H. Kim, Y. K. Kang and Y. K. Chung, *Chem. Eur. J.*, 2014, **20**, 9024-9036.
85. R. Liu, D. Yang, F. Chang, L. Giordano, G. Liu and A. Tenaglia, *Asian J. Org. Chem.*, 2019, **8**, 2011-2016.
86. A. Fürstner and P. W. Davies, *Angew. Chem. Int. Ed.*, 2007, **46**, 3410-3449.
87. C. Obradors and A. M. Echavarren, *Acc. Chem. Res.*, 2014, **47**, 902-912.
88. C. Gimeno, in *Modern Supramolecular Gold Chemistry*, 2008, DOI: https://doi.org/10.1002/9783527623778.ch1, pp. 1-63.
89. D. J. Gorin and F. D. Toste, *Nature*, 2007, **446**, 395-403.
90. C.-M. Chao, D. Beltrami, P. Y. Toullec and V. Michelet, *Chem. Commun.*, 2009, 6988-6990.
91. A. Pradal, C.-M. Chao, P. Y. Toullec and V. Michelet, *Beilstein J. Org. Chem.*, 2011, **7**, 1021-1029.
92. H. Teller, M. Corbet, L. Mantilli, G. Gopakumar, R. Goddard, W. Thiel and A. Fürstner, *J. Am. Chem. Soc.*, 2012, **134**, 15331-15342.
93. H. Teller and A. Fürstner, *Chem. Eur. J.*, 2011, **17**, 7764-7767.
94. N. M. Deschamps, V. I. Elitzin, B. Liu, M. B. Mitchell, M. J. Sharp and E. A. Tabet, *J. Org. Chem.*, 2011, **76**, 712-715.
95. P. Aillard, A. Voituriez, D. Dova, S. Cauteruccio, E. Licandro and A. Marinetti, *Chem. Eur. J.*, 2014, **20**, 12373-12376.
96. K. Yavari, P. Aillard, Y. Zhang, F. Nuter, P. Retailleau, A. Voituriez and A. Marinetti, *Angew. Chem. Int. Ed.*, 2014, **53**, 861-865.
97. C. Medena, F. Calogero, Q. Lemoine, C. Aubert, E. Derat, L. Fensterbank, G. Gontard, O. Khaled, N. Vanthuyne, J. Moussa, C. Ollivier, M. Petit and M. Barbazanges, *Eur. J. Org. Chem.*, 2019, **2019**, 2129-2137.

98. A. Vanitcha, C. Damelincourt, G. Gontard, N. Vanthuyne, V. Mouriès-Mansuy and L. Fensterbank, *Chem. Commun.*, 2016, **52**, 6785-6788.
99. Z. Wu, K. Isaac, P. Retailleau, J.-F. Betzer, A. Voituriez and A. Marinetti, *Chem. Eur. J.*, 2016, **22**, 3278-3281.
100. E. M. Barreiro, E. V. Boltukhina, A. J. P. White and K. K. Hii, *Chem. Eur. J.*, 2015, **21**, 2686-2690.
101. G. Zuccarello, J. G. Mayans, I. Escofet, D. Scharnagel, M. S. Kirillova, A. H. Pérez-Jimeno, P. Calleja, J. R. Boothe and A. M. Echavarren, *J. Am. Chem. Soc.*, 2019, **141**, 11858-11863.
102. Z. Zhuang, C. L. Li, Y. Xiang, Y. H. Wang and Z. X. Yu, *Chem. Commun.*, 2017, **53**, 2158-2161.
103. C. Nieto-Oberhuber, P. Pérez-Galán, E. Herrero-Gómez, T. Lauterbach, C. Rodríguez, S. López, C. Bour, A. Rosellón, D. J. Cárdenas and A. M. Echavarren, *J. Am. Chem. Soc.*, 2008, **130**, 269-279.
104. J. Sherwood, *Angew. Chem. Int. Ed.*, 2018, **57**, 14286-14290.
105. J. M. Schulman, A. A. Friedman, J. Panteleev and M. Lautens, *Chem. Commun.*, 2012, **48**, 55-57.
106. S. Y. Yun, M. Kim, D. Lee and D. J. Wink, *J. Am. Chem. Soc.*, 2009, **131**, 24-25.
107. H. Hofmeister, K. Annen, H. Laurent and R. Wiechert, *Angew. Chem. Int. Ed.*, 1984, **23**, 727-729.
108. C. García-Morales, B. Ranieri, I. Escofet, L. López-Suarez, C. Obradors, A. I. Konovalov and A. M. Echavarren, *J. Am. Chem. Soc.*, 2017, **139**, 13628-13631.
109. M. P. Muñoz, J. Adrio, J. C. Carretero and A. M. Echavarren, *Organometallics*, 2005, **24**, 1293-1300.
110. J. Schießl, J. Schulmeister, A. Doppiu, E. Wörner, M. Rudolph, R. Karch and A. S. K. Hashmi, *Adv. Synth. Catal.*, 2018, **360**, 2493-2502.
111. M. Jia and M. Bandini, *ACS Catal.*, 2015, **5**, 1638-1652.
112. Z. Lu, J. Han, O. E. Okoromoba, N. Shimizu, H. Amii, C. F. Tormena, G. B. Hammond and B. Xu, *Org. Lett.*, 2017, **19**, 5848-5851.
113. S. Lynn, R. Upton and S. Richards, *Unpublished work*.
114. L. M. Berkowitz and P. N. Rylander, *J. Am. Chem. Soc.*, 1958, **80**, 6682-6684.
115. P. H. J. Carlsen, T. Katsuki, V. S. Martin and K. B. Sharpless, *J. Org. Chem.*, 1981, **46**, 3936-3938.
116. T. K. M. Shing, V. W.-F. Tai and E. K. W. Tam, *Angew. Chem. Int. Ed.*, 1994, **33**, 2312-2313.
117. T. K. M. Shing, E. K. W. Tam, V. W.-F. Tai, I. H. F. Chung and Q. Jiang, *Chem. Eur. J.*, 1996, **2**, 50-57.
118. B. S. Bal, W. E. Childers and H. W. Pinnick, *Tetrahedron*, 1981, **37**, 2091-2096.
119. Y. Kogami, S. Shuto and M. Arisawa, *WO2014168262A1, 2014*
120. U. S. Bäumer and H. J. Schäfer, *Electrochim. Acta*, 2003, **48**, 489-495.
121. B. Plietker, M. Niggemann and A. Pollrich, *Org. Biomol. Chem.*, 2004, **2**, 1116-1124.
122. D. H. R. Barton, D. Crich and W. B. Motherwell, *J. Chem. Soc., Chem. Commun.*, 1983, 939-941.
123. M. F. Saraiva, M. R. C. Couri, M. Le Hyaric and M. V. de Almeida, *Tetrahedron*, 2009, **65**, 3563-3572.
124. K. Yotsuji, N. Hoshiya, T. Kobayashi, H. Fukuda, H. Abe, M. Arisawa and S. Shuto, *Adv. Synth. Catal.*, 2015, **357**, 1022-1028.
125. E. Hohn and J. Pietruszka, *Adv. Synth. Catal.*, 2004, **346**, 863-866.
126. C. Ollivier and P. Renaud, *Chem. Rev.*, 2001, **101**, 3415-3434.
127. S. Murarka, *Adv. Synth. Catal.*, 2018, **360**, 1735-1753.

128. J. Cornella, J. T. Edwards, T. Qin, S. Kawamura, J. Wang, C.-M. Pan, R. Gianatassio, M. Schmidt, M. D. Eastgate and P. S. Baran, *J. Am. Chem. Soc.*, 2016, **138**, 2174-2177.
129. K. M. M. Huihui, J. A. Caputo, Z. Melchor, A. M. Olivares, A. M. Spiewak, K. A. Johnson, T. A. DiBenedetto, S. Kim, L. K. G. Ackerman and D. J. Weix, *J. Am. Chem. Soc.*, 2016, **138**, 5016-5019.
130. J. Wang, T. Qin, T.-G. Chen, L. Wimmer, J. T. Edwards, J. Cornella, B. Vokits, S. A. Shaw and P. S. Baran, *Angew. Chem. Int. Ed.*, 2016, **55**, 9676-9679.
131. F. Toriyama, J. Cornella, L. Wimmer, T.-G. Chen, D. D. Dixon, G. Creech and P. S. Baran, *J. Am. Chem. Soc.*, 2016, **138**, 11132-11135.
132. F. Sandfort, M. J. O'Neill, J. Cornella, L. Wimmer and P. S. Baran, *Angew. Chem. Int. Ed.*, 2017, **56**, 3319-3323.
133. T.-G. Chen, H. Zhang, P. K. Mykhailiuk, R. R. Merchant, C. A. Smith, T. Qin and P. S. Baran, *Angew. Chem. Int. Ed.*, 2019, **58**, 2454-2458.
134. X. A. F. Cook, A. de Gombert, J. McKnight, L. R. E. Pantaine and M. C. Willis, *Angew. Chem. Int. Ed.*, 2021, **60**, 11068-11091.
135. S. L. Zultanski and G. C. Fu, *J. Am. Chem. Soc.*, 2013, **135**, 624-627.
136. X. Wang, S. Wang, W. Xue and H. Gong, *J. Am. Chem. Soc.*, 2015, **137**, 11562-11565.
137. S. Wang, Q. Qian and H. Gong, *Org. Lett.*, 2012, **14**, 3352-3355.
138. G. A. Molander, K. M. Traister and B. T. O'Neill, *J. Org. Chem.*, 2014, **79**, 5771-5780.
139. F. González-Bobes and G. C. Fu, *J. Am. Chem. Soc.*, 2006, **128**, 5360-5361.
140. A. S. Dudnik and G. C. Fu, *J. Am. Chem. Soc.*, 2012, **134**, 10693-10697.
141. N. A. Strotman, S. Sommer and G. C. Fu, *Angew. Chem. Int. Ed.*, 2007, **46**, 3556-3558.
142. D. A. Powell, T. Maki and G. C. Fu, *J. Am. Chem. Soc.*, 2005, **127**, 510-511.
143. A. Fawcett, J. Pradeilles, Y. Wang, T. Mutsuga, E. L. Myers and V. K. Aggarwal, *Science*, 2017, **357**, 283-286.
144. J. Wang, M. Shang, H. Lundberg, K. S. Feu, S. J. Hecker, T. Qin, D. G. Blackmond and P. S. Baran, *ACS Catal.*, 2018, **8**, 9537-9542.
145. C. Li, J. Wang, L. M. Barton, S. Yu, M. Tian, D. S. Peters, M. Kumar, A. W. Yu, K. A. Johnson, A. K. Chatterjee, M. Yan and P. S. Baran, *Science*, 2017, **356**, eaam7355.
146. D. Hu, L. Wang and P. Li, *Org. Lett.*, 2017, **19**, 2770-2773.
147. R. Hurley and A. C. Testa, *J. Am. Chem. Soc.*, 1968, **90**, 1949-1952.
148. R. Hurley and A. C. Testa, *J. Am. Chem. Soc.*, 1966, **88**, 4330-4332.
149. H. Shizunobu and K. Koji, *Bull. Chem. Soc. Jpn.*, 1972, **45**, 549-553.
150. A. Cu and A. C. Testa, *J. Phys. Chem.*, 1975, **79**, 644-646.
151. I. Kleban, D. S. Radchenko, A. V. Tymtsunik, S. Shuvakin, A. I. Konovets, Y. Rassukana and O. O. Grygorenko, *Monatsh. Chem.*, 2020, **151**, 953-962.
152. R. Robles-Machín, J. Adrio and J. C. Carretero, *J. Org. Chem.*, 2006, **71**, 5023-5026.
153. P. G. M. Wuts, R. L. Gu, N. M. Jill and C. L. Thomas, *Tetrahedron Lett.*, 1998, **39**, 9155-9156.
154. A. Gray, H. Olsson, I. H. Batty, L. Priganica and C. Peter Downes, *Anal. Biochem.*, 2003, **313**, 234-245.
155. J. Rowedder and K. Weis, *Unpublished work*.
156. L. Groenendaal, M. J. Bruining, E. H. J. Hendrickx, A. Persoons, J. A. J. M. Vekemans, E. E. Havinga and E. W. Meijer, *Chem. Mater.*, 1998, **10**, 226-234.
157. R. A. Aitken, N. Karodia, H. B. McCarron, C. Rouxel, N. Sahabo and A. M. Z. Slawin, *Org. Biomol. Chem.*, 2016, **14**, 1794-1804.
158. G. E. Boswell, R. W. Mcnutt, D. G. Bubacz, A. O. Davis and K.-J. Chang, *J. Heterocycl. Chem.*, 1995, **32**, 1801-1818.

159. J. F. Teichert, S. Zhang, A. W. v. Zijl, J. W. Slaa, A. J. Minnaard and B. L. Feringa, *Org. Lett.*, 2010, **12**, 4658-4660.
160. L. M. Geary, J. C. Leung and M. J. Krische, *Chem. Eur. J.*, 2012, **18**, 16823-16827.
161. H. Song, Y. Liu and Q. Wang, *Org. Lett.*, 2013, **15**, 3274-3277.
162. K. Yamamoto, T. Bruun, J. Y. Kim, L. Zhang and M. Lautens, *Org. Lett.*, 2016, **18**, 2644-2647.
163. D. P. Becker and D. L. Flynn, *Tetrahedron*, 1993, **49**, 5047-5054.
164. A. Hobbs, *Unpublished work*.
165. H. E. Bonfield, K. Mercer, A. Diaz-Rodriguez, G. C. Cook, B. S. J. McKay, P. Slade, G. M. Taylor, W. X. Ooi, J. D. Williams, J. P. M. Roberts, J. A. Murphy, L. Schmermund, W. Kroutil, T. Mielke, J. Cartwright, G. Grogan and L. J. Edwards, *ChemPhotoChem*, 2020, **4**, 45-51.
166. J. Boström, A. Hogner, A. Llinàs, E. Wellner and A. T. Plowright, *J. Med. Chem.*, 2012, **55**, 1817-1830.
167. J. A. Joule and K. Mills, *Heterocyclic Chemistry*, Wiley, London, 2013.
168. K. D. Patel, S. M. Prajapati, S. N. Panchal and H. D. Patel, *Synth. Commun.*, 2014, **44**, 1859-1875.
169. F. A. Omar, N. M. Mahfouz and M. A. Rahman, *Eur. J. Med. Chem.*, 1996, **31**, 819-825.
170. J. S. Warmus, C. Flamme, L. Y. Zhang, S. Barrett, A. Bridges, H. Chen, R. Gowan, M. Kaufman, J. Sebolt-Leopold, W. Leopold, R. Merriman, J. Ohren, A. Pavlovsky, S. Przybranowski, H. Tecle, H. Valik, C. Whitehead and E. Zhang, *Bioorg. Med. Chem. Lett.*, 2008, **18**, 6171-6174.
171. K. Goldberg, S. Groombridge, J. Hudson, A. G. Leach, P. A. MacFaul, A. Pickup, R. Poultney, J. S. Scott, P. H. Svensson and J. Sweeney, *MedChemComm*, 2012, **3**, 600-604.
172. O. Prakash, M. Kumar, R. Kumar, C. Sharma and K. R. Aneja, *Eur. J. Med. Chem.*, 2010, **45**, 4252-4257.
173. X. Ouyang, E. L. Piatnitski, V. Pattaropong, X. Chen, H.-Y. He, A. S. Kiselyov, A. Velankar, J. Kawakami, M. Labelle, L. Smith, J. Lohman, S. P. Lee, A. Malikzay, J. Fleming, J. Gerlak, Y. Wang, R. L. Rosler, K. Zhou, S. Mitelman, M. Camara, D. Surguladze, J. F. Doody and M. C. Tuma, *Bioorg. Med. Chem. Lett.*, 2006, **16**, 1191-1196.
174. Z. Li, P. Zhan and X. Liu, *Mini Rev. Med. Chem.*, 2011, **11**, 1130-1142.
175. V. Summa, A. Petrocchi, F. Bonelli, B. Crescenzi, M. Donghi, M. Ferrara, F. Fiore, C. Gardelli, O. Gonzalez Paz, D. J. Hazuda, P. Jones, O. Kinzel, R. Laufer, E. Monteagudo, E. Muraglia, E. Nizi, F. Orvieto, P. Pace, G. Pescatore, R. Scarpelli, K. Stillmock, M. V. Witmer and M. Rowley, *J. Med. Chem.*, 2008, **51**, 5843-5855.
176. R. M. Srivastava, R. A. W. Neves Filho, R. Schneider, A. A. Vieira and H. Gallardo, *Liq. Cryst.*, 2008, **35**, 737-742.
177. M. A. Omary and H. H. Patterson, in *Encyclopedia of Spectroscopy and Spectrometry (Third Edition)*, eds. J. C. Lindon, G. E. Tranter and D. W. Koppenaal, Academic Press, Oxford, 2017, DOI: https://doi.org/10.1016/B978-0-12-803224-4.00193-X, p. 648.
178. U. Mitschke and P. Bäuerle, *J. Mater. Chem.*, 2000, **10**, 1471-1507.
179. Y. Kaminorz, B. Schulz and L. Brehmer, *Synth. Met.*, 2000, **111-112**, 75-78.
180. Q. Pei and Y. Yang, *Chem. Mater.*, 1995, **7**, 1568-1575.
181. T. Tsutsui, E.-i. Aminaka and H. Tokuhisa, *Synth. Met.*, 1997, **85**, 1201-1204.
182. C. Adachi, T. Tsutsui and S. Saito, *Appl. Phys. Lett.*, 1989, **55**, 1489-1491.
183. A. P. Kulkarni, C. J. Tonzola, A. Babel and S. A. Jenekhe, *Chem. Mater.*, 2004, **16**, 4556-4573.
184. S. Oyston, C. Wang, G. Hughes, A. S. Batsanov, I. F. Perepichka, M. R. Bryce, J. H. Ahn, C. Pearson and M. C. Petty, *J. Mater. Chem.*, 2005, **15**, 194-203.

185. Y.-Z. Lee, X. Chen, S.-A. Chen, P.-K. Wei and W.-S. Fann, *J. Am. Chem. Soc.*, 2001, **123**, 2296-2307.
186. C. S. De Oliveira, B. F. Lira, J. M. Barbosa-Filho, J. G. F. Lorenzo and P. F. De Athayde-Filho, *Molecules*, 2012, **17**.
187. B. J. Brown, I. R. Clemens and J. K. Neesom, *Synlett*, 2000, 131-133.
188. D. Kovács, J. Wölfling, N. Szabó, M. Szécsi, R. Minorics, I. Zupkó and É. Frank, *Eur. J. Med. Chem.*, 2015, **98**, 13-29.
189. K. A. Milinkevich, C. L. Yoo, T. C. Sparks, B. A. Lorsbach and M. J. Kurth, *Bioorg. Med. Chem. Lett.*, 2009, **19**, 5796-5798.
190. A. B. Theocharis and N. E. Alexandrou, *J. Heterocycl. Chem.*, 1990, **27**, 1685-1688.
191. M.-F. Pouliot, L. Angers, J.-D. Hamel and J.-F. Paquin, *Org. Biomol. Chem.*, 2012, **10**, 988-993.
192. X. Zheng, Z. Li, Y. Wang, W. Chen, Q. Huang, C. Liu and G. Song, *J. Fluorine Chem.*, 2003, **123**, 163-169.
193. A. A. Kadi, N. R. El-Brollosy, O. A. Al-Deeb, E. E. Habib, T. M. Ibrahim and A. A. El-Emam, *Eur. J. Med. Chem.*, 2007, **42**, 235-242.
194. G. Nagendra, R. S. Lamani, N. Narendra and V. V. Sureshbabu, *Tetrahedron Lett.*, 2010, **51**, 6338-6341.
195. G. V. M. Sharma, A. Begum, Rakesh and P. R. Krishna, *Synth. Commun.*, 2004, **34**, 2387-2391.
196. S. Liras, M. P. Allen and B. E. Segelstein, *Synth. Commun.*, 2000, **30**, 437-443.
197. D. Ellis, P. S. Johnson, A. Nortcliffe and S. Wheeler, *Synth. Commun.*, 2010, **40**, 3021-3026.
198. C. Li and H. D. Dickson, *Tetrahedron Lett.*, 2009, **50**, 6435-6439.
199. H. A. Rajapakse, H. Zhu, M. B. Young and B. T. Mott, *Tetrahedron Lett.*, 2006, **47**, 4827-4830.
200. P. Stabile, A. Lamonica, A. Ribecai, D. Castoldi, G. Guercio and O. Curcuruto, *Tetrahedron Lett.*, 2010, **51**, 4801-4805.
201. J. K. Augustine, V. Vairaperumal, S. Narasimhan, P. Alagarsamy and A. Radhakrishnan, *Tetrahedron*, 2009, **65**, 9989-9996.
202. S. H. Mashraqui, S. G. Ghadigaonkar and R. S. Kenny, *Synth. Commun.*, 2003, **33**, 2541-2545.
203. F. Bentiss, M. Lagrenée and D. Barbry, *Synth. Commun.*, 2001, **31**, 935-938.
204. V. K. Tandon and R. B. Chhor, *Synth. Commun.*, 2001, **31**, 1727-1732.
205. M. Baumann and I. R. Baxendale, *Beilstein J. Org. Chem.*, 2013, **9**, 1613-1619.
206. I. Karlsson, K. Samuelsson, D. J. Ponting, M. Törnqvist, L. L. Ilag and U. Nilsson, *Scientific Reports*, 2016, **6**, 21203.
207. A.-M. M. E. Omar and O. M. Aboulwafa, *J. Heterocycl. Chem.*, 1984, **21**, 1415-1418.
208. F. Fülöp, é. Semega, G. Dombi and G. Bernáth, *J. Heterocycl. Chem.*, 1990, **27**, 951-955.
209. S. J. Dolman, F. Gosselin, P. D. O'Shea and I. W. Davies, *J. Org. Chem.*, 2006, **71**, 9548-9551.
210. P. S. Chaudhari, S. P. Pathare and K. G. Akamanchi, *J. Org. Chem.*, 2012, **77**, 3716-3723.
211. S.-J. Yang, S.-H. Lee, H.-J. Kwak and Y.-D. Gong, *J. Org. Chem.*, 2013, **78**, 438-444.
212. S. Maghari, S. Ramezanpour, F. Darvish, S. Balalaie, F. Rominger and H. R. Bijanzadeh, *Tetrahedron*, 2013, **69**, 2075-2080.
213. R. Hamdy, N. I. Ziedan, S. Ali, C. Bordoni, M. El-Sadek, E. Lashin, A. Brancale, A. T. Jones and A. D. Westwell, *Bioorg. Med. Chem. Lett.*, 2017, **27**, 1037-1040.
214. T. Li, G. Wen, J. Li, W. Zhang and S. Wu, *Molecules*, 2019, **24**, 1490.

215. R. S. Lamani, G. Nagendra and V. V. Sureshbabu, *Tetrahedron Lett.*, 2010, **51**, 4705-4709.
216. F. T. Coppo, K. A. Evans, T. L. Graybill and G. Burton, *Tetrahedron Lett.*, 2004, **45**, 3257-3260.
217. D. R. Guda, H. M. Cho and M. E. Lee, *RSC Adv.*, 2013, **3**, 7684-7687.
218. G. Prabhu and V. V. Sureshbabu, *Tetrahedron Lett.*, 2012, **53**, 4232-4234.
219. G. Majji, S. K. Rout, S. Guin, A. Gogoi and B. K. Patel, *RSC Adv.*, 2014, **4**, 5357-5362.
220. S. Guin, T. Ghosh, S. K. Rout, A. Banerjee and B. K. Patel, *Org. Lett.*, 2011, **13**, 5976-5979.
221. T. Chiba and M. Okimoto, *J. Org. Chem.*, 1992, **57**, 1375-1379.
222. S. P. Pardeshi, S. S. Patil and V. D. Bobade, *Synth. Commun.*, 2010, **40**, 1601-1606.
223. R. Yang and L. Dai, *J. Org. Chem.*, 1993, **58**, 3381-3383.
224. S. Rostamizadeh and S. A. G. Housaini, *Tetrahedron Lett.*, 2004, **45**, 8753-8756.
225. S. Singh, L. K. Sharma, A. Saraswat, I. R. Siddiqui, H. K. Kehri and R. K. P. Singh, *RSC Adv.*, 2013, **3**, 4237-4245.
226. C. Dobrotă, C. C. Paraschivescu, I. Dumitru, M. Matache, I. Baciu and L. L. Ruță, *Tetrahedron Lett.*, 2009, **50**, 1886-1888.
227. H. Rajak, M. D. Kharya and P. Mishra, *Arch. Pharm.*, 2008, **341**, 247-261.
228. G. Werber, F. Buccheri, R. Noto and M. Gentile, *J. Heterocycl. Chem.*, 1977, **14**, 1385-1388.
229. R. Kapoorr, S. N. Singh, S. Tripathi and L. D. S. Yadav, *Synlett*, 2015, **26**, 1201-1206.
230. E. A. Musad, R. Mohamed, B. Ali Saeed, B. S. Vishwanath and K. M. Lokanatha Rai, *Bioorg. Med. Chem. Lett.*, 2011, **21**, 3536-3540.
231. S. L. Gaonkar, K. M. L. Rai and B. Prabhuswamy, *Eur. J. Med. Chem.*, 2006, **41**, 841-846.
232. P. Niu, J. Kang, X. Tian, L. Song, H. Liu, J. Wu, W. Yu and J. Chang, *J. Org. Chem.*, 2015, **80**, 1018-1024.
233. W. Yu, G. Huang, Y. Zhang, H. Liu, L. Dong, X. Yu, Y. Li and J. Chang, *J. Org. Chem.*, 2013, **78**, 10337-10343.
234. D. M. Pore, S. M. Mahadik and U. V. Desai, *Synth. Commun.*, 2008, **38**, 3121-3128.
235. M. Dabiri, P. Salehi, M. Baghbanzadeh and M. Bahramnejad, *Tetrahedron Lett.*, 2006, **47**, 6983-6986.
236. J. N. Sangshetti, P. P. Dharmadhikari, R. S. Chouthe, B. Fatema, V. Lad, V. Karande, S. N. Darandale and D. B. Shinde, *Bioorg. Med. Chem. Lett.*, 2013, **23**, 2250-2253.
237. A. K. Yadav and L. D. S. Yadav, *Tetrahedron Lett.*, 2014, **55**, 2065-2069.
238. V. Polshettiwar and R. S. Varma, *Tetrahedron Lett.*, 2008, **49**, 879-883.
239. A. Kudelko and W. Zieliński, *Tetrahedron Lett.*, 2012, **53**, 76-77.
240. R. Huisgen, J. Sauer and H. J. Sturm, *Angew. Chem.*, 1958, **70**, 272-273.
241. R. Huisgen, J. Sauer, H. J. Sturm and J. H. Markgraf, *Chem. Ber.*, 1960, **93**, 2106-2124.
242. J. Sauer, R. Huisgen and H. J. Sturm, *Tetrahedron*, 1960, **11**, 241-251.
243. R. M. Herbst, *J. Org. Chem.*, 1961, **26**, 2372-2373.
244. Y. A. Efimova, T. V. Artamonova and G. I. Koldobskii, *Russ. J. Org. Chem.*, 2008, **44**, 1345.
245. B. Reichart and C. O. Kappe, *Tetrahedron Lett.*, 2012, **53**, 952-955.
246. H. Detert and D. Schollmeier, *Synthesis*, 1999, **1999**, 999-1004.
247. S. Fürmeier and Jürgen O. Metzger, *Eur. J. Org. Chem.*, 2003, **2003**, 885-893.
248. K. Geyl, S. Baykov, M. Tarasenko, L. E. Zelenkov, V. Matveevskaya and V. P. Boyarskiy, *Tetrahedron Lett.*, 2019, **60**, 151108.
249. M. Ichikawa, T. Kawaguchi, K. Kobayashi, T. Miki, K. Furukawa, T. Koyama and Y. Taniguchi, *J. Mater. Chem.*, 2006, **16**, 221-225.

250. E. Meyer, A. C. Joussef and H. Gallardo, *Synthesis*, 2003, 0899-0905.
251. N. D. Obushak, N. T. Pokhodylo, N. I. Pidlypnyi and V. S. Matiichuk, *Russ. J. Org. Chem.*, 2008, **44**, 1522.
252. L. I. Vereshchagin, A. V. Petrov, V. N. Kizhnyaev, F. A. Pokatilov and A. I. Smirnov, *Russ. J. Org. Chem.*, 2006, **42**, 1049-1055.
253. L. I. Vereshchagin, A. V. Petrov, A. G. Proidakov, F. A. Pokatilov, A. I. Smirnov and V. N. Kizhnyaev, *Russ. J. Org. Chem.*, 2006, **42**, 912-917.
254. J. Y. F. Wong, J. M. Tobin, F. Vilela and G. Barker, *Chem. Eur. J.*, 2019, **25**, 12439-12445.
255. J.-P. Hagenbuch, *CHIMIA*, 2003, **57**, 773-776.
256. R. J. Herr, *Biorg. Med. Chem.*, 2002, **10**, 3379-3393.
257. B. Gutmann, J.-P. Roduit, D. Roberge and C. O. Kappe, *Angew. Chem. Int. Ed.*, 2010, **49**, 7101-7105.
258. K. Ishihara, M. Kawashima, T. Matsumoto, T. Shioiri and M. Matsugi, *Synthesis*, 2018, **50**, 1293-1300.
259. K. Livingstone, S. Bertrand and C. Jamieson, *J. Org. Chem.*, 2020, **85**, 7413-7423.
260. Y.-H. Lin, H.-H. Wu, K.-T. Wong, C.-C. Hsieh, Y.-C. Lin and P.-T. Chou, *Org. Lett.*, 2008, **10**, 3211-3214.
261. S. U. Pandya, H. A. Al Attar, V. Jankus, Y. Zheng, M. R. Bryce and A. P. Monkman, *J. Mater. Chem.*, 2011, **21**, 18439-18446.
262. P. Venkatakrishnan, P. Natarajan, J. N. Moorthy, Z. Lin and T. J. Chow, *Tetrahedron*, 2012, **68**, 7502-7508.
263. M.-k. Leung, W.-H. Yang, C.-N. Chuang, J.-H. Lee, C.-F. Lin, M.-K. Wei and Y.-H. Liu, *Org. Lett.*, 2012, **14**, 4986-4989.
264. A. A. Vieira, E. Cavero, P. Romero, H. Gallardo, J. L. Serrano and T. Sierra, *J. Mater. Chem. C*, 2014, **2**, 7029-7038.
265. F. Považanec, J. Kováč and J. Svoboda, *Collect. Czech. Chem. Commun.*, 1980, **45**, 1299-1300.
266. N. A. Bumagin, A. V. Kletskov, S. K. Petkevich, I. A. Kolesnik, A. S. Lyakhov, L. S. Ivashkevich, A. V. Baranovsky, P. V. Kurman and V. I. Potkin, *Tetrahedron*, 2018, **74**, 3578-3588.
267. F. Fouad, D. R. Davis and R. Twieg, *Liq. Cryst.*, 2018, **45**, 1508-1517.
268. A. Jilale, P. Netchitaïlo, B. Decroix and D. Vegh, *J. Heterocycl. Chem.*, 1993, **30**, 881-885.
269. S. Kun, G. Z. Nagy, M. Tóth, L. Czecze, A. N. Van Nhien, T. Docsa, P. Gergely, M.-D. Charavgi, P. V. Skourti, E. D. Chrysina, T. Patonay and L. Somsák, *Carbohydr. Res.*, 2011, **346**, 1427-1438.
270. A. Kurowska, P. Zassowski, A. S. Kostyuchenko, T. Y. Zheleznova, K. V. Andryukhova, A. S. Fisyuk, A. Pron and W. Domagala, *PCCP*, 2017, **19**, 30261-30276.
271. N. N. Patwardhan, E. A. Morris, Y. Kharel, M. R. Raje, M. Gao, J. L. Tomsig, K. R. Lynch and W. L. Santos, *J. Med. Chem.*, 2015, **58**, 1879-1899.
272. K. Srinivas, G. Sivakumar, C. Ramesh Kumar, M. Ananth Reddy, K. Bhanuprakash, V. J. Rao, C.-W. Chen, Y.-C. Hsu and J. T. Lin, *Synth. Met.*, 2011, **161**, 1671-1681.
273. Y. Tan, Z. Wang, C. Wei, Z. Liu, Z. Bian and C. Huang, *Org. Electron.*, 2019, **69**, 77-84.
274. C. M. Tonge, N. R. Paisley, A. M. Polgar, K. Lix, W. R. Algar and Z. M. Hudson, *ACS Appl. Mater. Interfaces*, 2020, **12**, 6525-6535.
275. M. Tóth, S. Kun, É. Bokor, M. Benltifa, G. Tallec, S. Vidal, T. Docsa, P. Gergely, L. Somsák and J.-P. Praly, *Biorg. Med. Chem.*, 2009, **17**, 4773-4785.
276. F. Hundemer, L. Graf von Reventlow, C. Leonhardt, M. Polamo, M. Nieger, S. M. Seifermann, A. Colsmann and S. Bräse, *ChemistryOpen*, 2019, **8**, 1413-1420.
277. J. S. Clovis, A. Eckell, R. Huisgen and R. Sustmann, *Chem. Ber.*, 1967, **100**, 60-70.

278. V. Lohse, P. Leihkauf, C. Csongar and G. Tomaschewski, *J. Prakt. Chem.*, 1988, **330**, 406-414.
279. Y. Wang, C. I. Rivera Vera and Q. Lin, *Org. Lett.*, 2007, **9**, 4155-4158.
280. Y. Wang, W. J. Hu, W. Song, R. K. V. Lim and Q. Lin, *Org. Lett.*, 2008, **10**, 3725-3728.
281. R. Remy and C. G. Bochet, *Eur. J. Org. Chem.*, 2018, **2018**, 316-328.
282. S. Stewart, R. Harris and C. Jamieson, *Synlett*, 2014, **25**, 2480-2484.
283. Z. Li, L. Qian, L. Li, J. C. Bernhammer, H. V. Huynh, J.-S. Lee and S. Q. Yao, *Angew. Chem. Int. Ed.*, 2016, **55**, 2002-2006.
284. K. Livingstone, S. Bertrand, A. R. Kennedy and C. Jamieson, *Chemistry*, 2020, **26**, 10591-10597.
285. K. Livingstone, S. Bertrand, J. Mowat and C. Jamieson, *Chem. Sci.*, 2019, **10**, 10412-10416.
286. C. P. Ramil and Q. Lin, *Curr. Opin. Chem. Biol.*, 2014, **21**, 89-95.
287. N. H. Toubro and A. Holm, *J. Am. Chem. Soc.*, 1980, **102**, 2093-2094.
288. A. Tartar and J. C. Gesquiere, *J. Org. Chem.*, 1979, **44**, 5000-5002.
289. K. Livingstone, *Preliminary work*, 2018
290. J. Choina, D. Dolat, E. Kusiak, M. Janus and A. Morawski, *Pol. J. Chem. Tech.*, 2009, **11**, 1-6.
291. K. Zając, A. Czyżewski, M. Kaszyńska and M. Janus, *Catalysts*, 2020, **10**, 385.
292. Y. Matsumura and H. N. Ananthaswamy, *Toxicol. Appl. Pharmacol.*, 2004, **195**, 298-308.
293. F. Albericio and A. El-Faham, *Org. Process. Res. Dev.*, 2018, **22**, 760-772.
294. S. R. Buzilova, N. I. Kuznetsova, V. M. Shul'gina, G. A. Gareev and L. I. Vereshchagin, *Chem. Heterocycl. Compd.*, 1983, **19**, 107-109.
295. Q. Wang, Y. Wang and M. Kurosu, *Org. Lett.*, 2012, **14**, 3372-3375.
296. W. Gordy and W. J. O. Thomas, *J. Chem. Phys.*, 1956, **24**, 439-444.
297. MOE Version 2019.01, Chemical Computing Group, 2019.
298. F. Politano and G. Oksdath-Mansilla, *Org. Process Res. Dev.*, 2018, **22**, 1045-1062.
299. B. D. A. Hook, W. Dohle, P. R. Hirst, M. Pickworth, M. B. Berry and K. I. Booker-Milburn, *J. Org. Chem.*, 2005, **70**, 7558-7564.
300. J. E. Baldwin and S. Y. Hong, *Chem. Commun. (London)*, 1967, 1136a-1136a.
301. S.-Y. Hong and J. E. Baldwin, *Tetrahedron*, 1968, **24**, 3787-3794.
302. C. Jamieson and K. Livingstone, *The Nitrile Imine 1,3-Dipole Properties, Reactivity and Applications* Springer, Cham, Switzerland, 2020.
303. E. Blasco, Y. Sugawara, P. Lederhose, J. P. Blinco, A.-M. Kelterer and C. Barner-Kowollik, *ChemPhotoChem*, 2017, **1**, 159-163.
304. J. P. Menzel, B. B. Noble, A. Lauer, M. L. Coote, J. P. Blinco and C. Barner-Kowollik, *J. Am. Chem. Soc.*, 2017, **139**, 15812-15820.
305. G. Bertrand and C. Wentrup, *Angew. Chem. Int. Ed.*, 1994, **33**, 527-545.
306. B. García, S. Ibeas and J. M. Leal, *J. Phys. Org. Chem.*, 1996, **9**, 593-597.
307. C.-C. Yang, C.-J. Hsu, P.-T. Chou, H. C. Cheng, Y. O. Su and M.-k. Leung, *J. Phys. Chem. B*, 2010, **114**, 756-768.
308. G. B. Barlin and T. J. Batterham, *J. Chem. Soc. B Phys. Org.*, 1967, 516-518.
309. L. I. Vereshchagin, O. N. Verkhozina, F. A. Pokatilov, S. K. Strunevich, A. G. Proidakov and V. N. Kizhnyaev, *Russ. J. Org. Chem.*, 2007, **43**, 1710-1714.
310. E. Havinga and H. Veldstra, *Recl. Trav. Chim. Pays-Bas*, 1947, **66**, 257-272.
311. I. Saito, S. Muramatsu, H. Sugiyama, A. Yamamoto and T. Matsuura, *Tetrahedron Lett.*, 1985, **26**, 5891-5894.
312. P.-S. Song and W. E. Kurtin, *J. Am. Chem. Soc.*, 1969, **91**, 4892-4906.
313. C. Pac and H. Sakurai, *Tetrahedron Lett.*, 1968, **9**, 1865-1870.

314. J. Pazinato, O. M. Cruz, K. P. Naidek, A. R. A. Pires, E. Westphal, H. Gallardo, H. Baubichon-Cortay, M. E. M. Rocha, G. R. Martinez, S. M. B. Winnischofer, A. Di Pietro and H. Winnischofer, *Eur. J. Med. Chem.*, 2018, **148**, 165-177.
315. S. Bansal, M. Bala, S. K. Suthar, S. Choudhary, S. Bhattacharya, V. Bhardwaj, S. Singla and A. Joseph, *Eur. J. Med. Chem.*, 2014, **80**, 167-174.
316. L. Pitzer, F. Schäfers and F. Glorius, *Angew. Chem. Int. Ed.*, 2019, **58**, 8572-8576.
317. F. G. Fallon and R. M. Herbst, *J. Org. Chem.*, 1957, **22**, 933-936.
318. D. Cambié, C. Bottecchia, N. J. W. Straathof, V. Hessel and T. Noël, *Chem. Rev.*, 2016, **116**, 10276-10341.
319. C. Sambiagio and T. Noël, *Trends Chem.*, 2020, **2**, 92-106.
320. J. P. Knowles, L. D. Elliott and K. I. Booker-Milburn, *Beilstein J. Org. Chem.*, 2012, **8**, 2025-2052.
321. R. Huisgen, H. J. Sturm and M. Seidel, *Chem. Ber.*, 1961, **94**, 1555-1562.
322. Y. A. Efimova, G. G. Karabanovich, T. V. Artamonova and G. I. Koldobskii, *Russ. J. Org. Chem.*, 2009, **45**, 1241-1243.
323. J. Sauer, Gunther R. Pabst, U. Holland, H.-S. Kim and S. Loebbecke, *Eur. J. Org. Chem.*, 2001, **2001**, 697-706.
324. T. Curtius, *Ber. Dtsch. Chem. Ges.*, 1890, **23**, 3023-3033.
325. Y. A. Efimova, G. G. Karabanovich, T. V. Artamonova and G. I. Koldobskii, *Russ. J. Org. Chem.*, 2009, **45**, 631-632.
326. A. Maciejewski and R. P. Steer, *Chem. Rev.*, 1993, **93**, 67-98.
327. S. Yamada, T. Misono and S. Tsuzuki, *J. Am. Chem. Soc.*, 2004, **126**, 9862-9872.
328. T. Kawano, T. Yoshizumi, K. Hirano, T. Satoh and M. Miura, *Org. Lett.*, 2009, **11**, 3072-3075.
329. L. Wang, J. Cao, Q. Chen and M. He, *J. Org. Chem.*, 2015, **80**, 4743-4748.
330. S. Dailey, W. J. Feast, R. J. Peace, I. C. Sage, S. Till and E. L. Wood, *J. Mater. Chem.*, 2001, **11**, 2238-2243.
331. W. Zhang, Y. Su, S. Chong, L. Wu, G. Cao, D. Huang, K.-H. Wang and Y. Hu, *Org. Biomol. Chem.*, 2016, **14**, 11162-11175.
332. X.-Y. Fan, X. Jiang, Y. Zhang, Z.-B. Chen and Y.-M. Zhu, *Org. Biomol. Chem.*, 2015, **13**, 10402-10408.
333. Z. Li, A. Zhu, X. Mao, X. Sun and X. Gong, *J. Braz. Chem. Soc.*, 2008, **19**, 1622-1626.
334. S. N. R. Mule, S. K. Battula, G. Velupula, D. R. Guda and H. B. Bollikolla, *RSC Adv.*, 2014, **4**, 58397-58403.